NASA-TM-104,937

NASA-TM-104937 19910073923

THEORETICAL AERODYNAMICS CONTRACTORS' WORKSHOP

N A S A LANGLEY RESEARCH CENTER

Hampton, VA

October 18 - 19, 1983

Volume II

LIBRARY COPY
AUG 1 6 1991
LANGLEY RESEARCH CENTER
LIBRARY, NASA, HAMPTON, VA

CONTENTS OF VOL II

WEDNESDAY, OCTOBER 19

			page
	POTENTIAL FLOW		
8:30 - 8:55	MCAERO Subsonic Wing Design Panel Method for Complex Configurations	Dean Bristow McDonnell-Douglas	365
8:55 - 9:20	Cartesian Finite-Volume Full-Potential Method for General Configurations	Bruce Wedan Northrop	383
9:20 - 9:55	Transonic Wing-Body Simulations with Multiple-Canted Winglets and Swept-Planform Pylons	Charles Boppe B. S. Rosen Grumman	407
9:55 - 10:25	BREAK		
10:25 - 10:50	Embedded Mesh Multi-Grid Treatment of 2-D Transonic Flows	Doug McCarthy Purdue	435
10:50 - 11:15	Computational Methods for Vortex Dominated Compressible Flows	Earll Murman MIT	445
11:15 - 11:40	Entropy Effects and Shock Fitting in Conical Supersonic Full-Potential Flows	Mike Siclari Grumman	461
11:40 - 12:40	LUNCH		
12:40 - 1:05	Supersonic Potential for Three-Dimensional Configurations	V. Shankar Rockwell	495

N91-71478 #

VICOUS/INVISCID INTERACTION

1:05 - 1:30	Numerical Methods for Computing Airfoil Leading-Edge Separation Bubbles	Jim Carter UTRC	539
1:30 - 1:55	Recent Improvements in GRUMFOIL	Bob Melnik Grumman	557
1:55 - 2:20	Interacted Euler/Boundary Layer Methods for Airfoil Flows	Dave Whitfield MSU	583
2:20 - 2:45	Development of Viscous Wing Theory	Reuben Chow Grumman	607
2:45 - 3:15	BREAK		
3:15 - 3:40	Computation of Flow Fields in Unbounded Domains	Lu Ting NYU	635

GRID GENERATION

3:40 - 4:05	Solution Adaptive Grid Generation	Pete Eiseman Columbia	651
4:05 - 4:20	Application of Variational Methods for Generating Adaptive Grids	Rick Kreis NCSU	689

MCAERO Subsonic Wing Design Panel Method for Complex Configurations

Dean R. Bristow

McDonnell Aircraft Company
St. Louis, Missouri

MCDONNELL AIRCRAFT COMPANY

BRISTOW

SEQUENCE OF COMPUTER PROGRAMS FOR ANALYSIS AND DESIGN

Geometry Input

500 - 1000 Panels

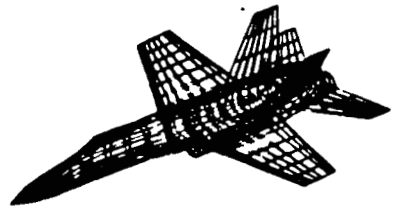

① MCAERO

Conventional Subsonic Analysis

- Calculate Φ_i, $\vec{V}_i$, C_{p_i}
- \$100 - \$200 per case

② DMCAERO

Geometry Sensitivity Coefficients

- Calculates $\frac{\partial \Phi_i}{\partial z_k}$
- \$200 - \$500 per case

③ DESIGN

Pressures Prescribed

- Calculates Twist, Camber, Thickness
- \$2 - \$5 per case
- Interactive Graphics

MCAERO Prediction Accuracy for Clean and Takeoff Configurations

Flaps	MCAERO	Wind tunnel data
Undeflected	——	○
15° Deflected 30°	- - - -	△

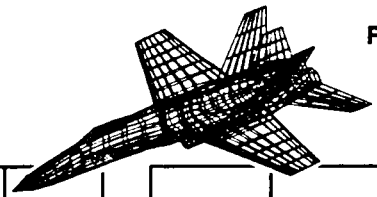

F-18 Full 3-D Panelling
($\delta_{horizontal} = -5°$)

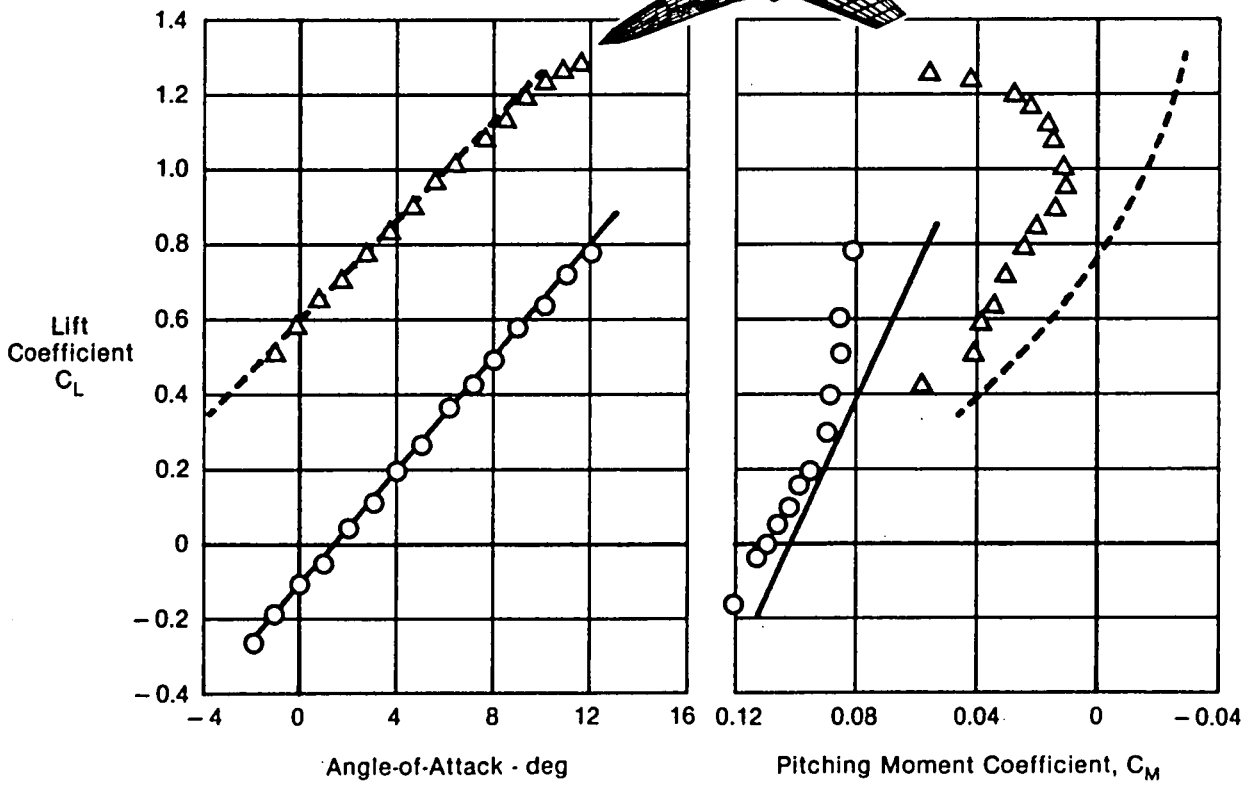

GP33-0692-2

SOLUTION APPROACH FOR MCAERO AND DMCAERO

MCAERO - CONVENTIONAL ANALYSIS

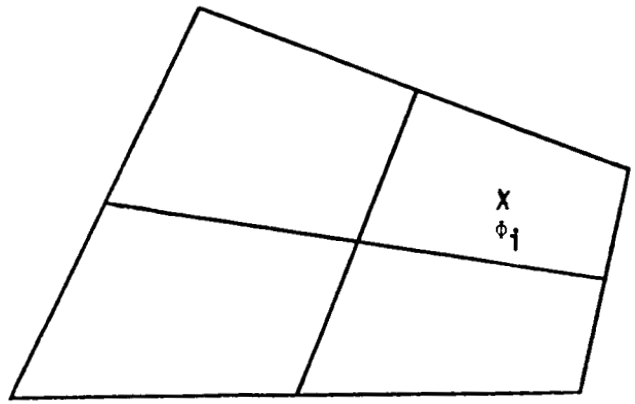

$(x,y,z)_k$

1. $\left[A_{ij}\right]\left[\Phi_j\right] = \left[BC_i\right]$

2. $\left[\Phi_i\right] = \left[A_{ij}\right]^{-1}\left[BC_j\right]$

3. Solution: $\left[\Phi_i\right]$

DMCAERO - GEOMETRY SENSITIVITY COEFFICIENTS

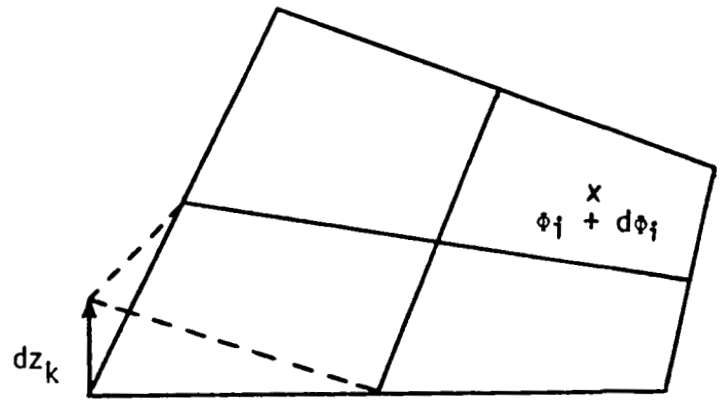

$(x,y,z)_k$

1. $\left[A_{ij}\right]\left[d\Phi_j\right] + \left[\frac{\partial A_{ij}}{\partial z_k} \cdot dz_k\right]\left[\Phi_j\right] = 0$

2. $\left[d\Phi_i\right] = \left[A_{ij}\right]^{-1} \cdot \left[\frac{\partial A_{ij}}{\partial z_k} \cdot \Phi_j\right]\left[dz_k\right]$

3. Solution: $\left[\frac{\partial \Phi_j}{\partial z_k}\right]$

SIGNIFICANCE OF GEOMETRY SENSITIVITY COEFFICIENTS $\frac{\partial \Phi_i}{\partial z_k}$

(1) Efficient Perturbation Analysis by Extrapolation

$$\Delta \Phi_i \cong \sum_k \left(\frac{\partial \Phi_i}{\partial z_k} \right) \cdot \Delta z_k$$

(2) Accurate for Large Changes in Wing Section Geometry

(3) $\frac{\partial \Phi_i}{\partial z_k}$ can be converted to $\frac{\partial c_{p_i}}{\partial z_k}$ for Wing Design

COMPARISON OF TWO EXTRAPOLATION APPROACHES FOR THICK DISPLACEMENT MODELING

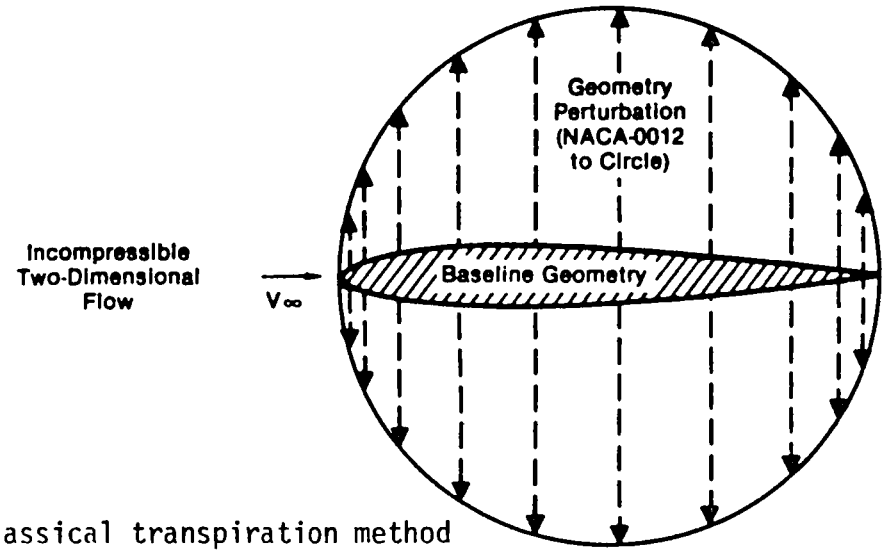

□ Classical transpiration method of Lighthill

○ MCAERO Perturbation Analysis Method

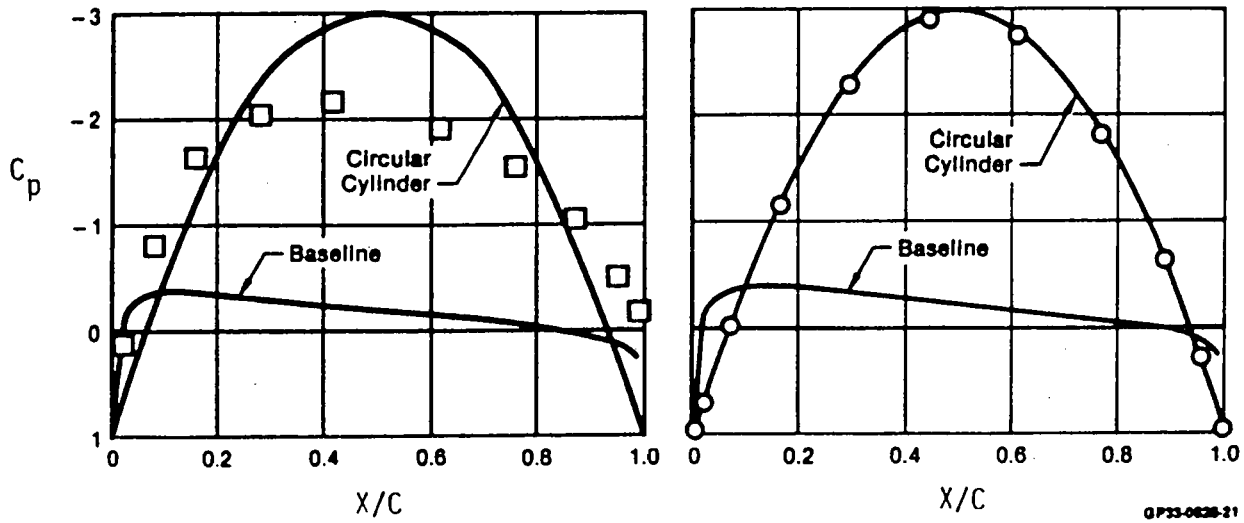

VARIATION OF FLOW PROPERTIES WITH THICKNESS

ELLIPTICAL CYLINDER AT 0° INCIDENCE

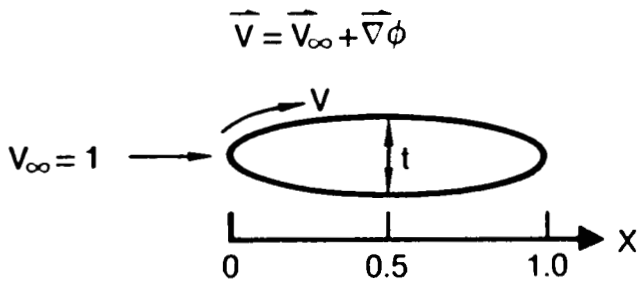

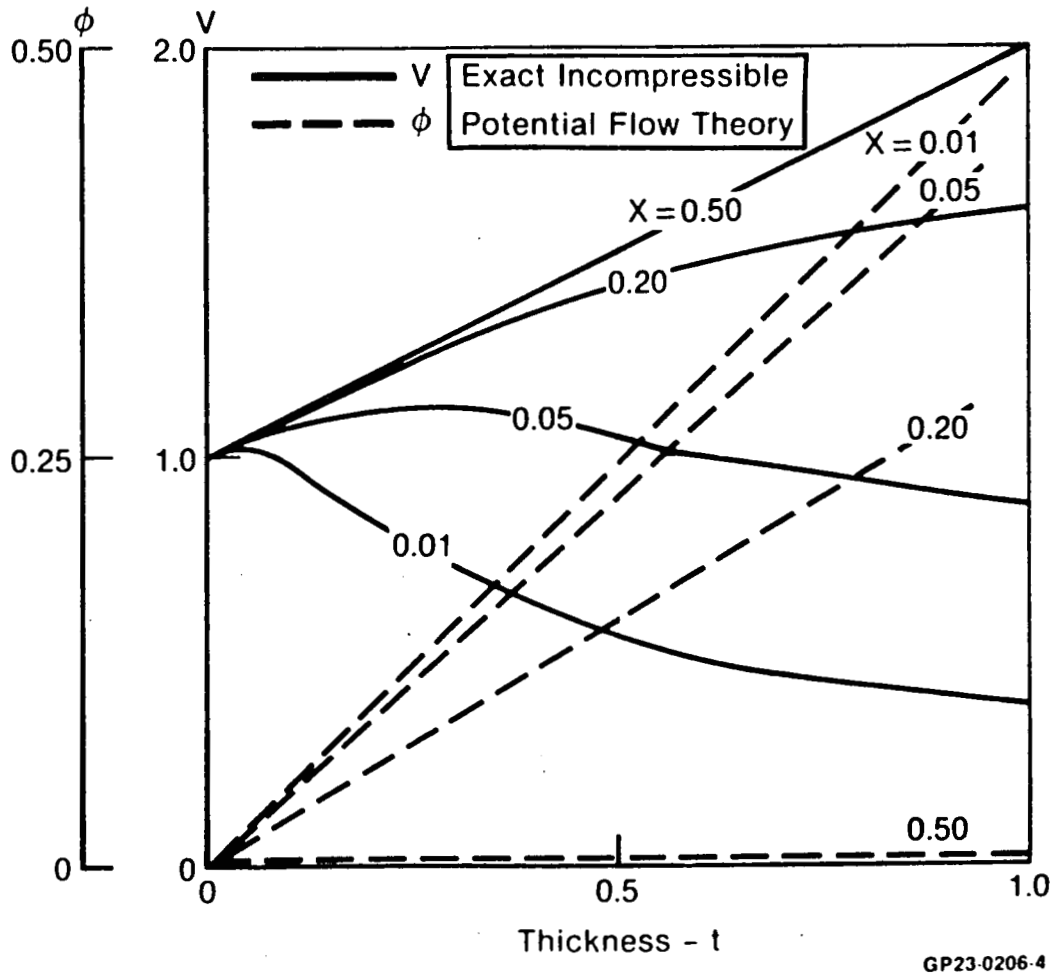

GP23-0206-4

BASELINE WING PANELING FOR PERTURBATION ANALYSIS TEST CASES

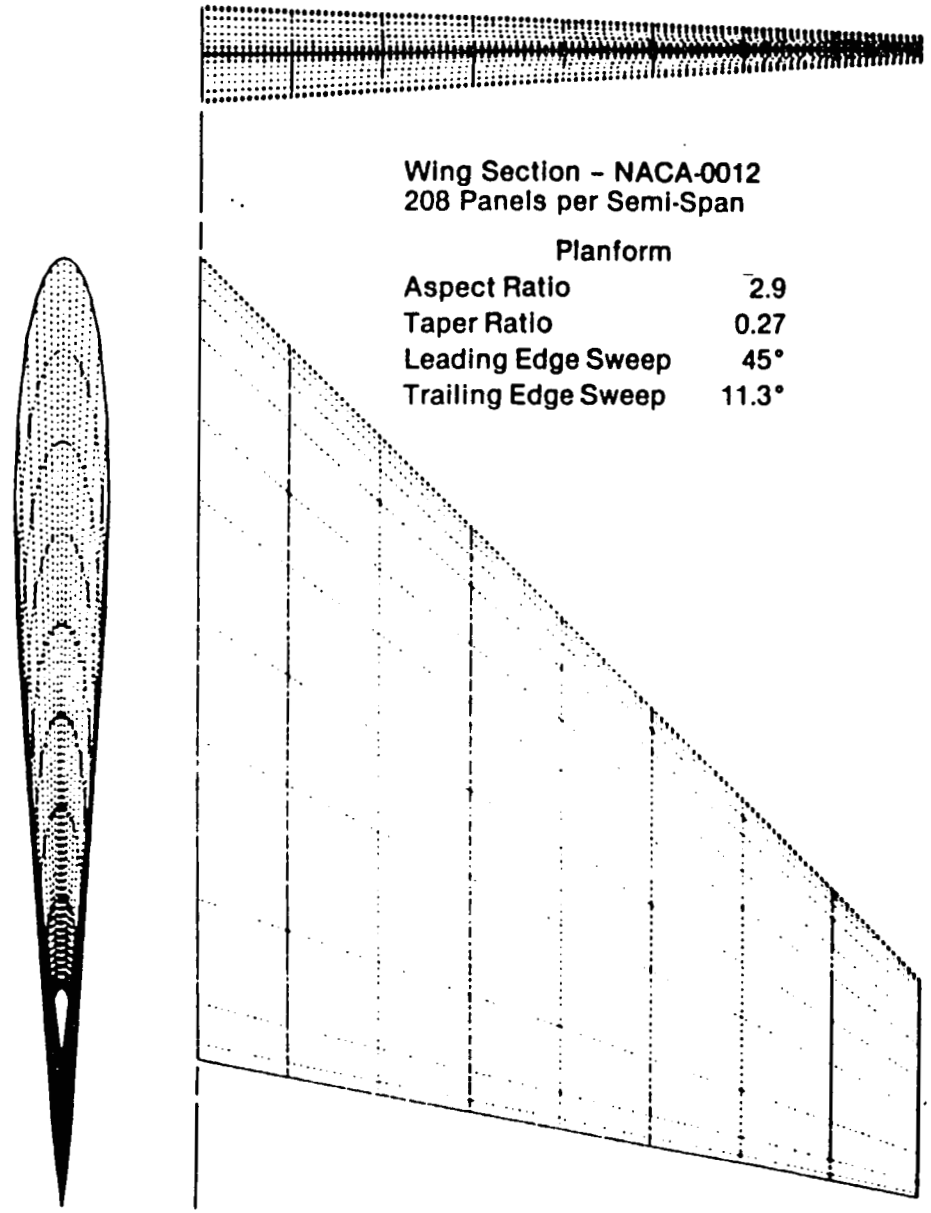

GP23-0206-11

GEOMETRY PERTURBATION TEST CASES
FIXED PLANFORM GEOMETRY

	Root Section	Tip Section	CPU Seconds
Baseline Wing (NACA-0012)	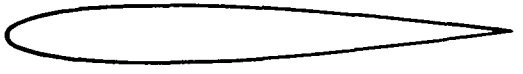	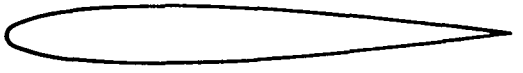	120
Case A (10° Twist)	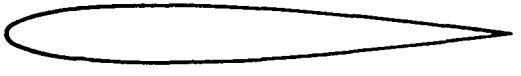	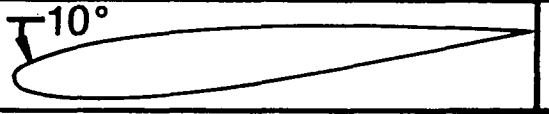	4
Case B (Supercritical)			4
Case C (Fighter)	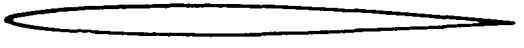	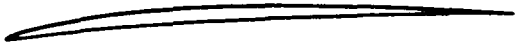	4

GP23-0206-9

PRESSURE DISTRIBUTION AT 5° ANGLE-OF-ATTACK
FIGHTER

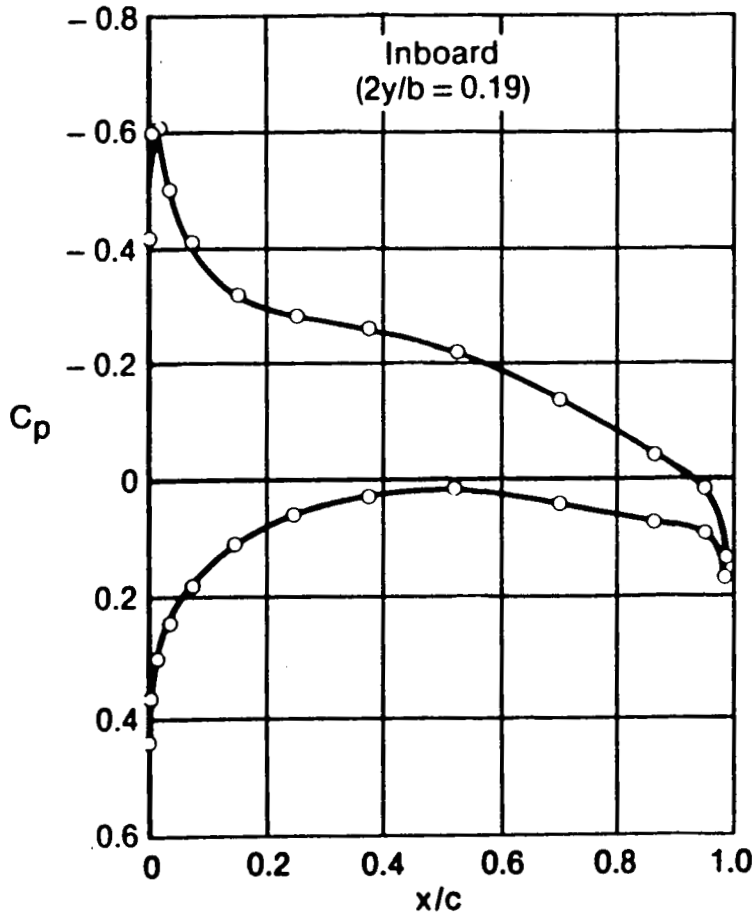

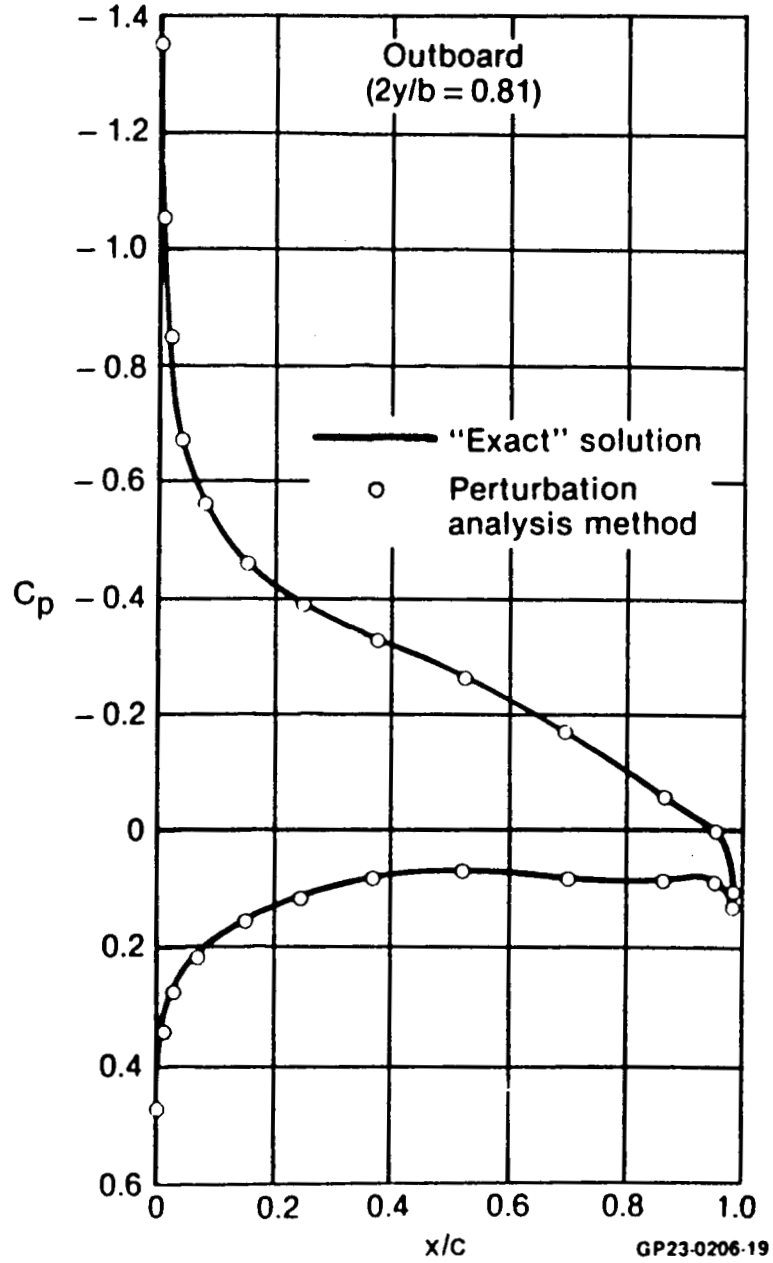

Schematic of MCAIR 3-D Wing Design Method

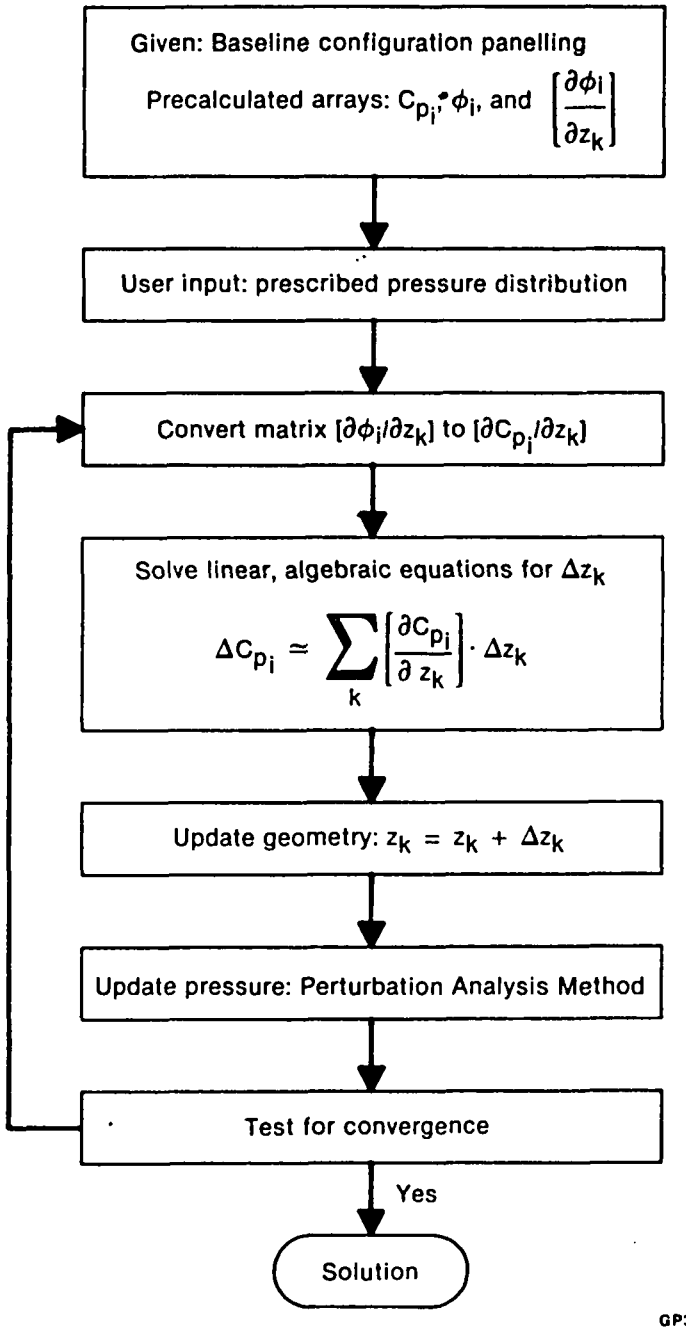
Given: Baseline configuration panelling
Precalculated arrays: C_{p_i}, ϕ_i, and $\left[\frac{\partial \phi_i}{\partial z_k}\right]$
User input: prescribed pressure distribution
Convert matrix $[\partial \phi_i / \partial z_k]$ to $[\partial C_{p_i} / \partial z_k]$
Solve linear, algebraic equations for Δz_k
$\Delta C_{p_i} \simeq \sum_k \left[\frac{\partial C_{p_i}}{\partial z_k}\right] \cdot \Delta z_k$
Update geometry: $z_k = z_k + \Delta z_k$
Update pressure: Perturbation Analysis Method
Test for convergence
Yes
Solution

GP33-0151-10

CONVERSION OF $\frac{\partial \Phi i}{\partial z_k}$ TO $\frac{\partial c_p}{\partial z_k}$

(2-D Incompressible Assumed for Clarity)

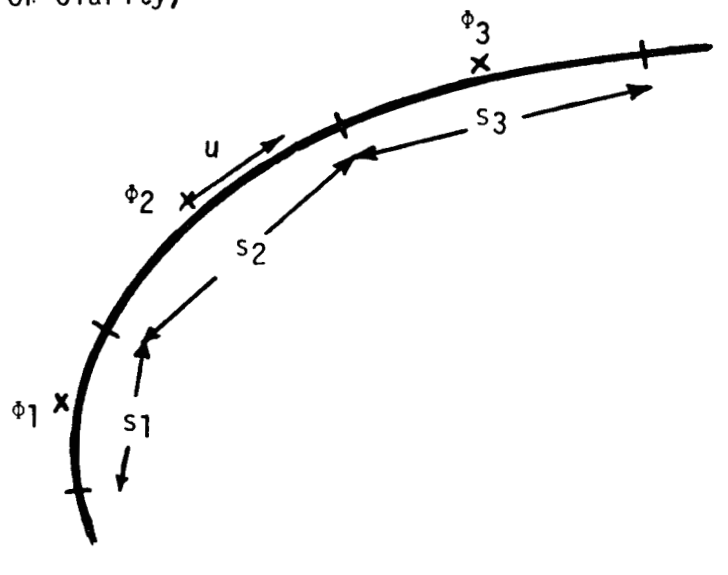

1. Convert Φ_1, Φ_2, Φ_3 to u by Numerical Differentiation

$$u = f_1(s_1, s_2, s_3) \cdot \Phi_1 + f_2(s_1, s_2, s_3) \cdot \Phi_2 + f_3(s_1, s_2, s_3) \cdot \Phi_3$$

2. $C_p = 1-u^2 \Rightarrow dc_p = -2udu$

3. $$\frac{\partial c_p}{\partial z_k} = -2u \cdot \left\{ \sum_{i=1}^{3} \left[f_i \frac{\partial \Phi i}{\partial z_k} \right] + \sum_{i=1}^{3} \left[\frac{\partial f_i}{\partial z_k} \Phi_i \right] \right\}$$

Updated Each Iteration — Reused — Updated

DEMONSTRATION OF WAVY WALL DESIGN INSTABILITY

Fighter wing tip

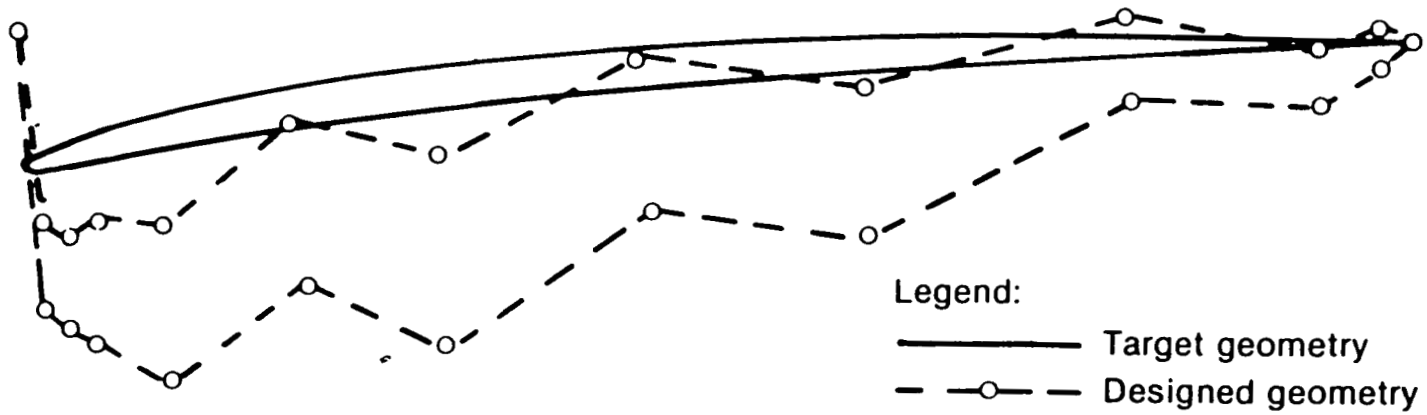

GP33-0151-12

TYPICAL WING DESIGN SOLUTION INSTABILITIES

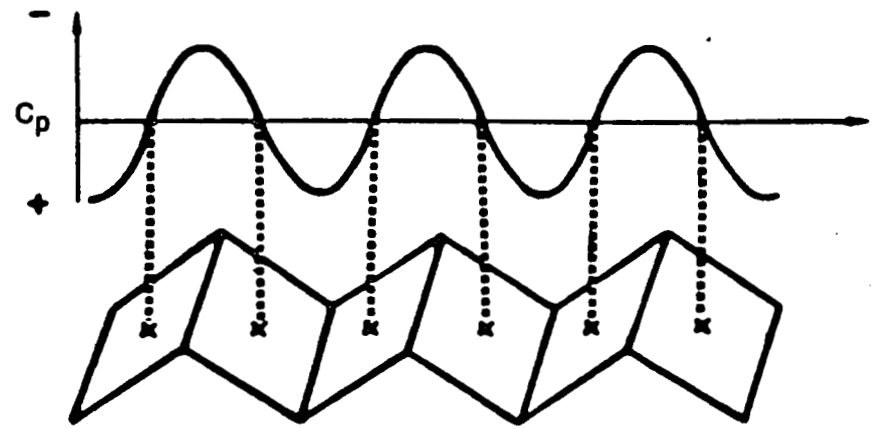

WAVY WALL INSTABILITY

Pressure at Panel Center Does Not Control Streamwise Slope Oscillations

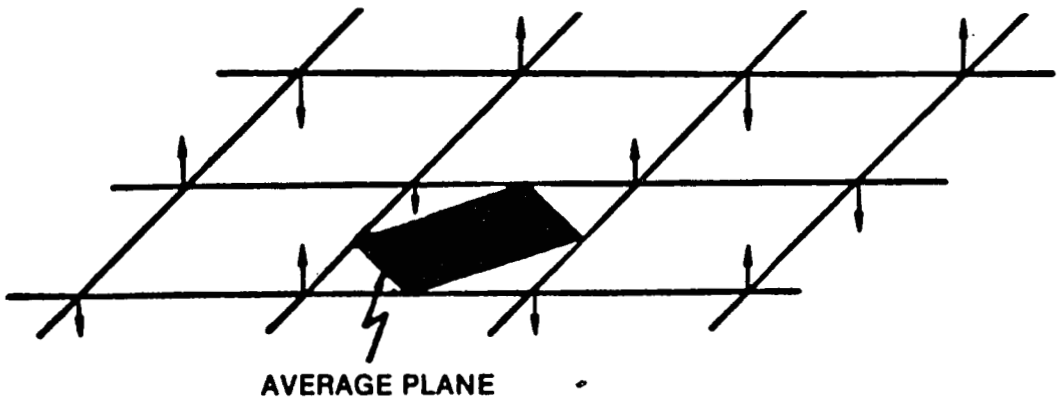

FOUR-CORNER INSTABILITY

Average Plane of Panel Does Not Control Corner Point Oscillations

REMEDY:
- MORE PRESSURES THAN UNKNOWNS
- LEAST SQUARES

Example Wing Design Solution

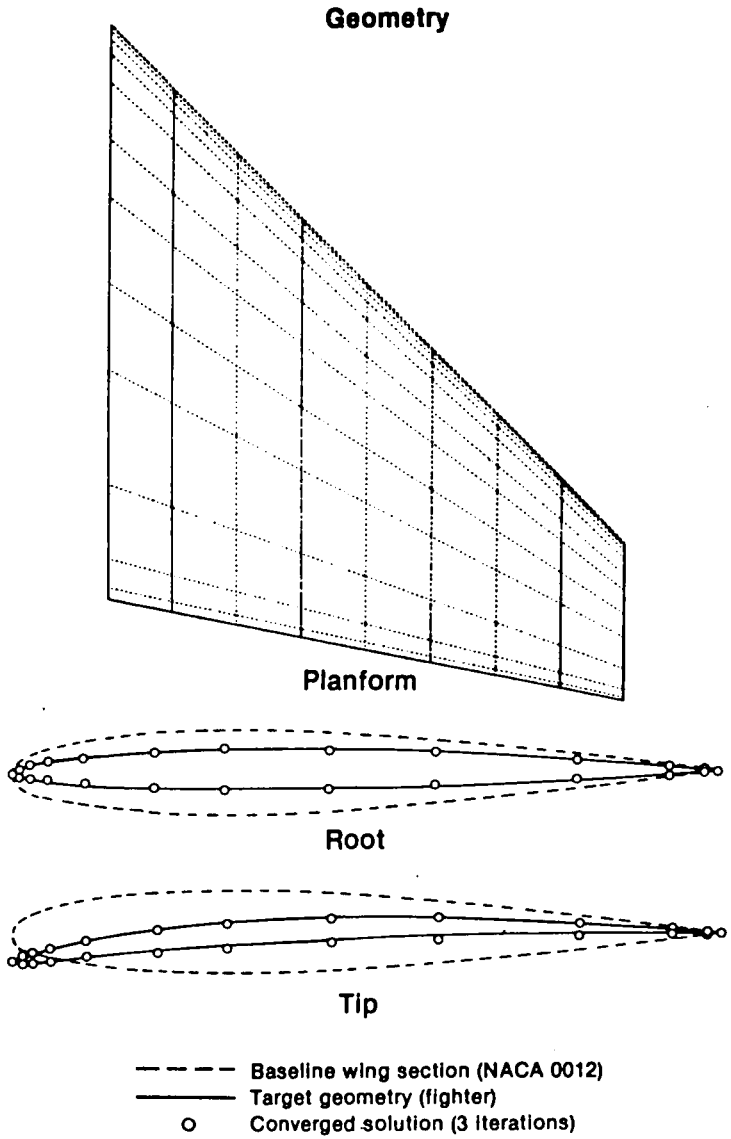

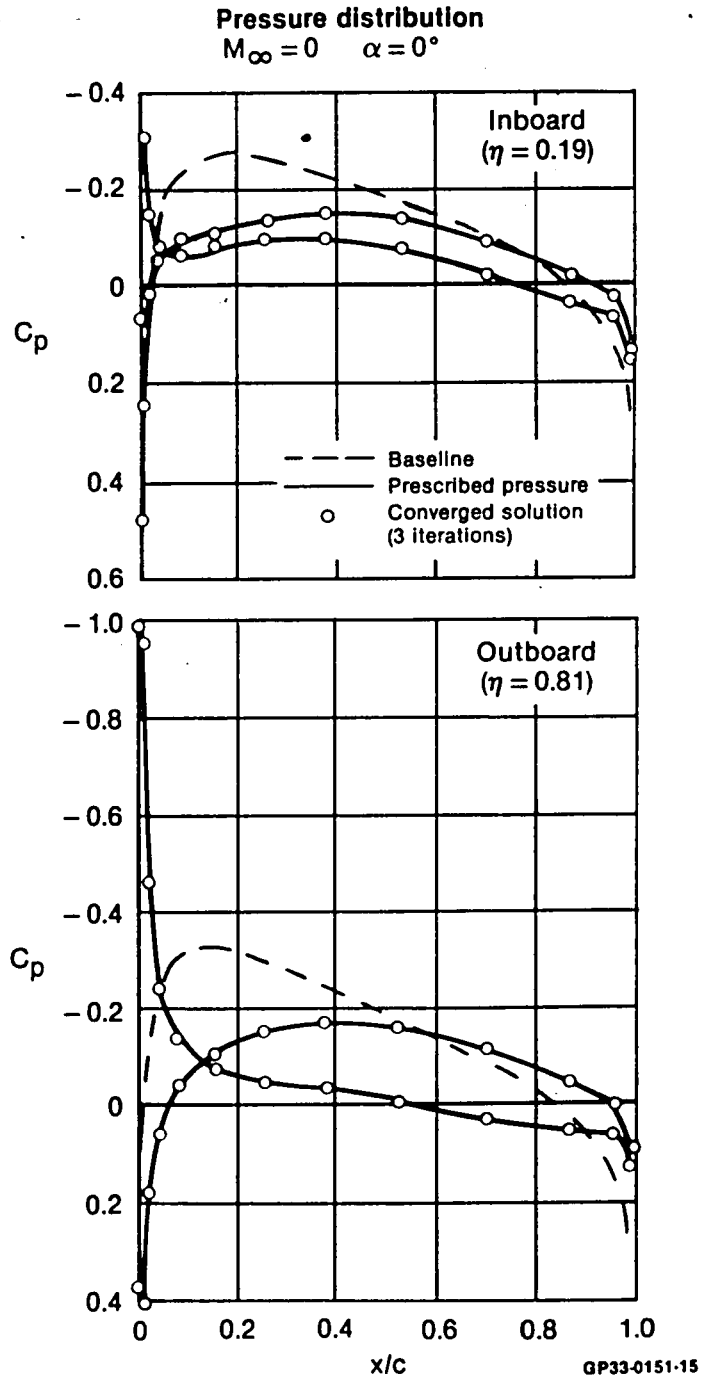

MCAERO WING-ON-FUSELAGE SUBSONIC DESIGN OPTION

DEMONSTRATION CASE: MODIFY CAMBER TO REMOVE PRESSURE PEAK (8°α, LOW SPEED)

—— BASELINE PRESSURES

— — PRESCRIBED UPPER SURFACE PRESSURES

• SOLUTION PRESSURE DISTRIBUTION (FIVE DOLLARS)

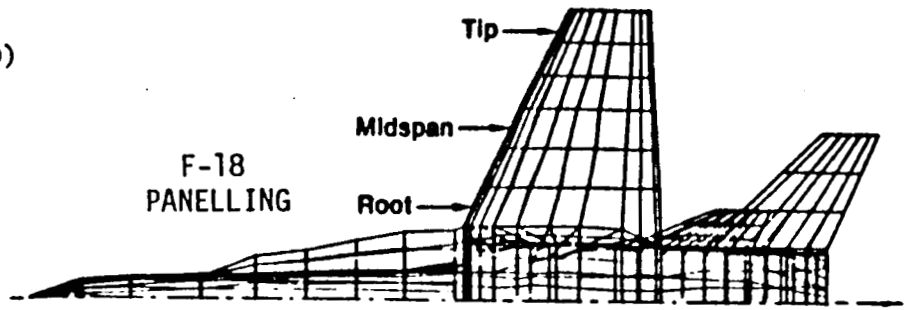

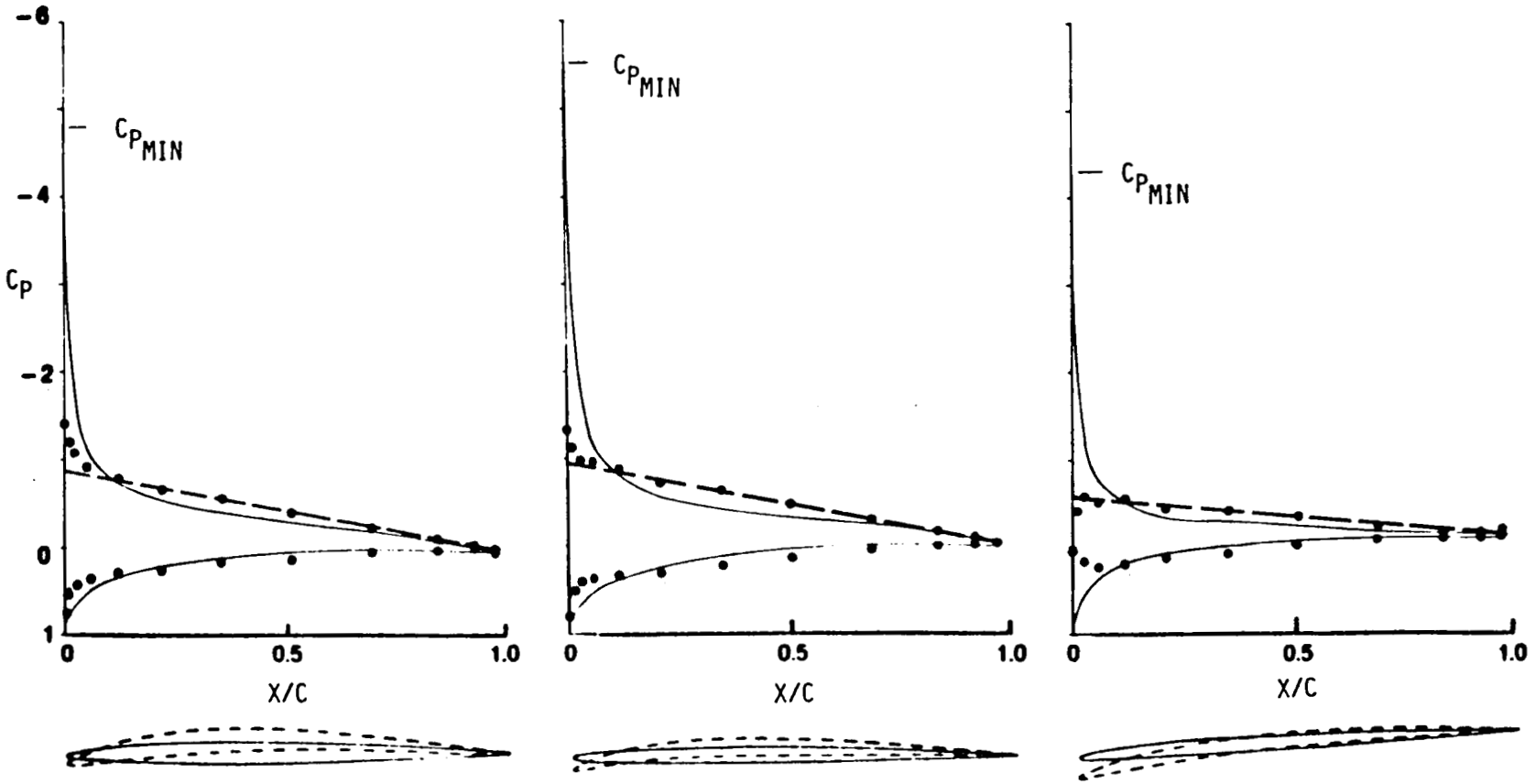

GEOMETRIC TAILORING OF MULTI-MISSION WING

MACH = .9

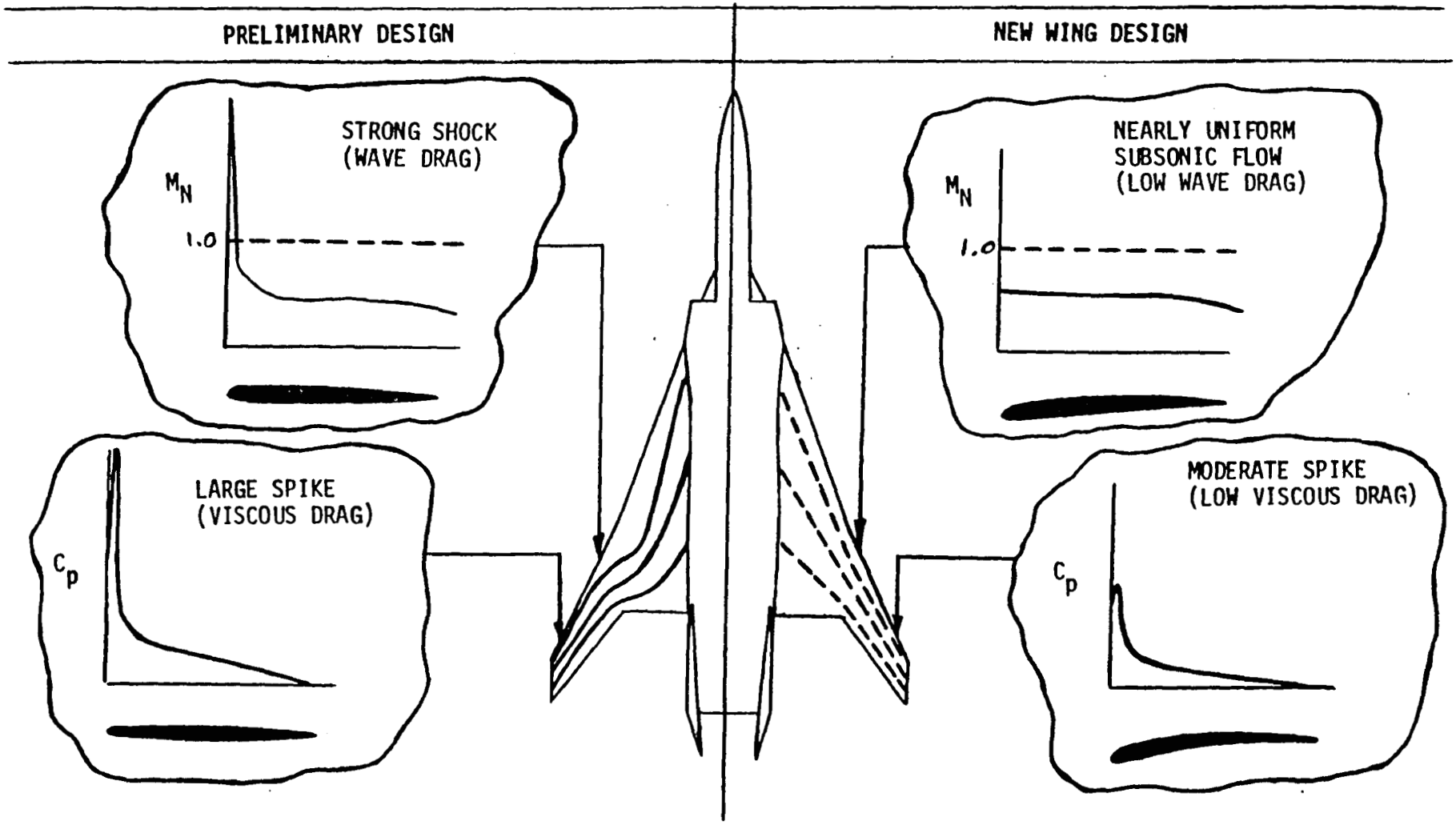

WIND TUNNEL VERIFICATION

WIND TUNNEL TEST - 1984

WING FABRICATION - 1983

MCDONNELL AIRCRAFT COMPANY

STATUS OF PANEL METHOD TECHNOLOGY

- NO FURTHER DEVELOPMENTS NEEDED FOR SUBSONIC ATTACHED FLOW
- FUTURE PLANS - DEVELOP FIELD PANEL METHOD FOR HIGH AOA
  - REATTACHING SEPARATION BUBBLES
  - HIGHLY VORTICAL FLOW
  - VORTEX - CONTROL SURFACE INTERACTIONS

(14)

A METHOD FOR SOLVING THE TRANSONIC FULL-POTENTIAL EQUATION FOR GENERAL CONFIGURATIONS

B. WEDAN
NORTHROP AIRCRAFT DIVISION
HAWTHORNE, CALIFORNIA

J. C. SOUTH, JR.
NASA LANGLEY RESEARCH CENTER
HAMPTON, VIRGINIA

WEDAN

PURPOSE

DEVELOP ENGINEERING-TYPE METHOD FOR THE SOLUTION OF THE TRANSONIC F.P.E. FOR COMPLEX GEOMETRIES

APPROACH

- COMBINE IMPROVED ACCURACY OF F.P.E. WITH GRID SIMPLICITY OF T.S.D.
- FINITE-VOLUME FORMULATION WITH CARTESIAN GRID
- SIMPLE APPROACH TO APPLYING B.C.
- SACRIFICE SOME LOCAL RESOLUTION FOR MORE COMPLEX GEOMETRY MODELING
- VALIDATE APPROACH INITIALLY FOR 2-D FLOWS

FIELD CELL

$$\rho u S_3 - \rho u S_1 + \rho v S_4 - \rho v S_2 = 0$$

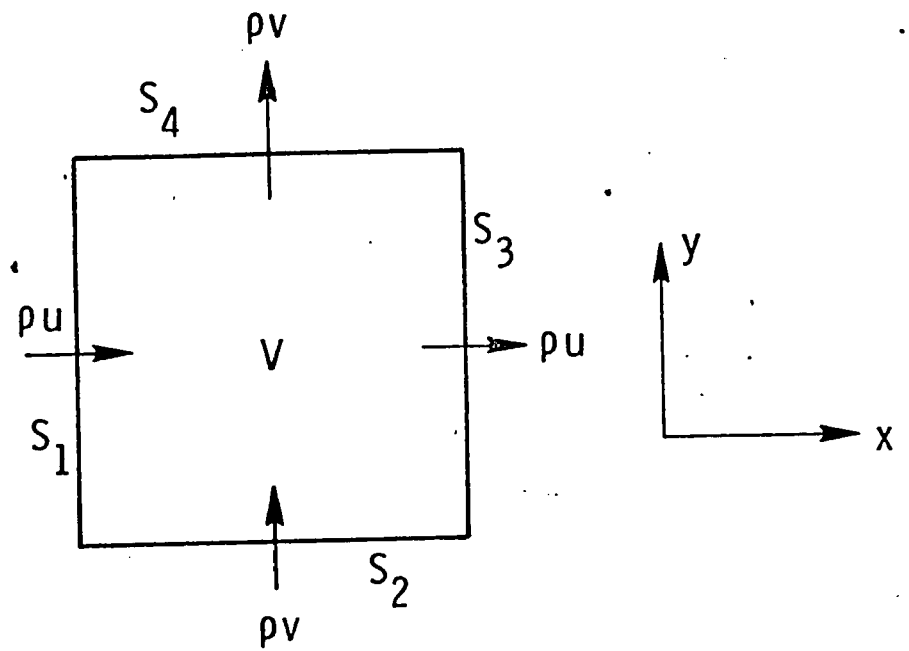

BODY BOUNDARY CELL

$$\rho u S_{BC} - \rho u S_{AD} + \rho v S_{CD} = 0$$

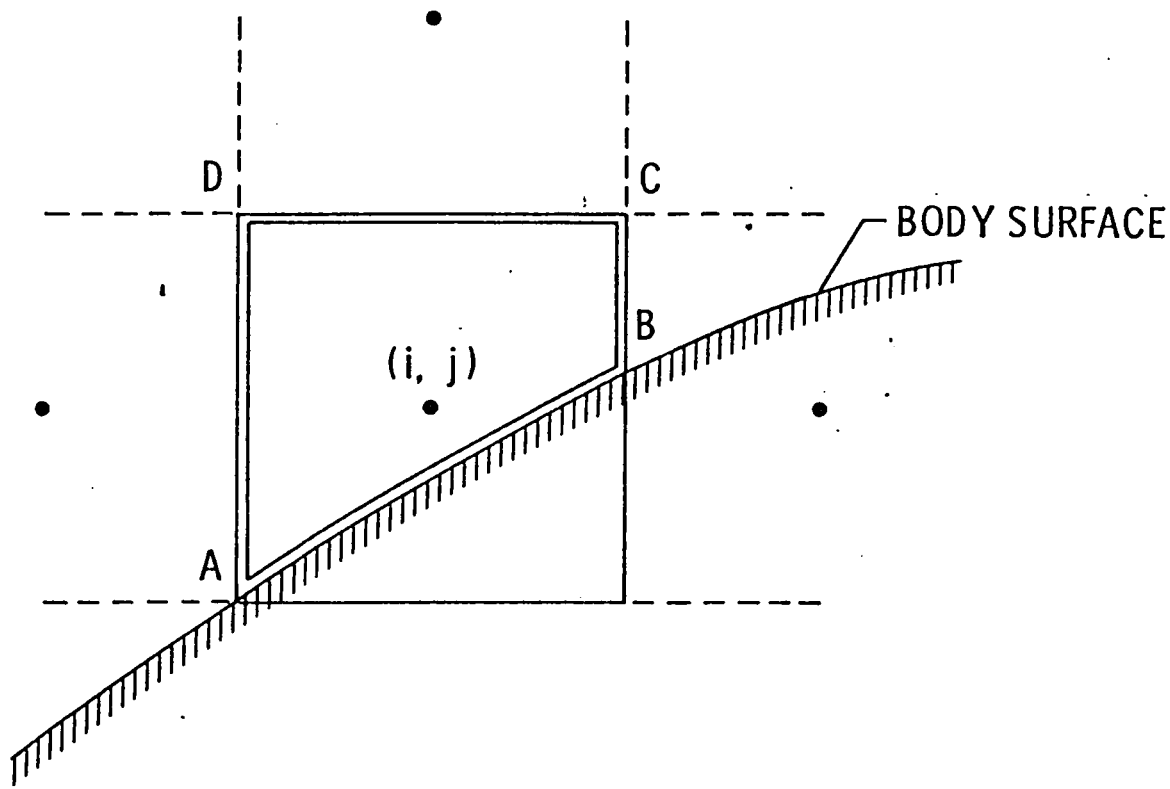

GRID FOR CIRCULAR CYLINDER — 59 x 56 CELLS

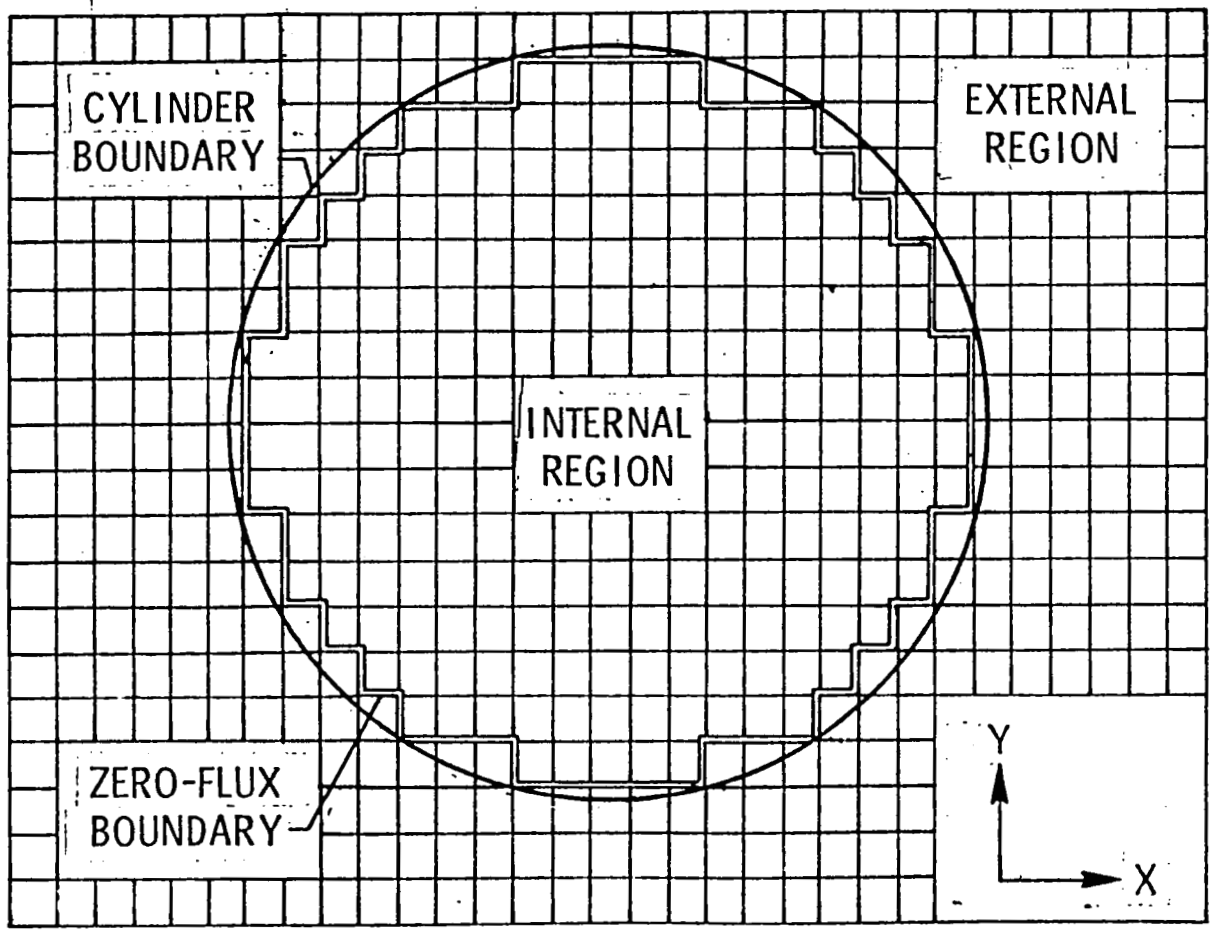

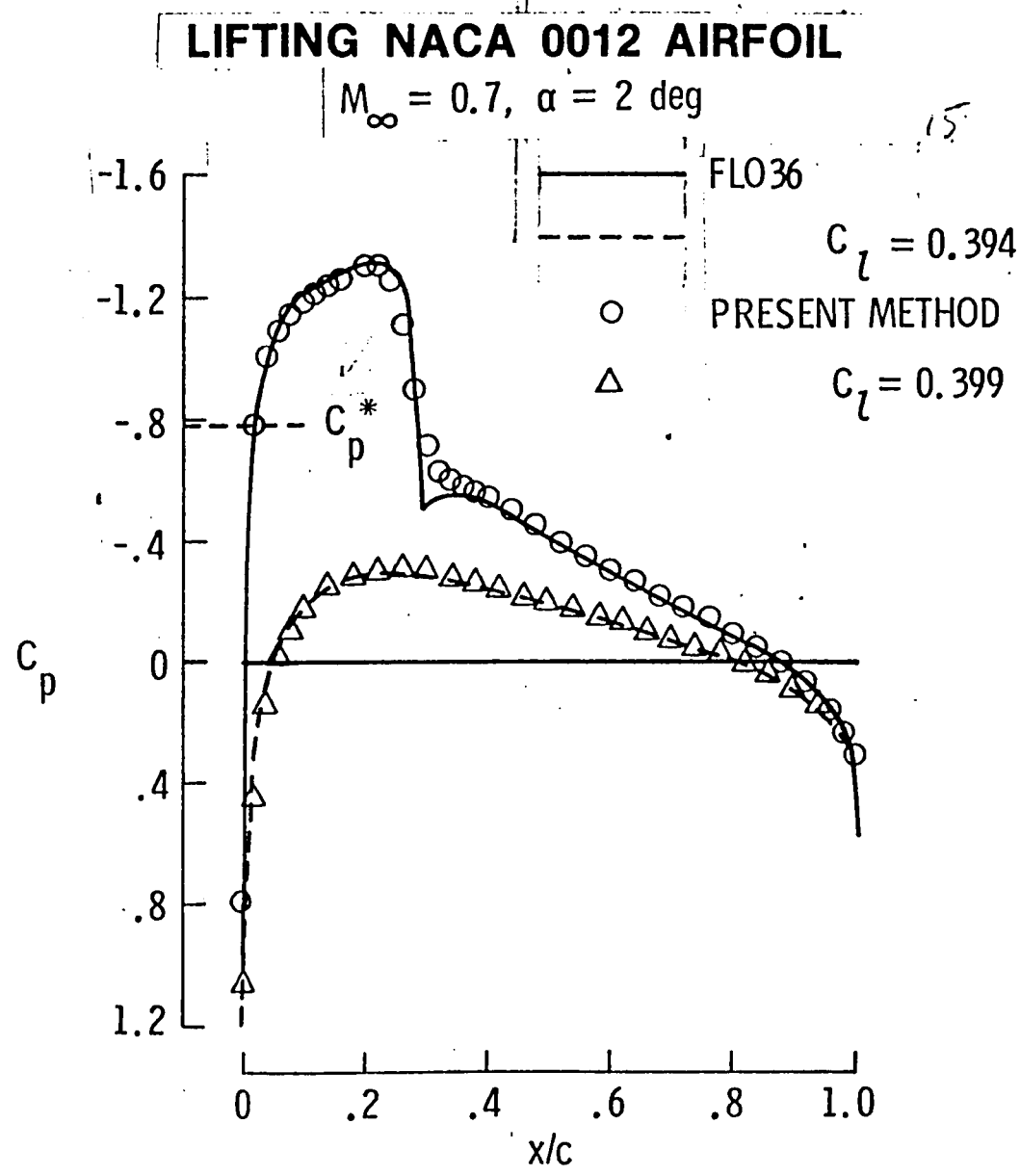
LIFTING NACA 0012 AIRFOIL
$M_\infty = 0.7,\ \alpha = 2$ deg
FLO36
$C_l = 0.394$
PRESENT METHOD
$C_l = 0.399$
C_p^*
C_p
-1.6
-1.2
-.8
-.4
0
.4
.8
1.2
0
.2
.4
.6
.8
1.0
x/c

SYMETRIC 5 DEGREE DOUBLE WEDGE WITH ATTACHED SHOCK

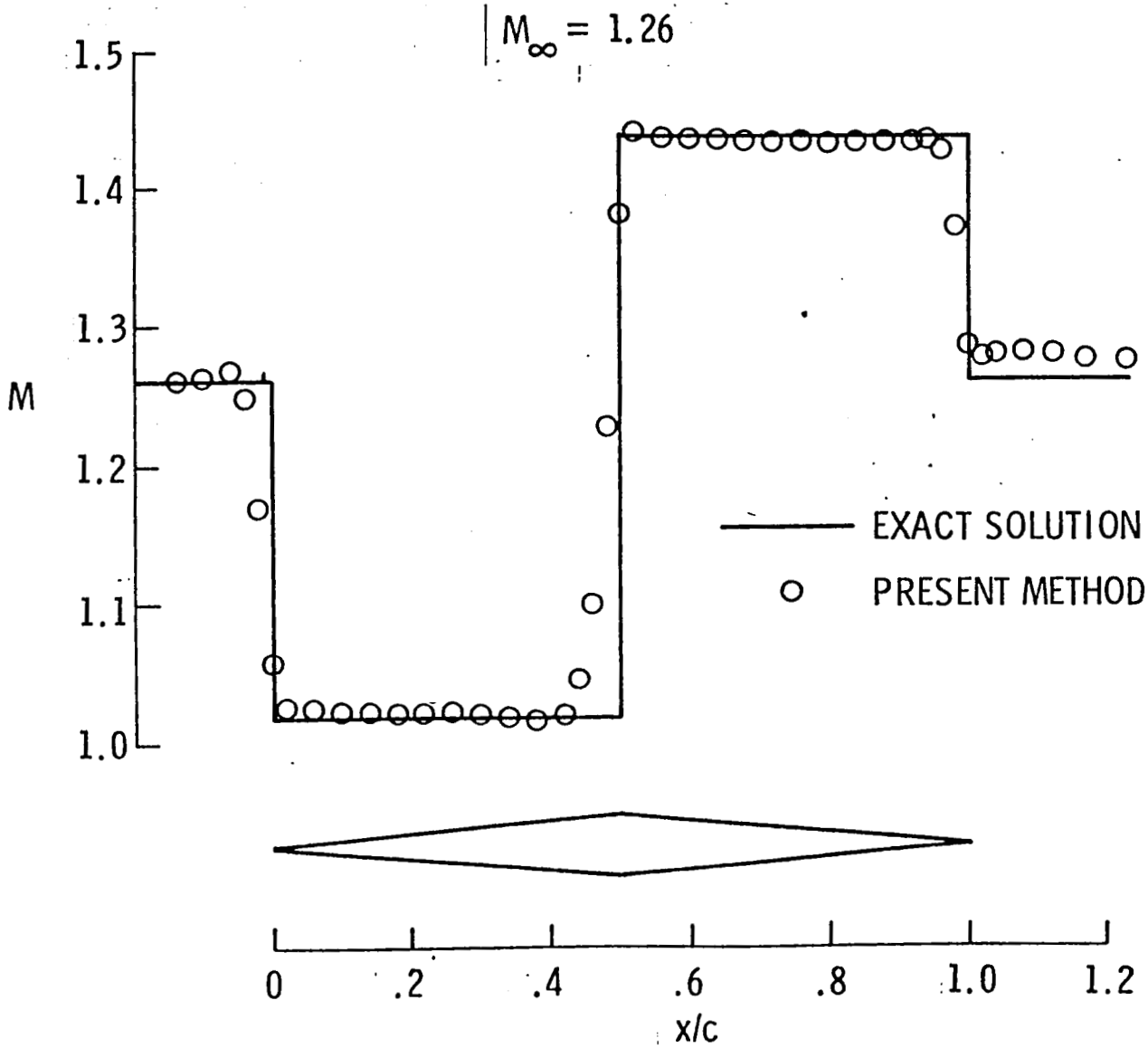

MACH CONTOURS FOR 5 DEGREE DOUBLE WEDGE

$M_\infty = 1.26$

LOCAL MACH NUMBER

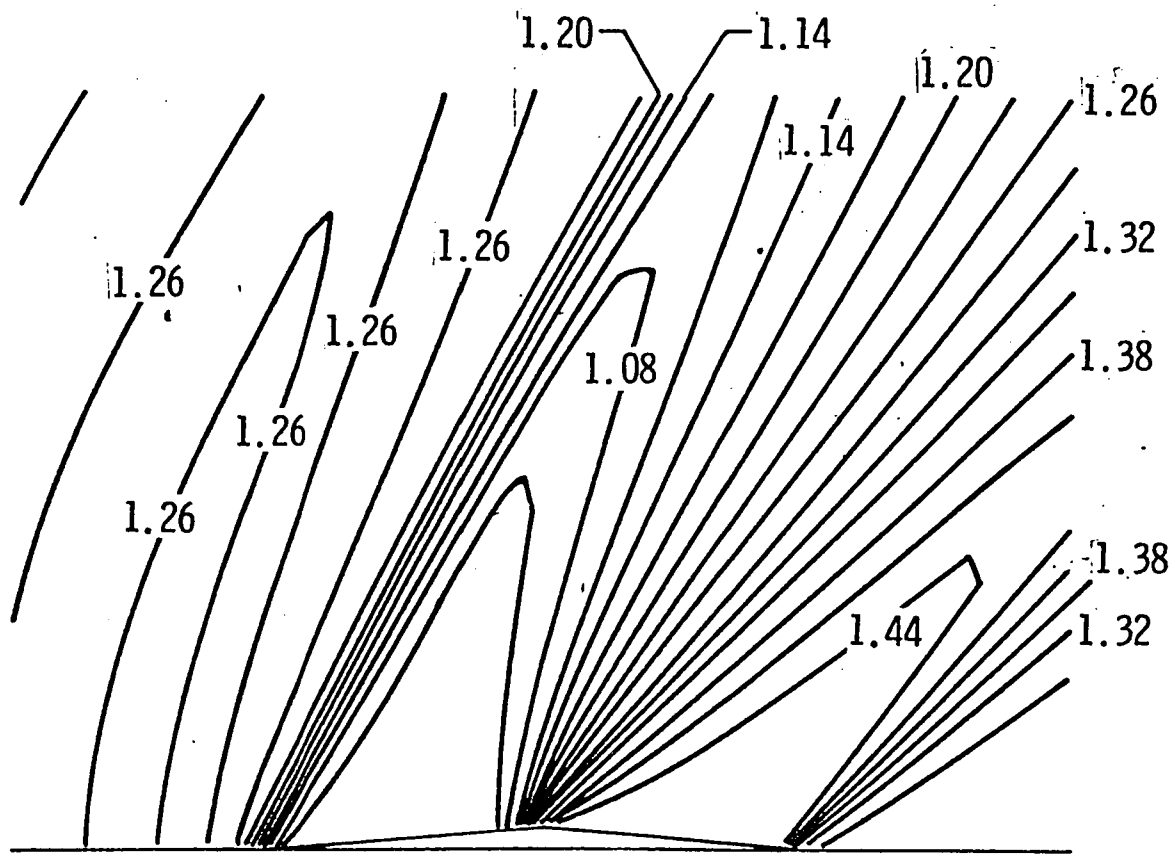

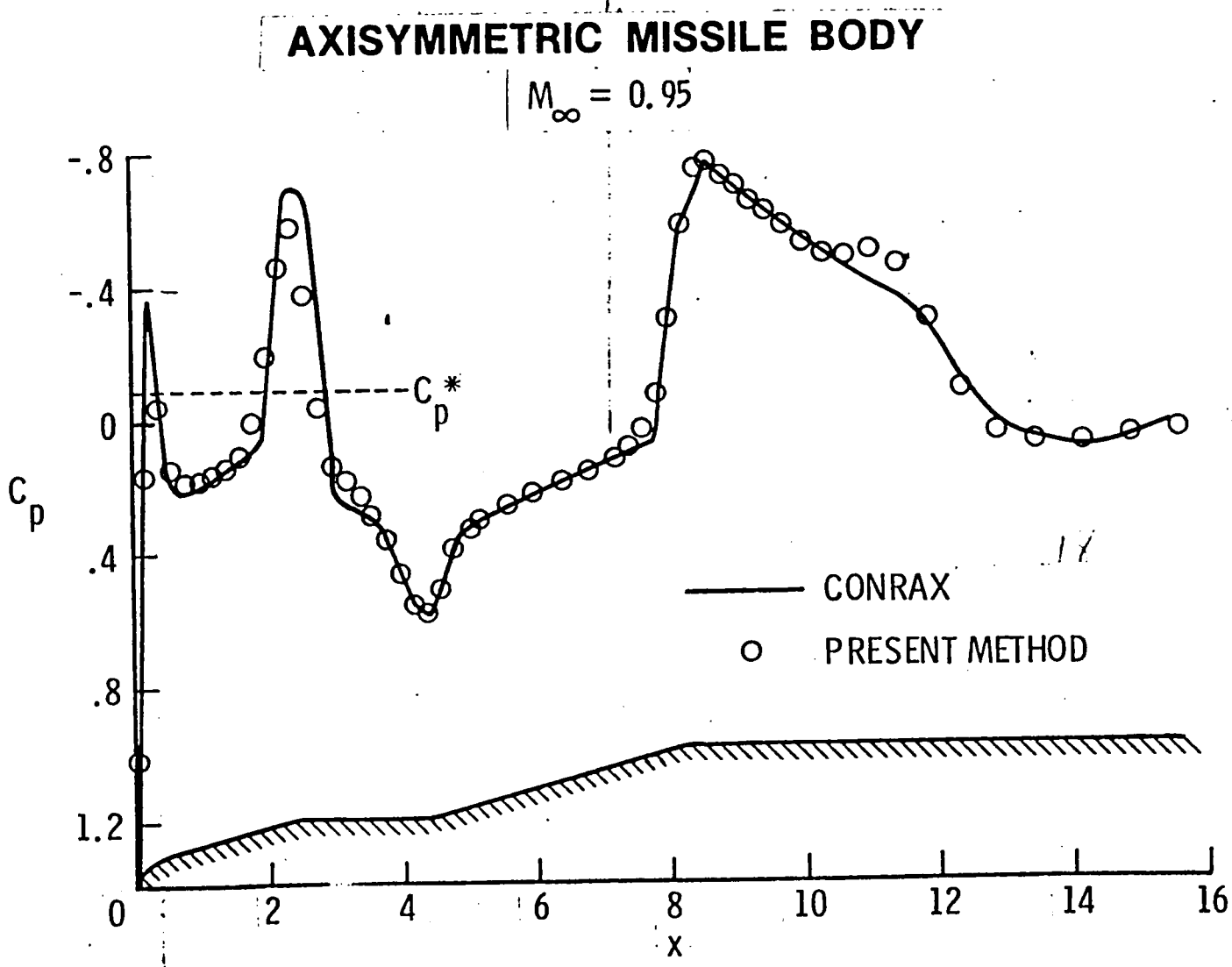
AXISYMMETRIC MISSILE BODY
$M_\infty = 0.95$
-.8
-.4
0
.4
.8
1.2
C_p
C_p^*
0
2
4
6
8
10
12
14
16
x
CONRAX
PRESENT METHOD

AXISYMMETRIC CONVERGING DUCT

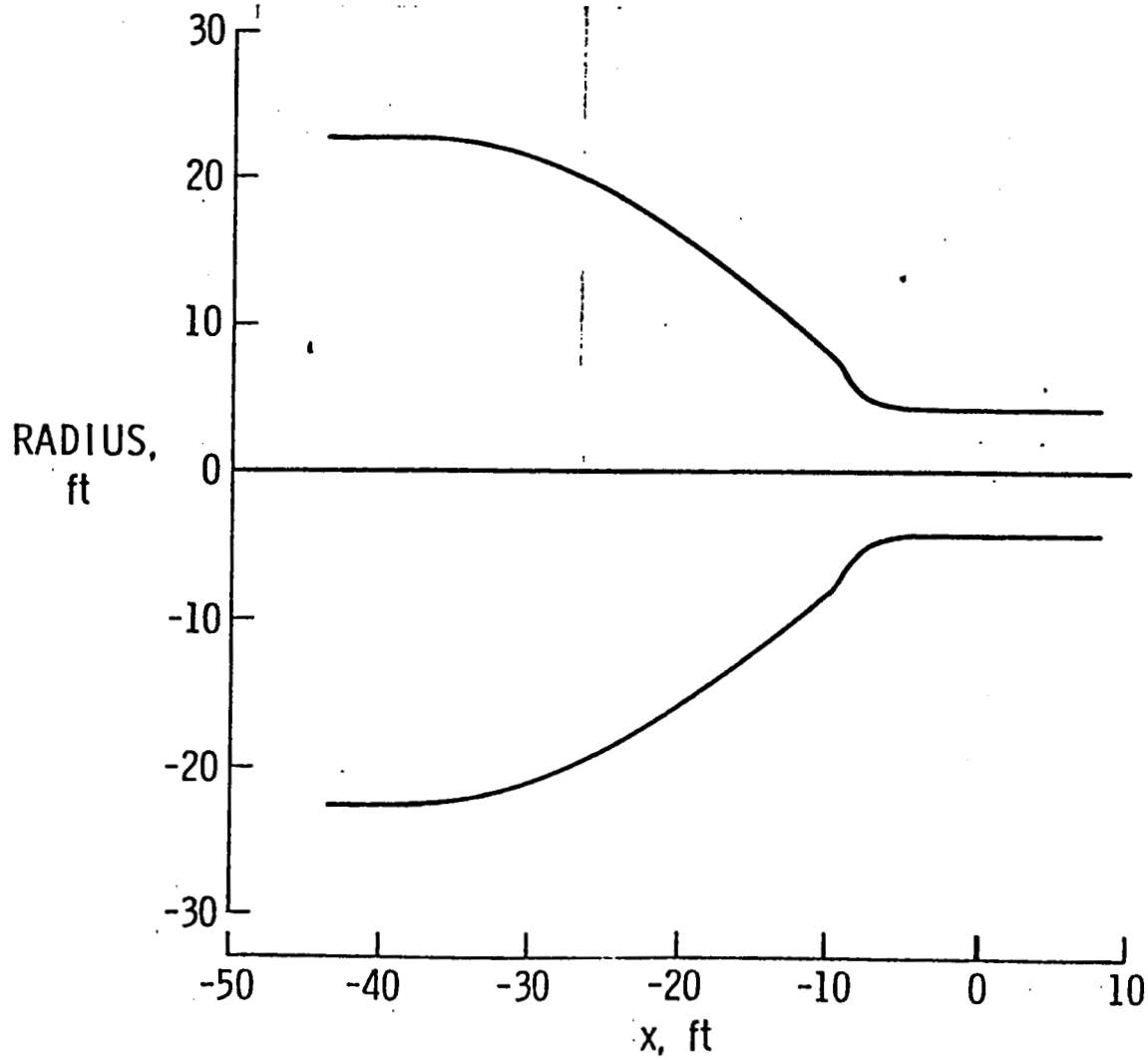

WALL AND CENTERLINE MACH NUMBER FOR AXISYMMETRIC CONVERGING DUCT

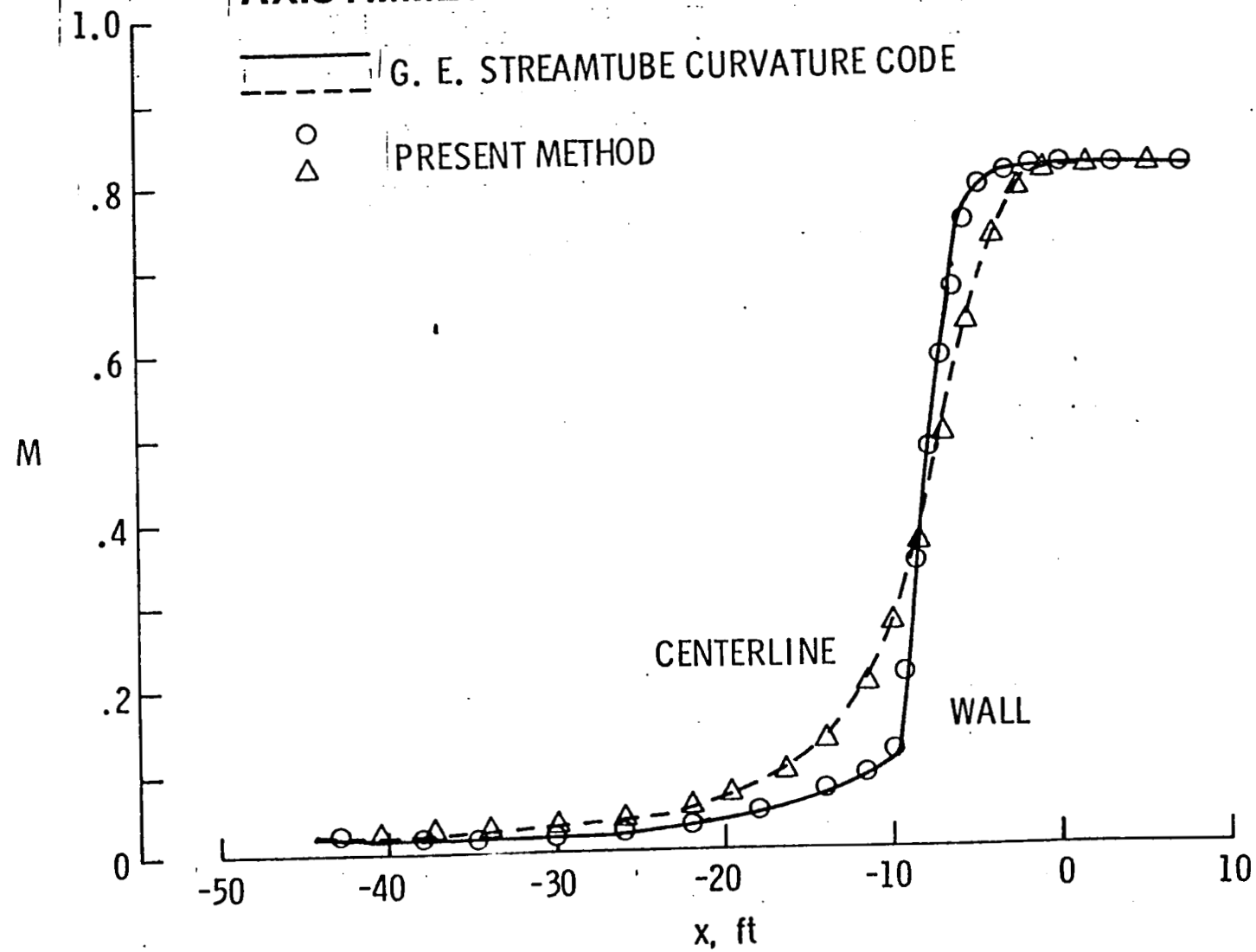

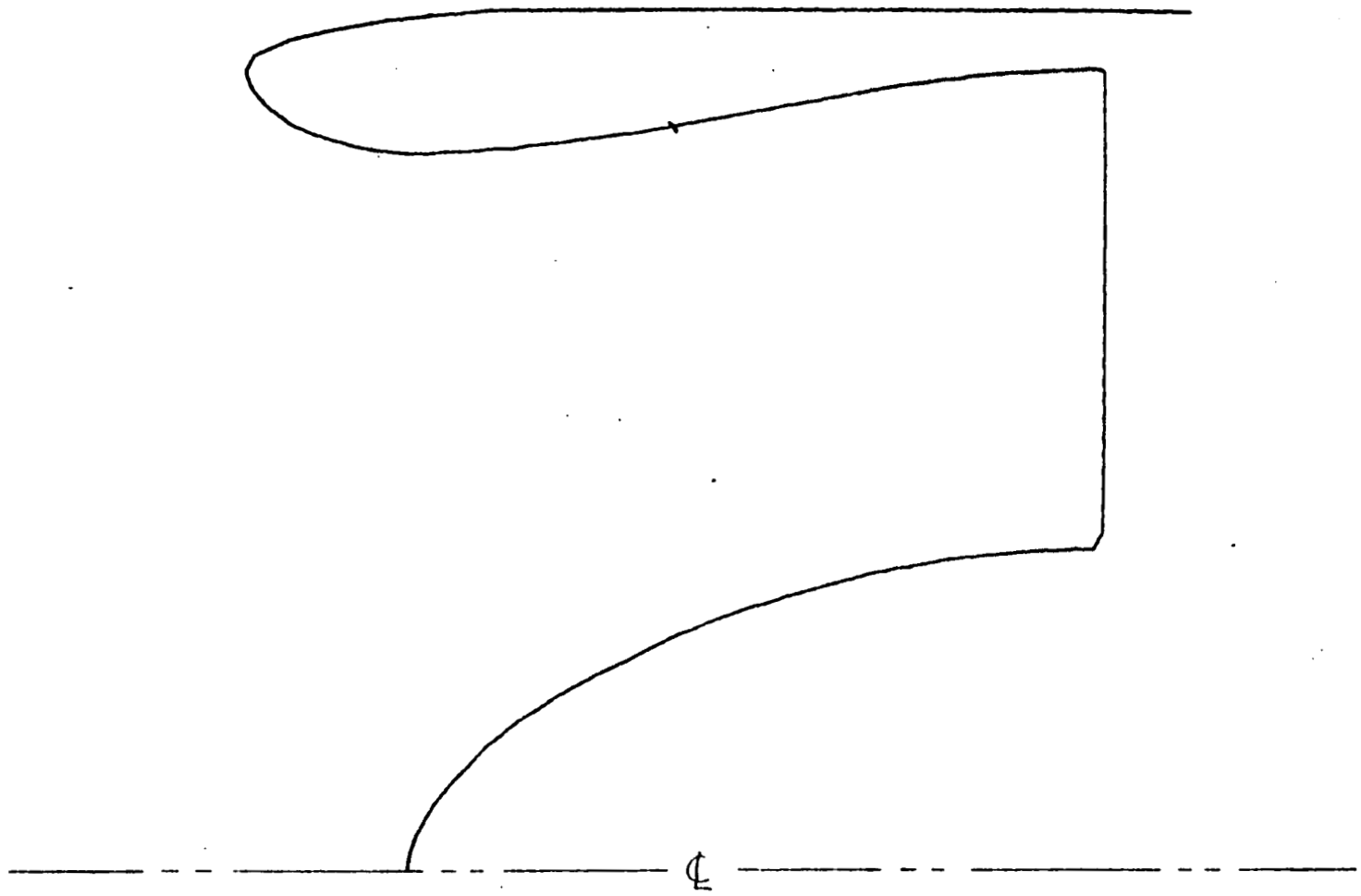

INLET TEST CASE

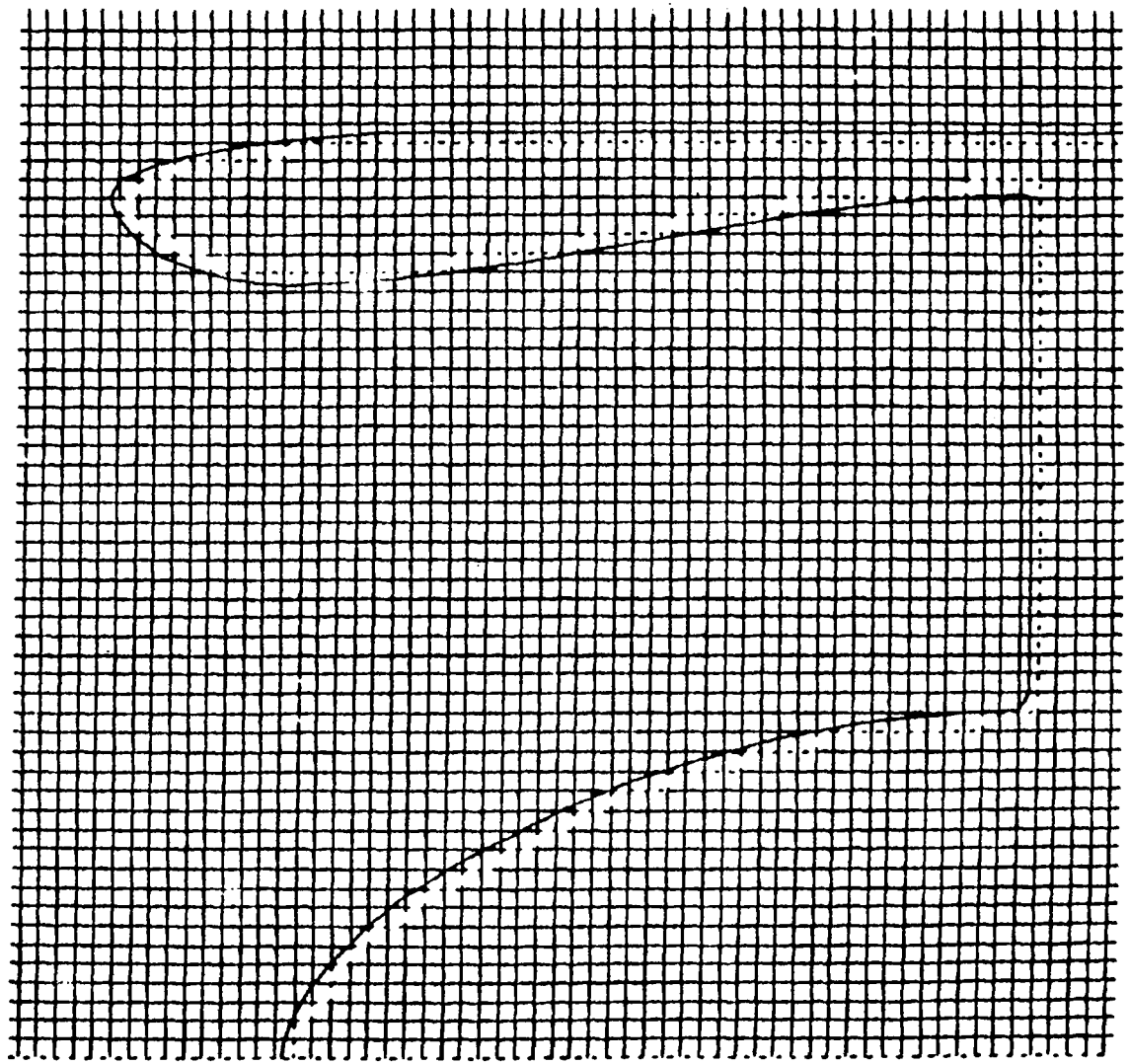

INLET TEST CASE

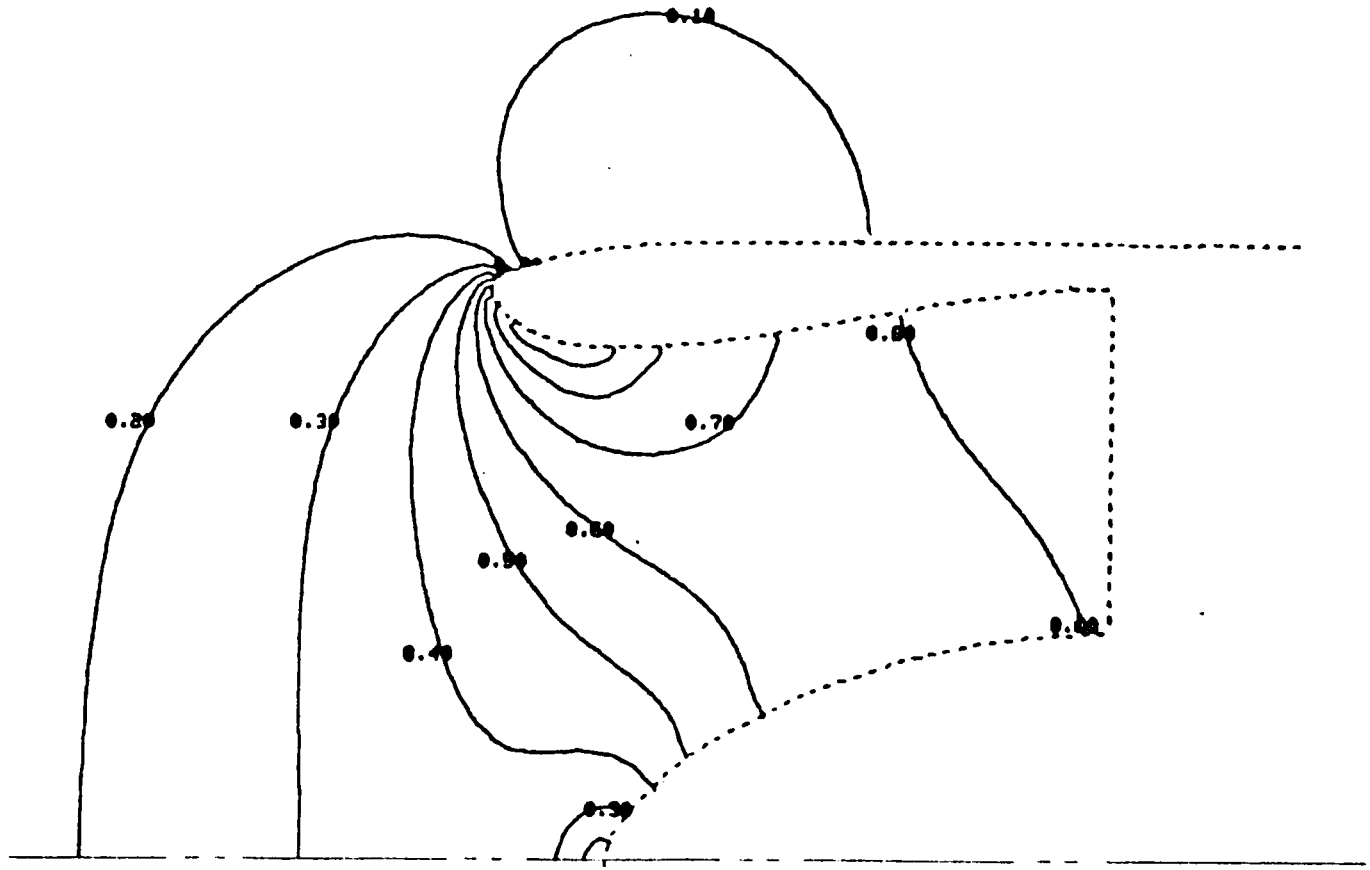

MACH NUMBER
INLET TEST CASE

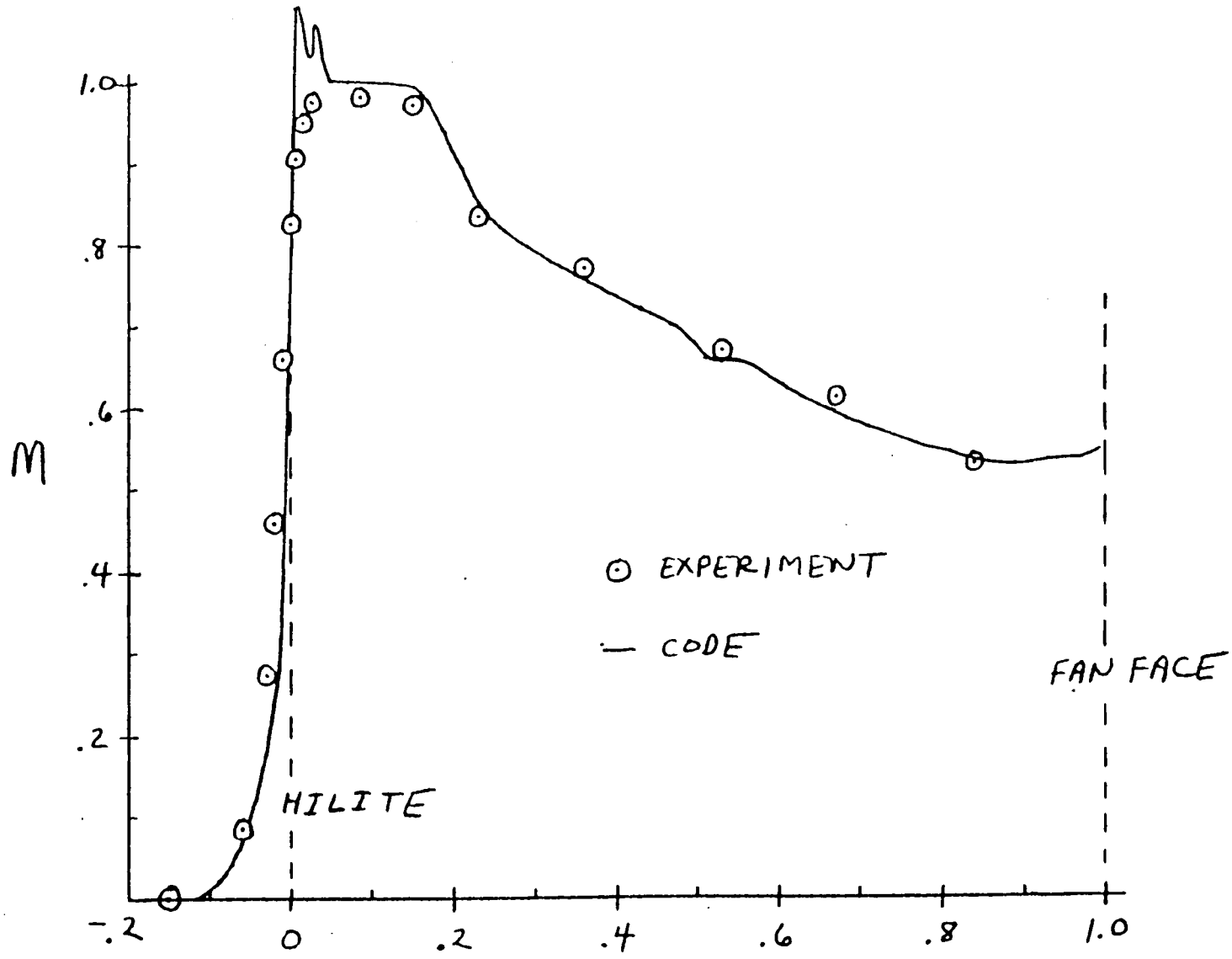

MACH NO. DISTRIBUTION ON FAN COWL

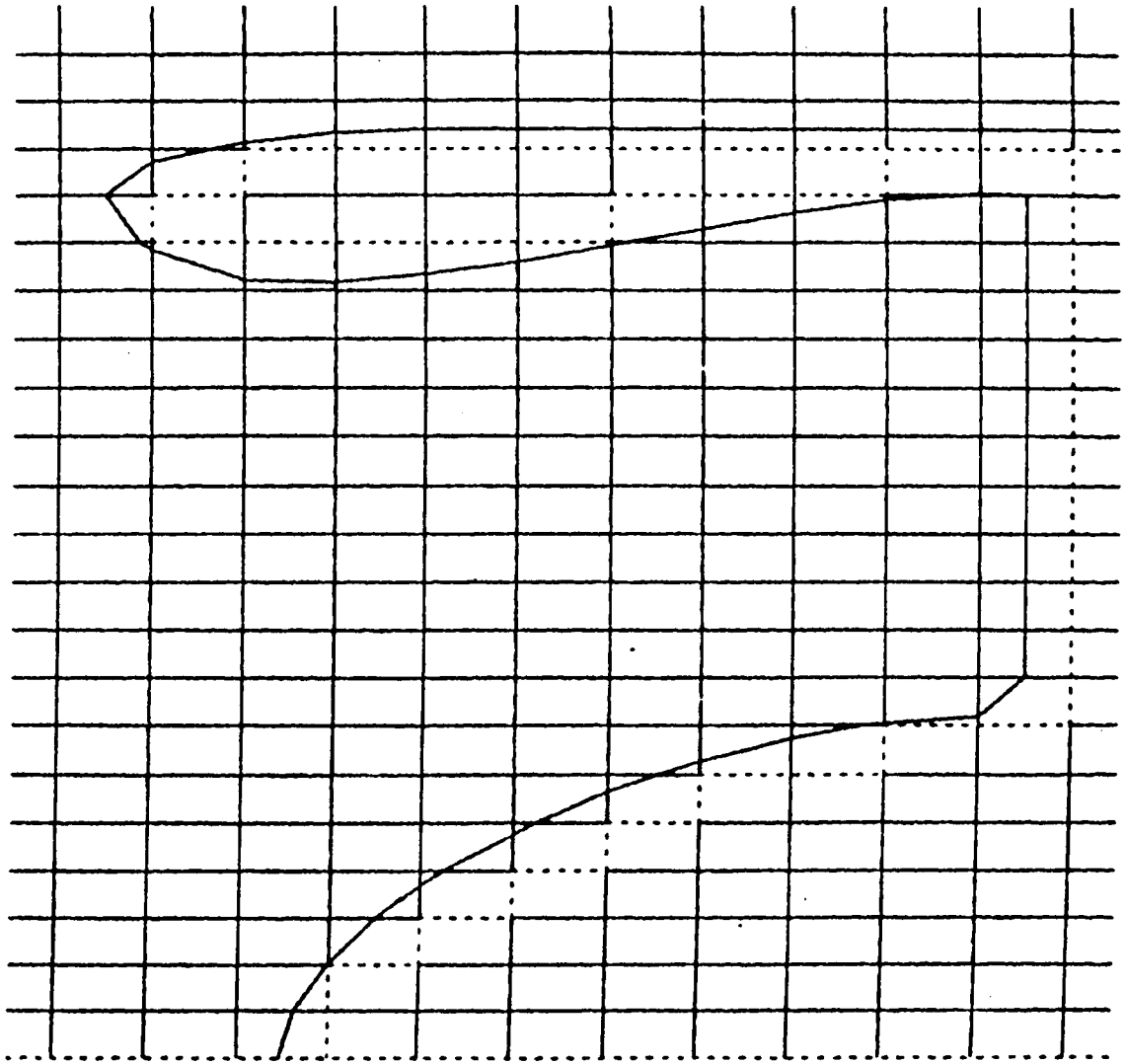

INLET TEST CASE - CRUDE GRID

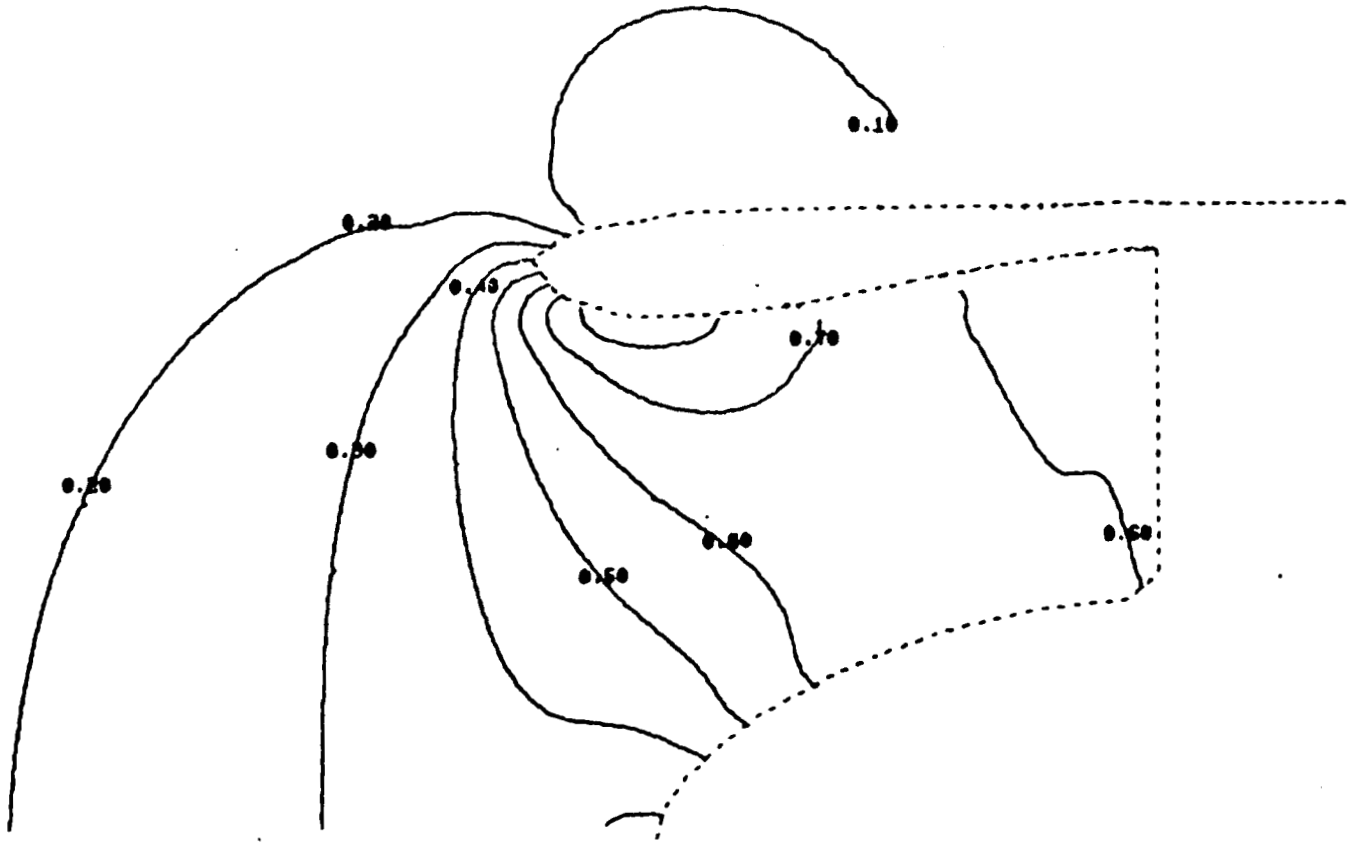

MACH NUMBER

INLET TEST CASE - CRUDE GRID

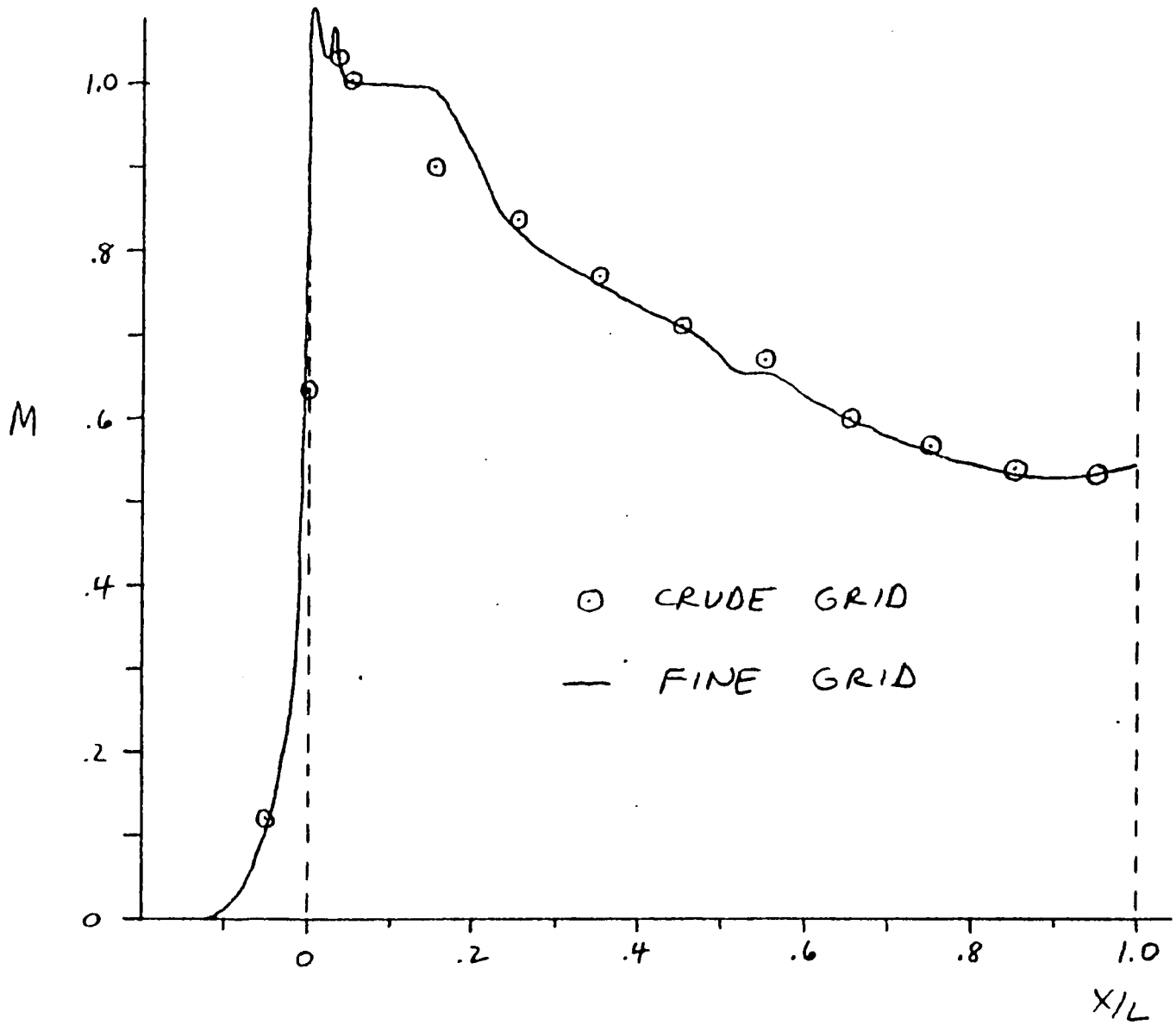

MACH NO. DISTRIBUTION ON FAN COWL

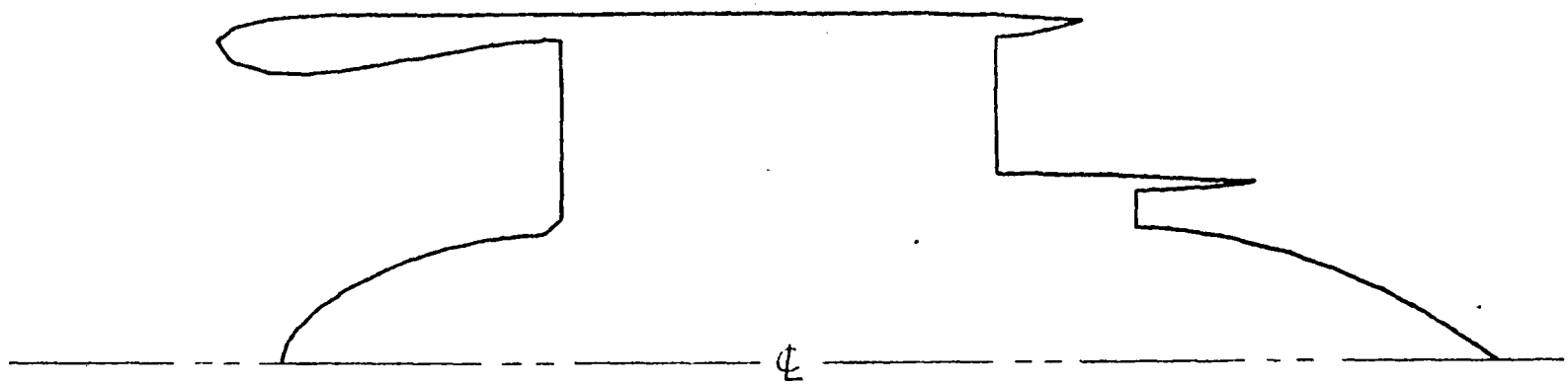

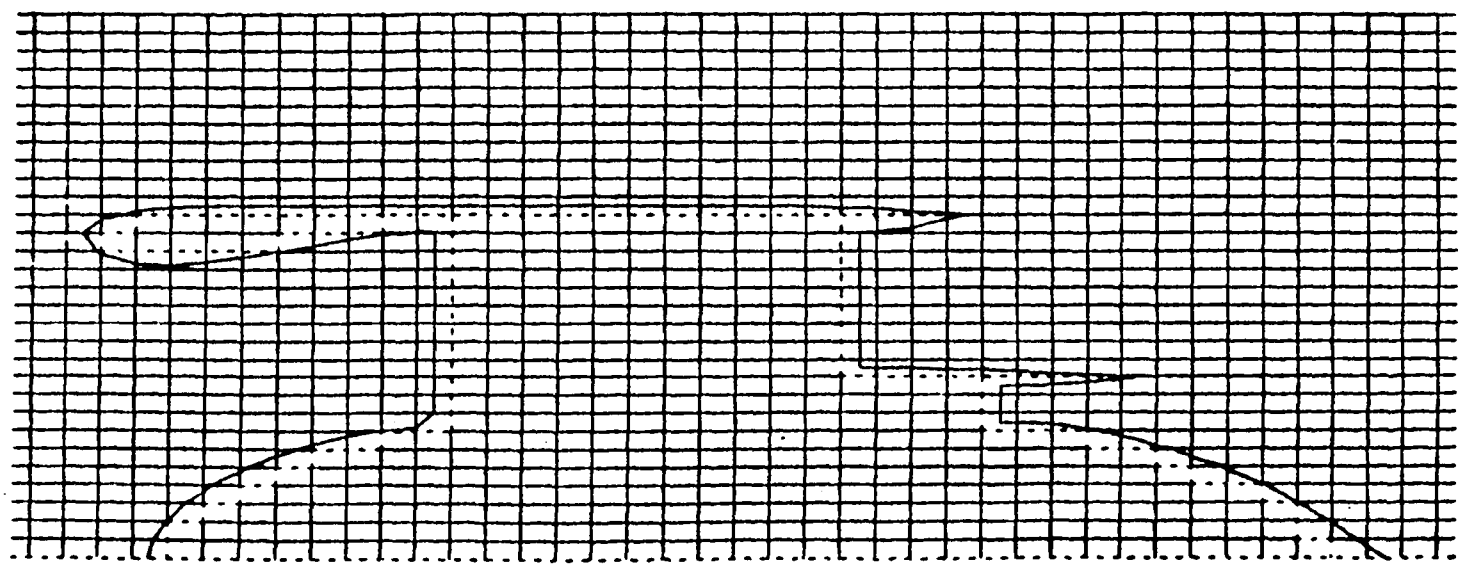

NACELLE TEST CASE - NO KUTTA CONDITION

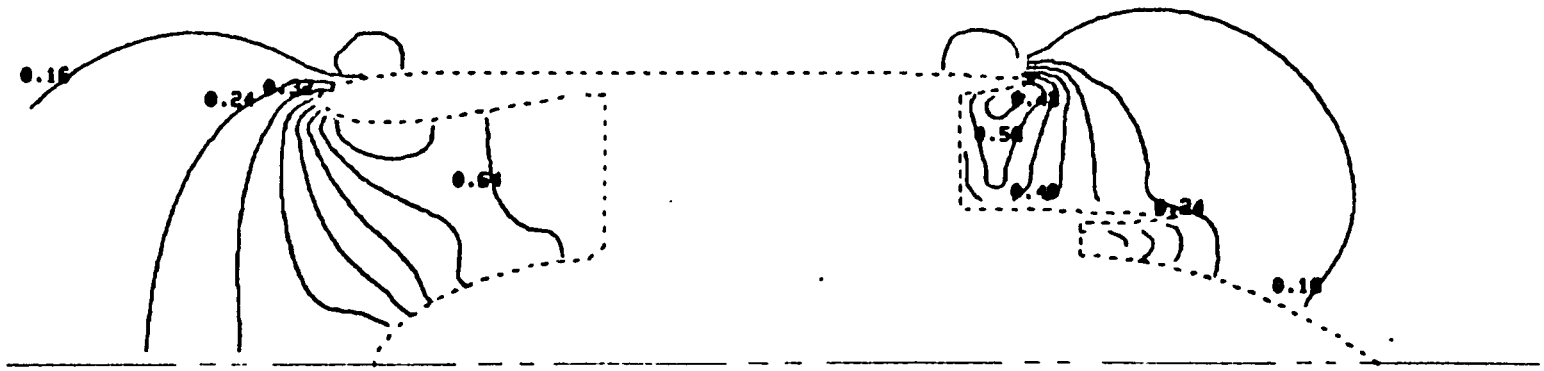

MACH NUMBER

NACELLE TEST CASE - NO KUTTA CONDITION

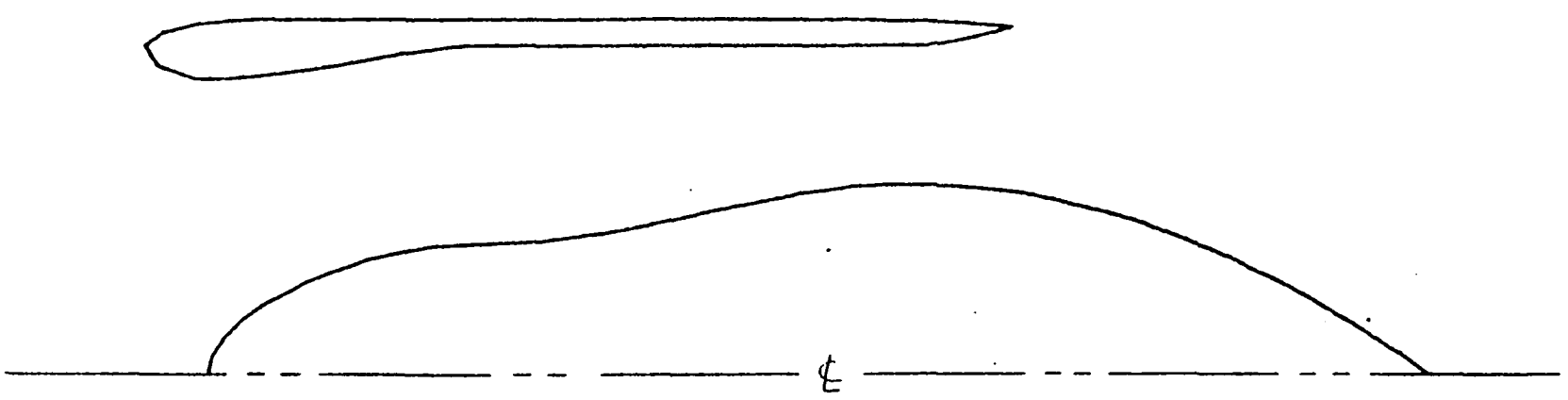

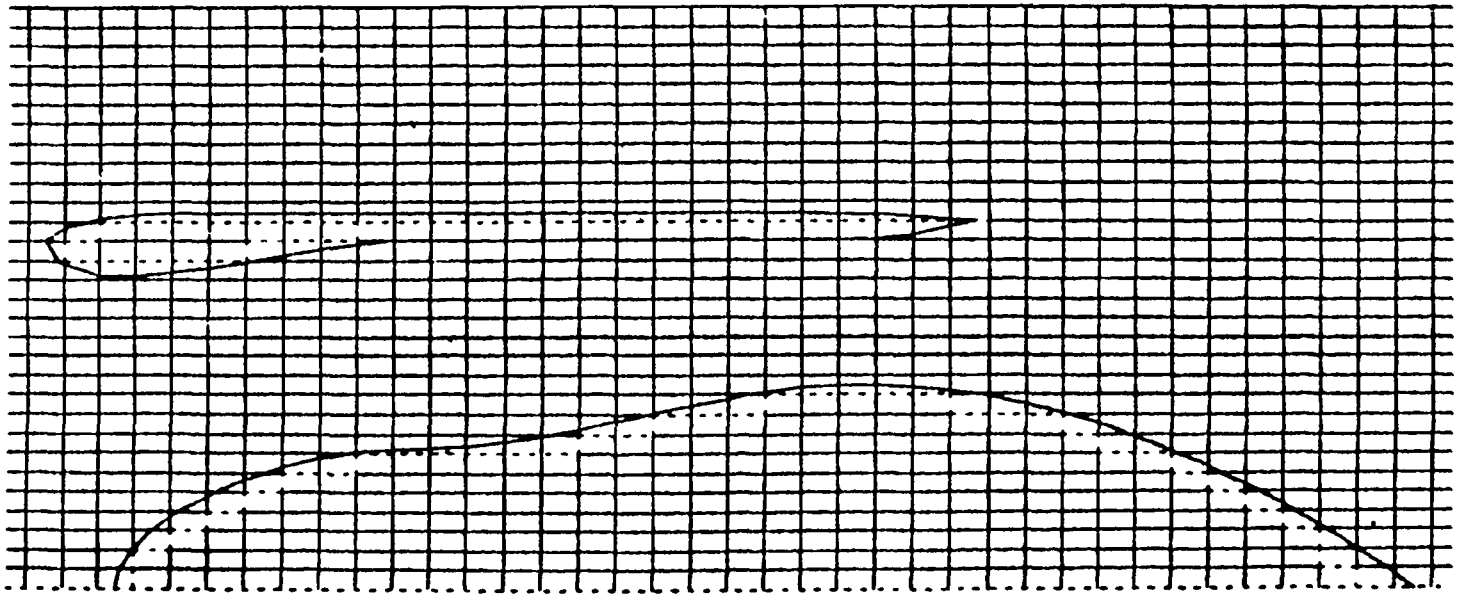

FLOW-THROUGH NACELLE CASE

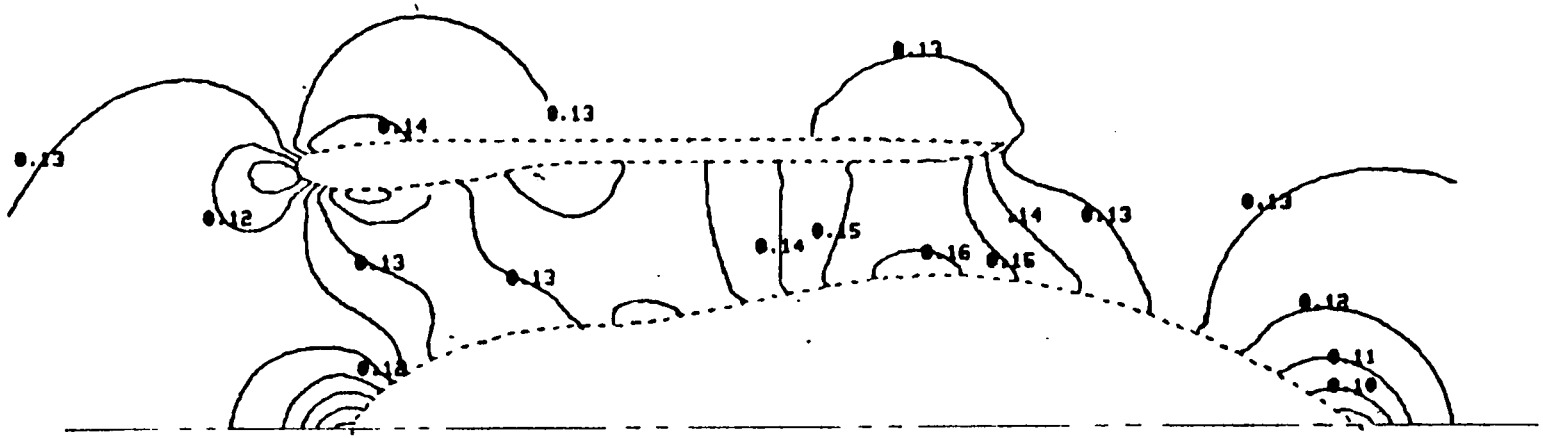

MACH NUMBER
FLOW-THROUGH NACELLE CASE

CURRENT STATUS

- 2-D AND AXISYMMETRIC, INTERNAL AND EXTERNAL FLOWS
- MULTIPLE SURFACE CAPABILITY
- SIX SOLUTION ALGORITHMS
  VLOR, HLOR, HZEBRA, AF2X, ADI, SIP
- MASS FLOW RATES AND POINT SOURCES MAY BE SPECIFIED
  ANYWHERE IN COMPUTATIONAL DOMAIN
- SEMI-INVERSE MODE WITH LIFT COEFFICIENT SPECIFIED
- 3-D GEOMETRY CODE COMPLETED

ADDITIONAL WORK REQUIRED

- IMPROVE KUTTA CONDITION TREATMENT
- IMPROVE SURFACE POTENTIAL INTERPOLATION
- INCLUDE JUMP CONDITIONS FOR REGIONS OF DIFFERRING P_o AND T_o
- INCLUDE MESH EMBEDDING CAPABILITY
- CONTINUE VERIFICATION OF 2-D CODE
- CONTINUE DEVELOPMENT OF 3-D CODE

(15)

TRANSONIC WING-BODY FLOW SIMULATIONS

UPPER/LOWER CANTED WINGLETS AND ARBITRARY PLANFORM PYLONS

CHARLIE BOPPE
BRUCE ROSEN

(516) 575-3671

CONTRACT NAS 1-14732

19 OCTOBER 1983

BOPPE

MULTIPLE EMBEDDED GRID APPROACH

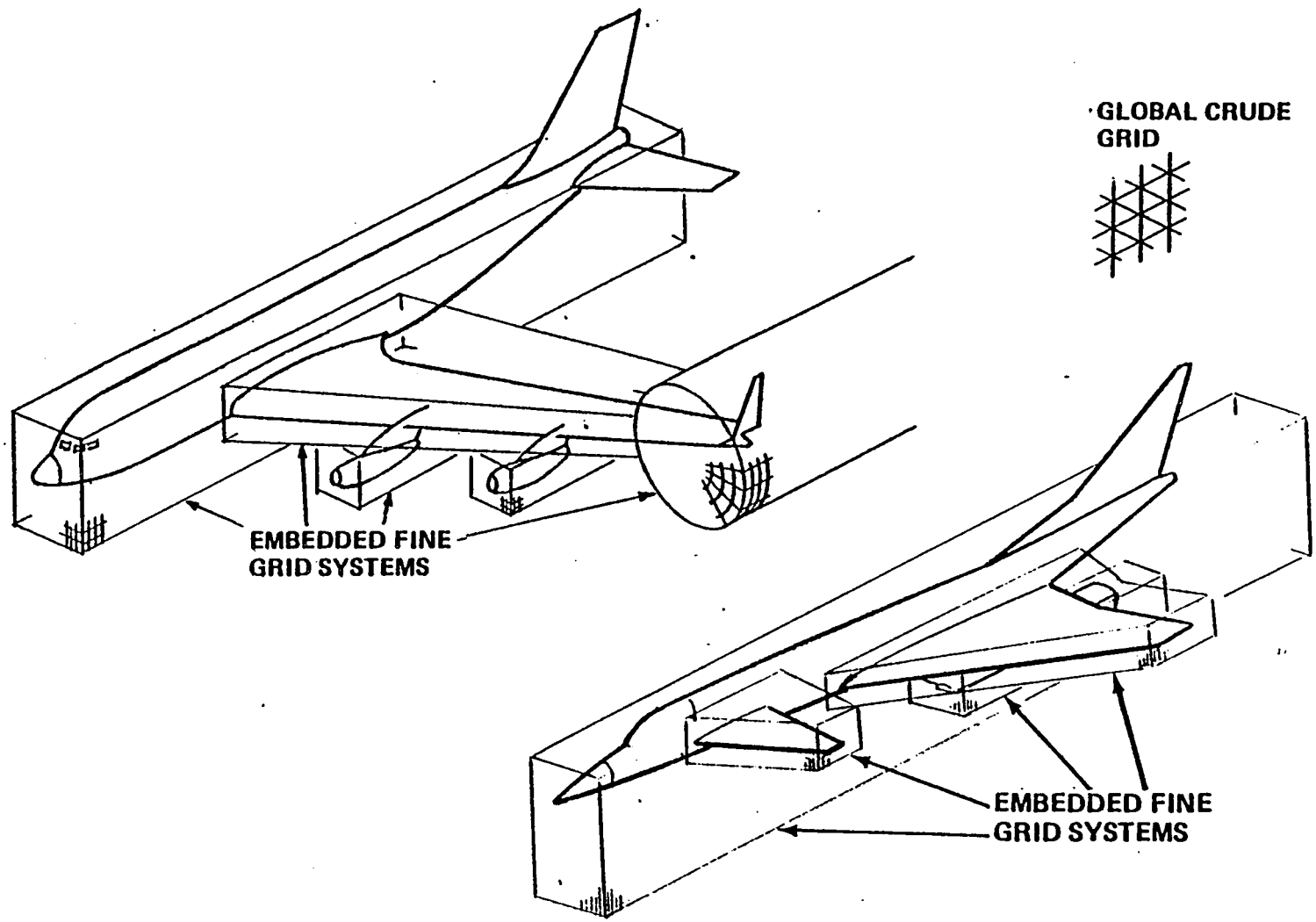

GRUMMAN

USE OF MORE THAN ONE FLOW EQUATION FOR MULTIPLE GRID SYSTEM

FLOW EQUATION FOR PLANAR WING AND GLOBAL FLOW FIELD

$$\left[1 - M_\infty^2 - (\gamma + 1) M_\infty^2 \varphi_x - \frac{\gamma + 1}{2} M_\infty^2 \varphi_x^2\right] \varphi_{xx} - 2M_\infty^2 \varphi_y \varphi_{xy}$$

$$+ \left[1 - (\gamma - 1) M_\infty^2 \varphi_x\right] \varphi_{yy} + \varphi_{zz} = 0$$

FLOW EQUATION FOR VERTICAL PYLON SURFACE

$$\left[1 - M_\infty^2 - (\gamma + 1) M_\infty^2 \varphi_x - \frac{\gamma + 1}{2} M_\infty^2 \varphi_x^2\right] \varphi_{xx} - 2M_\infty^2 \varphi_z \varphi_{xz}$$

$$+ \left[1 - (\gamma - 1) M_\infty^2 \varphi_x\right] \varphi_{zz} + \varphi_{yy} = 0$$

PYLON-WING-NACELLE GRID ARRANGEMENT

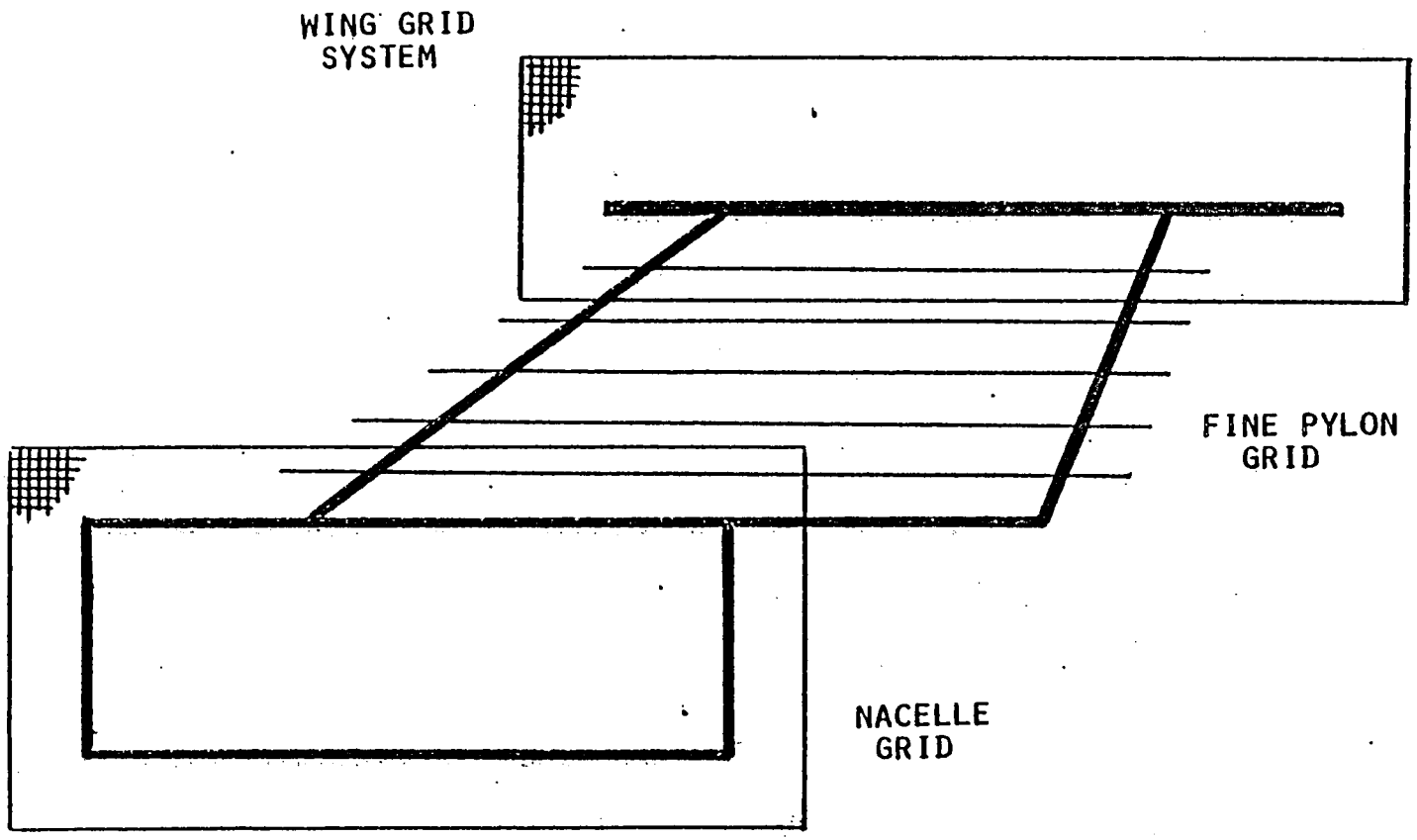

CASES FOR PYLON CODE VALIDATION

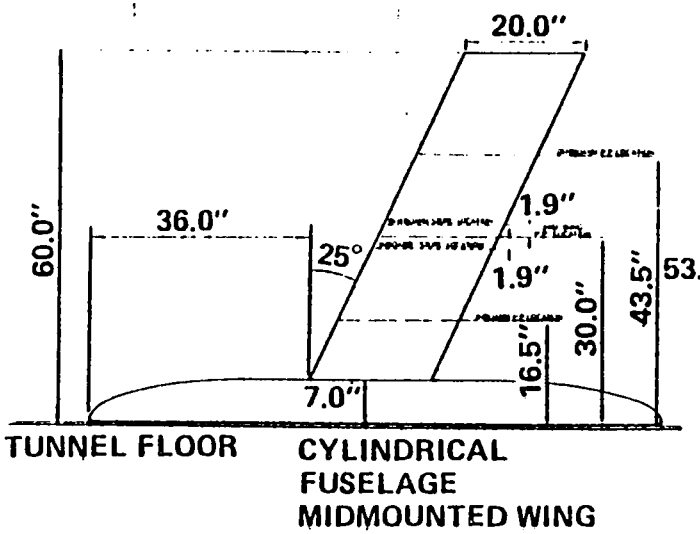

BRITISH AEROSPACE/ARA MODEL M-64
(DETAILED PYLON PRESSURES)

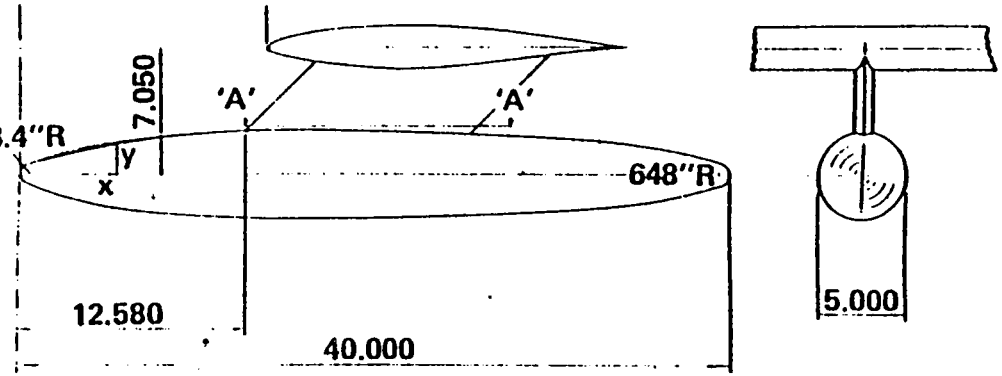

C-5A/NASA TM X-2530
(PYLON SHAPE EFFECTS)

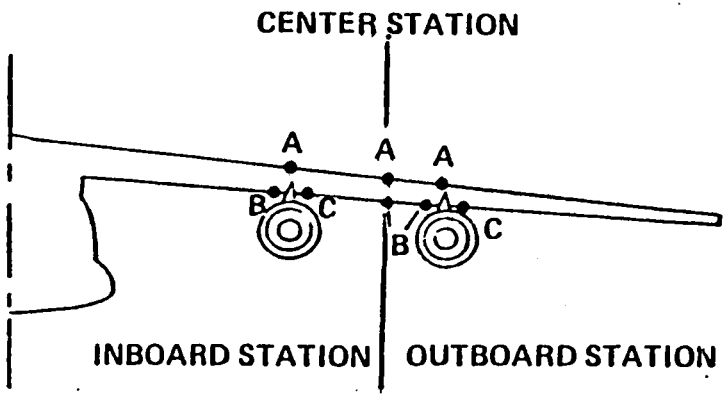

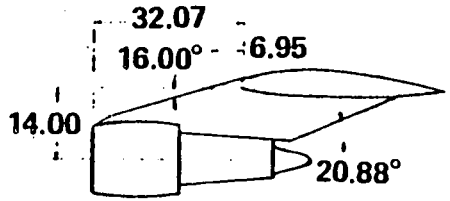

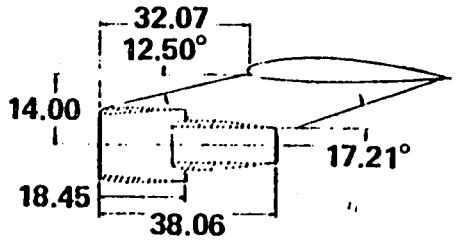

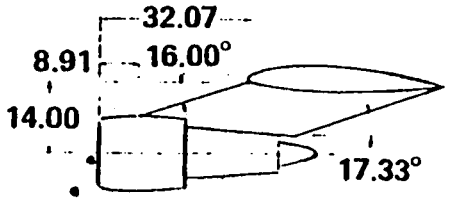

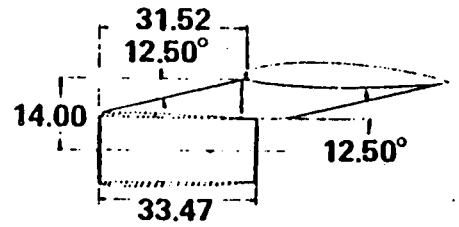

GRUMMAN

C-5A PYLON PRESSURE CORRELATION
M = 0.775 $\alpha = 2°$

NASA TM X-2530

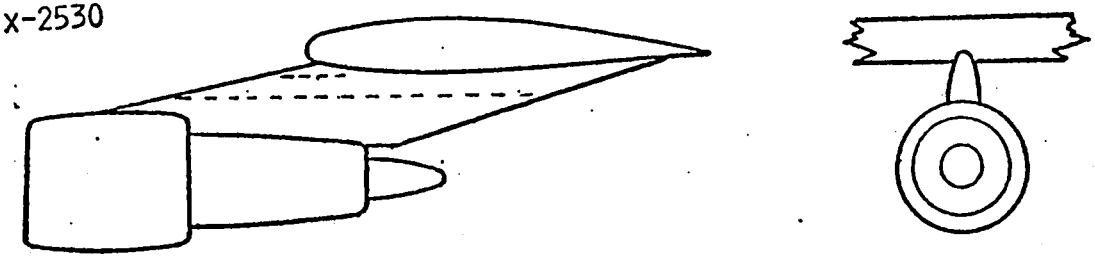

EXPERIMENT ANALYSIS

INBOARD

OUTBOARD

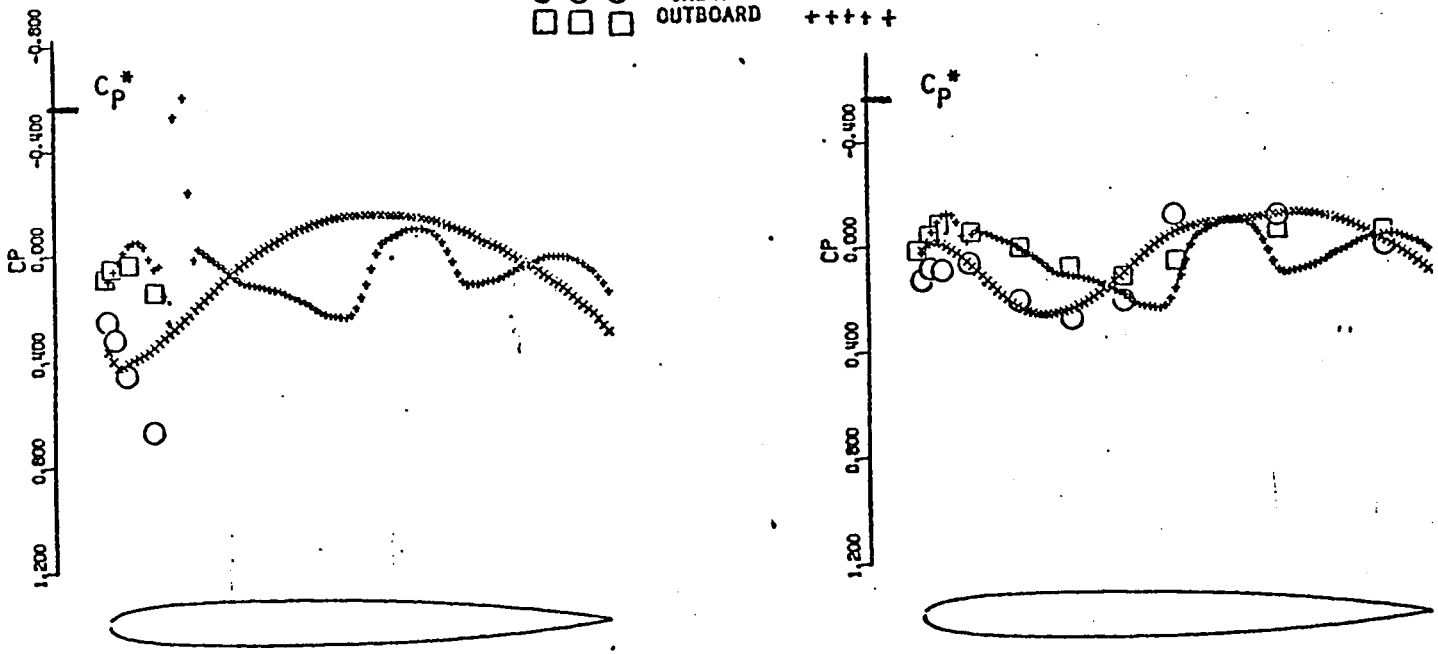

C-5A PYLON PRESSURE CORRELATION
M = 0.775 α = -2°

NASA TM X-2530

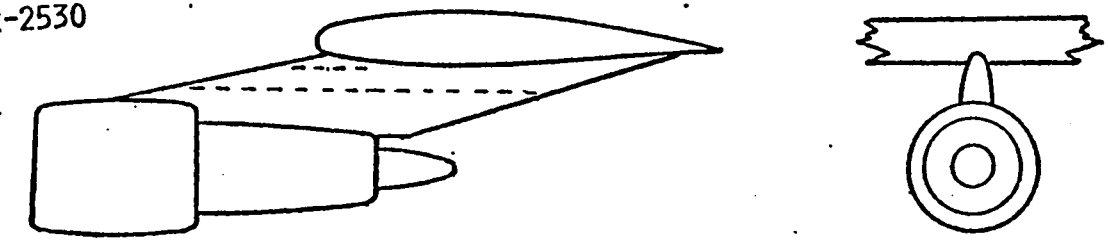

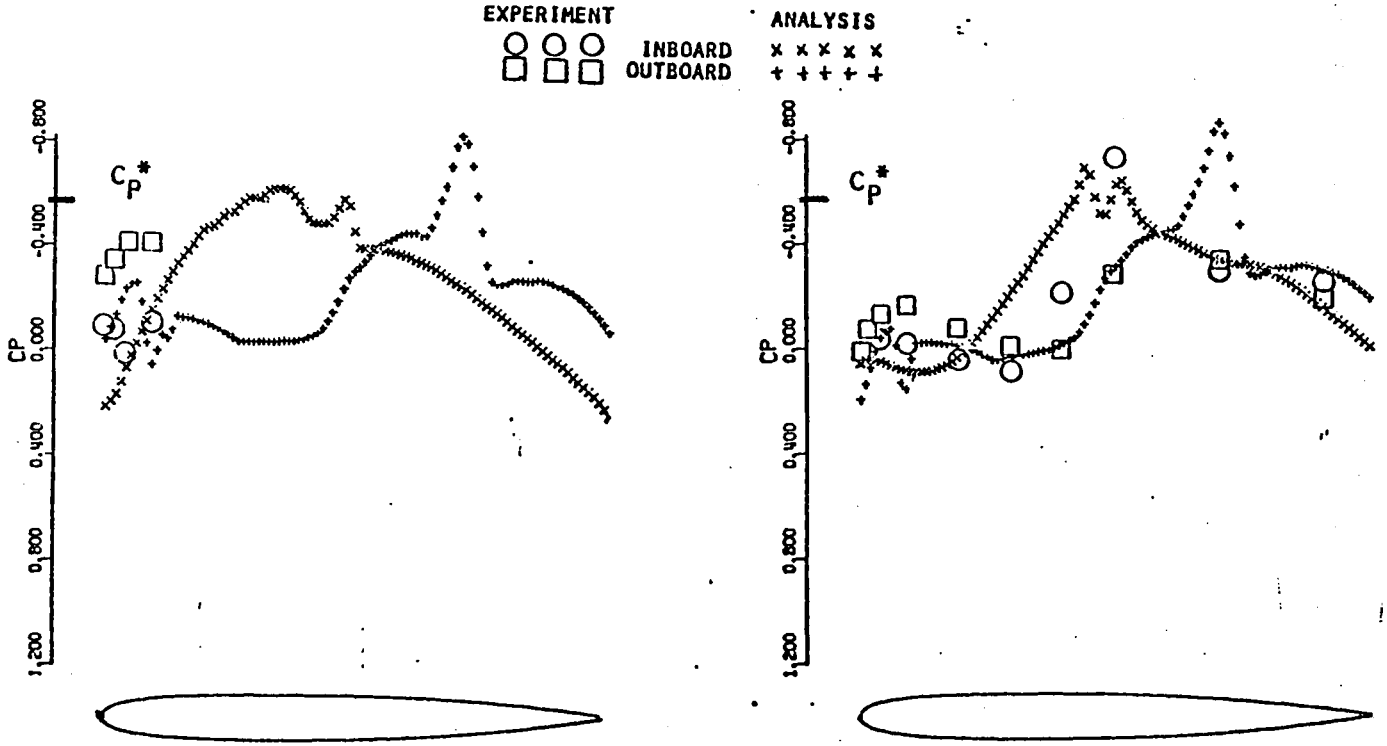

CYLINDRICAL EMBEDDED WING TIP GRID FOR MODELING CANTED WINGLETS

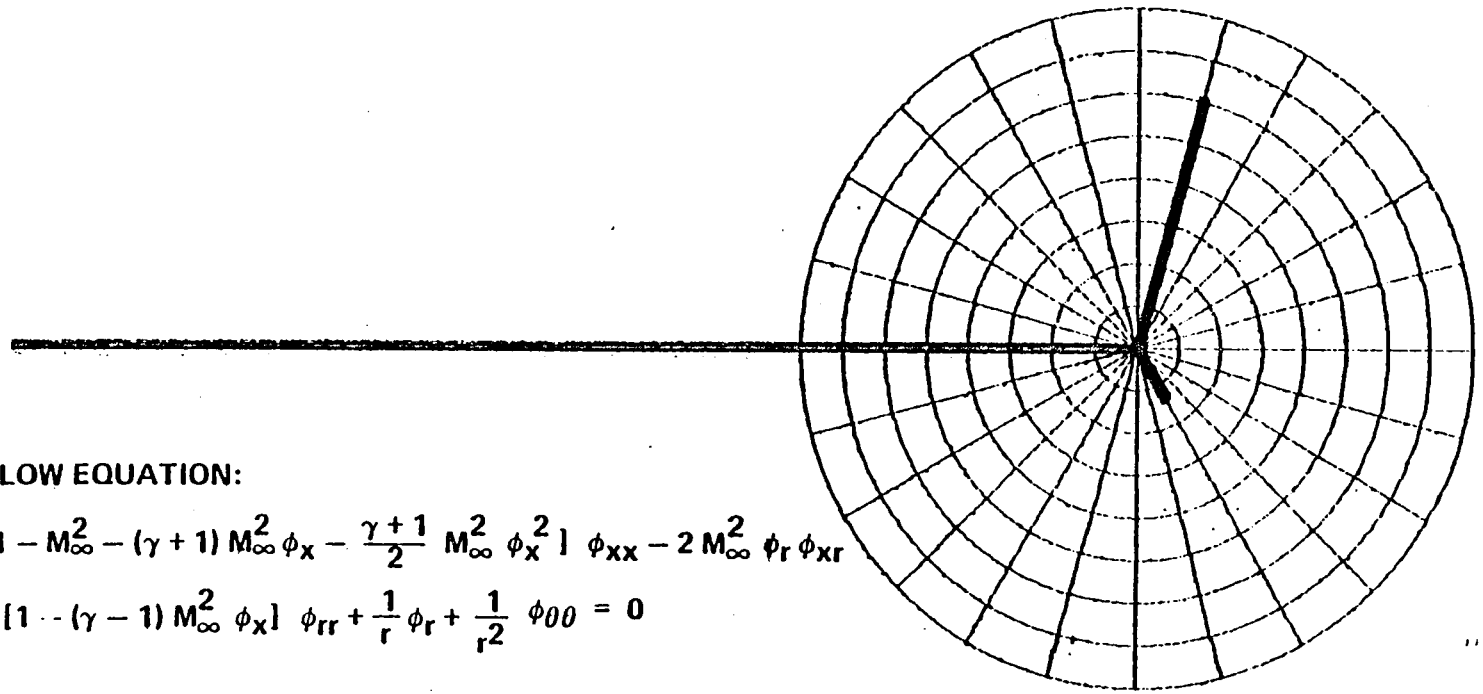

FLOW EQUATION:

$$[1 - M_\infty^2 - (\gamma + 1) M_\infty^2 \phi_x - \frac{\gamma + 1}{2} M_\infty^2 \phi_x^2] \phi_{xx} - 2 M_\infty^2 \phi_r \phi_{xr}$$

$$+ [1 - (\gamma - 1) M_\infty^2 \phi_x] \phi_{rr} + \frac{1}{r} \phi_r + \frac{1}{r^2} \phi_{00} = 0$$

GRUMMAN

CRUDE/MEDIUM/FINE GRID ARRANGEMENT FOR ARBITRARY CANTED WINGLETS

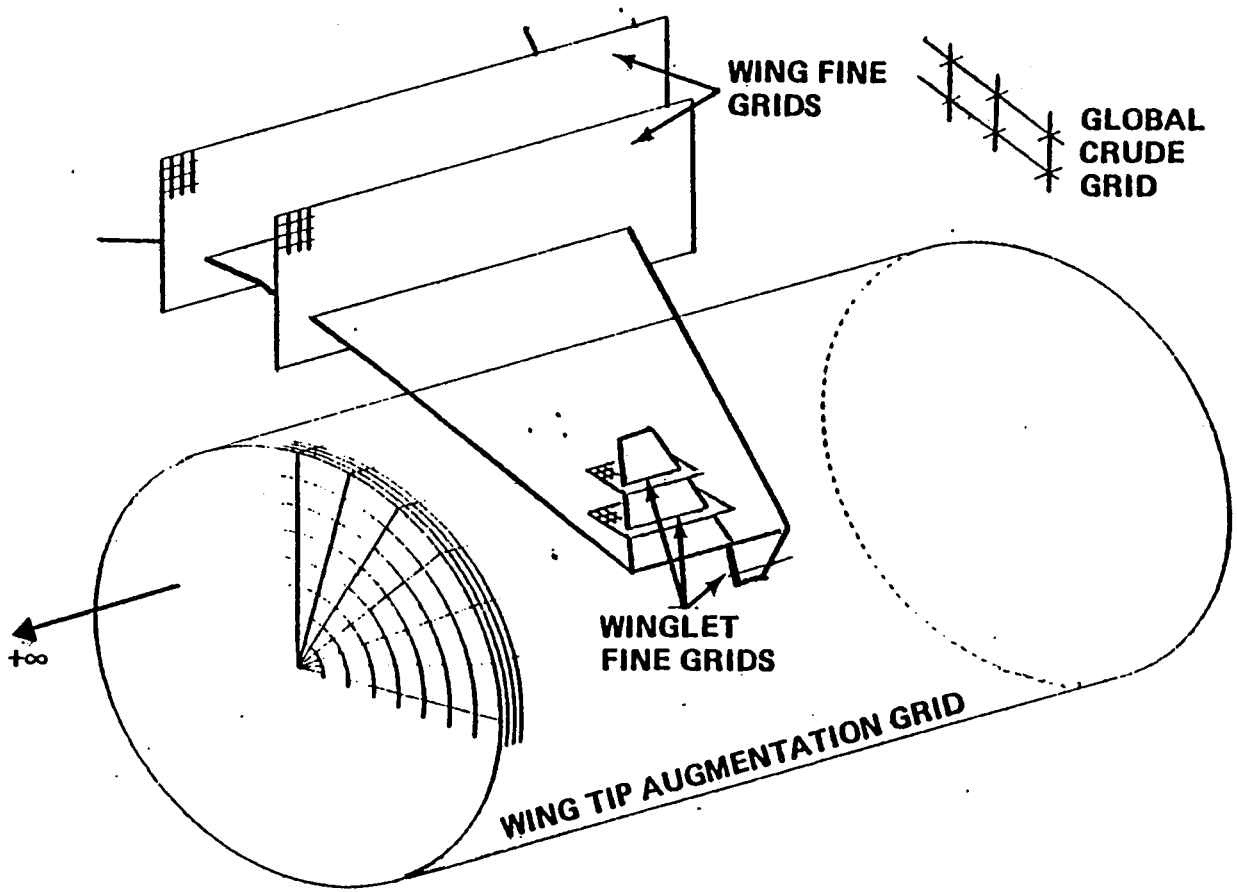

GRUMMAN

CRUDE-MEDIUM GRID INTERACTION

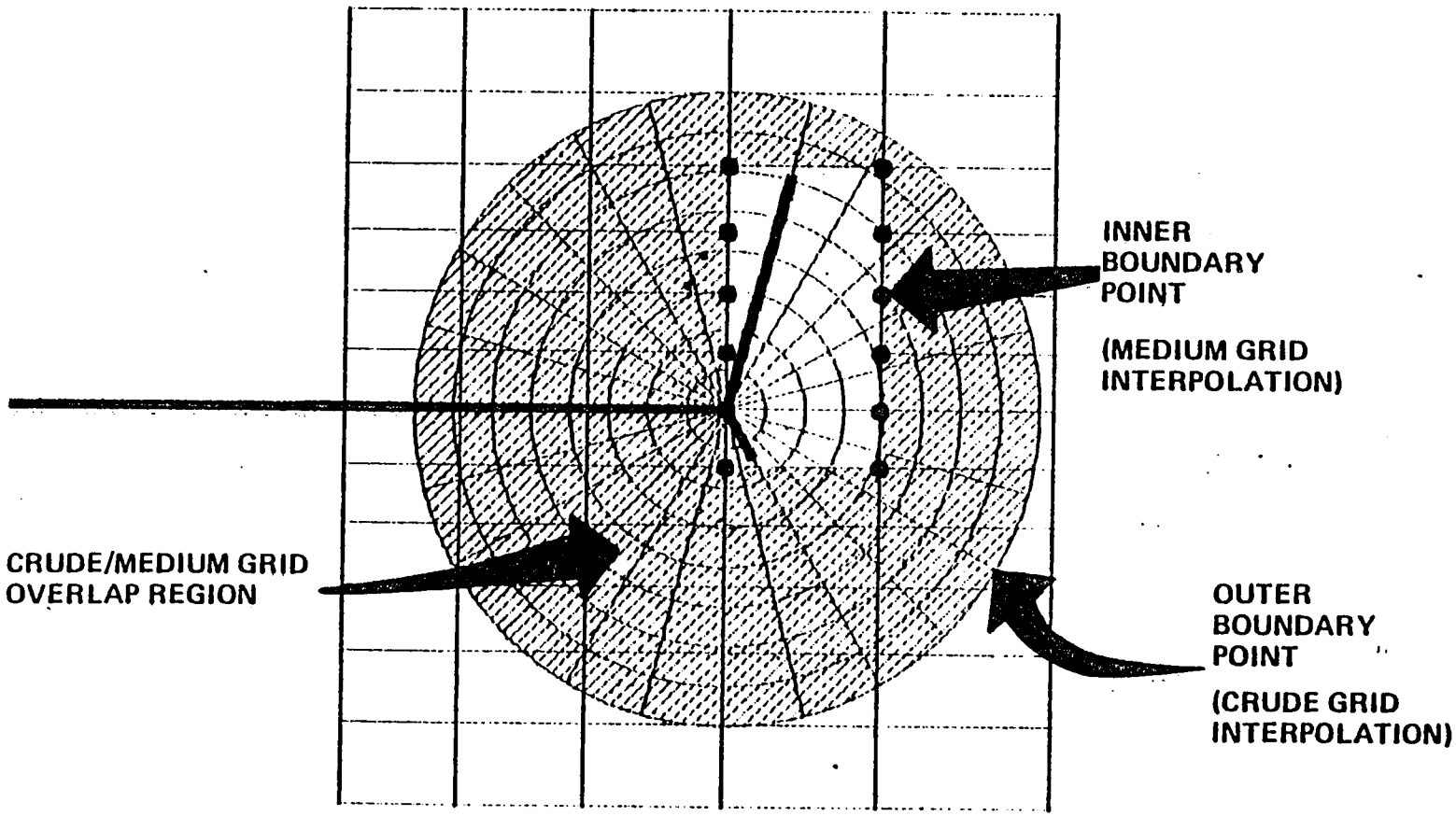

GRUMMAN

CASES FOR WINGLET VALIDATION

- BOEING KC-135

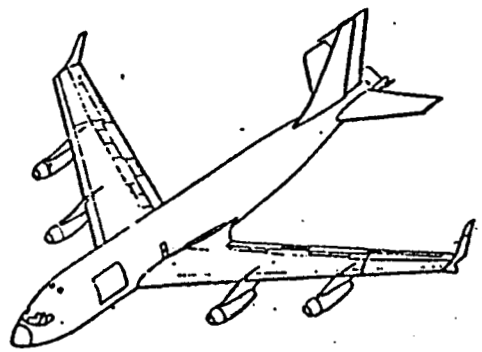

- DOUGLAS DC-10
  (FEDD RESTRICTED)

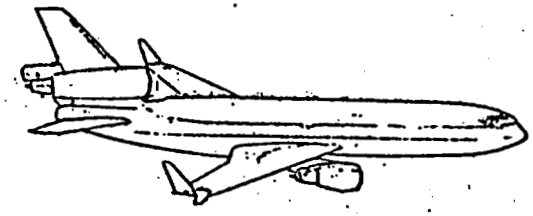

- GULFSTREAM AEROSPACE GIII

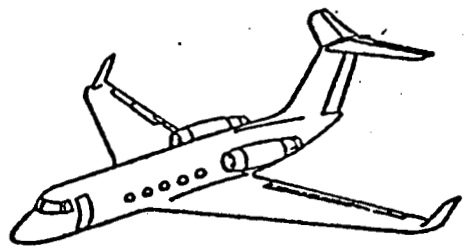

KC-135 WINGLET PRESSURE CORRELATION

M = 0.78 α = 2°

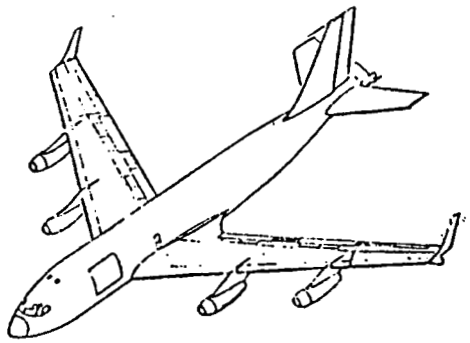

DATA: NASA TN D-8474

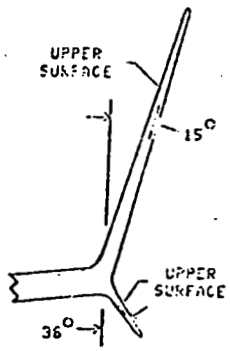

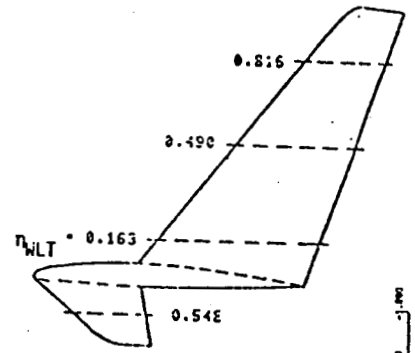

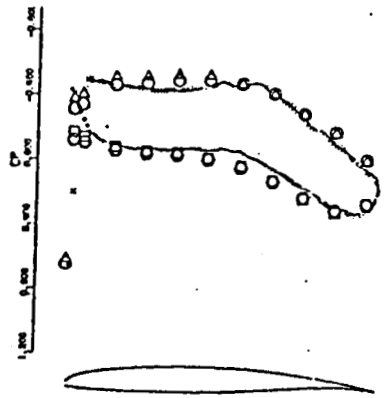

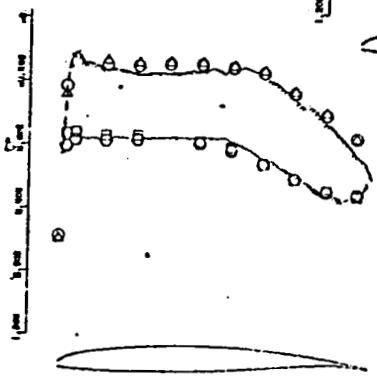

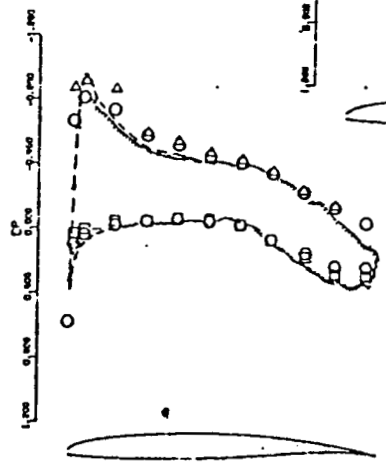

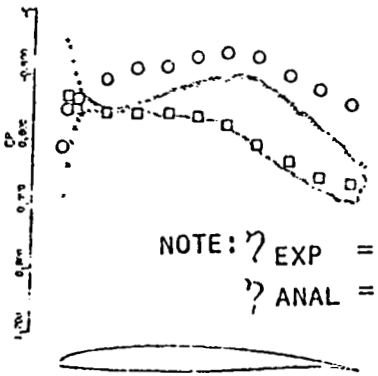

NOTE: η_{EXP} = 0.55

η_{ANAL} = 0.67

KC-135 SPANLOAD CORRELATION WITH WINGLETS
M = 0.78 α = 2°

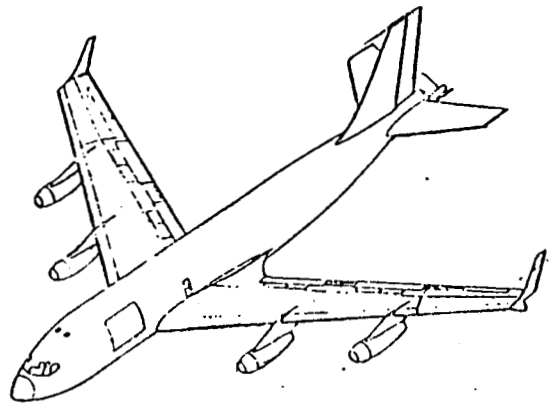

EXPERIMENT
- ○ LOWER WLT. ON
- □ LOWER WLT. OFF

ANALYSIS
- LOWER WLT. ON ——————
- LOWER WLT. OFF - - - -

DATA: NASA TN D-8474

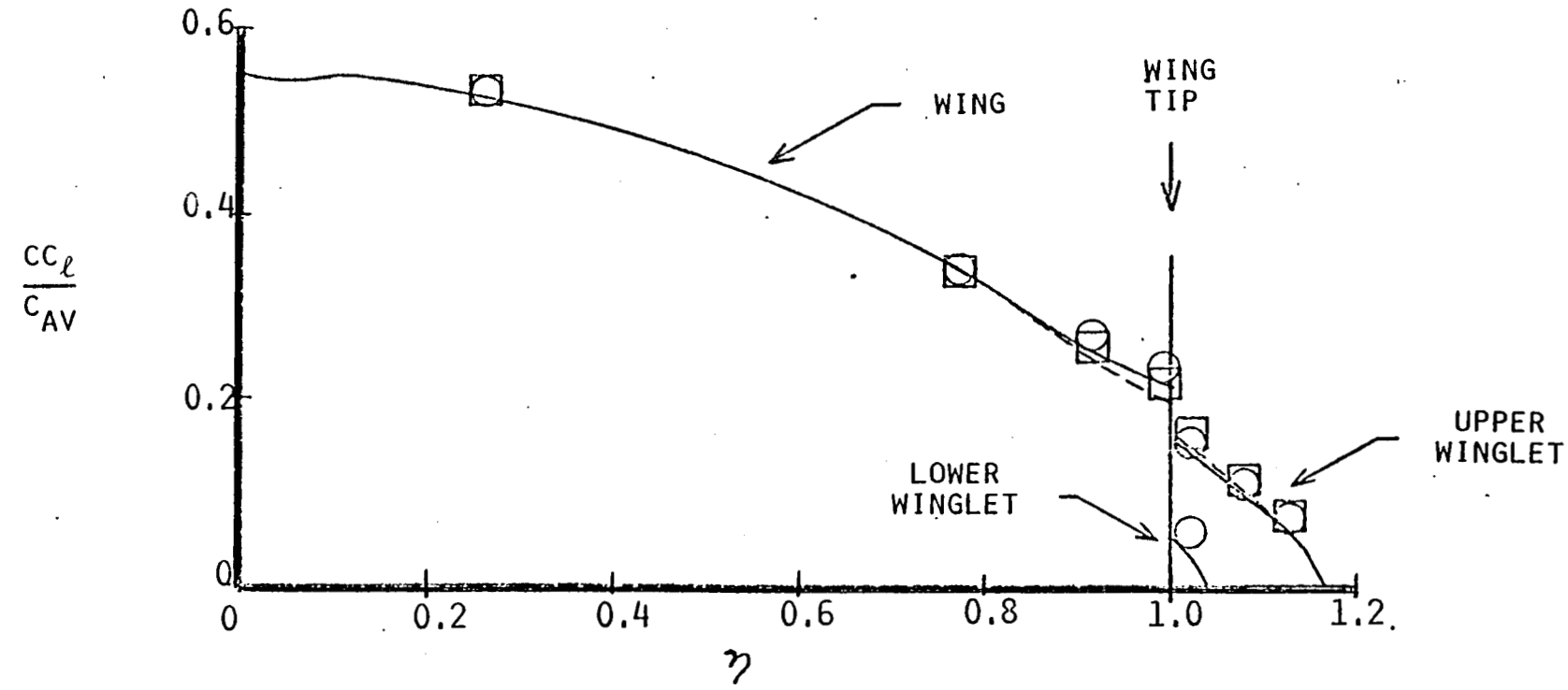

KC-135 WINGLET PRESSURE CORRELATION
M = 0.80 α = 3.5°

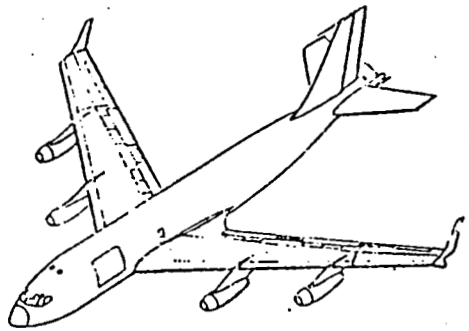

DATA: NASA TN D-8474

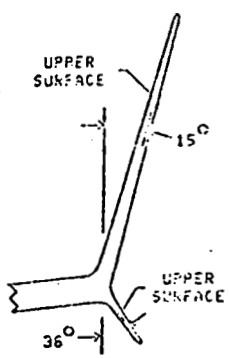

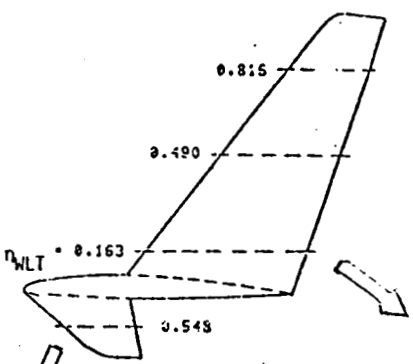

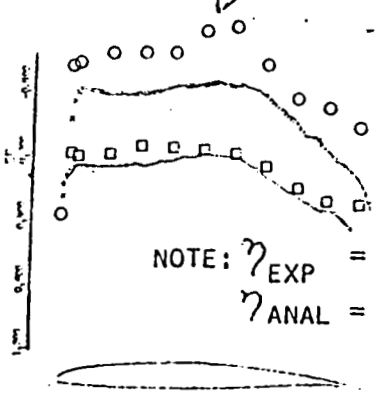

NOTE: η_{EXP} = 0.55
η_{ANAL} = 0.67

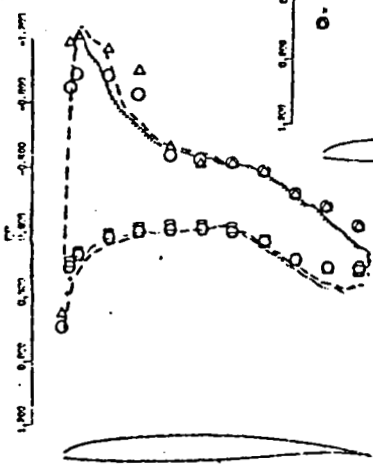

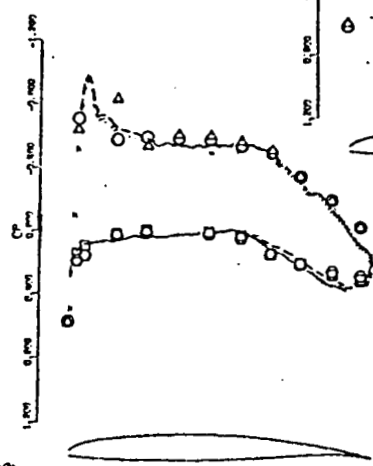

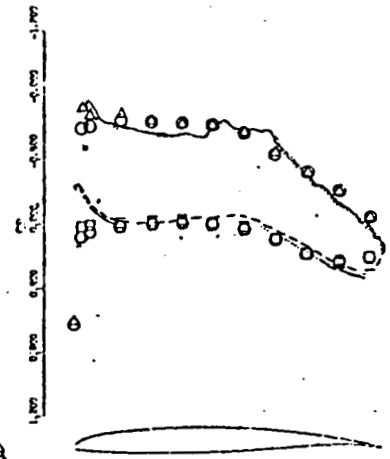

G-III WINGLET PRESSURE CORRELATION

M = 0.75 α = 4°

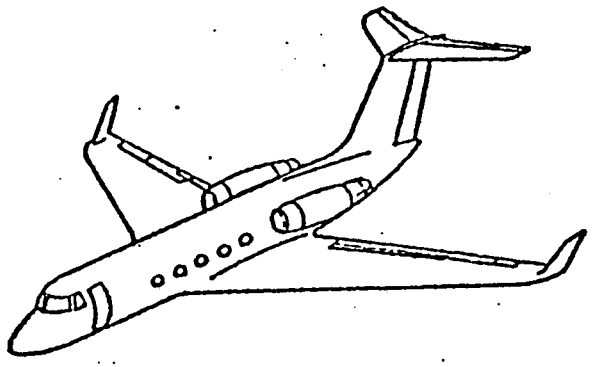

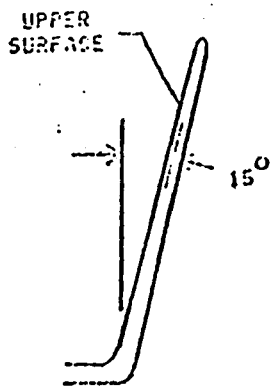

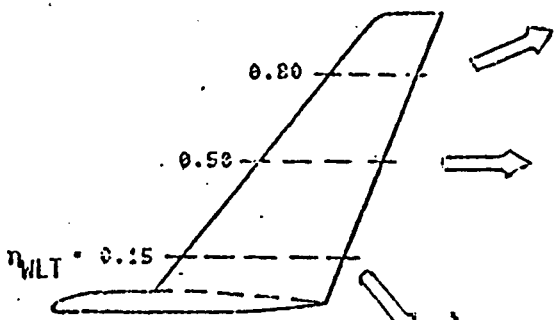

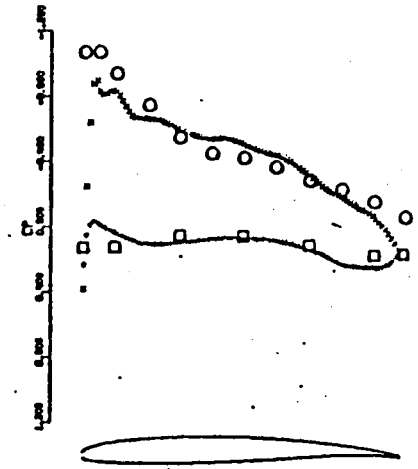

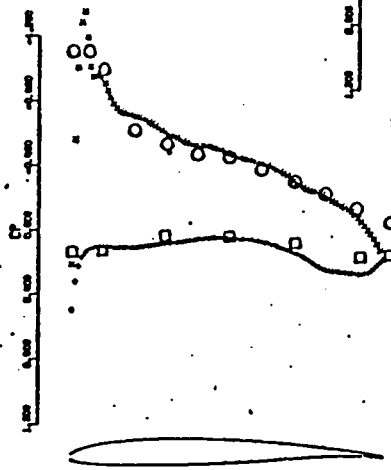

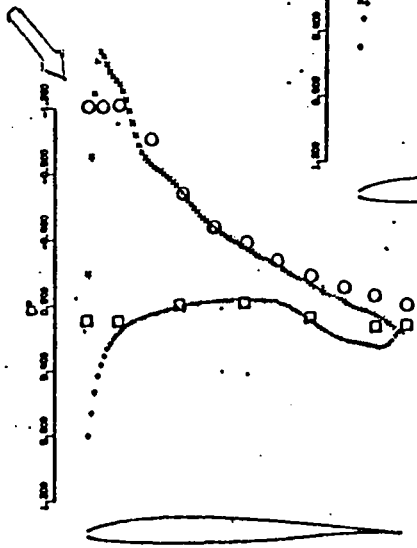

NASA/GRUMMAN TRANSONIC WING-BODY CODE RELATED EFFORTS 1983

- WING/PROP SLIPSTREAM INTERACTION
- NACELLE EMBEDDED IN WING ANALYSIS
- CANARD-WING-FUSELAGE CORRELATION
- G-IV "TAY" ENGINE STUDY
- ROTATED DIFF. SCHEME FOR SEVERE PLANFORM/FLOW COMBINATIONS
- LFC AIRFOIL ANALYSIS
- NON-SYMMETRIC CONFIGURATIONS

WING PRESSURE COMPARISON FOR POSITIVE/NEGATIVE SLIPSTREAM SWIRL

M = 0.80 α = 3°

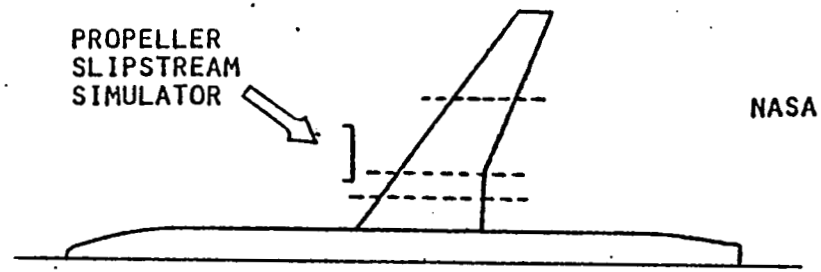

NASA CR-152138

EXPERIMENT ANALYSIS

POSITIVE 7° SWIRL XXXXXX
NEGATIVE 7° SWIRL

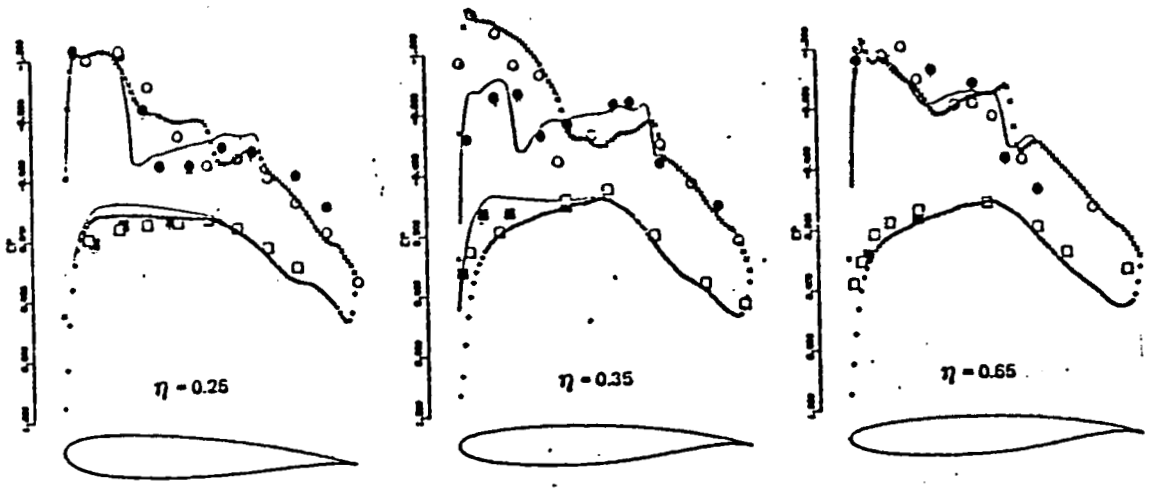

EFFECT OF PROPELLER SLIPSTREAM ON SPANLOAD, LIFT & DRAG
M = 0.80

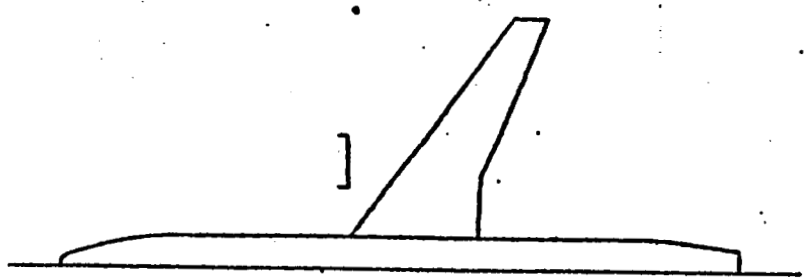

EXPERIMENT ANALYSIS

SWIRL +7° ——
SWIRL -7° - - - -

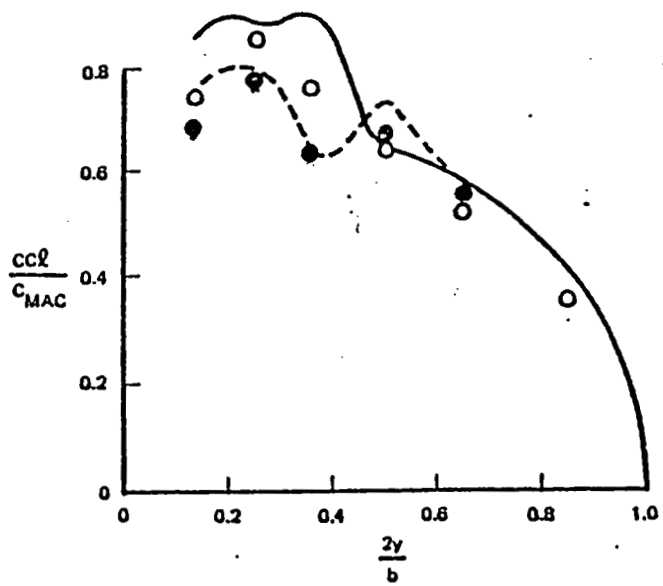

NASA CR-152138

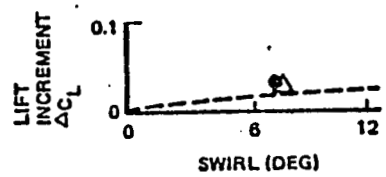

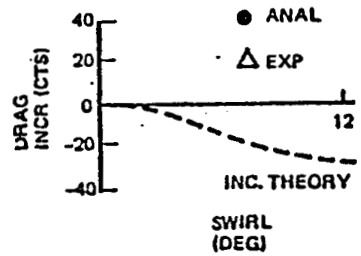

EFFECT OF EMBEDDED-NACELLE ON WING SHOCK WAVE PATTERN

M = 0.80 · C_L ~ 0.43

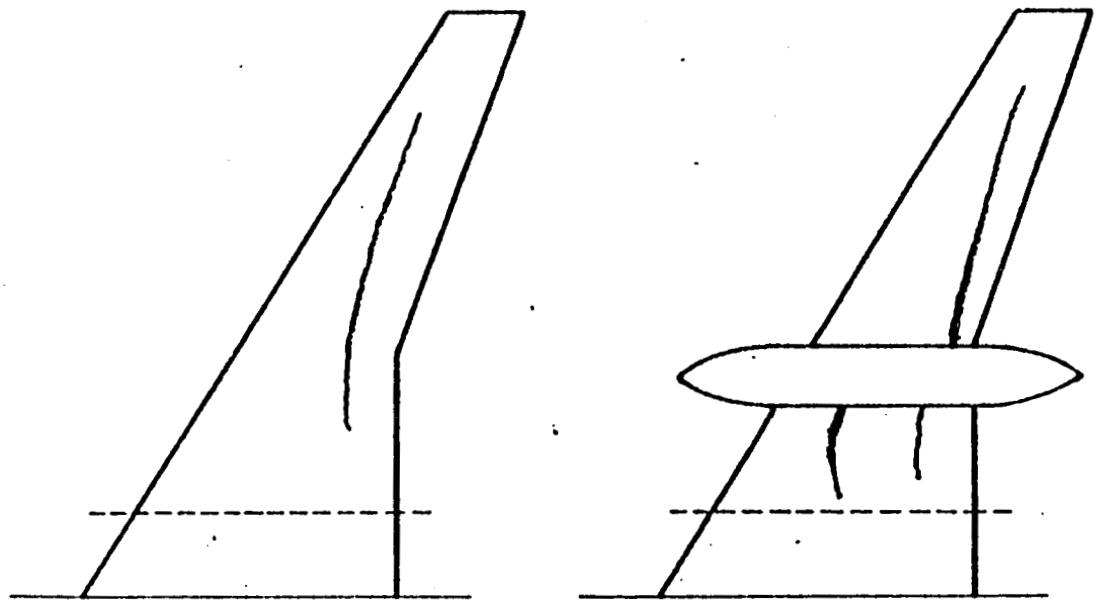

NASA EXP./GRUMMAN ANALYSIS CO-OP
PRESSURE COMPARISONS: NOV. 1983

CANARD-WING-FUSELAGE PRESSURE CORRELATION
M = 0.90 α = 6°

AIR FORCE CANARD VERSION OF CODE

DATA: AIAA 83-1850

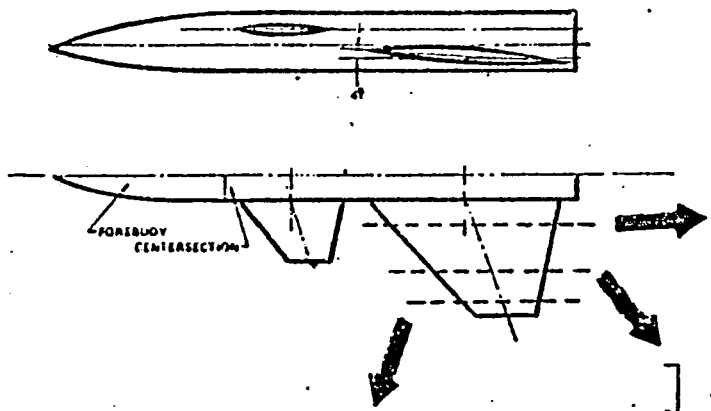

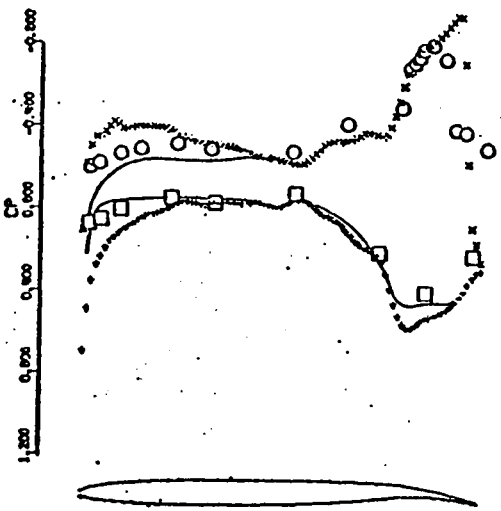

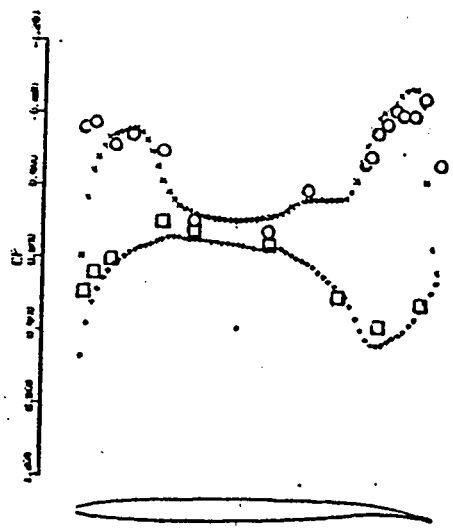

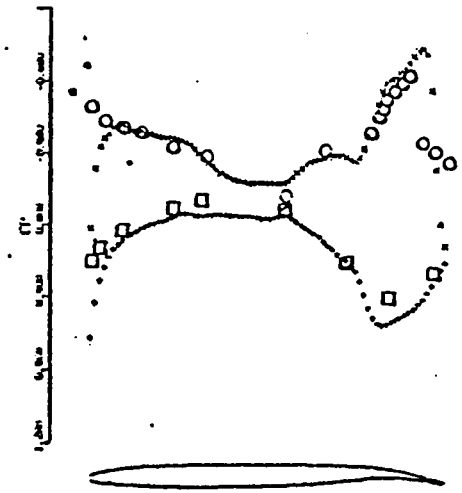

G-IV "TAY" WING ROOT PRESSURE CORRELATION
M = 0.78 α = 4°

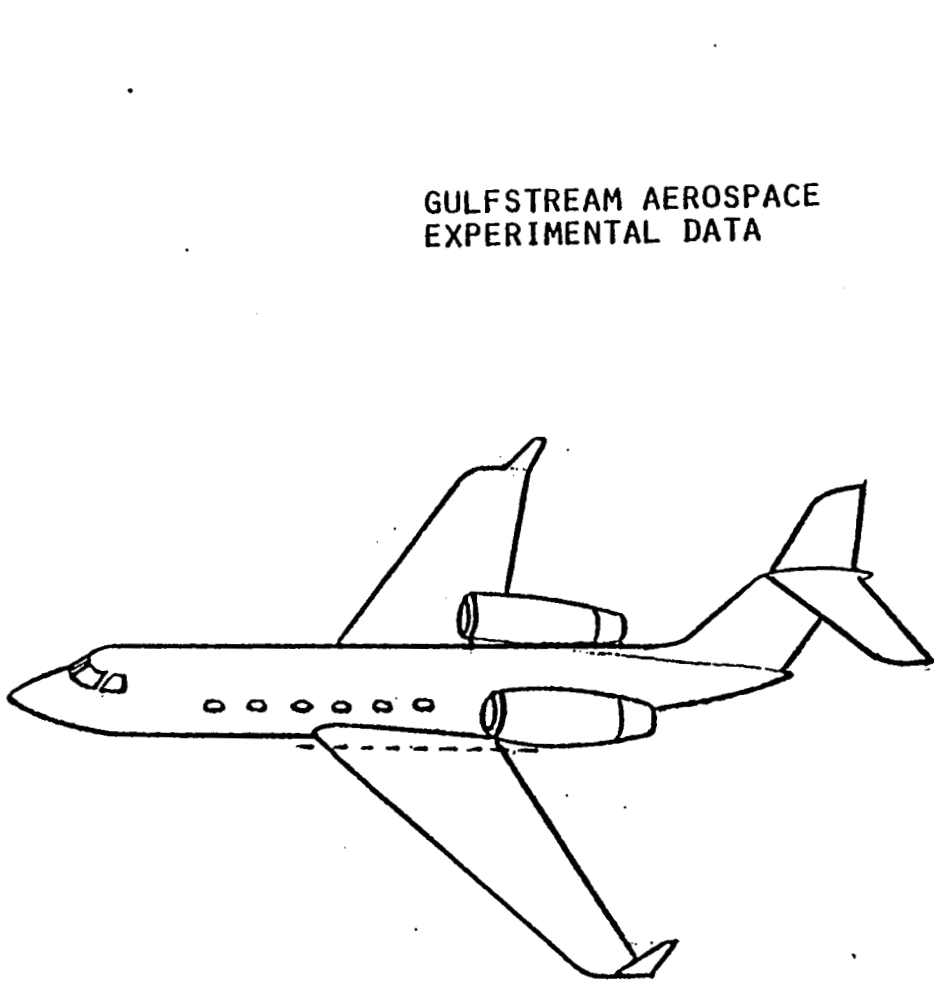

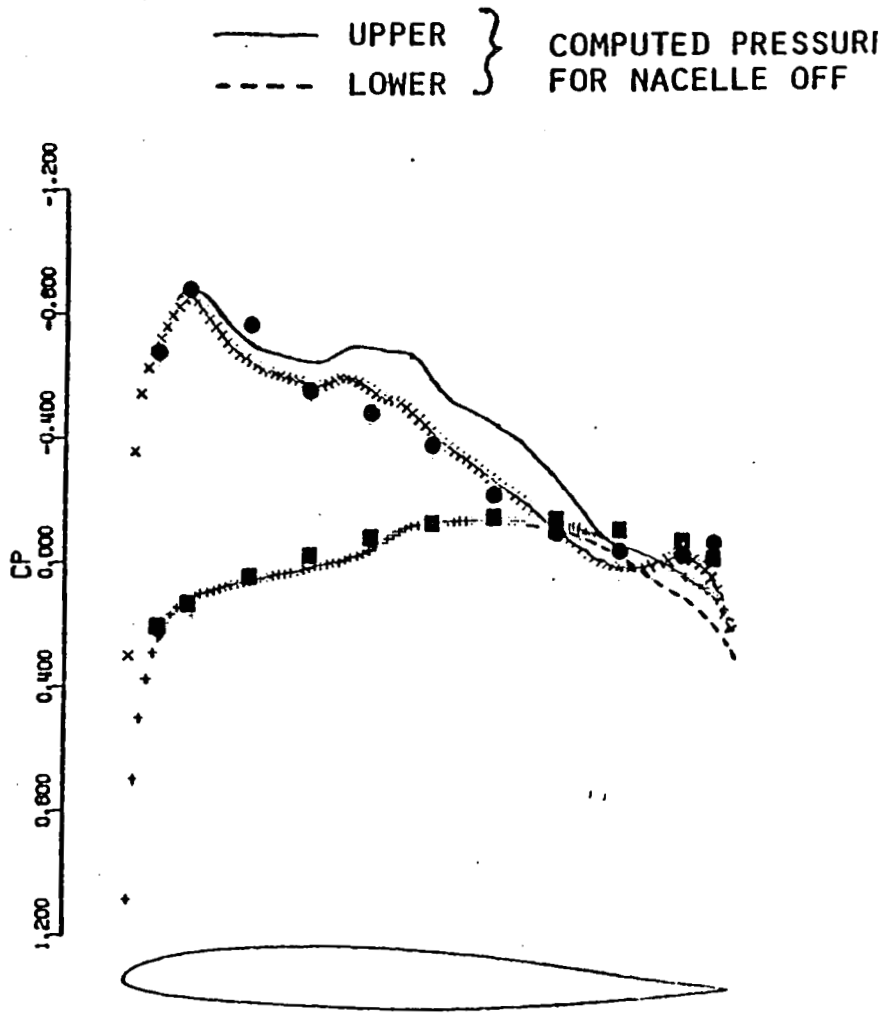

WING TIP STABILITY PROBLEM . . .

A NEW APPROACH

PROBLEM:	HIGHLY LOADED WINGS OR WINGS WITH STEEP PRESSURE GRADIENTS ON PLANFORMS HAVING HIGH SWEEP AND SEVERE TAPER (LOW AR) OFTEN DEVELOP UNSTABLE FLOW NEAR THE WING TIP.
1982 SOLUTION: (SEE LAST YEARS CONTRACTOR REVIEW)	DEVELOP MODIFIED (ADJUSTABLE) WING TIP GRID TO AUTOMATICALLY REDUCE TIP GRID RESOLUTION
BUT...	LOSS OF GRID RESOLUTION COMPROMISED SOME COMPARISONS
1983 SOLUTION:	X-Y ROTATED DIFF SCHEME

$$T\phi_{xx} + U\phi_{xy} + V\phi_{yy} + \phi_{zz} = 0$$

DUE TO INCLUSION OF THIS CROSSFLOW TERM, THE DOMAIN OF DEPENDENCE OF THE FLOW EQUATION WILL ROTATE IN THE X-Y (WING) PLANE, USE ROTATED DIFFERENCES (IN THE X-Y PLANE ONLY)

H28

NEW SCHEME IMPROVES SOLUTION STABILITY FOR EXTREME PLANFORM/FLOW COMBINATIONS

M = 0.90 α = 8°

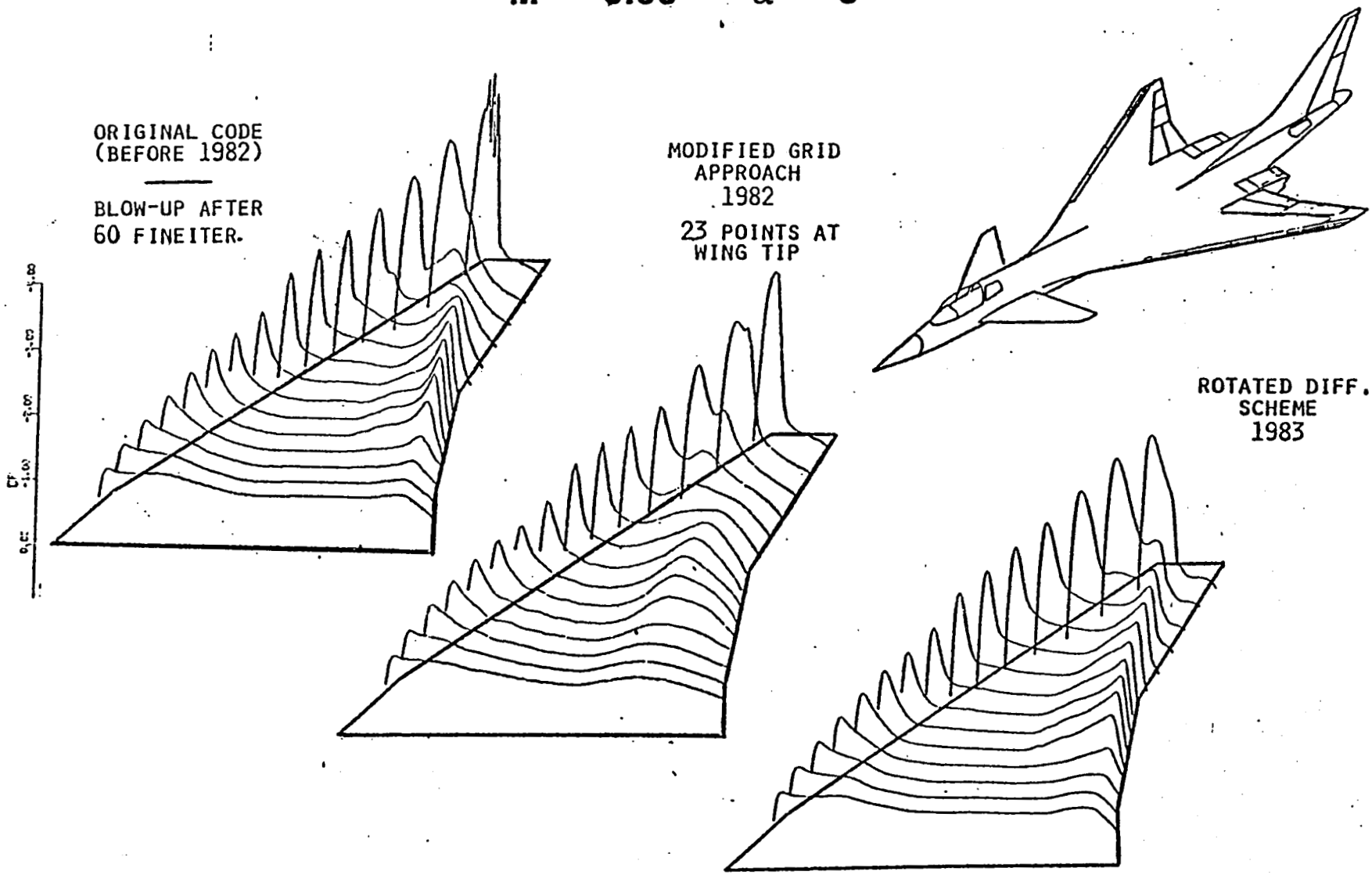

REFINED WING ROOT SIMULATION USING ROTATED DIFF. SCHEME

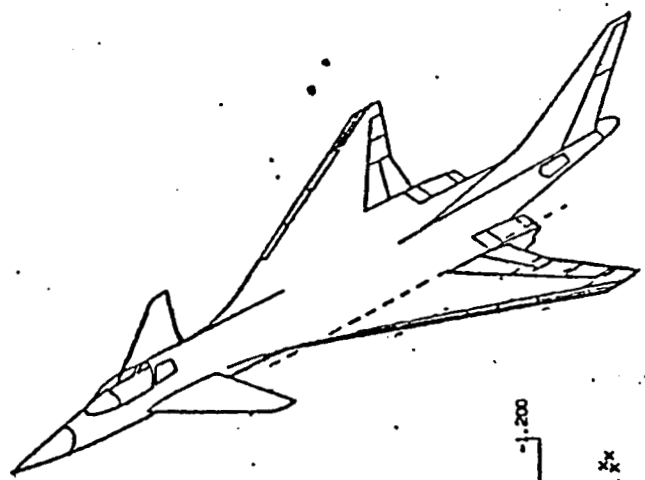

MODIFIED GRID APPROACH 1982

23 POINTS AT WING TIP

GRUMMAN CDAF DATA

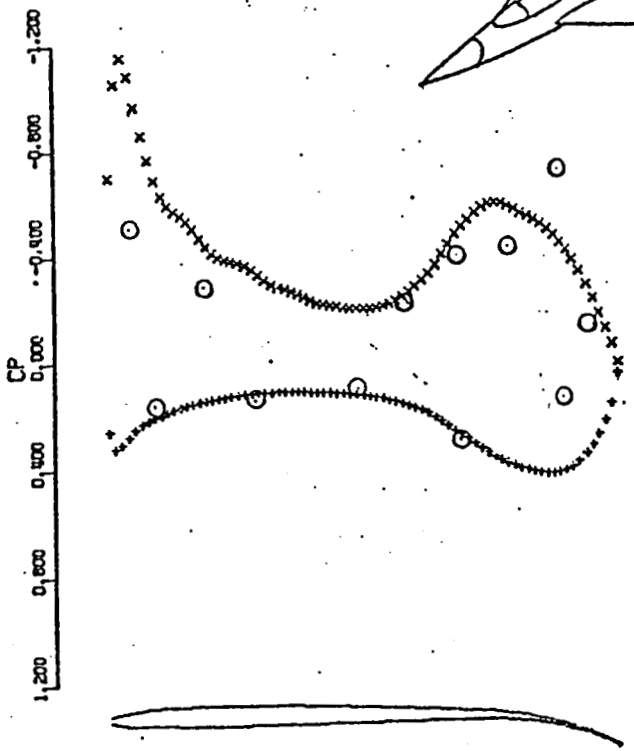

ROTATED DIFF. SCHEME 1983

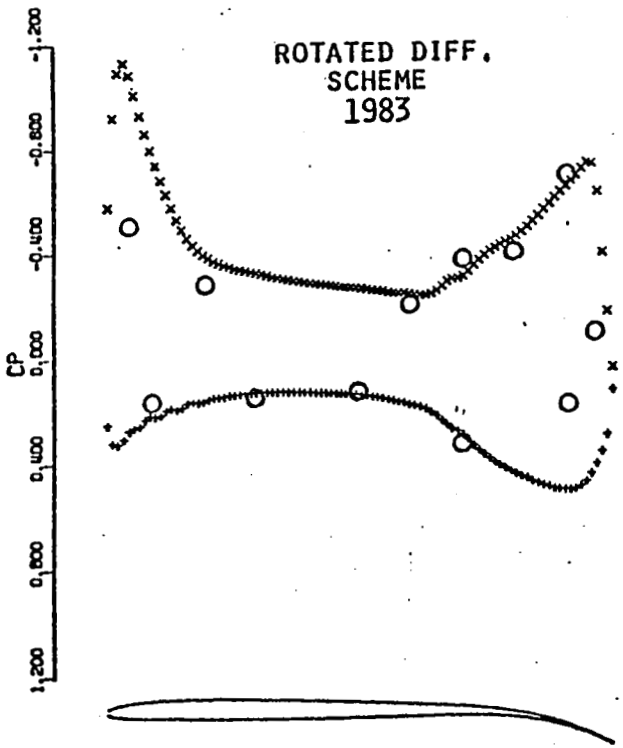

FUSELAGE PRESSURE CORRELATION FOR NON-SYMMETRIC CONFIGURATION

M = 0.90 α = 0°

NACA RM A58C03

NOTE: NO FORWARD SWEPT JUNCTURE PRESSURES AVAIL.

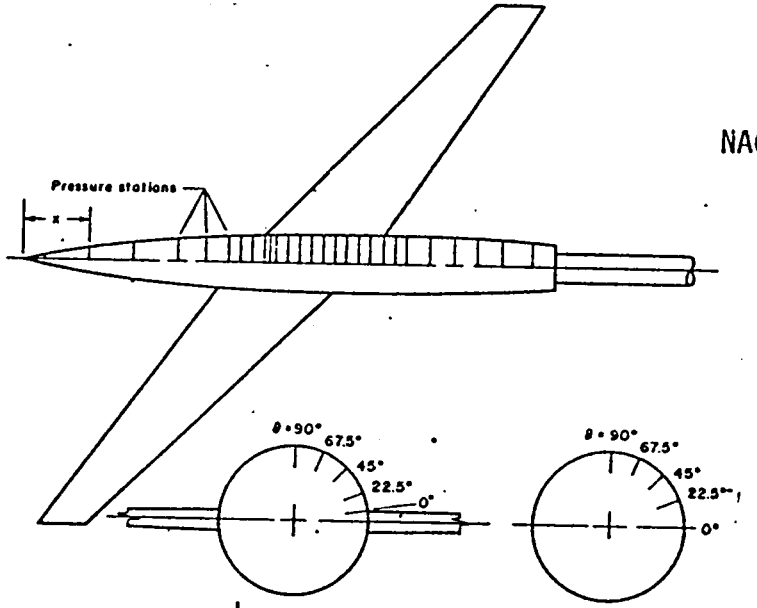

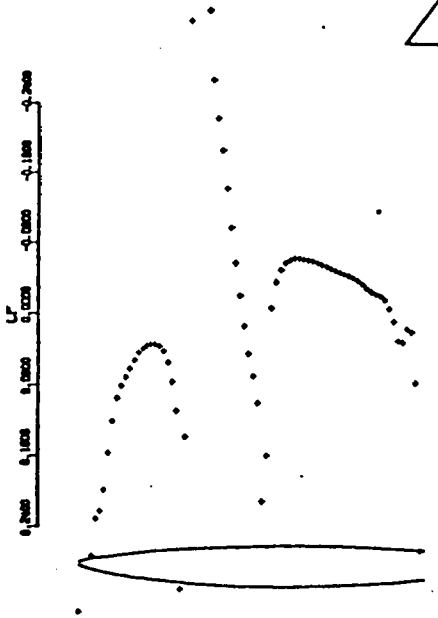

FORWARD SWEPT JUNCTURE

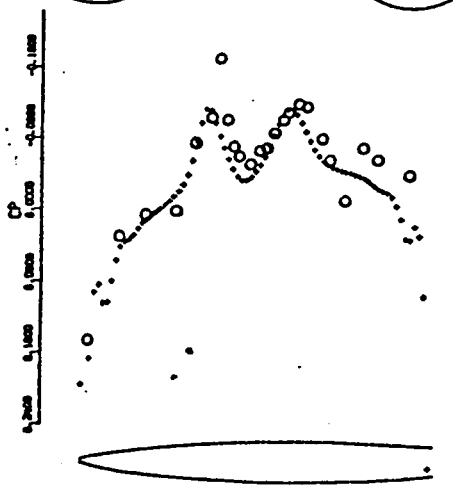

TOP CENTERLINE

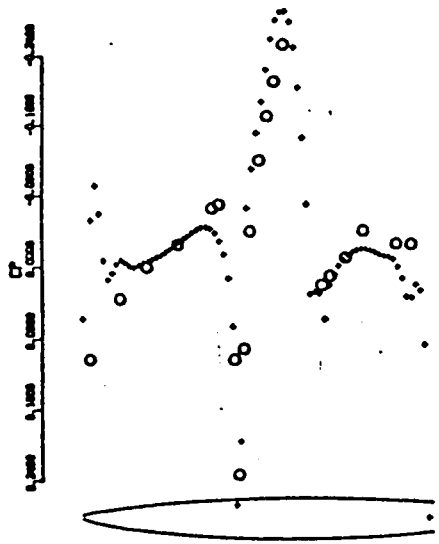

AFT SWEPT JUNCTURE

WING PRESSURE CORRELATION FOR NON-SYMMETRIC CONFIGURATION

M = 0.90 α = 0°

NACA RM A58C03

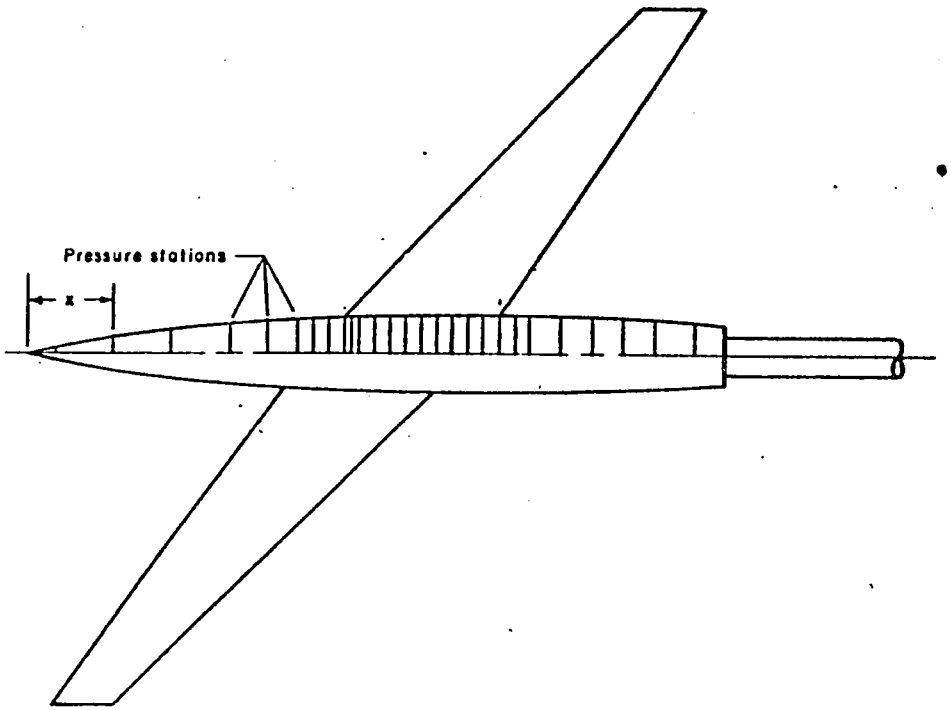

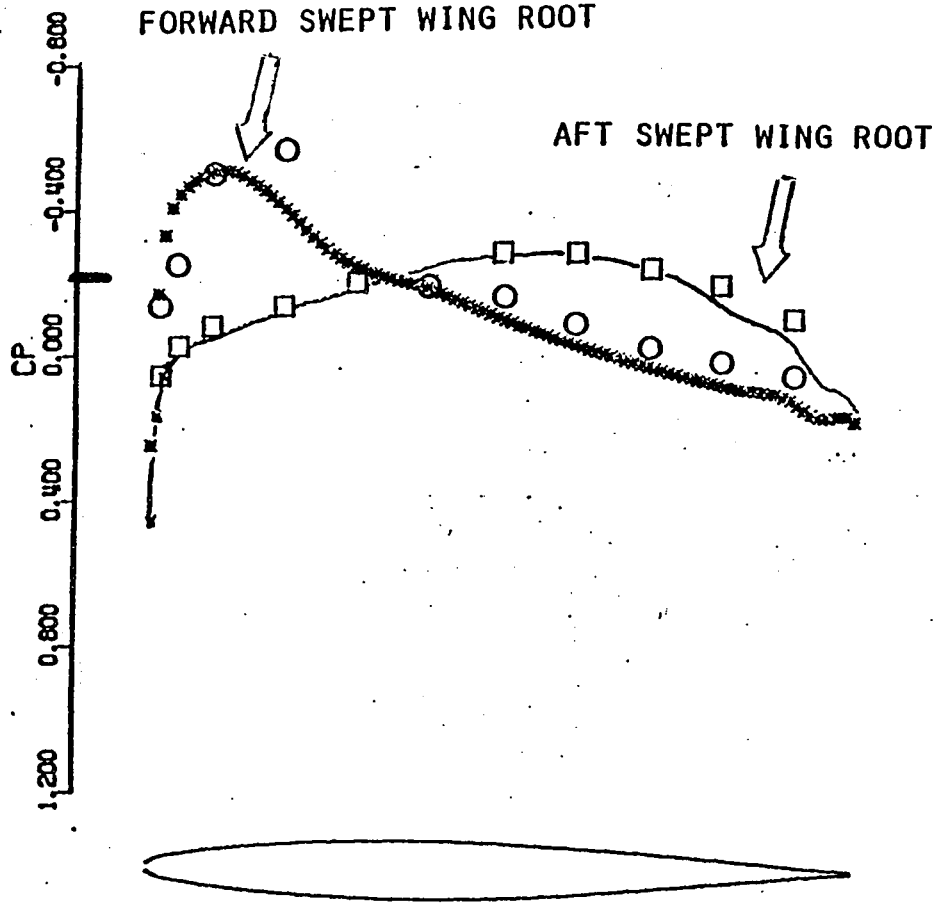

SUPERIMPOSED WING PRESSURES FOR NON-SYMMETRIC DESIGN APPLICATION
M = 0.90 α = 2°

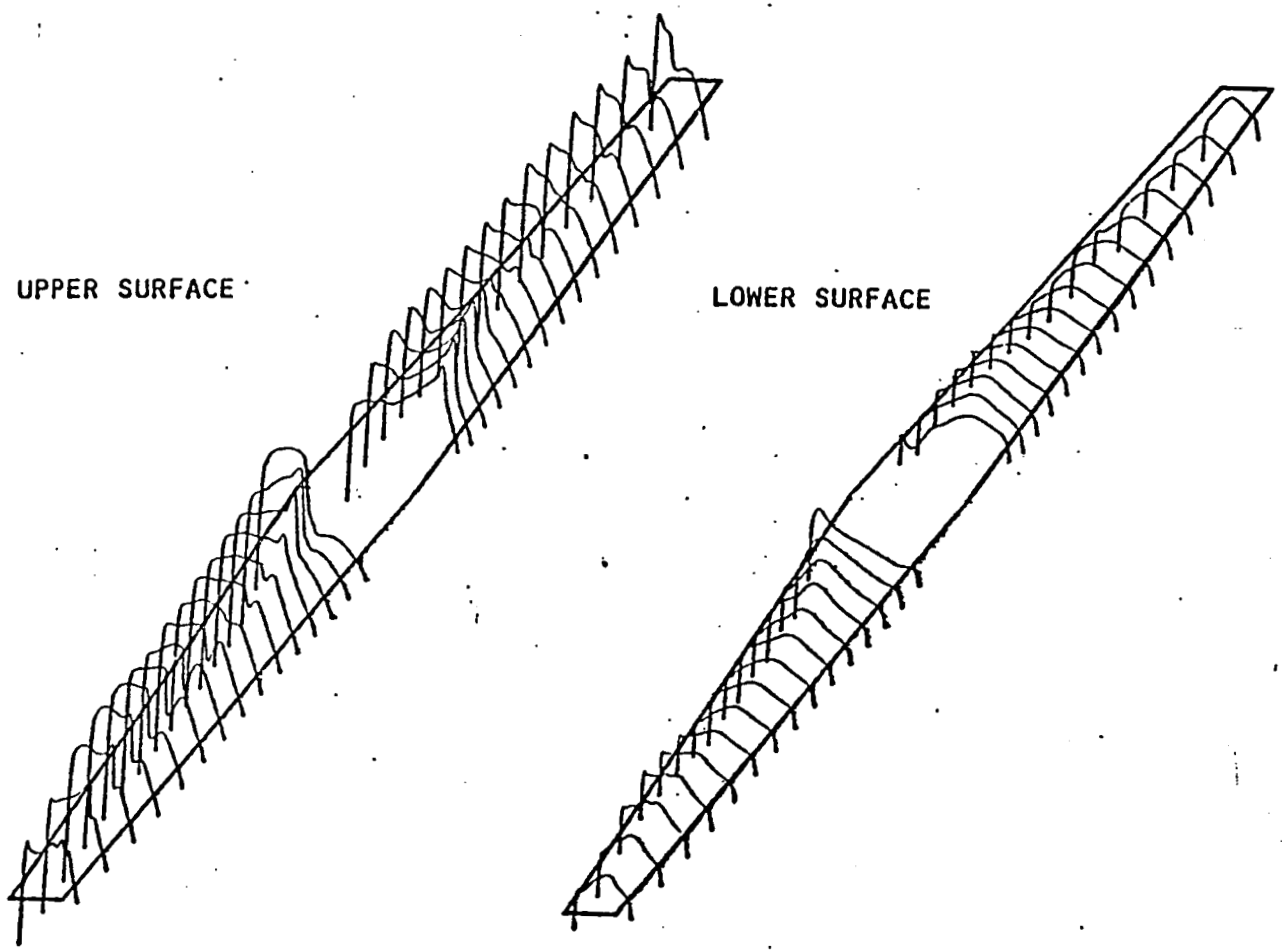

STATUS OF PYLON & WINGLET TASKS FOR CONTRACT NAS1-14732

- TECH PAPER DOCUMENTATION
  - WINGLET AIAA 84-0302
  - PYLON AIAA 84-0117 (INVITED)
- WINGLET CODING COMPLETE - CODE OPERATIONAL ON LaRC COMPUTING SYSTEM
  - UPPER/LOWER CANTED WINGLETS
  - 2-D "STRIP" B.L.
- WINGLET CODE VALIDATED USING 3 CONFIGURATIONS
- PYLON CODING COMPLETE - CODE TRANSFER PLANNED FOR NOV. '83
- PYLON PREDICTIONS COMPARED WITH C-5A DATA
  - SOME SENSITIVITY NOTED...WING/PYLON, NACELLE/PYLON, NPR VARIATIONS (PYLON SWEEP $\sim 80°$)
  - PYLON T.E. MATCH PROBLEM

EMBEDDED MESH MULTIGRID TREATMENT OF TWO-DIMENSIONAL TRANSONIC FLOWS

D. R. McCarthy*

Purdue University
West Lafayette, Indiana
and
Indiana University - Purdue University
Fort Wayne, Indiana

and

R. C. Swanson

NASA - Langley Research Center
Hampton, Virginia

Presented at the
International Multigrid Conference
Copper Mountain, CO
April 1983

* Work of this author supported by a grant from NASA-Langley Research Center, Hampton, VA.

McCARTHY

FIGURE 1

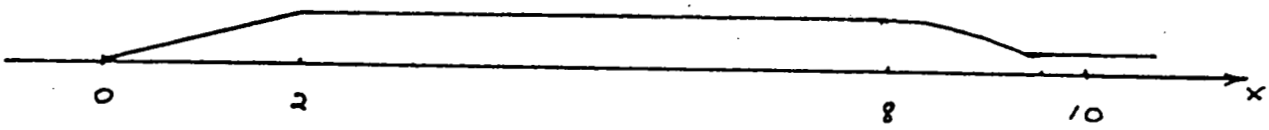

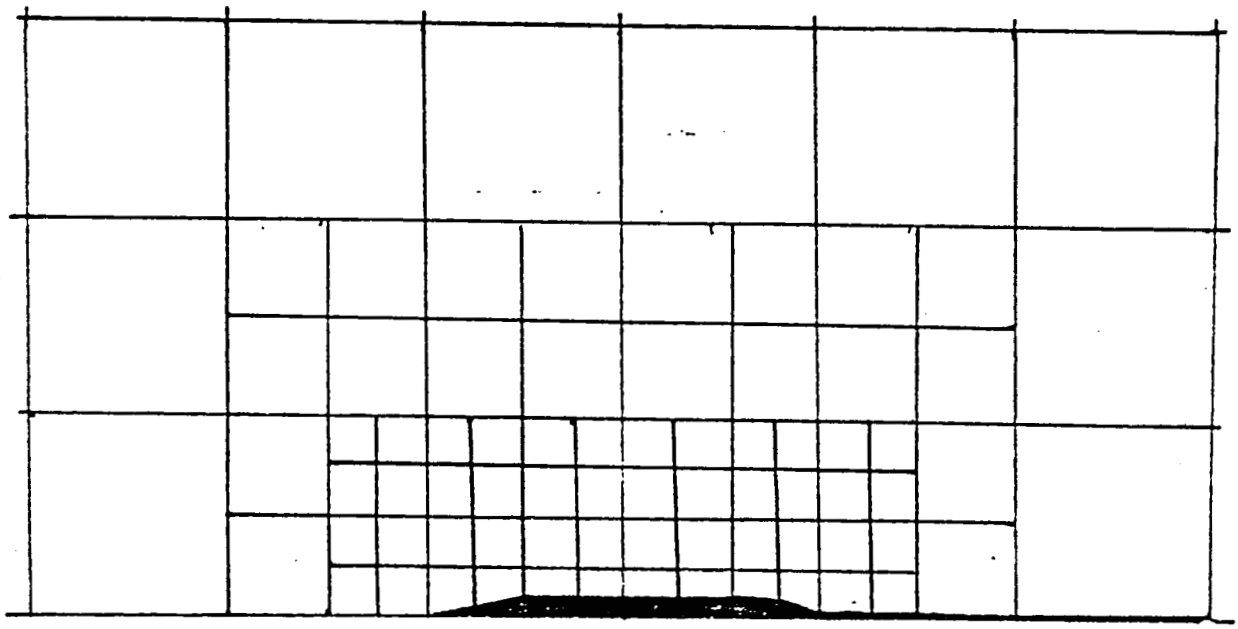

FIGURE 2

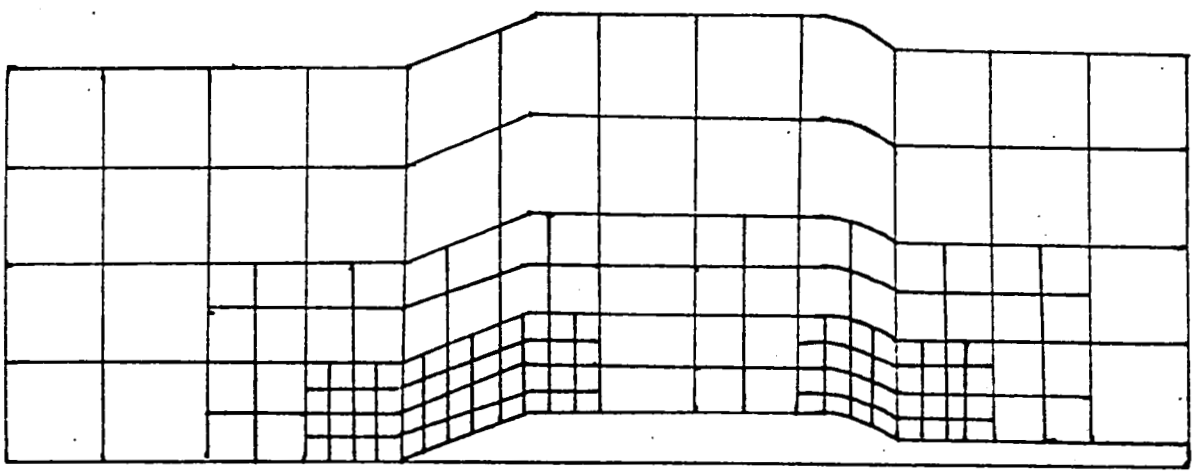

FIGURE 3

Type	CPU sec.	r_{avg}	r_{max}
FI (1)	47	3×10^{-4}	1×10^{-3}
FI (5)	144	3×10^{-6}	4×10^{-5}
GSVLR (1)	30	1×10^{-4}	1×10^{-3}
GSVLR (5)	87	3×10^{-6}	3×10^{-5}
JCVLR (1)	20	6×10^{-3}	3×10^{-2}
JCVLR (5)	55	2×10^{-4}	9×10^{-4}
PJ (1)	18	8×10^{-3}	4×10^{-2}
PJ (5)	52	9×10^{-4}	3×10^{-3}
FI (1) 6 levels	82	5×10^{-4}	2×10^{-3}

$M_\infty = 0.80$

TYPE	CPU sec.	r_{avg}	r_{max}
GSVLR (1)	21	1×10^{-3}	8×10^{-3}
GSVLR (5)	88	3×10^{-4}	7×10^{-3}
FI (1)	48	2×10^{-3}	8×10^{-3}
FI (5)	212	5×10^{-4}	6×10^{-3}
FI (10) (5×5)	542	3×10^{-5}	3×10^{-4}

$$M_\infty = 0.96$$

FIGURE 7

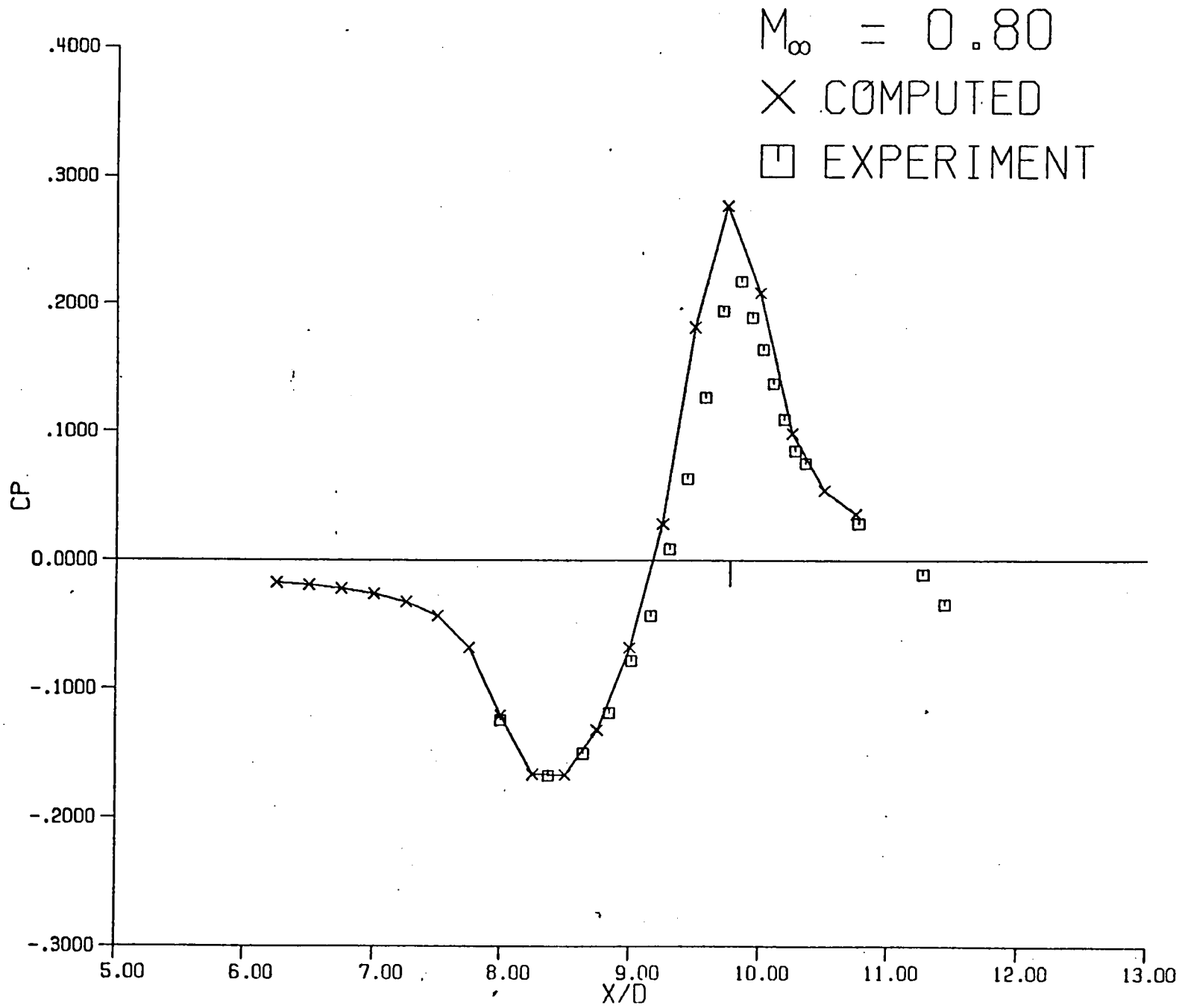
M_∞ = 0.80
X COMPUTED
EXPERIMENT
.4000
.3000
.2000
.1000
0.0000
-.1000
-.2000
-.3000
CP
5.00
6.00
7.00
8.00
9.00
10.00
11.00
12.00
13.00
X/D

FIGURE 9

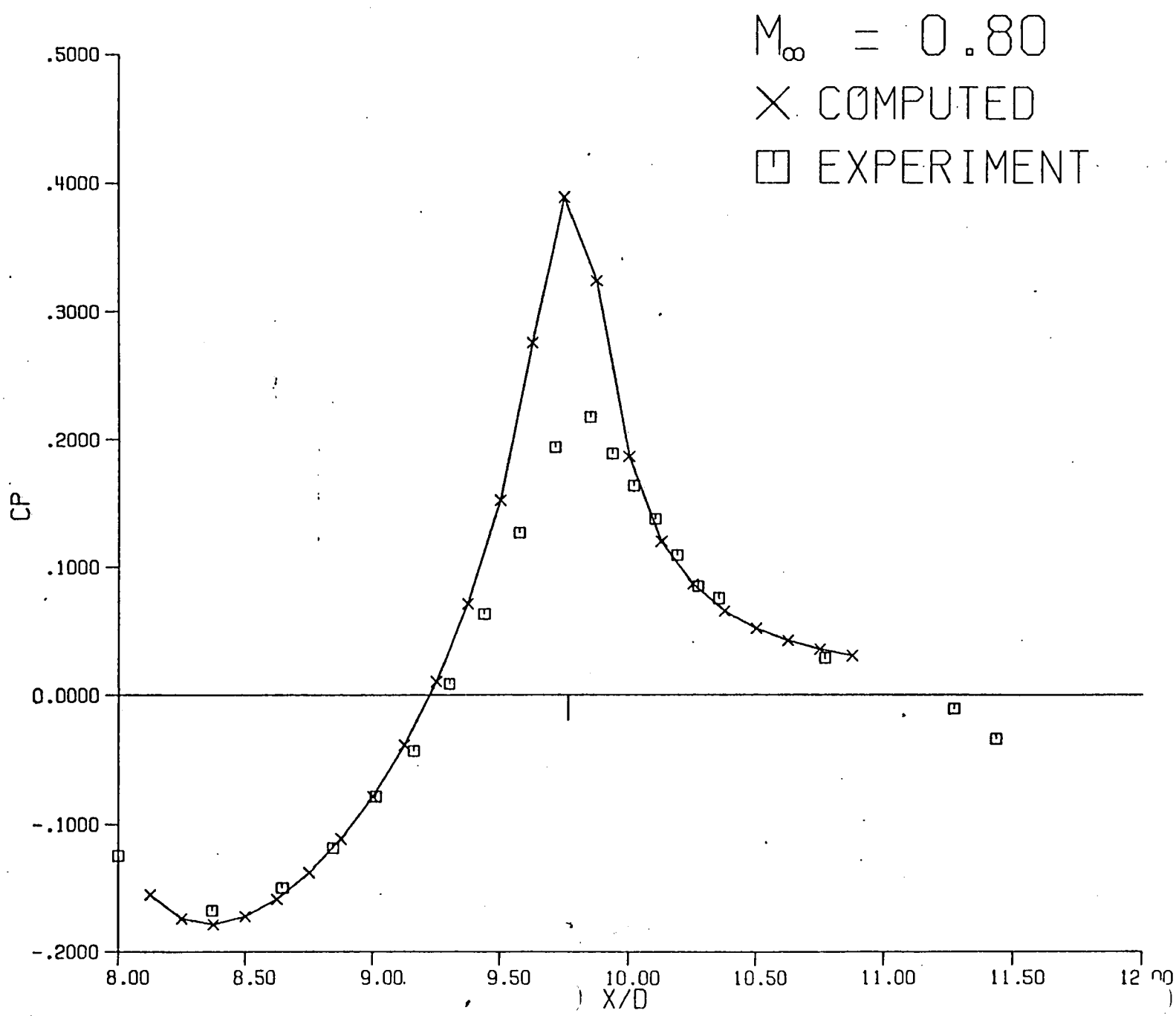
$M_\infty = 0.80$
X COMPUTED
□ EXPERIMENT
.5000
.4000
.3000
.2000
.1000
0.0000
-.1000
-.2000
CP
8.00
8.50
9.00
9.50
10.00
10.50
11.00
11.50
12.00
X/D

440

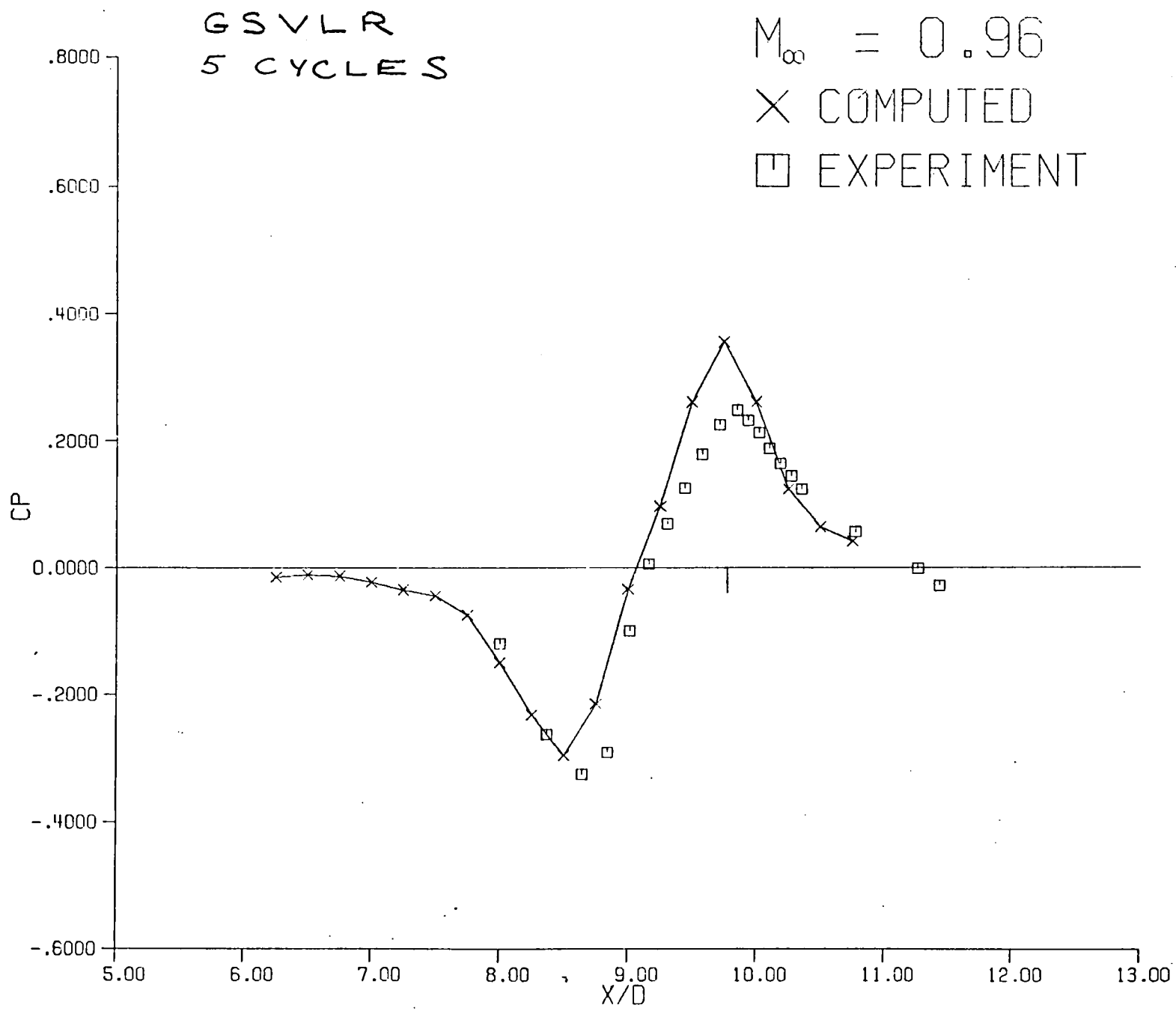
GSVLR
5 CYCLES
M_∞ = 0.96
X COMPUTED
EXPERIMENT
.8000
.6000
.4000
.2000
0.0000
-.2000
-.4000
-.6000
CP
5.00
6.00
7.00
8.00
9.00
10.00
11.00
12.00
13.00
X/D

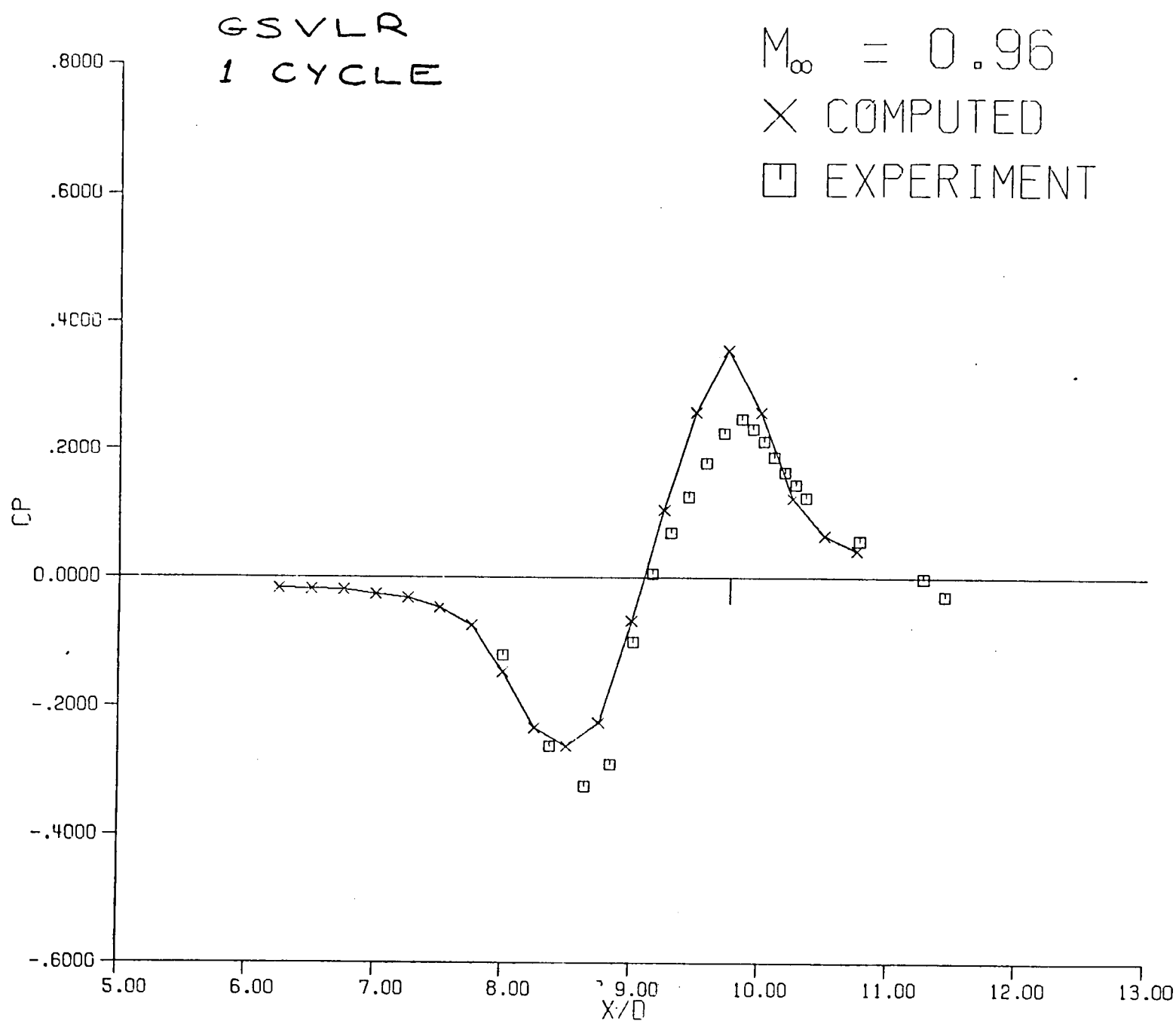
GSVLR
1 CYCLE
M_∞ = 0.96
X COMPUTED
EXPERIMENT
.8000
.6000
.4000
.2000
0.0000
-.2000
-.4000
-.6000
CP
5.00
6.00
7.00
8.00
9.00
10.00
11.00
12.00
13.00
X/D

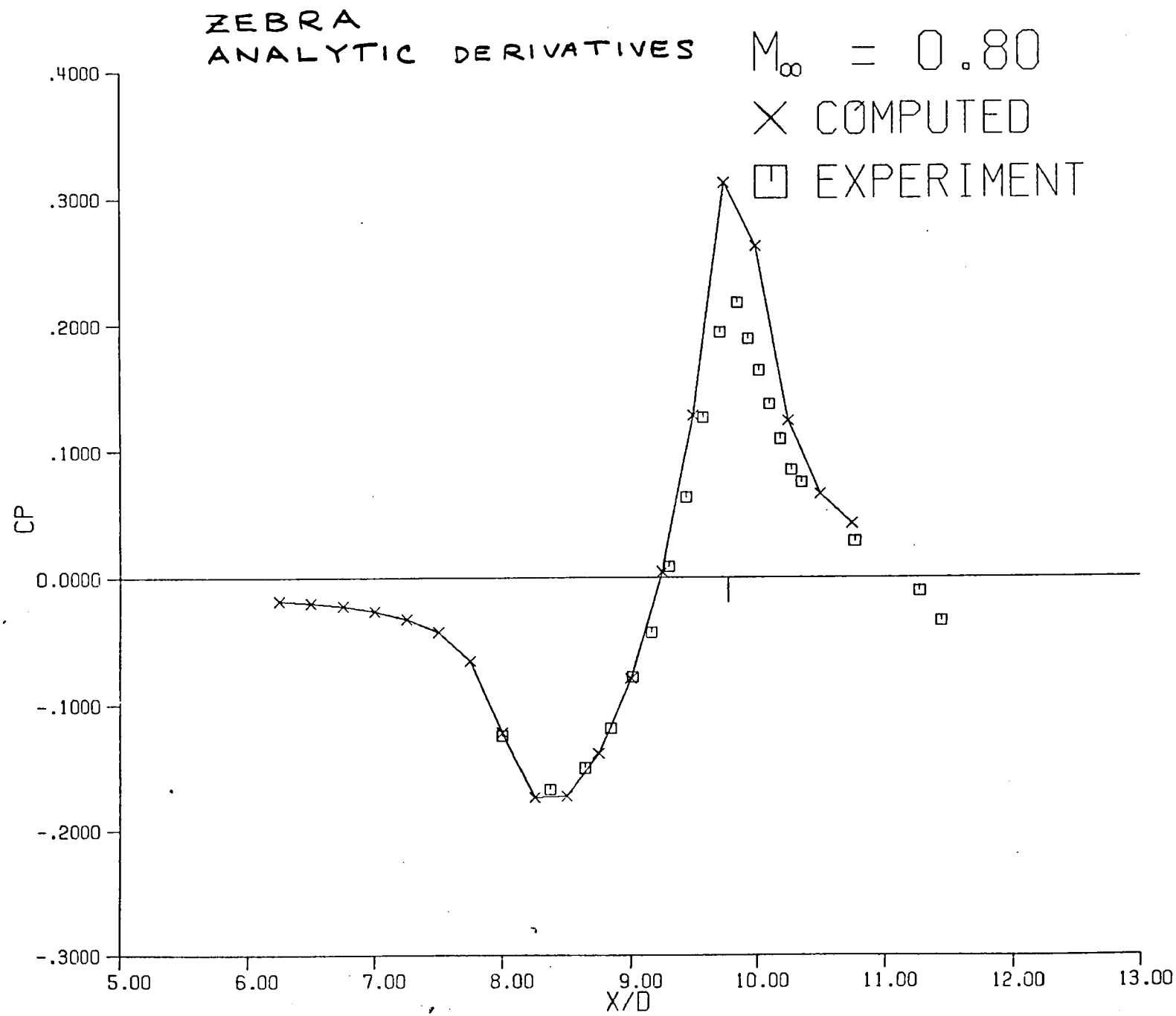
ZEBRA
ANALYTIC DERIVATIVES
$M_\infty = 0.80$
COMPUTED
EXPERIMENT
.4000
.3000
.2000
.1000
0.0000
-.1000
-.2000
-.3000
CP
5.00
6.00
7.00
8.00
9.00
10.00
11.00
12.00
13.00
X/D

(17)

Progress Report

Computational Methods for Vortex Dominated Compressible Flows

NASA Grant NAG-1-358

Principal Investigator

Earll M. Murman

Department of Aeronautics & Astronautics

Massachusetts Institute of Technology

October 19, 1983

MURMAN

445

Objective of Research

To investigate and understand

- structure of vortex dominated compressible flow
- numerical methods used to predict these flows

Activities to date

- Grant initiated April 1, 1983
- Attended AGARD Meeting on "Aerodynamics of Vortical Type Flows in Three Dimensions" - April 1983
- Background reading & planing - summer 1983
- Initiated active work - Sept 15, 1983

SESSION I – FUNDAMENTALS, GENERATION AND STRUCTURE OF VORTICAL FLOWS

ON ISSUES CONCERNING FLOW SEPARATION AND VORTICAL FLOWS IN THREE DIMENSIONS
by D.J.Peake and M.Tobak 1

THE VORTEX SKELETON MODEL FOR THREE-DIMENSIONAL STEADY FLOWS
by H.G.Hornung 2

ON THE STRUCTURE OF THE TURBULENT VORTEX
by L.Roberts 3

INSTABILITIES IN TRAILING VORTICES: FLOW VISUALISATION USING HOT-WIRE ANEMOMETRY
by C.Strange and J.K.Harvey 4

INTERACTION ENTRE UNE ONDE DE CHOC ET UNE STRUCTURE TOURBILLONNAIRE ENROULEE
par J.Delery et E.Horowitz 5

ON THE GENERATION AND SUBSEQUENT DEVELOPMENT OF SPIRAL VORTEX FLOW OVER A SWEPT-BACK WING
by D.E.A.Poll 6

AN EXPERIMENTAL INVESTIGATION OF THE VORTEX FLOW OVER DELTA AND DOUBLE-DELTA WINGS AT LOW SPEED
by N.G.Verhaagen 7

VISUALISATION DES ECOULEMENTS TOURBILLONNAIRES TRIDIMENSIONNELS
par H.Werle 8

LASER VELOCIMETRY STUDY OF COMPRESSIBILITY EFFECTS ON THE FLOW FIELD OF A DELTA WING
by G.Vorropoulos and J.F.Wendt 9

SESSION II – INTERACTION OF VORTICAL FLOW WITH SURFACES

RECENT STUDIES AT NASA-LANGLEY OF VORTICAL FLOWS INTERACTING WITH NEIGHBORING SURFACES
by J.E.Lamar and J.F.Campbell 10

EXPERIMENTAL INVESTIGATION OF FOREBODY AND WING LEADING EDGE VORTEX INTERACTIONS AT HIGH ANGLES OF ATTACK
by G.E.Erickson and W.P.Gilbert 11

SOME RESULTS FROM A PROGRAMME OF RESEARCH INTO THE STRUCTURE OF VORTEX FLOW FIELDS AROUND MISSILE SHAPES
by F.Byrom, A.Petersen and S.T.Kitson 12

PREDICTING AERODYNAMIC CHARACTERISTICS OF VORTICAL FLOWS ON THREE-DIMENSIONAL CONFIGURATIONS USING A SURFACE-SINGULARITY PANEL METHOD
by B.Maskew 13

SEPARATION AND VORTICAL TYPE FLOW AROUND A PROLATE SPHEROID – EVALUATION OF RELEVANT PARAMETERS
by H.Vollmers, H.P.Kreplin and H.U.Meier 14

ON THE GENERATION OF VORTICAL FLOWS AT HYPERSONIC SPEEDS OVER ELLIPTICAL CONES
by P.Evangelou 15

VISCOUS THREE-DIMENSIONAL FLOW SEPARATION FROM HIGH-WING PROPELLER TURBINE NACELLE MODELS
by R.H.Wickens 16

Papers in AGARD CP-342, April 1983

SESSION III – MODELLING AND COMPUTING

THEORETICAL MODELLING OF THREE-DIMENSIONAL VORTEX FLOWS IN AERODYNAMICS
by J.H.B.Smith 17

COMPUTATIONAL VORTEX FLOW AERODYNAMICS
by H.W.M.Hoeijmakers 18

VORTEX FLOW SIMULATIONS PAST WINGS USING THE EULER EQUATIONS
by C.Weiland 19

SIMULATION D'ECOULEMENTS TURBULENTS PAR UNE METHODE DE TOURBILLONS PONCTUELS
par S.Huberson 20

NUMERICAL SOLUTIONS OF THE EULER EQUATIONS SIMULATING VORTEX FLOWS AROUND WINGS
by A.Rizzi, L-E.Eriksson, W.Schmidt and S.Hitzel 21

THE TREATMENT OF CONVECTED VORTICES IN COMPRESSIBLE POTENTIAL FLOW
by J.Steinhoff, K.Ramachandran and K.Suryanarayanan 22

SESSION IV – STABILITY AND BREAKDOWN OF VORTICAL FLOWS

VORTEX STABILITY AND BREAKDOWN
by S.Leibovich 23

THE BREAK-UP MECHANISM OF A STREAMWISE DIRECTED VORTEX
by L.N.Persen 24

VORTEX BREAKDOWN: A TWO-STAGE TRANSITION
by M.P.Escudier and J.J.Keller 25

A CONTRIBUTION TO THE PROBLEM OF VORTEX BREAKDOWN
by E.Krause 26

NUMERICAL SIMULATION OF VORTEX BREAKDOWN BY THE VORTEX FILAMENT METHOD
by Y.Nakamura, A.Leonard and P.R.Spalart 27

ETUDES EXPERIMENTALES D'ECOULEMENTS TOURBILLONNAIRES SOUMIS A DES EFFETS DE GRADIENT DE PRESSION ADVERSE
par J.L.Solignac et O.Leuchter 28

WAVES ON VORTEX CORES AND THEIR RELATION TO VORTEX BREAKDOWN
by T.Maxworthy, M.Mory and E.J.Hopfinger 29

SESSION V – CONTROL AND EXPLOITATION OF VORTICAL FLOWS

VORTICAL FLOW MANAGEMENT FOR IMPROVED CONFIGURATION AERODYNAMICS – RECENT EXPERIENCES
by D.M.Rao 30

THE EFFECTS OF WING TIP DEVICES ON THE PERFORMANCE OF THE B.Ae JETSTREAM
by J.J.Spillman and M.J.Bell 31A

THE EFFECT OF WING TIP DEVICES ON THE FAR-FIELD WAKE OF A PARIS AIRCRAFT
by J.J.Spillman 31B

BOUNDARY LAYER SEGMENTATION ON SHARP HIGHLY SWEPT LOADING EDGES AND ITS EFFECTS ON SECONDARY VORTICES
by A.Baron and S.de Ponte 32

AUGMENTATION OF FIGHTER AIRCRAFT PERFORMANCE BY SPANWISE BLOWING OVER THE WING LEADING EDGE
by A.Segner and M.Salomon 33

ROUND TABLE DISCUSSION RTD

Numerical Methods for 3-D Compressible Vortical Flows.

Potential Methods

- Panel or Boundary Integral
  Extensive Incompressible Vortex Flows.
  Maybe extendable to compressible flows using Boeing/Ames ideas

- Finite Volume
  Shock generated vorticity (Hafez & Lovell, Klopfer & Nixon, Grossman)
  Shed Vortex Wakes (Steinhoff, et. al)

  Extension of existing potential flow codes, less storage than Euler
  Analysis & numerical methods more difficult
  Hard to extend to viscous flow.

Euler Equations

- Pseudo time marching method
  3D delta, arrow, trapezodial wings (Rizzi, Eriksson, Schmidt, Hitzel)
- Space marching
  Delta wing (Weilderd), Cones (Marconi), missiles (Klopfer et al)

- Vortex flows captured using finite volume method
- Effects of artifical & physical viscosity not well understood.

Navier-Stokes

- Needed for Viscous Dominated Flows.

Classes of 3D Problems

- Subsonic or Supersonic

  Freestream Mach Number $M_\infty \lessgtr 1 \Rightarrow$ Outer B.C.
  Streamwise Mach Number $M_s \gtrless 1 \Rightarrow$ Space Marching vs Time Marching
  Mach Number normal to L.E. $M_n \gtrless 1 \Rightarrow$ Flow Structure

- Body Geometry

  Conical or Non conical $\Rightarrow$ Conical flow approximation valid for $M_\infty > 1$; $M_\infty < 1$ slender body

  Sharp leading edge $\Rightarrow$ separation point fixed by geometry

  Round leading edge $\Rightarrow$ separation point fixed by viscous effects empirical Kutta cond. or N.S.
  - wing like geometries (ellipses)
  - body like geometries (cones)

  Real geometries wing - body - $\begin{matrix}\text{canard}\\ \text{tail}\end{matrix}$ - inlet

- Viscous Dominated vs Inviscid Dominated Free Vortex Flows
- Vortex Bursting.

Issues

Methods - Can the Euler Eqns. be used to model vortex flows? - Yes

- Can the modified potential eqns be used to model vortex flows? - Probably yes.
- Maybe 3D stream function methods

Flow Structures

- Lots of investigations of topology (kinematics)
- Don't understand too well possible vortex & shock type flows.

Viscosity

- What is role of artificial viscosity vs physical viscosity?

  creation of vorticity

  shedding of vorticity (Kutta condition, separation)

  convection of vorticity - diffusion

  bursting

Uniqueness ?
Steady ?

Experiments - Not much comparison with data.

Results fair but not perfect.

SHARP L.E. DELTA WING FLOW REGIMES

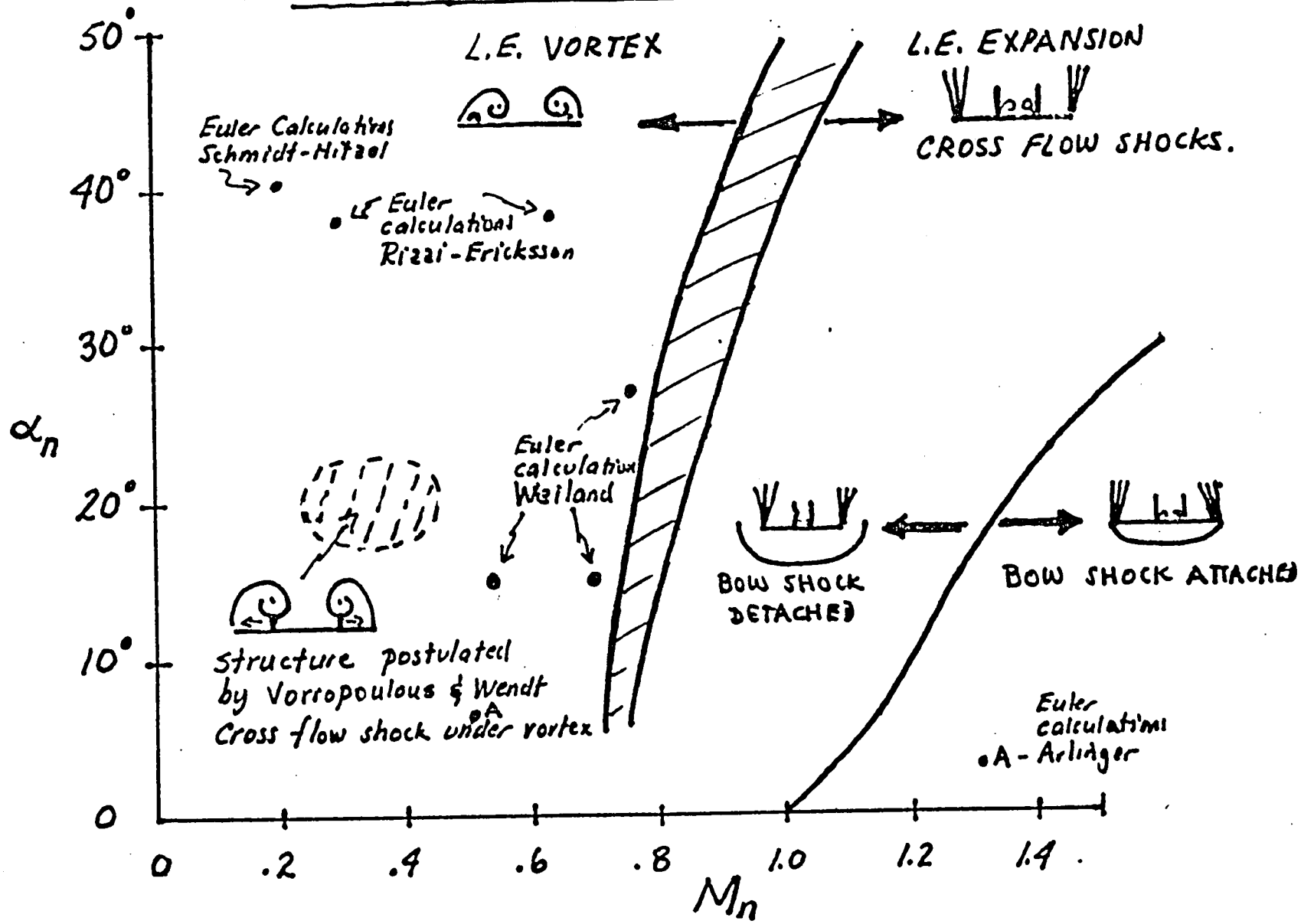

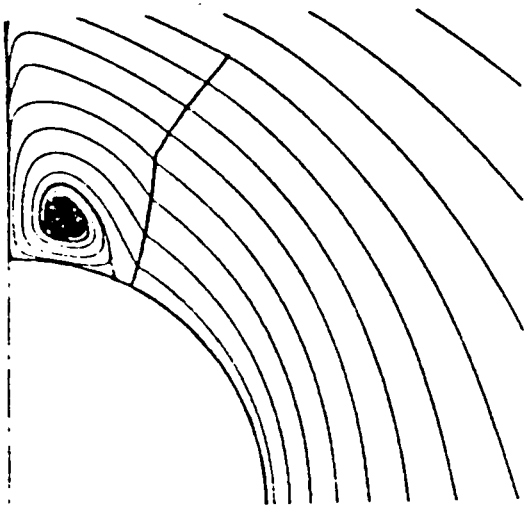

Fig. 13 Cross Flow Streamlines Near Lee Plane ($M_\infty = 3, \delta = 9.46°, \alpha = 25°$)

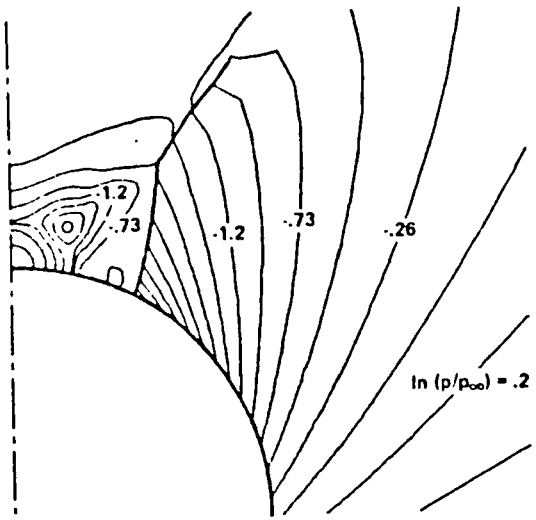

Fig. 14 Isobars Near Lee Plane ($M_\infty = 3, \delta = 9.46°, \alpha = 25°$)

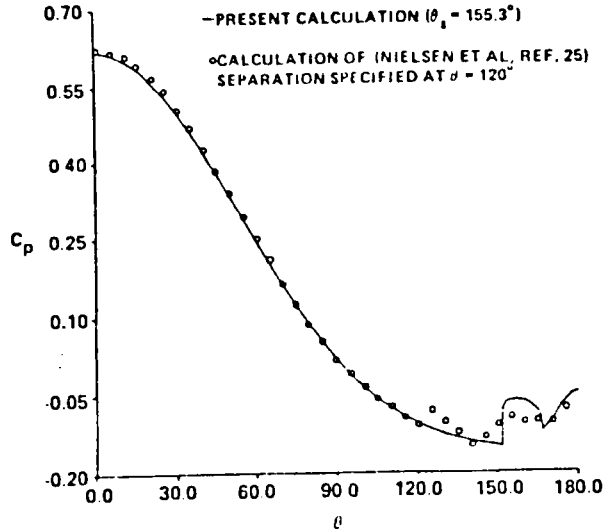

Fig. 15 Surface Pressure Comparison ($M_\infty = 3, \delta = 9.46°, \alpha = 25°$)

Results of Marconi (AIAA Paper 83-1665, July 1983) showing shock wave under vortex.

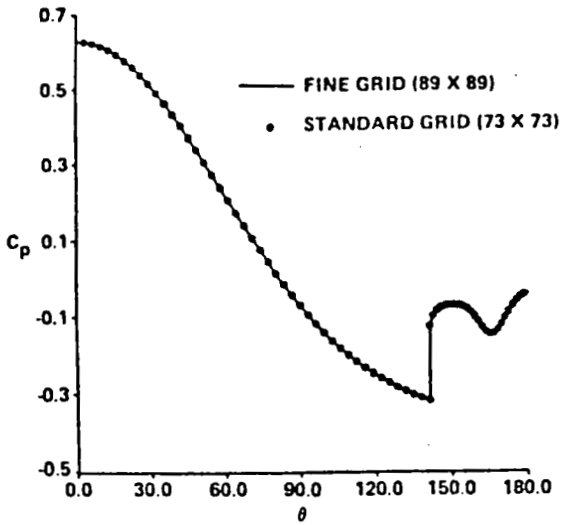

Fig. 3 Comparison of Computation with Two Grids, Surface Pressure ($M_\infty = 2, \delta = 10°, \alpha = 25°$)

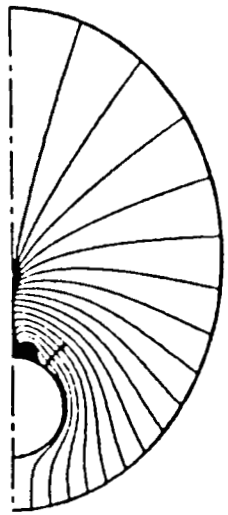

Fig. 4 Cross Flow Streamlines in Field ($M_\infty = 2, \delta = 10°, \alpha = 25°$)

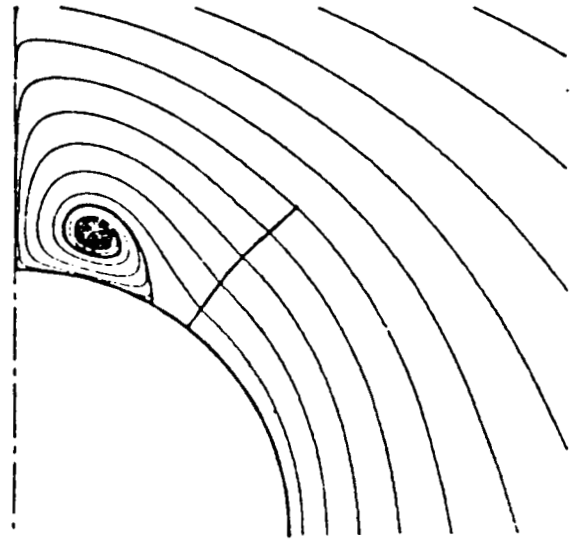

Fig. 5 Cross Flow Streamlines Near Lee Plane ($M_\infty = 2, \delta = 10°, \alpha = 25°$)

Results of Marconi (AIAA Paper 83-1665) showing separation and vortex formed by shock generated vorticity. - Conical flow Euler calculation.

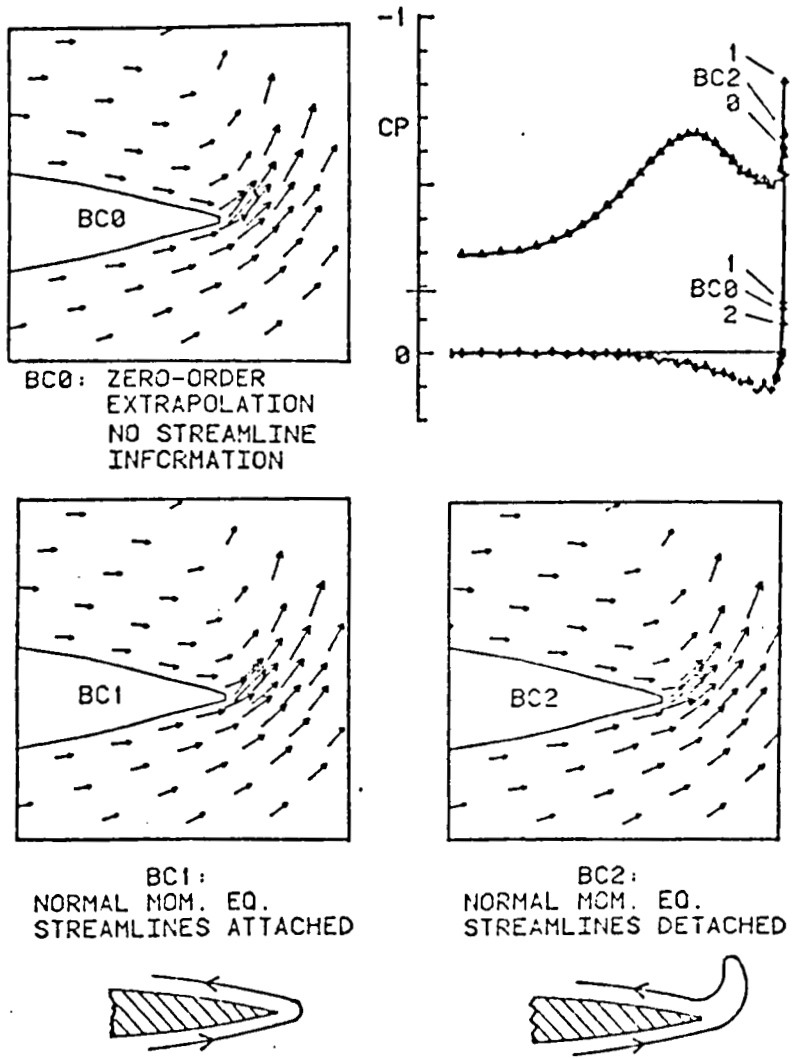

FIG. 9 DEMONSTRATION THAT A KUTTA CONDITION IS INESSENTIAL FOR THE COMPUTATION OF SEPARATED FLOW. 85% SECTION DELTA WING $M_\infty = 0.9$ $\alpha = 15°$

Rizzi & Eriksson - IV · CANM Conf. Oct. 81

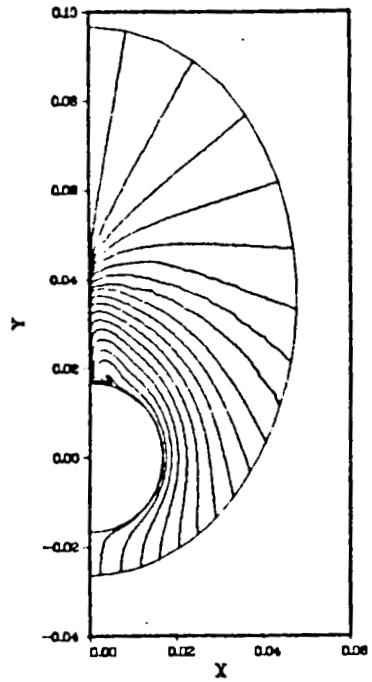

Figure 5.- Conical streamlines from Euler solution for cone without the Kutta condition imposed

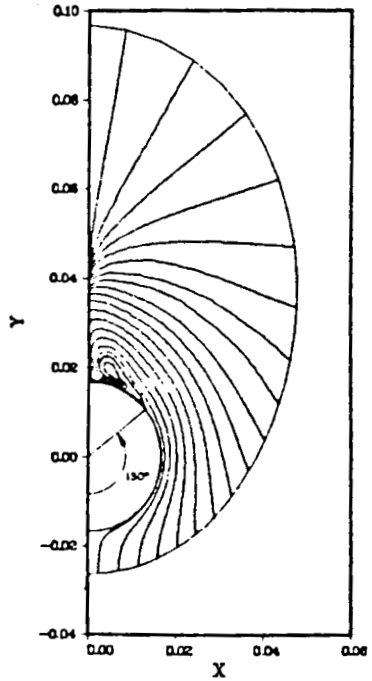

Figure 7.- Conical streamlines from Euler solution for cone with kutta condition imposed

Klopfer, Kuhn, & Nielsen (AIAA Paper 83-0460 Jan 83)

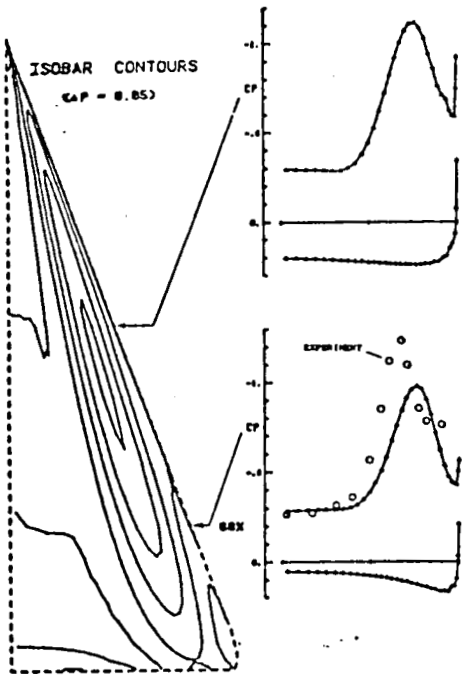

Fig. 12

Imprint of computed pressure trough given by isobar contours on wing surface together with two spanwise section plots of C_p of which one (80% chord) is compared with experimental values (FFA Report AU-295) M_∞=0.7 α=15°. Delta wing.

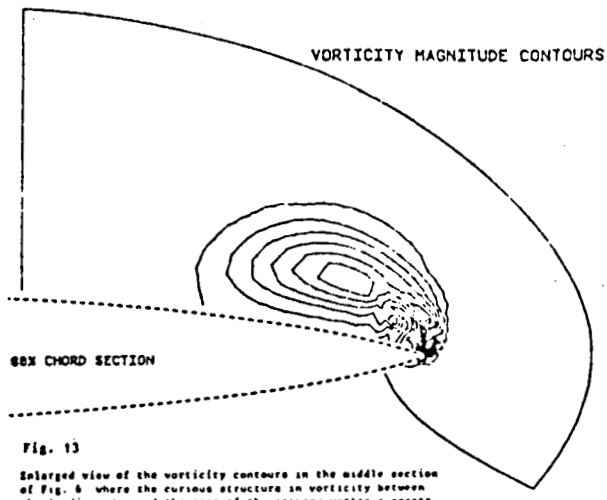

Fig. 13

Enlarged view of the vorticity contours in the middle section of Fig. 6 where the curious structure in vorticity between the leading edge and the core of the primary vortex suggests the presence of a secondary vortex. M_∞=0.7 α=15°.

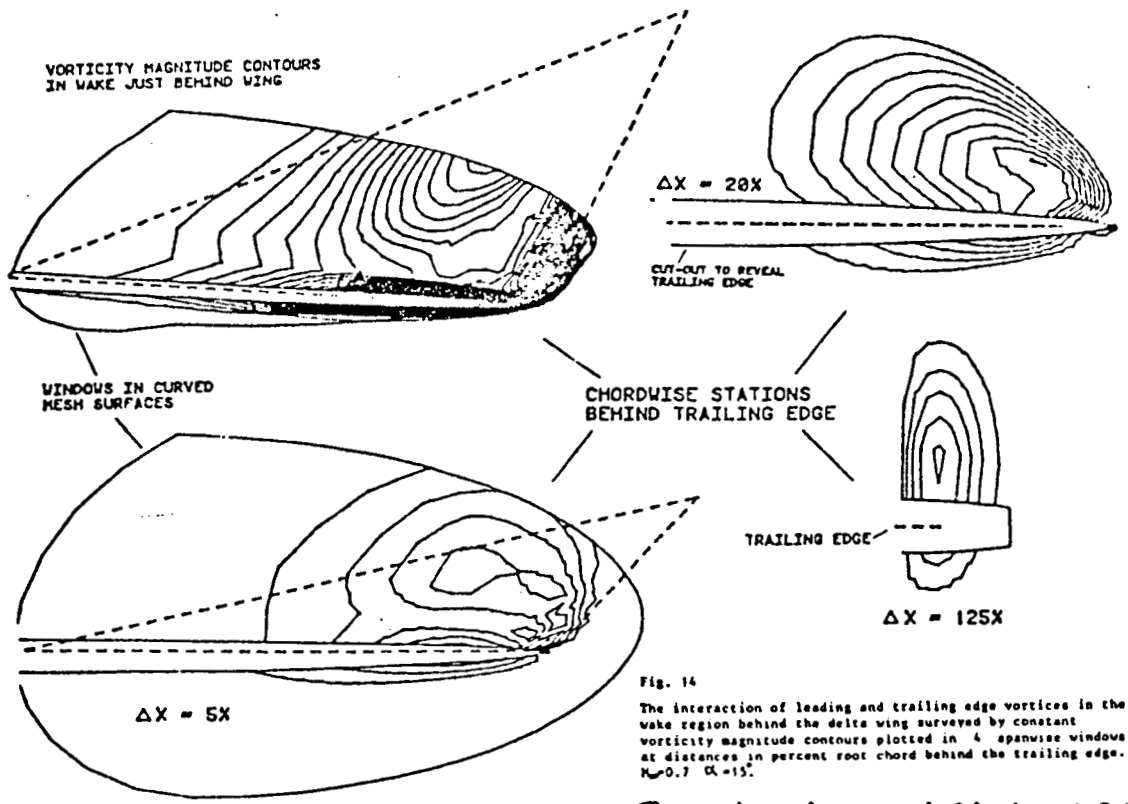

Fig. 14

The interaction of leading and trailing edge vortices in the wake region behind the delta wing surveyed by constant vorticity magnitude contours plotted in 4 spanwise windows at distances in percent root chord behind the trailing edge. M_∞=0.7 α=15°.

Rizzi, et al AGARD CP 342

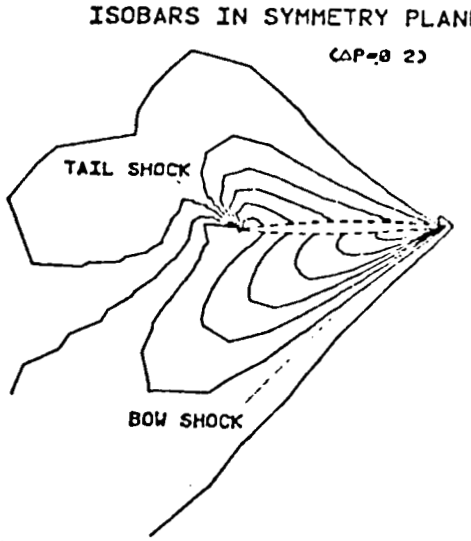

Fig. 17

Contours of isobars in the plane of symmetry of the delta wing showing the compression regions of the bow and tail shocks. M_∞=1.5 α=15°. Sweep 70°.

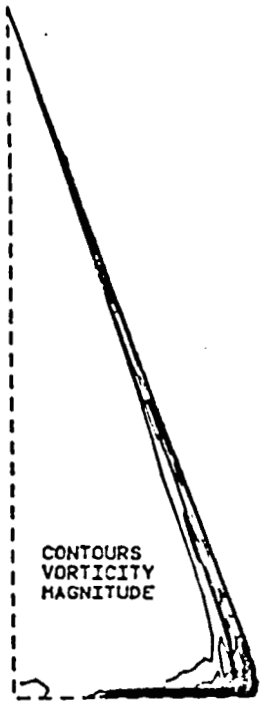

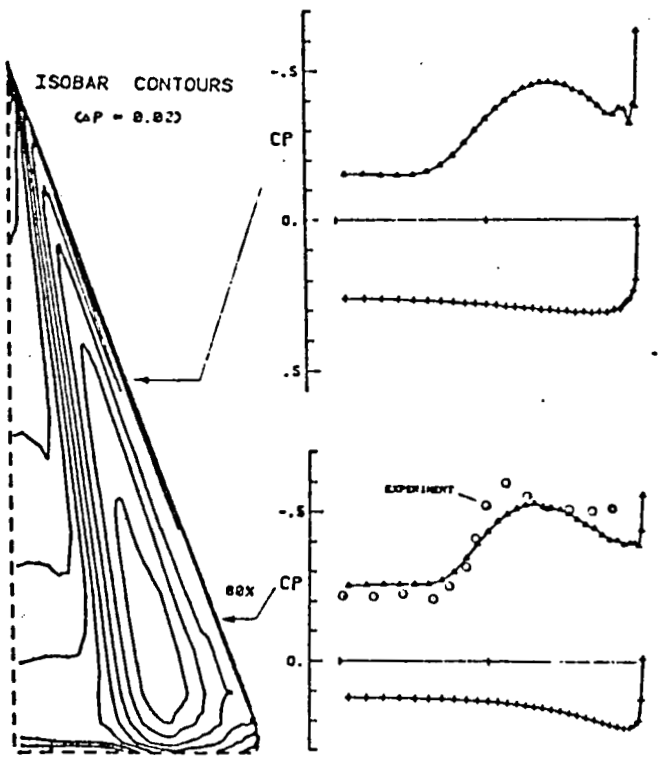

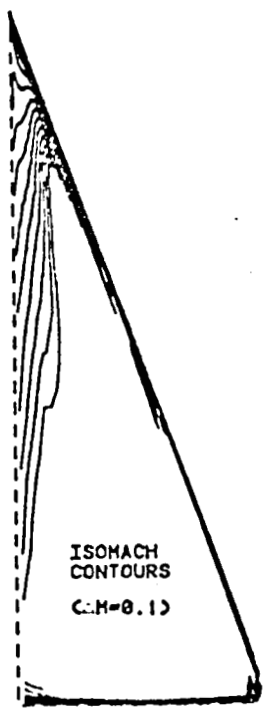

Fig. 18

Contours of constant vorticity magnitude, Mach number, and isobars on the wing surface together with two spanwise section plots of c_p of which one (80%) is compared with experimental values (FFA Report AU-295) M =1.5 α=15°. Delta wing.

Rizzi, Eriksson, Schmidt, Hitzel - AGARD CP 342

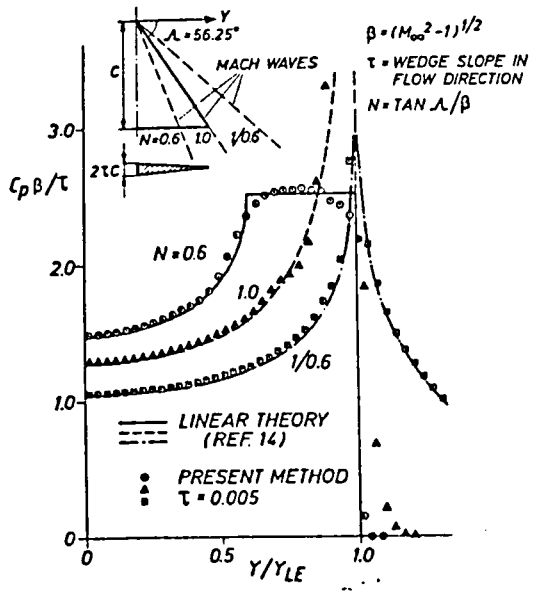

Fig 7. Pressure coefficient parameter for single-wedge delta at α=0

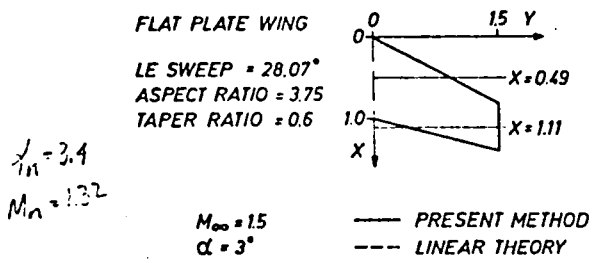

$\gamma_{in} = 3.4$
$M_n = 1.32$

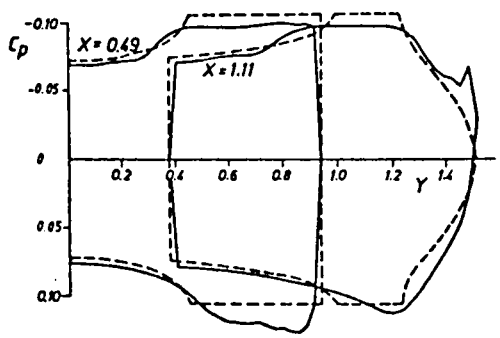

Fig 8. Spanwise pressure distributions for thin swept wing

$d_n = 17°$
$M_n = .715$

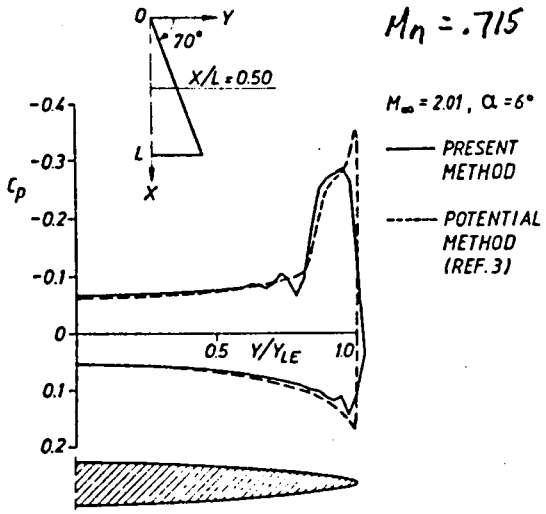

Fig 9. Calculated cross flow pressure distribution at x/L=0.5 on delta wing

$M_n = .5$ $d_n = 5.8°$

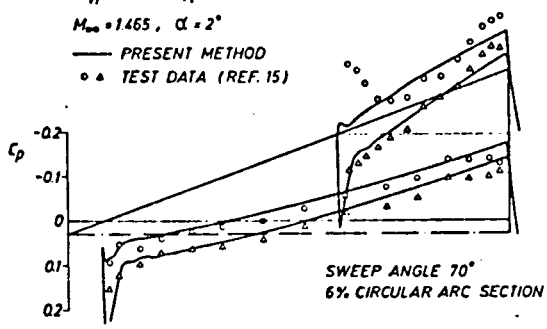

Fig 10. Calculated and experimental pressure distributions for delta wing

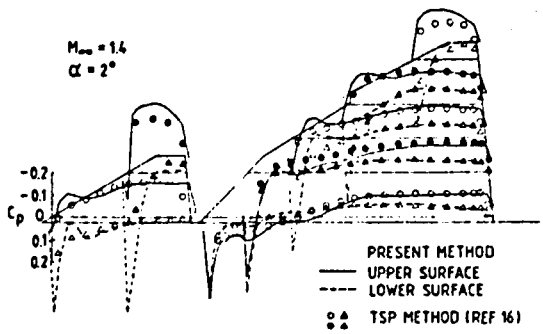

Fig 11. Calculated pressure distribution for canard configuration

Plans for next year's research

- Conical flow model $M_\infty > 1$ $M_n, M_s \geq 1$
  - better resolution & simpler than full 3D
  - complements 3D studies elsewhere
- Euler equation model
  - Pseudo time finite volume method
  - Mainstream interest now, methods developing rapidly
- Sharp leading edge geometries
  - separation point fixed
- Investigate role of numerical viscosity on results.
  - Capture Vortex - effect of grid resolution / grid embedding
    - effect of artificial viscosity parameter
  - Fit Vortex - companion study supported by CFD training grant
- Investigate types of flow structure.

  $0 < M_n \leq 1.5$ $0 < \delta_n \leq 50°$

- Comparison with experiments. (?)

(18)

ENTROPY EFFECTS AND SHOCK FITTING IN CONICAL SUPERSONIC FULL POTENTIAL FLOWS

M.J. SICLARI
GRUMMAN AEROSPACE CORPORATION
BETHPAGE, NY 11714

GRUMMAN

1773-001D

SICLARI

GRUMMAN SUPERSONIC NONLINEAR FULL POTENTIAL TECHNOLOGY

HISTORICAL PERSPECTIVE

- COREL (Grossman/1978)
  - Conical Flows
  - Shocks captured (Nonconservative)
- NCOREL (Grossman & Siclari/1980)
  - Nonconical flows (nonconservative)
  - Bow shock fit (Siclari/1981)
    - Isentropic conservative
  - Subsonic Regions (Siclari/1981)
    - Transonic total Mach numbers
    - Conical flows (implicit)
    - Axisymmetric flows
- APPLICATIONS (Siclari/1982)
  - Arbitrary bodies
  - Wings
  - Wing-body

ENGINEERING DERIVATIVE APPLICATIONS

- CONCEPTUAL WING DESIGN (Mason/1979)
  - NASA/Grumman
  - SC3 concept
  - Shockless high lift ($C_L \sim 0.40$)
- DEMONSTRATION WING (Mason/1982)
  - NASA/Grumman
  - Fighter planform/Supersonic maneuver
  - High lift/attached flow
- ATF STUDIES (Meyer/Mason)
  - Future fighter wing design
- MISSILE TECHNOLOGY
  - Supersonic hybrid code (Laiosa & Boppe/1983)
  - NASA (Pittman)

GRUMMAN

GRUMMAN CURRENT DEVELOPMENTS

- NCOREL
  - Computational efficiency
    - Approximate factorization (Siclari/1982)
    - Cut CPU by factor of three (fine meshes)
  - Improve wing-body computations — wake
  - Wing-body-canard computations
- CORELF
  - New conical flow code
  - Fits both bow and crossflow shocks implicitly
  - Fully conservative
- ENTROPY EFFECTS (NCORELS, CORELFS)
  - Extend accuracy of full potential equation to include large entropy flows (High Mach number/ large deflections)
  - Rankine-Hugoniot fitted shocks
  - Approximate pressure-entropy streamline model

APPROXIMATE FACTORIZATION

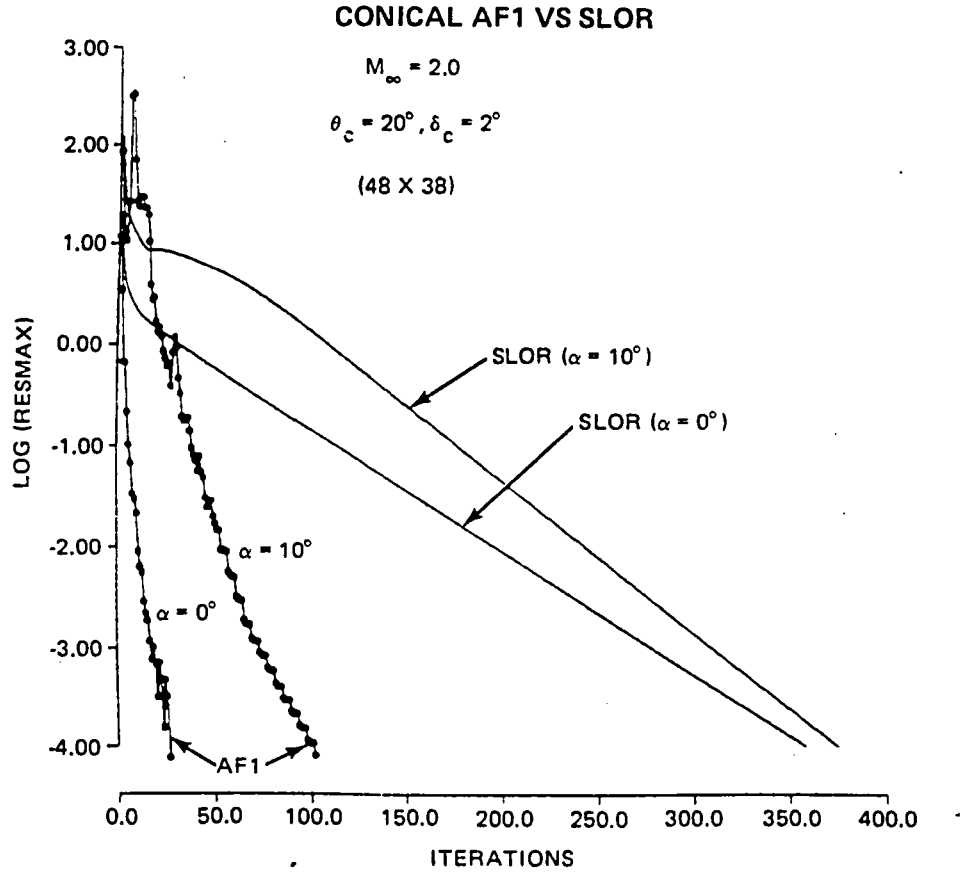

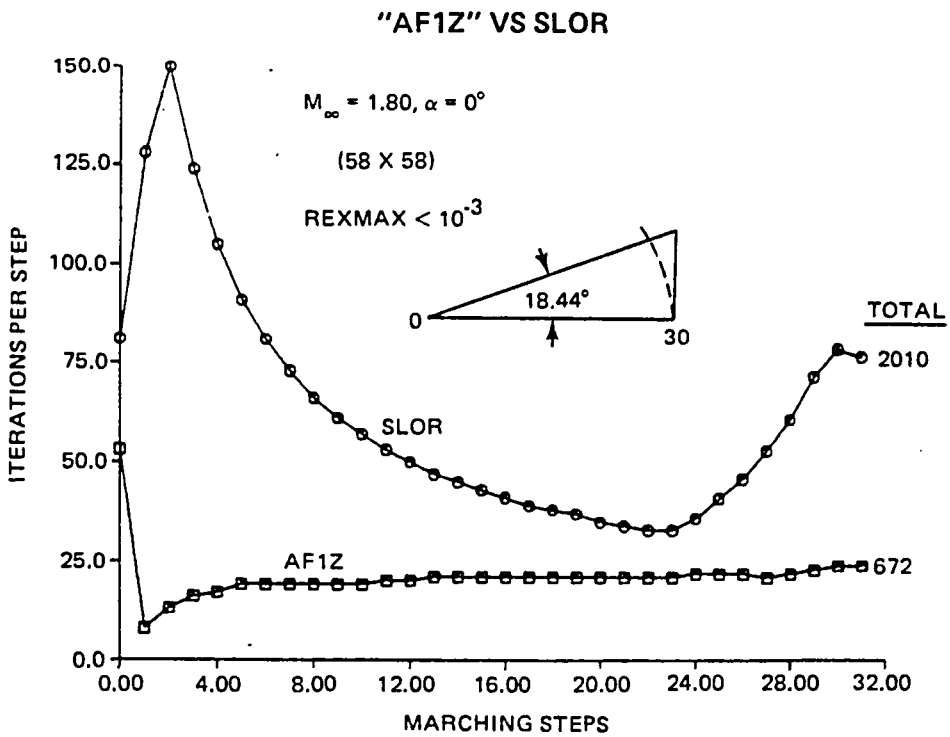

SQUIRE WING COMPUTATION
AIAA-83-0376

GRUMMAN

NCOREL APPLICATIONS

GRUMMAN

GRUMMAN/NASA CONICAL WING (SC3) CONCEPT, $C_L \sim 0.40$

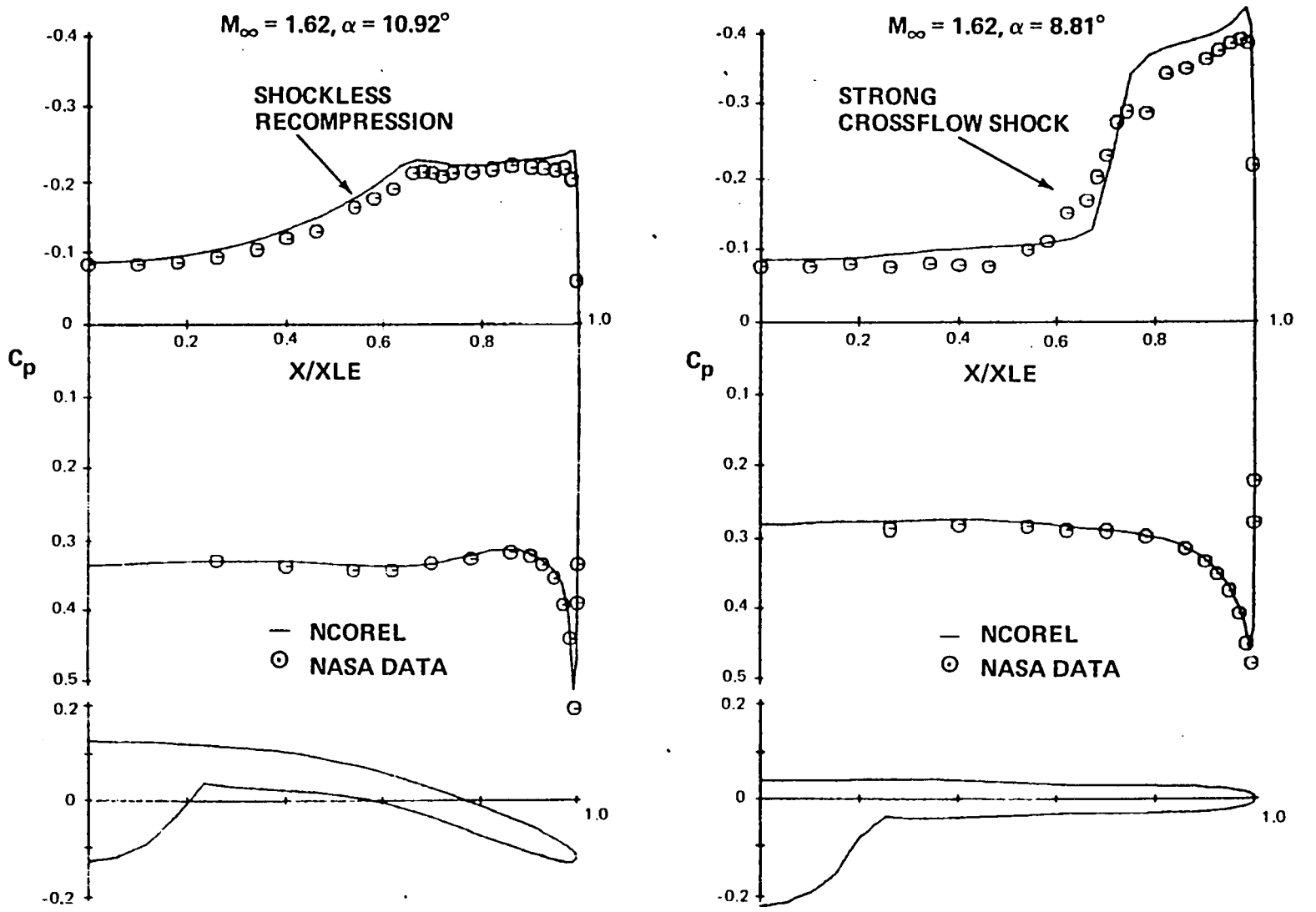

AIAA 80-1421

GRUMMAN

1773-022D

CONICAL SOLUTIONS (BSF)

EMBEDDED SUBSONIC TOTAL MACH NUMBER REGIONS

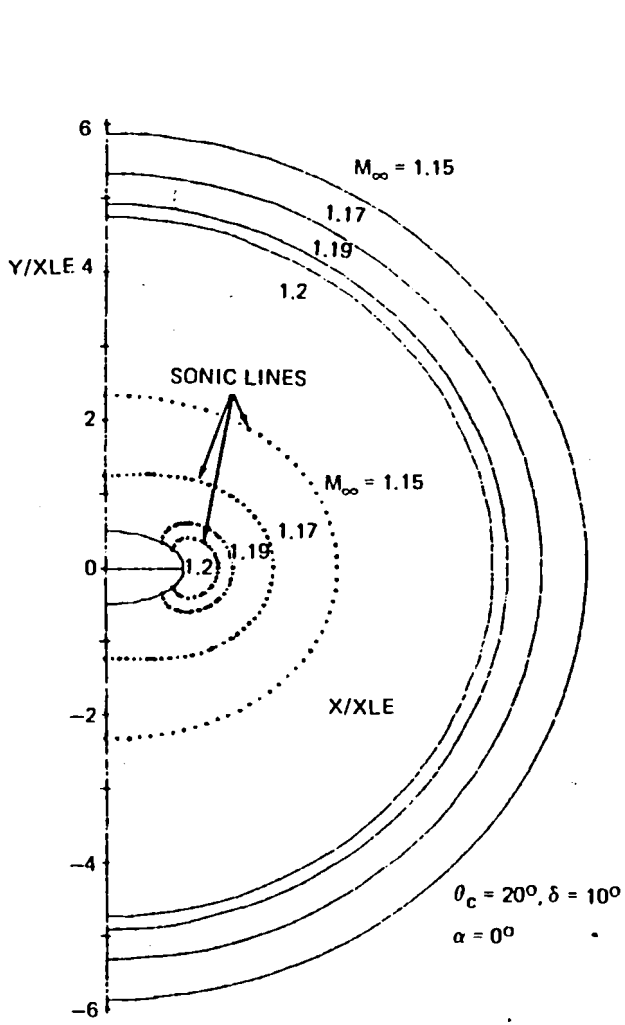

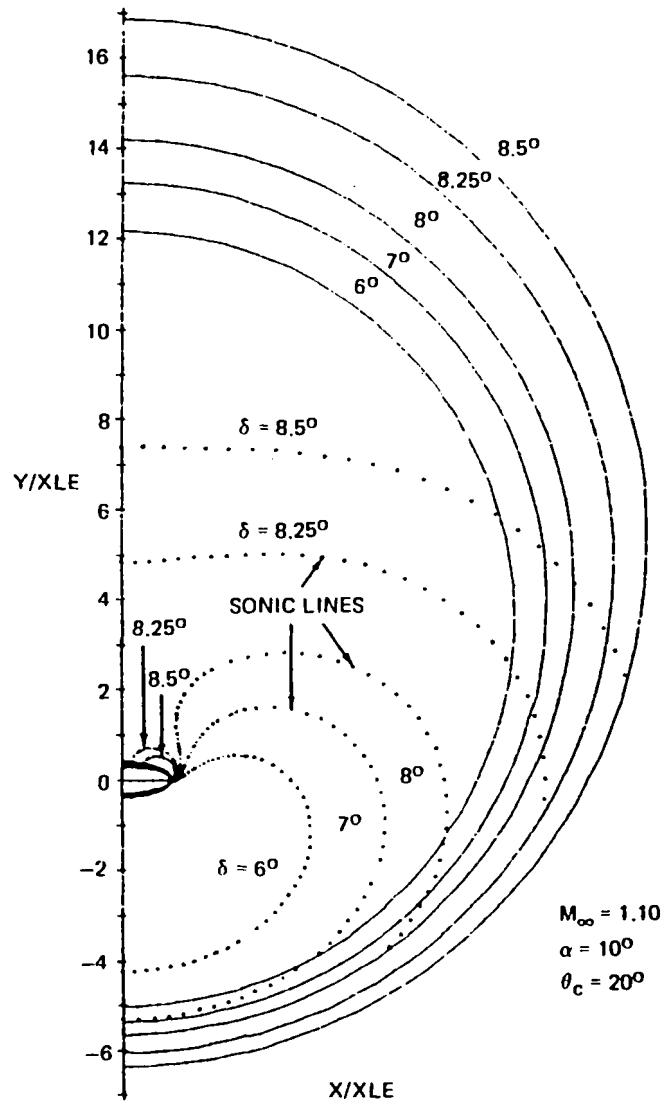

AIAA 81-1262

GRUMMAN

1773-023D

AXISYMMETRIC SOLUTIONS (BSF) SUBSONIC TOTAL MACH NUMBER REGIONS

BOW SHOCK AND MACH NUMBER CONTOURS

TRANSONIC CONE

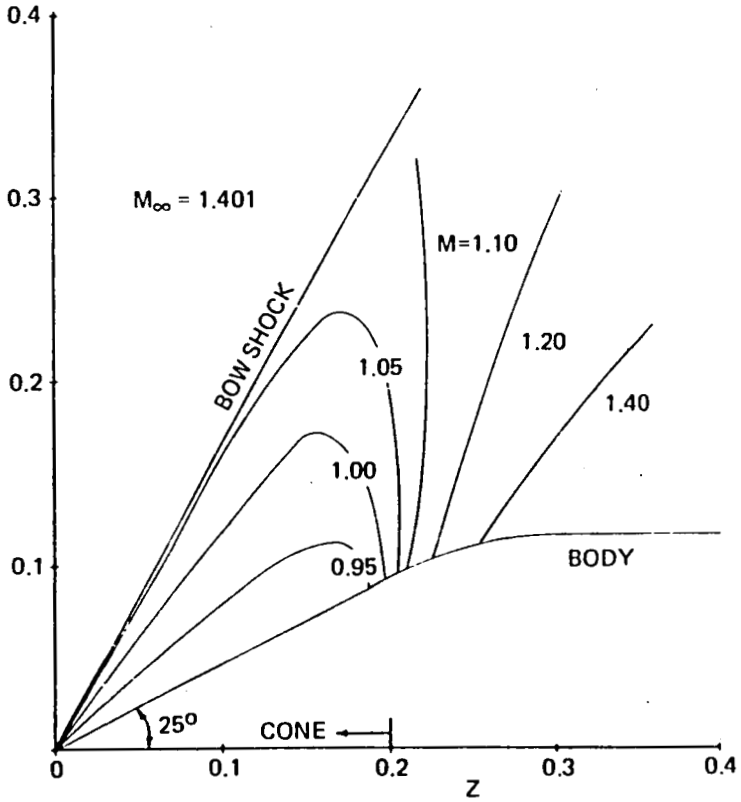

COMPRESSION SURFACE

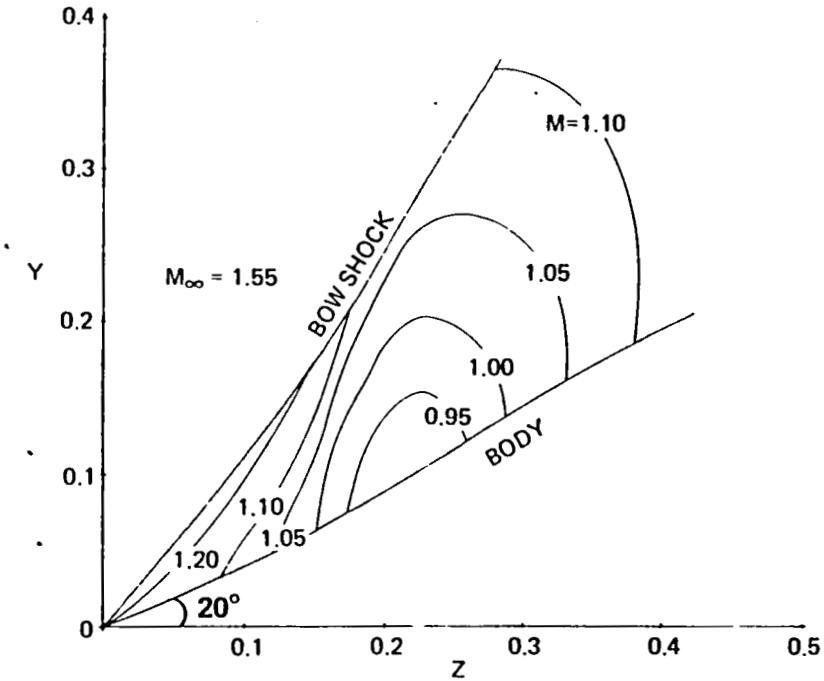

AIAA 81-1202

GRUMMAN

1773-024D

NCOREL ARBITRARY BODY CAPABILITY

α =10.35°

M_∞=1.70

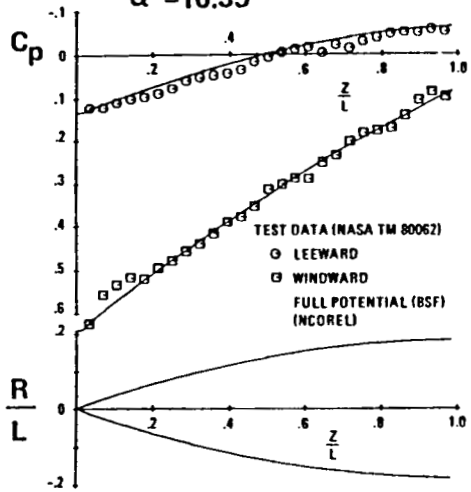

WINDWARD AND LEEWARD AXIAL DISTRIBUTION OF PRESSURE

α =5.01°

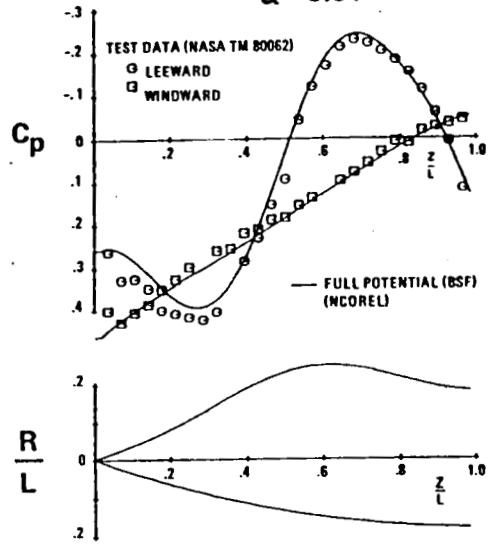

WINDWARD AND LEEWARD AXIAL DISTRIBUTION OF PRESSURE

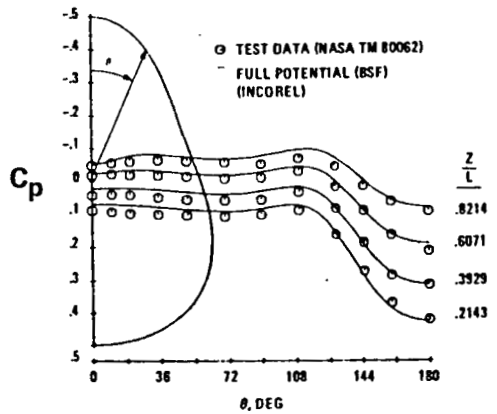

DETAILED AZIMUTHAL DISTRIBUTIONS OF PRESSURE AT SEVERAL AXIAL LOCATIONS

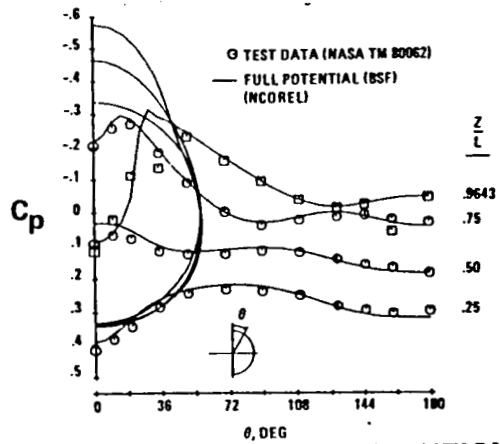

COMPARISON OF AZIMUTHAL DISTRIBUTIONS OF PRESSURE AT SEVERAL AXIAL STATIONS

GRUMMAN

AIAA 82-0167

ZERO LIFT WAVE DRAG PREDICTIONS
"SQUIRE DELTA WING"

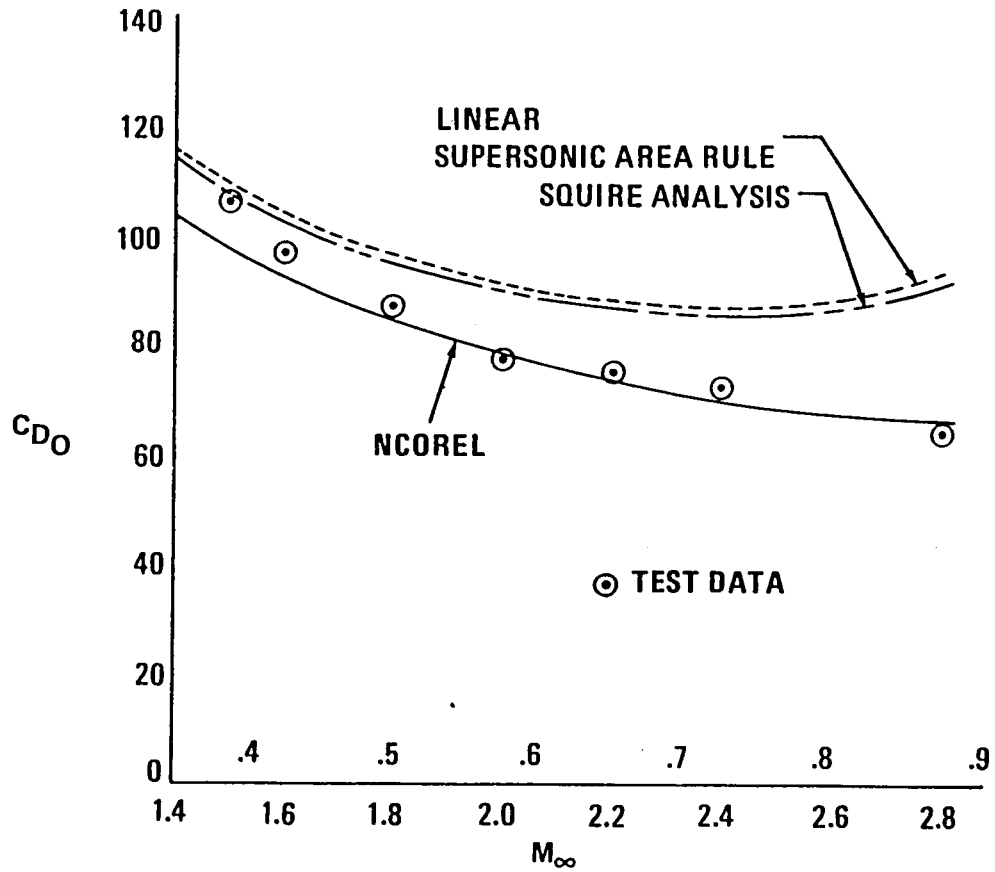

AIAA 82-0167

GRUMMAN

1773-028D

COMPUTED ISOBAR PATTERNS AT $C_L = 0.40, M_\infty = 1.62$

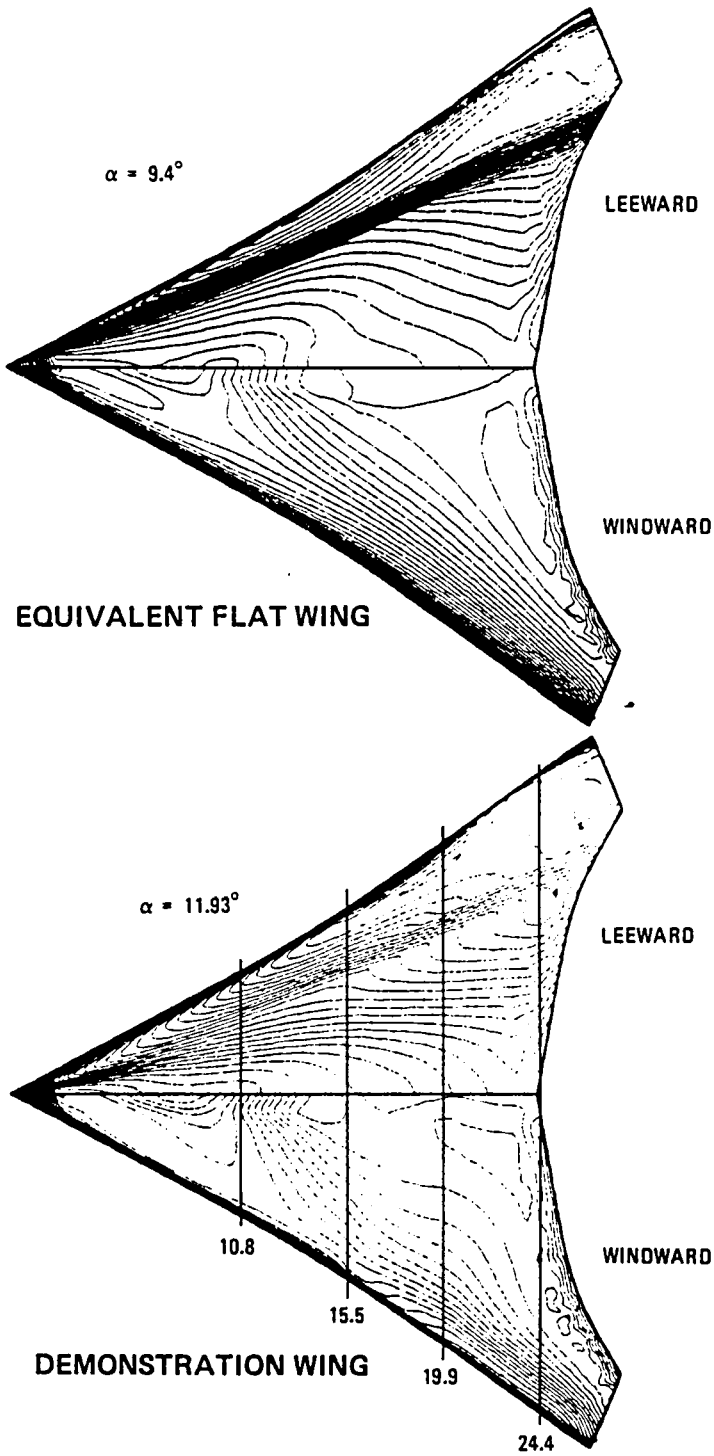

1773-026D

GRUMMAN

COMPARISON OF NCOREL PRETEST PREDICTIONS WITH NASA/GRUMMAN DEMO WING DATA AT DESIGN CONDITION

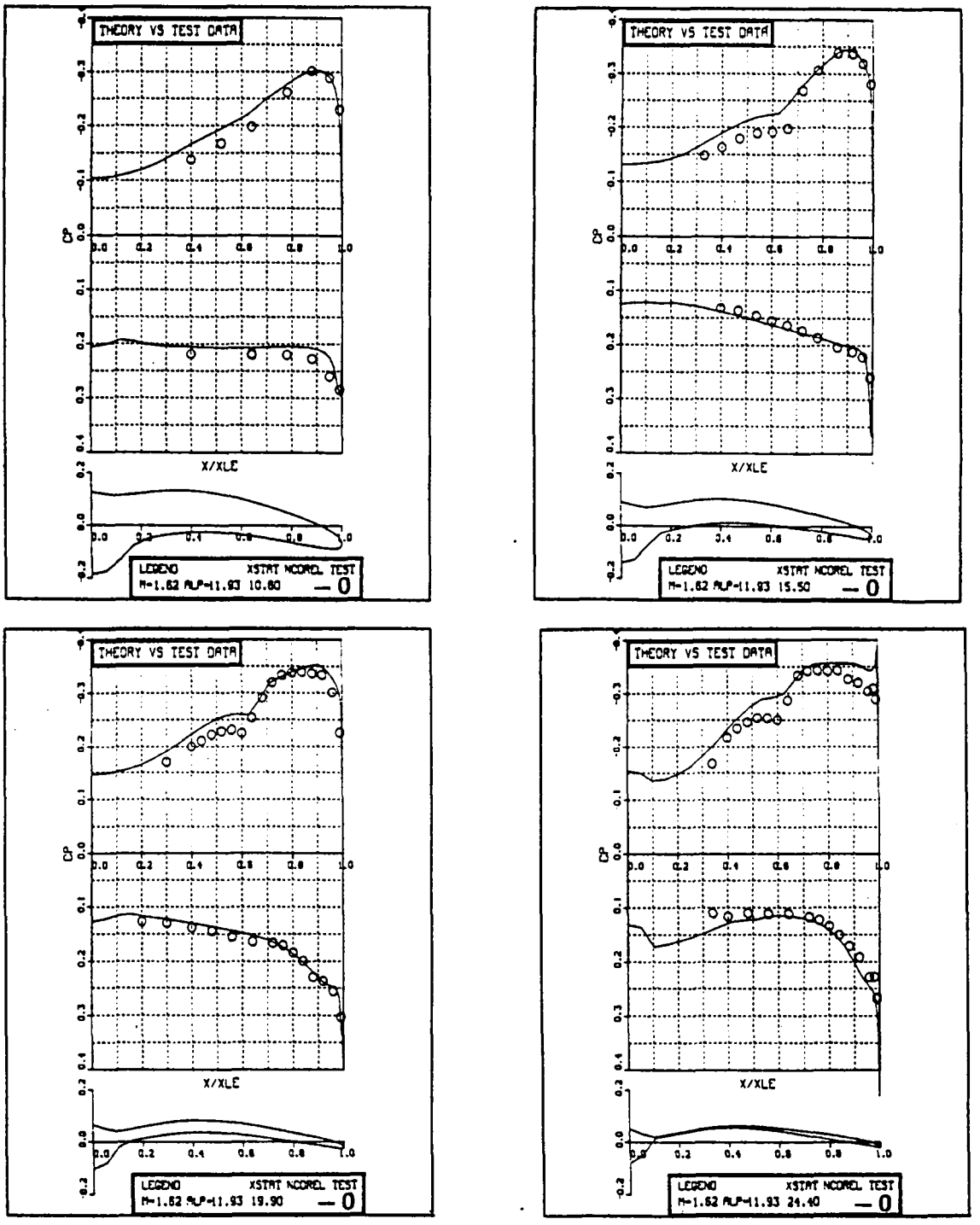

AIAA-83-0425

1773-027D

GRUMMAN

NCOREL MISSILE BODY AERODYNAMICS

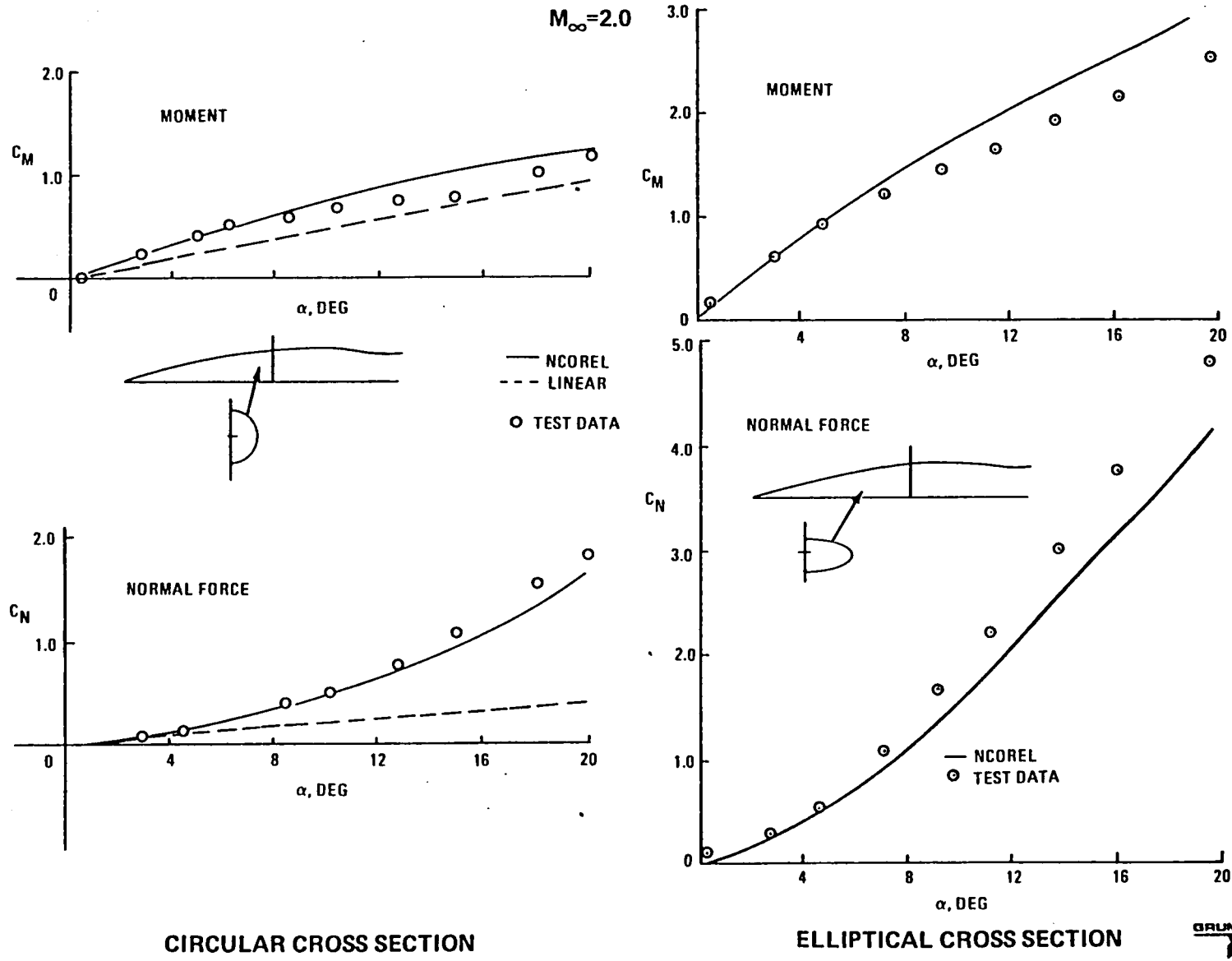

CIRCULAR CROSS SECTION

ELLIPTICAL CROSS SECTION

GRUMMAN

1773-029D

MISSILE TECHNOLOGY
GRUMMAN SUPERSONIC "HYBRID CODE"
$M_\infty = 2.0$

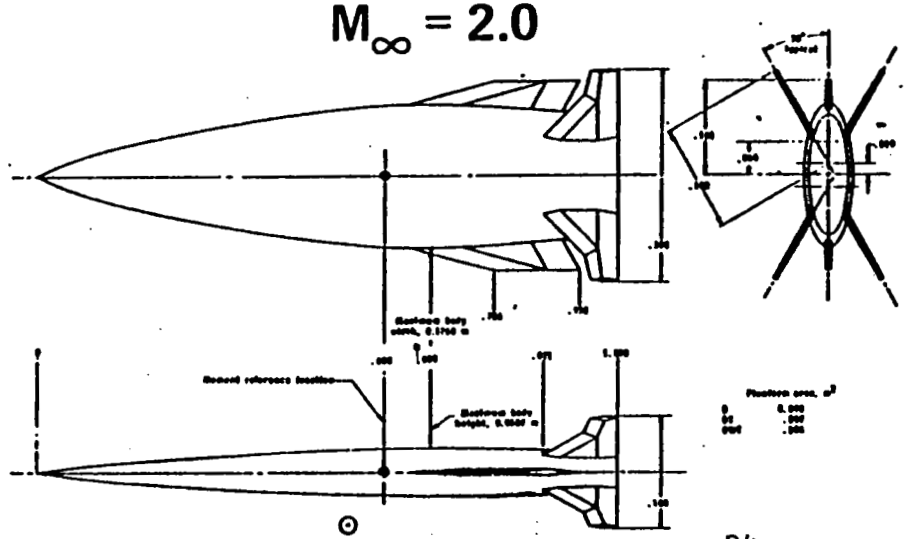

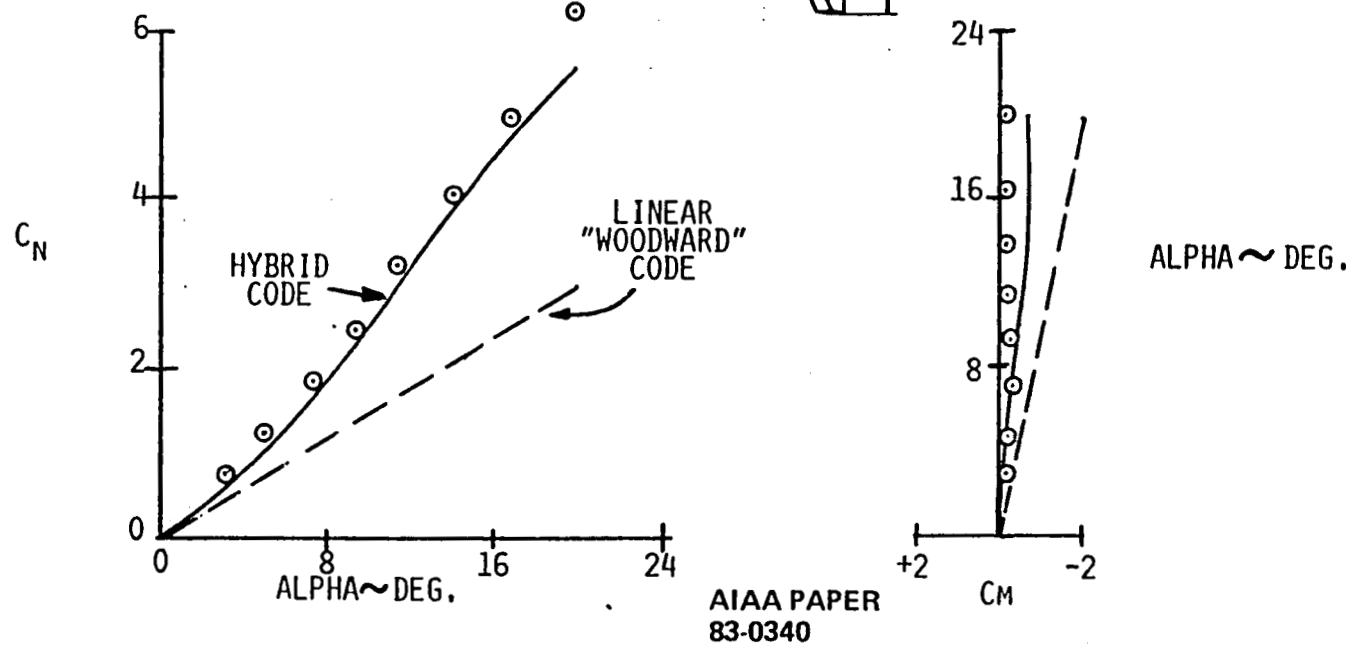

AIAA PAPER
83-0340

GRUMMAN

1773-037D

CORELF
CROSSFLOW SHOCK FITTING

SHOCK FITTING IN FULL POTENTIAL FLOWS

- SHOCK AS A BOUNDARY
  - $\|\phi\| = 0$
  - Insures continuity of tangential flow
- SHOCK JUMP CONDITION
  - $\|\rho Q_{NORM}\| = 0$
    - Isentropic $\rho = \rho_{ISEN}(M)$
    - Rankine-Hugoniot $\rho = \rho_{ISEN}\, e^{-\frac{AS}{R}}$

      (Hafez & Lovell)
      (Klopfer & Nixon)

GRUMMAN

1773-035D

CROSSFLOW SHOCK FITTING

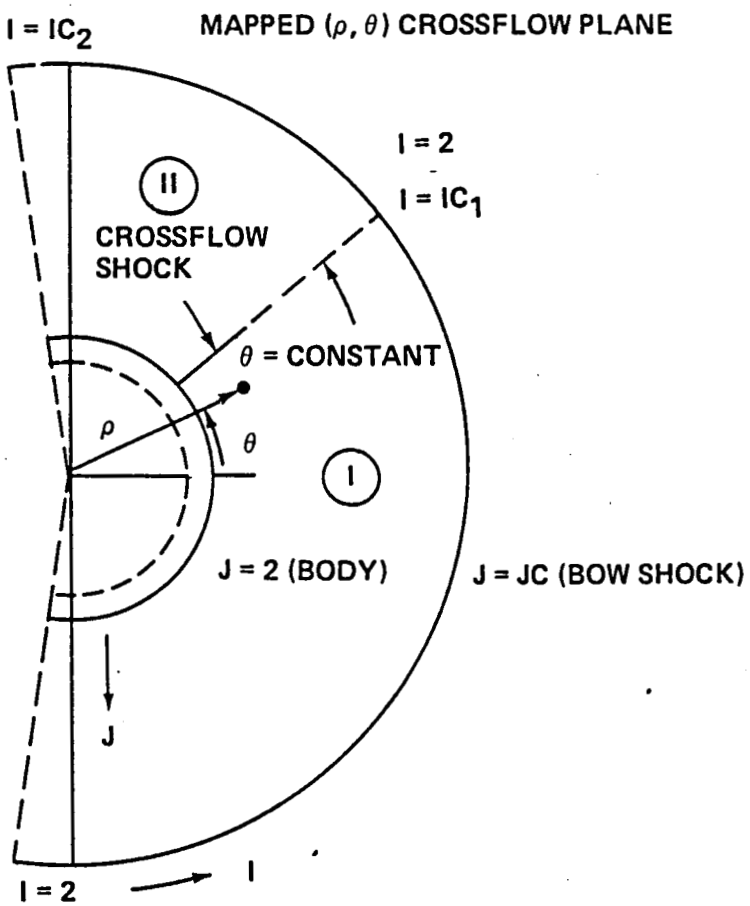

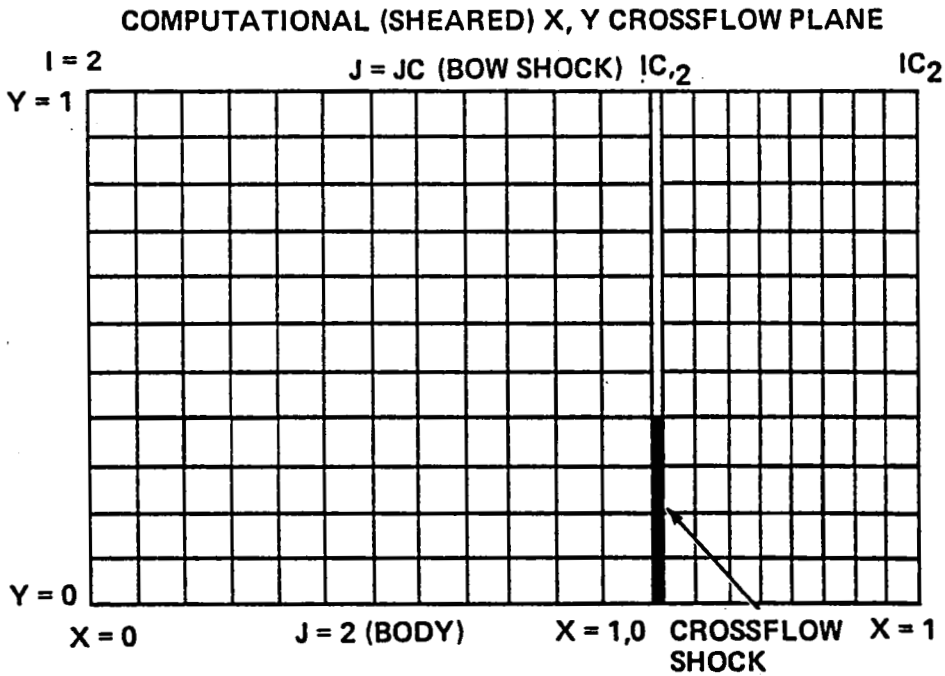

1773-034D

GRUMMAN

CROSSFLOW SHOCK FIT SHAPES

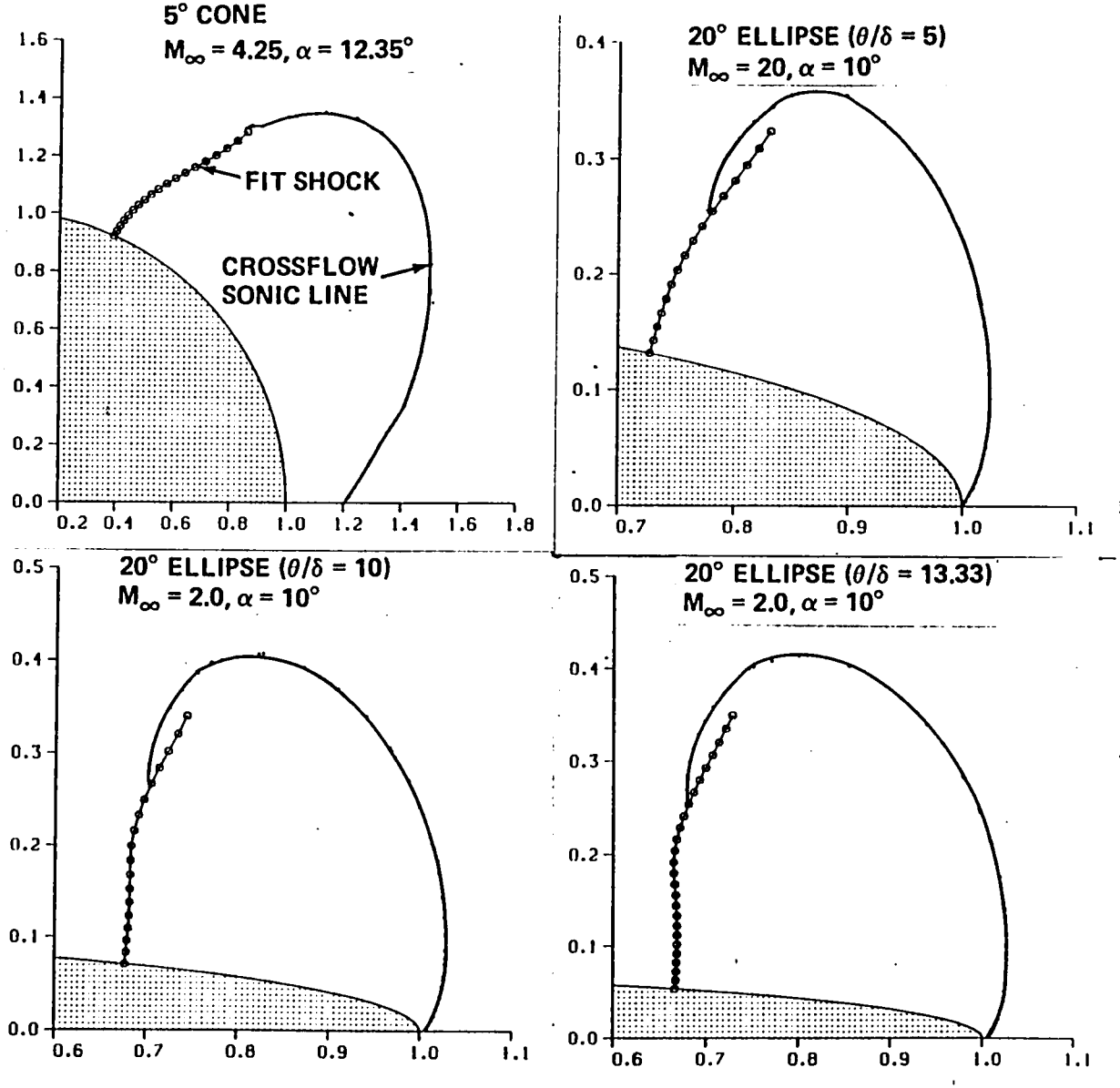
5° CONE
$M_\infty = 4.25, \alpha = 12.35°$
FIT SHOCK
CROSSFLOW SONIC LINE
20° ELLIPSE ($\theta/\delta = 5$)
$M_\infty = 20, \alpha = 10°$
20° ELLIPSE ($\theta/\delta = 10$)
$M_\infty = 2.0, \alpha = 10°$
20° ELLIPSE ($\theta/\delta = 13.33$)
$M_\infty = 2.0, \alpha = 10°$

1773-015D

CROSSFLOW SHOCK FIT EULER vs POTENTIAL

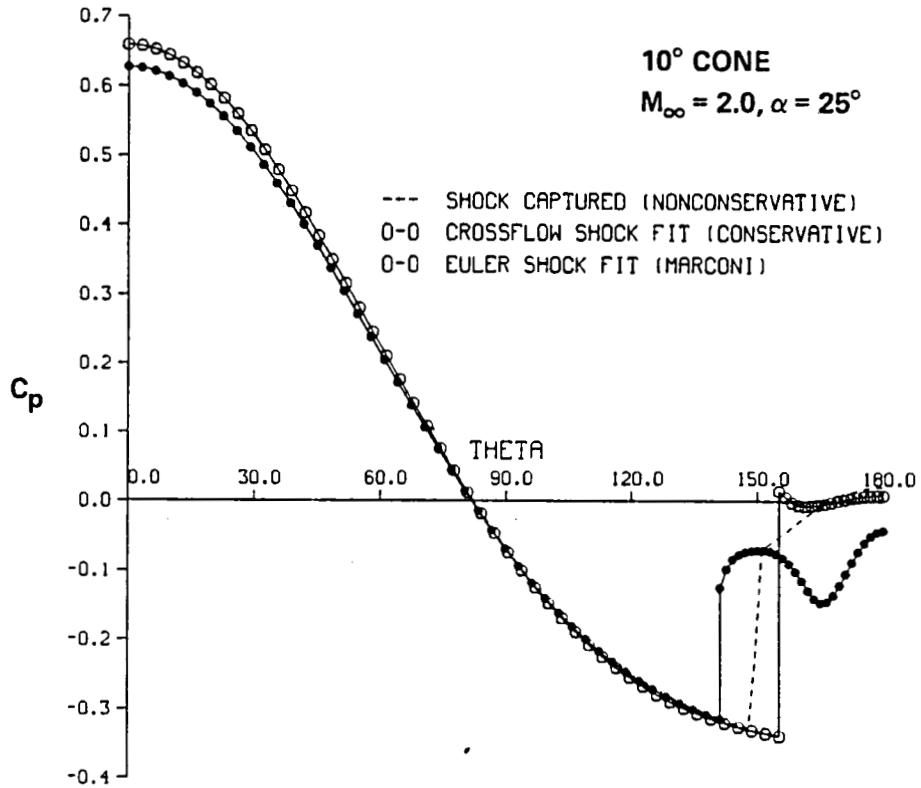

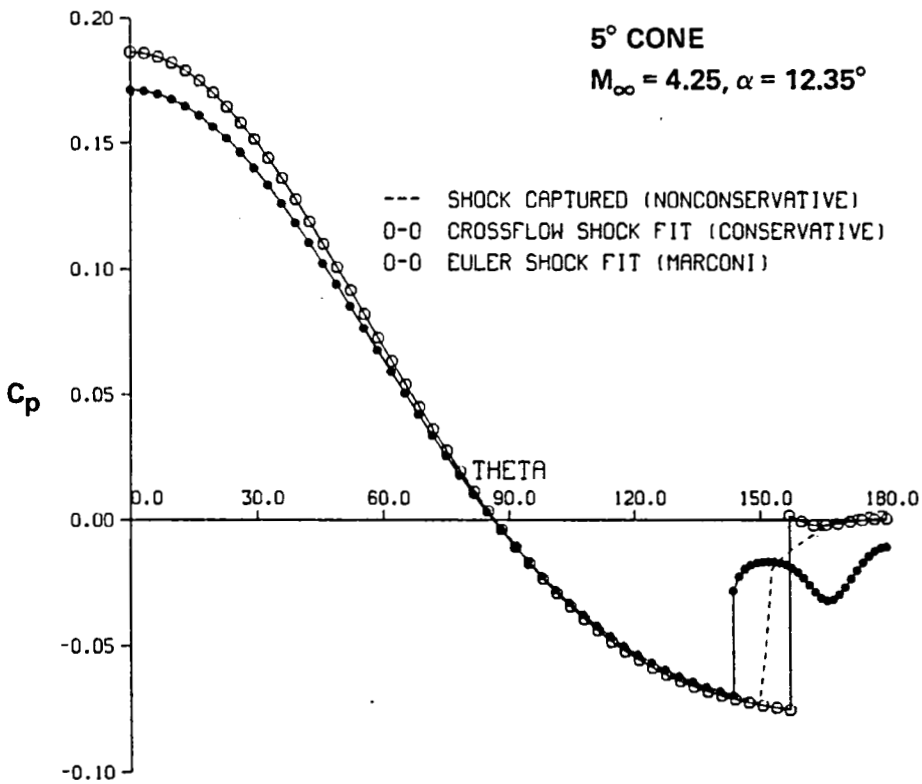

1773-016D

GRUMMAN

5° CIRCULAR CONE CROSSFLOW SHOCK FIT

$M_\infty = 4.25, \alpha = 12.35°$

ISOBARS

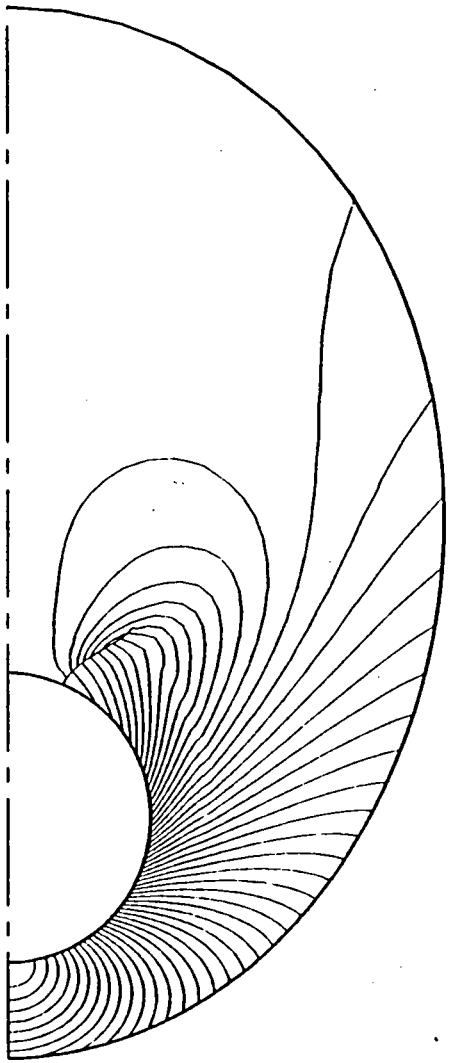

CROSSFLOW ISOMACHS

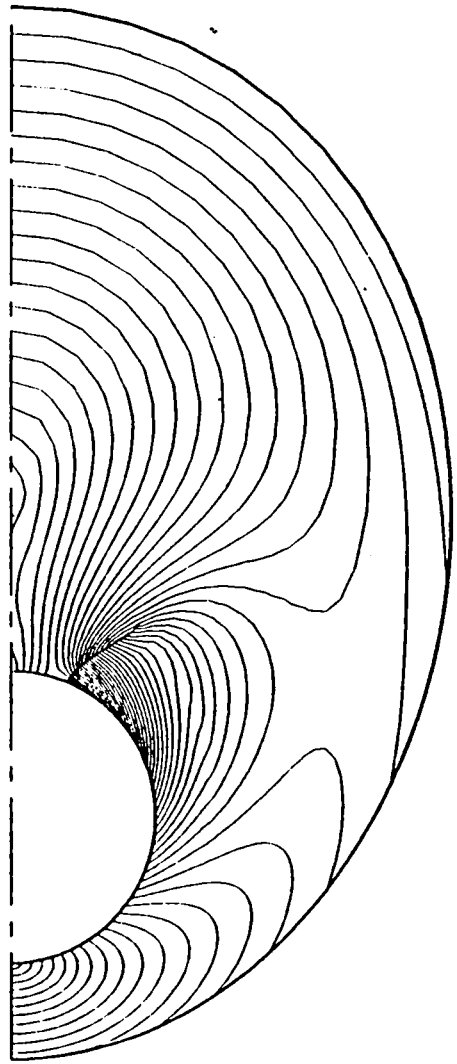

GRUMMAN

1773-018D

CROSSFLOW SHOCK FIT vs CAPTURED

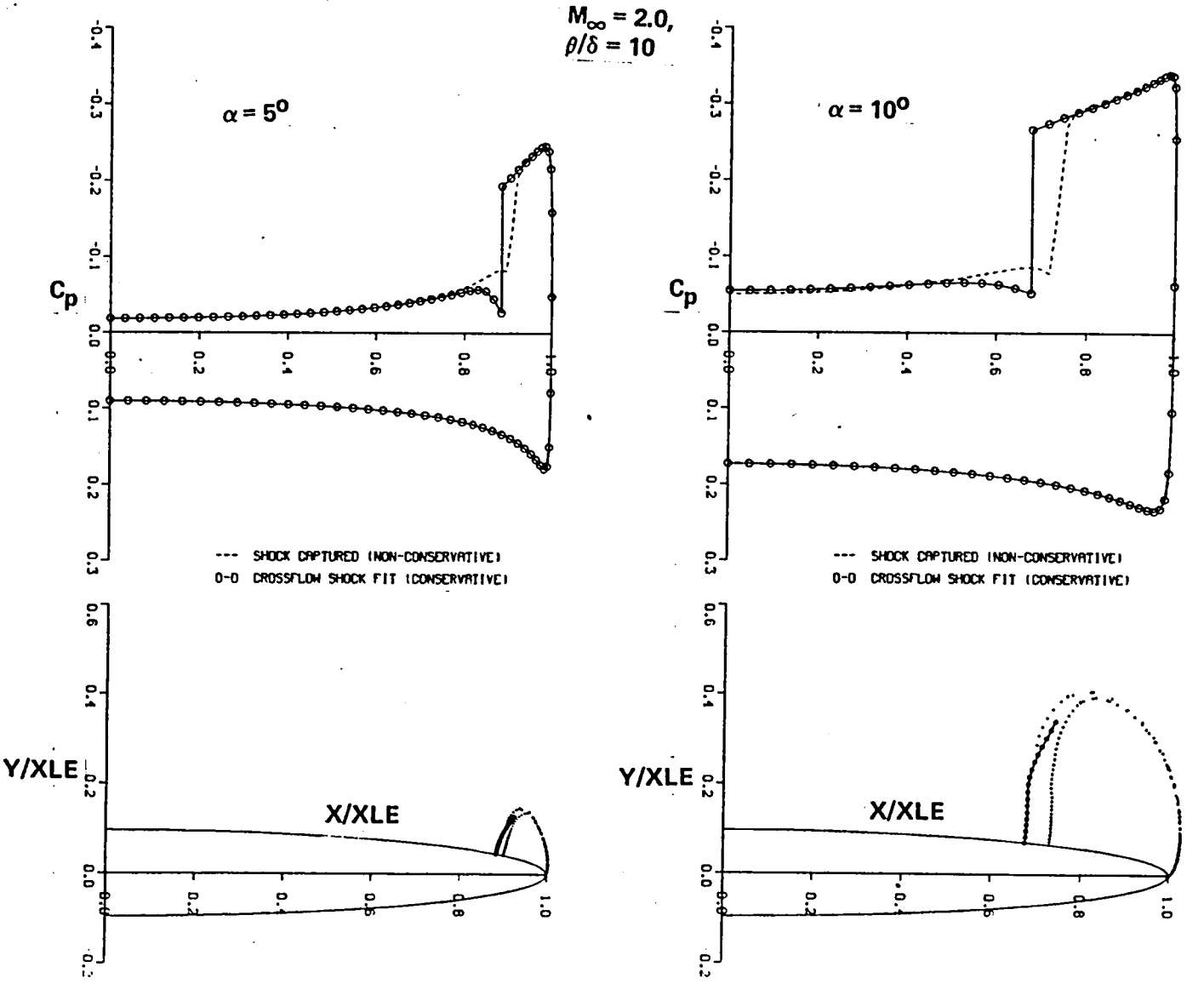

1773-017D

20° ELLIPTIC CONE ($\theta/\delta = 5$)

$M_\infty = 2.0, \alpha = 10°$

ISOBARS

CROSSFLOW ISOMACHS

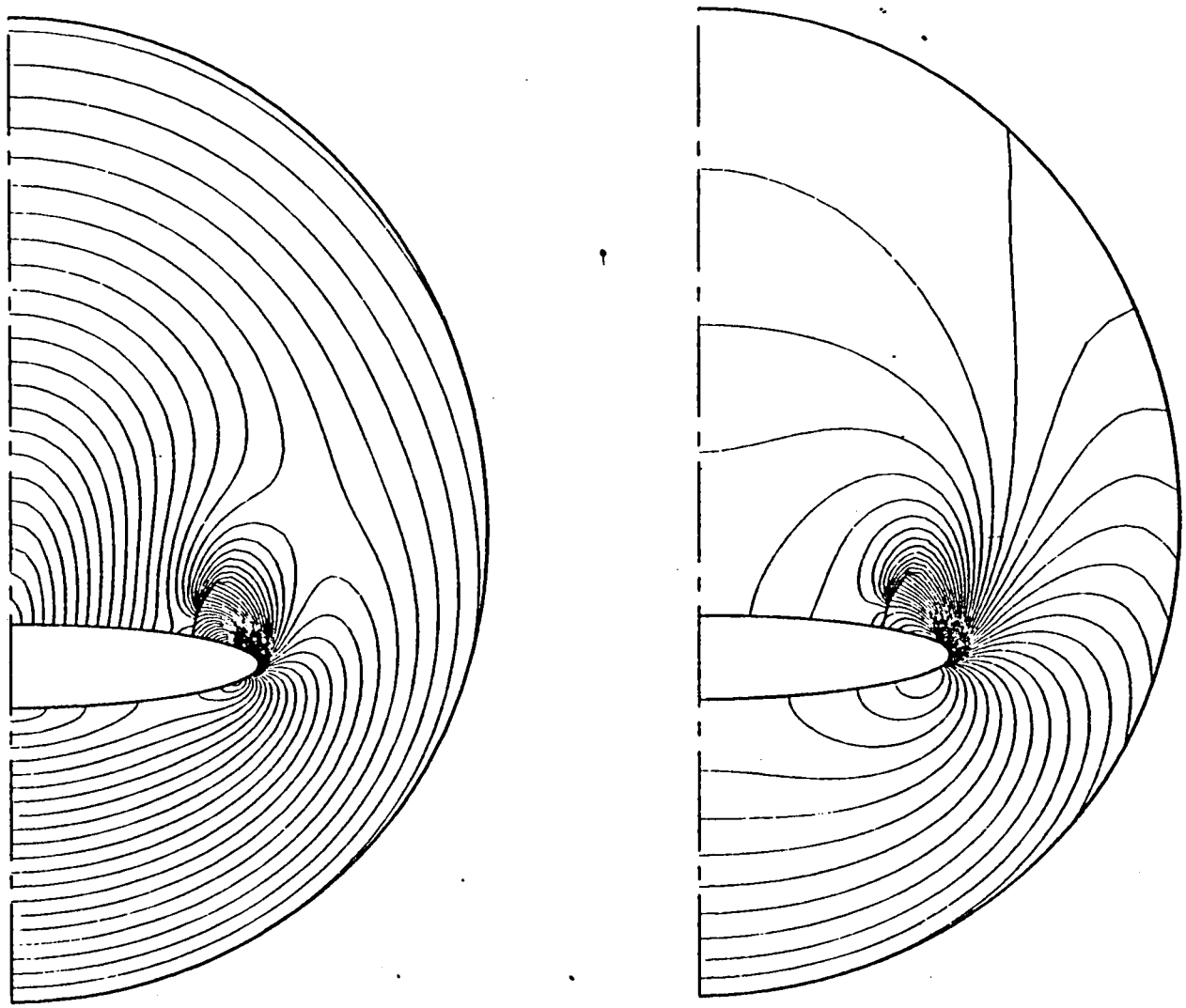

GRUMMAN

1773-019D

20° ELLIPTIC CONE (θ/δ = 13.33)

$M_\infty = 2.0, \alpha = 10°$

ISOBARS

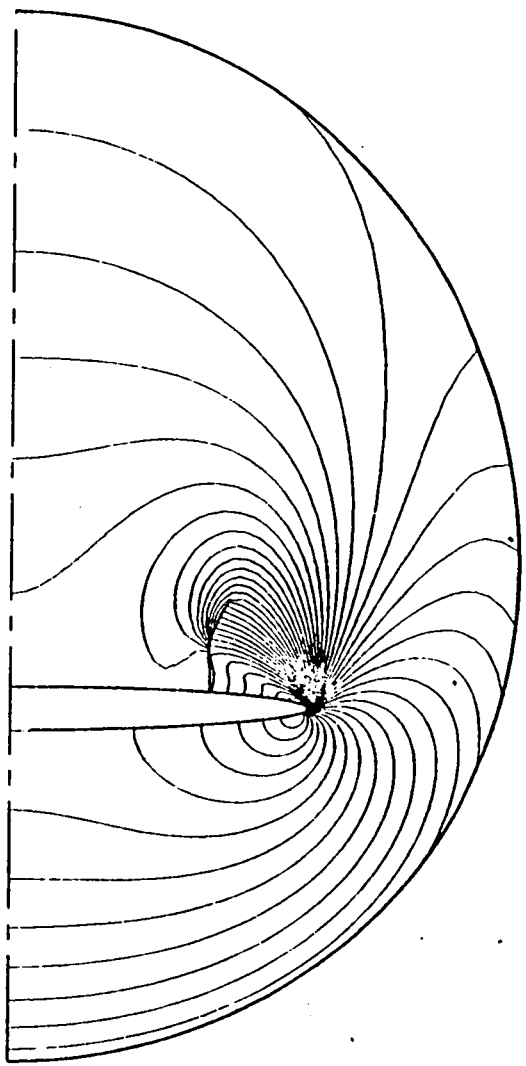

CROSSFLOW ISOMACHS

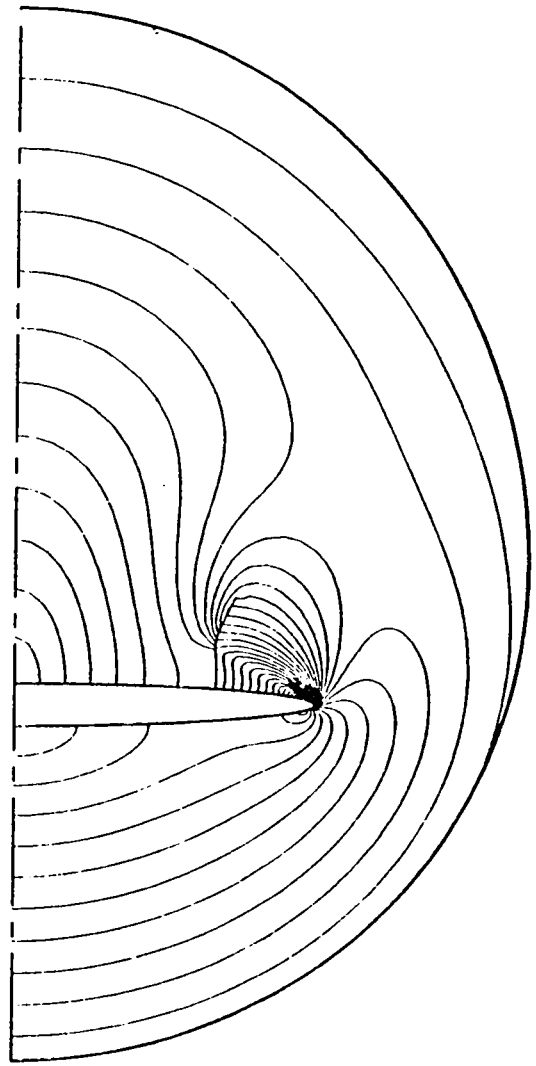

GRUMMAN

1773-020D

METHODS COMPARISON - ELLIPTIC CONES ($\alpha = 10°$)

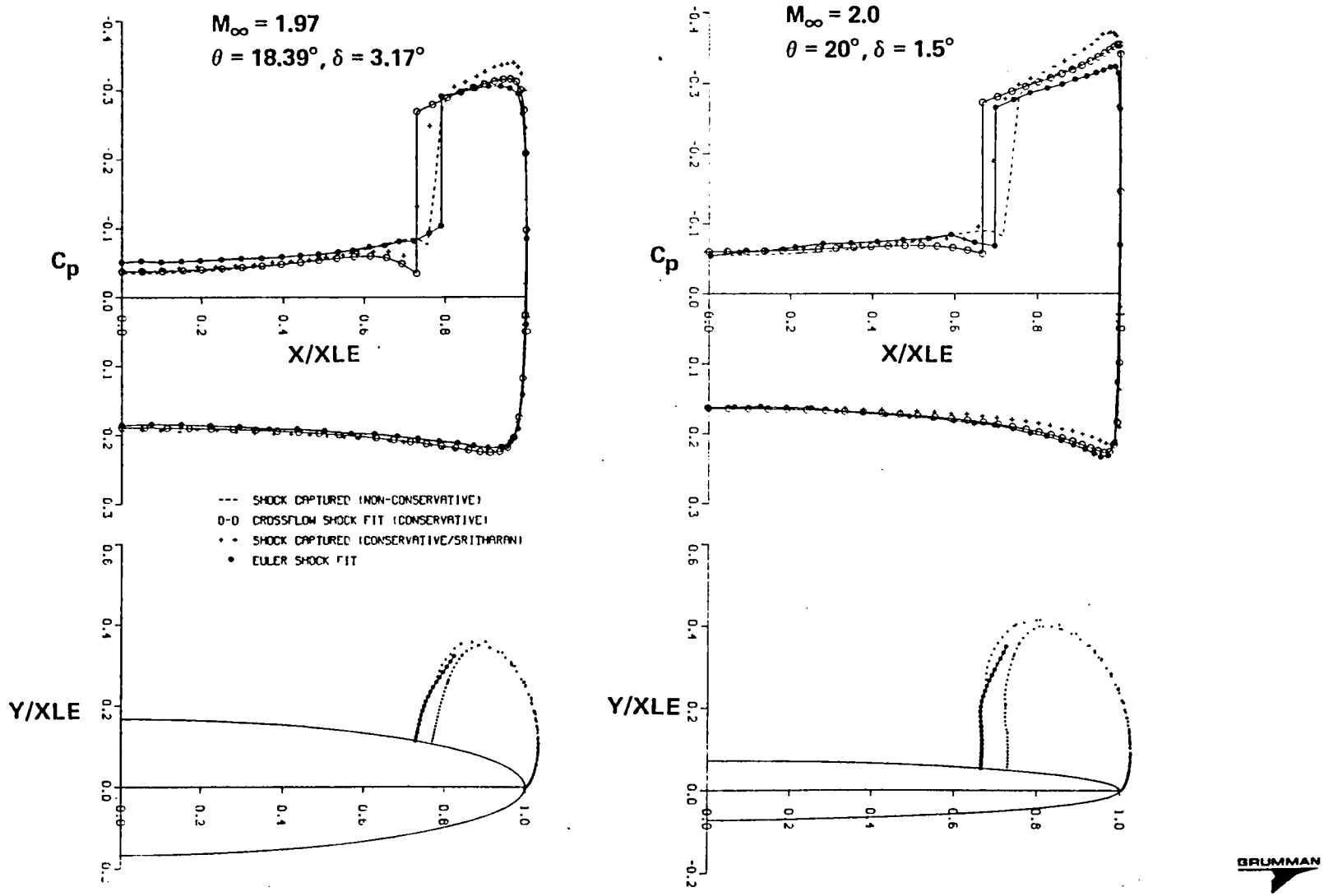

1773-021D

GRUMMAN

ENTROPY EFFECTS

30° CONE (α = 0°)

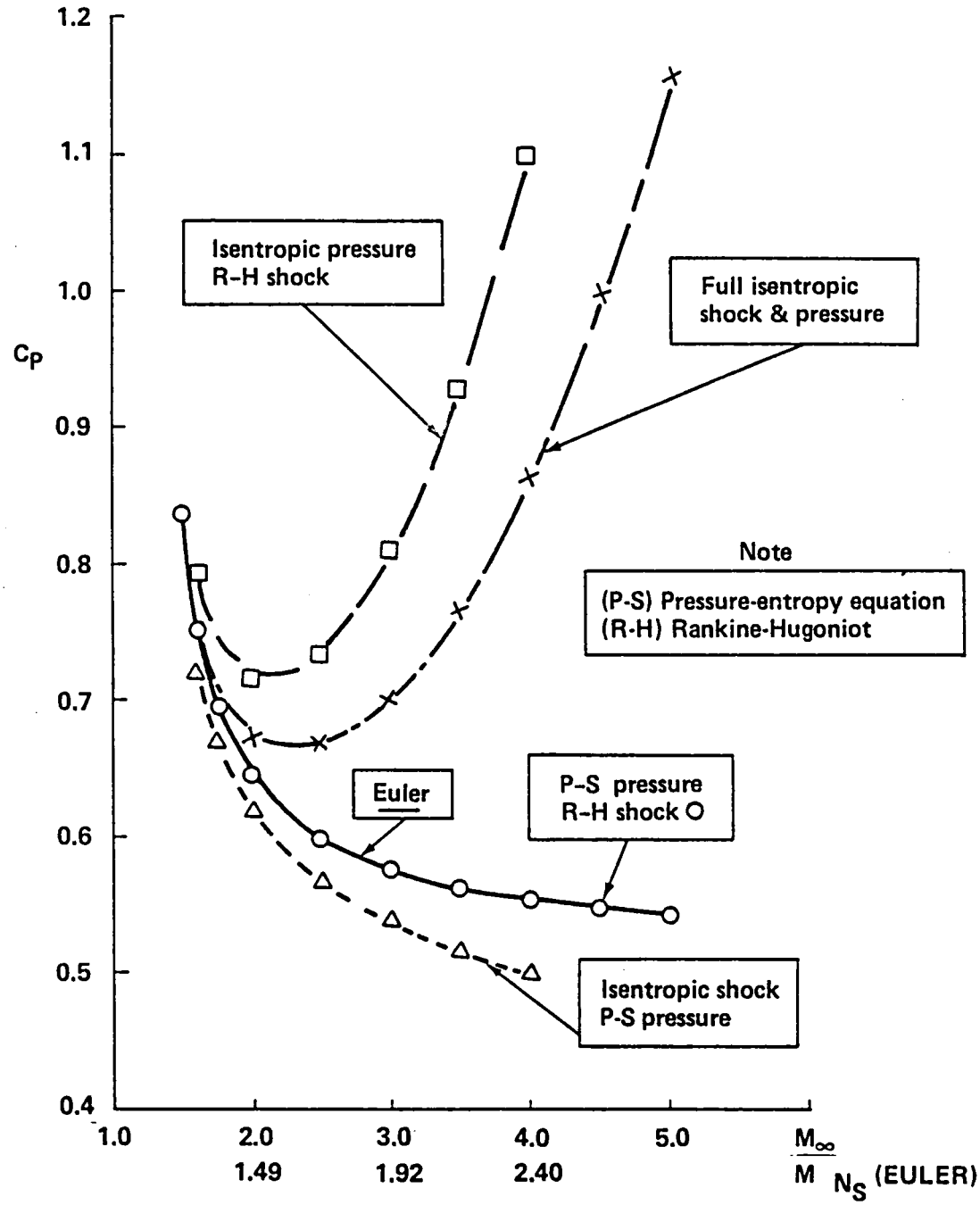

GRUMMAN

1773-005D

BOW SHOCK ENTROPY EFFECT

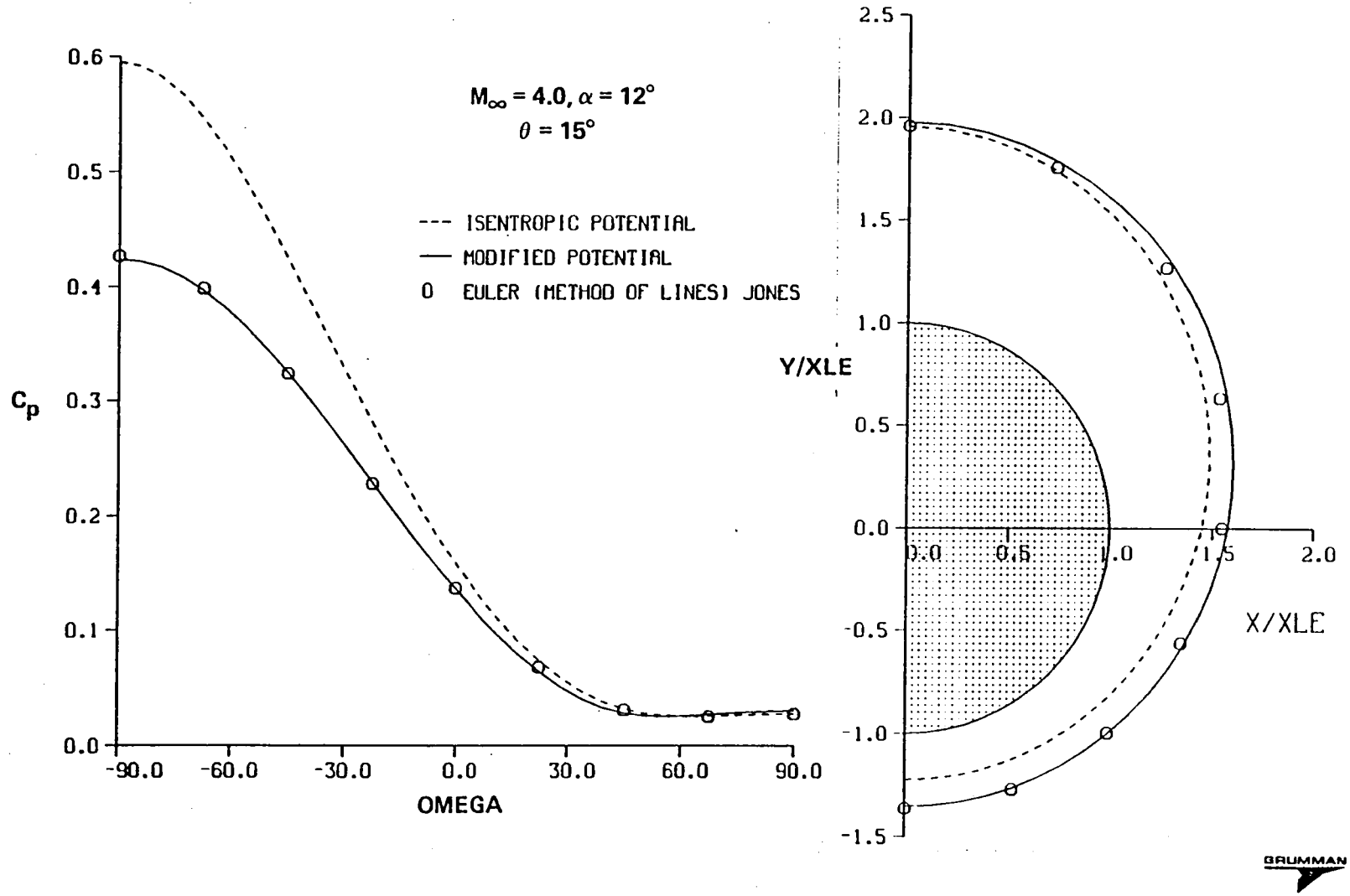

GRUMMAN

1773-013D

BOW SHOCK ENTROPY EFFECT

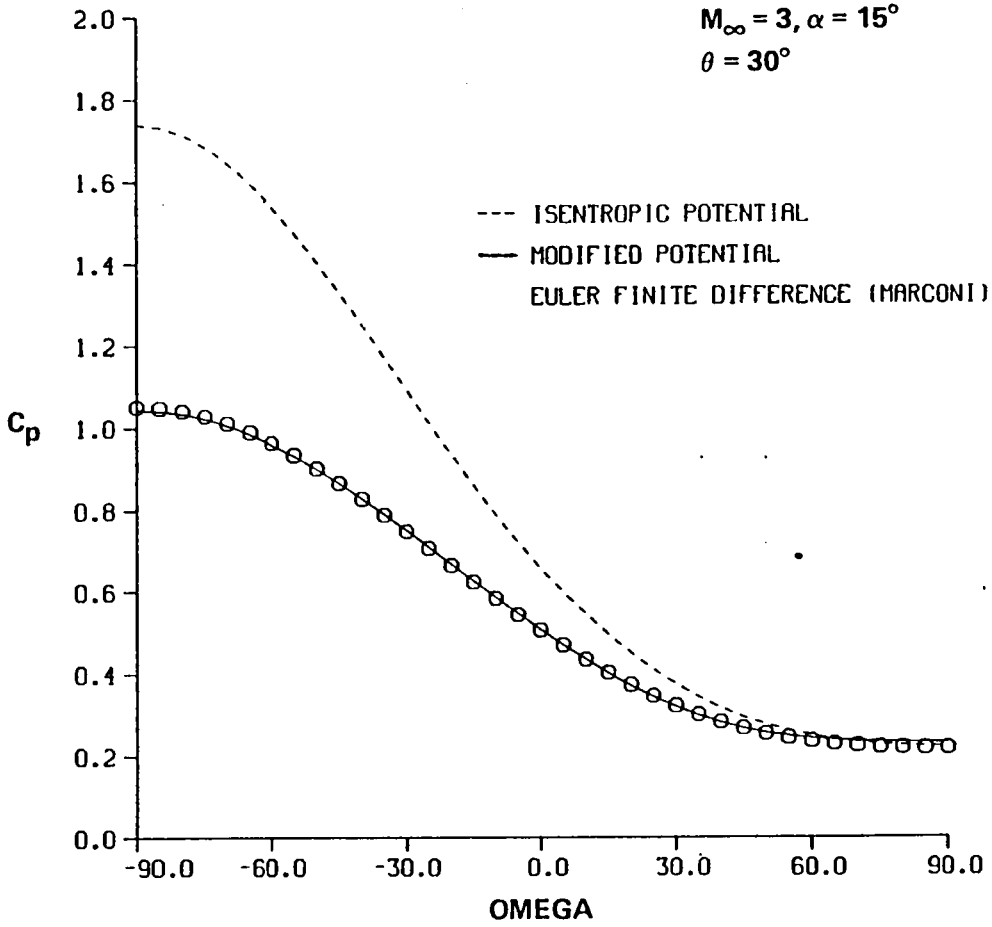

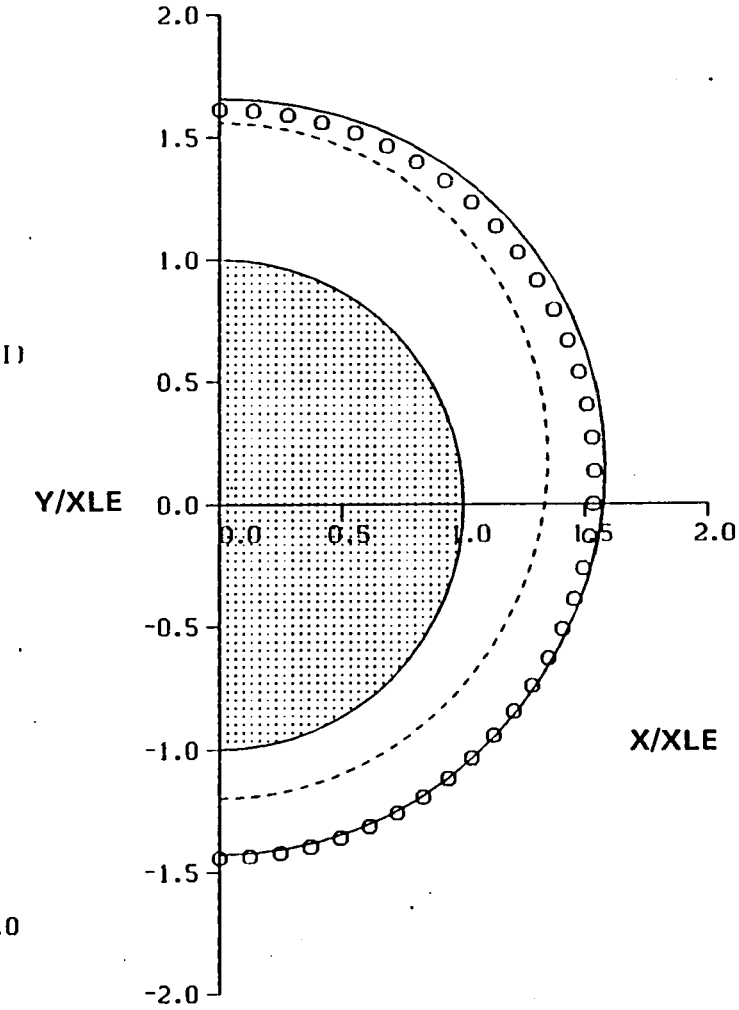

GRUMMAN

1773-006D

BOW SHOCK ENTROPY EFFECT

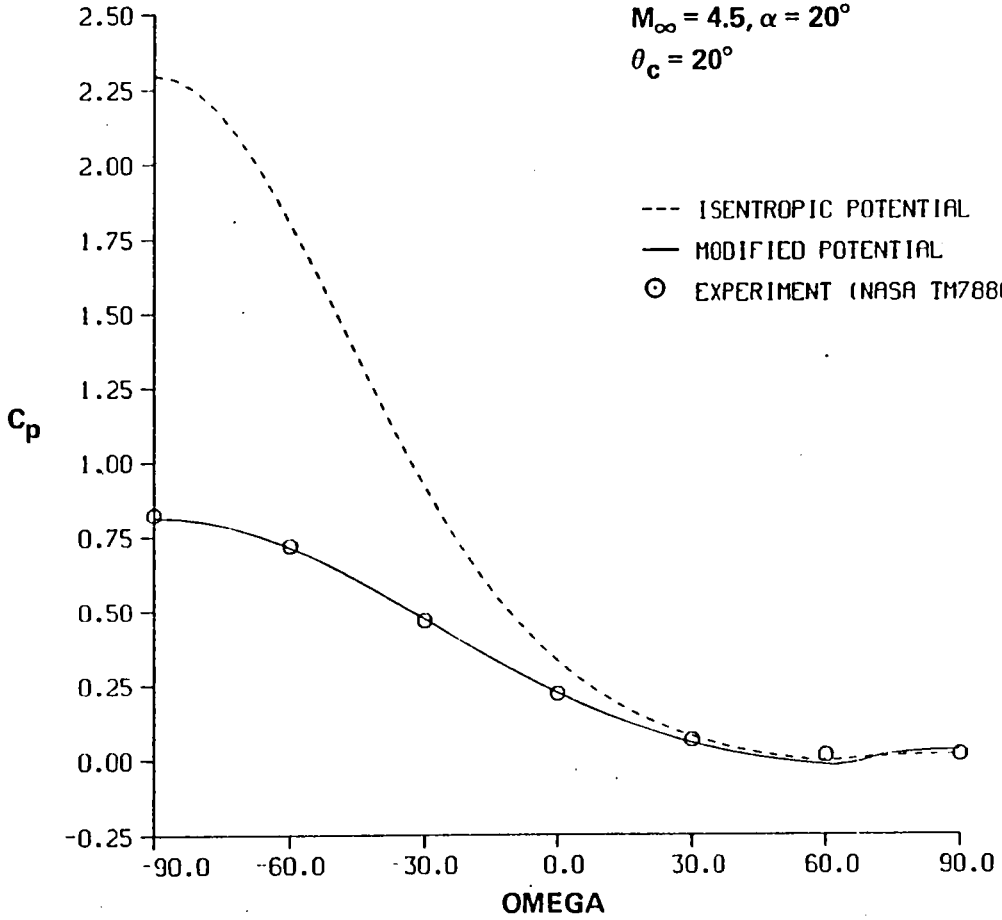

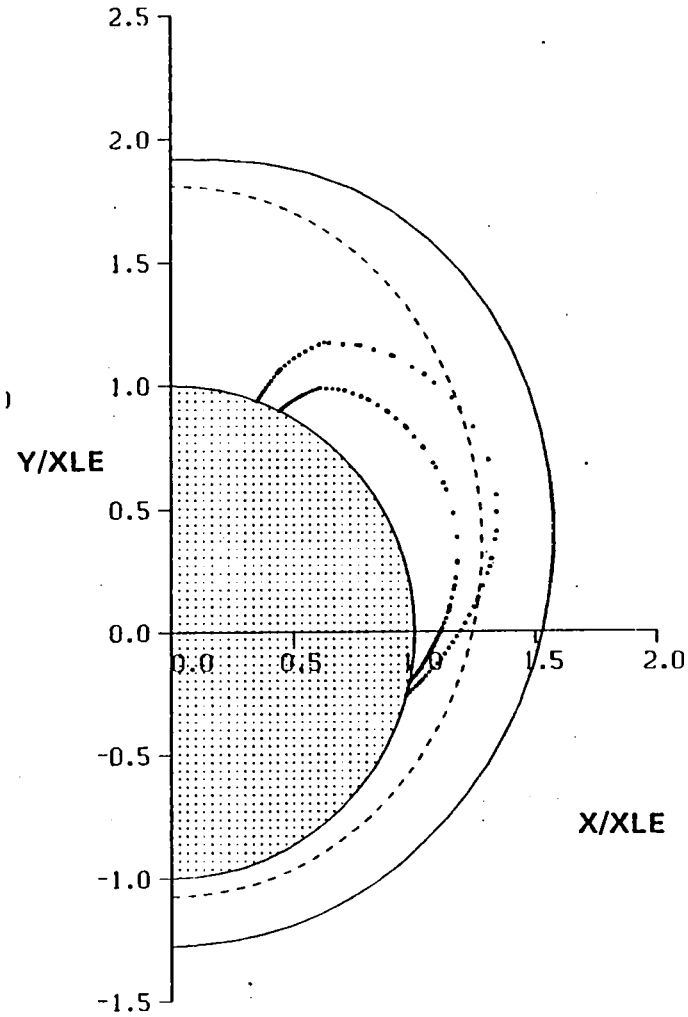

GRUMMAN

1773-008D

488

BOW SHOCK ENTROPY EFFECT

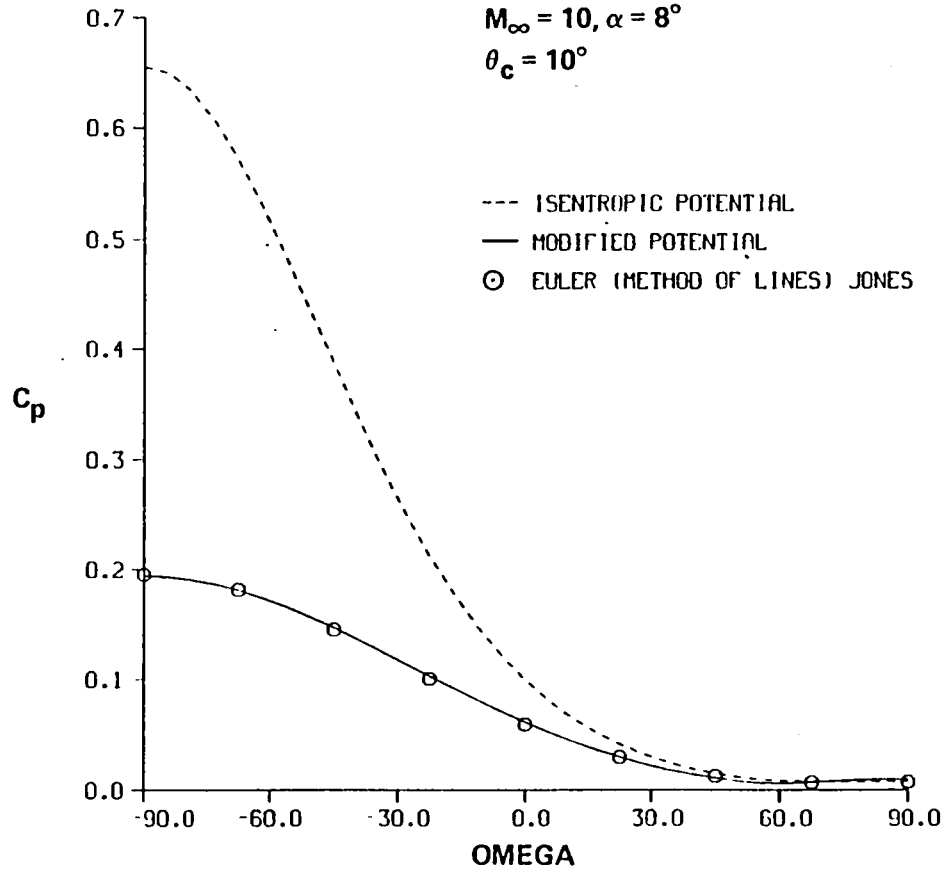

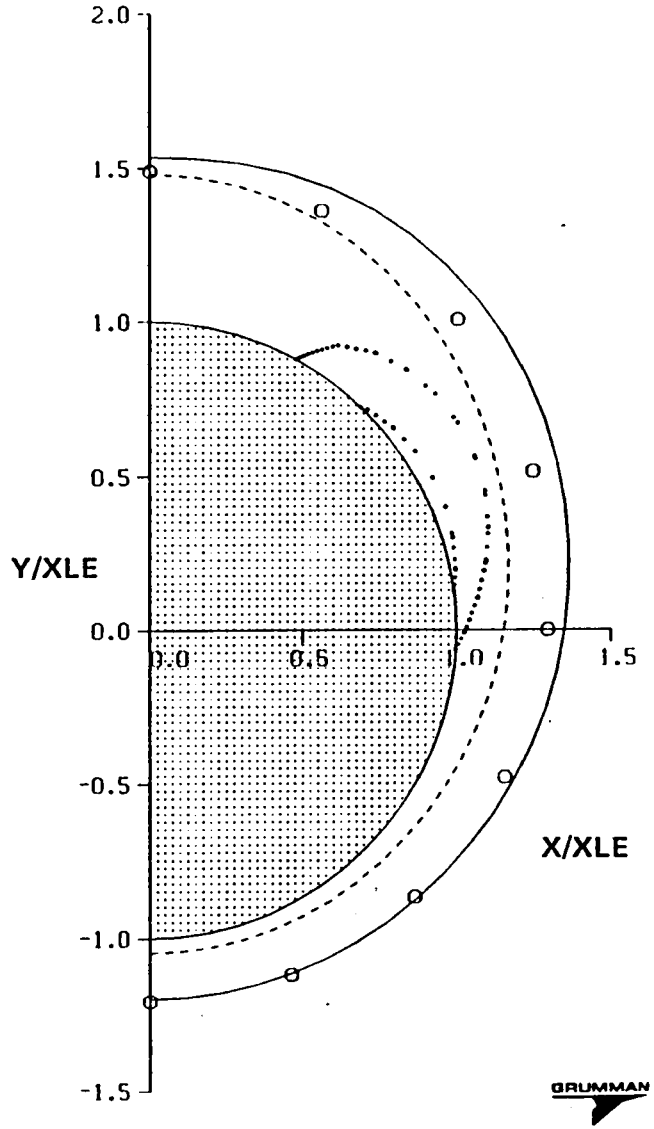

GRUMMAN

1773-009D

BOW SHOCK ENTROPY EFFECT

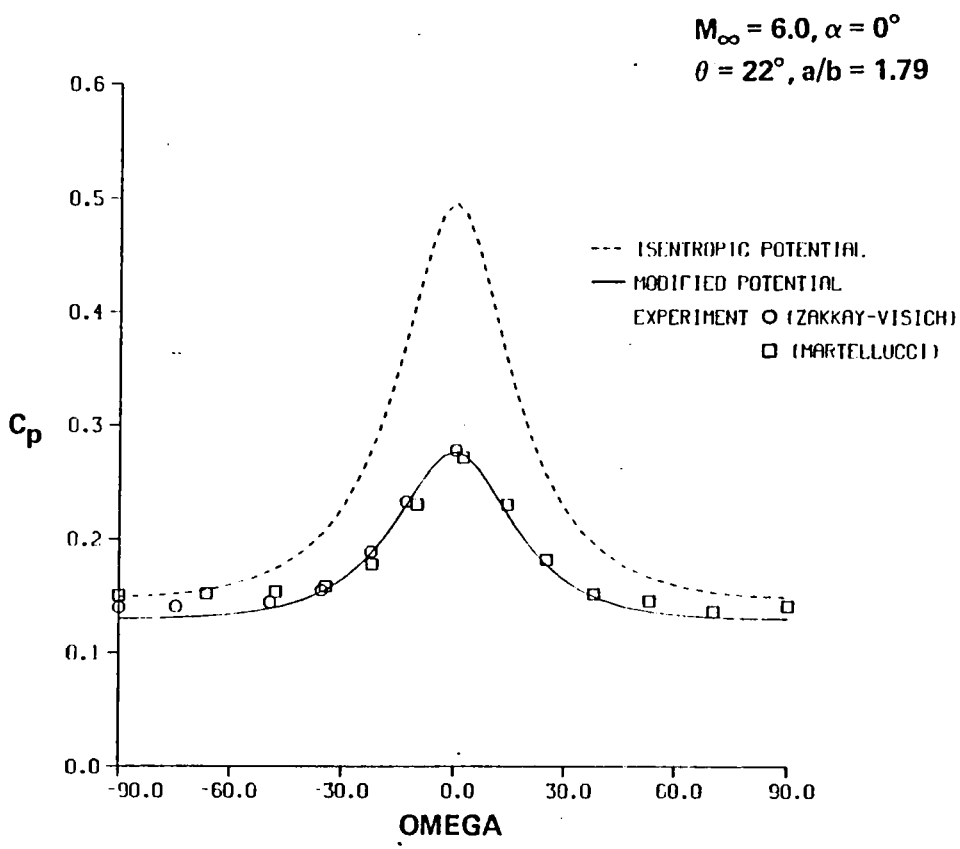

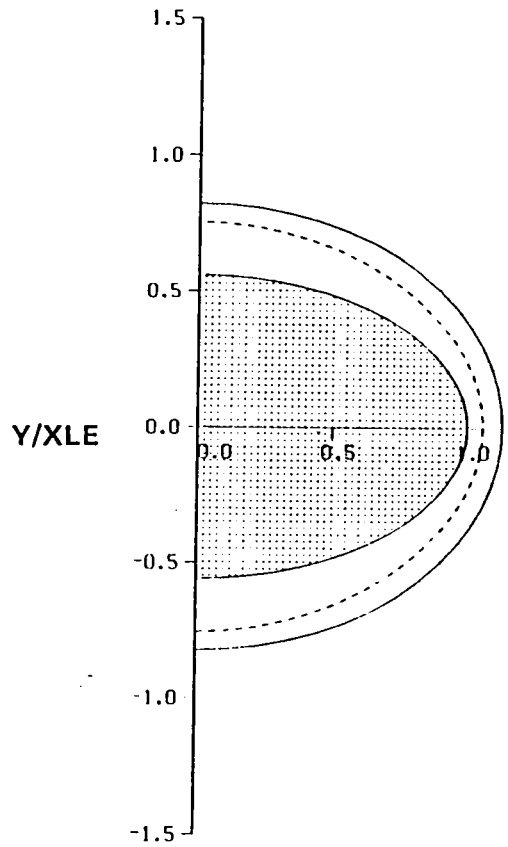

GRUMMAN

1773-007D

BOW SHOCK ENTROPY EFFECT

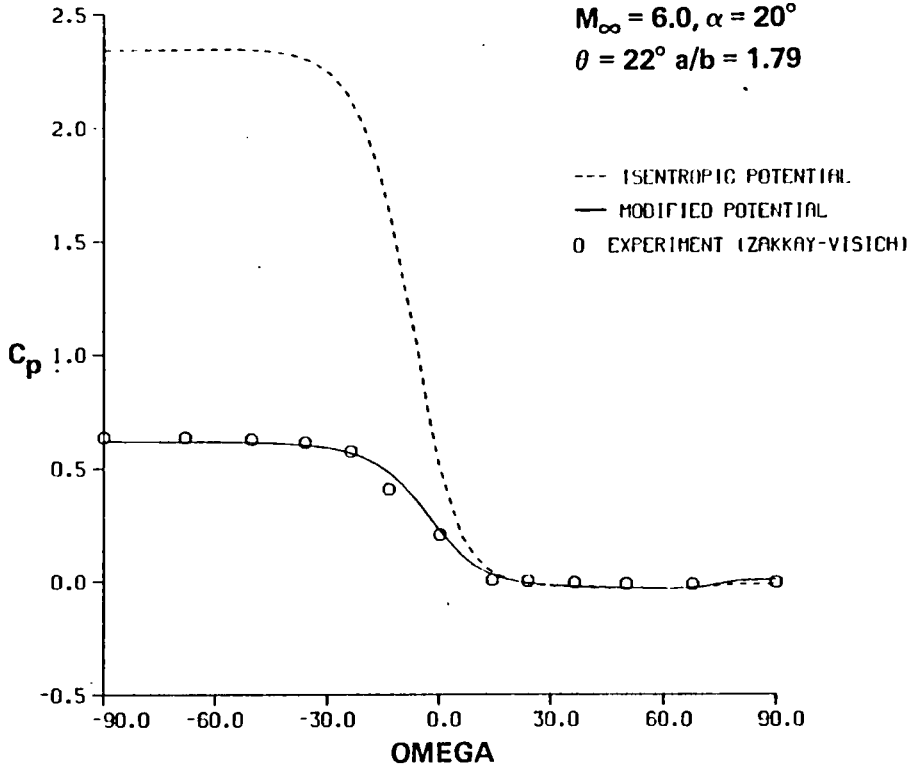

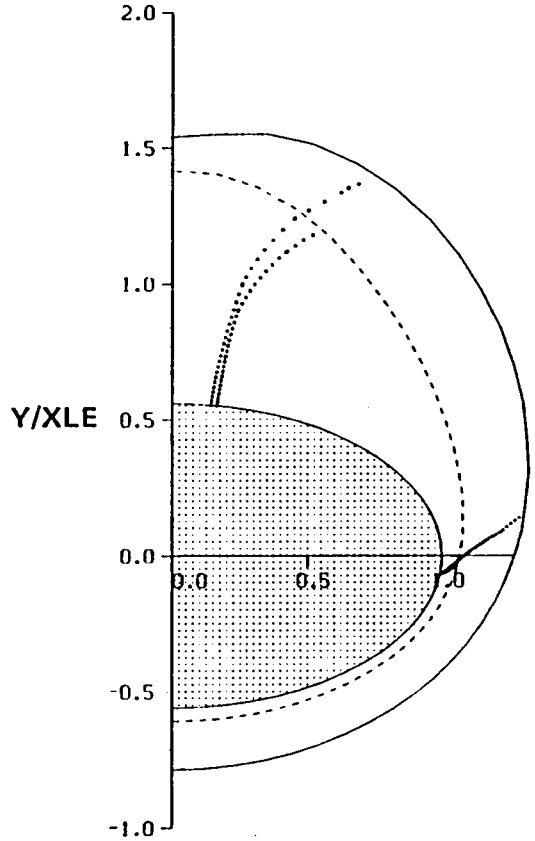

GRUMMAN

1773-014D

ENTROPY EFFECTS ON FORCE AND MOMENT PREDICTION
20° CIRCULAR CONE $M_\infty = 4.5$

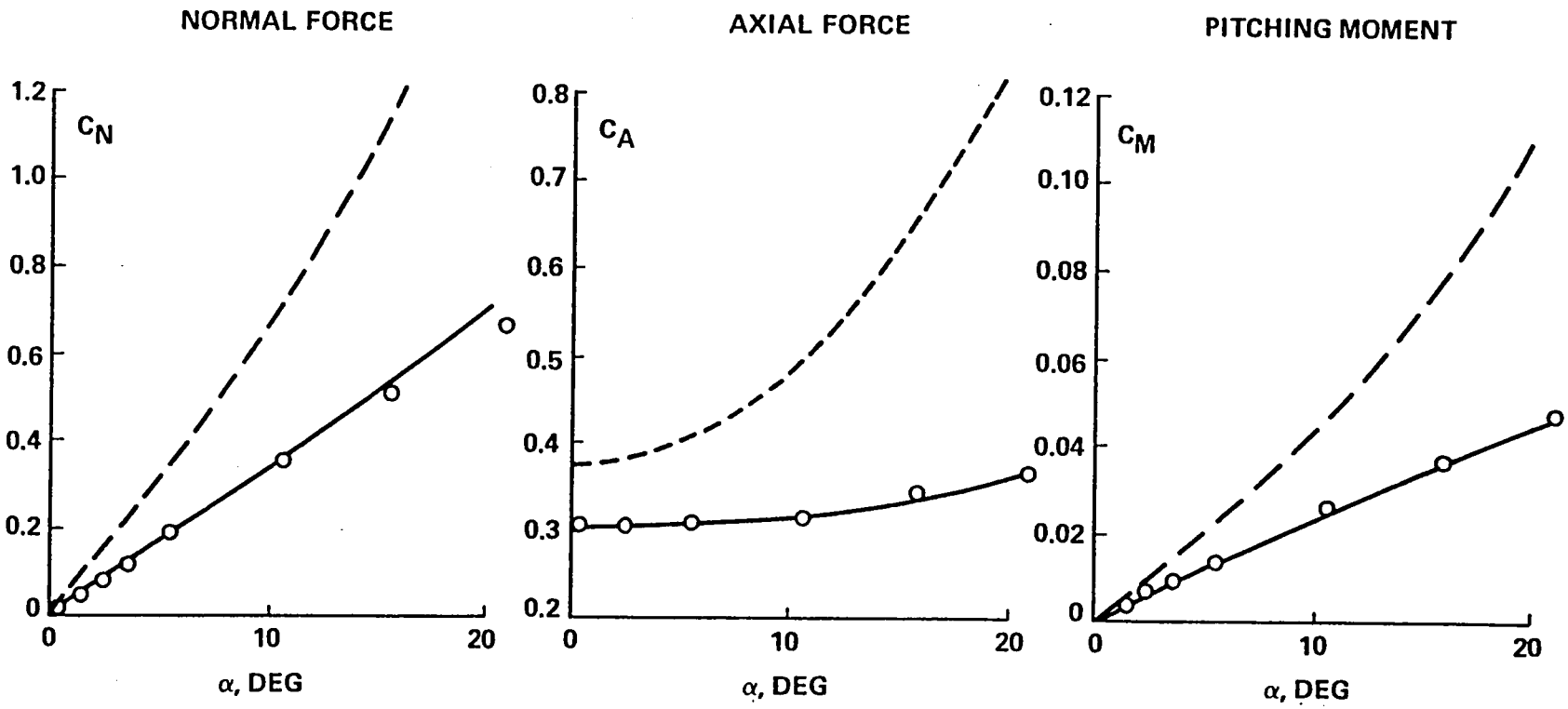

AIAA 84-0231
PITTMAN & SICLARI

- – – – ISENTROPIC POTENTIAL
- ——— MODIFIED POTENTIAL
- o EXPERIMENT

GRUMMAN

1773-031D

ENTROPY EFFECTS ON FORCE & MOMENT PREDICTION
20° ELLIPTIC CONE (3:1 AXIS RATIO) $M_\infty = 4.5$

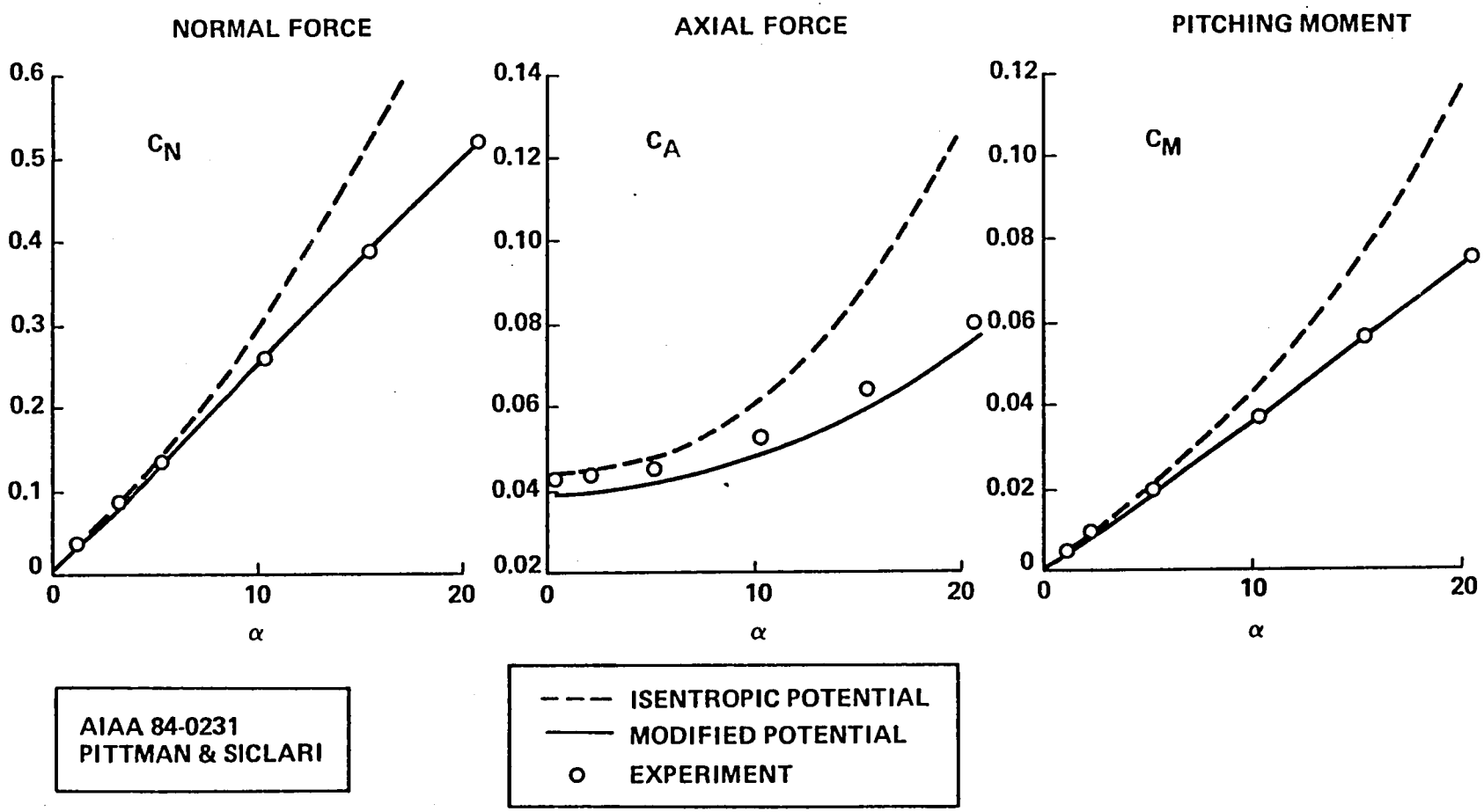

(19)

FULL POTENTIAL AERODYNAMIC PREDICTION CAPABILITY FOR COMPLEX CONFIGURATIONS

VIJAYA SHANKAR
AND
KUO-YEN SZEMA

ROCKWELL INTERNATIONAL SCIENCE CENTER
THOUSAND OAKS, CA

NASA LANGLEY CONTRACT - NAS1-15820

CONTRACT MONITORS - KEN JONES
NOEL TALCOTT

Rockwell International
Science Center

SHANKAR

HIGHLIGHTS

- FULL POTENTIAL EQUATION IN CONSERVATION FORM
- CONSERVATIVE SWITCHES FOR THE TREATMENT OF SUPERSONIC (HYPERBOLIC) AND SUBSONIC (ELLIPTIC) REGIONS
- FLUX BIASING AND DENSITY BIASING METHODS FOR ARTIFICIAL VISCOSITY GENERATION
- IMPLICIT FACTORIZATION ALGORITHM
- NUMERICAL MAPPING
- WAKE TREATMENT
- RESULTS

Rockwell International
Science Center

EQUATION AND CHARACTERISTIC THEORY

$$\left(\rho\frac{U}{J}\right)_{\zeta}+\left(\rho\frac{V}{J}\right)_{\eta}+\left(\rho\frac{W}{J}\right)_{\xi}=0$$

COMBINE FULL POTENTIAL EQUATION AND IRROTATIONALITY CONDITION

$$A f_{\zeta} + B f_{\eta} + C f_{\xi} = 0$$

$$A=\begin{bmatrix} \frac{1}{J}(\rho U)_{\phi_\zeta} & \frac{1}{J}(\rho U)_{\phi_\eta} & \frac{1}{J}(\rho U)_{\phi_\xi} \\ 0 & 1 & 0 \\ 0 & 0 & 1 \end{bmatrix}$$

. SIMILARLY B AND C, $f=\begin{pmatrix}\phi_\zeta\\ \phi_\eta\\ \phi_\xi\end{pmatrix}$.

ζ IS HYPERBOLIC IF, $(\rho U)_{\phi_\zeta}=\rho\left(a_{11}-\frac{U^2}{a^2}\right)<0$

ζ IS ELLIPTIC IF, $\left(a_{11}-\frac{U^2}{a^2}\right)>0$

<u>THREE POSSIBILITIES</u>

1. $\left(a_{11}-\frac{U^2}{a^2}\right)<0$; $q>a$ (q = TOTAL VELOCITY), MARCHING SUPERSONIC

2. $\left(a_{11}-\frac{U^2}{a^2}\right)>0$; $q>a$, MARCHING SUBSONIC

3. $\left(a_{11}-\frac{U^2}{a^2}\right)>0$; $q<a$, TOTAL SUBSONIC

Rockwell International
Science Center

EMBEDDED SUBSONIC BUBBLE IN A SUPERSONIC FLOW

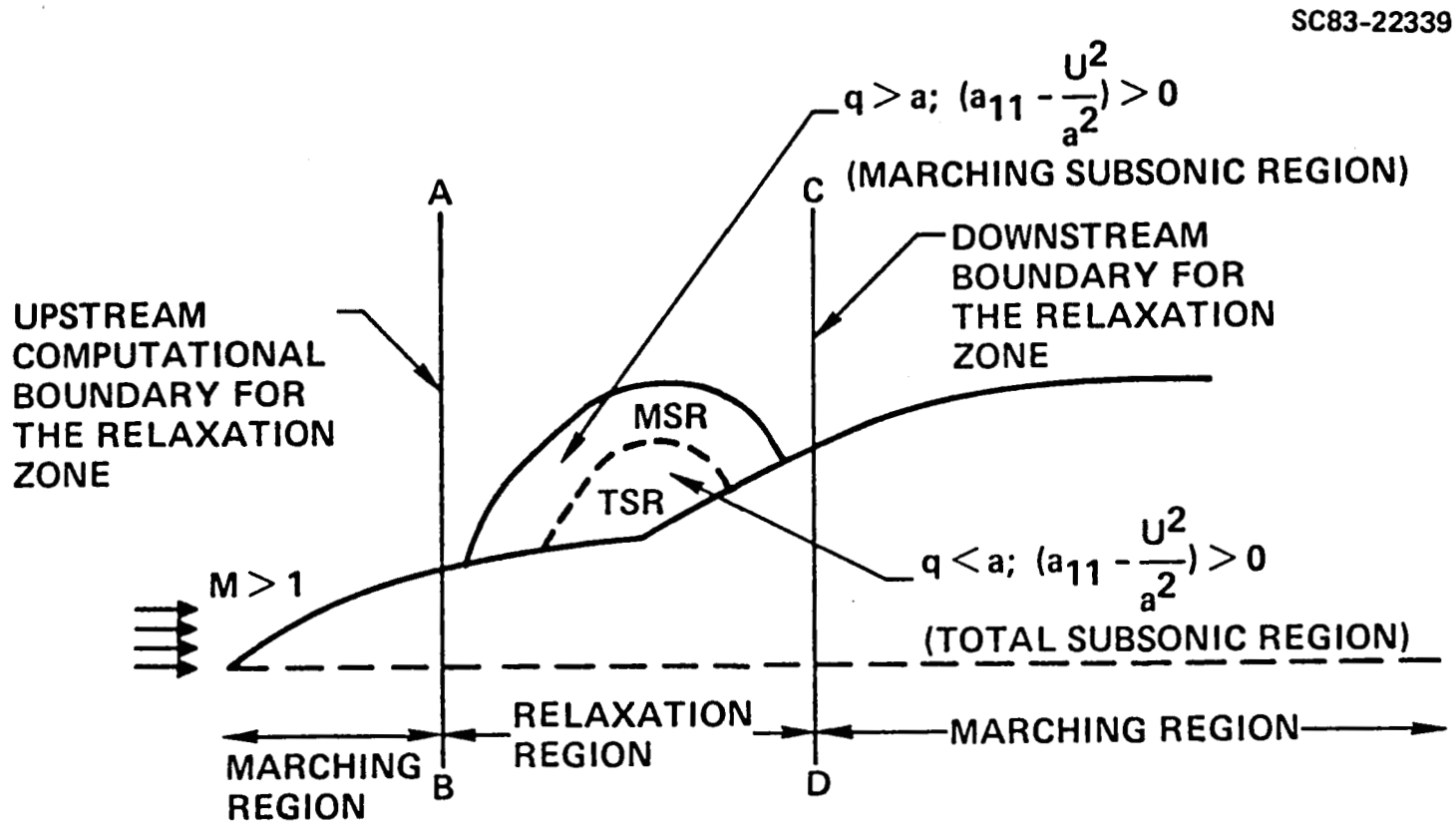

Rockwell International
Science Center

ROLE OF CHARACTERISTICS IN DEFINING SUPERSONIC REGION, MARCHING SUBSONIC REGION (MSR), AND TOTAL SUBSONIC REGION (TSR)

SC83-22352

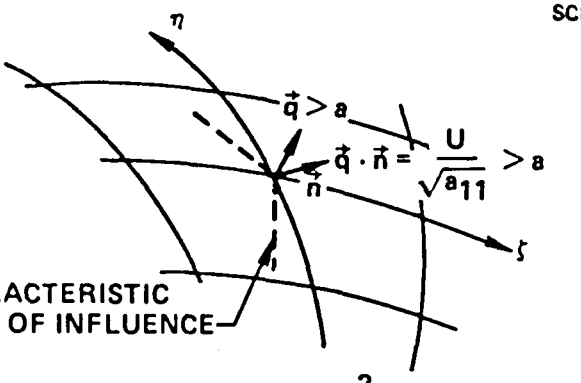

a) PURE SUPERSONIC REGION, $(a_{11} - \frac{U^2}{a^2}) < 0$.
MARCHING ALONG ζ IS VALID.

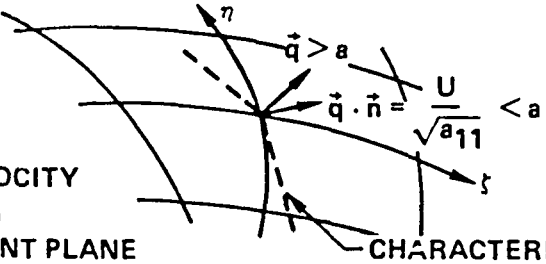

$\vec{q}$ = TOTAL VELOCITY
$\vec{n}$ = NORMAL TO
ζ = CONSTANT PLANE
a = SPEED OF SOUND

b) MARCHING SUBSONIC REGION (MSR), $(a_{11} - \frac{U^2}{a^2}) > 0$, $q > a$.
MARCHING ALONG ζ IS NOT VALID.

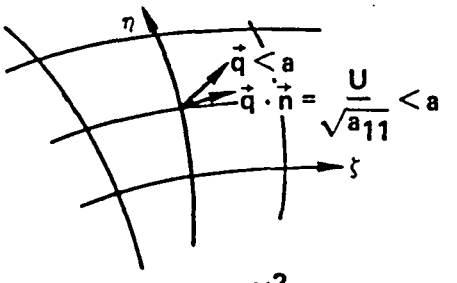

c) TOTAL SUBSONIC REGION (TSR), $(a_{11} - \frac{U^2}{a^2}) > 0$, $q < a$.
COMPLEX CHARACTERISTICS.

Rockwell International
Science Center

SWITCHING OPERATOR FOR $(\rho \frac{U}{J})_\zeta$

$$\frac{\partial}{\partial \zeta}\left(\rho \frac{U}{J}\right) = \theta_i \underbrace{\frac{\overleftarrow{\partial}}{\partial \zeta}\left(\rho \frac{U}{J}\right)_{i+1}}_{\text{SUPERSONIC}}$$

$$+ (1 - \theta_{i+1}) \underbrace{\frac{\overrightarrow{\partial}}{\partial \zeta}\left(\tilde{\rho} \frac{U}{J}\right)_{i+1}}_{\substack{\text{MARCHING} \\ \text{SUBSONIC}}}$$

WHERE

$\overleftarrow{\partial}$ REFERS TO BACKWARD DIFFERENCING

$\overrightarrow{\partial}$ REFERS TO FORWARD DIFFERENCING

$$\theta_i = 1 \text{ IF } \left(a_{11} - \frac{U^2}{a^2}\right) < 0$$

$$= 0 \text{ IF } \left(a_{11} - \frac{U^2}{a^2}\right) > 0$$

FLUX BIASING CONCEPT

$$\frac{\partial}{\partial \zeta}\left(\rho \frac{U}{J}\right) = \underbrace{\frac{\overrightarrow{\partial}}{\partial \zeta}\left(\rho \frac{U}{J}\right)_{i+1}}_{\substack{\text{ELLIPTIC} \\ \text{OPERATOR}}}$$

$$\underbrace{- \Delta\zeta \frac{\overleftarrow{\partial}}{\partial \zeta} \theta_{i+1} \frac{\overleftarrow{\partial}}{\partial \zeta}\left(\rho \frac{U}{J}\right)_{i+2}}_{\substack{\text{FLUX BIASING TO PRODUCE} \\ \text{THE ARTIFICAL VISCOSITY}}}$$

Rockwell International
Science Center

CONSERVATIVE TYPE-DEPENDENT SWITCHING SCHEME FOR THE TREATMENT OF SUBSONIC BUBBLE IN A SUPERSONIC FLOW

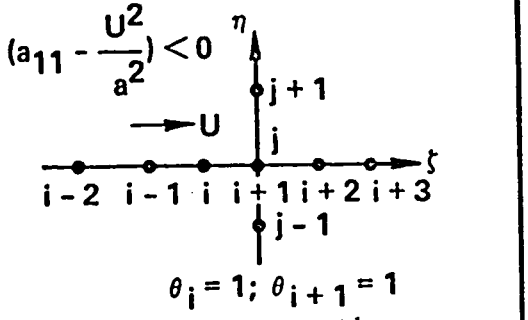

$\frac{\delta}{\delta\zeta}(\frac{\rho U}{J}) = \frac{\overleftarrow{\delta}}{\delta\zeta}(\frac{\rho U}{J})_{i+1}$ (FROM EQ. 10)

a) SUPERSONIC UPWIND OPERATOR

SC83-22353

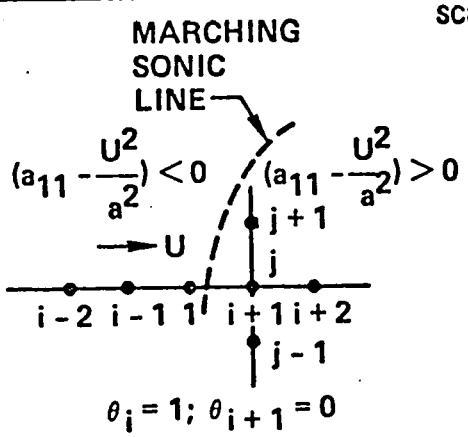

$\frac{\delta}{\delta\zeta}(\frac{\rho U}{J}) = \frac{\overleftarrow{\delta}}{\delta\zeta}(\frac{\rho U}{J})_{i+1} + \frac{\overrightarrow{\delta}}{\delta\zeta}(\frac{\widetilde{\rho U}}{J})_{i+1}$

b) BEGINING OF SUBSONIC BUBBLE.

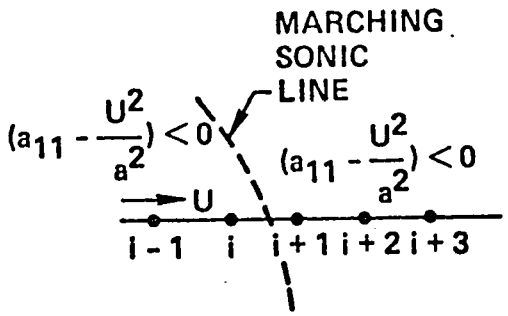

$\frac{\delta}{\delta\zeta}(\frac{\rho U}{J}) = 0$

c) END OF SUBSONIC BUBBLE.

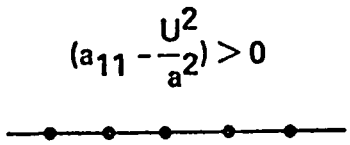

$\theta_i = 0;\ \theta_{i+1} = 0$

$\frac{\delta}{\delta\zeta}(\frac{\rho U}{J}) = \frac{\overrightarrow{\delta}}{\delta\zeta}(\frac{\widetilde{\rho U}}{J})_{i+1}$

d) PURE SUBSONIC REGION. CENTRAL DIFFERENCE OPERATOR (ϕ_ζ IS BACKWARD DIFFERENCED)

Rockwell International
Science Center

SUPERSONIC AND MARCHING SUBSONIC OPERATORS

SUPERSONIC

$$\frac{\overleftarrow{\partial}}{\partial\zeta}\left(\rho\frac{U}{J}\right)_{i+1} \doteq \frac{\overleftarrow{\partial}}{\partial\zeta}\rho_i\left[\left(a_{11}-\frac{U^2}{a^2}\right)_i\frac{\overleftarrow{\partial}}{\partial\zeta}\Delta\phi + \left(a_{12}-\frac{UV}{a^2}\right)_i\frac{\partial}{\partial\eta}\Delta\phi + \left(a_{13}-\frac{UW}{a^2}\right)\frac{\partial}{\partial\xi}\Delta\phi + U_i\right],$$

$$\Delta\phi = (\phi_{i+1}-\phi_i).$$

MARCHING SUBSONIC

$$\frac{\overrightarrow{\partial}}{\partial\zeta}\tilde{\rho}\frac{U}{J}_{i+1} \doteq \frac{\overrightarrow{\partial}}{\partial\zeta}\left[\frac{\tilde{\rho}^{n+1}_{i+1}}{J}\left(a_{11}\overleftarrow{\phi_\zeta}+a_{12}\phi_\eta+a_{13}\phi_\xi\right)_{i+1}\right]$$

WHERE

$$\tilde{\rho}^{n+1}_{i+1} = \rho^{n}_{i+1} - \nu(\rho^{n}_{i+1}-\rho^{n}_{i}), \text{ FOR } U>0$$

$$\nu = \text{MAX}\left(0, 1-\frac{a^2}{q^2}\right).$$

Rockwell International
Science Center

TREATMENT OF $(\rho \frac{V}{J})_\eta$

$$\frac{\partial}{\partial \eta}\left(\rho \frac{V}{J}\right) = \theta_{i+1} \underbrace{\frac{\overleftarrow{\partial}}{\partial \eta}\left(\bar{\rho} \frac{V}{J}\right)_{j+\frac{1}{2}}}_{\text{SUPERSONIC}} + (1 - \theta_{i+1}) \underbrace{\frac{\overleftarrow{\partial}}{\partial \eta}\left(\tilde{\rho} \frac{V}{J}\right)_{j+\frac{1}{2}}}_{\substack{\text{MARCHING} \\ \text{SUBSONIC}}}$$

WHERE

$$\theta_{i+1} = 1 \text{ IF } \left(a_{11} - \frac{U^2}{a^2}\right)_{i+1} < 0 \quad \text{(SUPERSONIC POINT)}$$

$$= 0 \text{ IF } \left(a_{11} - \frac{U^2}{a^2}\right)_{i+1} \geq 0 \quad \text{(MSR)}$$

DENSITY BIASING

$$\bar{\rho}_{j+\frac{1}{2}} = (1 - \bar{\nu}_{j+\frac{1}{2}})\rho^*_{j+\frac{1}{2}} + \frac{1}{2}\bar{\nu}_{j+\frac{1}{2}}(\rho^*_j + \rho^*_{j-1})$$

WHERE

$$\bar{\nu} = \text{MAX}\left(0, 1 - a_{22}\frac{a^2}{V^2}\right) .$$

$$\tilde{\rho}^{n+1}_{j+\frac{1}{2}} = (1 - \tilde{\nu}_{j+\frac{1}{2}})\rho^n_{j+\frac{1}{2}} + \frac{1}{2}\tilde{\nu}_{j+\frac{1}{2}}(\rho^n_j + \rho^n_{j-1})$$

WHERE $\tilde{\nu} = \text{MAX}\left(0, 1 - \frac{a^2}{q^2}\right)$

Rockwell International
Science Center

IMPLICIT APPROXIMATE FACTORIZATION

$$\left[1+\frac{A_3}{\beta\Delta\zeta}\frac{\partial}{\partial\xi}+\frac{1}{\beta}\frac{\partial}{\partial\xi}\left(\frac{\hat{\rho}}{J}\frac{a_{31}}{\Delta\zeta}\right)+\frac{1}{\beta}\frac{\partial}{\partial\xi}\frac{\hat{\rho}a_{33}}{J}\frac{\partial}{\partial\xi}\right]$$

$$L_\xi L_\eta(\Delta\phi) = R$$

$$\times\left[1+\frac{A_2}{\beta\Delta\zeta}\frac{\partial}{\partial\eta}+\frac{1}{\beta}\frac{\partial}{\partial\eta}\frac{\hat{\rho}a_{21}}{J\Delta\zeta}\right.$$

$$\left.+\frac{1}{\beta}\frac{\partial}{\partial\eta}\frac{\hat{\rho}a_{22}}{J}\frac{\partial}{\partial\eta}\right]\Delta\phi = R\,.$$

$$L_\xi(\Delta\phi)^* = R \quad L_\eta(\Delta\phi) = (\Delta\phi)^* \quad \phi_{i+1} = \phi_i + \Delta\phi\ .$$

$$\beta = \frac{1}{\Delta\zeta^2}\left[\theta_i A_1 - (1-\theta_{i+1})\frac{\Delta\zeta}{\Delta\zeta_0}\left(\frac{\tilde{\rho}a_{11}}{J}\right)_{i+1}\right]$$

$$A_1 = \frac{\rho_i}{J_{i+1}}\left(a_{11}-\frac{U^2}{a^2}\right)$$

$$A_2 = \theta_i\left[\frac{\rho_i}{J_{i+1}}\left(a_{12}-\frac{UV}{a^2}\right)\right] - (1-\theta_{i+1})\frac{\Delta\zeta}{\Delta\zeta_0}\left(\frac{\tilde{\rho}a_{12}}{J}\right)_{i+1}$$

$$A_3 = \theta_i\left[\frac{\rho_i}{J_{i+1}}\left(a_{13}-\frac{UW}{a^2}\right)\right] - (1-\theta_{i+1})\frac{\Delta\zeta}{\Delta\zeta_0}\left(\frac{\tilde{\rho}a_{13}}{J}\right)_{i+1}$$

$$\Delta\zeta_0 = \zeta_{i+2} - \zeta_{i+1}$$

$$\Delta\zeta = \zeta_{i+1} - \zeta_i$$

Rockwell International
Science Center

AXIAL SURFACE PRESSURE DISTRIBUTION FOR A DEVELOPED CROSS-SECTION FOREBODY; $M_\infty = 1.7$, $\alpha = -5^o$

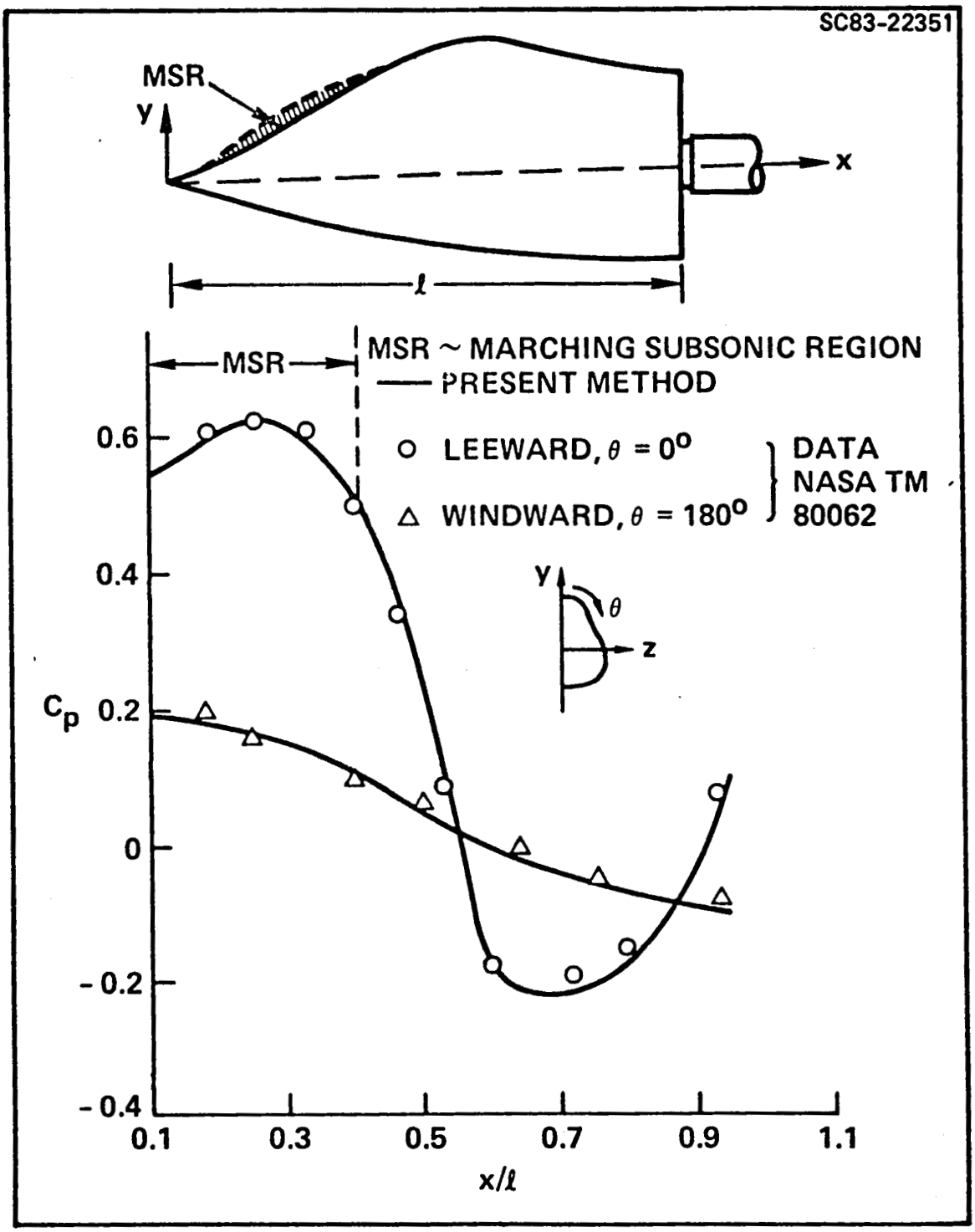

Rockwell International
Science Center

CIRCUMFERENTIAL PRESSURE DISTRIBUTION FOR A DEVELOPED CROSS-SECTION FOREBODY; $M_\infty = 1.7$, $\alpha = -5^o$, $x/\ell = 0.28$

SC83-22350

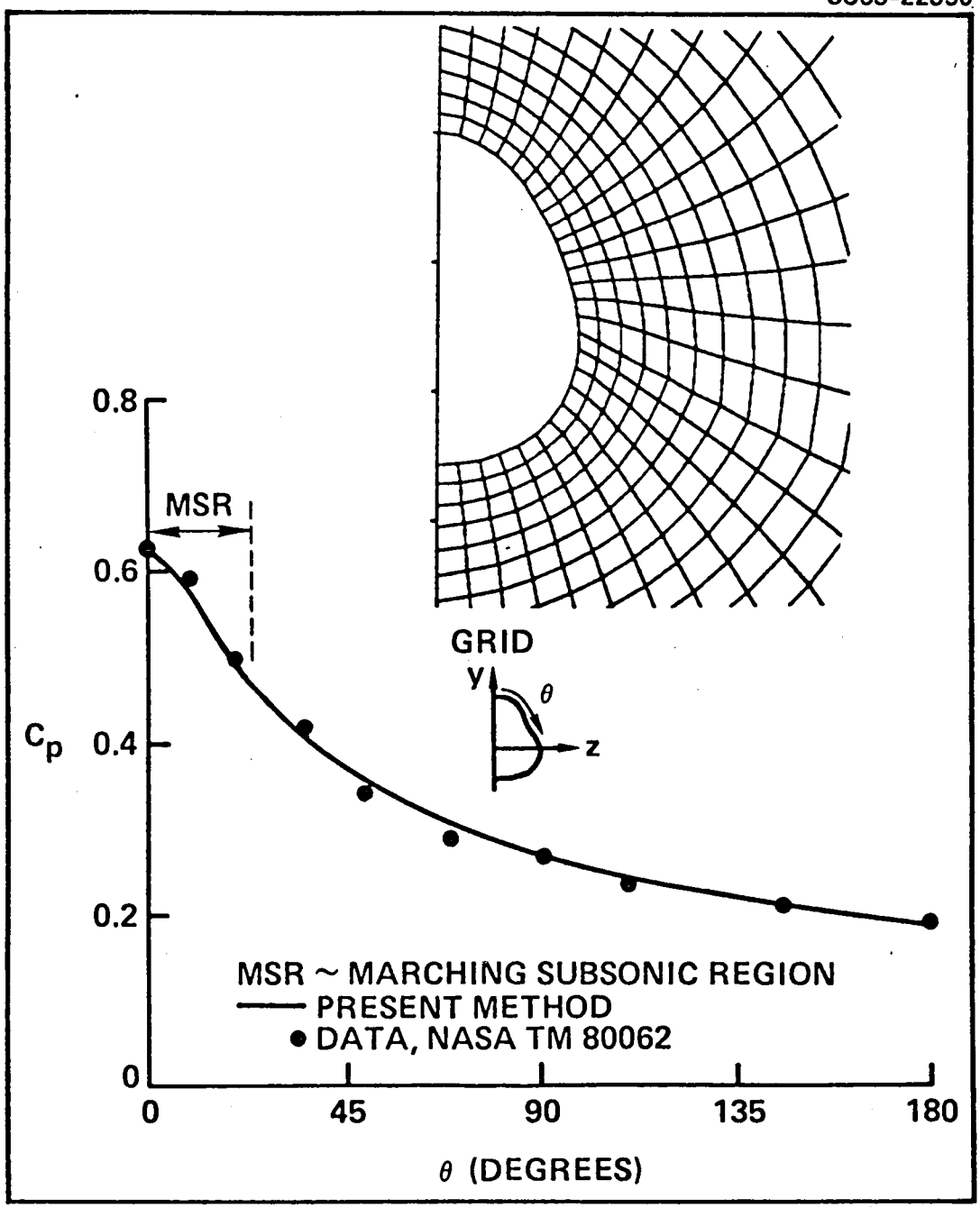

Rockwell International
Science Center

NUMERICAL APPROACH TO DRAG AND LIFT ESTIMATES

SC82-19737

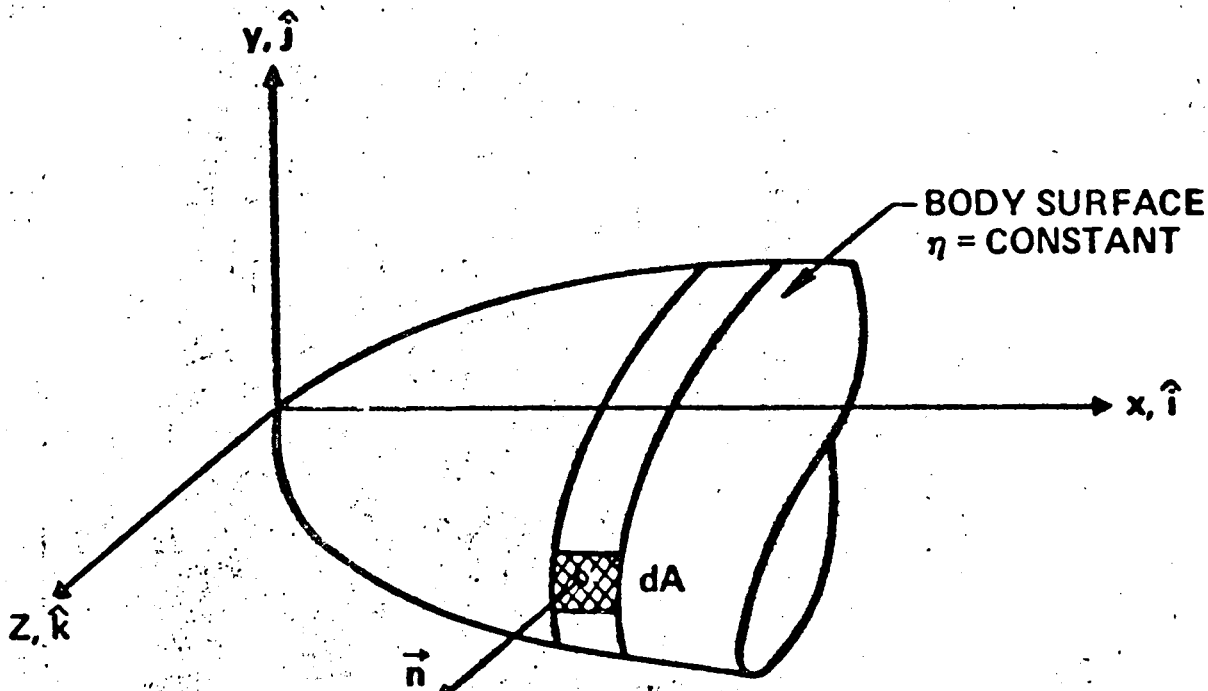

$$\vec{n} = \frac{\eta_x \hat{i} + \eta_y \hat{j} + \eta_z \hat{k}}{\sqrt{\eta_x^2 + \eta_y^2 + \eta_z^2}}$$

ELEMENTAL AREA (dA) CALCULATION

SC83-21579

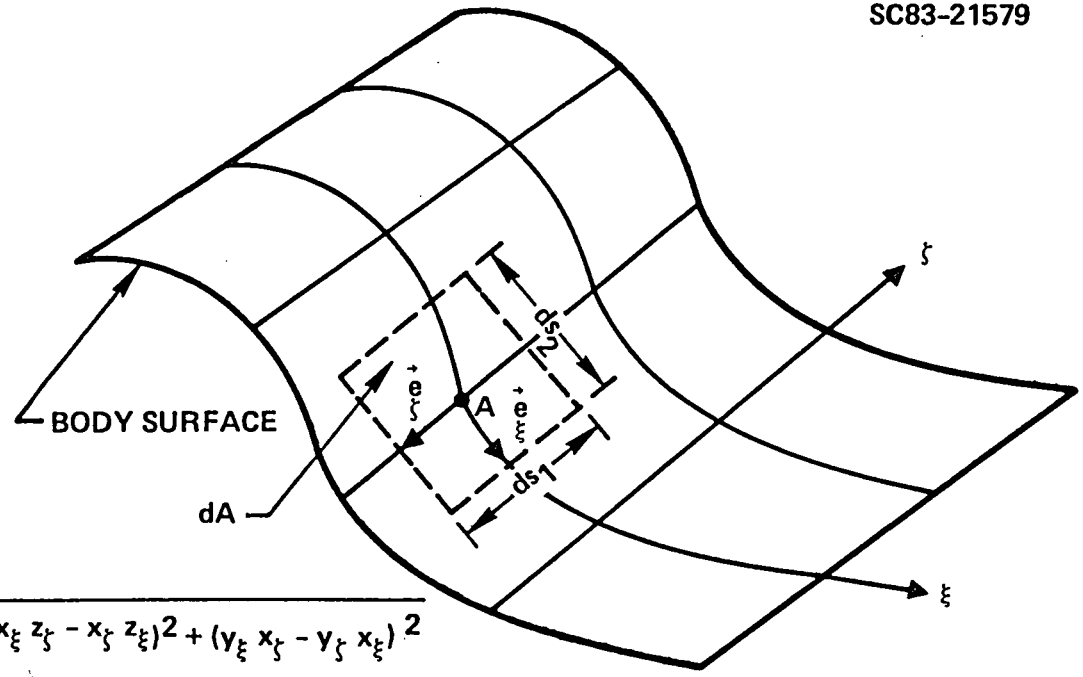

$$\vec{e}_\zeta = (x_\zeta \hat{i} + y_\zeta \hat{j} + z_\zeta \hat{k}) / \sqrt{x_\zeta^2 + y_\zeta^2 + z_\zeta^2}$$

$$\vec{e}_\xi = (x_\xi \hat{i} + y_\xi \hat{j} + z_\xi \hat{k}) / \sqrt{x_\xi^2 + y_\xi^2 + z_\xi^2}$$

$$ds_1 = \sqrt{x_\zeta^2 + y_\zeta^2 + z_\zeta^2}\ d\zeta$$

$$ds_2 = \sqrt{x_\xi^2 + y_\xi^2 + z_\xi^2}\ d\xi$$

$$dA = ds_1 \vec{e}_\zeta \times ds_2 \vec{e}_\xi = d_\zeta\, d_\xi \sqrt{(y_\zeta z_\xi - z_\zeta y_\xi)^2 + (x_\xi z_\zeta - x_\zeta z_\xi)^2 + (y_\xi x_\zeta - y_\zeta x_\xi)^2}$$

$$C_y = \frac{-1}{A_{REF}} \Sigma\ C_p\, (\eta_y / \sqrt{\eta_x^2 + \eta_y^2 + \eta_z^2})\, dA$$

$$C_x = \frac{-1}{A_{REF}} \Sigma\ C_p\, (\eta_x / \sqrt{\eta_x^2 + \eta_y^2 + \eta_z^2})\, dA$$

$$C_\ell = C_y \cos\alpha - C_x \sin\alpha$$

$$C_d = C_y \sin\alpha + C_x \cos\alpha$$

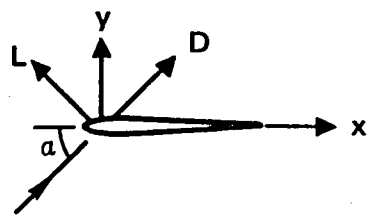

Rockwell International
Science Center

GRIDDING FOR A DOUBLE WEDGED DELTA WING

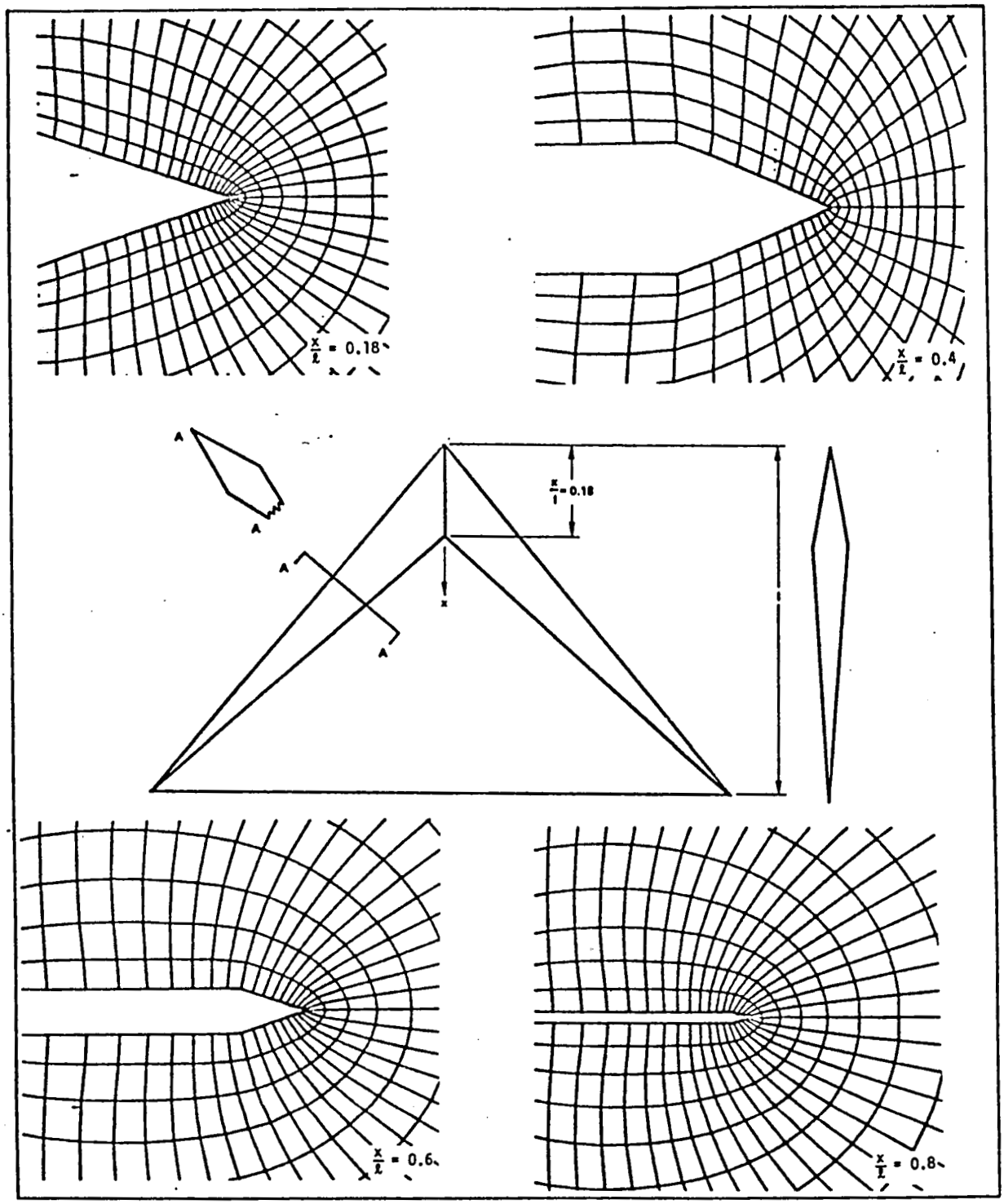

Rockwell International
Science Center

PRESSURE CONTOURS AT $x/\ell = 0.4$ FOR THE DELTA WING AT $M_\infty = 1.92$

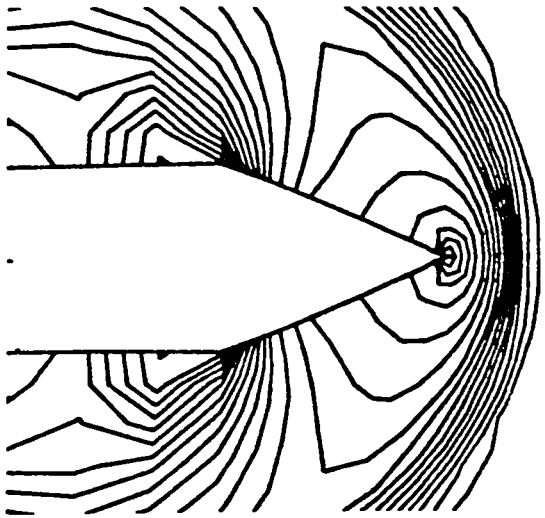

MINIMUM DRAG COEFFICIENTS FOR THE DELTA WING

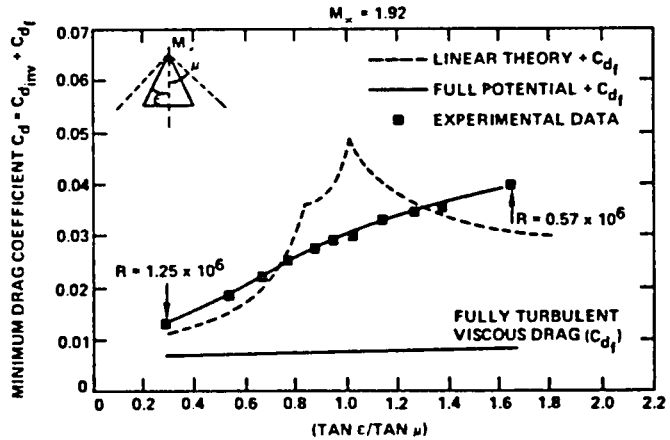

Rockwell International
Science Center

DRAG PREDICTION FOR A DOUBLE WEDGE DELTA WING AT $M_\infty = 1.62$, $\alpha = 0^o$

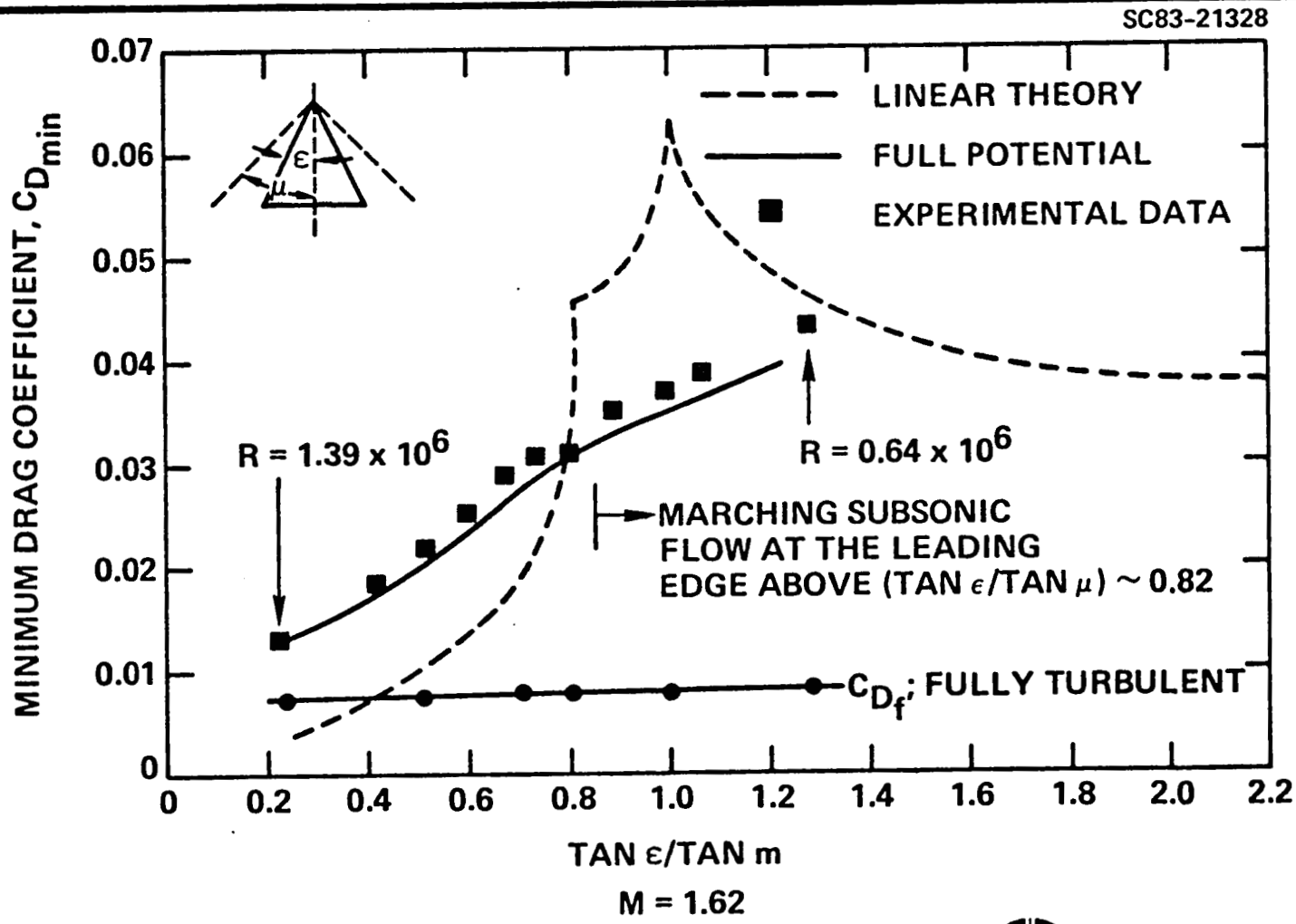

Rockwell International
Science Center

WAKE BOUNDARY CONDITION

SC83-22341

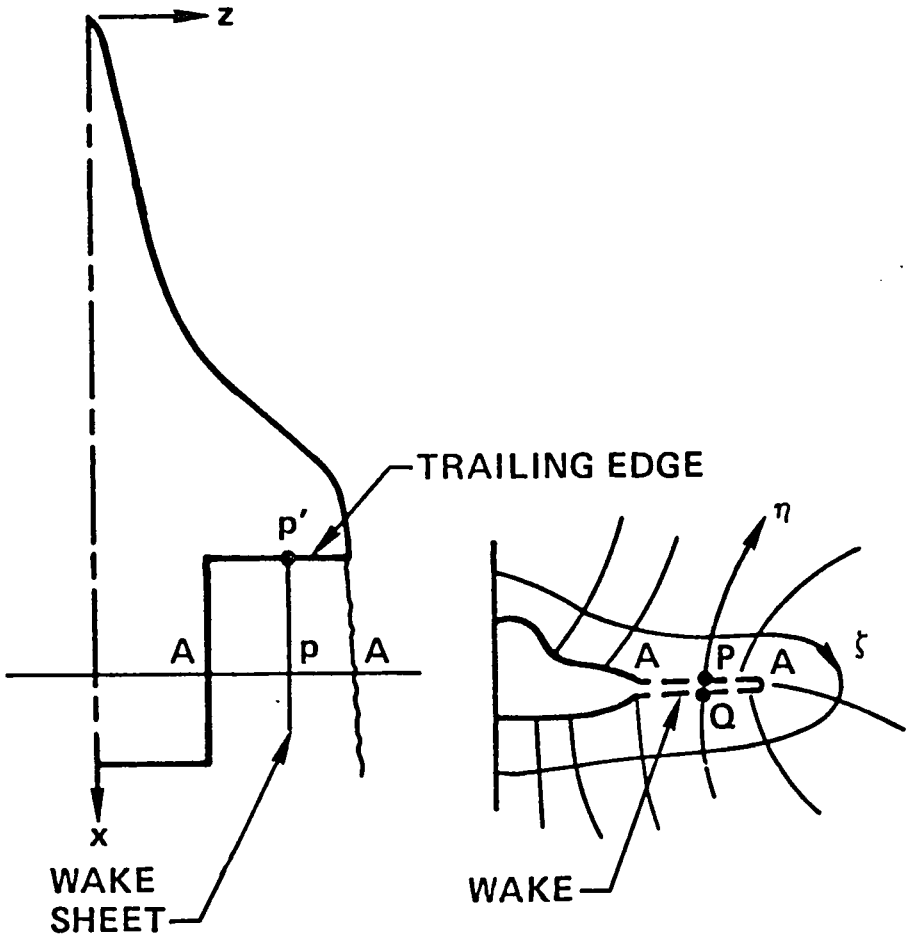

WAKE MODEL

$\phi_P - \phi_Q = \phi_{P'} - \phi_{Q'}$ (JUMP IN ϕ)

$(\phi_\zeta)_P - (\phi_\zeta)_Q \doteq 0$

$(\phi_\eta)_P - (\phi_\eta)_Q \doteq 0 \rightarrow (\phi_{\eta\eta})_P = 0$

Rockwell International
Science Center

SCHEMATIC OF AN ARROW WING

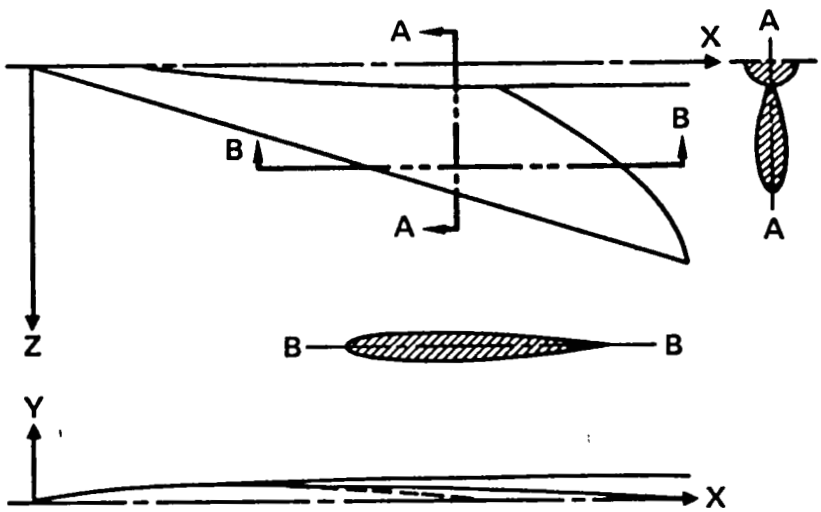

ARROW-WING CALCULATION, $M_\infty = 2.96$, $\alpha = 10^o$

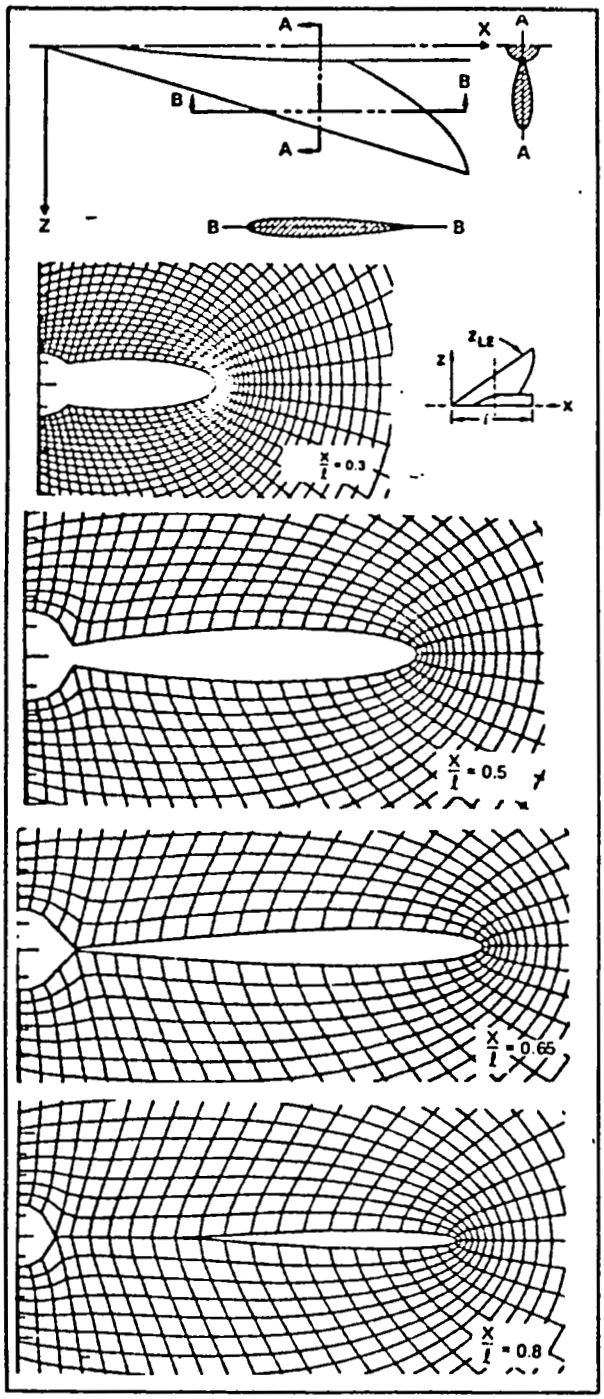

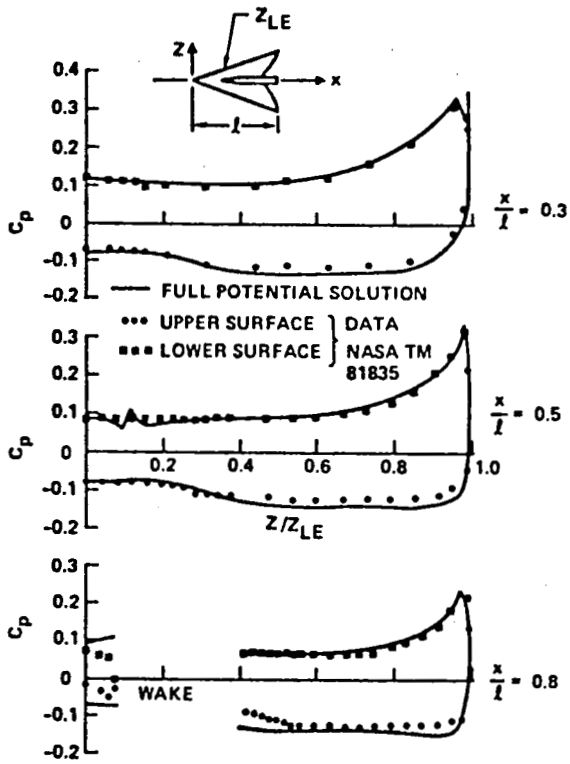

Rockwell International
Science Center

NO WAKE MODEL

PRESSURE PROFILES

$M = 2.96$, $\alpha = 10.01^{\circ}$, $\frac{x}{\ell} = 0.8$

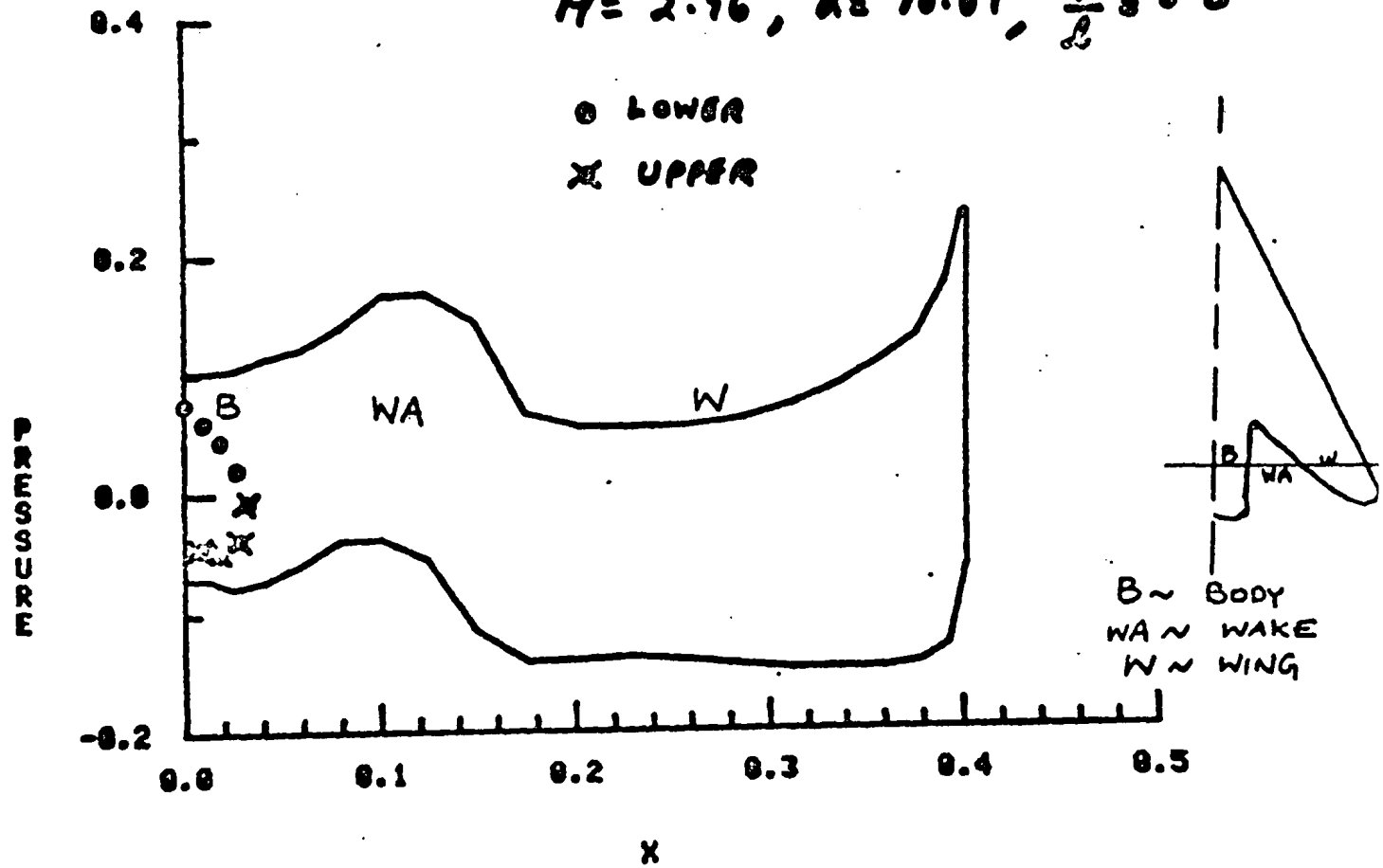

WAKE MODEL

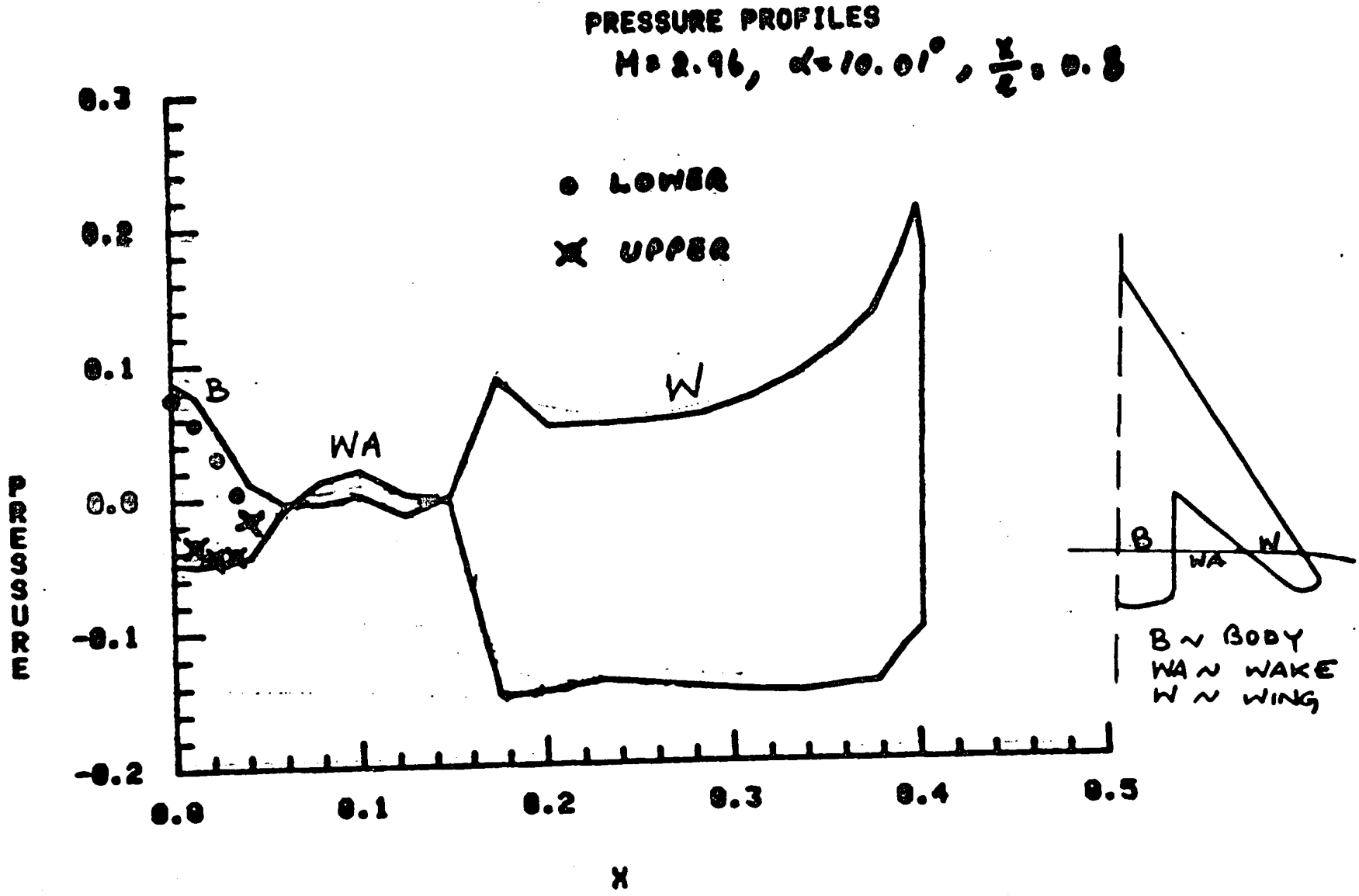

516

SUPERSONIC FIGHTER WITH AN EMBEDDED MARCHING SUBSONIC REGION NEAR THE LEADING EDGE

SC83-22343

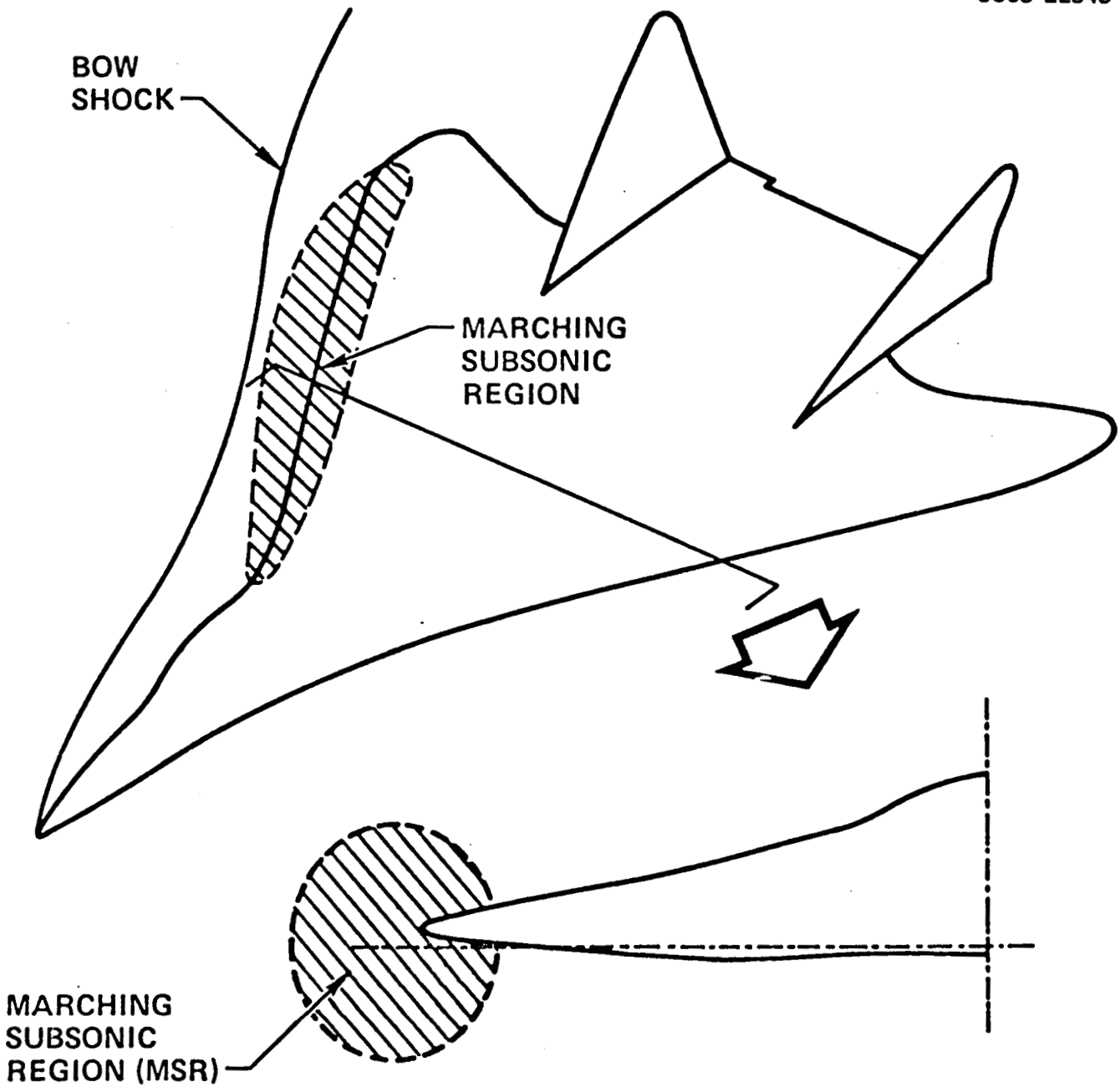

Rockwell International
Science Center

PRESSURE DISTRIBUTION ON A FIGHTER-LIKE CONFIGURATION, $M_\infty = 1.6$, $\alpha = 5^o$

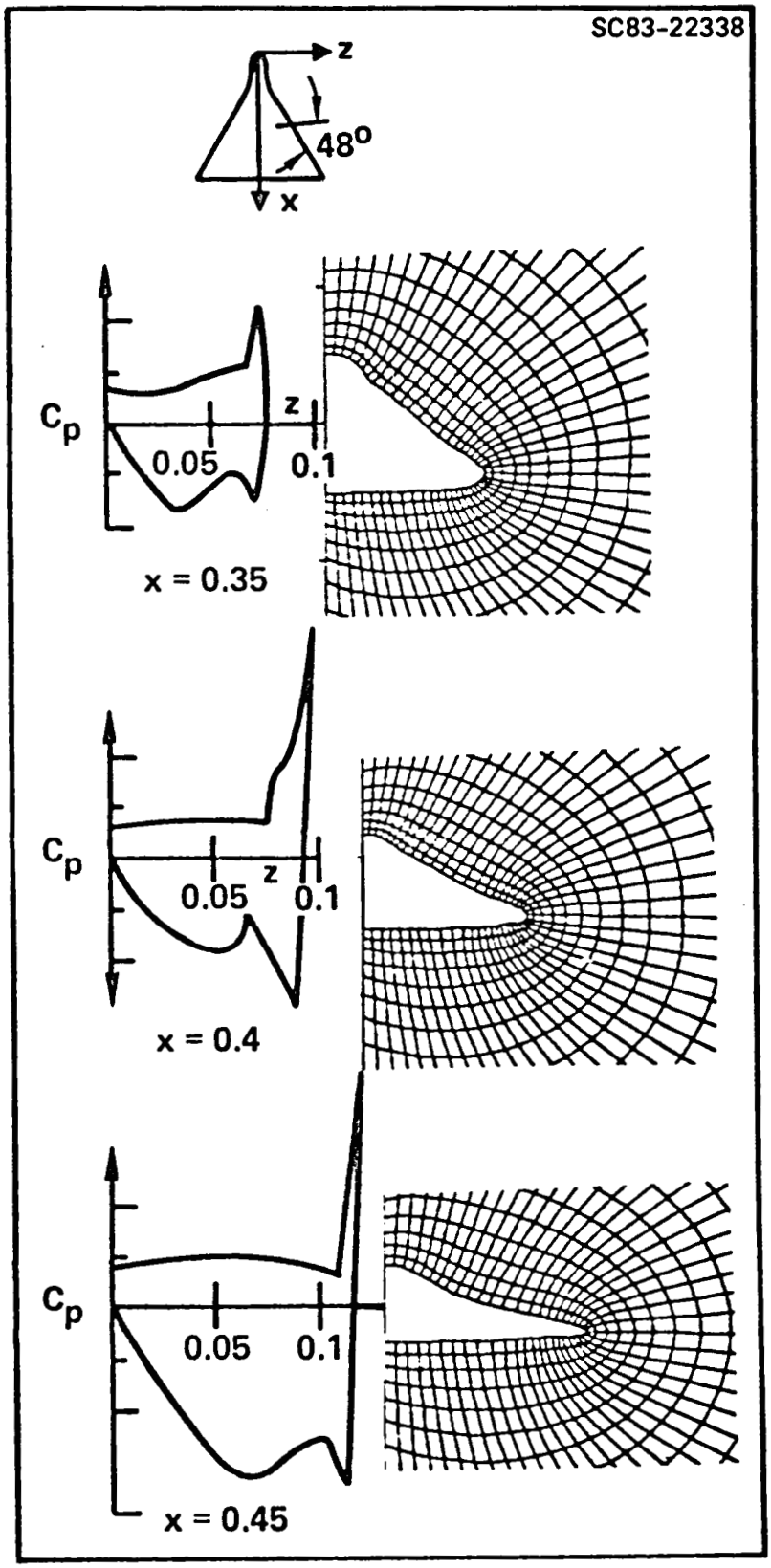

Rockwell International
Science Center

GRID AND PRESSURE DISTRIBUTION IN THE WAKE REGION; $M_\infty = 1.6, \alpha = 5^o$

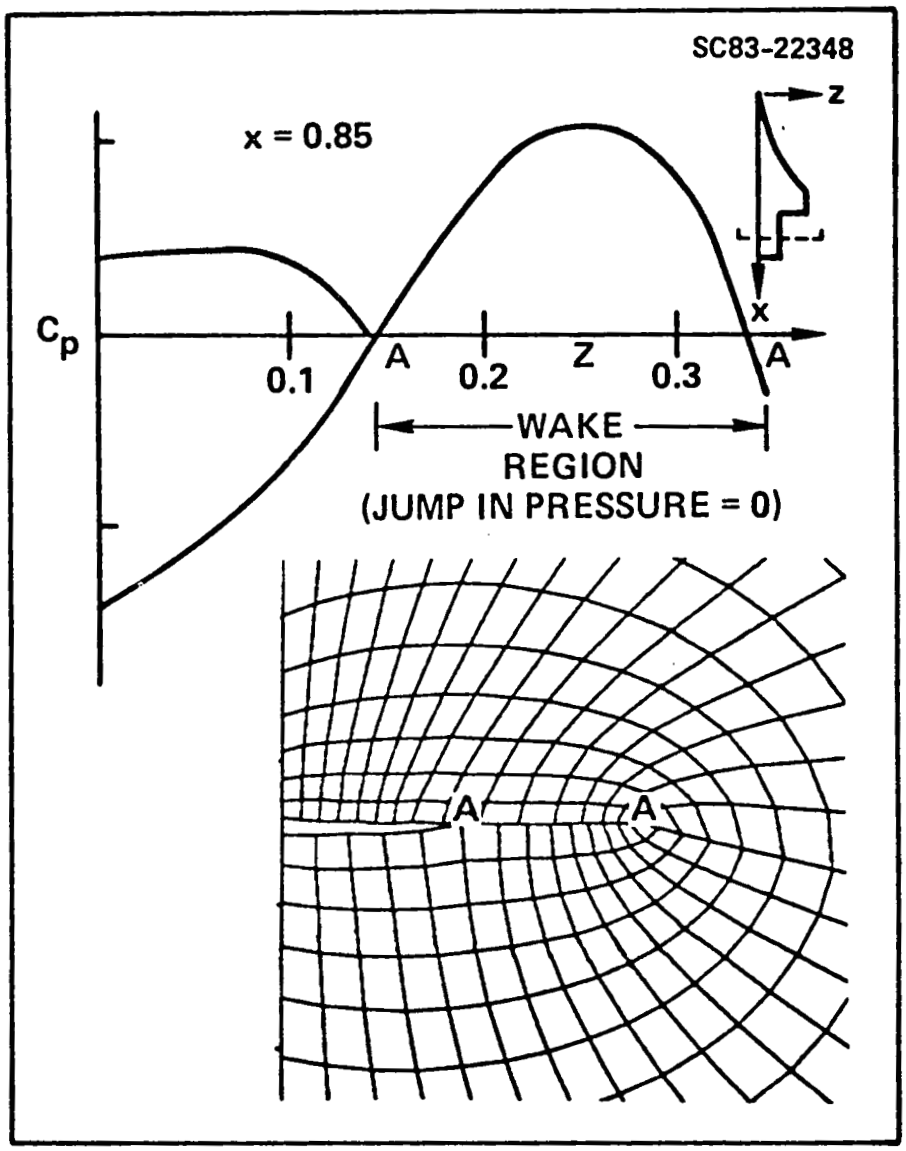

Rockwell International
Science Center

WING-TAIL-WAKE TREATMENT

SC83-22807

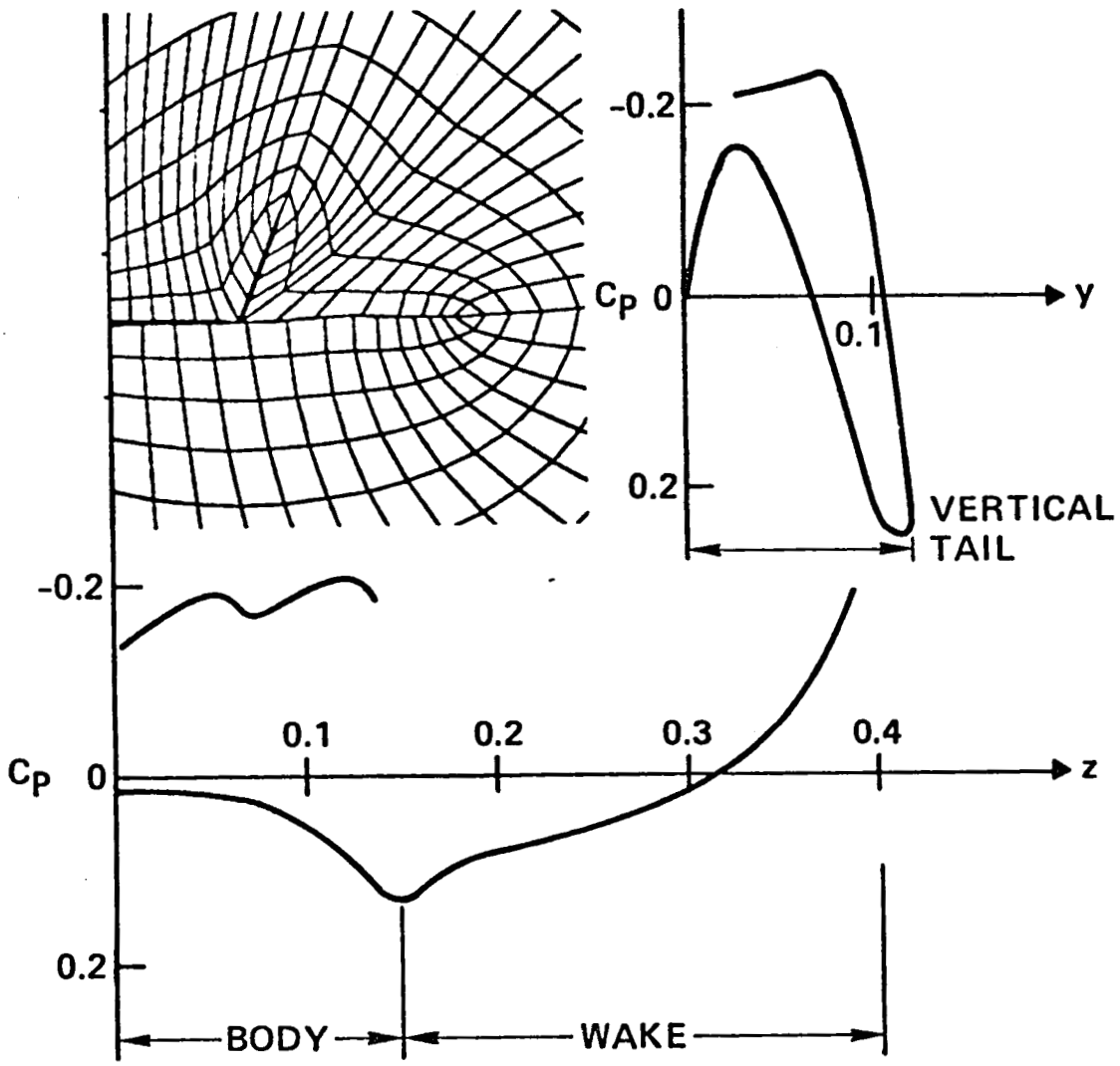

Rockwell International
Science Center

ADVANCED TACTICAL FIGHTER GEOMETRY

SC83-24366

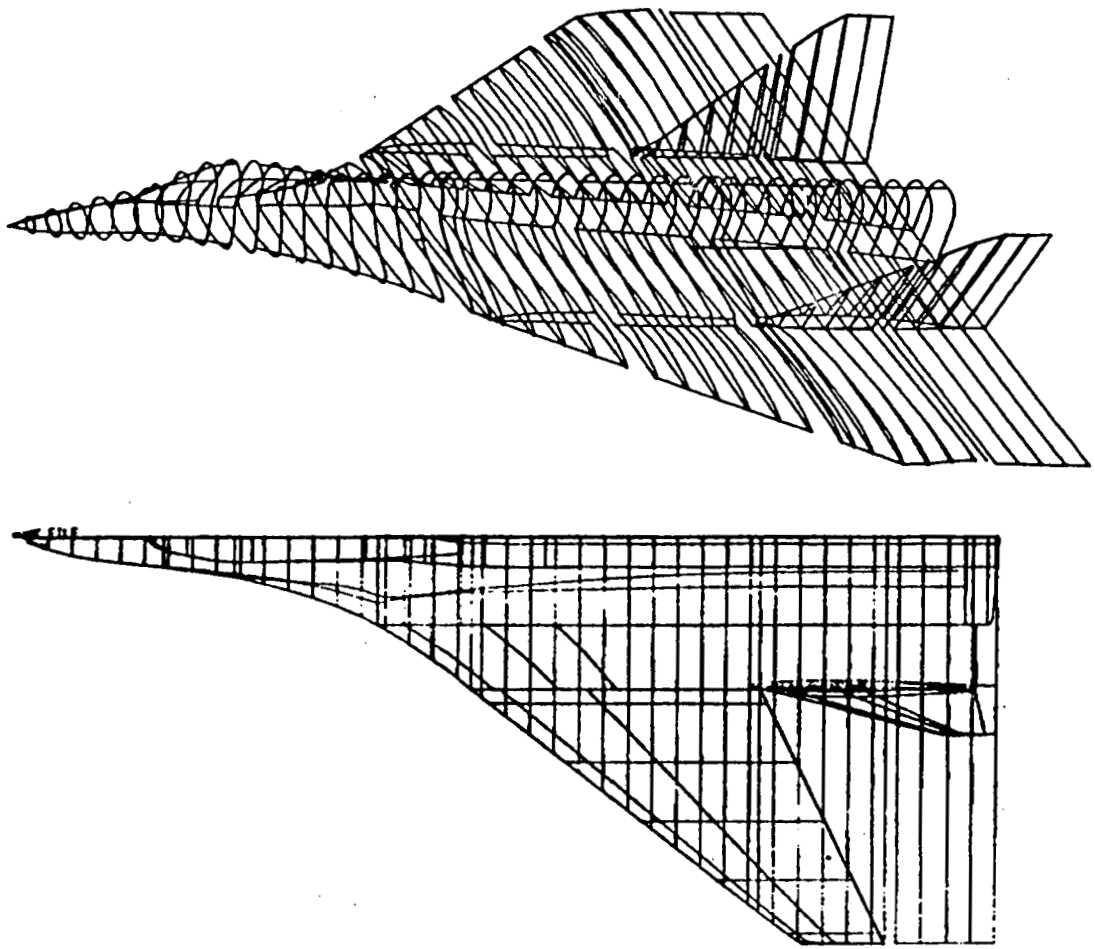

Rockwell International
Science Center

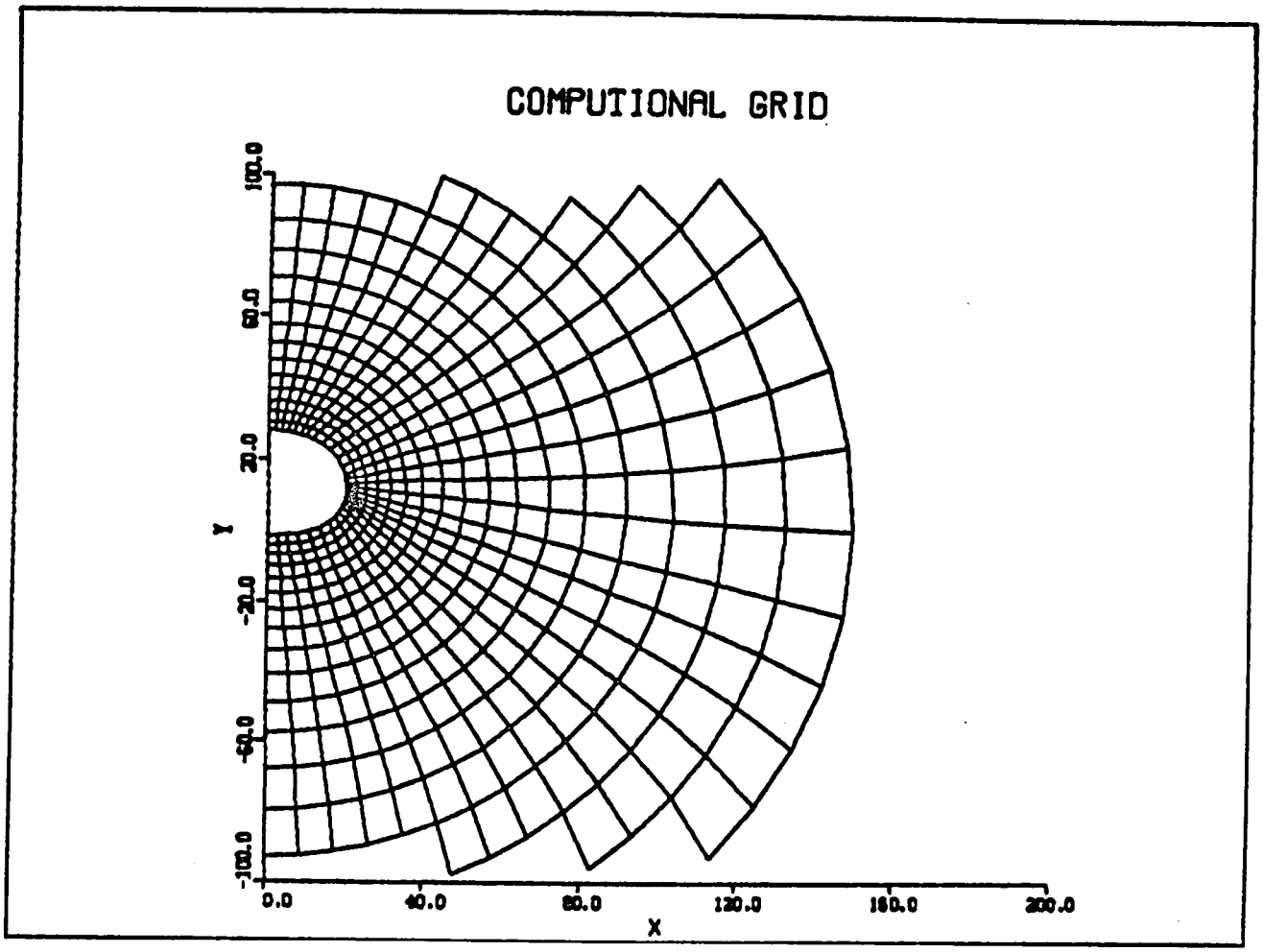
COMPUTIONAL GRID
100.0
60.0
20.0
-20.0
-60.0
-100.0
Y
0.0
40.0
80.0
120.0
160.0
200.0
X

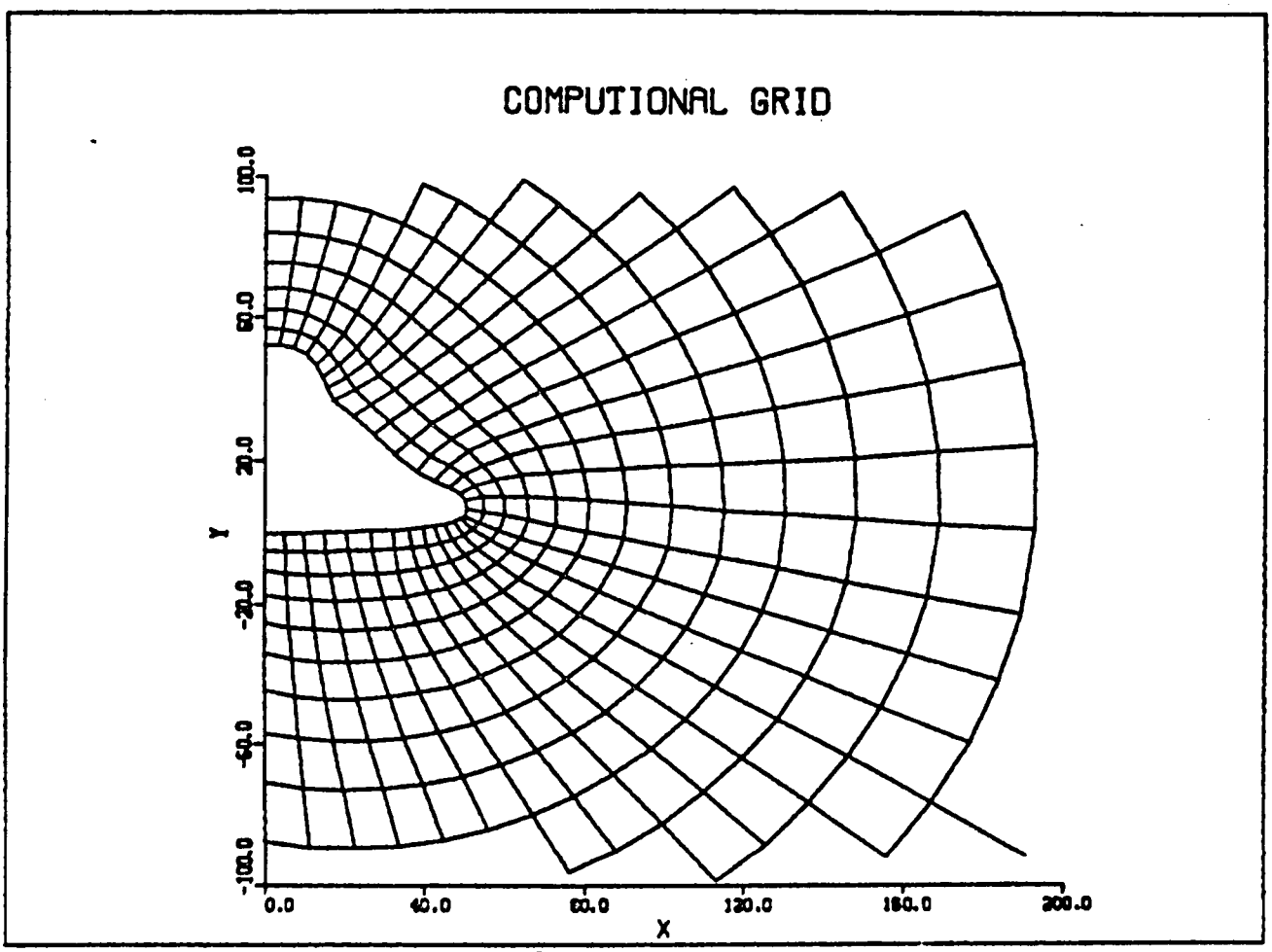
COMPUTIONAL GRID
100.0
60.0
20.0
-20.0
-60.0
-100.0
Y
0.0
40.0
80.0
120.0
160.0
200.0
X

COMPUTIONAL GRID

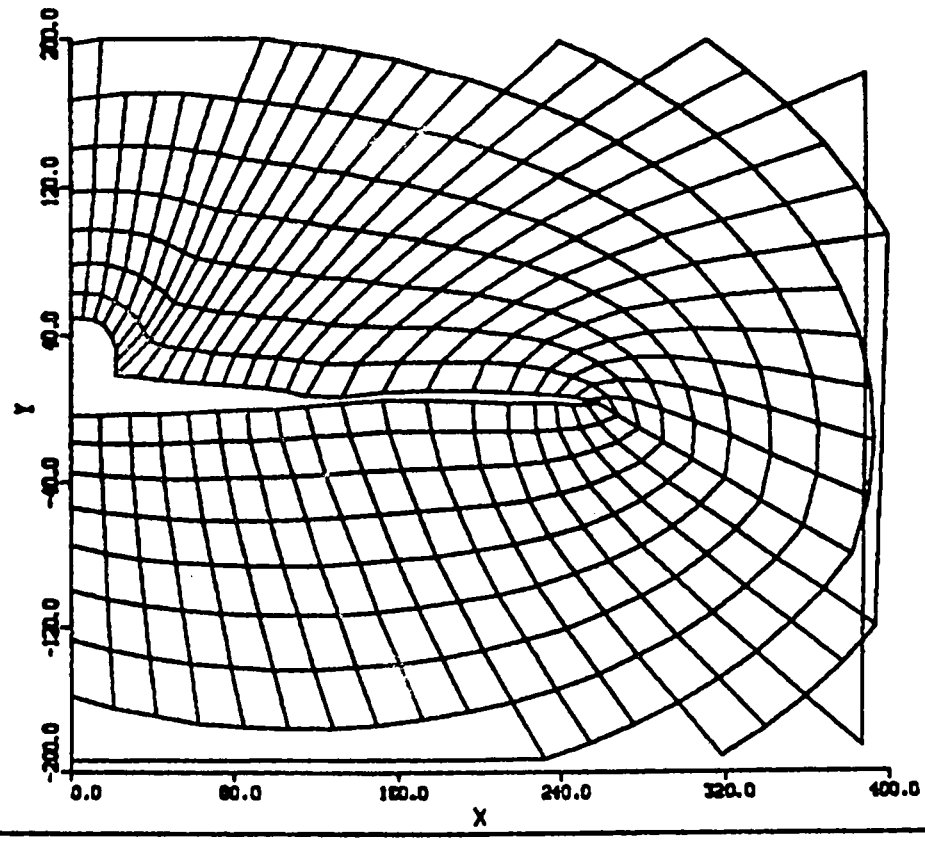

COMPUTIONAL GRID

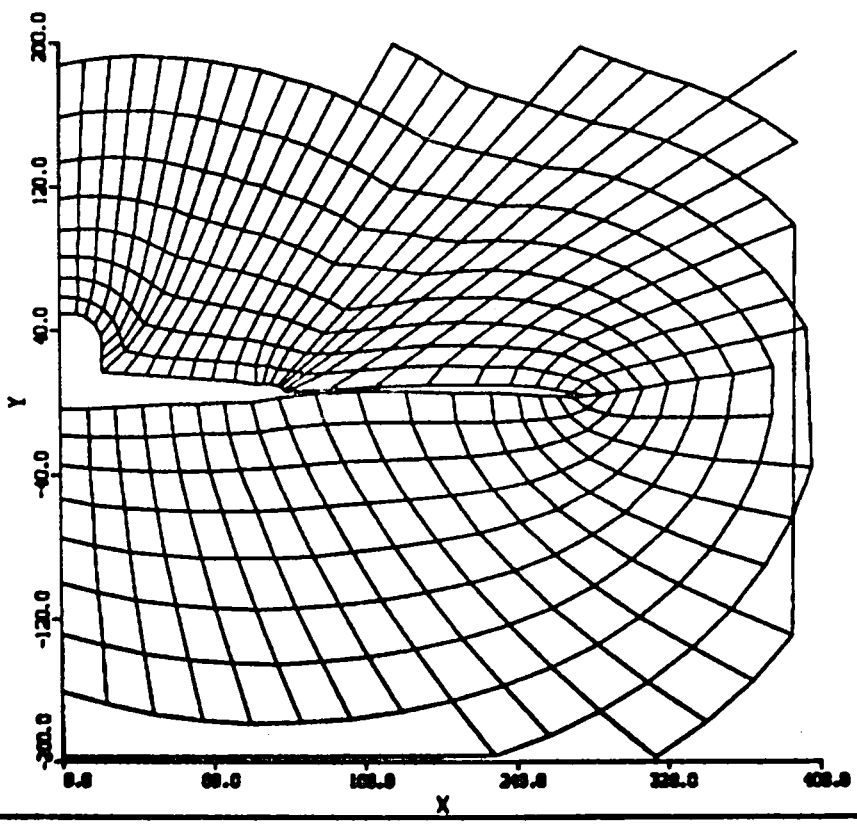

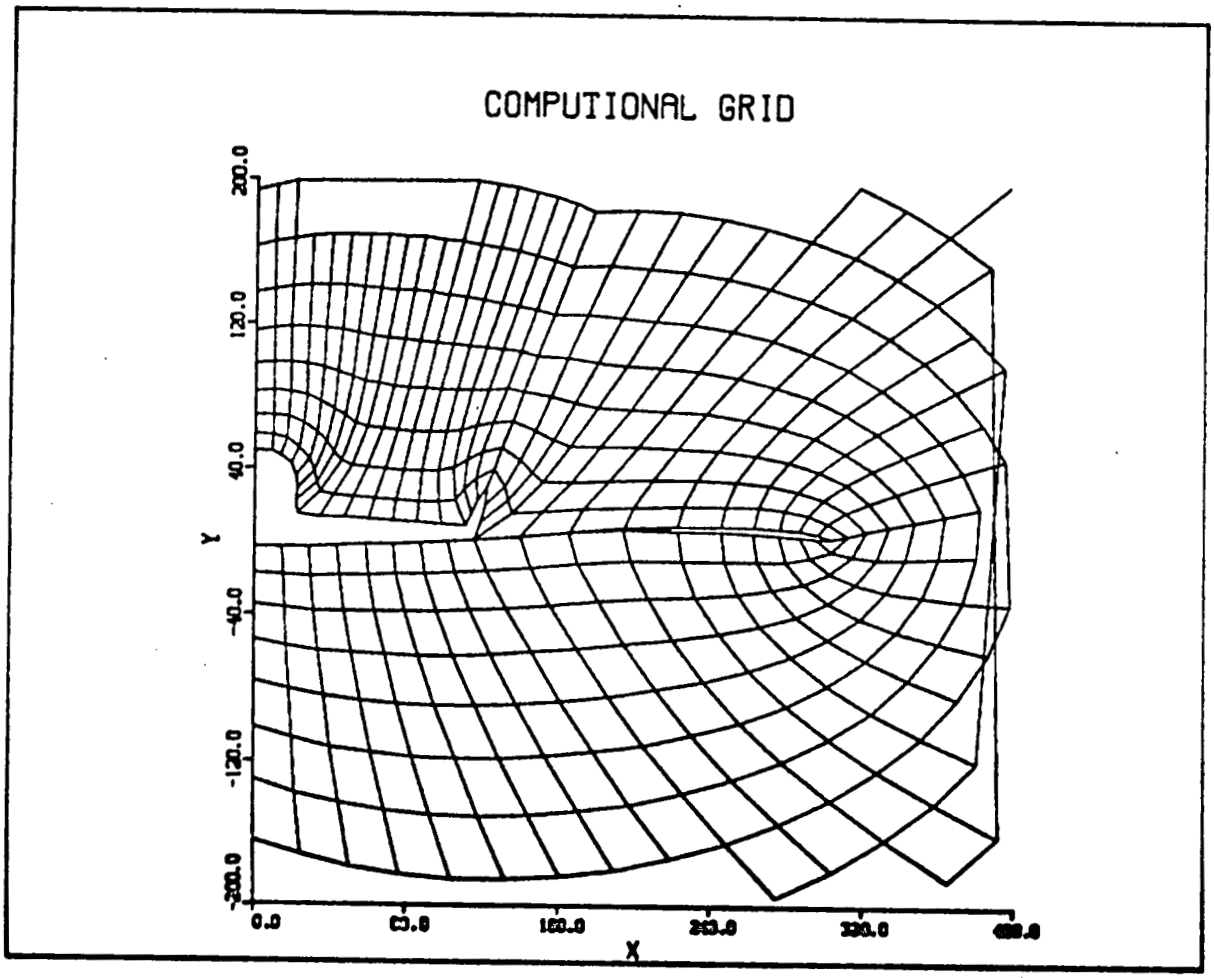
COMPUTIONAL GRID
200.0
120.0
40.0
-40.0
-120.0
-200.0
Y
0.0
80.0
160.0
240.0
320.0
X

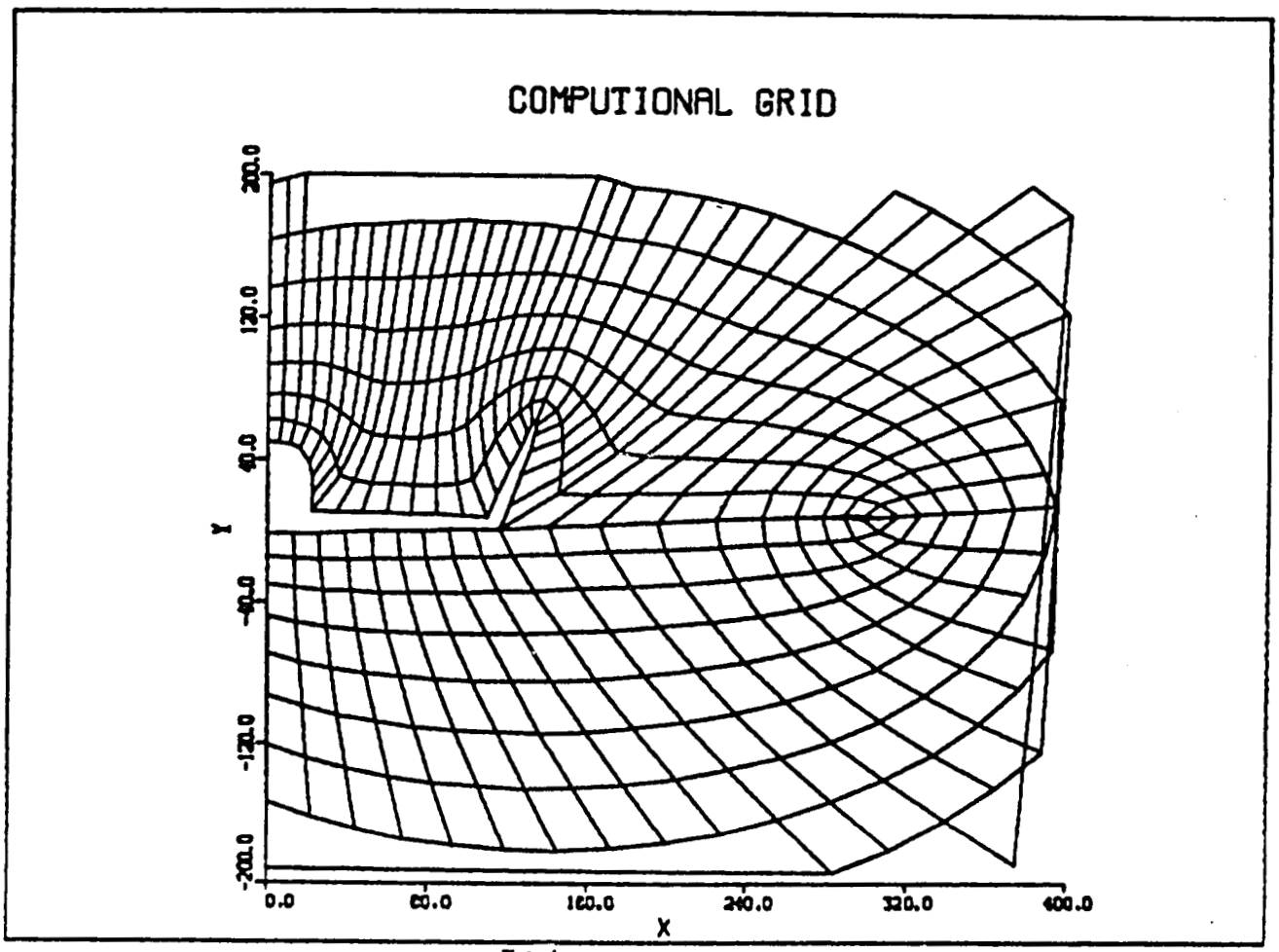
COMPUTIONAL GRID
200.0
120.0
40.0
-40.0
-120.0
-200.0
Y
0.0
80.0
160.0
240.0
320.0
400.0
X

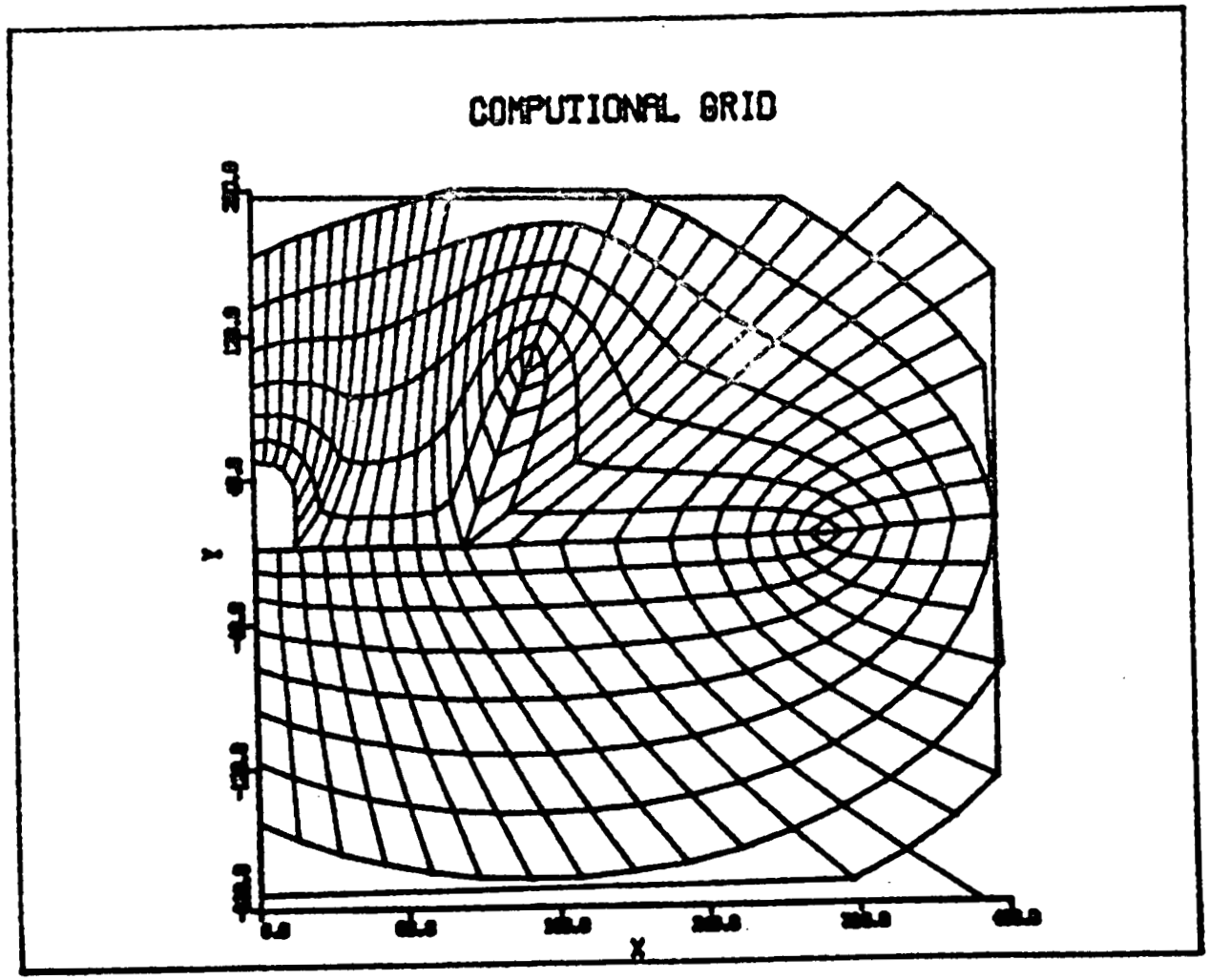
COMPUTIONAL GRID
Y
X

SC83-24368

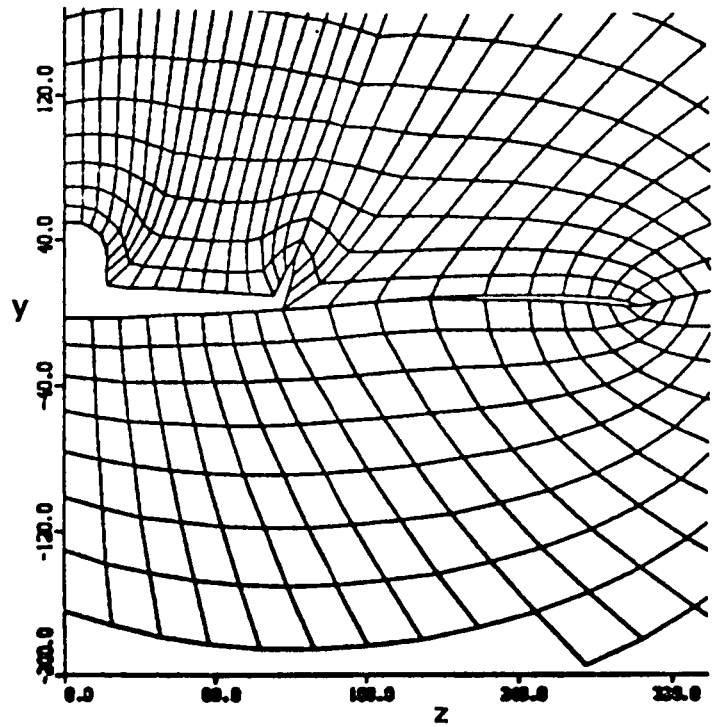

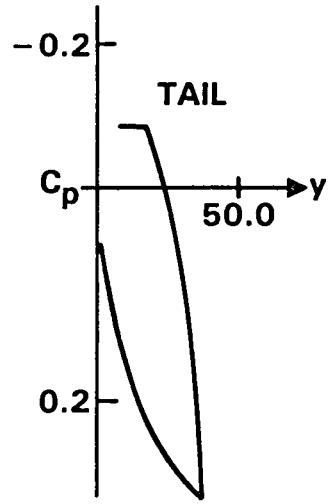

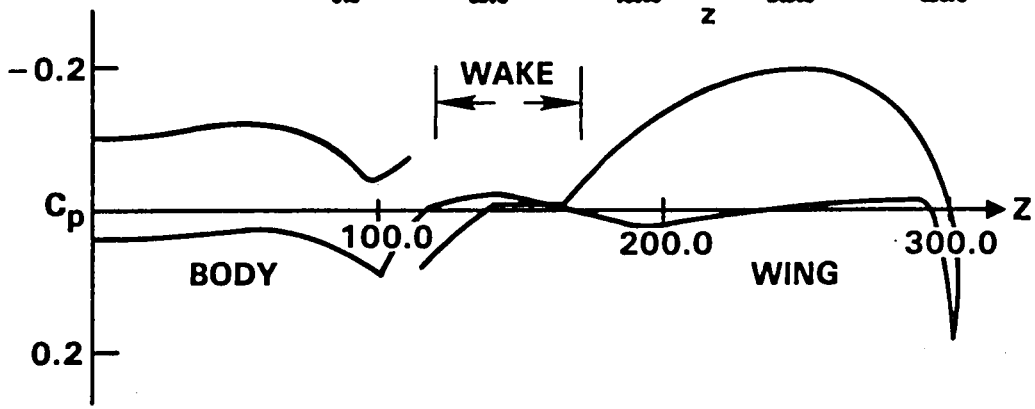

Rockwell International
Science Center

SC83-24367

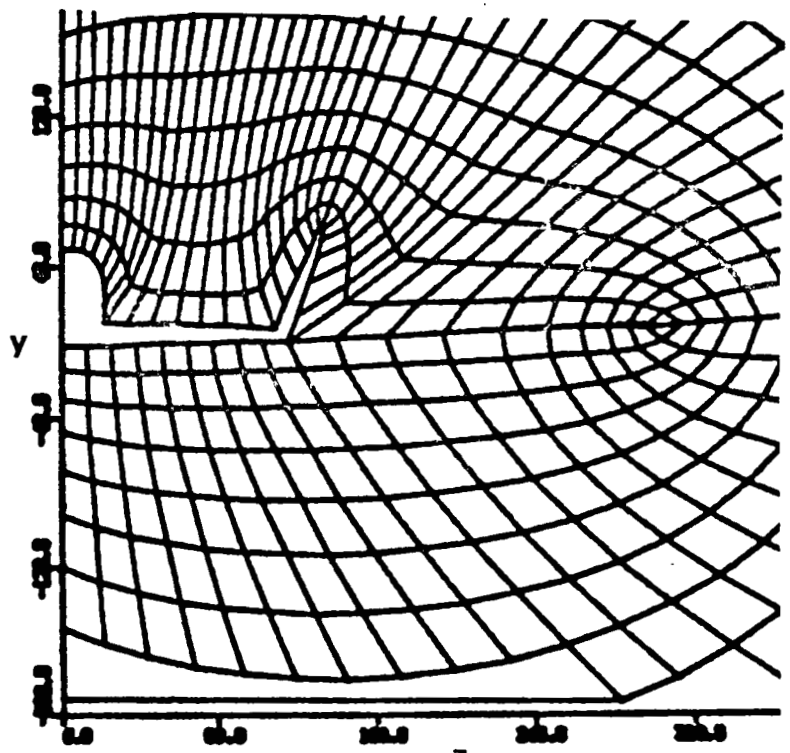

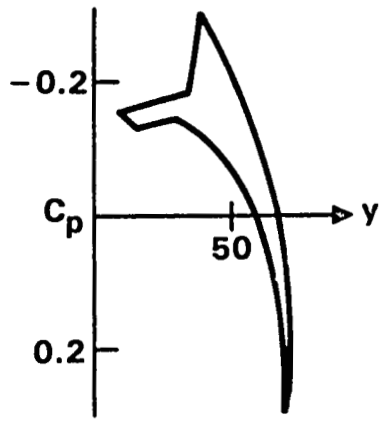

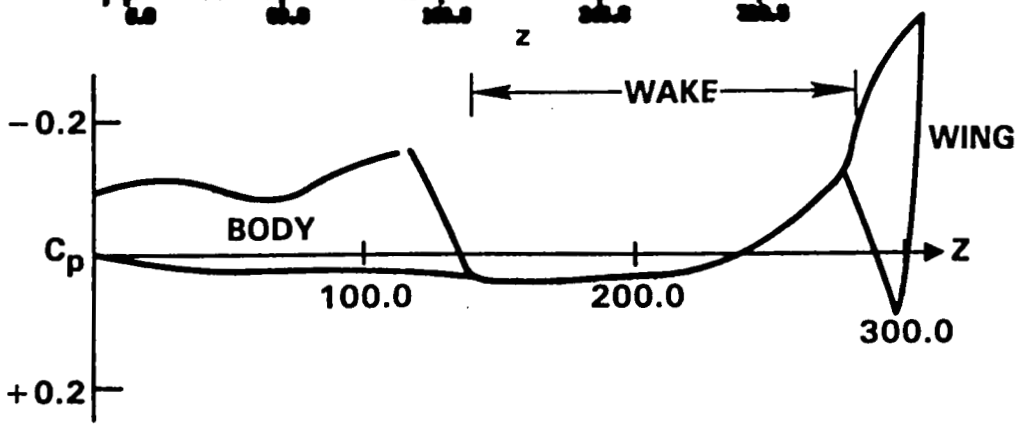

Rockwell International
Science Center

COMPARISON OF NUMERICAL PREDICTION WITH WIND TUNNEL DATA

ATF TEST CASES

α		5°	5°	5°	5°
M_∞		1.6*	1.6†	1.4†	1.6†
Λ		48°	48°	48°	55°
C_L	CODE	0.298	0.3016	0.3561	0.29186
	DATA	0.277	0.295	0.342	0.3
C_D	CODE	0.0462	0.04916	0.04117	0.028129
	DATA	0.0457	0.0493	0.0425	0.0301

* TAIL OFF
† TAIL ON

ONGOING PROJECTS

1. FOREBODY CANARD-WING FIGHTER GEOMETRY (KEN JONES)
2. ATF DESIGN (BONNER/SZEMA)
3. FULL 3-D CAPABILITY (YAW, OBLIQUE WING) (SHANKAR)
4. FLEXIBLE ADAPTIVE WING (IDE/NAAO)
5. WAVE RIDERS (KEN JONES)

FOLLOW-ON ACTIVITIES

1. CANARD-WING SIMULATION
2. FLOW THROUGH NACELLE MODELING

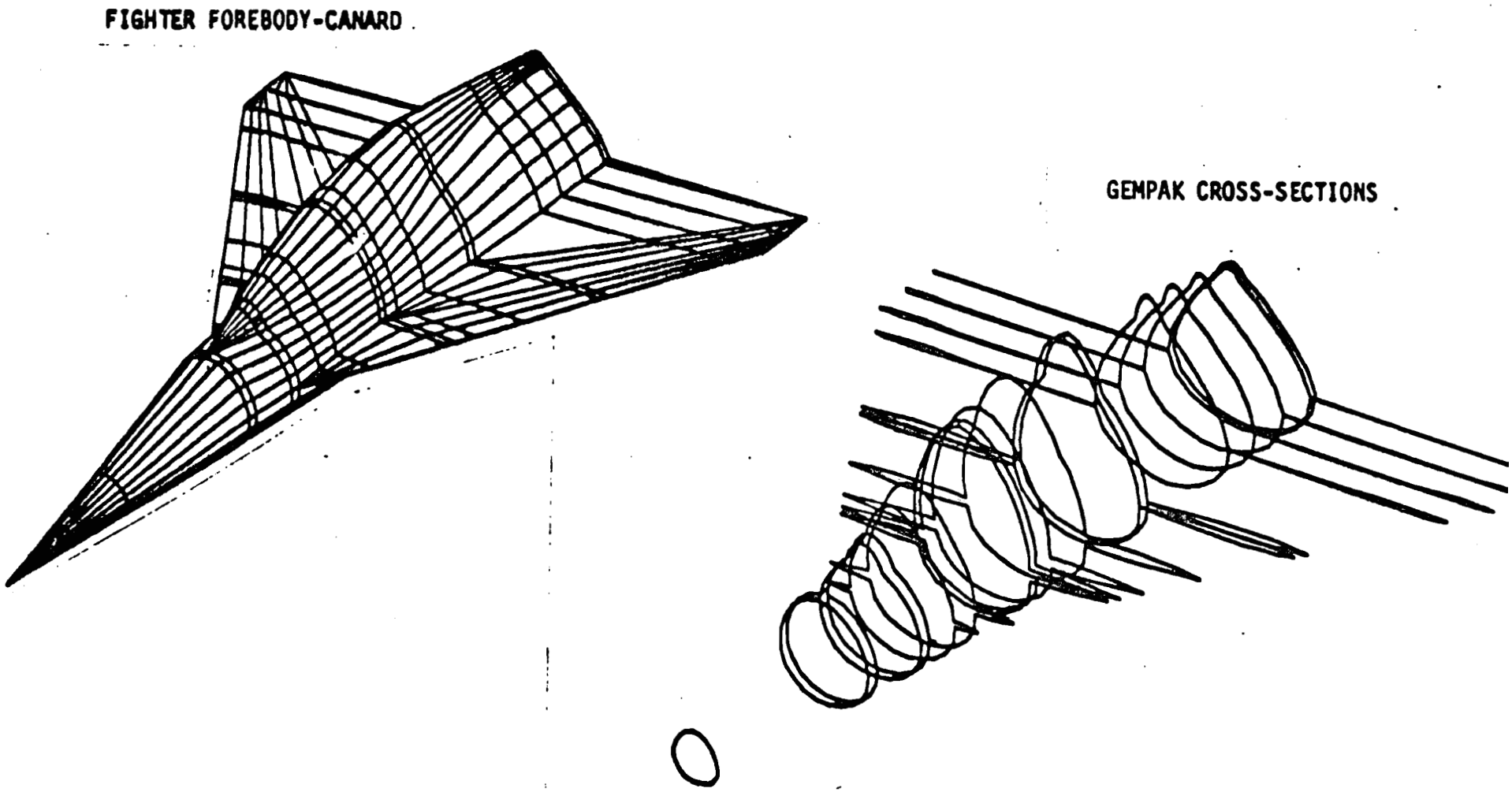

Figure 11.- GEMPAK generated cross sections for the advanced fighter model.

TPR23

COMPUTATIONAL GRID

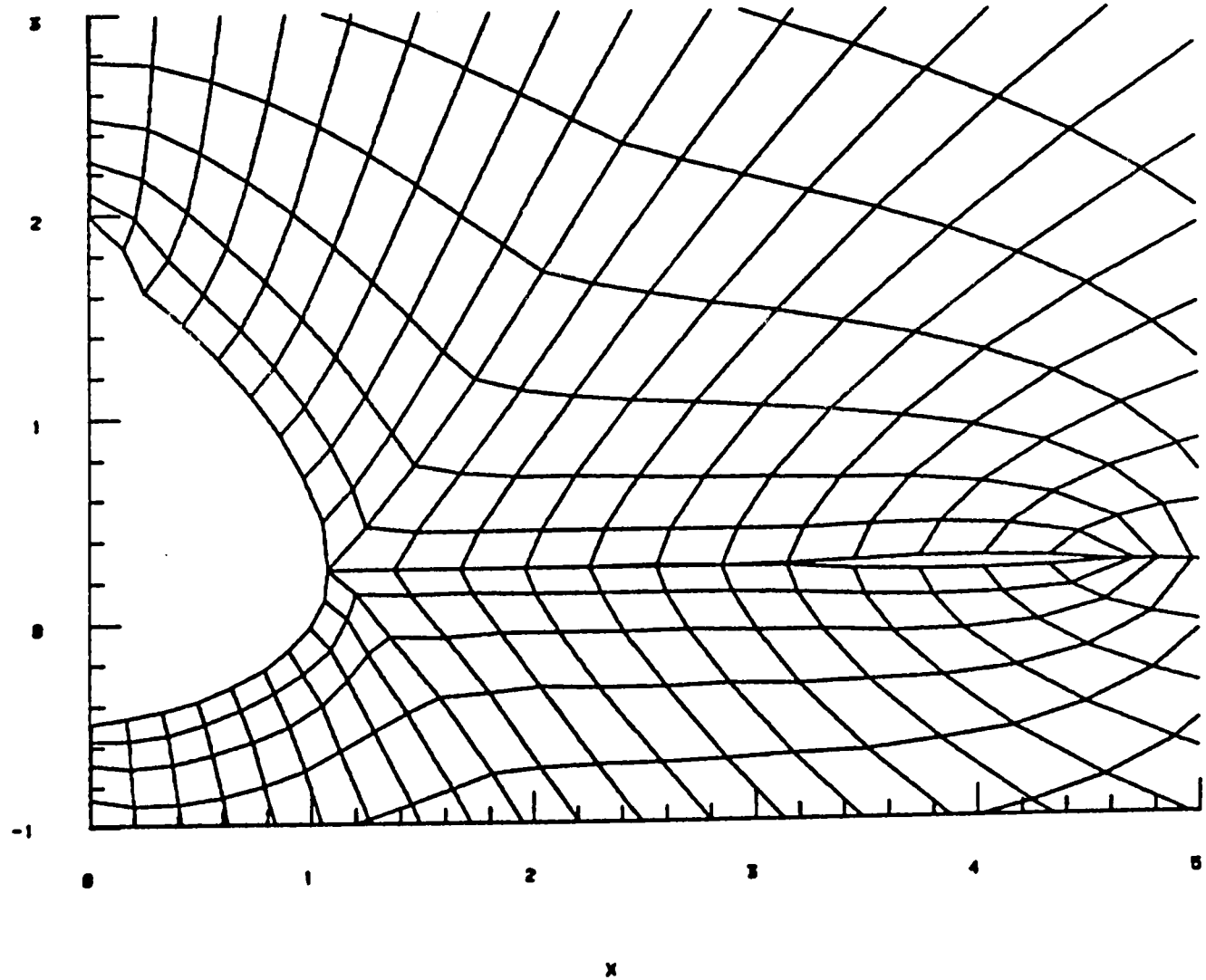

MACH NO. = 2.00

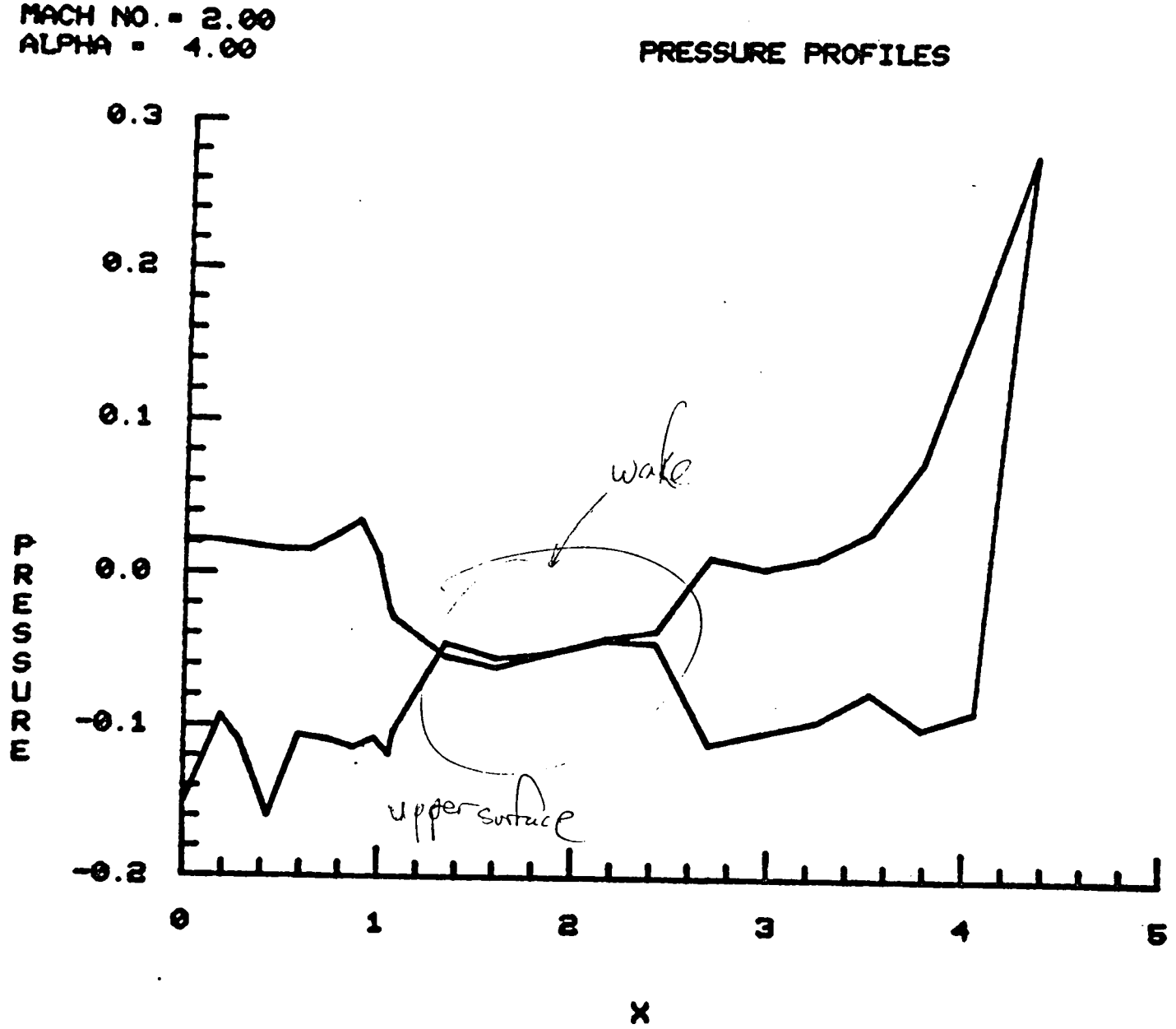

flow field analysis upto 11.00

PRESSURE DISTRIBUTION ON A FOREBODY IN SIDESLIP
$M = 2.5, \beta = 5.02, \alpha = 0°$

SC83-24361

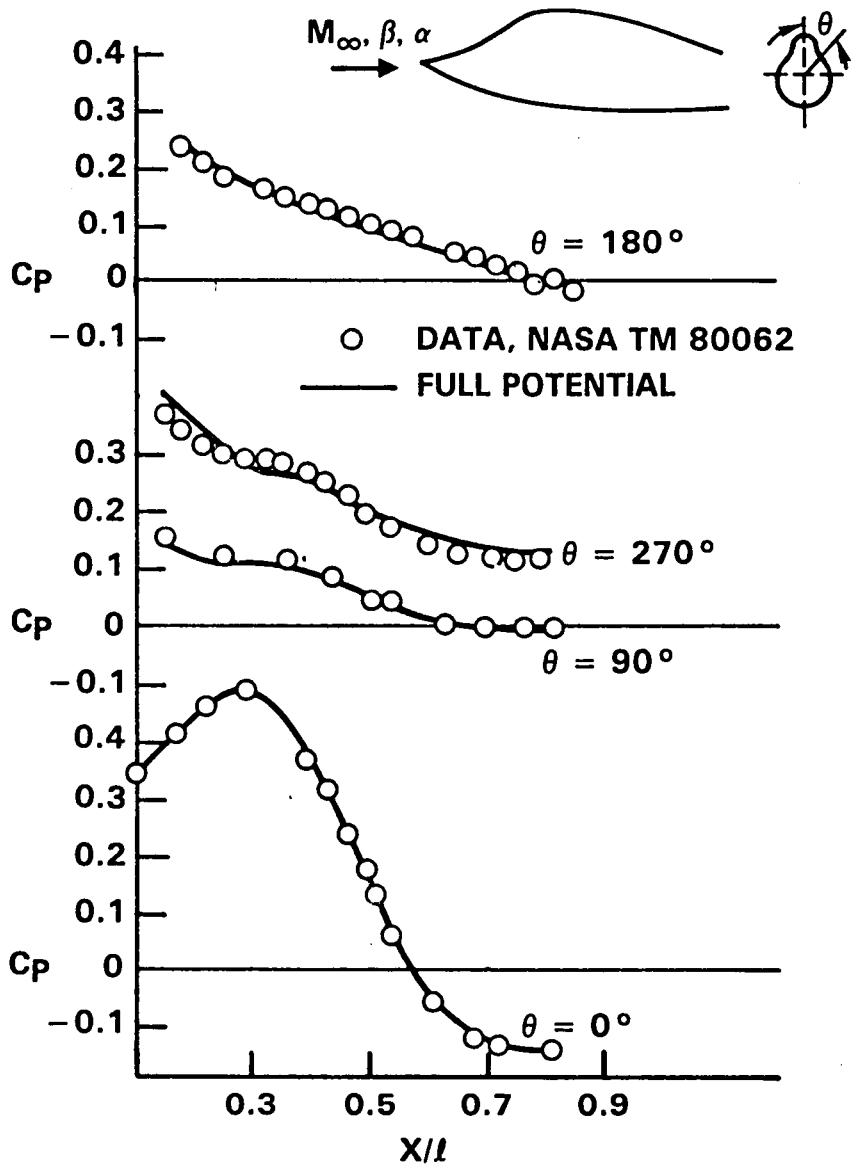

Rockwell International
Science Center

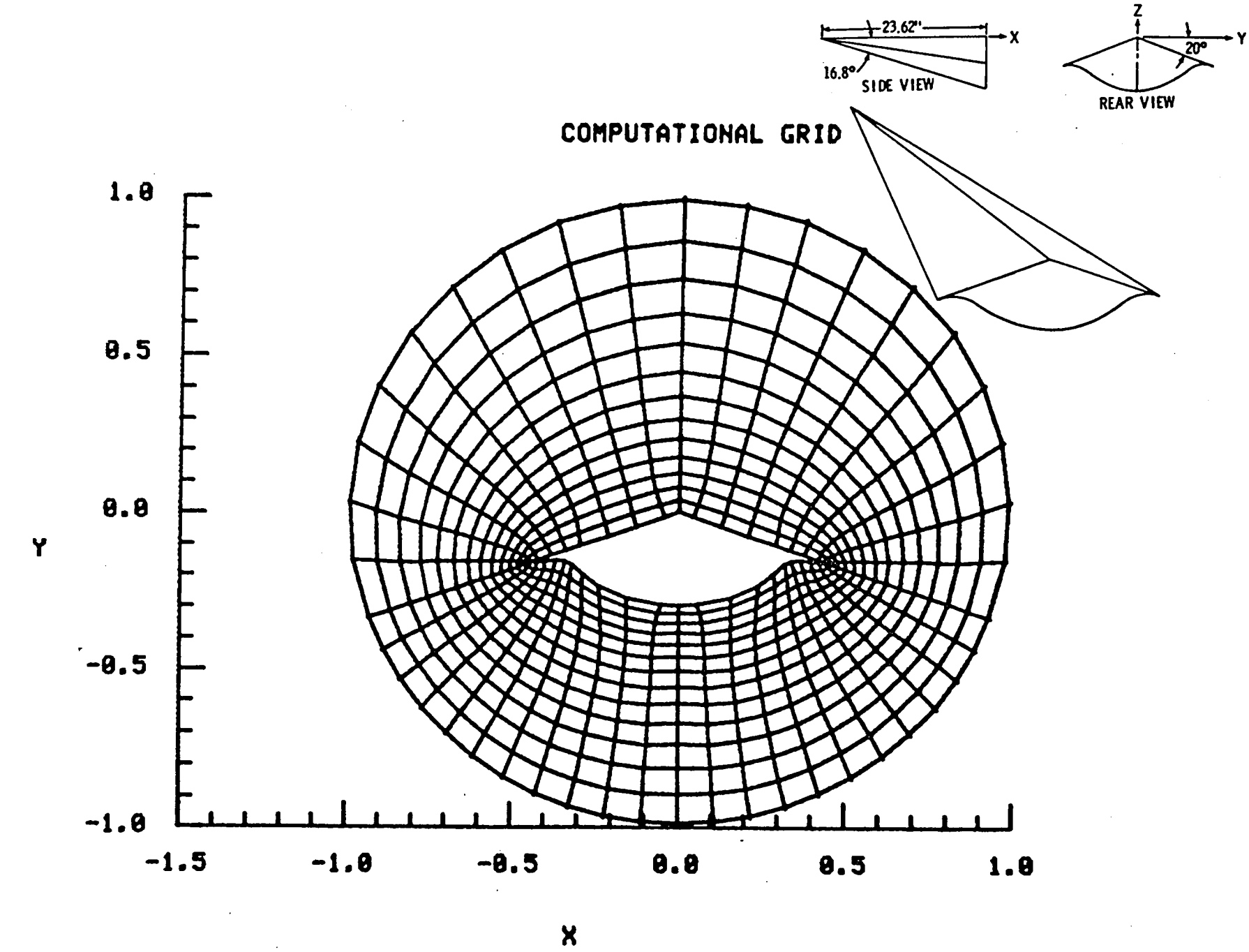
23.62"
X
16.8°
SIDE VIEW
Z
Y
20°
REAR VIEW
COMPUTATIONAL GRID
1.0
0.5
0.0
-0.5
-1.0
Y
-1.5
-1.0
-0.5
0.0
0.5
1.0
X

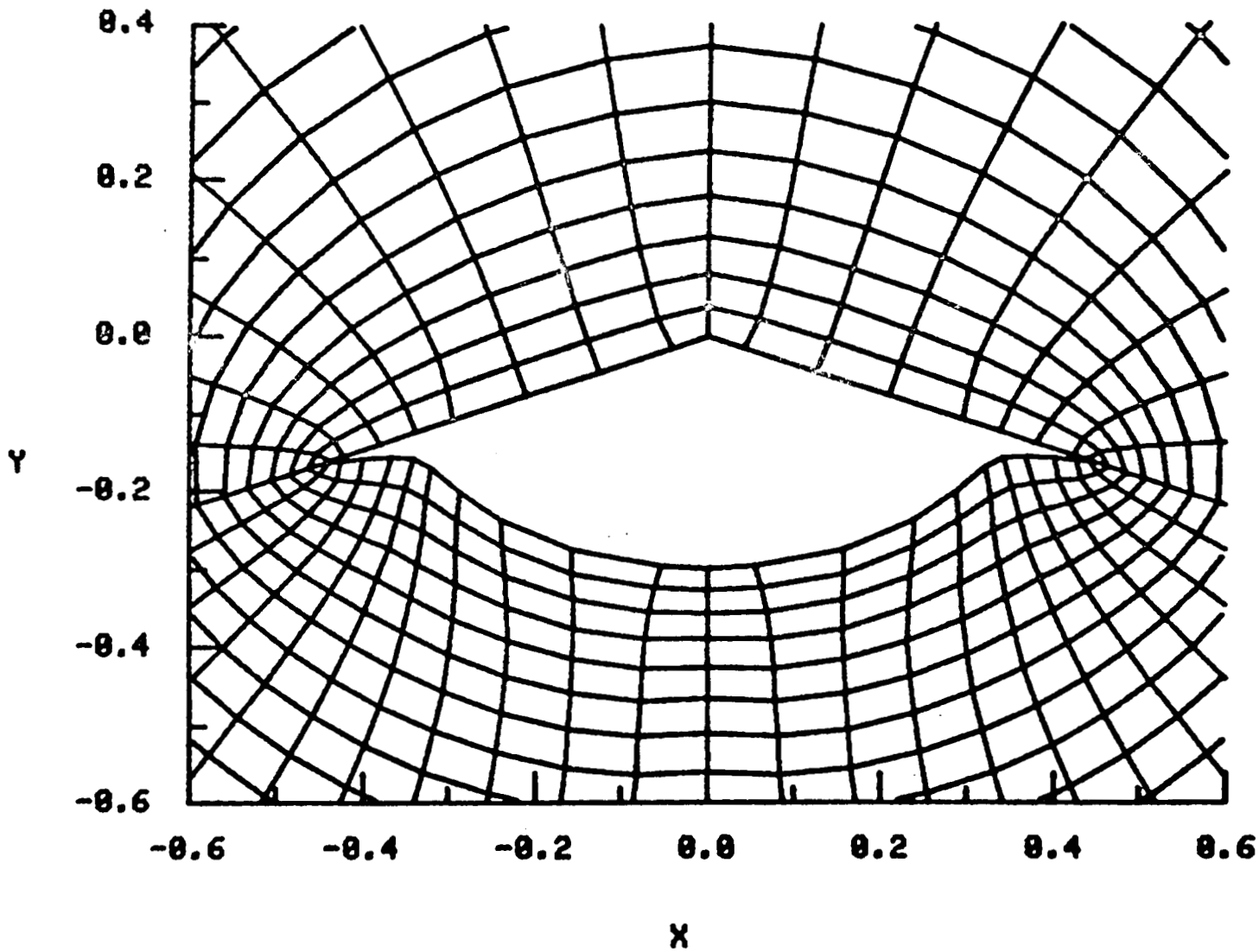
COMPUTATIONAL GRID
0.4
0.2
0.0
-0.2
-0.4
-0.6
Y
-0.6
-0.4
-0.2
0.0
0.2
0.4
0.6
X

PRESSURE CONTOURS

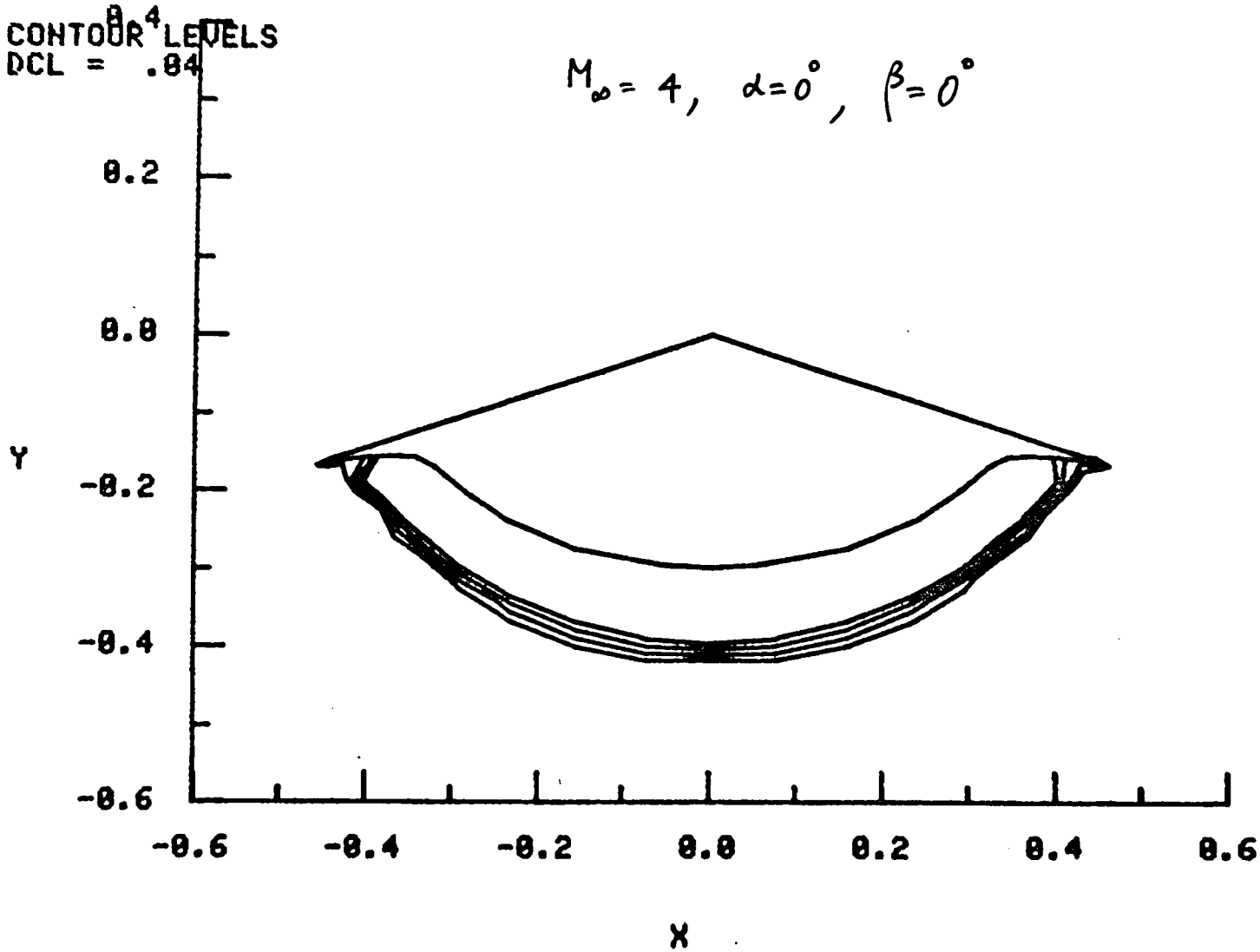

PRESSURE CONTOURS

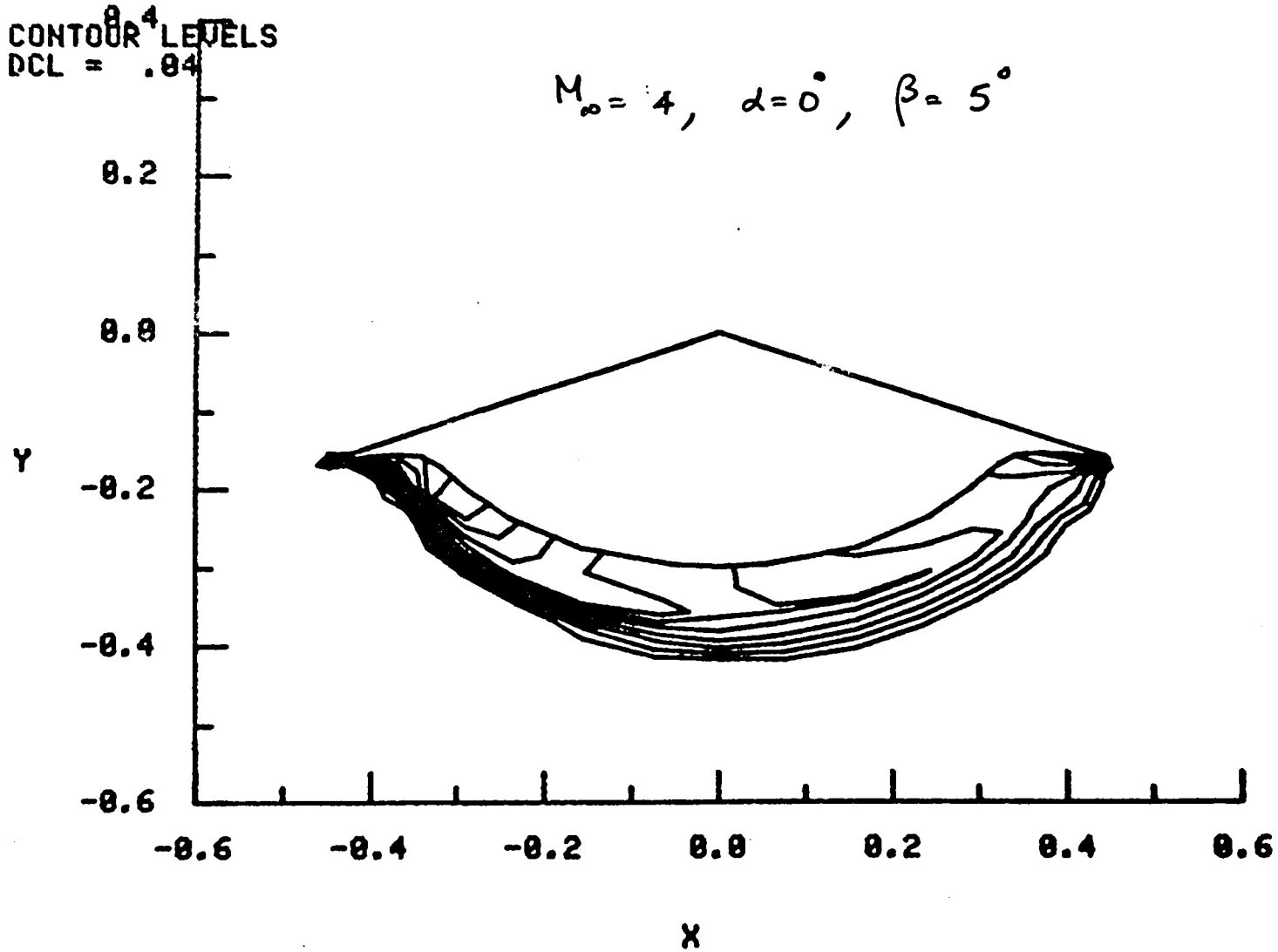

PRESSURE CONTOURS

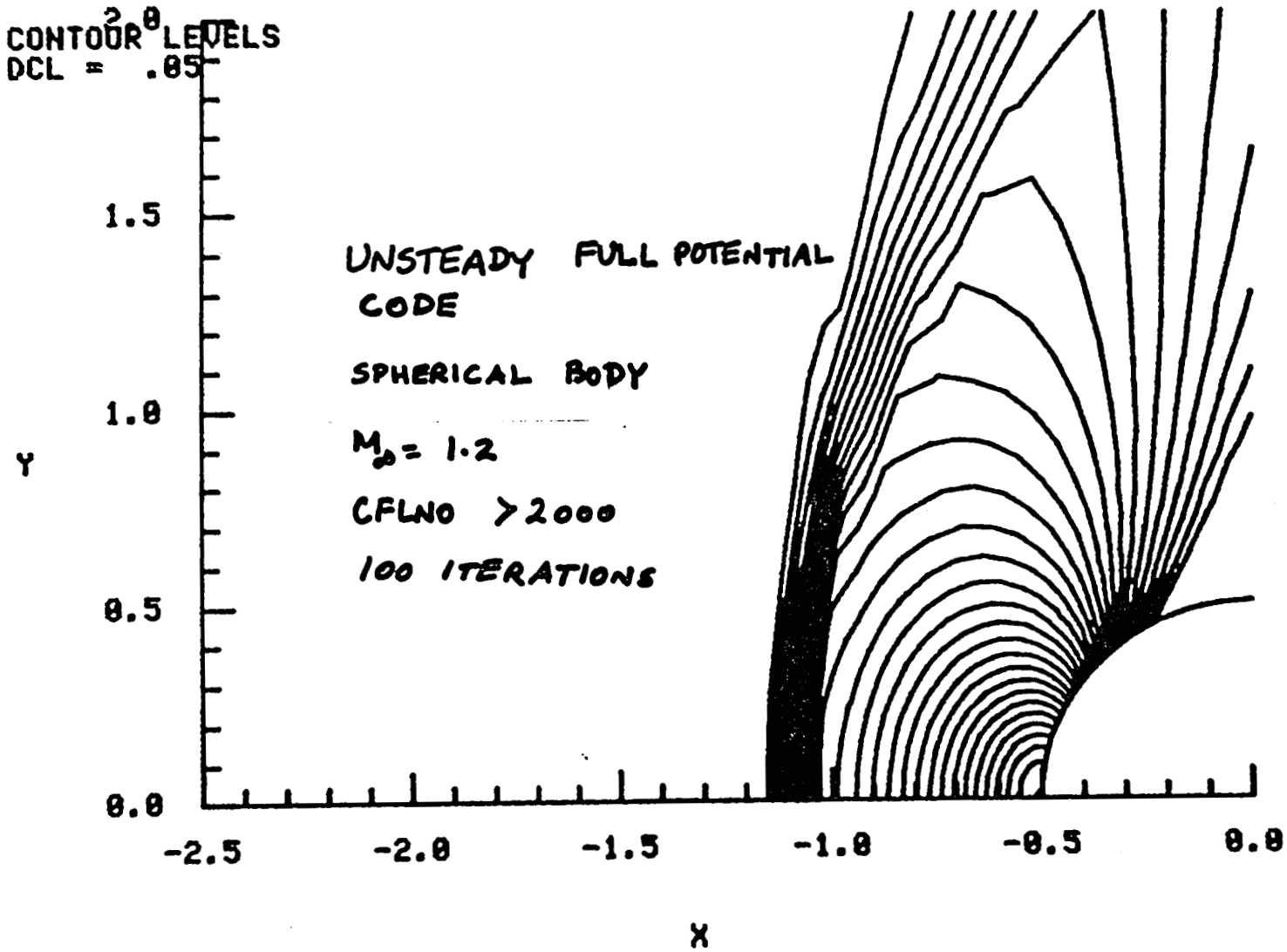

(20)

ANALYSIS OF AIRFOIL TRANSITIONAL SEPARATION BUBBLES

R.L. Davis
J.E. Carter

RB660TX.003

CARTER

AIRFOIL SEPARATED FLOW ANALYSIS

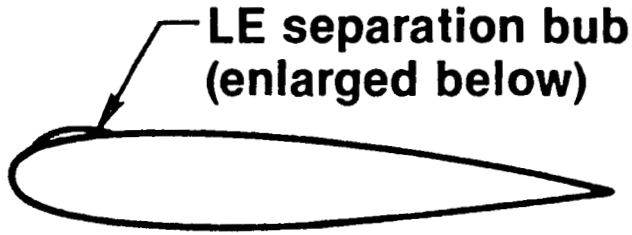

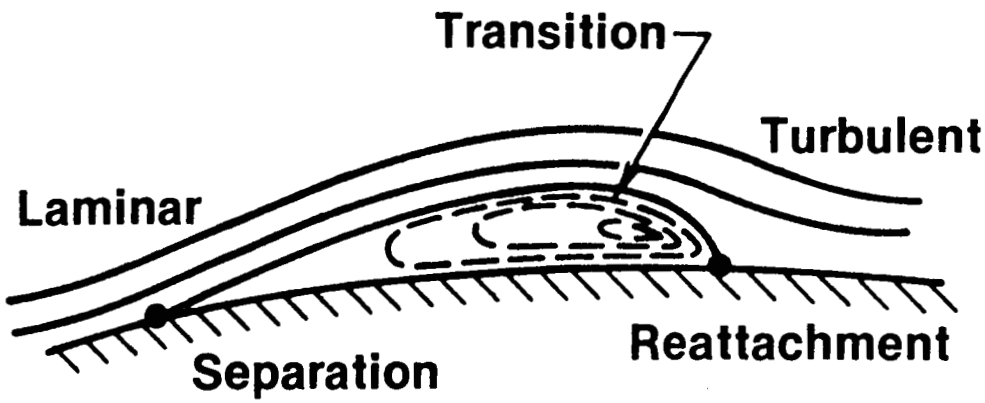

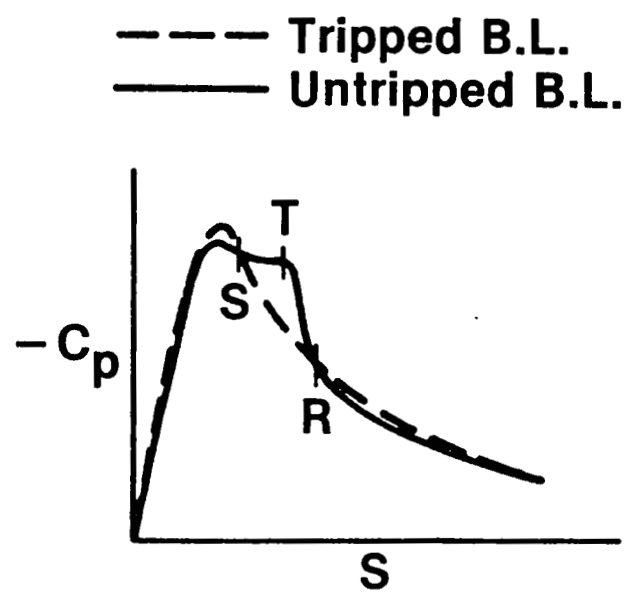

81-8-80-4

INTRODUCTION

Approach

- Interacting boundary layer theory
  - Local analysis
  - Global analysis - GRUMFOIL

Current focus

- Asymptotic analysis of airfoil protrusion
- Windward vs FLARE differencing
- Evaluation of natural transition model
- Experimental comparisons

AIRFOIL WITH A SMALL PROTRUSION

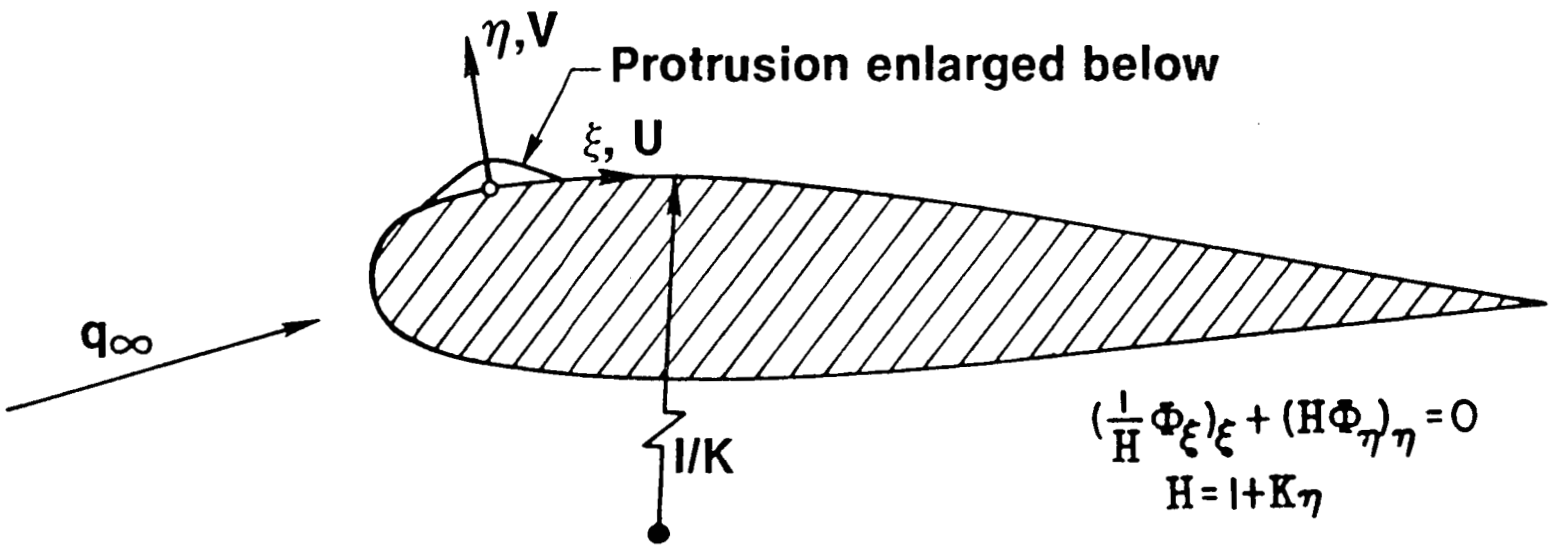

$$\left(\frac{1}{H}\Phi_\xi\right)_\xi + (H\Phi_\eta)_\eta = 0$$

$$H = 1 + K\eta$$

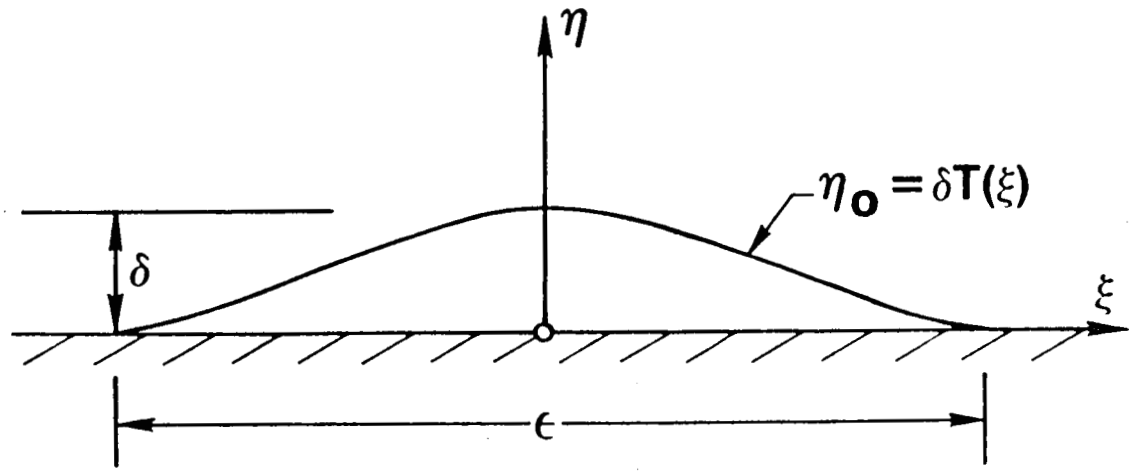

$$\Phi_\eta = \frac{1}{H^2}\eta_o'\Phi_\xi \quad \text{at} \quad \eta = \eta_o$$

$$\left.\begin{aligned}\Phi_\xi &\to H\cos\theta \\ \Phi_\eta &\to -\sin\theta\end{aligned}\right\} \quad \xi, \eta \to \infty$$

83-10-17-1

ASYMPTOTIC ANALYSIS OF A THIN PROTRUSION ON AN AIRFOIL

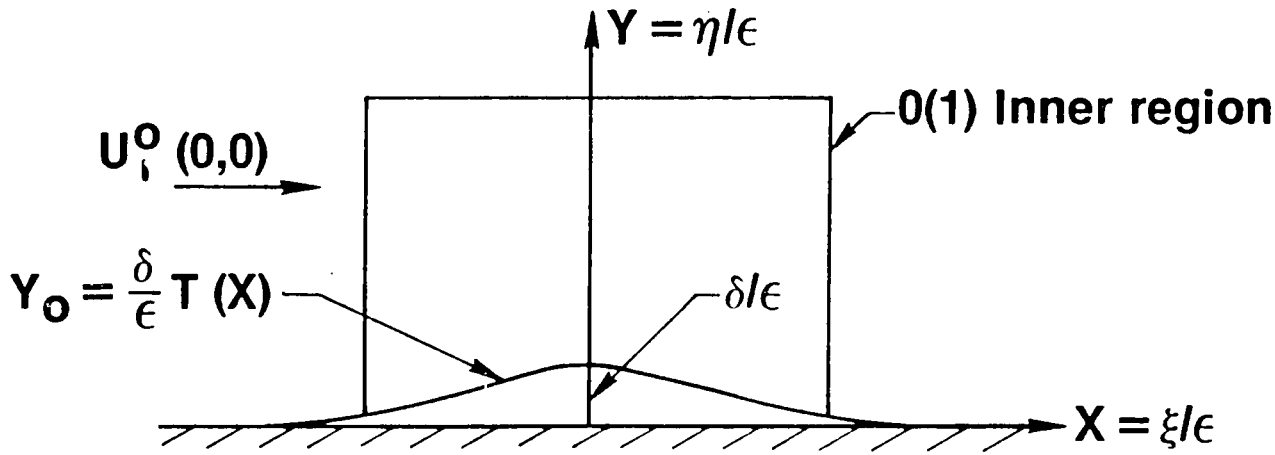

Outer: $\Phi^o(\xi,\eta;\epsilon) = \Phi_1^o(\xi,\eta) + \Delta_2(\epsilon)\Phi_2^o(\xi,\eta) + \ldots$ ($\Phi_2^o \to 0$)

Inner: $\Phi^i(\xi,\eta;\epsilon) = \epsilon U_1^o(0,0)X + \delta\phi_2^i(X,Y) + \ldots$

$$\phi_{2XX}^i + \phi_{2YY}^i = 0$$

$$\phi_{2Y}^i(X,0) = U_1^o(0,0)T'(X)$$

$$\phi_2^i(\infty,\infty) = 0$$

For the limit $\epsilon^2 < \delta < \epsilon$

SKIN FRICTION-NACA 0010 AIRFOIL

$\alpha = 8°$

$Re_c = 2 \times 10^6$

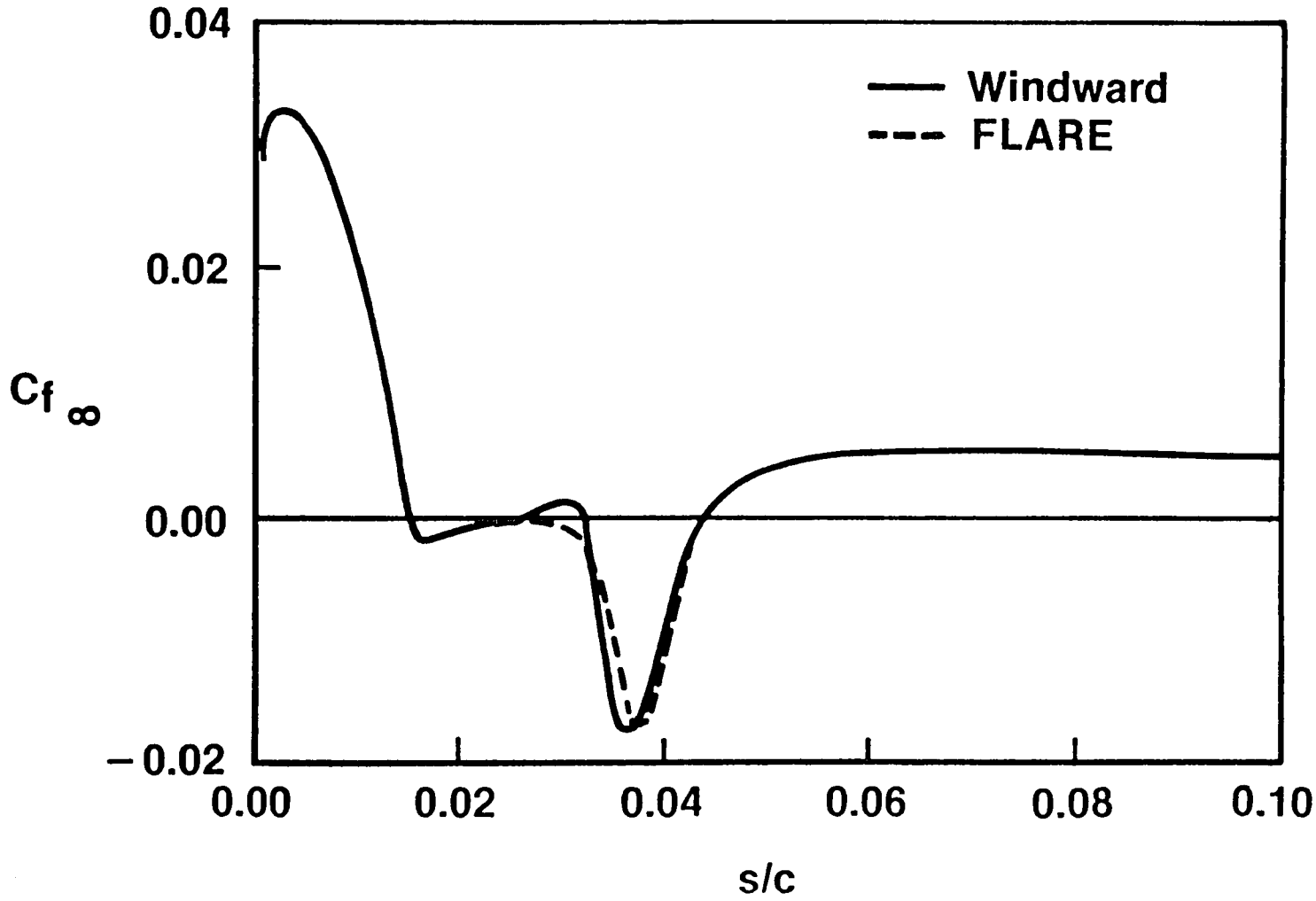

83 10 17 3

VISCOUS STREAMLINES- WINDWARD

$\alpha = 8°$

$Re_c = 2 \times 10^6$

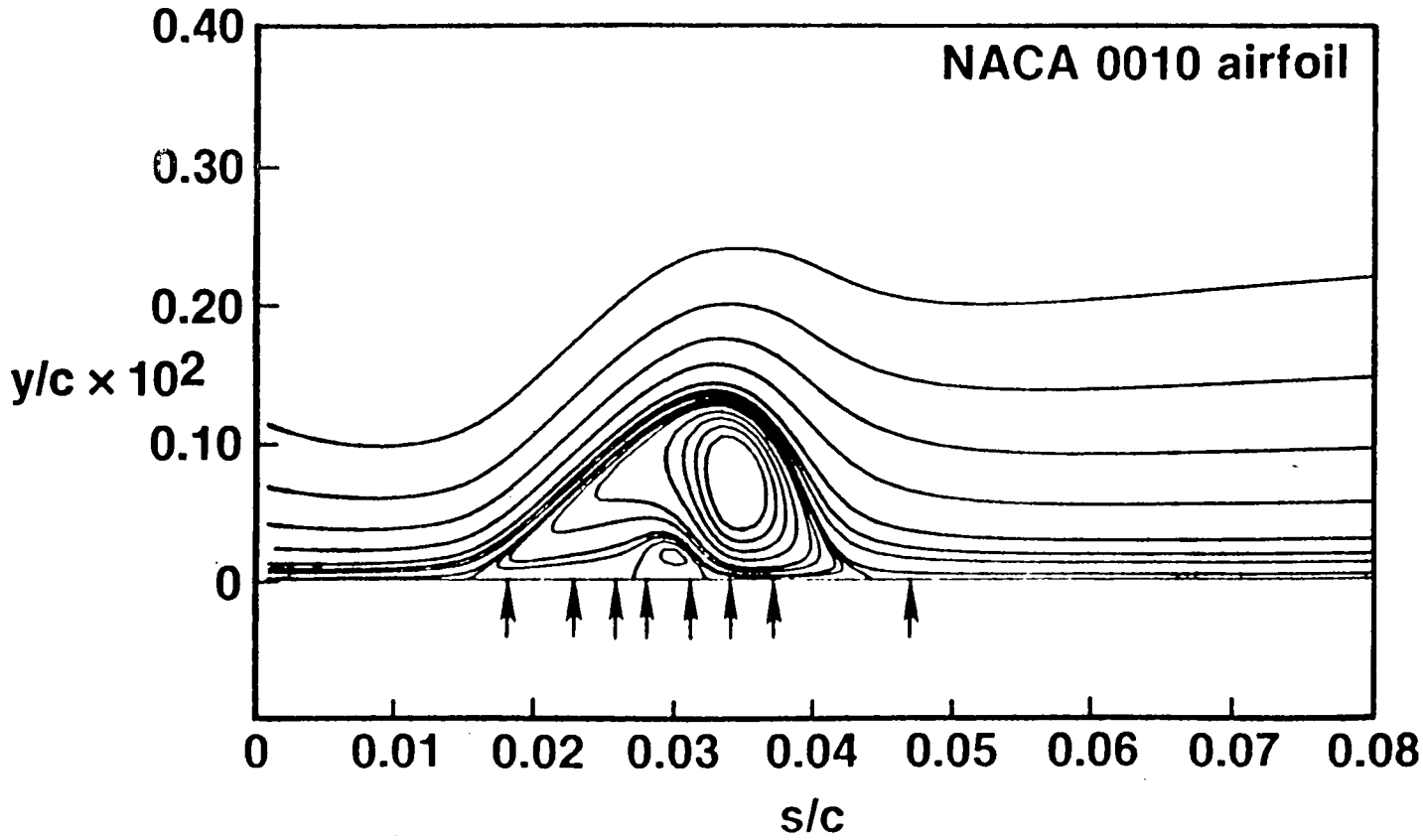

83-10-17-4

VISCOUS STREAMLINES-FLARE

$\alpha = 8°$

$Re_c = 2 \times 10^6$

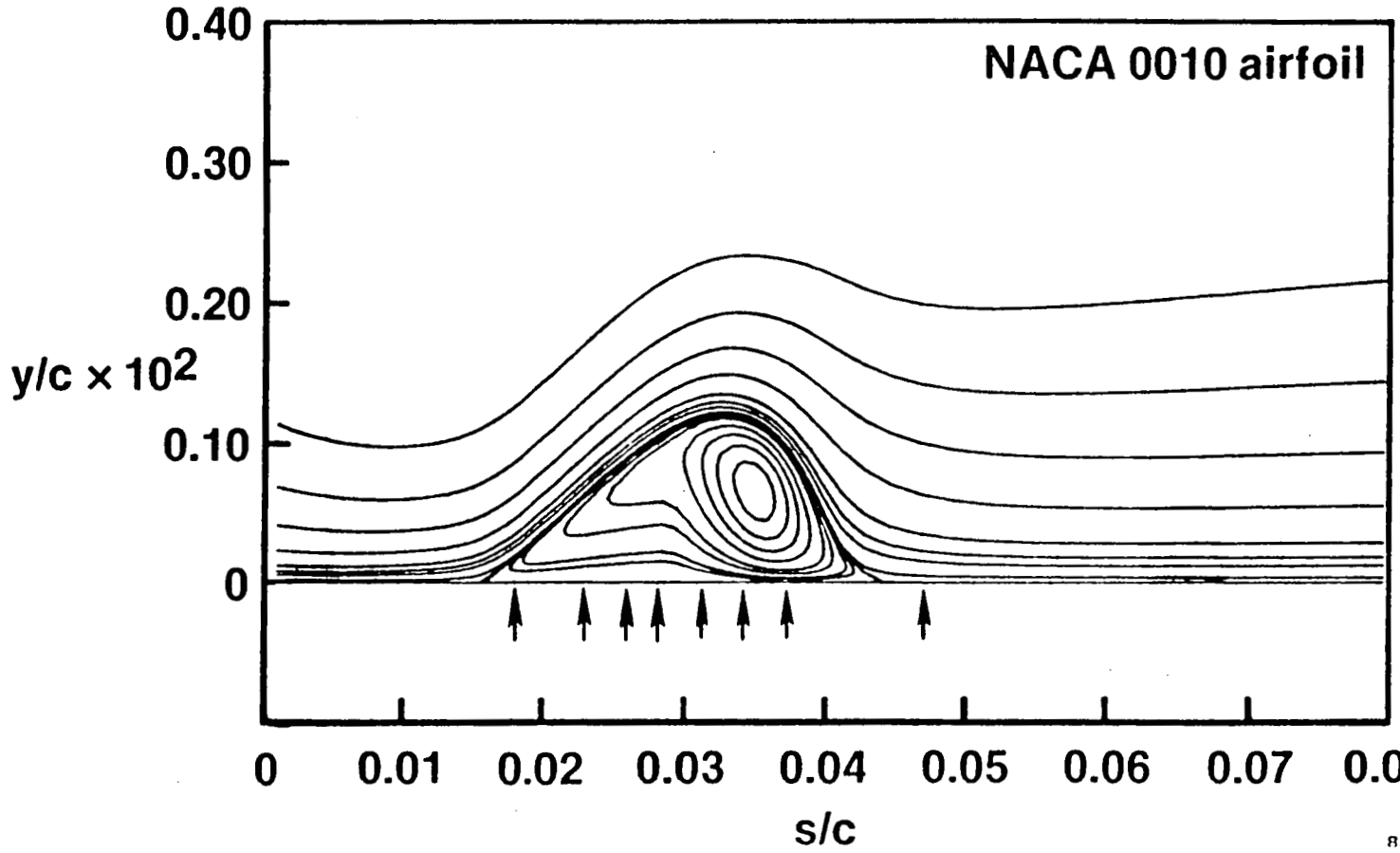

83-10-17-5

VELOCITY PROFILES—NACA-0010 AIRFOIL

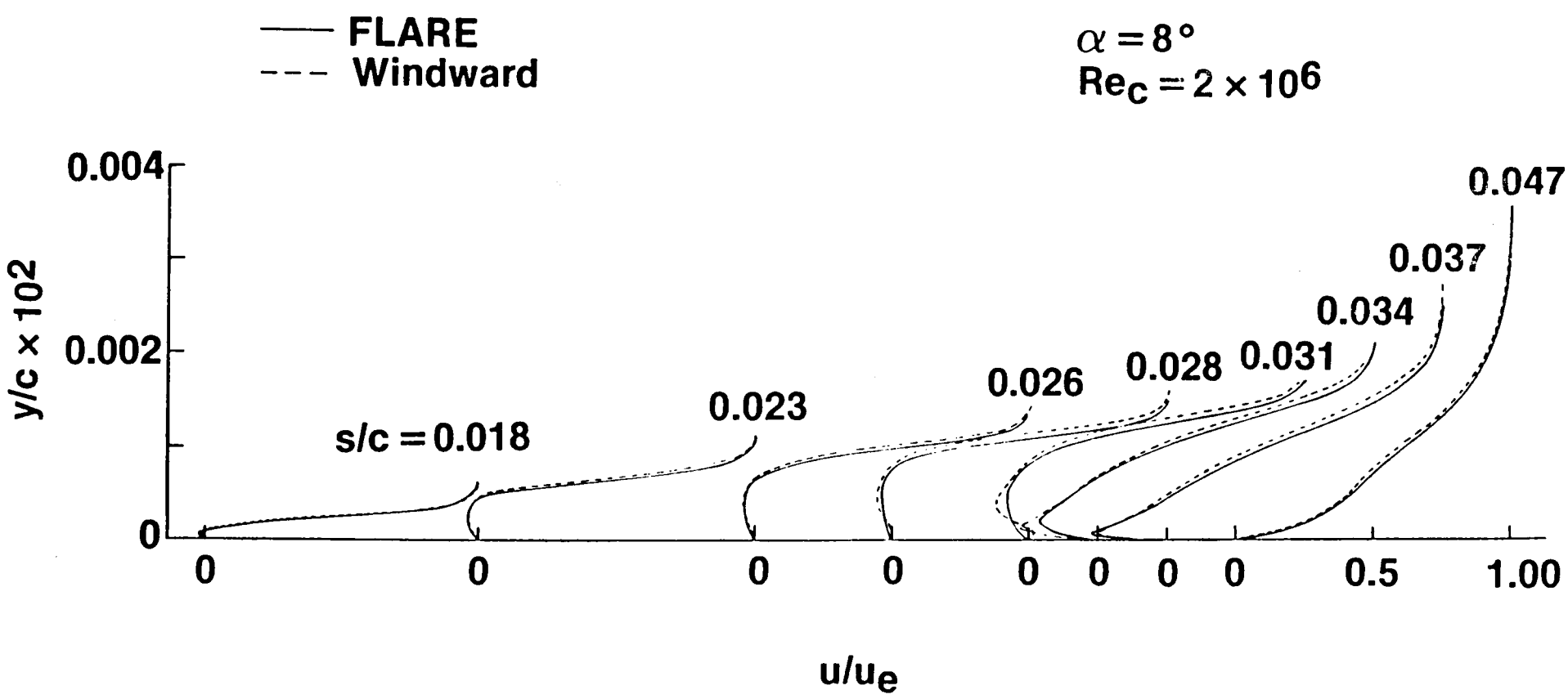

83-10-17-6

CONVERGENCE HISTORY
NACA 0010 AIRFOIL

$\alpha = 8°$

$Re_c = 2 \times 10^6$

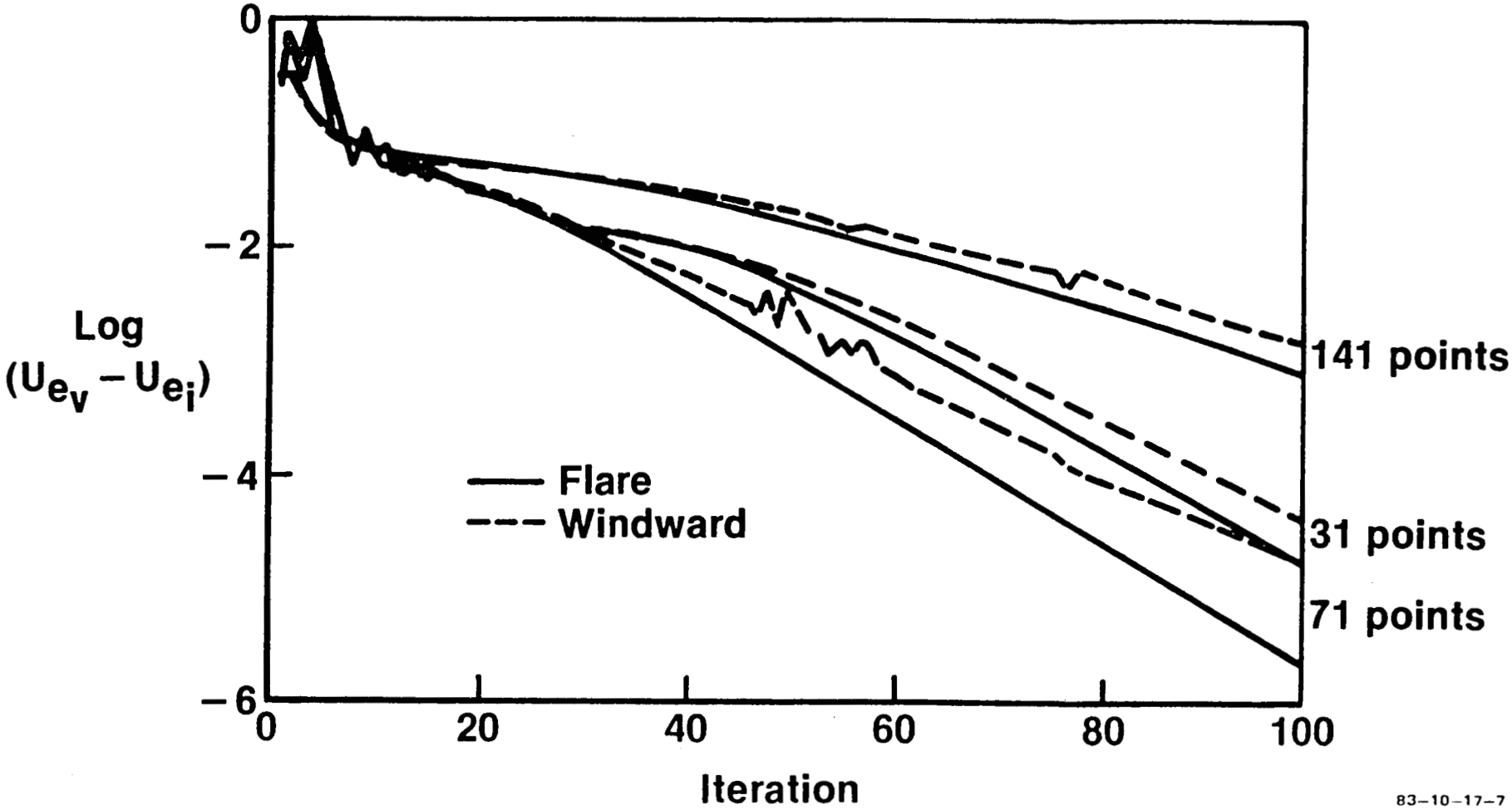

83-10-17-7

ISO-VELOCITY CONTOURS-GASTER CASE

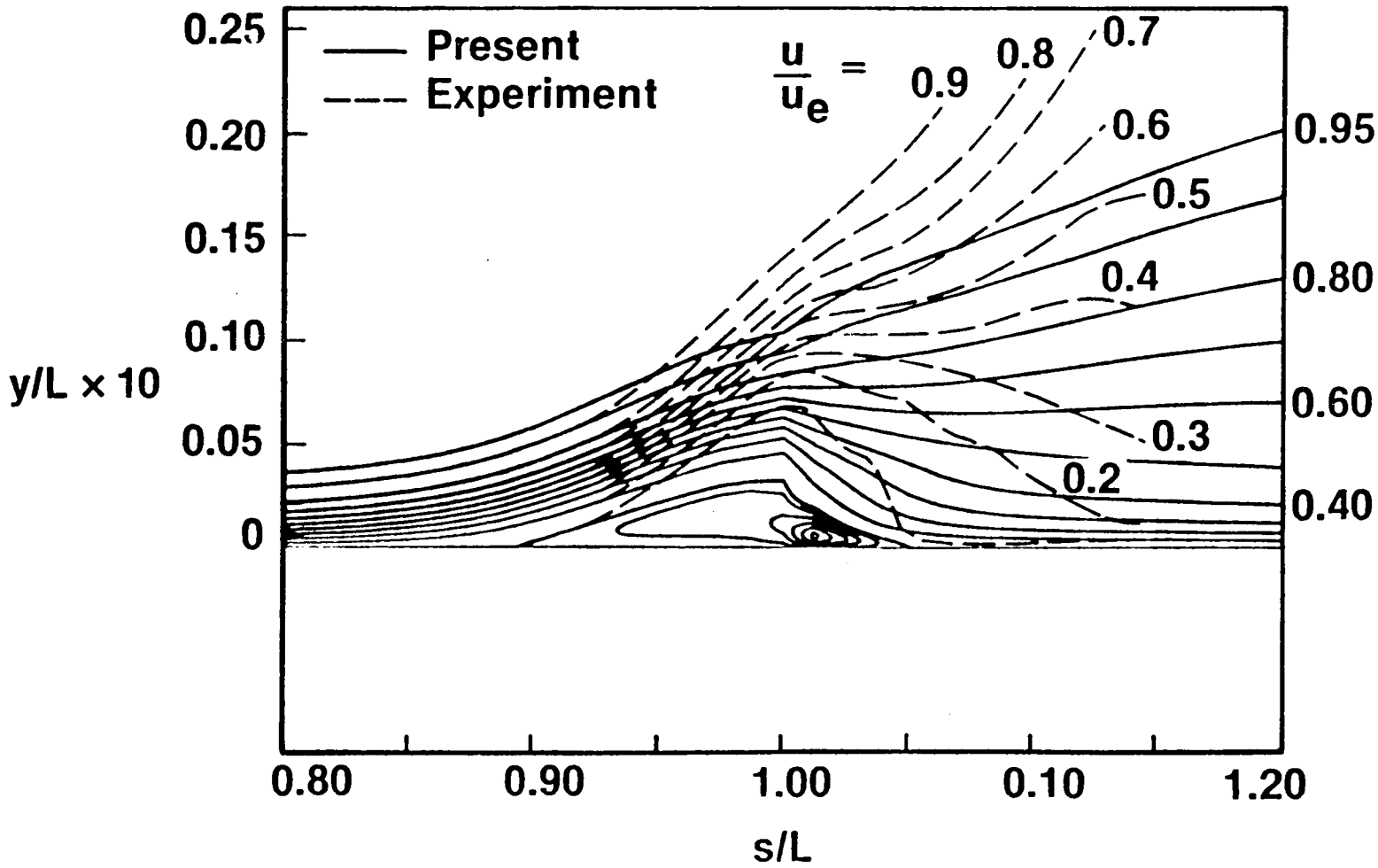

83-10-17-8

McDONALD-FISH TRANSITION/TURBULENCE MODEL

Integral form of turbulent kinetic energy equation

$$\frac{d\phi_1}{dx} = \phi_2 - \phi_3 + E$$

ϕ_1 = **streamwise convection of turbulence energy**

ϕ_2 = **net production of turbulence**

ϕ_3 = **normal stress production**

E = **turbulence energy entrained from the free stream**

$$-\overline{u'v'} = a_1 \overline{q^2}$$

$$\overline{u'^2} = a_2 \overline{q^2}$$

$$\overline{v'^2} = a_3 \overline{q^2}$$

a_1, a_2, a_3 – **empirical structural coefficients**

$$-\overline{u'v'} = \ell^2 \left|\frac{\partial u}{\partial y}\right| \frac{\partial u}{\partial y}$$

$$\ell = \ell_\infty \tanh(\kappa y/\ell_\infty)$$

Solve TKE for ℓ_∞

83-10-17-13

FLAT PLATE SKIN FRICTION
LOW Tu_∞

$u_\infty = 100$ ft/sec
$Re = 5.105 \times 10^4$ /in.
$Tu_\infty = 0.0025$

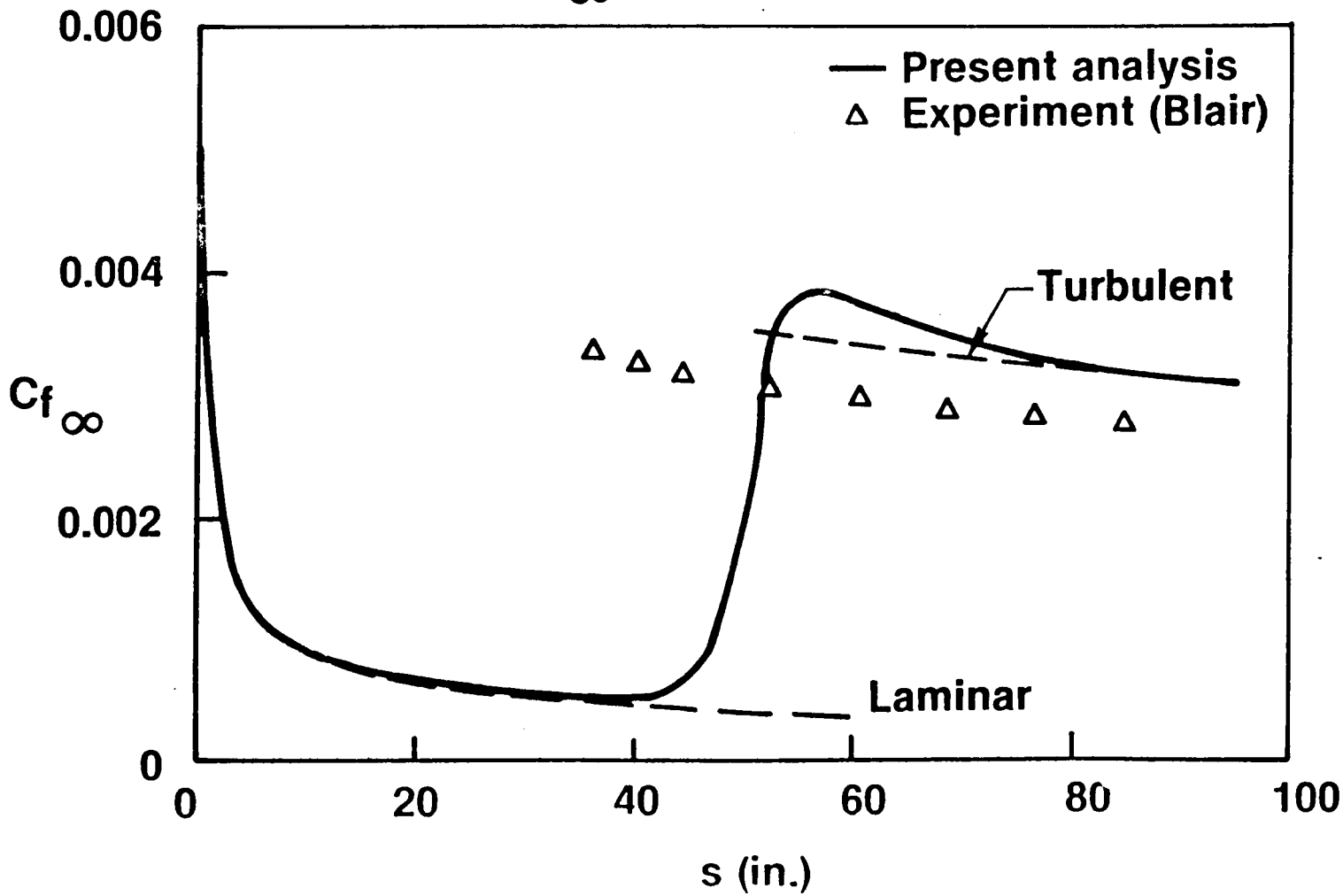

83 10 17 9

FLAT PLATE DISPLACEMENT THICKNESS — LOW Tu_∞

$U_\infty = 100$ ft/sec

$Re = 5.105 \times 10^4$ /in.

$Tu_\infty = 0.0025$

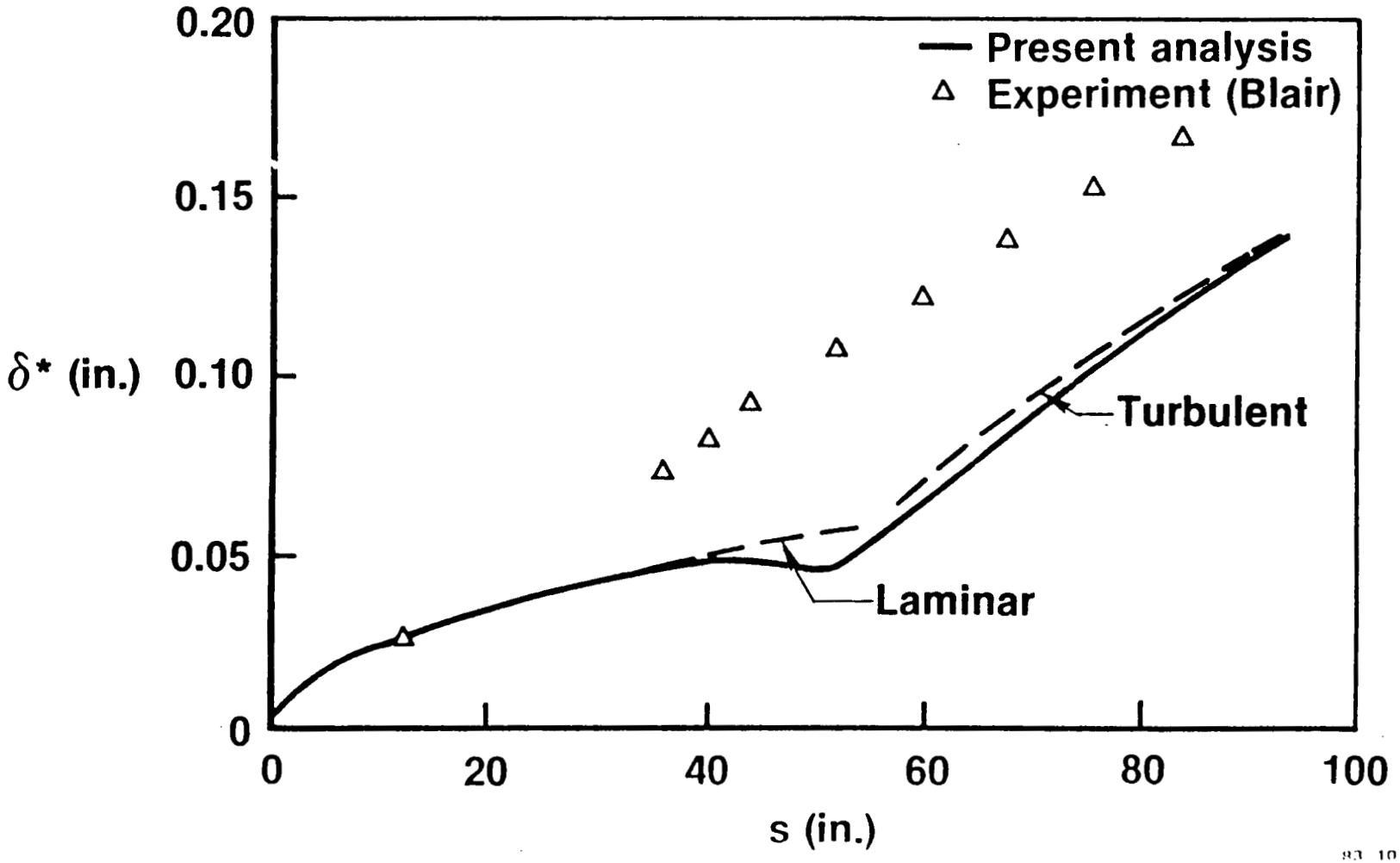

557

PRESSURE-NACA 663-018 AIRFOIL

$\alpha = 0°$

$Re_c = 2.0 \times 10^6$

$Tu_\infty = 0.002$

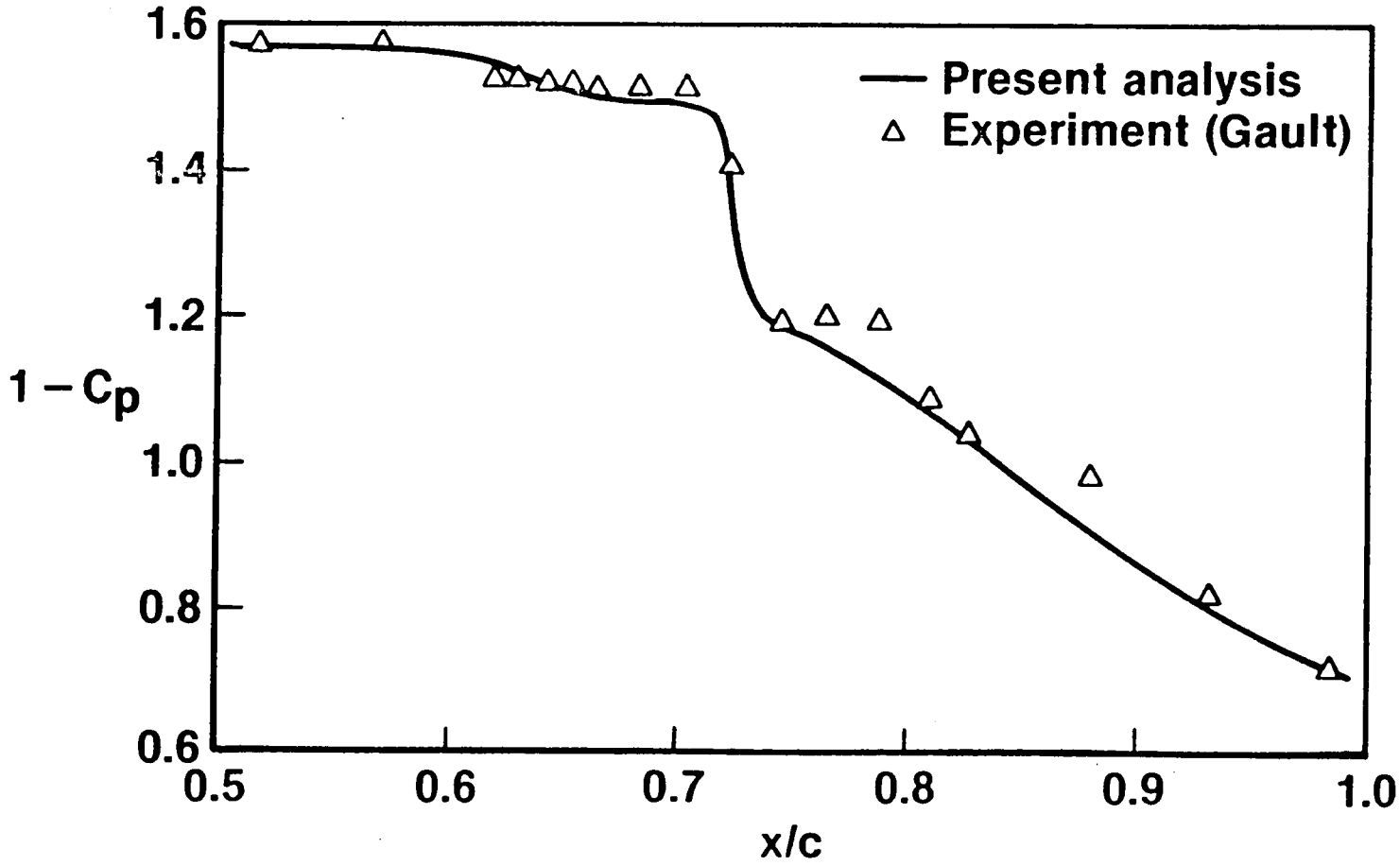

83-10-17-11

VELOCITY PROFILES-NACA 663-018 AIRFOIL

— FLARE
--- Windward
△ Experiment (Gault)

$\alpha = 0°$
$Re_c = 2.0 \times 10^6$
$Tu_\infty = 0.002$

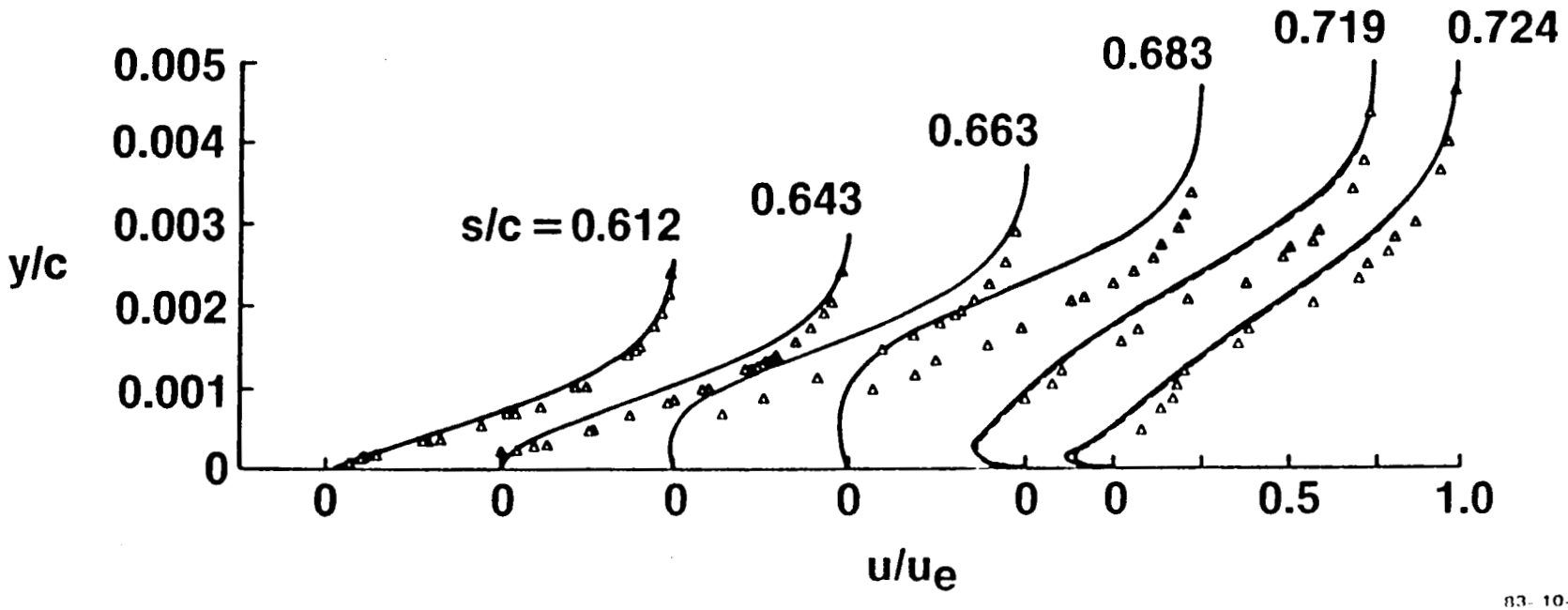

83-10-17-12

CONCLUSIONS

- Windward differencing reveals "double bubble" structure
- FLARE is good approximation even for large reversed flow velocity
- McDonald-Fish transition model predicts delayed transition for low Tu_∞
- Future directions
  - Utilize code to develop improved transition model
    - Exp. study/correlations
    - "1st principles" stability analysis
  - Extend method to 3-D wing flow

RB668TX.001

COMPUTATION OF SEPARATED FLOW ON AIRFOILS WITH THE GRUMFOIL CODE

R.E. MELNIK

J.W. BROOK

GRUMMAN AEROSPACE CORPORATION

OCTOBER 19, 1983

GRUMMAN

VISCID/INVISCID INTERACTIONS ON AIRFOILS

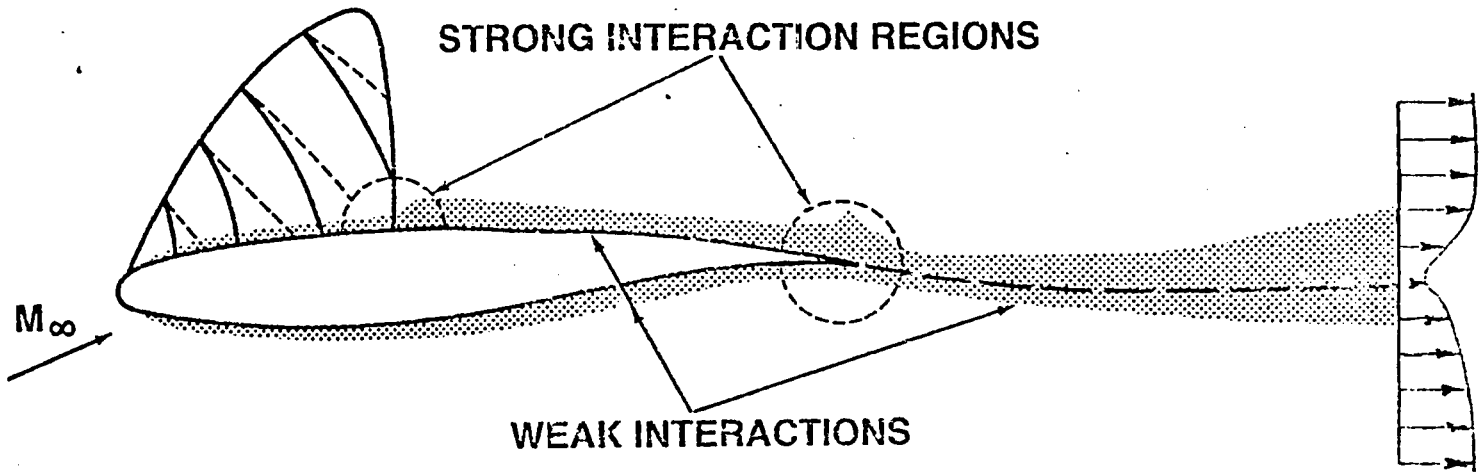

1. DISPLACEMENT EFFECTS ON THE AIRFOIL
2. DISPLACEMENT EFFECTS IN THE WAKE
3. WAKE CURVATURE EFFECTS
4. SHOCK-WAVE BOUNDARY-LAYER INTERACTIONS
5. TRAILING EDGE BOUNDARY-LAYER INTERACTIONS

} WEAK INTERACTIONS

} STRONG INTERACTIONS

GRUMMAN

2376-001W

SUMMARY OF THE GRUMFOIL CODE

(AIAA PAPER-83-0234)

INVISCID SOLUTION

- o FULL POTENTIAL FLOW EQUATION
- o CIRCLE PLANE GRID
- o FULLY CONSERVATIVE ROTATED SCHEME
- o MULTIGRID/ADI SOLVER

BOUNDARY LAYER SOLUTION

- o LAMINAR INTEGRAL METHOD STARTING SOLUTION
- o GREENS LAG ENTRAINMENT METHOD FOR TURBULENT FLOW
- o GREEN/LEBALLEUR VELOCITY PROFILES FOR SEPARATED FLOW

VISCID INVISCID INTERACTION MODEL

- o EQUIVALENT SOURCE FLOW FORMULATION
- o WAKE THICKNESS/CURVATURE EFFECTS INCLUDED
- o STRONG INTERACTION AT (CUSPED) TRAILING EDGES
- o CARTER SEMI-INVERSE ITERATIVE SCHEME

GRUMMAN

RECENT DEVELOPMENTS

- TURBULENCE MODEL
  - VELOCITY PROFILES
  - ENTRAINMENT RELATION
- ENTROPY CORRECTION
- NUMERICS
  - TRAILING EDGE POTENTIAL
  - CELL CENTERED FINITE DIFFERENCE SCHEME

GRUMMAN

RAE 2822 AIRFOIL CASE 10

UPPER SURFACE SOURCE VELOCITY

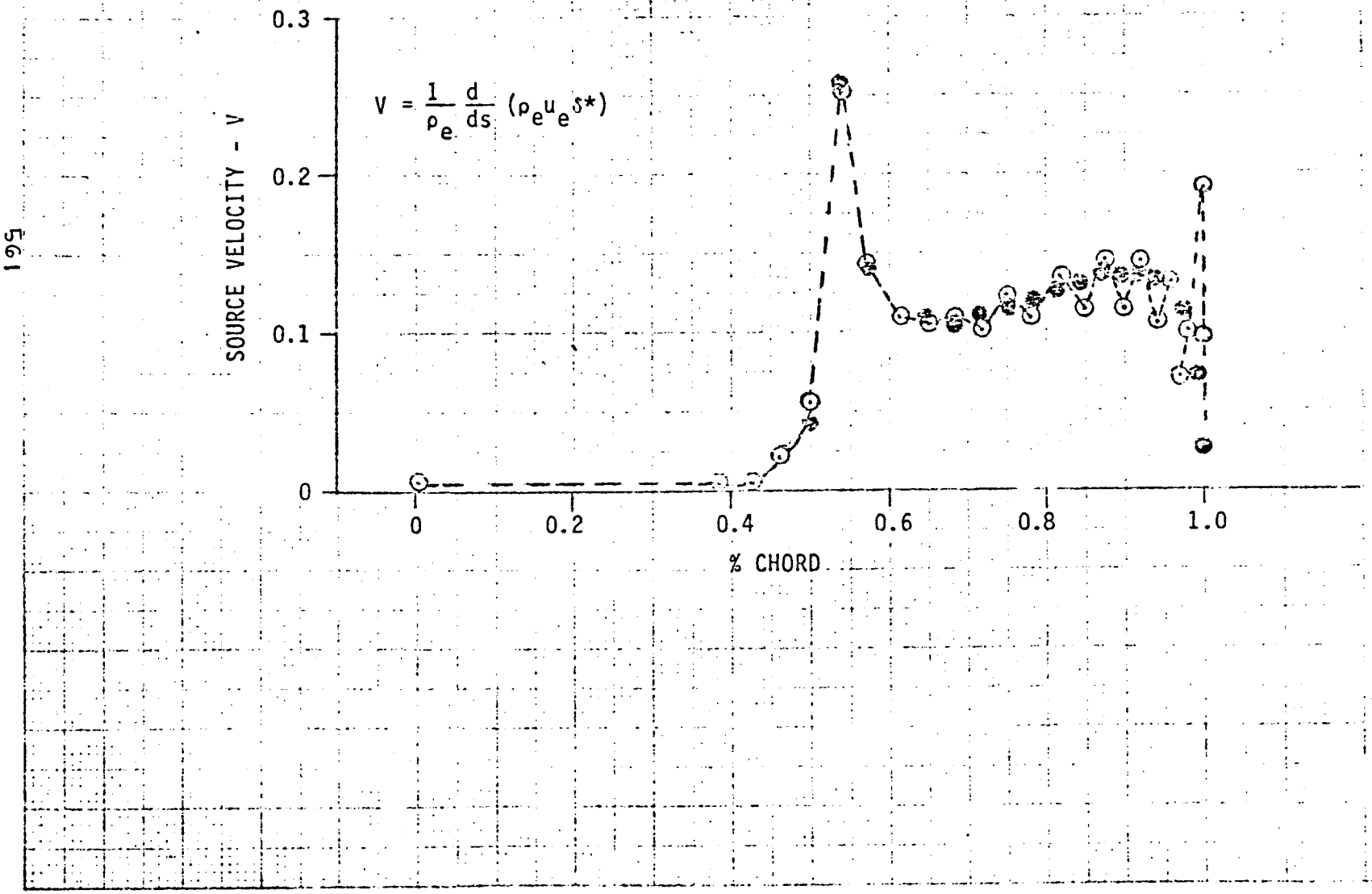

INVERSE BOUNDARY LAYER EQUATIONS

$Q = \rho_e U_e \delta^*$ PRESCRIBED

$$\frac{du_e}{ds} = \frac{C_1 \rho_e u_e - K\, dQ/ds}{C_2 \rho_e \Theta}$$

Q ⇨ $$\frac{d\bar{H}}{ds} = \frac{(C_3 \rho_e u_e - H_1\, dQ/ds)(H+1)}{C_2 \rho_e u_e \Theta}$$ ⇨ U_e, H, C_E

$$\frac{dC_E}{ds} = \left\{ \frac{\qquad}{\Theta} \right\}$$

$H = \delta^*/\Theta \quad \bar{H} = \tfrac{1}{2}(C_r+1)(\bar{H}+1)-1 \quad H_1 = (\delta-\delta^*)/\Theta$

SHAPE FACTOR RELATIONS $H_1 = H_1(\bar{H})$ $\quad K = dH_1(\bar{H})/d\bar{H}$

SEPARATION: $K=0$ $\quad C_2 \neq 0$ NO SINGULARITY

LEBALLEUR/GREEN VELOCITY PROFILE FOR SEPARATED FLOW

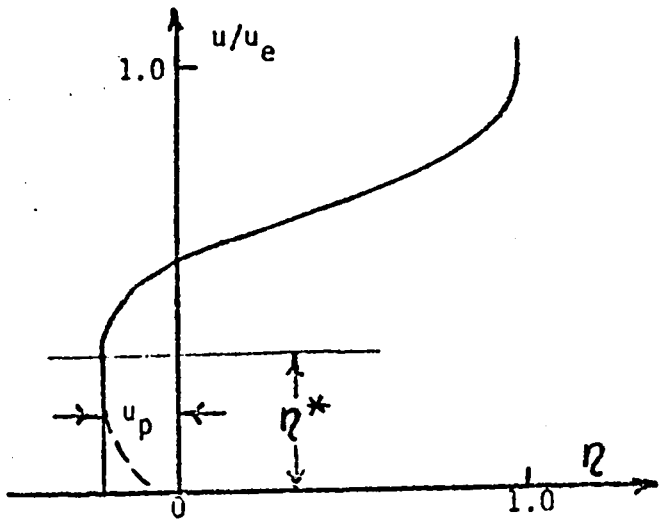

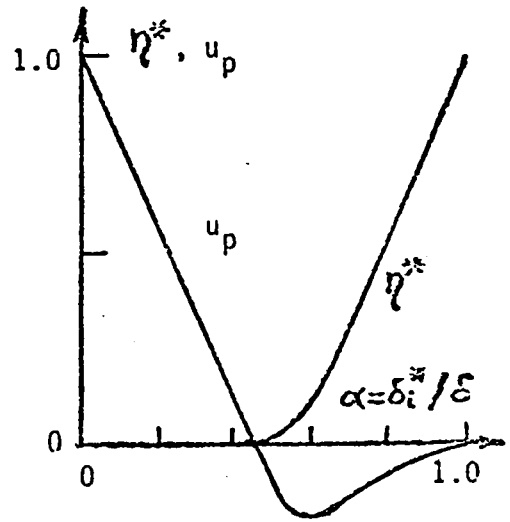

$$\frac{U}{U_E} = 1 + C_1 \text{ LOG } \eta - C_2\tilde{F}(\eta) \quad ; \quad \eta = \frac{Y}{\delta}$$

$$F(\eta) = 1 \qquad \eta < \eta^*$$

$$\tilde{F}(\eta) = F(\bar{\eta}) \qquad \eta > \eta^* \ , \qquad \bar{\eta} = (\eta-\eta^*)/(1-\eta^*)$$

GRUMMAN

SHAPE FACTOR RELATIONSHIP

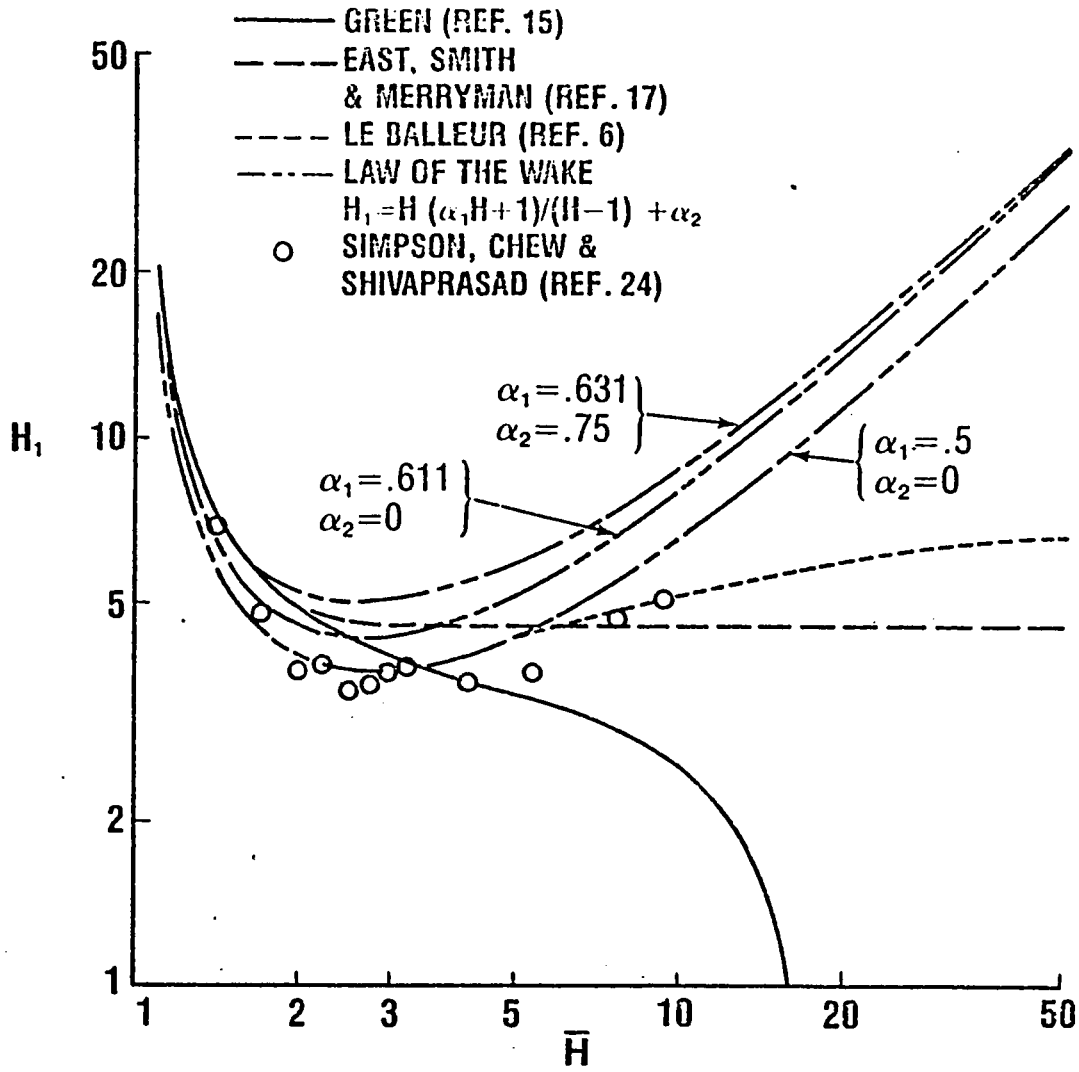

2376-002W

GRUMMAN

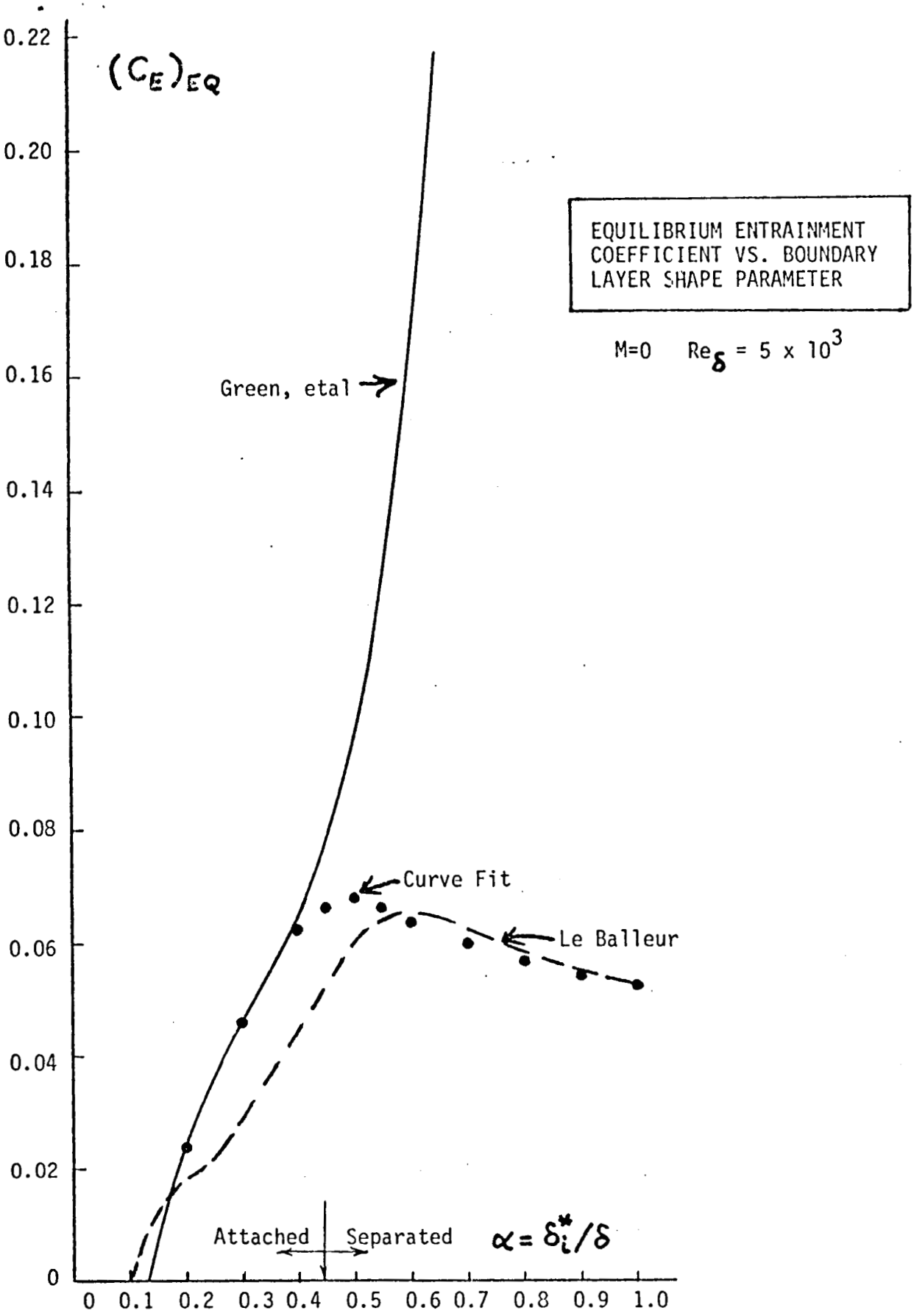
$(C_E)_{EQ}$
0.22
0.20
0.18
0.16
0.14
0.12
0.10
0.08
0.06
0.04
0.02
0
Green, etal
Curve Fit
Le Balleur
Attached
Separated
$\alpha = \delta_i^*/\delta$
0 0.1 0.2 0.3 0.4 0.5 0.6 0.7 0.8 0.9 1.0
EQUILIBRIUM ENTRAINMENT COEFFICIENT VS. BOUNDARY LAYER SHAPE PARAMETER
M=0 $Re_\delta = 5 \times 10^3$

RAE 2822 AIRFOIL-CASE 10
EFFECT OF VELOCITY PROFILE RELATION
(UNCORRECTED POTENTIAL FLOW)

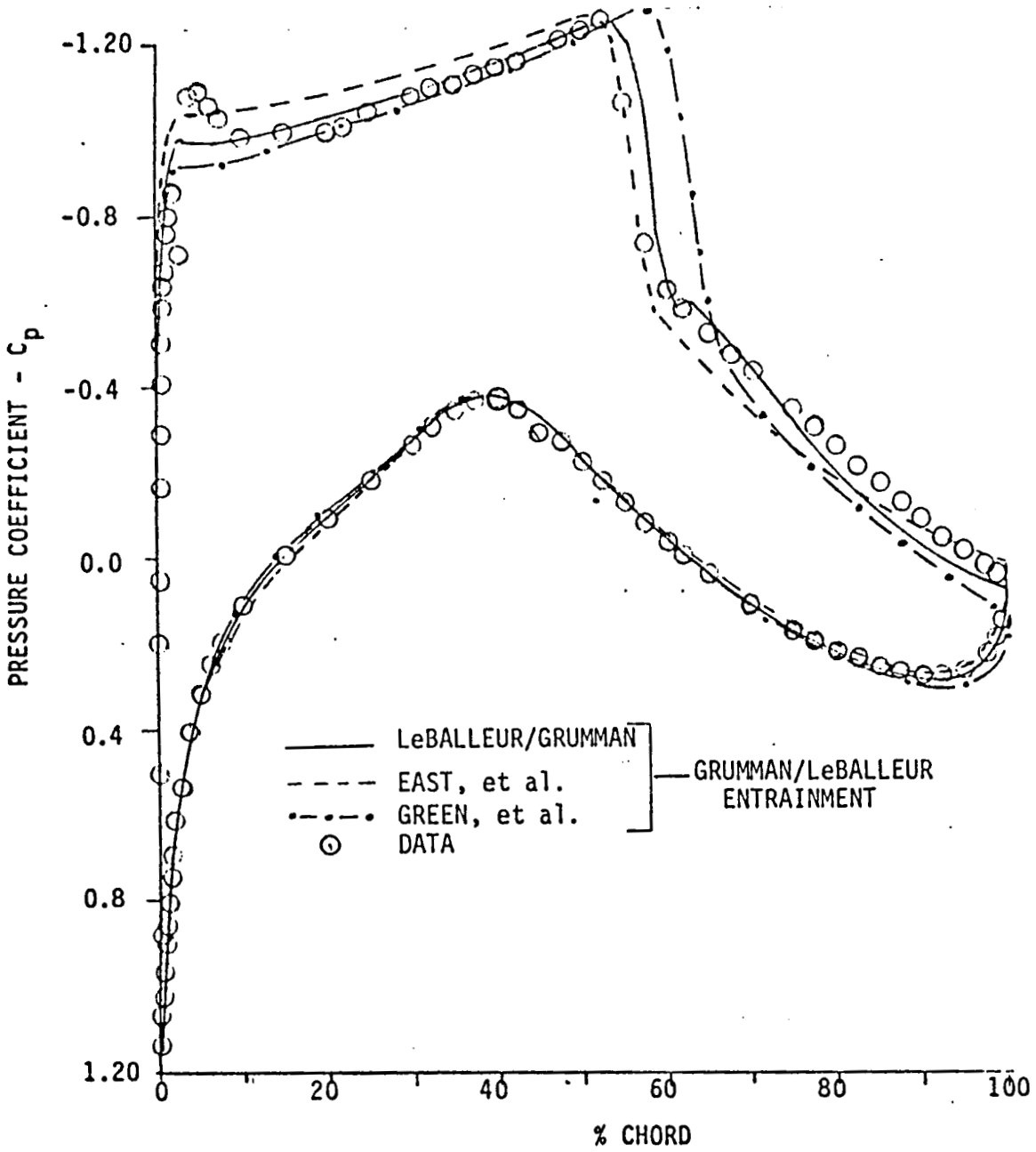

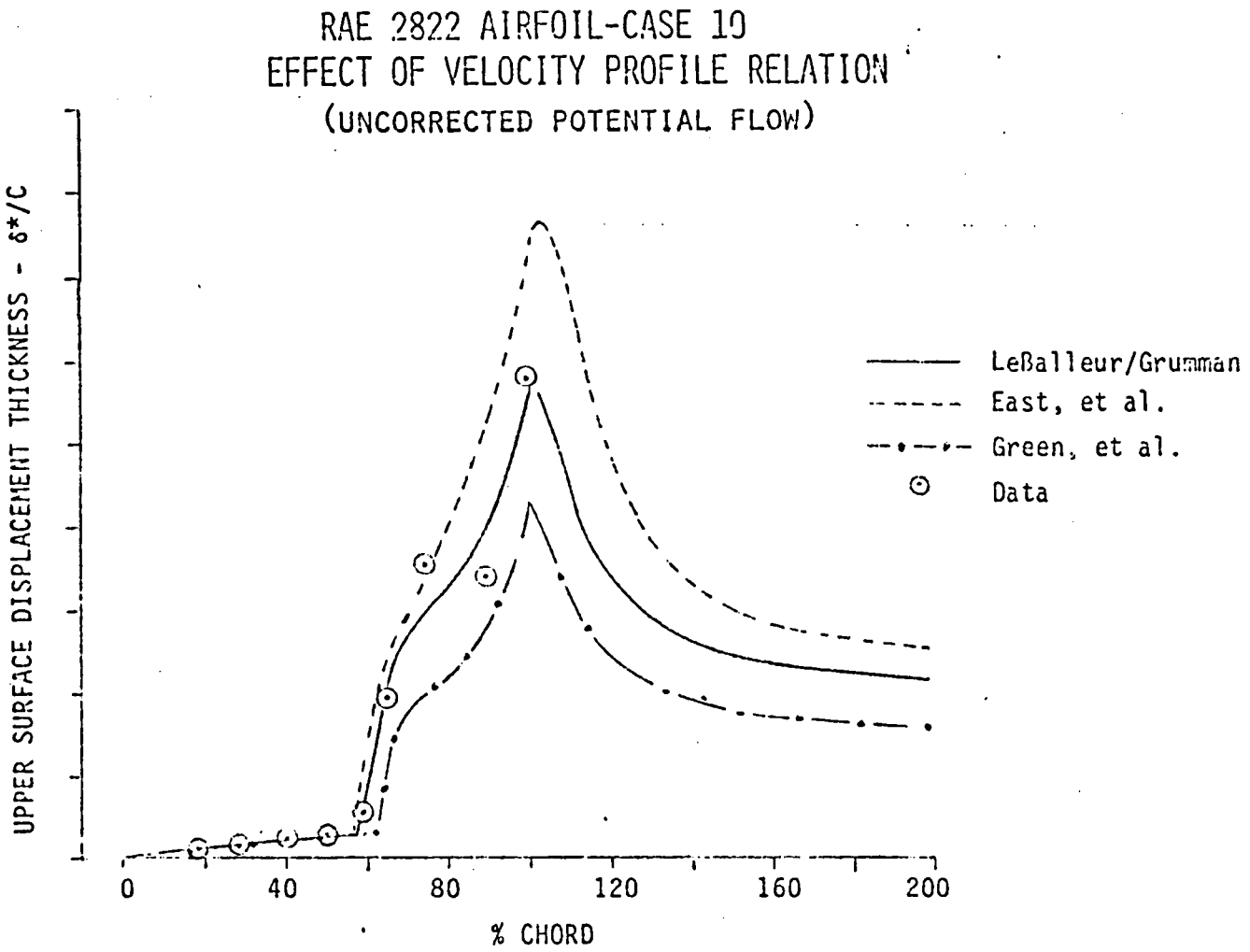
RAE 2822 AIRFOIL-CASE 10
EFFECT OF VELOCITY PROFILE RELATION
(UNCORRECTED POTENTIAL FLOW)
UPPER SURFACE DISPLACEMENT THICKNESS - δ*/C
0
40
80
120
160
200
% CHORD
Leßalleur/Grumman
East, et al.
Green, et al.
Data

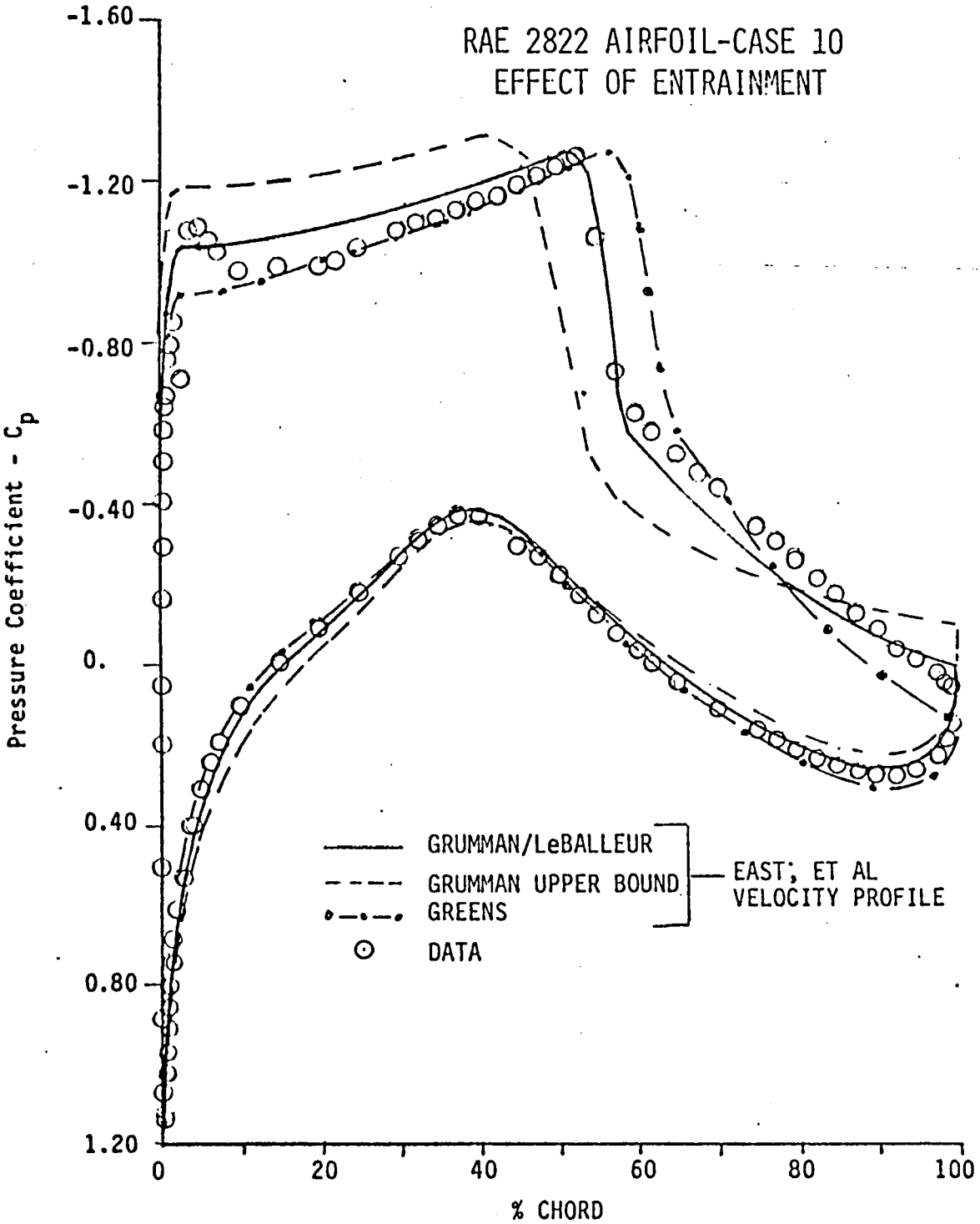
RAE 2822 AIRFOIL-CASE 10
EFFECT OF ENTRAINMENT
-1.60
-1.20
-0.80
-0.40
0.
0.40
0.80
1.20
Pressure Coefficient - C_p
0
20
40
60
80
100
% CHORD
GRUMMAN/LeBALLEUR
GRUMMAN UPPER BOUND
GREENS
DATA
EAST, ET AL VELOCITY PROFILE

RAE 2822 AIRFOIL-CASE 10
EFFECT OF ENTRAINMENT
ON DISPLACEMENT THICKNESS

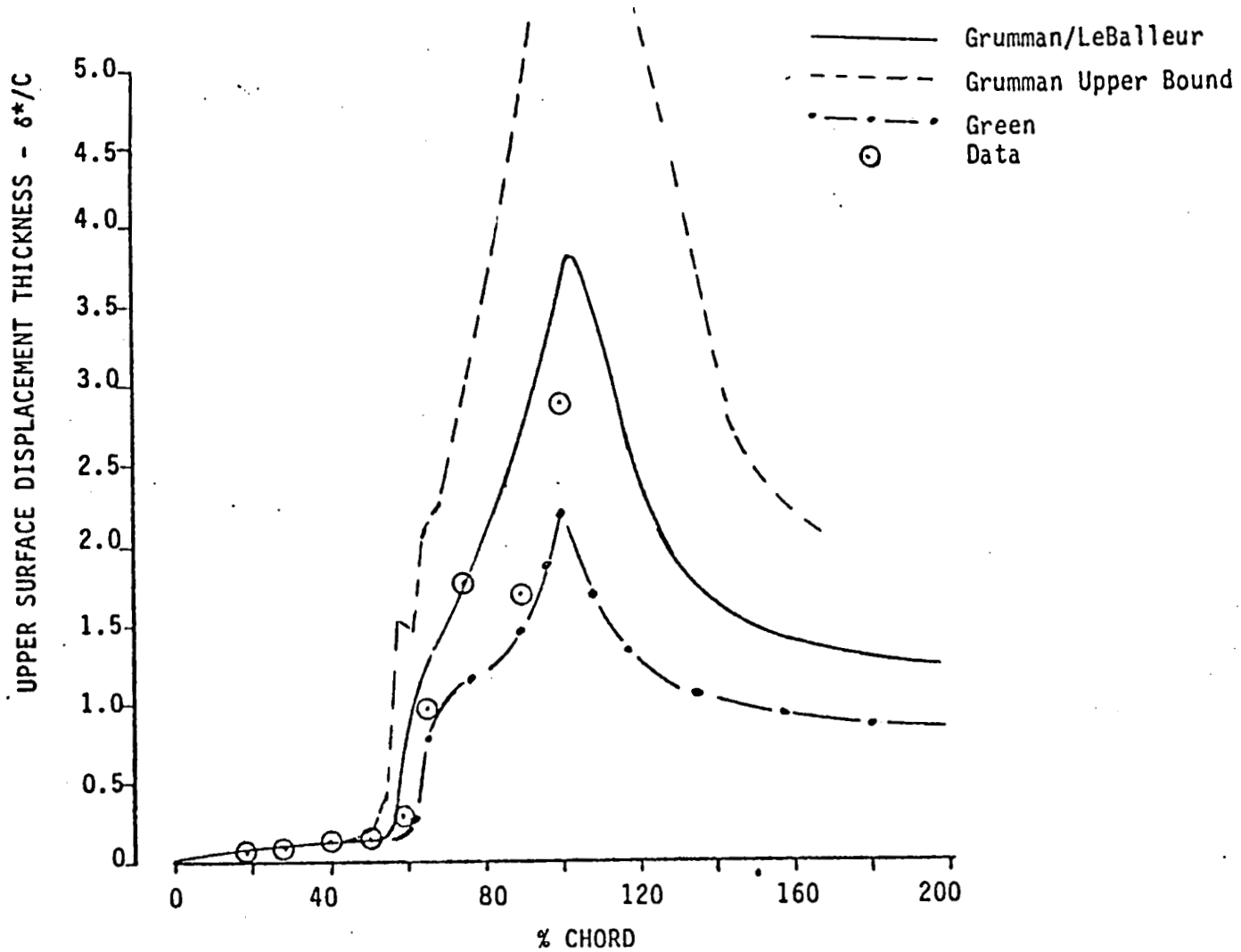

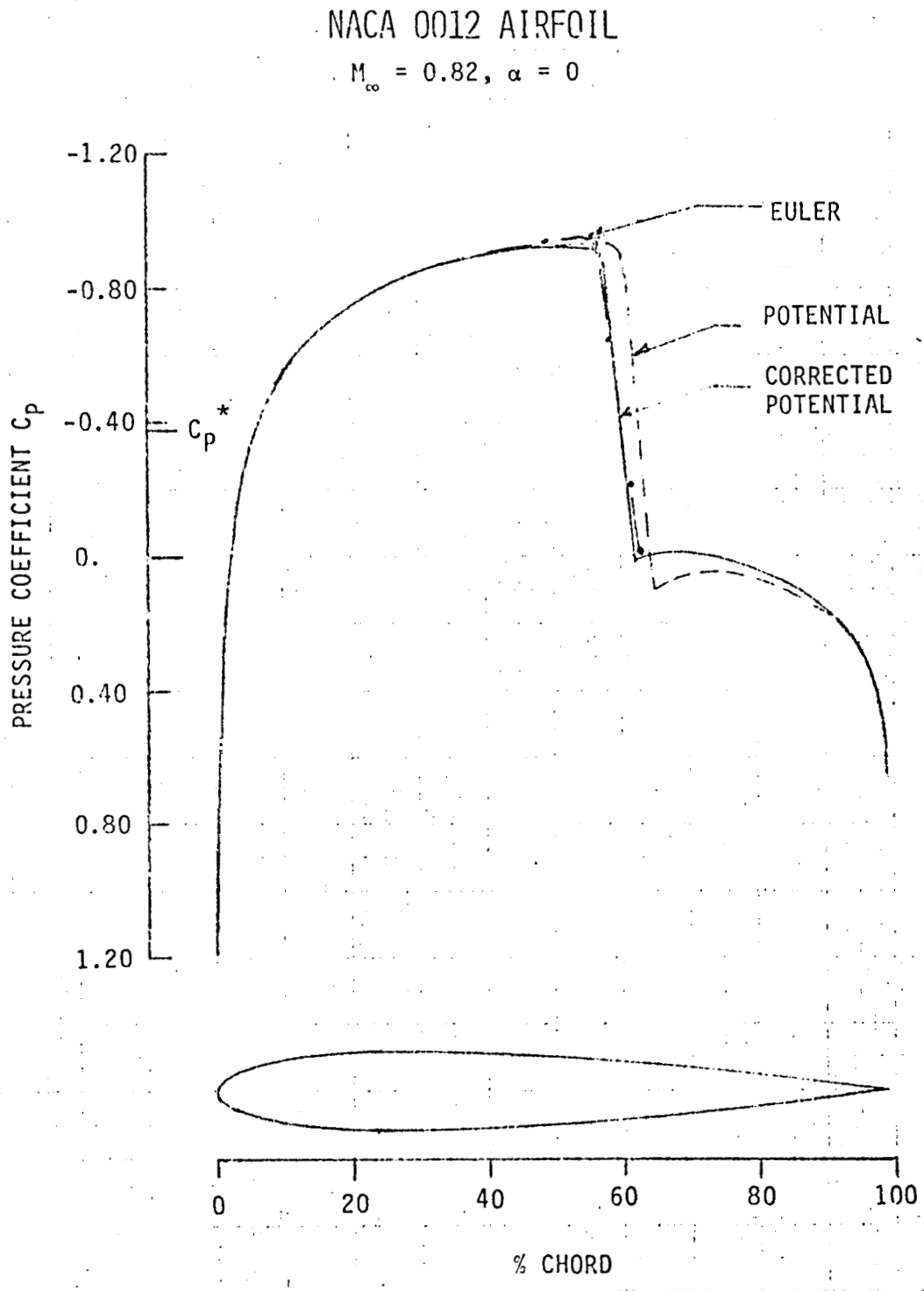
NACA 0012 AIRFOIL
$M_\infty = 0.82, \alpha = 0$
-1.20
-0.80
-0.40
0.
0.40
0.80
1.20
C_p^*
PRESSURE COEFFICIENT C_p
EULER
POTENTIAL
CORRECTED POTENTIAL
0
20
40
60
80
100
% CHORD

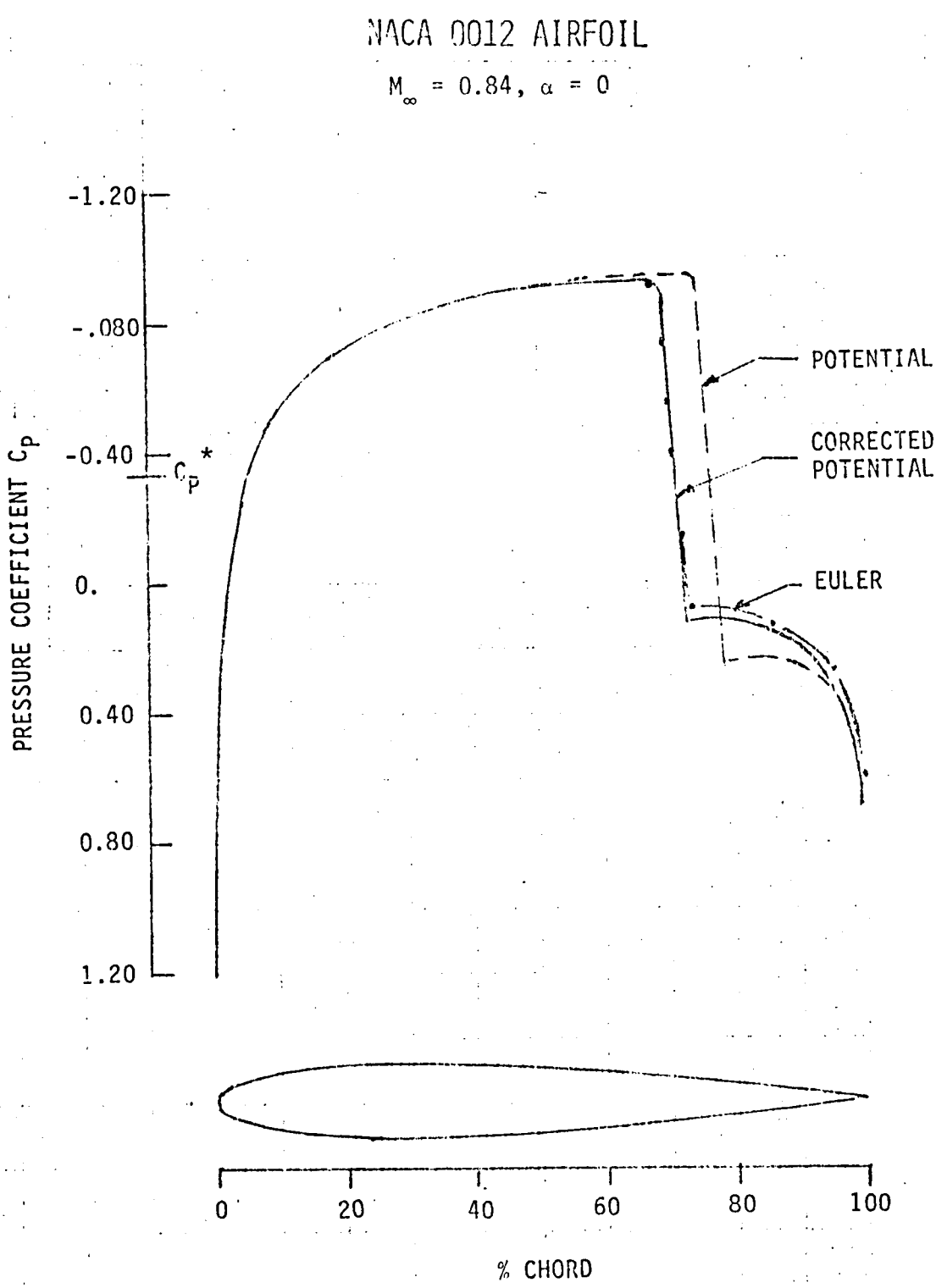
NACA 0012 AIRFOIL
$M_\infty = 0.84, \alpha = 0$
-1.20
-.080
-0.40
C_P^*
0.
0.40
0.80
1.20
PRESSURE COEFFICIENT C_p
POTENTIAL
CORRECTED POTENTIAL
EULER
0
20
40
60
80
100
% CHORD

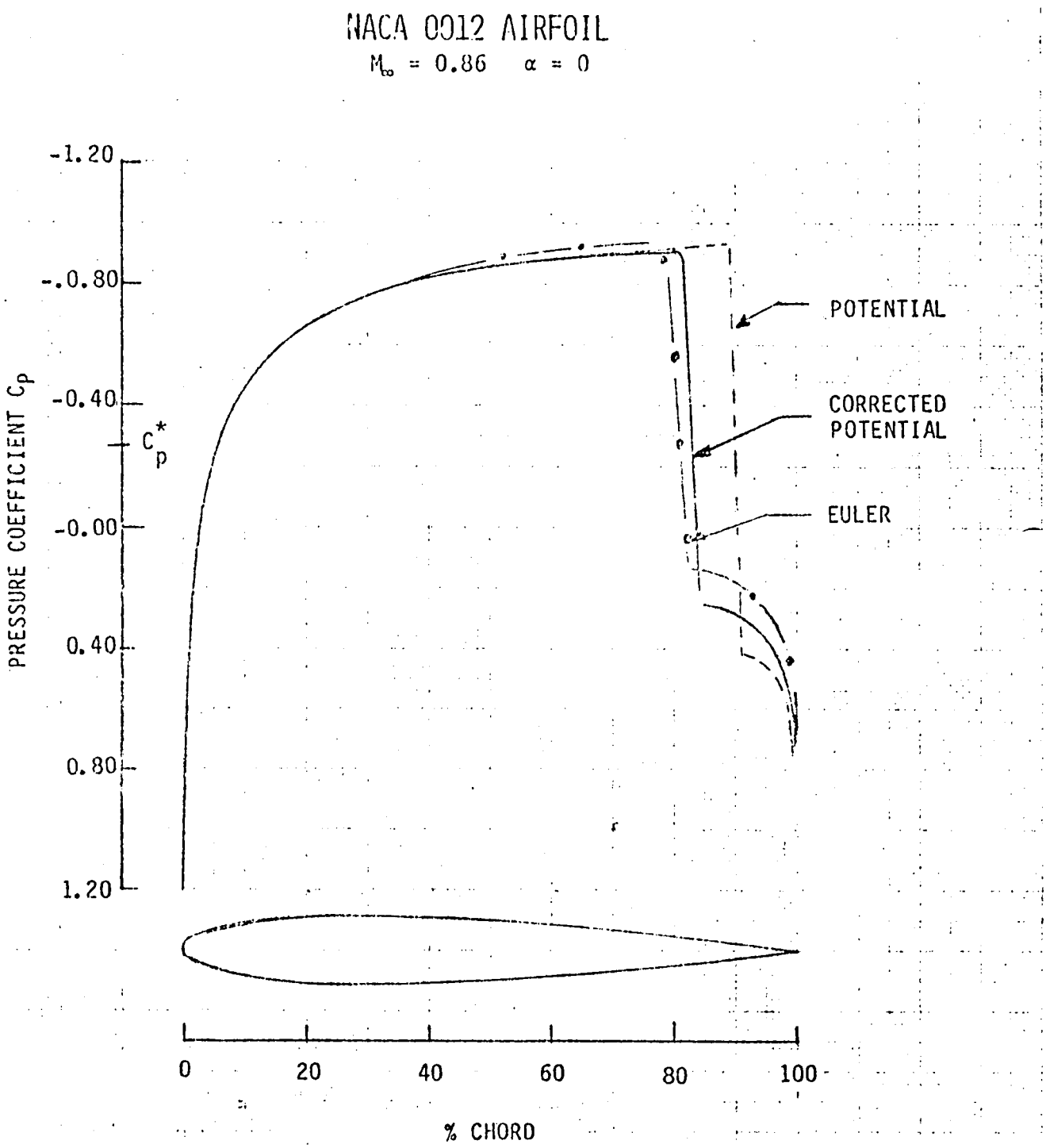
NACA 0012 AIRFOIL
$M_\infty = 0.86 \quad \alpha = 0$
-1.20
-.0.80
-0.40
-0.00
0.40
0.80
1.20
PRESSURE COEFFICIENT C_p
C_p^*
POTENTIAL
CORRECTED POTENTIAL
EULER
0
20
40
60
80
100
% CHORD

NACA 0012 AIRFOIL INVISCID SHOCK POSITION

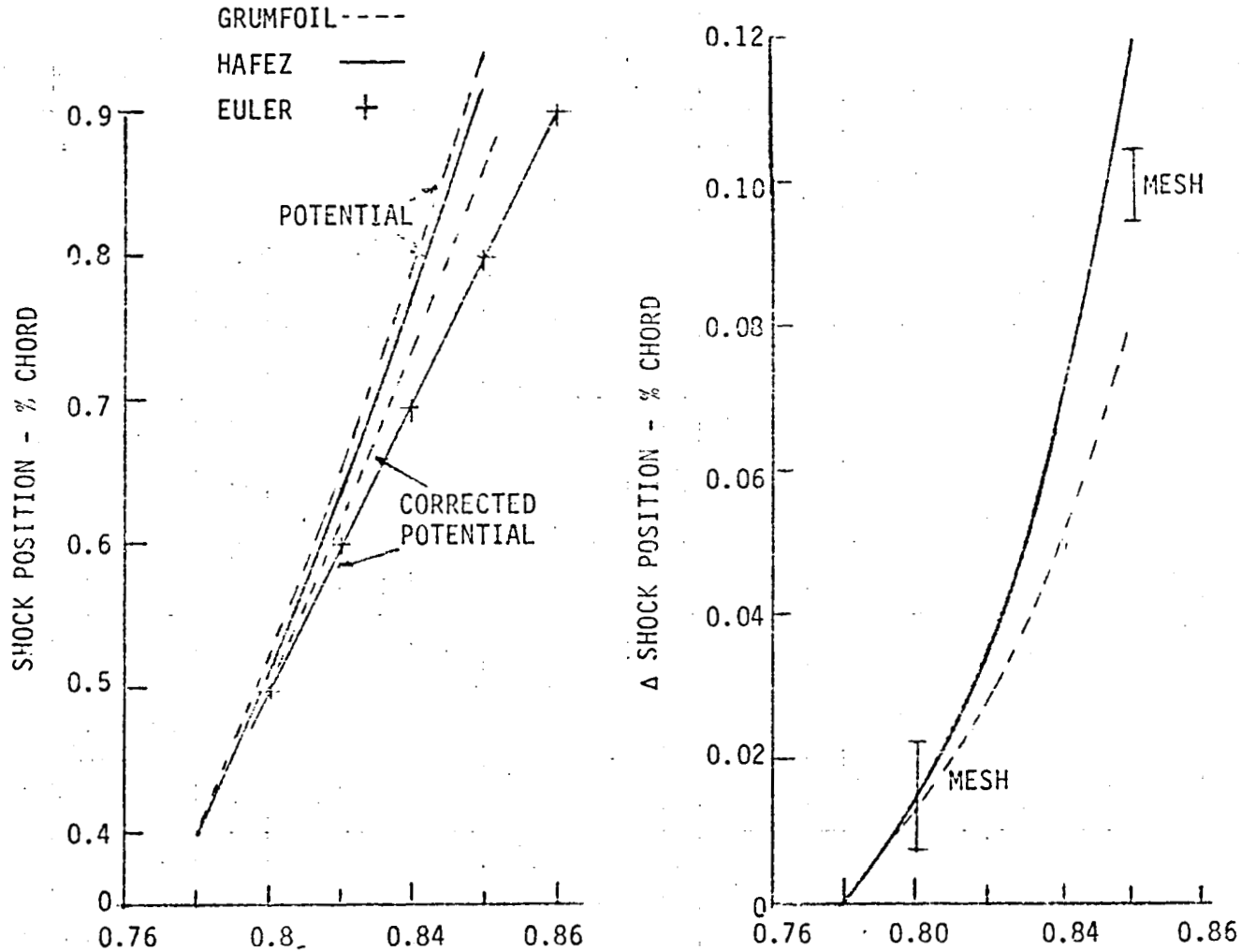

NACA 0012 AIRFOIL INVISCID LIFT

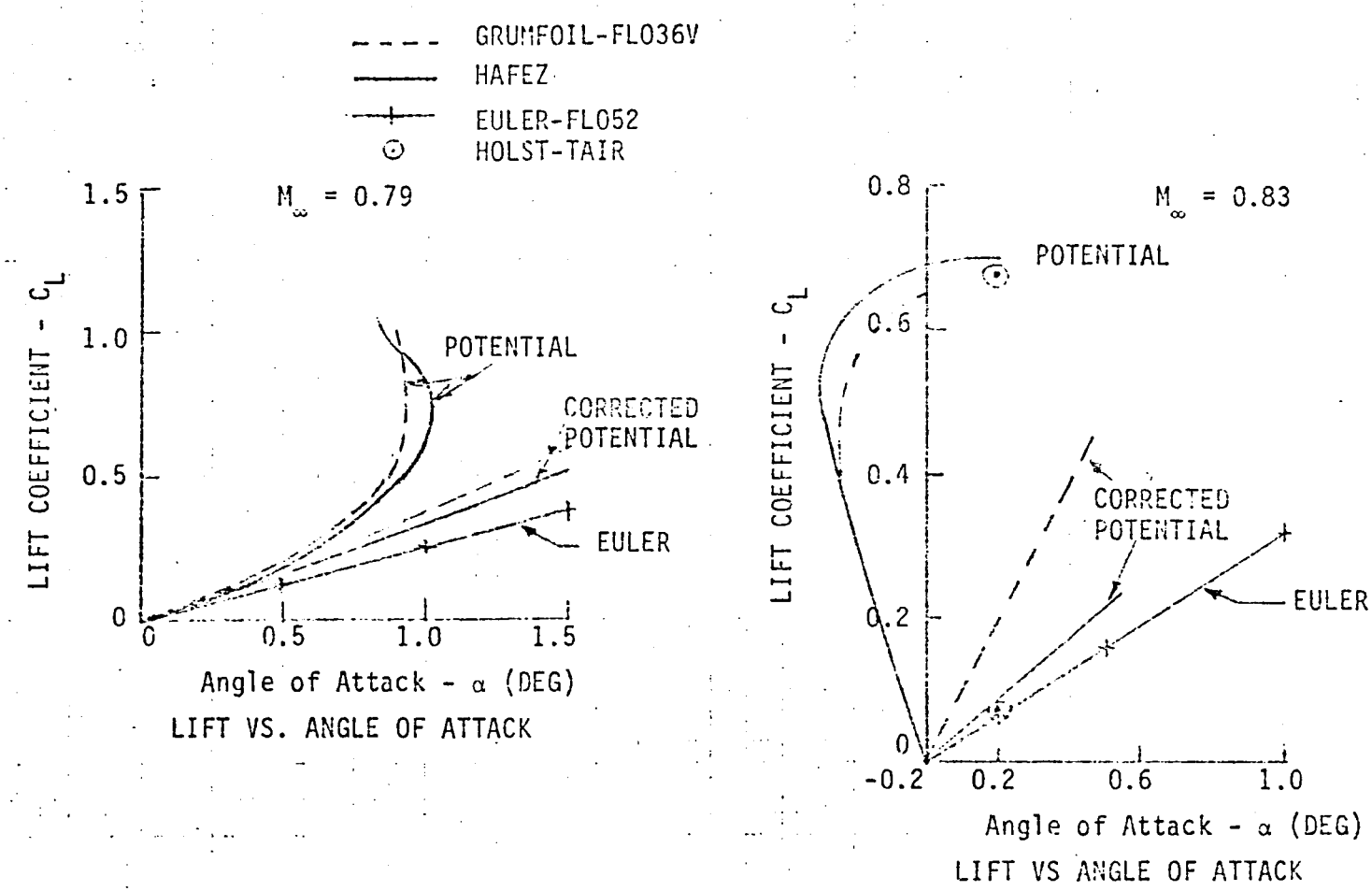

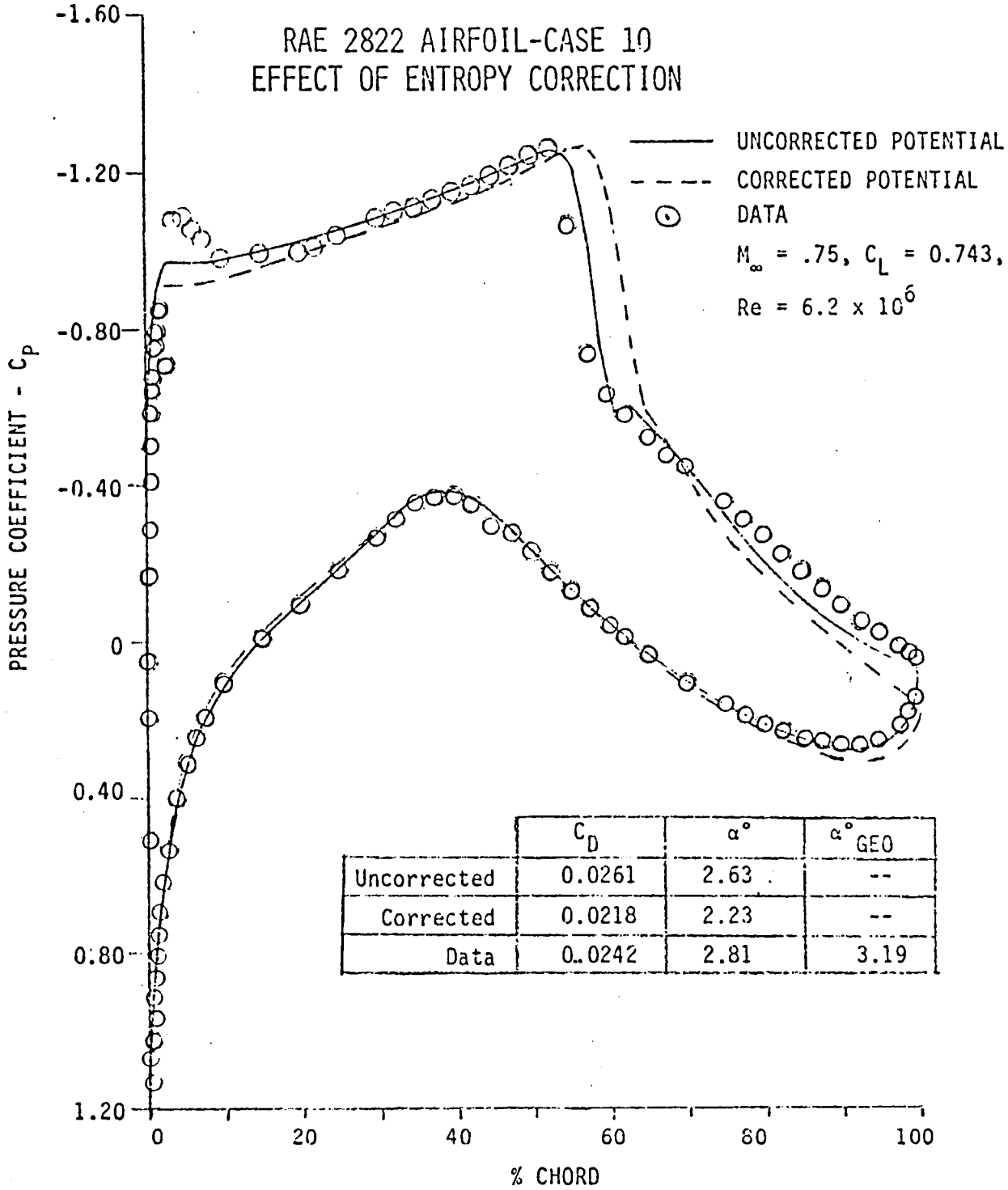

	C_D	α°	α°_{GEO}
Uncorrected	0.0261	2.63	--
Corrected	0.0218	2.23	--
Data	0.0242	2.81	3.19

RAE 2822 AIRFOIL-CASE 10
EFFECT OF ENTROPY CORRECTION

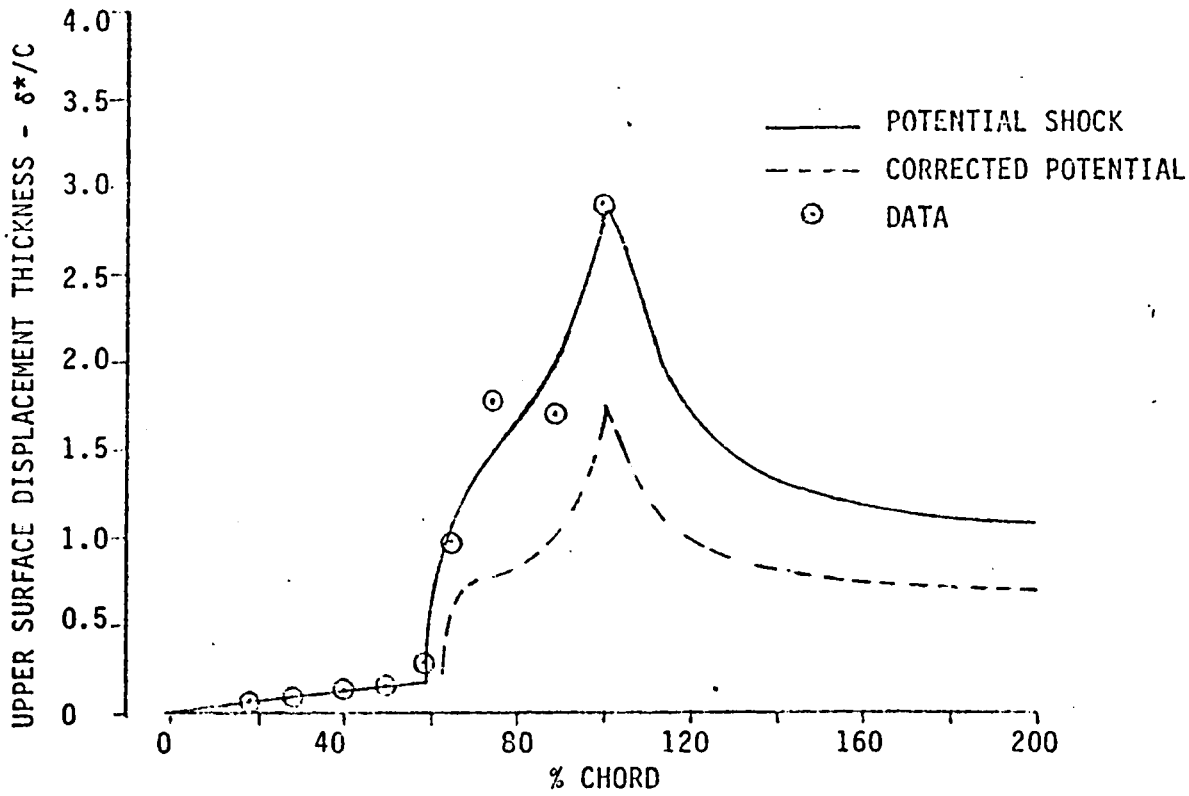

EFFECT OF ENTROPY CORRECTION ON THE COMPUTED LIFT OF THE RAE 2822 AIRFOIL AT $M_\infty = 0.75$

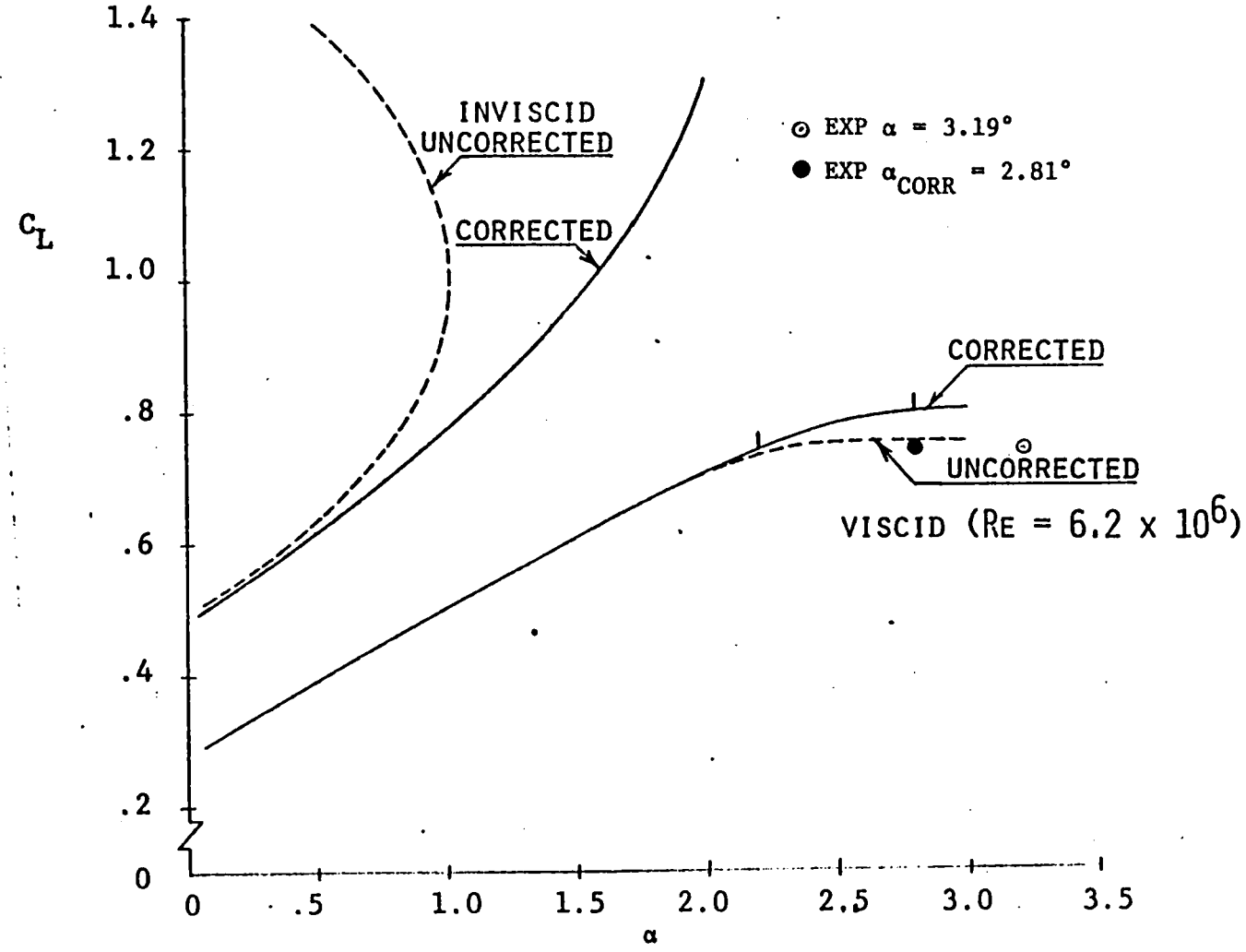

GRUMMAN

FORMULATION OF INVERSE PROBLEM WITH TRAILING EDGE CLOSURE

- AIRFOIL SOUGHT FOR $\frac{q}{q_\infty} = f_1(\omega; a_1)\left[f_o(s) + a_2 f_2(\omega) + a_3 f_3(\omega)\right]$
- q_∞ FIXED; a_1, a_2, a_3 FOUND AS PART OF THE SOLUTION
- PROPER CHOICES OF f_1, f_2, f_3 UNCOUPLE SEARCH FOR a_1, a_2, a_3
- $f_3(\omega) = \text{MAX}(1, \mu) \qquad \frac{3\pi}{4} \leqslant \omega \leqslant \frac{5\pi}{4}$

  $\mu = \text{MAX}\left[1, 0.4\left(\frac{dq_o}{d\omega} - 1\right)\right]$

  THIS f_3 SHIFTS L.E. STAGNATION POINT ⇒ CONTROLS T.E. Δx
- f_2 USED TO CONTROL Δy
- f_1 USED TO SATISFY FIRST CONSTRAINT

GRUMMAN

1606-014D

EFFECT OF CLOSURE SCHEME ON AIRFOIL SOLUTIONS; COMPUTED PRESSURES AND ORIGINAL TARGET; CASE A2, $M_\infty = 0.800$

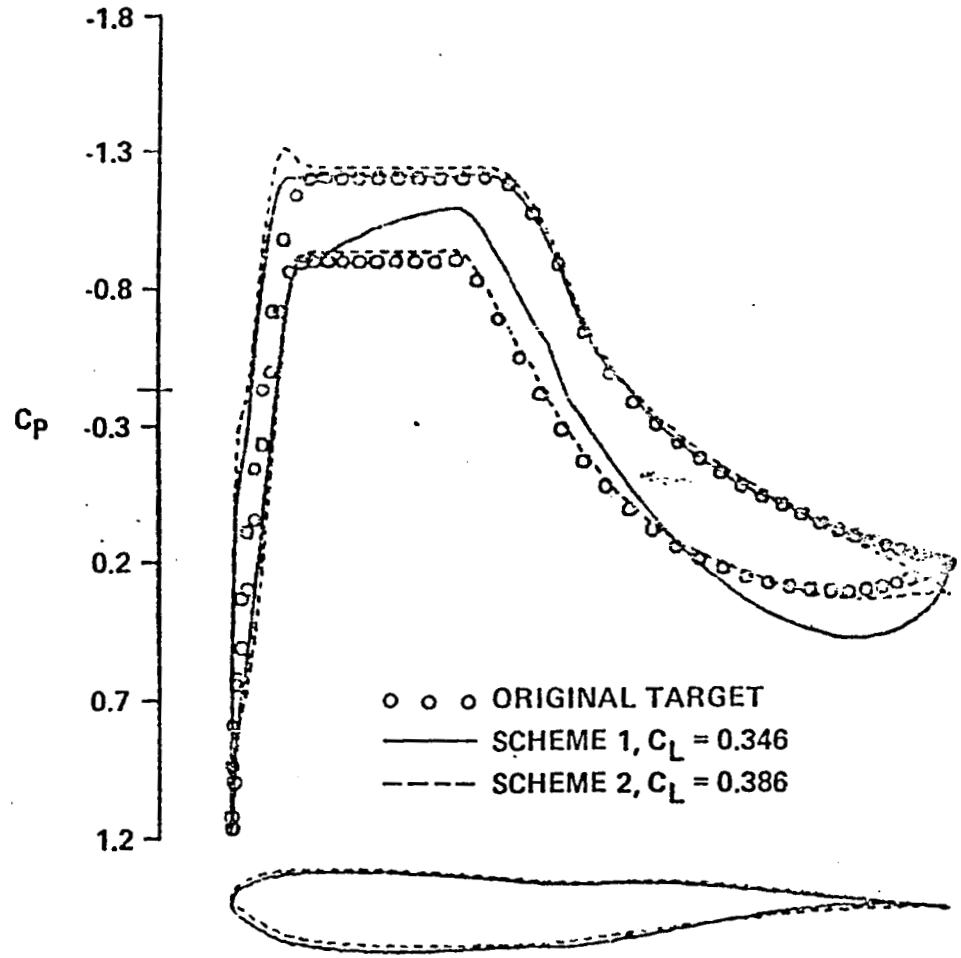

DESIGNED CONTOUR, COMPUTED PRESSURES AND ORIGINAL TARGET; CASE E1, $M_\infty = 0.683$

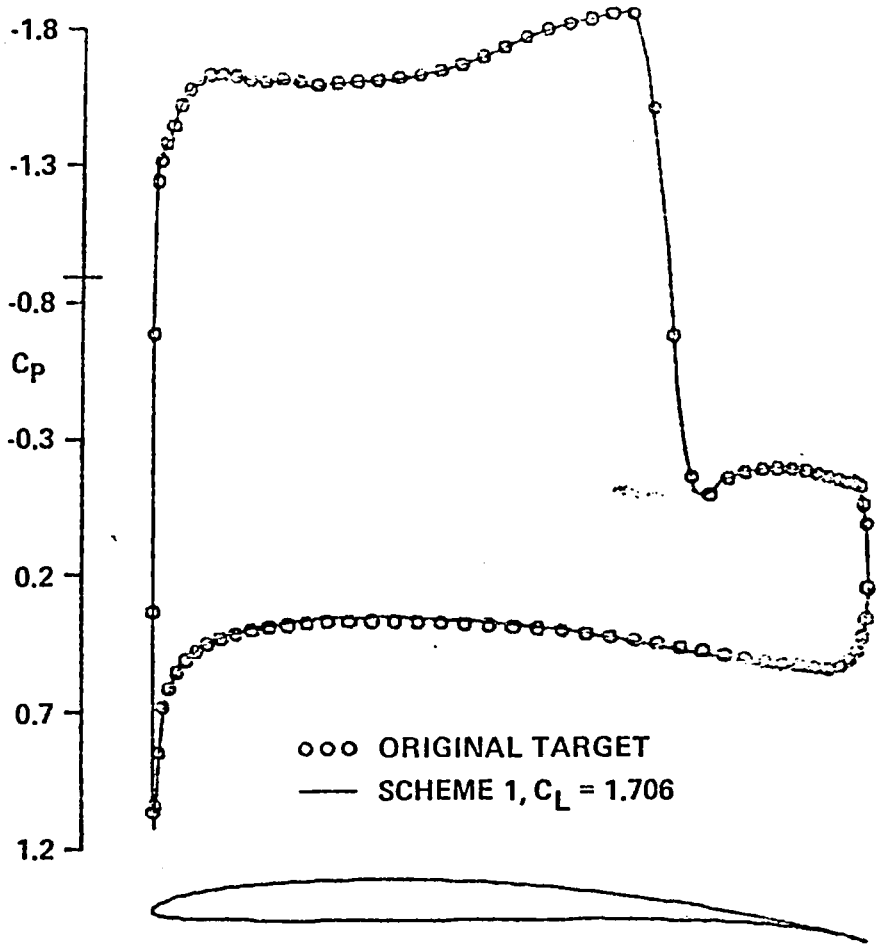

GRUMMAN

1606-026D

CONCLUSIONS

- SOLUTIONS ARE SENSITIVE TO ENTRAINMENT AND VELOCITY PROFILE RELATIONS WHEN SEPARATION IS PRESENT
- ENTROPY CORRECTIONS ARE LESS IMPORTANT WHEN BOUNDARY LAYER IS INCLUDED
- POTENTIAL FLOW/BOUNDARY LAYER CODE IS USEFUL UP TO MAXIMUM LIFT
- SEMI-INVERSE METHOD IS USEFUL BUT NEEDS TO BE IMPROVED UPON FOR LARGE SEPARATION ZONES
- CANNOT YET PREDICT SEPARATED FLOWS WITH CONFIDENCE
- "COMPLETE" AND CORRECT FORMULATION OF INVERSE DESIGN METHOD ACHIEVED FOR COMPRESSIBLE FLOW

GRUMMAN

TRANSONIC VISCOUS-INVISCID INTERACTION USING EULER AND INVERSE BOUNDARY-LAYER EQUATIONS

GRANT NO. NASA NAG-1-226

PRINCIPAL INVESTIGATOR:
DAVE WHITFIELD
MISSISSIPPI STATE UNIVERSITY

TECHNICAL OFFICER:
FRANK THAMES
NASA LANGLEY RESEARCH CENTER

OCTOBER 1983

APPROACH

- EULER EQUATIONS (THREE-DIMENSIONAL)
    1. Jameson and Turkel's Runge-Kutta Code
    2. Upwind (Flux-Vector-Split) Code

- INVERSE INTEGRAL BOUNDARY LAYER
    - Momentum Equation
    - Mean Flow Kinetic Energy Equation
    - Dissipation Equation

- VISCOUS-INVISCID INTERACTION
    1. Displacement Surface
    2. Surface Porosity
    3. Vorticity

OUTLINE

- 3-D EULER SOLUTIONS WITH BODY FORCE TERMS
- 3-D FLUX-VECTOR-SPLIT EULER CODE
- PSEUDO NAVIER-STOKES
- RESULTS

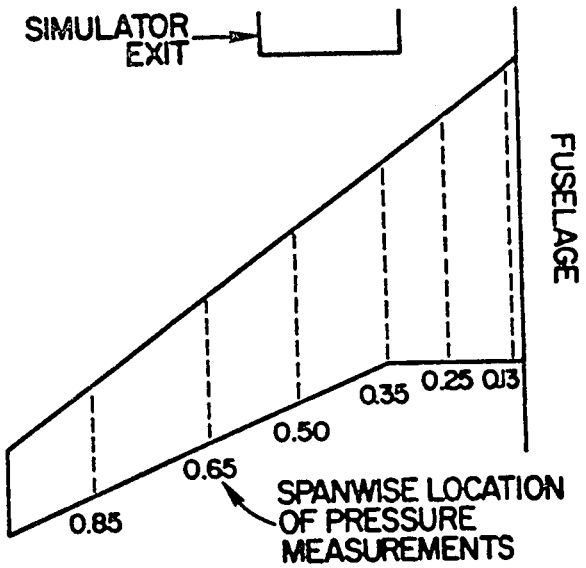

Schematic of Simulator and Wing

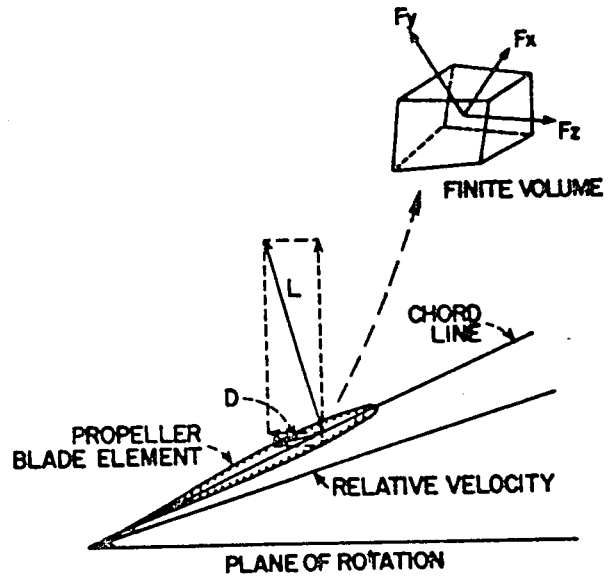

Force Diagram of a Propeller Blade Element

EULER EQUATIONS WITH FORCE TERMS

$$\int_{V_o} \frac{\partial \vec{G}}{\partial t}\, dV + \int_{S_o} (\vec{F}_x n_x + \vec{F}_y n_y + \vec{F}_z n_z) dS - \int_{V_o} \vec{B} dV = 0$$

where

$$\vec{G} = [\rho,\ \rho u,\ \rho v,\ \rho w,\ \rho E]^T$$

$$\vec{F}_x = [\rho u,\ \rho uu+p,\ \rho vu,\ \rho wu,\ \rho(E+p/\rho)u]^T$$

$$\vec{F}_y = [\rho v,\ \rho uv,\ \rho vv+p,\ \rho wv,\ \rho(E+p/\rho)v]^T$$

$$\vec{F}_z = [\rho w,\ \rho uw,\ \rho vw,\ \rho ww+p,\ \rho(E+p/\rho)w]^T$$

$$\vec{B} = [0,\ \rho f_x,\ \rho f_y,\ \rho f_z,\ \rho(f_x u + f_y v + f_z w)]^T$$

$$\int_{V_o} \vec{B} dV = \int_{V_o} \text{div}\, \vec{\vec{\tau}} dV = \int_{S_o} \vec{\tilde{B}} dS$$

where

$$\vec{\tilde{B}} = \vec{\vec{\tau}} \cdot \vec{n} = [0,\ \tilde{f}_x,\ \tilde{f}_y,\ \tilde{f}_z,\ \tilde{f}_x u + \tilde{f}_y v + \tilde{f}_z w]^T$$

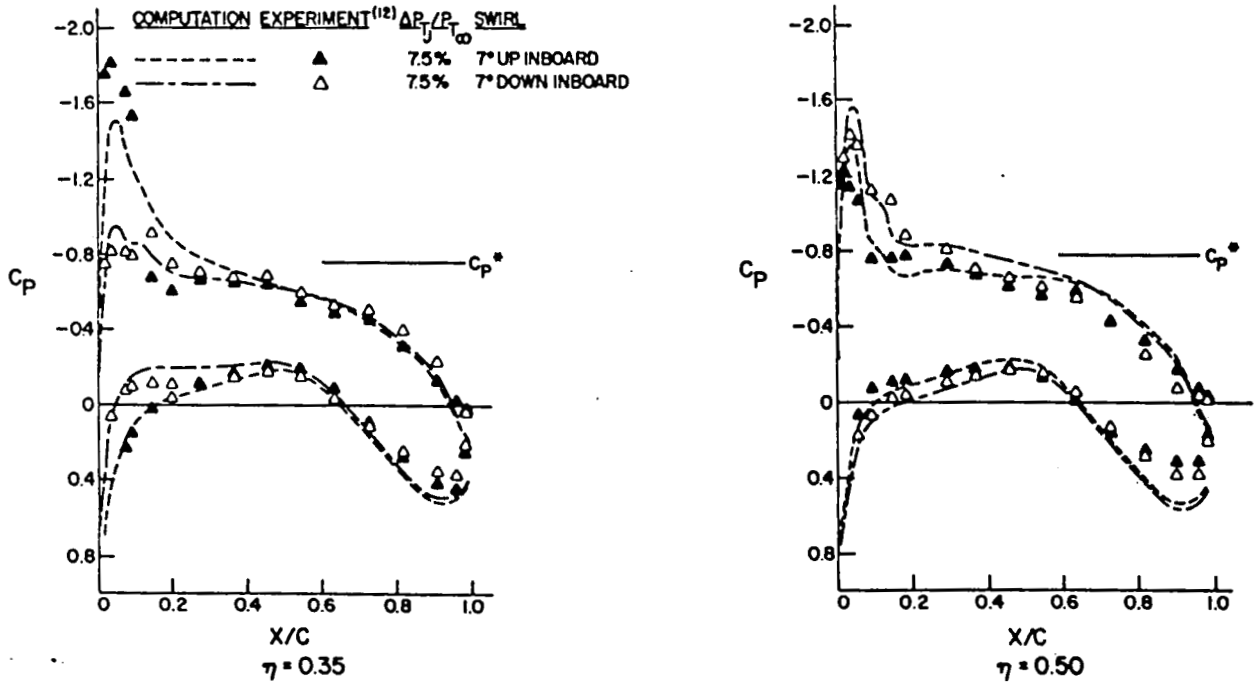

Numerical and Experimental Wing Surface Pressures
With and Without Simulator for $M_\infty = 0.70$, $Re = 2.3 \times 10^6$,
and $\alpha = 3°$

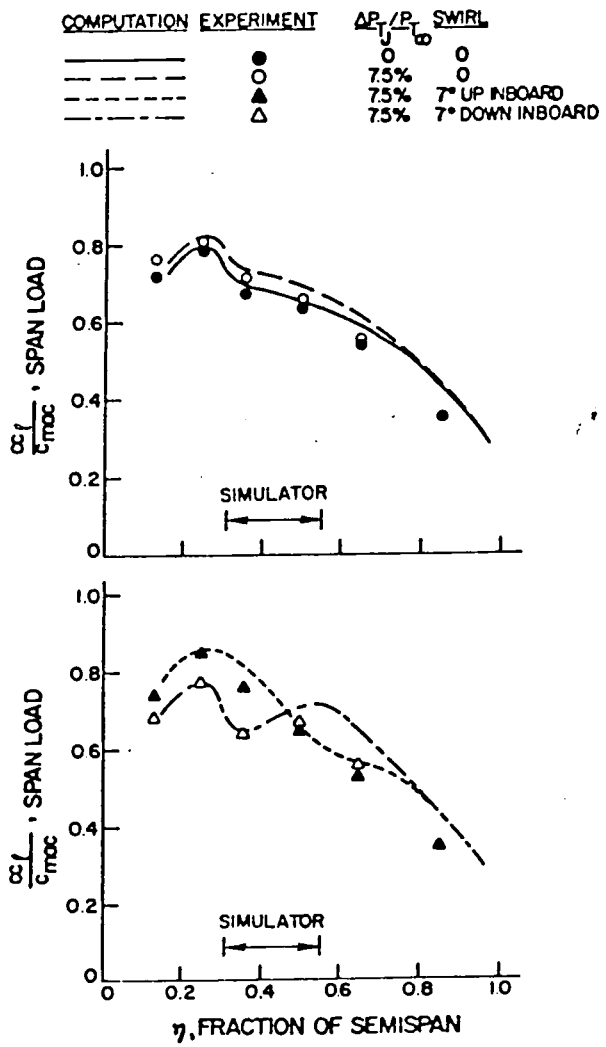

Numerical and Experimental Spanwise Load Distributions for $M_\infty = 0.80$, $Re = 2.3 \times 10^6$, and $\alpha = 3°$

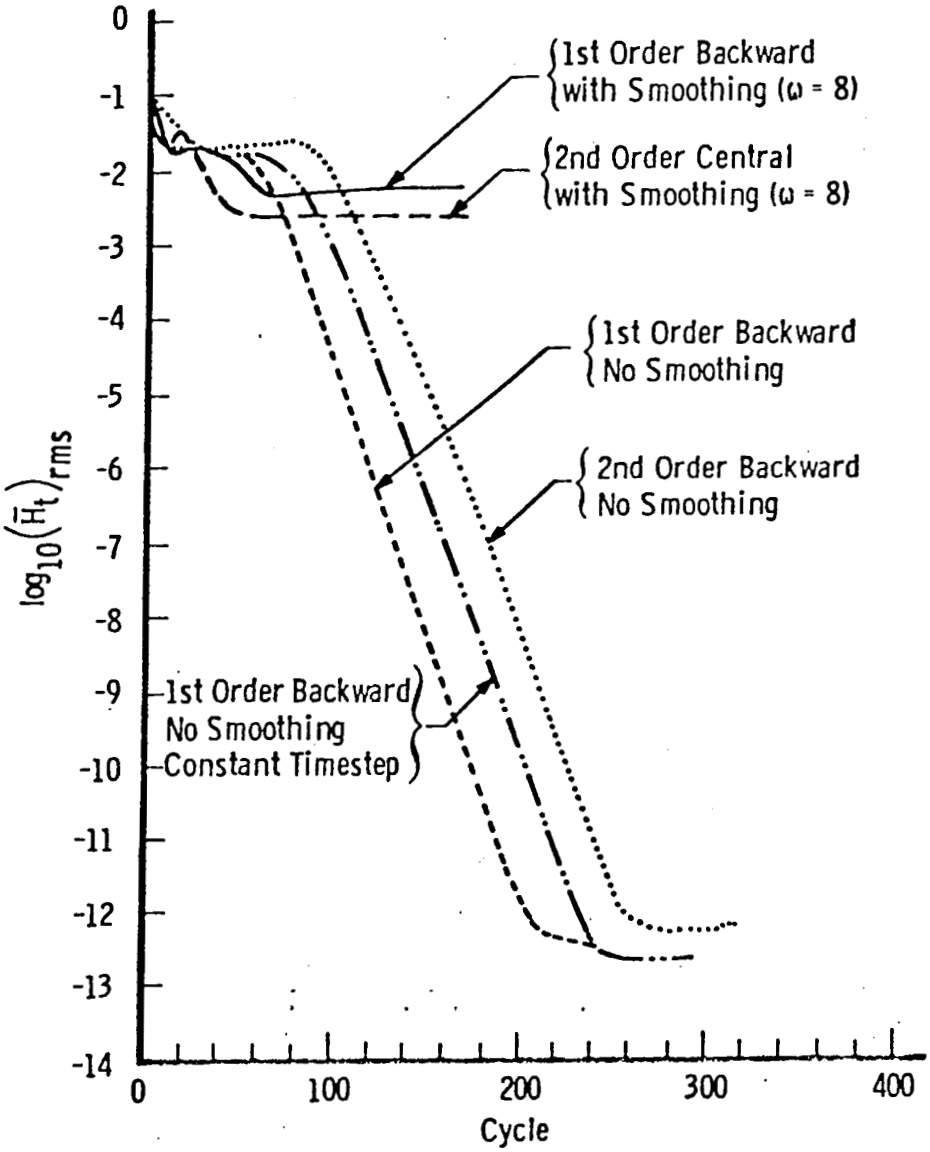

Convergence Histories for the Cumpsty and Head Infinite Swept-Wing Dummy Test Case.

FLUX-VECTOR-SPLIT (SKOAL) CODE

- THREE-DIMENSIONAL UNSTEADY EULER EQUATIONS
- FINITE VOLUME DISCRETIZATION
- EXPLICIT SECOND-ORDER UPWIND SCHEME
- STABLE FOR A CFL OF 2
- CHARACTERISTIC BOUNDARY CONDITIONS IN THE FAR FIELD AND AT THE SURFACE
- NO ADDITIONAL ARTIFICIAL DISSIPATION TERMS ADDED

EIGENVALUE INTERROGATION

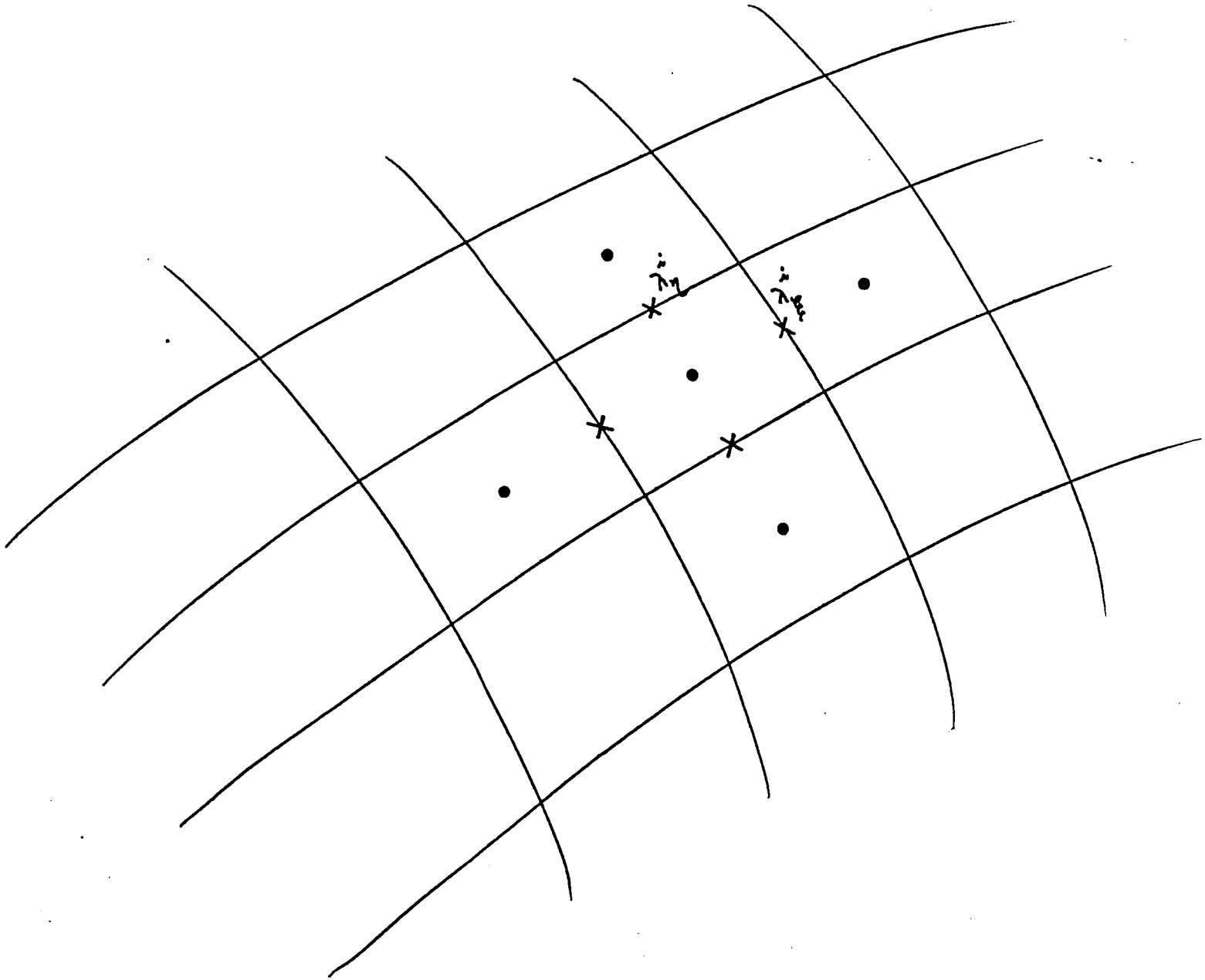

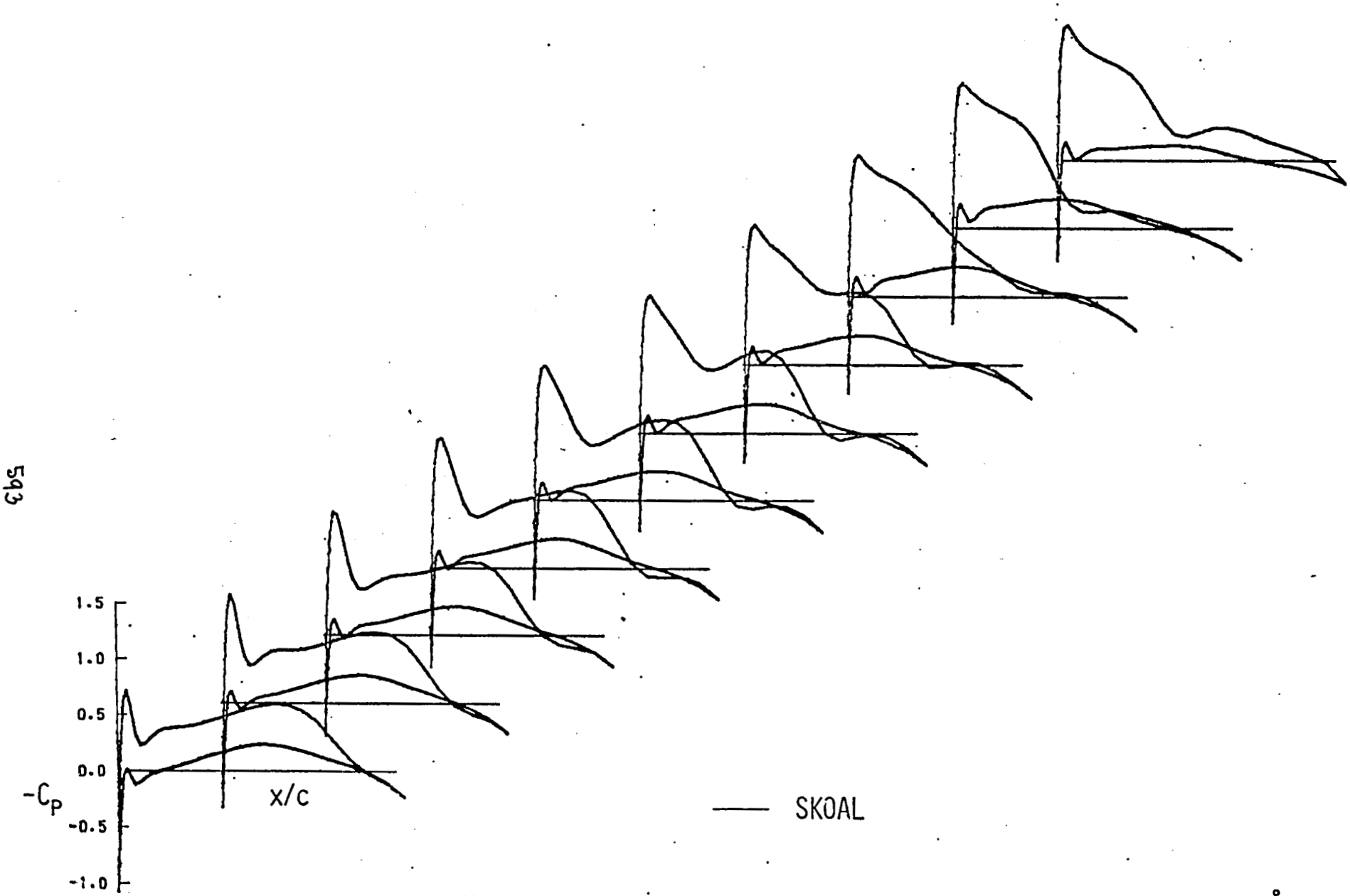

PRESSURE DISTRIBUTIONS ON THE ONERA M6 WING FOR $M_\infty = 0.84$ AND $\alpha = 3.06^\circ$

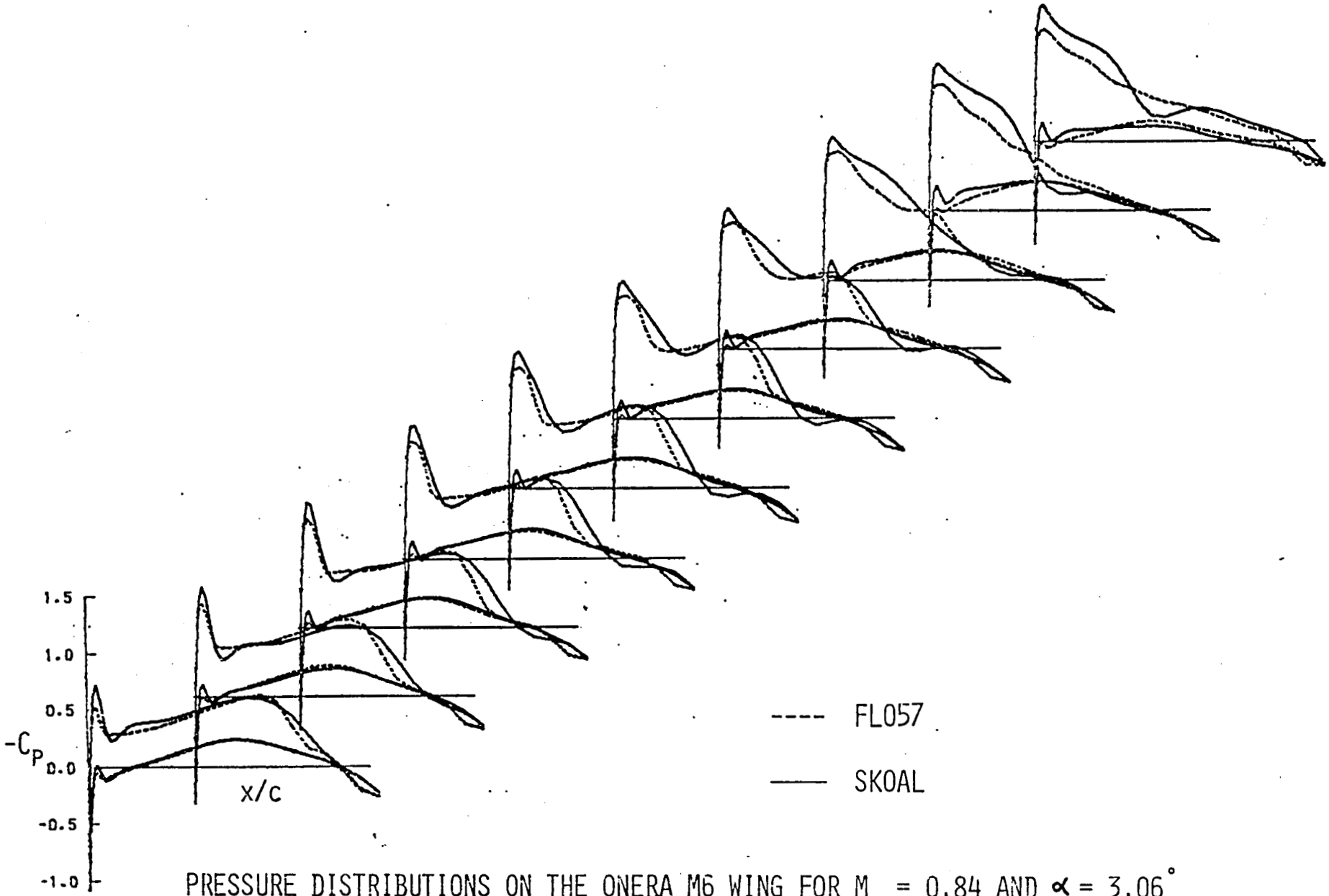

PRESSURE DISTRIBUTIONS ON THE ONERA M6 WING FOR $M_\infty = 0.84$ AND $\alpha = 3.06^\circ$

ONERA M6 WING

$M_\infty = 0.84$

$\alpha = 3.06^\circ$

$\eta = 0.45$

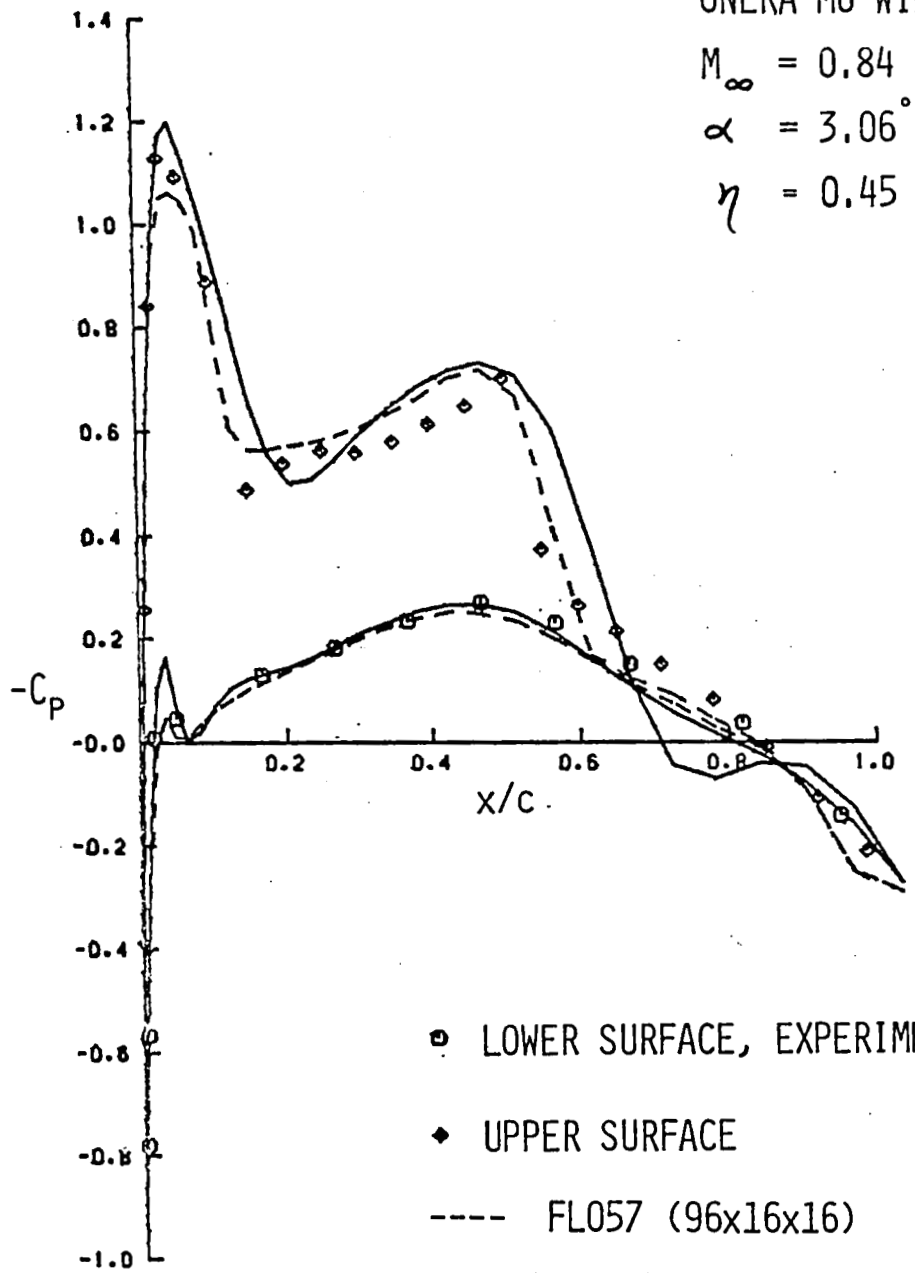

- LOWER SURFACE, EXPERIMENT (AGARD AR-138)
- UPPER SURFACE
---- FLO57 (96x16x16)
____ SKOAL (96x16x16)

EULER EQUATIONS WITH FORCE TERMS

$$\int_{V_o} \frac{\partial \vec{G}}{\partial t}\, dV + \int_{S_o} (\vec{F}_x n_x + \vec{F}_y n_y + \vec{F}_z n_z) dS - \int_{V_o} \vec{B} dV = 0$$

where

$$\vec{G} = [\rho,\ \rho u,\ \rho v,\ \rho w,\ \rho E]^T$$

$$\vec{F}_x = [\rho u,\ \rho uu+p,\ \rho vu,\ \rho wu,\ \rho(E+p/\rho)u]^T$$

$$\vec{F}_y = [\rho v,\ \rho uv,\ \rho vv+p,\ \rho wv,\ \rho(E+p/\rho)v]^T$$

$$\vec{F}_z = [\rho w,\ \rho uw,\ \rho vw,\ \rho ww+p,\ \rho(E+p/\rho)w]^T$$

$$\vec{B} = [0,\ \rho f_x,\ \rho f_y,\ \rho f_z,\ \rho(f_x u + f_y v + f_z w)]^T$$

$$\int_{V_o} \vec{B} dV = \int_{V_o} \text{div}\, \vec{\vec{\tau}} dV = \int_{S_o} \vec{\tilde{B}} dS$$

where

$$\vec{\tilde{B}} = \vec{\vec{\tau}} \cdot \vec{n} = [0,\ \tilde{f}_x,\ \tilde{f}_y,\ \tilde{f}_z,\ \tilde{f}_x u + \tilde{f}_y v + \tilde{f}_z w]^T$$

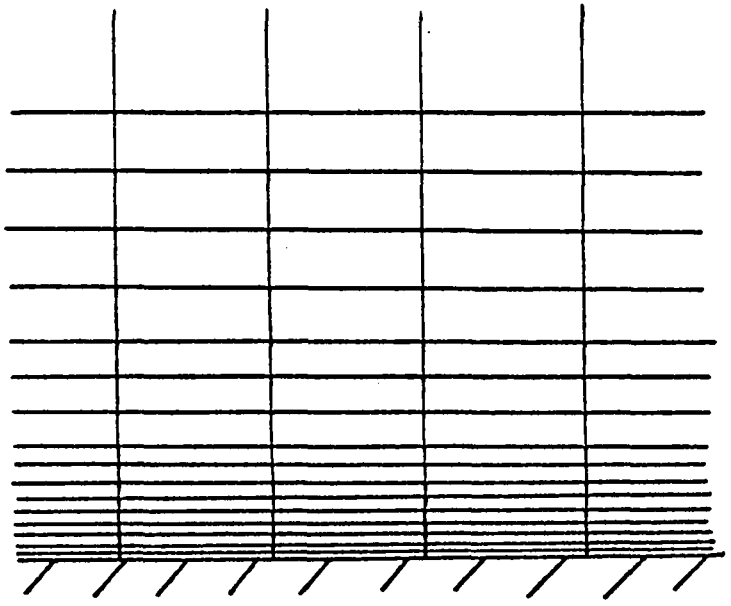

Navier-Stokes Grid

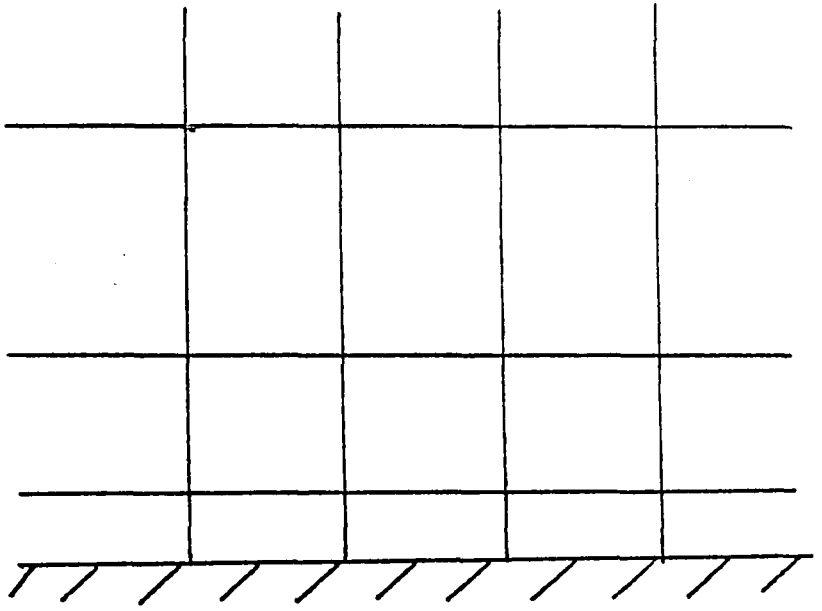

Euler Grid

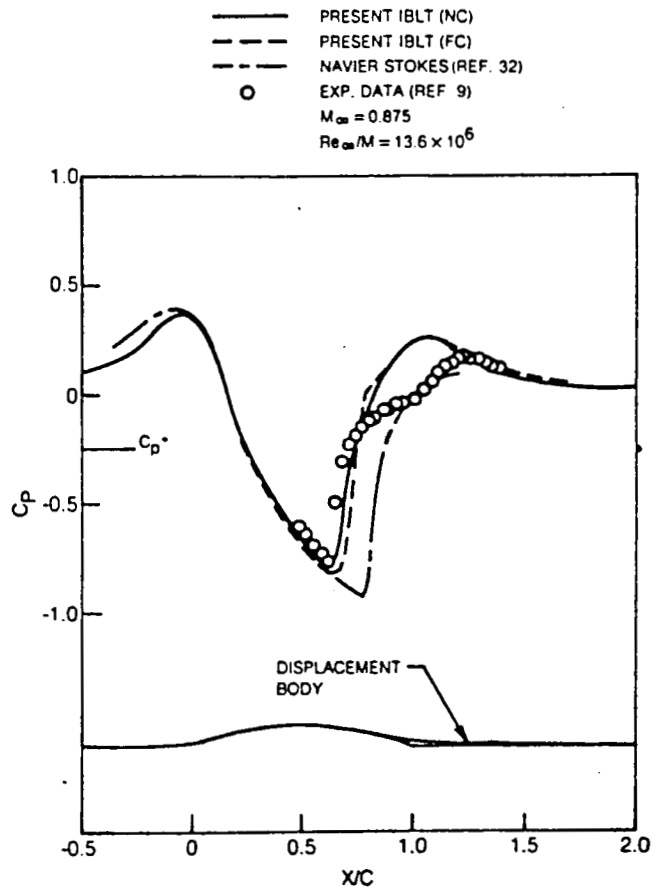

Interacted pressure distributions

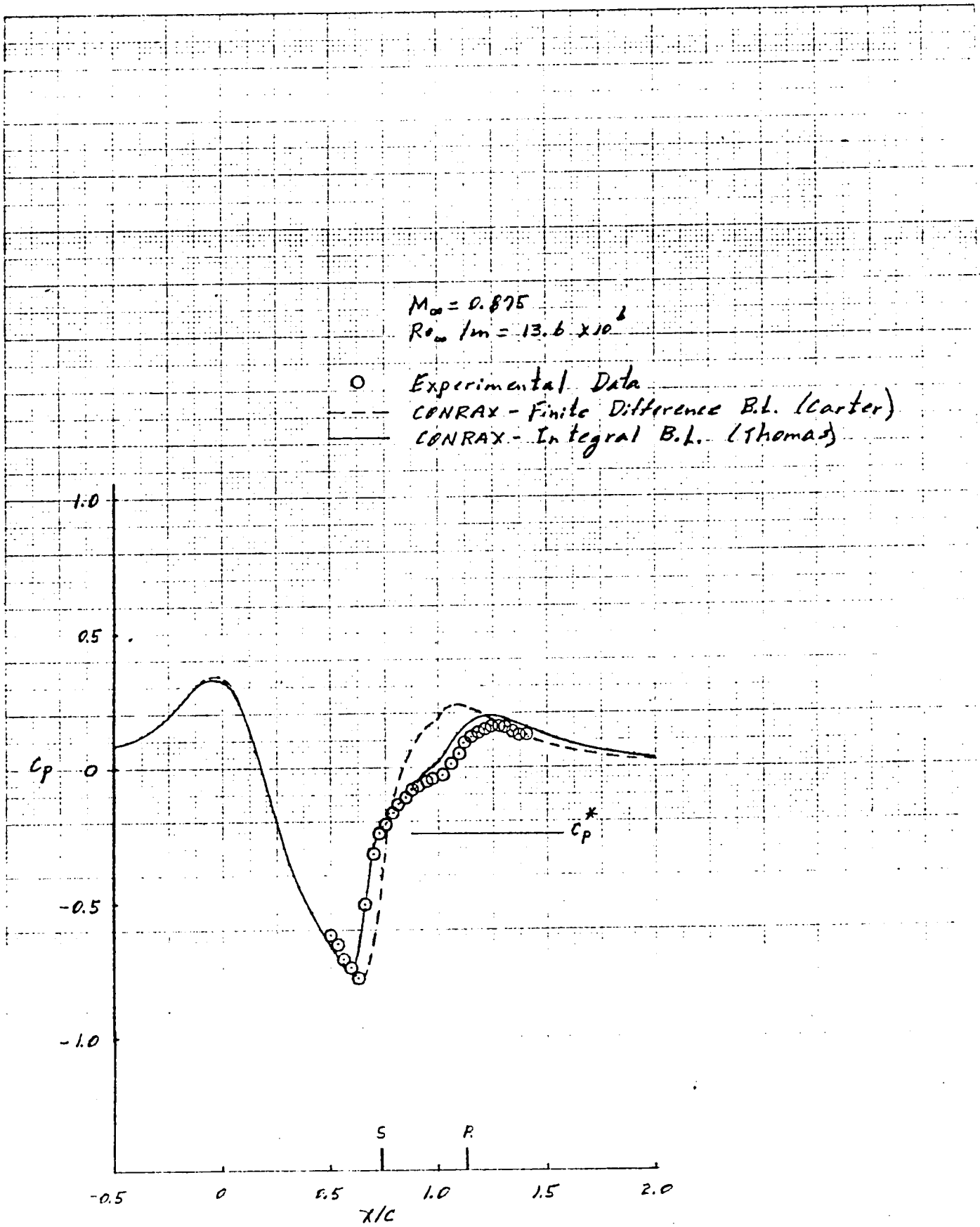

Pressure Distributions on the Bachalo-Johnson Axisymmetric Bump

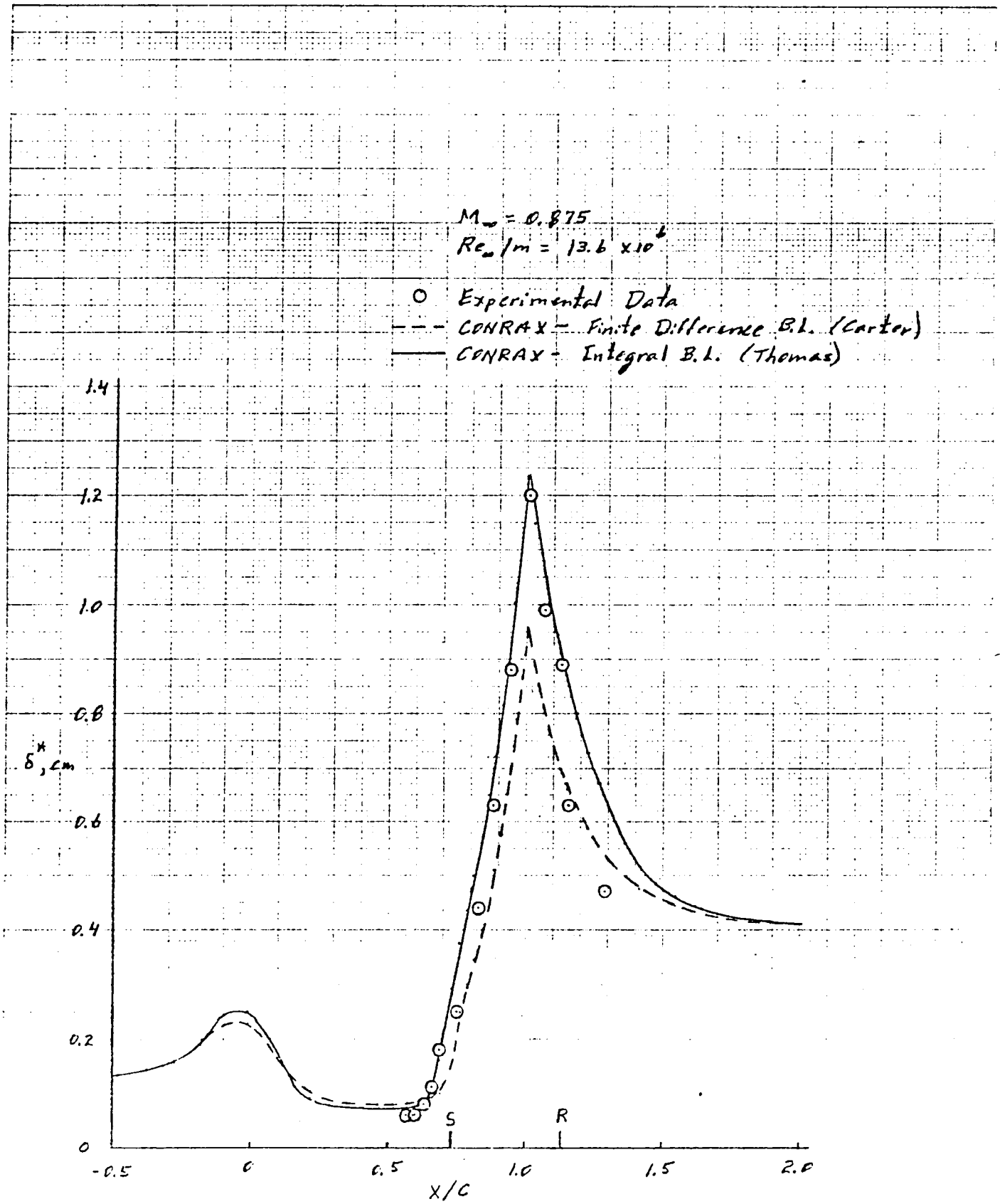

Displacement Thickness Distributions on the Bachalo-Johnson Axisymmetric Bump

O EXPERIMENT (CASE 8611 - BACHALO AND JOHNSON)

—— VELOCITY PROFILE MODEL

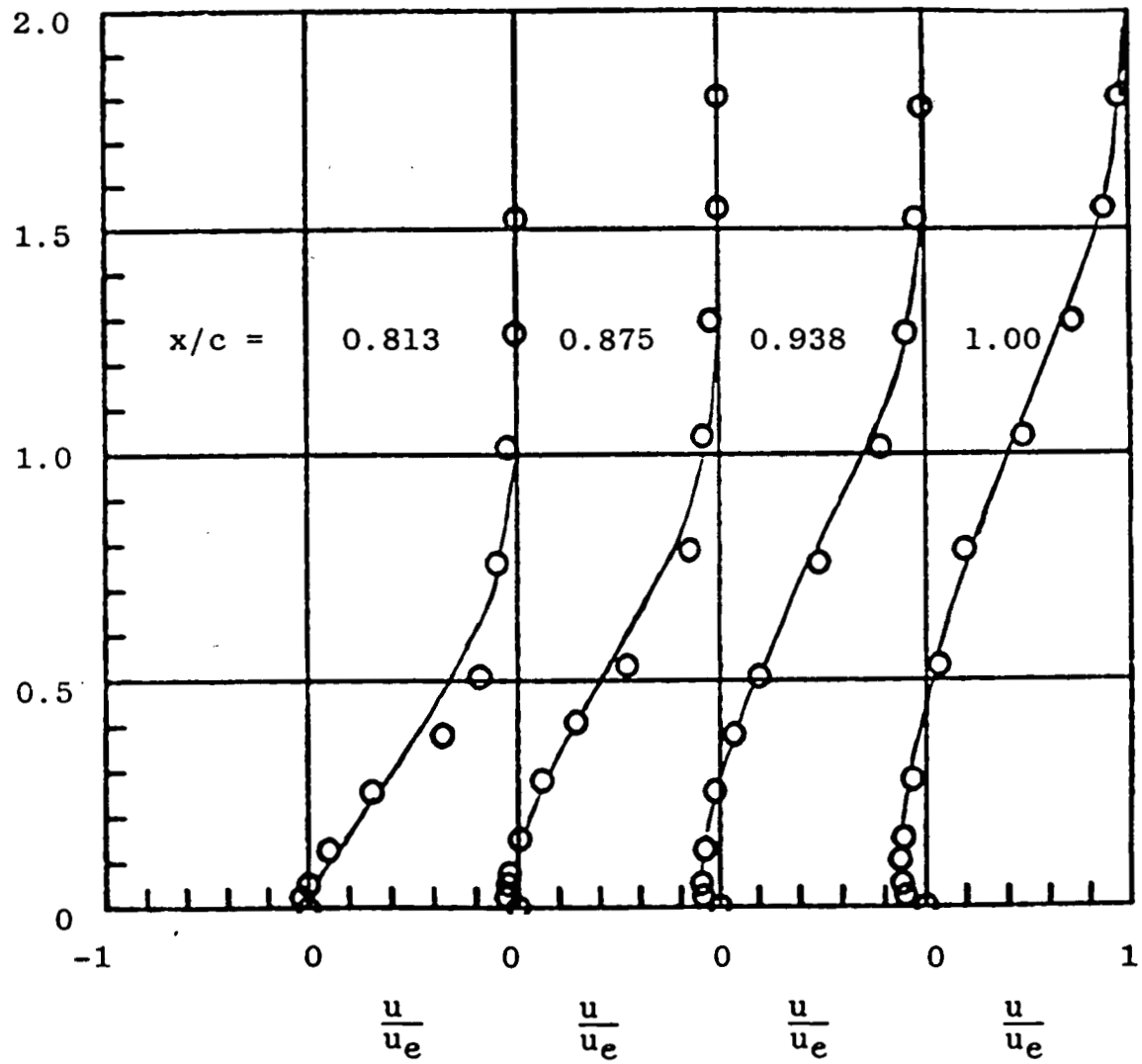

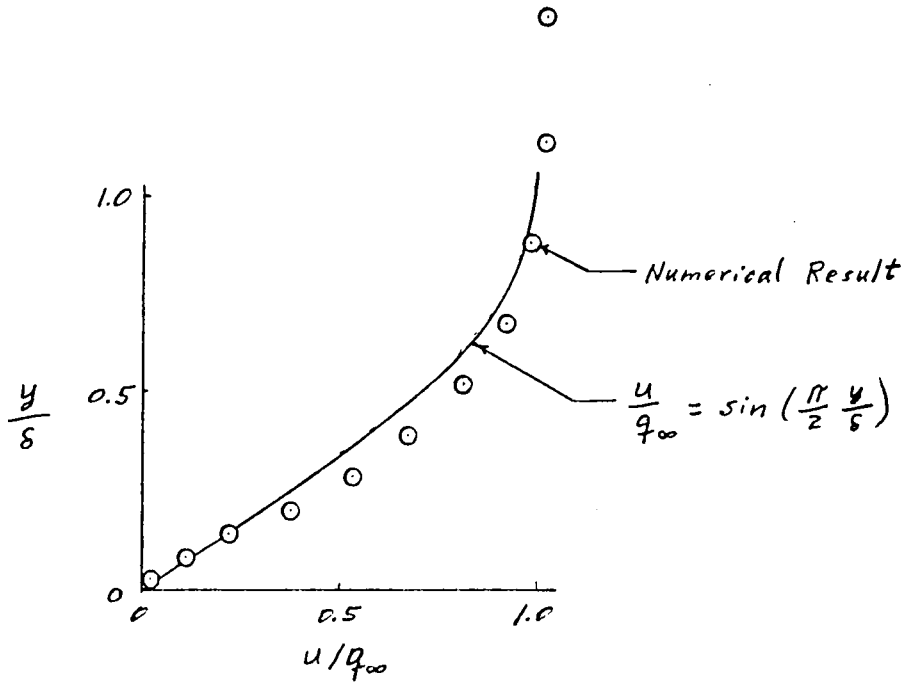

INTERACTION RESULT USING LAMINAR BOUNDARY-LAYER STRESS TERMS IN THE EULER EQUATIONS

18% CIRCULAR ARC AIRFOIL

$M_\infty = 0.7425$

VELOCITY PROFILE AT THE TRAILING EDGE

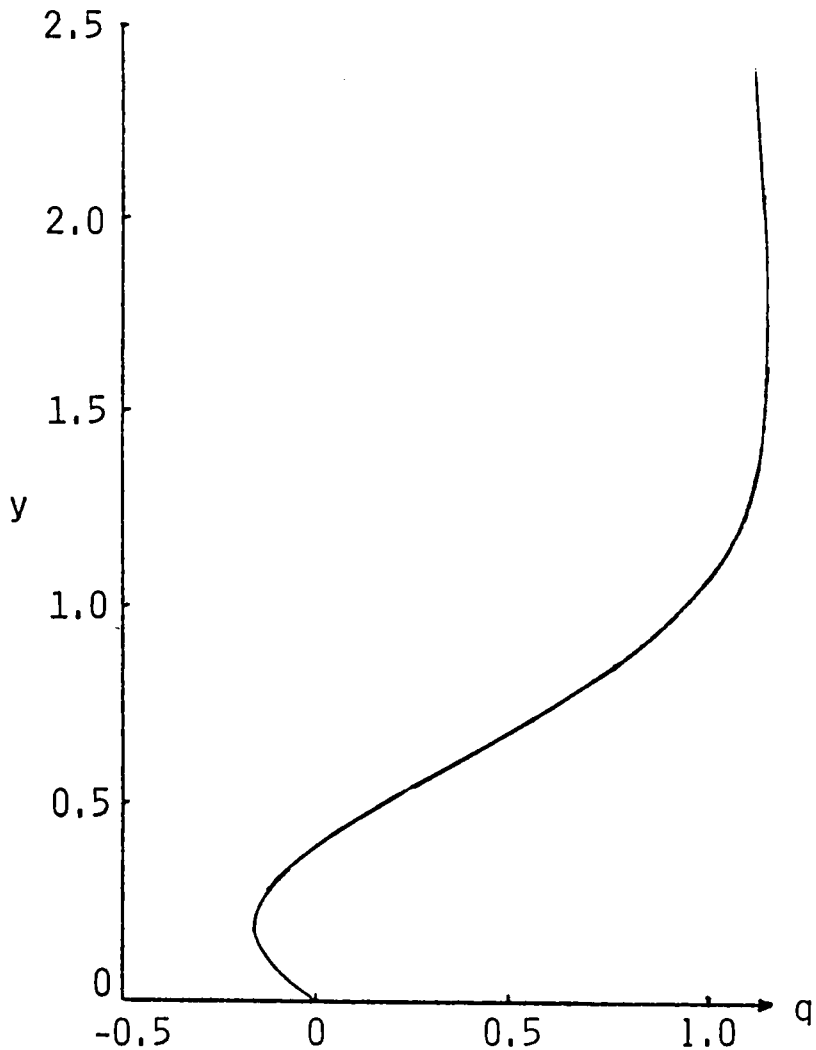

VORTICITY INTERACTION USING LAMINAR STRESSES IN EULER EQUATIONS (PSEUDO NAVIER-STOKES)

SUMMARY

- OBTAINED NUMERICAL SOLUTIONS USING BODY FORCES IN THE EULER EQUATIONS
- THOMAS EXTENDED THE INVERSE COMPRESSIBLE TURBULENT INTEGRAL BOUNDARY-LAYER METHOD TO INCLUDE A DISSIPATION EQUATION
- NEW THREE-DIMENSIONAL UNSTEADY EULER CODE WRITTEN BASED ON FLUX-VECTOR-SPLITTING
- PSEUDO NAVIER-STOKES (VORTICITY INTERACTION) FORMULATED

It appears that presently, integral methods work better than more "advanced" models, especially when the flow separates. We have also made calculations with other turbulence models (including a three transport equation model) on the O.N.E.R.A. M= 1.3 test case (see paper enclosed). The agreement with experiment is not better. Research is now in progress to try to improve these turbulence models.

The calculation of the most separated cases with the ASM model failed .. because of severe numerical instabilities. I hope that these difficulties will be overcome in the near future.

I am still waiting for LE BALLEUR's results ; also, the data have been transmitted to J. DUNHAM of the Royal Aircraft Establishment in U.K. Of course, I will communicate you these new results as soon as I receive them.

Please feel free to use the here enclosed results as needed and do not hesitate to contact me if you want any further information.

Still thank you very much for your kind cooperation.

Sincerely yours,

J Delery

J. DELERY

Enclosures.

(23)

VISCOUS WING CODE DEVELOPMENT – A 3-D VISCID-INVISCID INTERACTIVE ANALYSIS

R. CHOW

R.E. MELNIK

F. MARCONI

L09

GRUMMAN

VISCOUS FLOW OVER WINGS

OBJECTIVE

DEVELOP METHOD TO COMPUTE VISCOUS TRANSONIC FLOW OVER WINGS

APPROACH

- COUPLED INVISCID/BOUNDARY LAYER EQUATIONS
- AFZ SCHEME FOR FULL POTENTIAL FLOW EQUATION
- 3 D INTEGRAL METHODS FOR BOUNDARY LAYER & WAKE
- FULL SET OF COUPLING CONDITIONS
  - WING DISPLACEMENT EFFECT
  - WAKE DISPLACEMENT EFFECT
  - WAKE CURVATURE EFFECT
  - TRAILING EDGE STRONG INTERACTION

809

GRUMMAN

ITERATION STEPS FOR 3-D VISCOUS WING PROGRAM

STEP (1) OBTAIN INVISCID SOLUTION USING FINITE VOLUME AFZ CODE – FLO47 (OR FLO27, FLO27M)

STEP (2) COMPUTE SURFACE VELOCITIES AND SURFACE FLOW ANGLES FROM 3-D INVISCID SOLUTION

STEP (3) OBTAIN 3-D LAMINAR-TURBULENT BOUNDARY LAYER/WAKE SOLUTION

STEP (4a) COMPUTE SURFACE SOURCE FROM BOUNDARY LAYER/WAKE SOLUTION USING 3-D ENTRAINMENT EQUATION

(4b) COMPUTE FLOATING WAKE SURFACE COORDINATES (STREAM SURFACE) USING THE INVISCID VELOCITIES

(4c) COMPUTE VELOCITY POTENTIAL JUMP DUE TO VISCOUS WAKE CURVATURE EFFECT (LONGITUDINAL CURVATURE ONLY)

(4d) COMPUTE THE NEW SHEAR COORDINATES IN THE INVISCID CALCULATION DUE TO FLOATING WAKE

STEP (5) GO TO STEP (1)

609

GRUMMAN

RECENT DEVELOPMENTS

- o INVISCID SOLUTION (AFZ CODE)
  - FAR FIELD BOUNDARY CONDITIONS
  - 2ND ORDER ARTIFICIAL VISCOSITY
- o VISCOUS SOLUTION
  - TRAILING EDGE STRONG INTERACTION SOLUTION
- o APPLICATIONS
  - VECTORIZED INTERACTION CODE FOR CRAY-1S AND CYBER-205
  - LOCKHEED WING (WING A)

GRUMMAN

PRANDTL - GLAUERT FAR FIELD BOUNDARY CONDITION

$$G \sim G_{lift} + 0\left(\frac{x}{R^3}\right) + 0\left(\frac{1}{R^3}\right)$$

$0\left(\frac{1}{R^3}\right)$ — VOLUME INTEGRAL

$0\left(\frac{x}{R^3}\right)$ — WING THICKNESS INTEGRAL

THE LIFT INTEGRAL;

$$G_{lift} = \frac{y}{4\pi} \iint_{W.S.} \frac{\frac{\partial G(\xi,\zeta)}{\partial \xi}}{(Z-\zeta)^2 + y^2} \left[1 + \frac{x-\xi}{R}\right] d\xi\, d\zeta$$

$$R \doteq \left\{(x-\xi)^2 + \beta^2 \left[(Z-\zeta)^2 + (y-\eta)^2\right]\right\}^{1/2}$$

$$\beta^2 = 1 - M_\infty^2$$

ξ, η, ζ = surface coordinates of the wing.

ON C-MESH BOUNDARY:

$$\frac{x-\xi}{R} \doteq \frac{x-\xi}{\left\{(x-\xi)^2 + \beta^2 \left[y^2 + (Z-\zeta)^2\right]\right\}^{1/2}}.$$

GRUMMAN

BOUNDARY OF C-MESH IN Z = CONSTANT PLANE

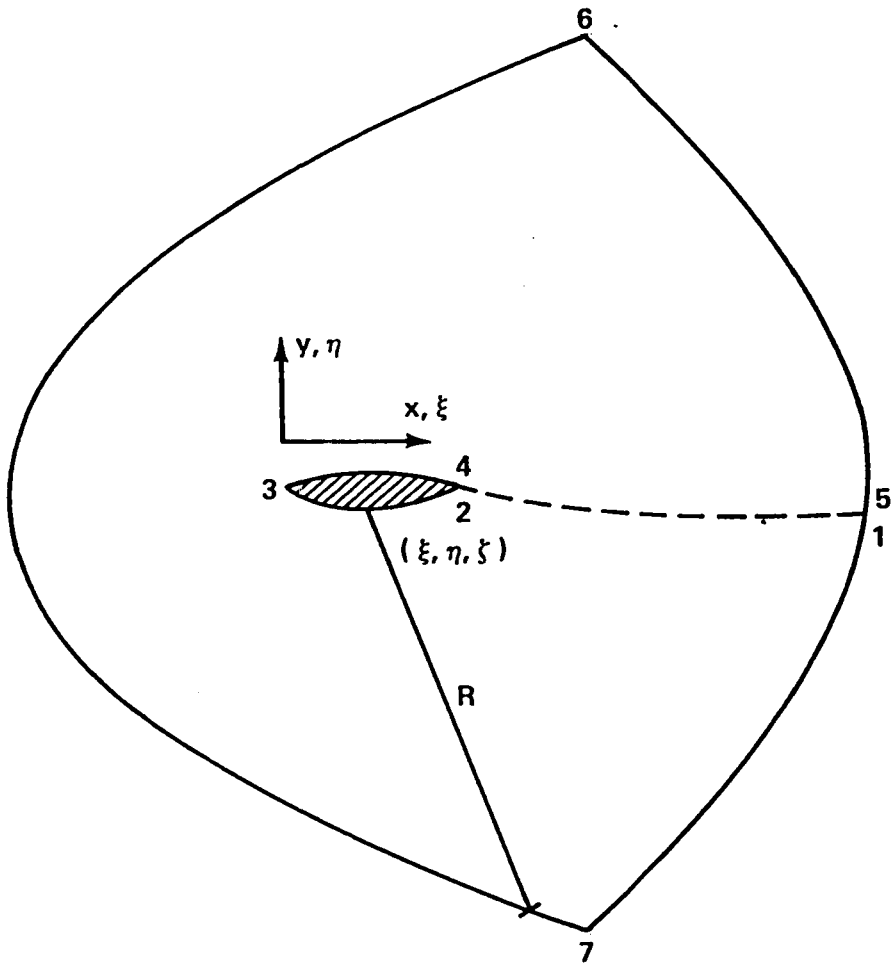

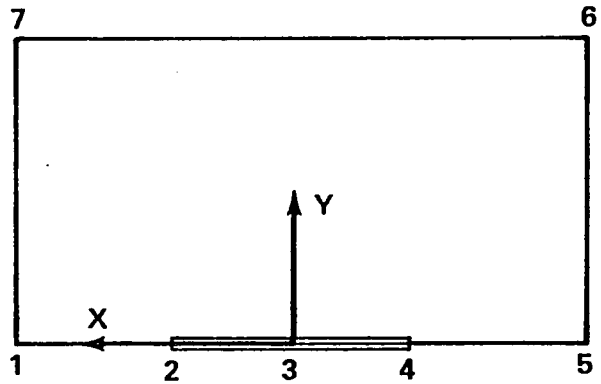

GRUMMAN

1583-055PP

TRANSONIC WING THEORY

FLO47 CONVERGENCE HISTORY

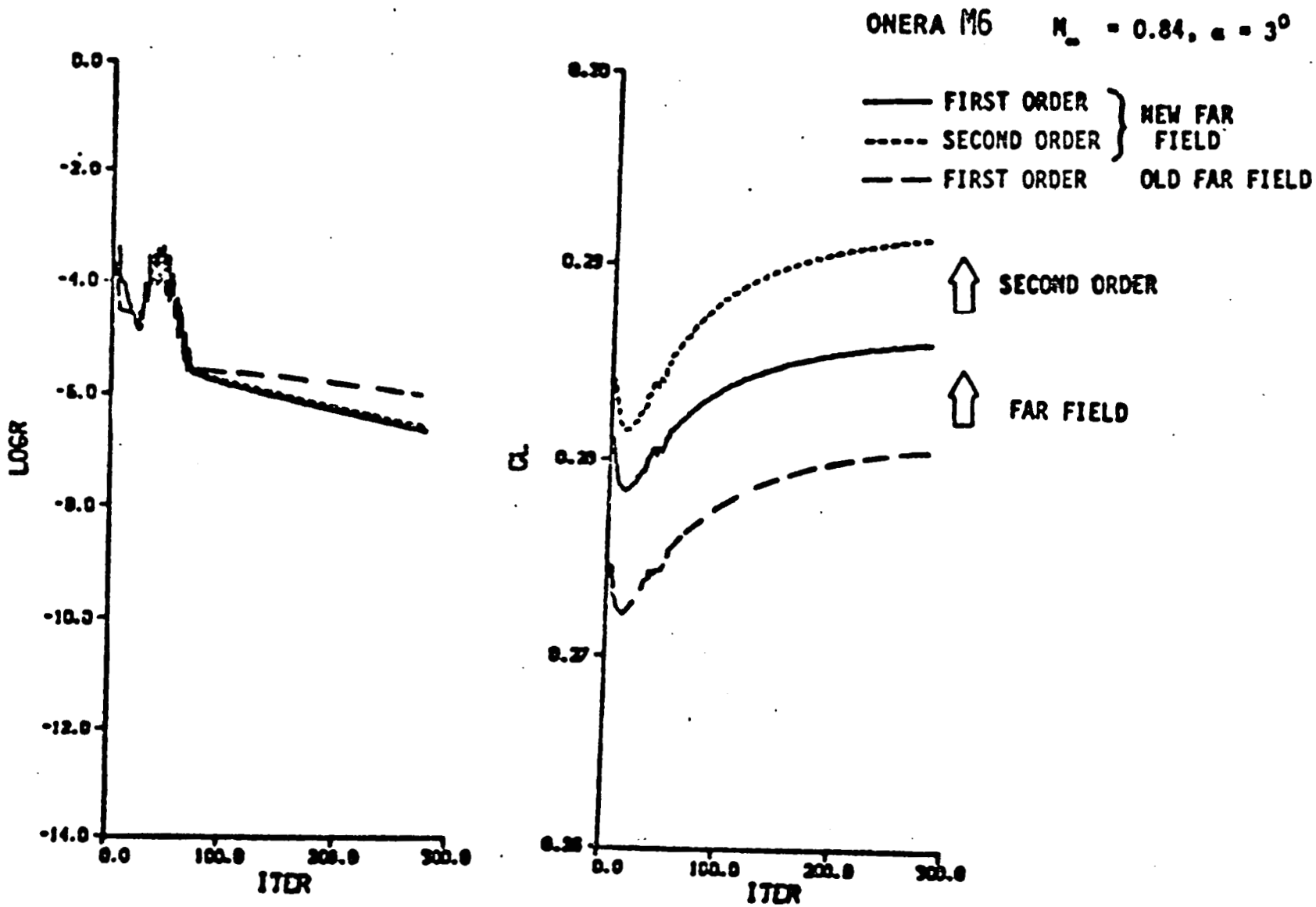

COMPARISON OF 1st AND 2nd ORDER ARTIFICIAL VISCOSITY LOCKHEED WING A, $M_\infty = 0.82$, $\alpha = 1.5°$

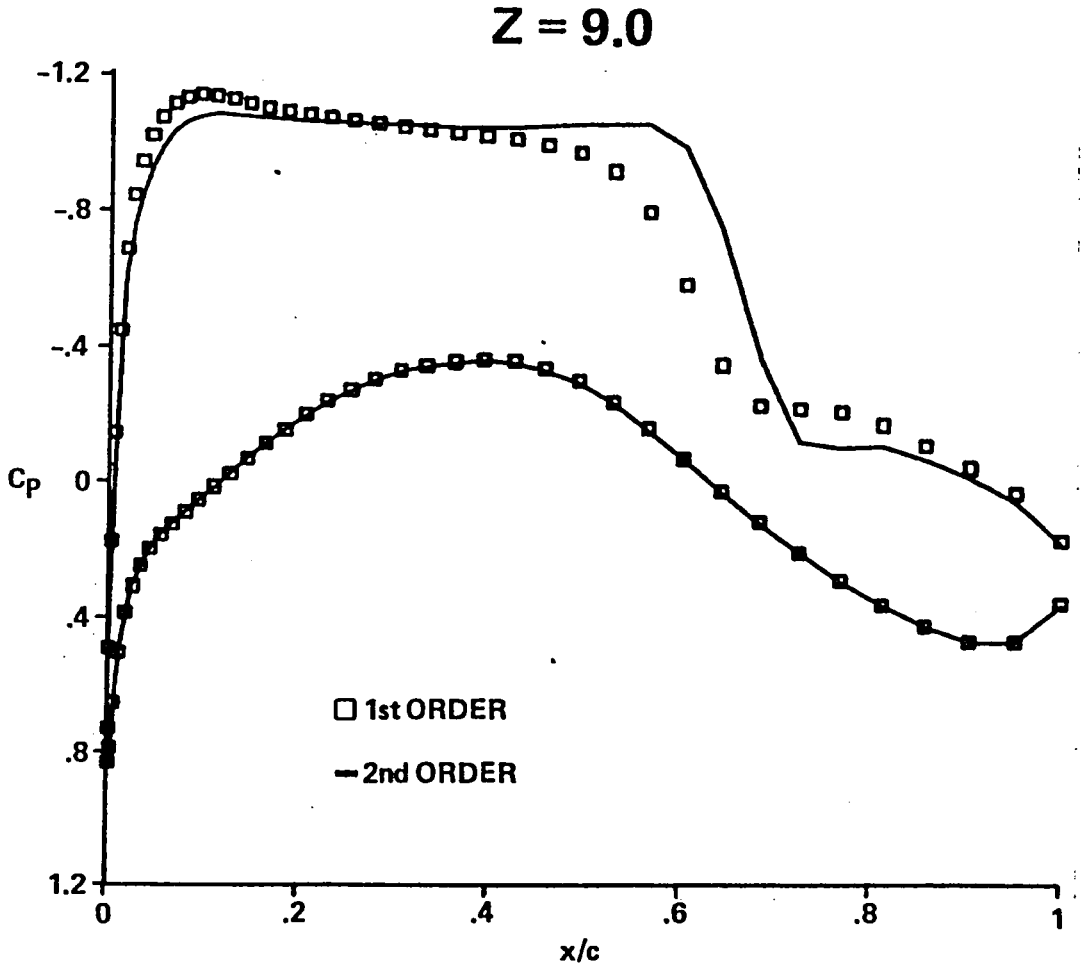

GRUMMAN

1583-021PP

SAMPLE WING 2, $M_\infty = 0.9$, $\alpha = 8°$

Planform & Isobars

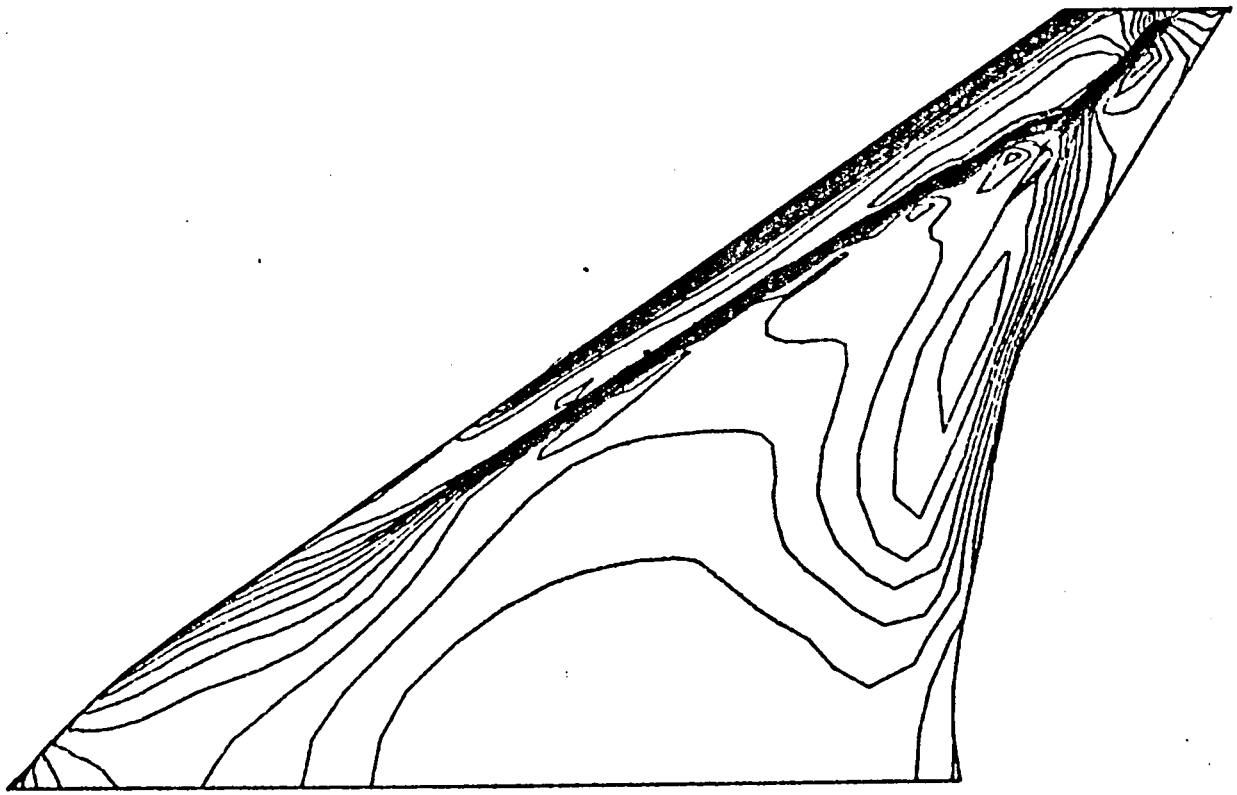

GRUMMAN

1583-010PP

CONVERGENCE HISTORY OF NO. OF SUPERSONIC POINTS & WING ROOT CIRCULATION

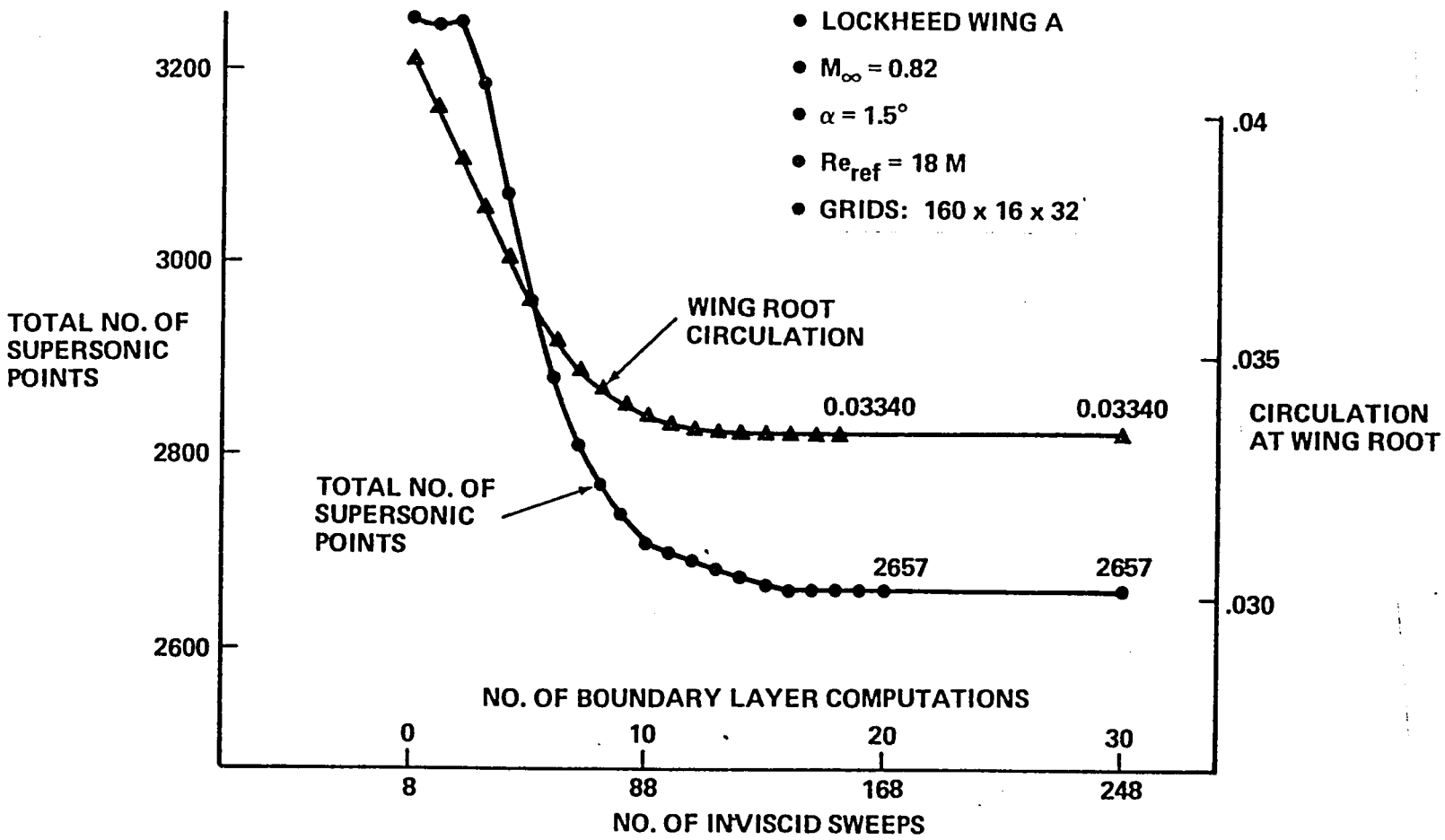

GRUMMAN

1583-059PP

CONVERGENCE HISTORY OF NO. OF SUPERSONIC POINTS & WING ROOT CIRCULATION

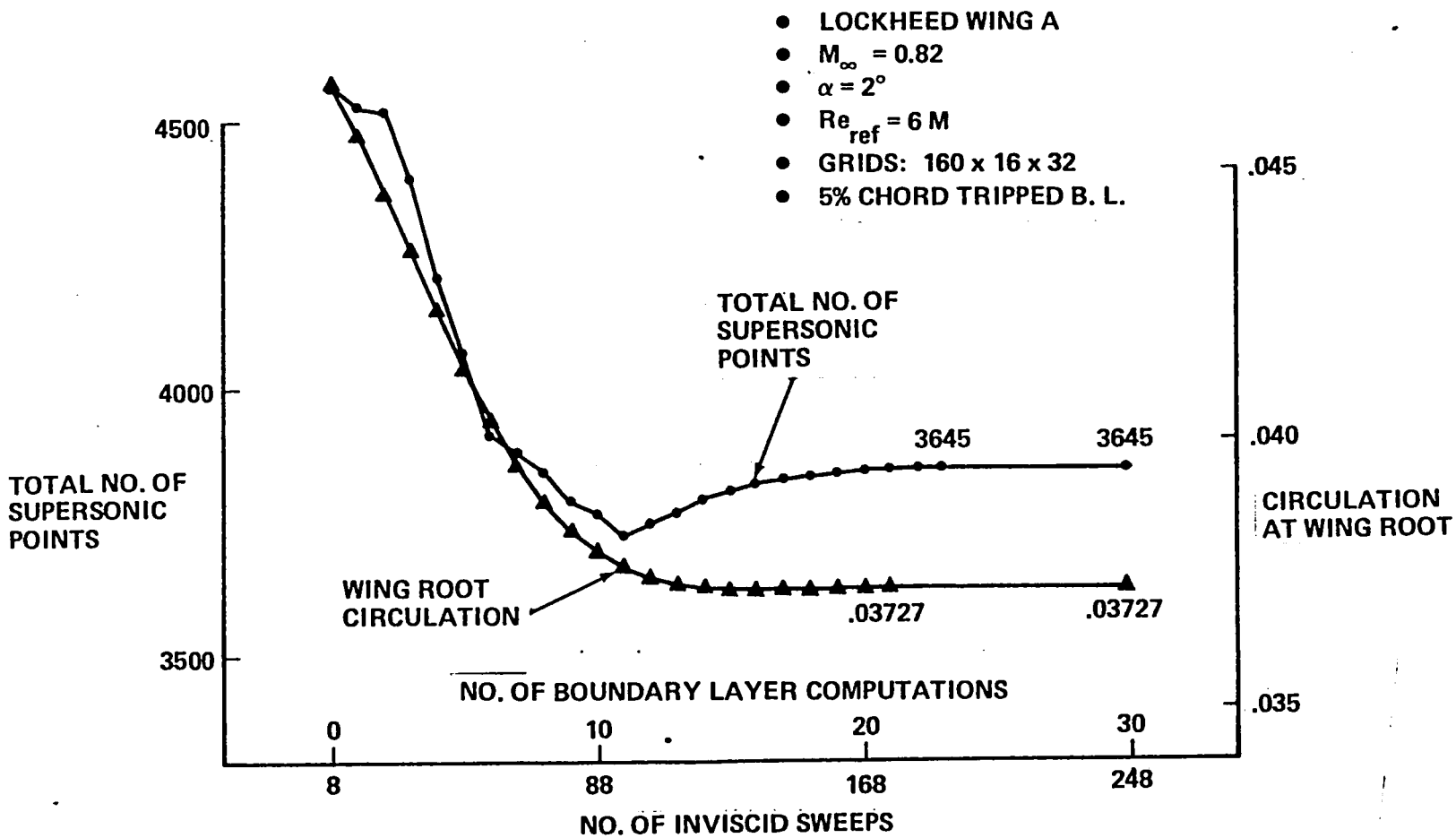

GRUMMAN

1583-029PP

CONVERGENCE HISTORY OF LAST VISCOUS FLOATING WAKE POINT AT WING ROOT SECTION

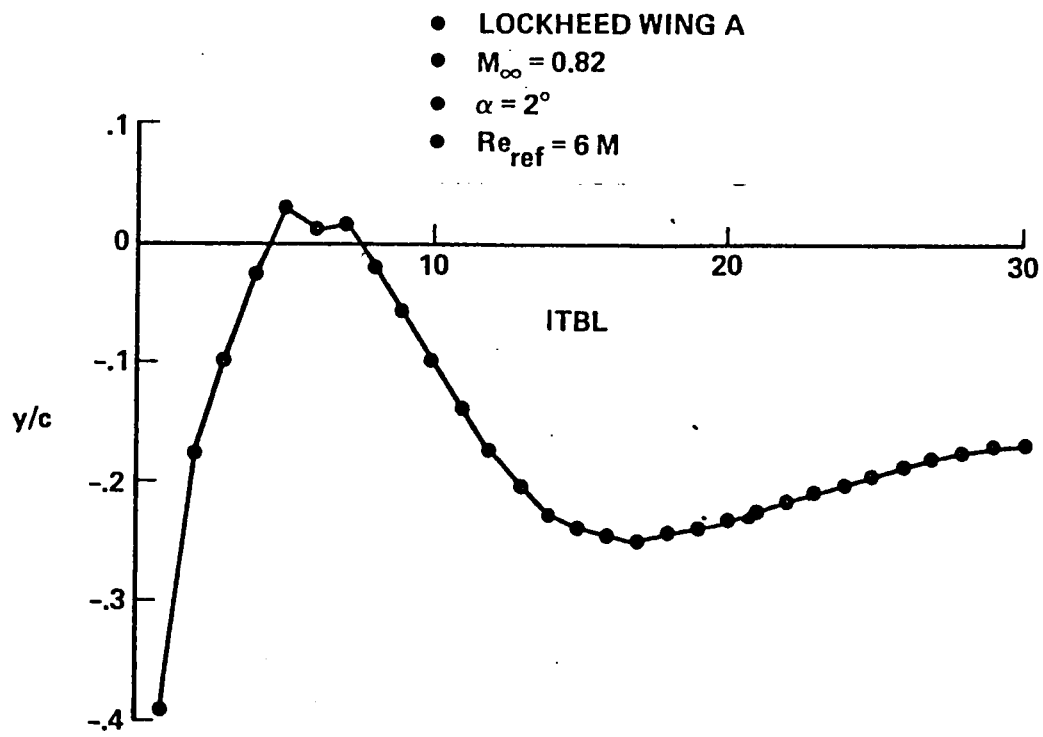

1583-030PP

LOCKHEED WING A

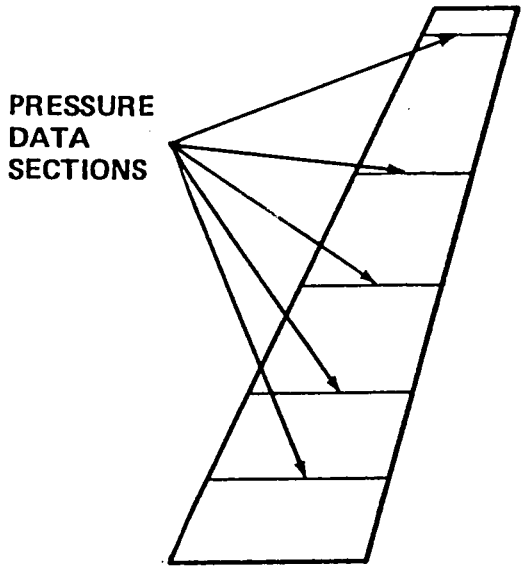

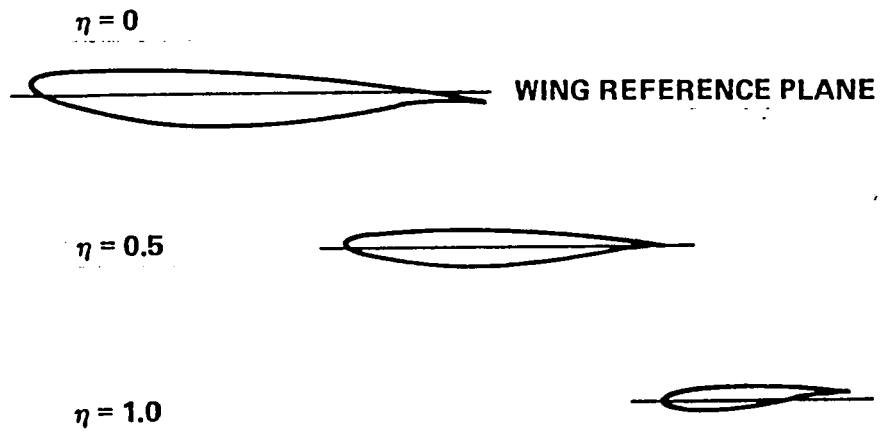

- WING A AIRFOIL SECTIONS IN RIGGED POSITION

GRUMMAN

COMPARISONS OF SECTIONAL PRESSURE DISTRIBUTIONS FOR LOCKHEED WING A

$\eta = 0.15$

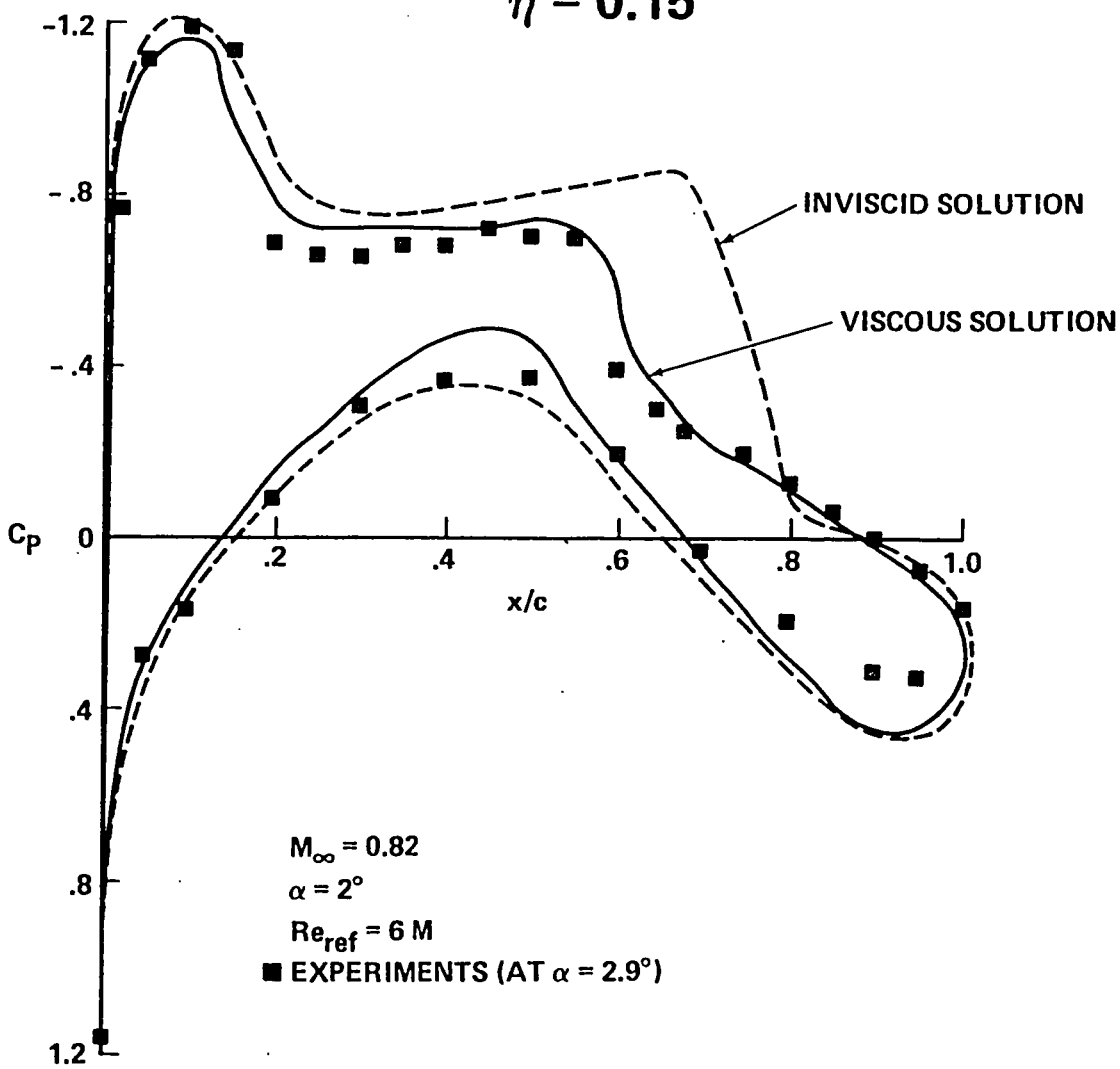

GRUMMAN

1583-032PP

COMPARISONS OF SECTIONAL PRESSURE DISTRIBUTIONS FOR LOCKHEED WING A

$\eta = 0.30$

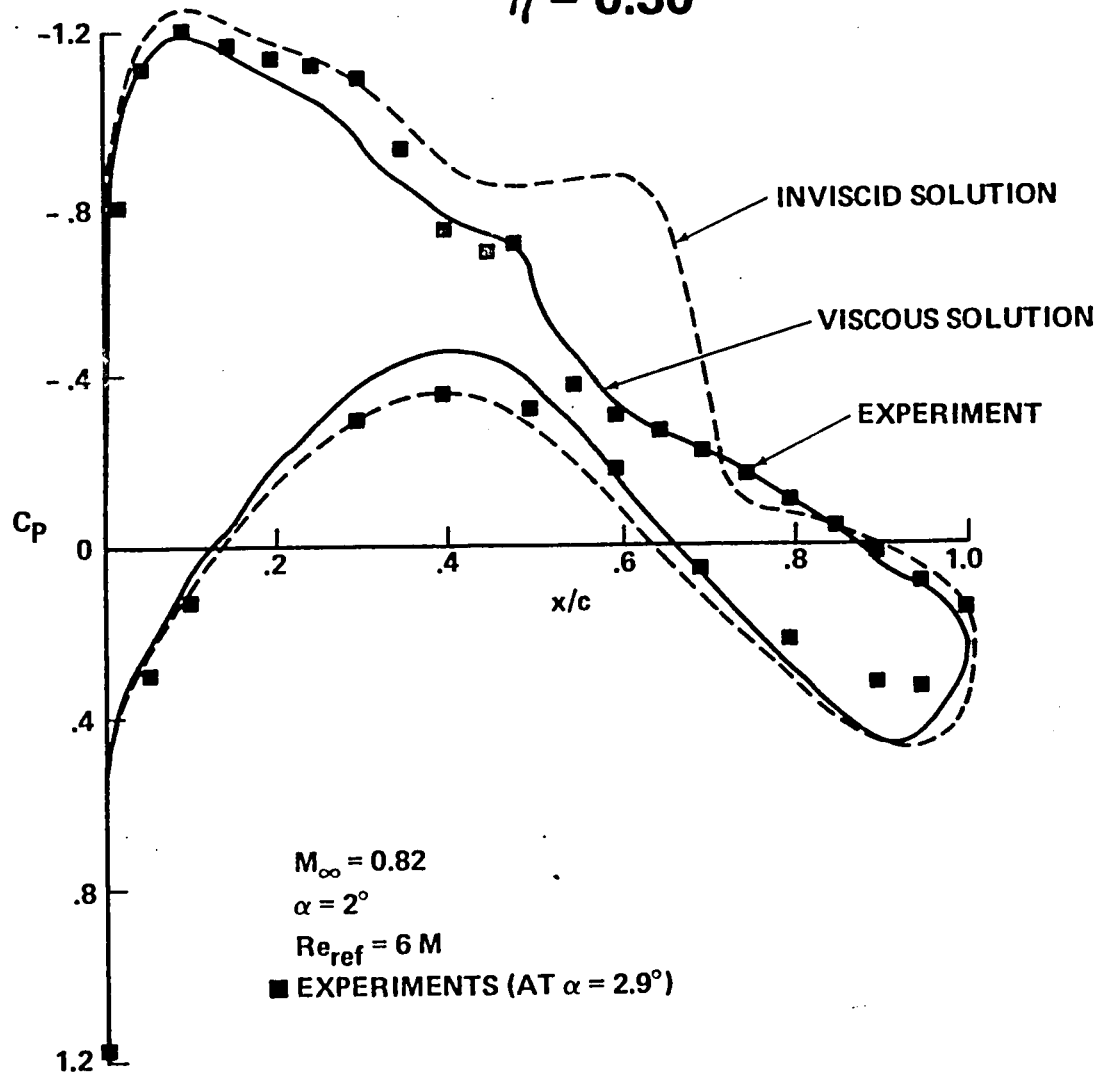

GRUMMAN

1583-033PP

COMPARISONS OF SECTIONAL PRESSURE DISTRIBUTIONS FOR LOCKHEED WING A

$\eta = 0.50$

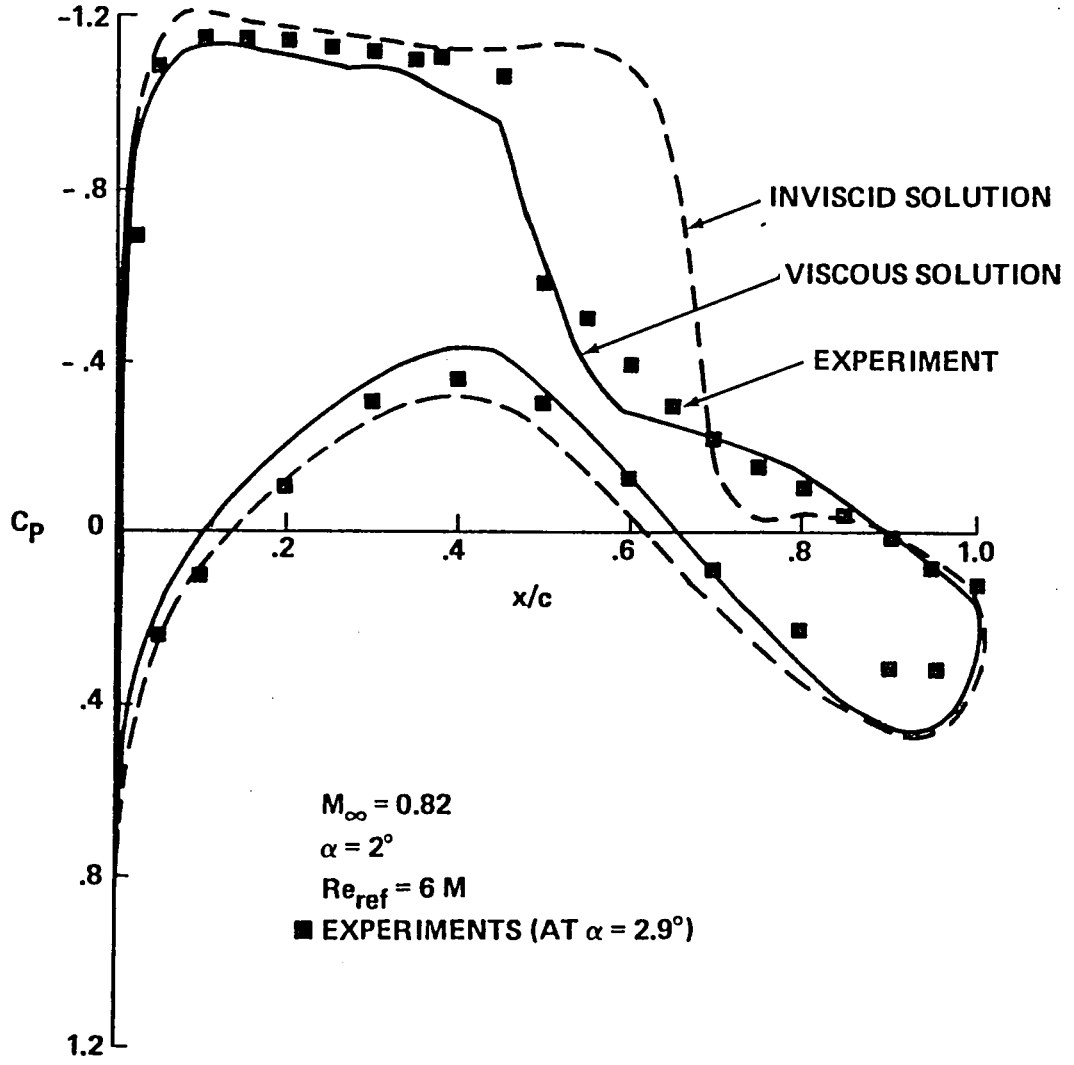

1583-034PP

GRUMMAN

COMPARISONS OF SECTIONAL PRESSURE DISTRIBUTIONS FOR LOCKHEED WING A

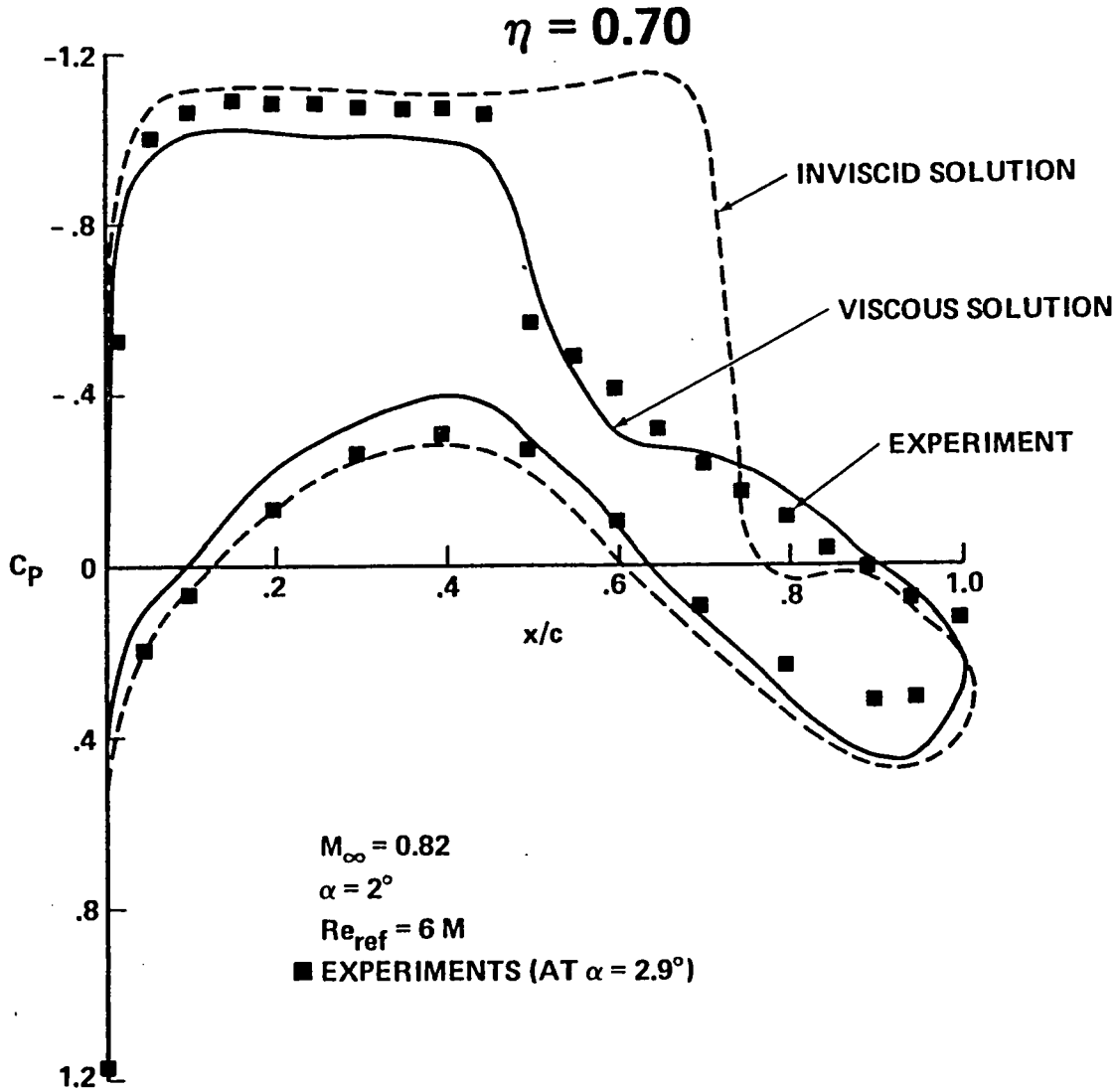

623

GRUMMAN

1583-035PP

COMPARISONS OF SECTIONAL PRESSURE DISTRIBUTIONS FOR LOCKHEED WING A

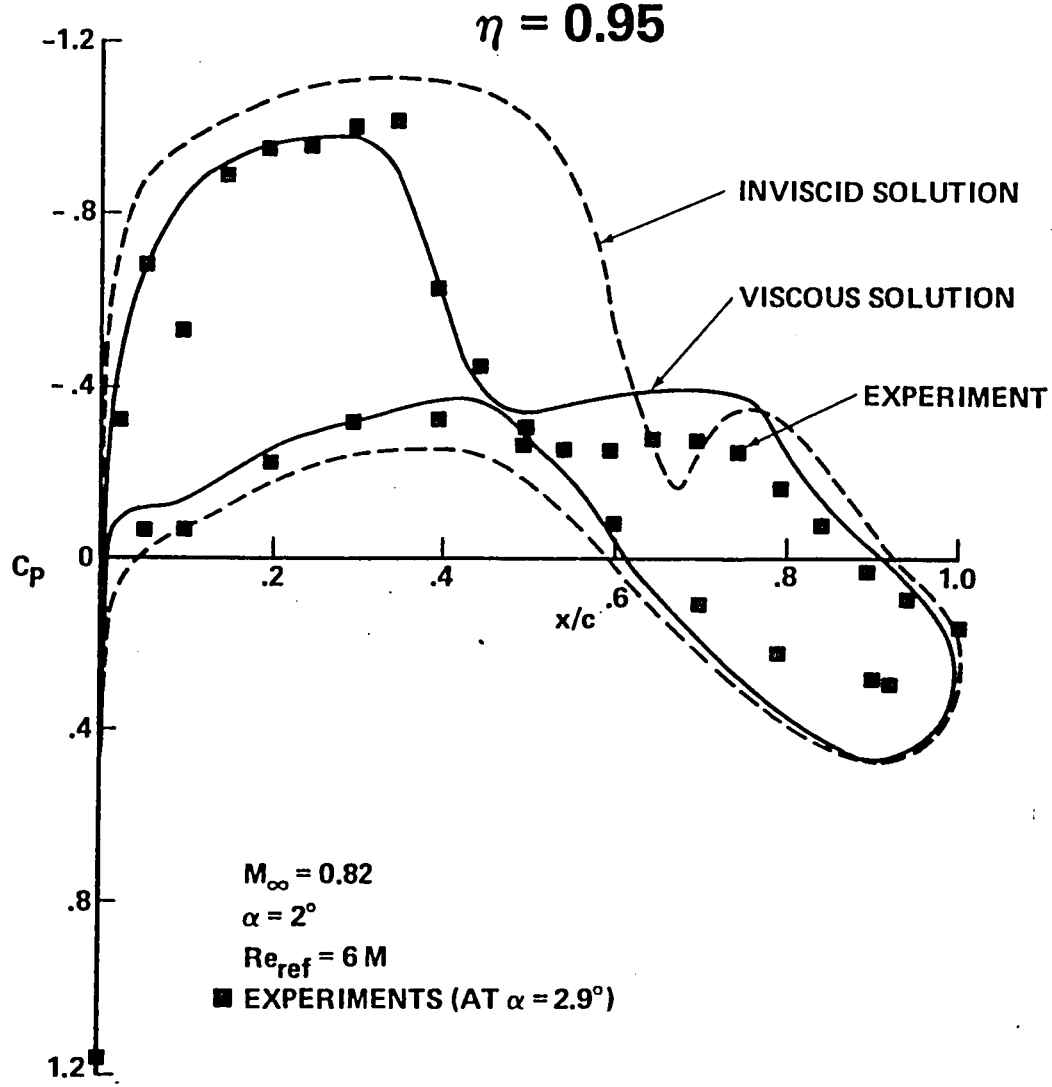

624

GRUMMAN

1583-036PP

COMPARISONS OF SPAN LOAD DISTRIBUTION FOR LOCKHEED WING A

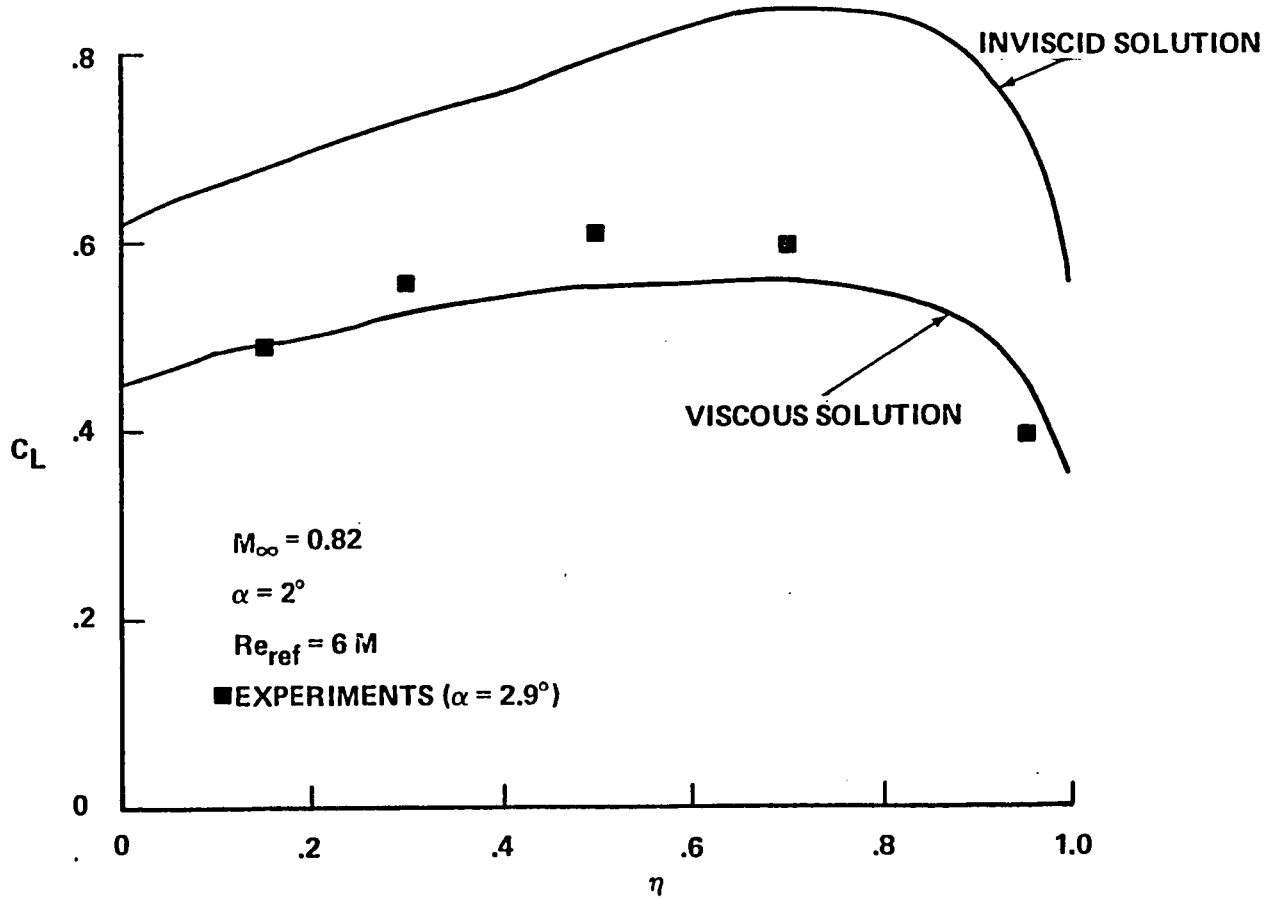

GRUMMAN

1583-043PP

EFFECT OF METRIC COEFFICIENTS ON 3-D BOUNDARY LAYER AND WAKE SOLUTION

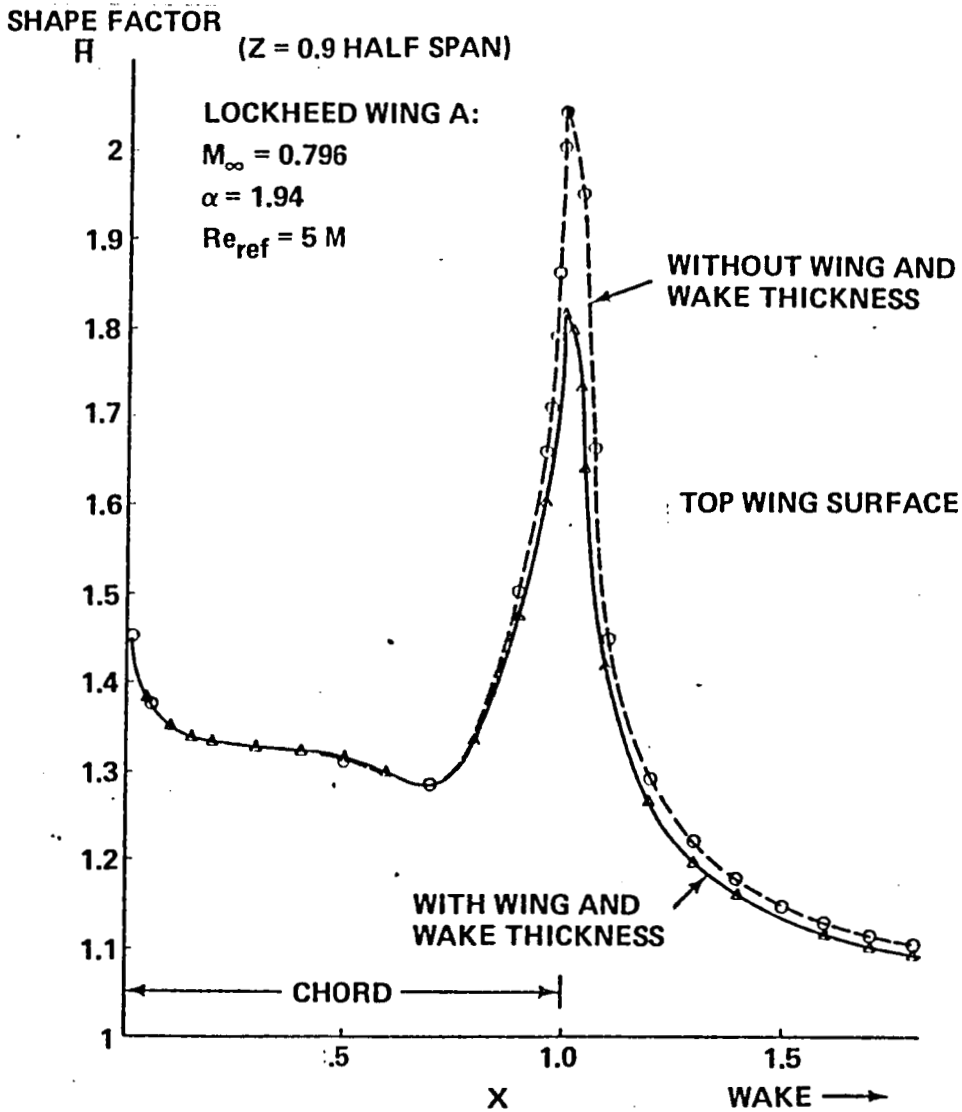

GRUMMAN

1583-005PP

DISPLACEMENT THICKNESS DISTRIBUTION AT MID-HALF-SPAN STATION

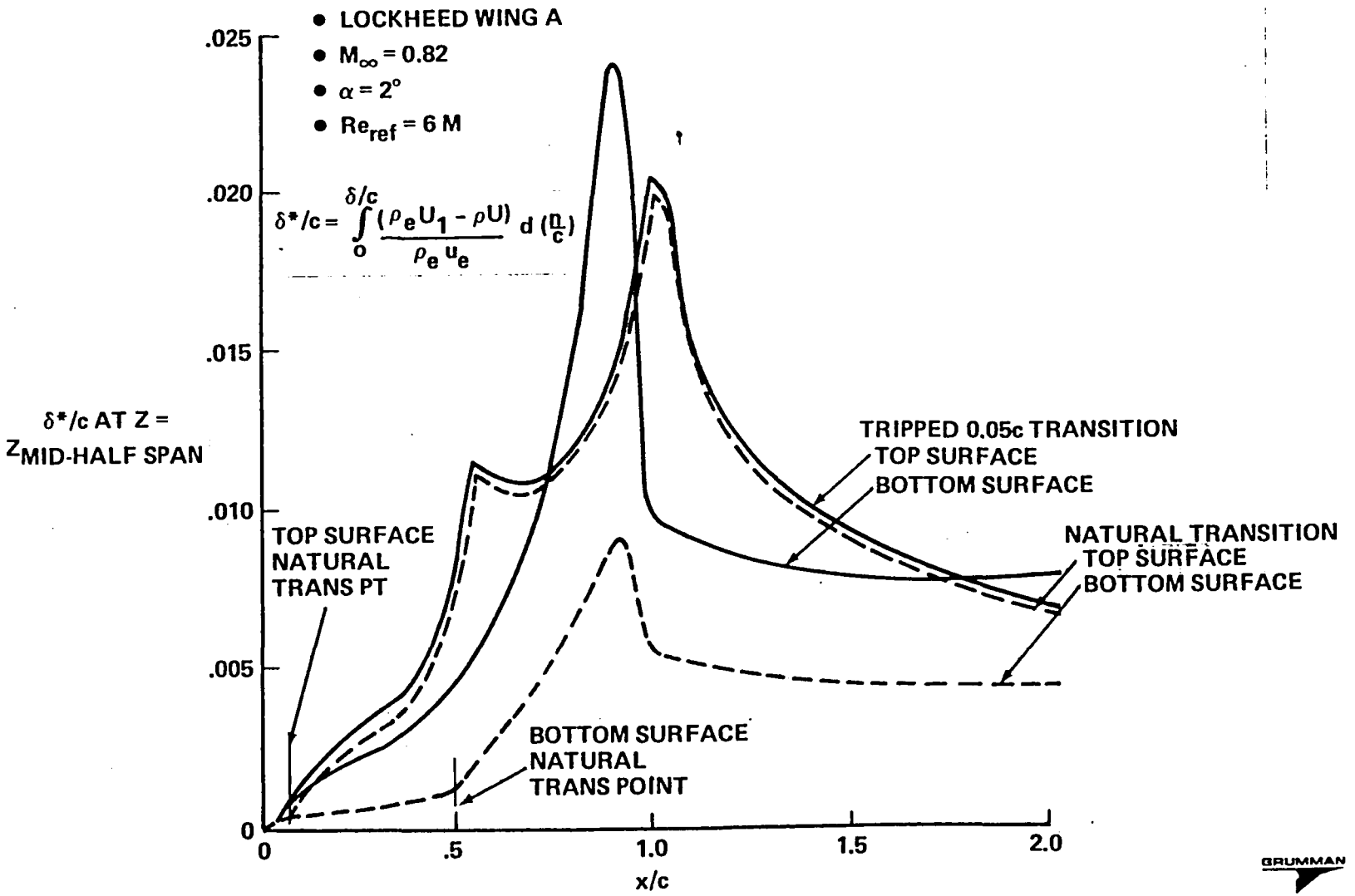

GRUMMAN

1583-045PP

LOWER WING SURFACE SKIN FRICTION DISTRIBUTION AT MID-HALF-SPAN SECTION

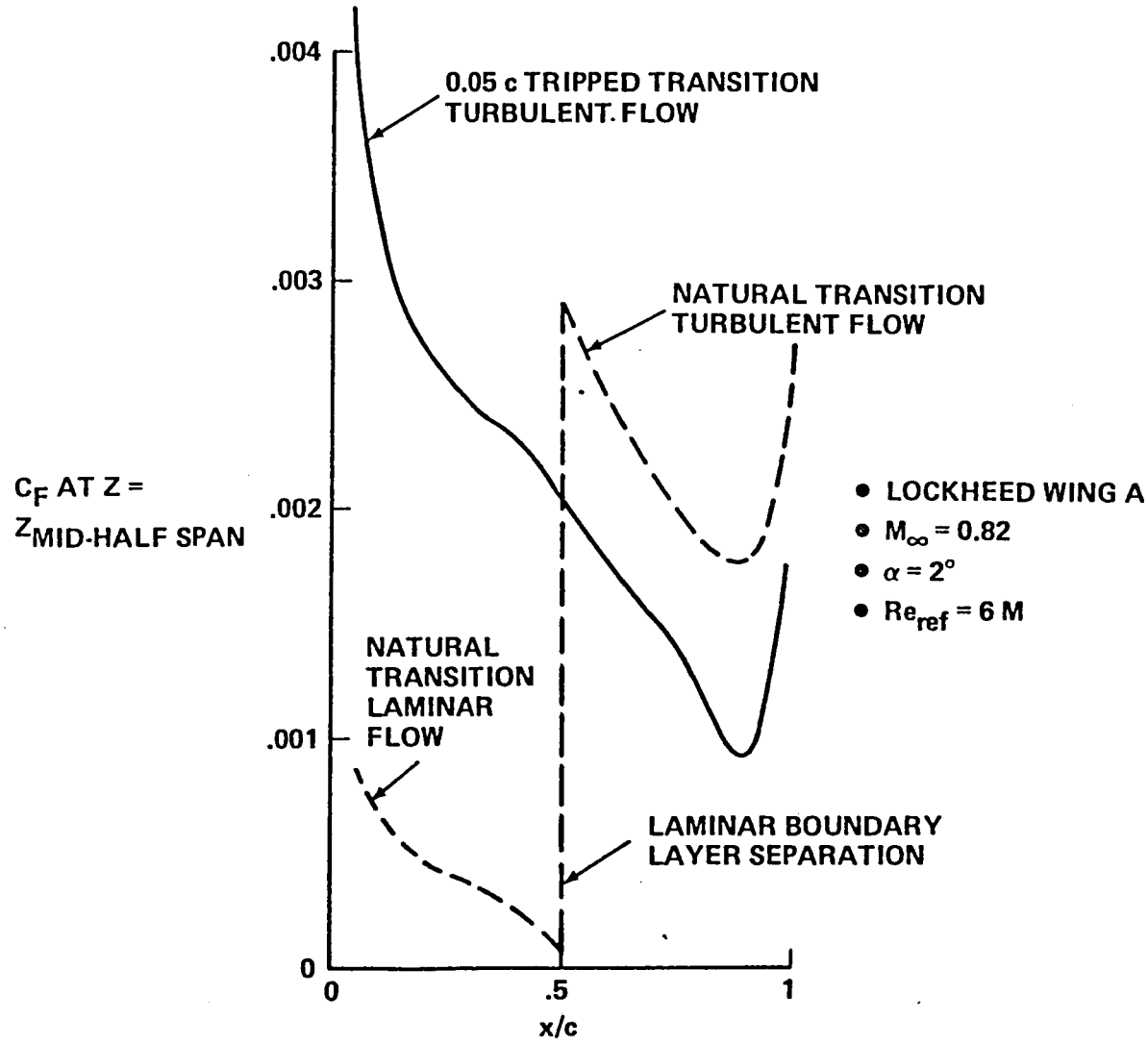

GRUMMAN

1583-047PP

CONVERGED VISCOUS WING SOLUTION – SURFACE ISOBARS

- LOCKHEED WING A
- $M_\infty = 0.82$
- $\alpha = 2°$
- $Re_{ref} = 6\ M$

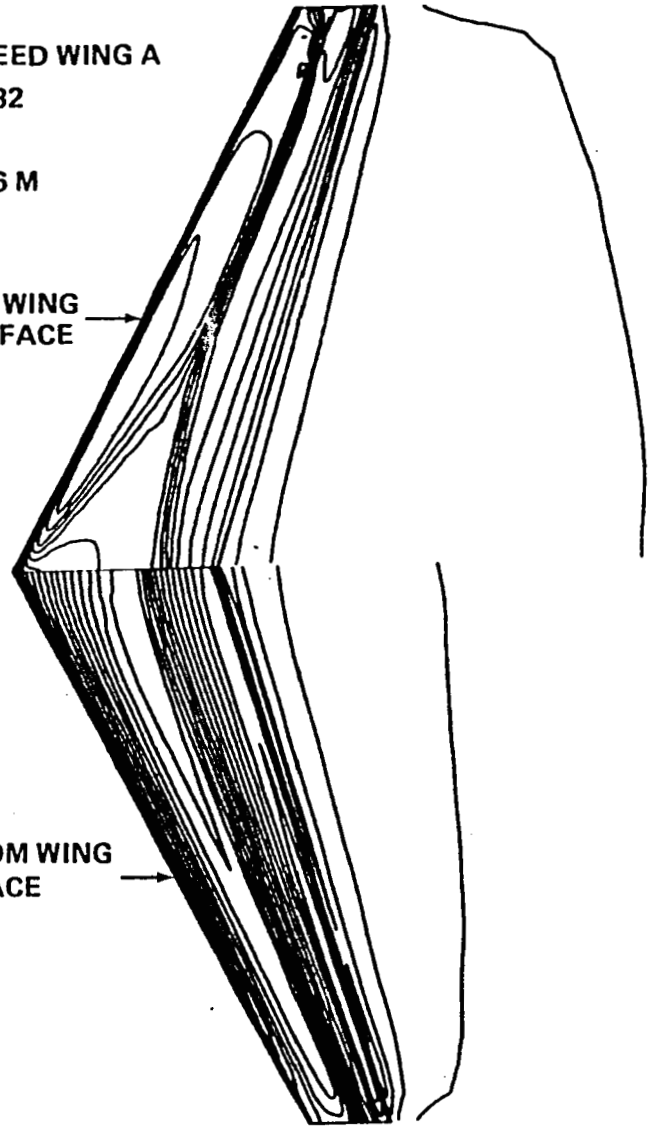

GRUMMAN

629

1583-044PP

CONVERGED ISOCLINES FOR VISCOUS WING SOLUTION

Shape Factor

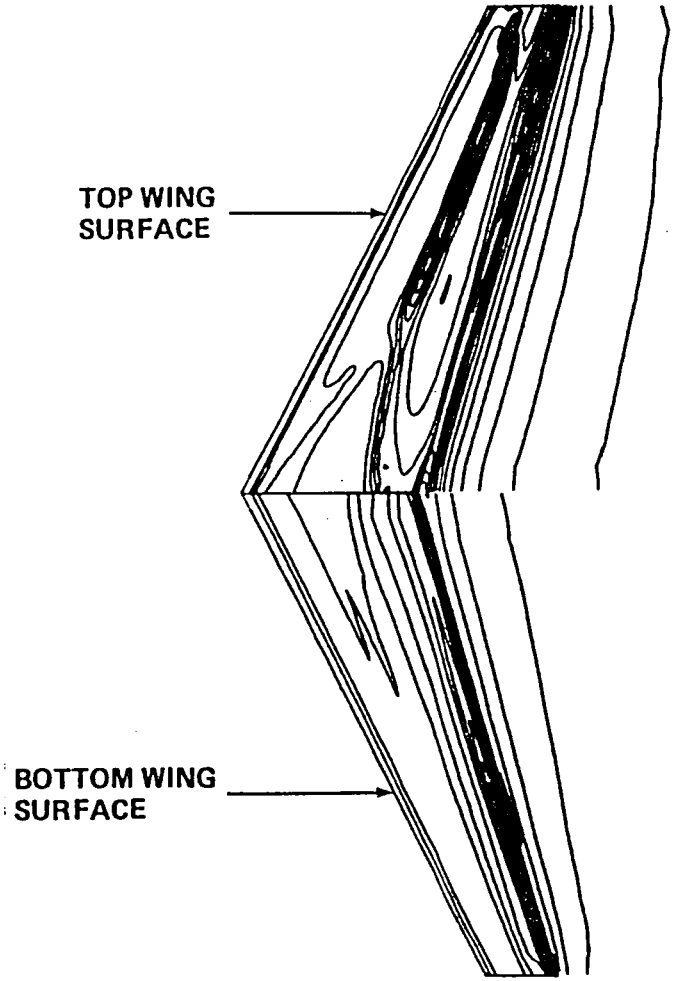

- LOCKHEED WING A
- $M_\infty = 0.82$
- $\alpha = 2°$
- $Re_{ref} = 6\ M$

$$\bar{H} = \frac{c}{\theta_{11}} \int_0^{\delta/c} \frac{\rho}{\rho_e} \left(1 - \frac{U}{u_e}\right) d\left(\frac{n}{c}\right)$$

GRUMMAN

1583-053PP

CONVERGED ISOCLINES FOR VISCOUS WING SOLUTION

Surface Velocity Angle Alpha

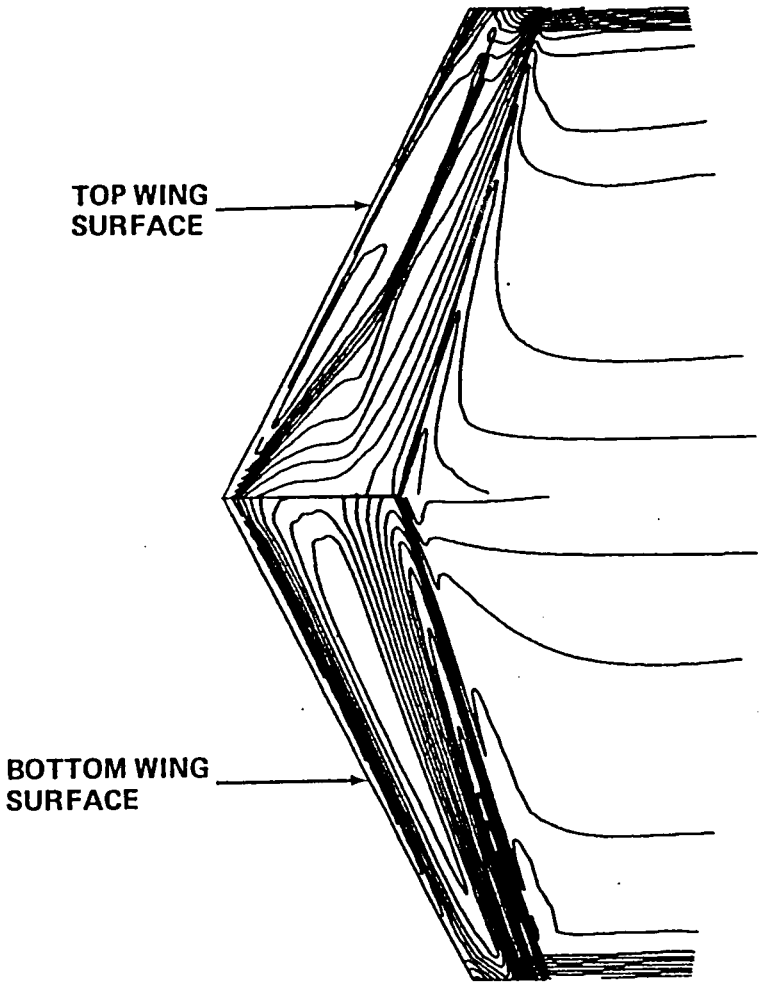

- LOCKHEED WING A
- $M_\infty = 0.82$
- $\alpha = 2°$
- $Re_{ref} = 6\ M$

GRUMMAN

1583-050PP

CONVERGED ISOCLINES FOR VISCOUS WING SOLUTION

Limiting Wall Streamline Angle β

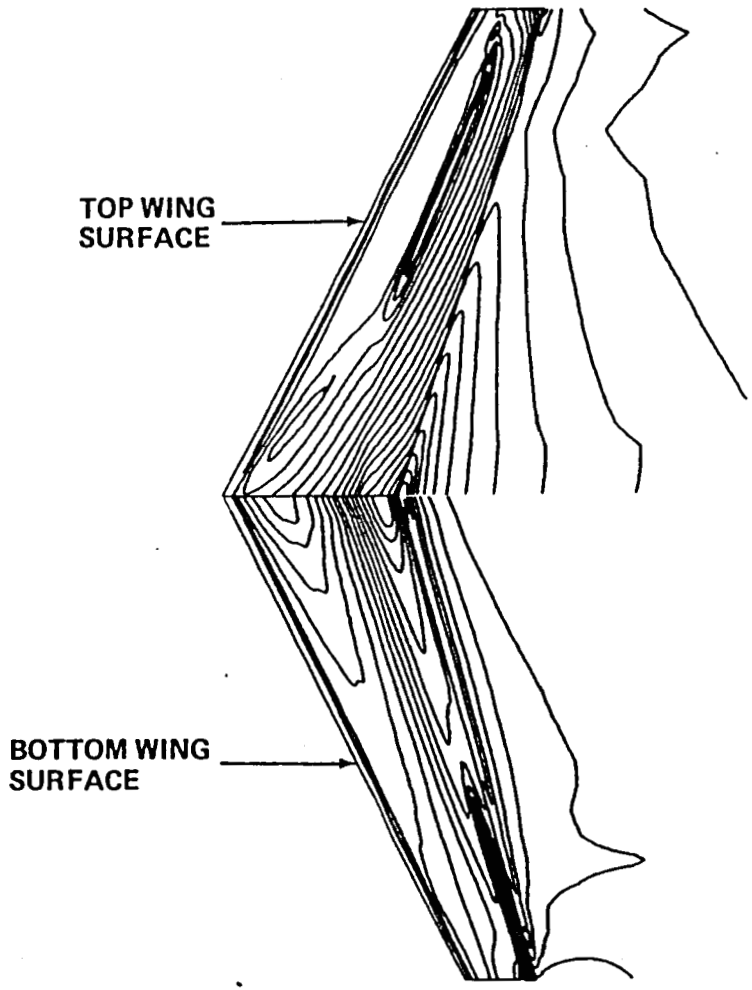

- LOCKHEED WING A
- $M_\infty = 0.82$
- $\alpha = 2°$
- $Re_{ref} = 6$ M

GRUMMAN

1583-054PP

REYNOLDS NUMBER DEPENDENCE OF VISCOUS WING SOLUTION

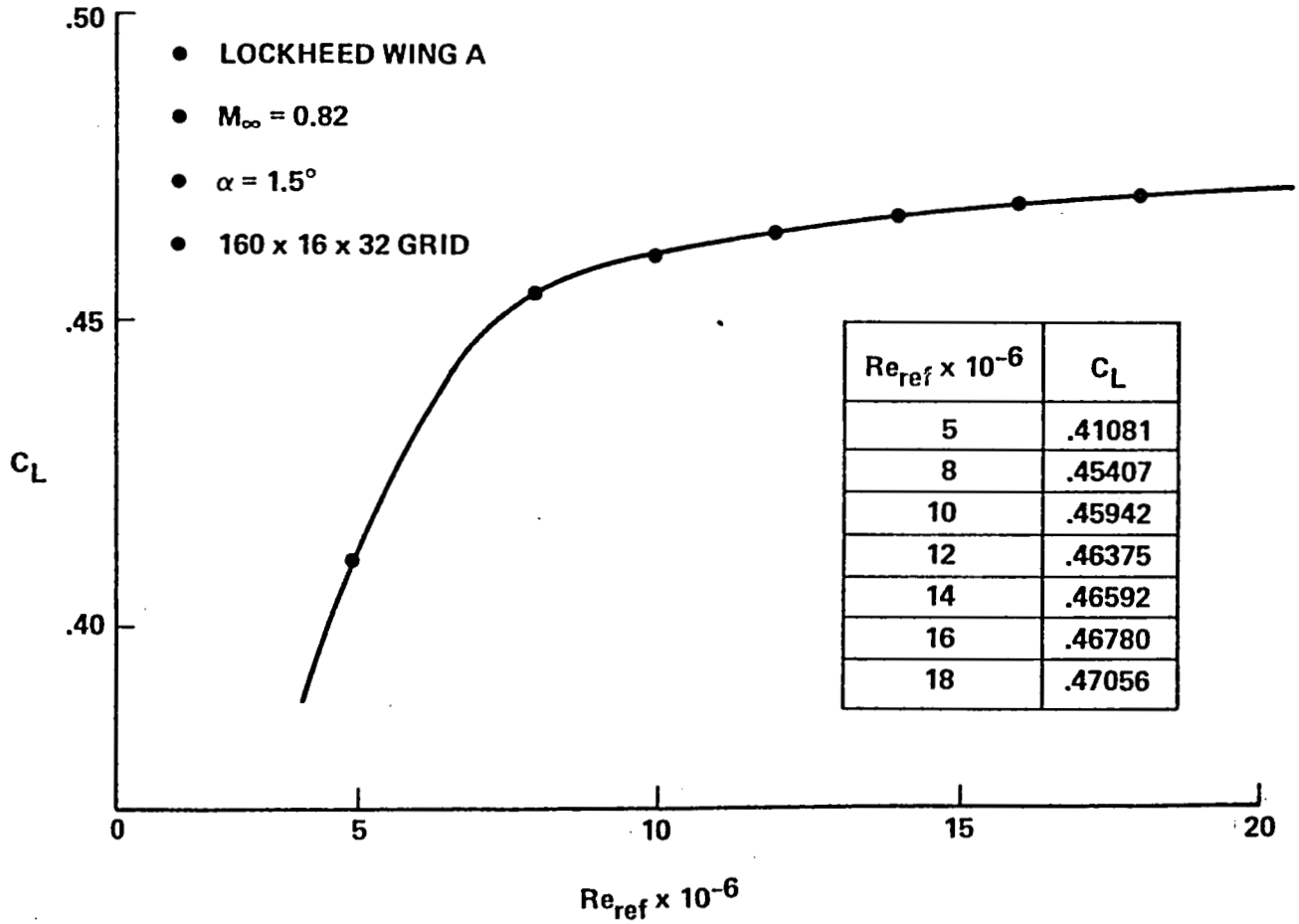

$Re_{ref} \times 10^{-6}$	C_L
5	.41081
8	.45407
10	.45942
12	.46375
14	.46592
16	.46780
18	.47056

GRUMMAN

1583-028PP

FUTURE AREAS OF INTEREST

- BETTER SOLUTION METHODS FOR BOUNDDARY LAYER/WAKE FOR MODERATE AR WINGS (EFFECTS OF WING ROOT AND TIP BOUNDARY CONDITIONS)
- INVERSE MODE TURBULENT BOUNDARY LAYER ANALYSIS
- IMPROVED TURBULENCE MODEL FOR SEPARATED FLOW
- IMPROVED WING TIP TREATMENT FOR POTENTIAL FLOW SOLUTION
- INCLUSION OF FUSELAGE
- IMPLEMENT 3-D EULER INVISCID SOLVER

GRUMMAN

(24)

COMPUTATION OF FLOW FIELDS IN UNBOUNDED DOMAINS

635

NASA NCCI-58

L. TING
COURANT INSTITUTE
NEW YORK UNIV.
OCT. 19, 1983

Two Topics

I, Boundary Conditions for Navier Stokes Solutions Merging with Boundary Layer and Potential Solutions

II, Motion and Decay of Strong Vortical Spots Submerged in a Background Rotational Flow and Their Interactions

I, Physical Problems in Which N S Solutions Merge with

Boundary Layer (or Wake) and Potential Solutions

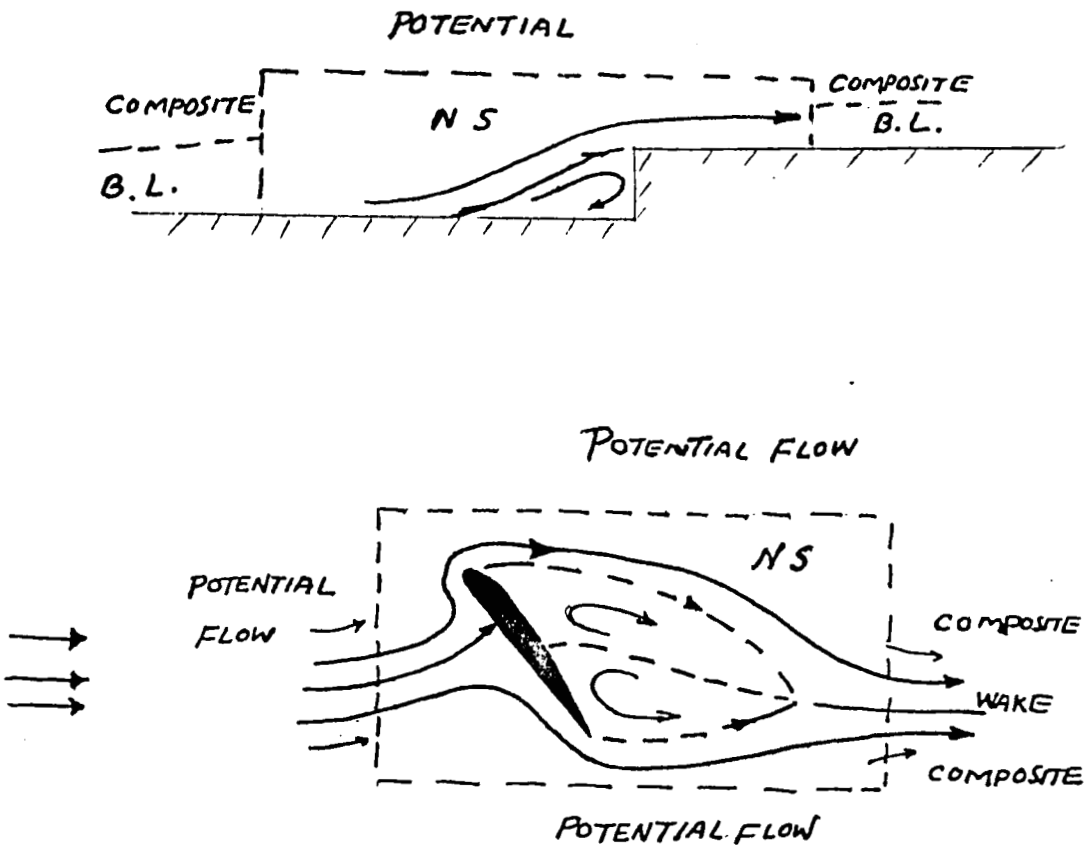

AND THREE DIMENSIONAL PROBLEMS

II) PROBLEMS INVOVING STRONG VORTEX SPOTS IN A SHEAR FLOW

(i) VORTICAL SPOTS IN A BOUNDARY LAYER (2-D unsteady)

(ii) TRAILING VORTICES IN A CROSS (SHEAR) FLOW

$x, y, z \qquad \delta \to U_\infty t$

THERE TWO REFERENCE LENGTH SCALES AND TWO VORTICITY SCALES

$H = 1$, FOR THE SHEAR FLOW OR THICKNESS OF B.L.

δ SIZE OF A VORTICAL SPOT

$$H \gg \delta$$

Γ STRENGTH OF A SPOT $= O(U_\infty H)$ "STRONG"

ζ VORTICITY IN A SPOT $O\left(\frac{\Gamma}{\delta^2}\right)$

ω VORTICITY OF SHEAR FLOW $O(U_\infty / H)$

$$\zeta / \omega = O(\delta^{-2})$$

$$Re_L = \frac{U_\infty H}{\nu} \gg 1 \quad \Rightarrow \text{VISCOSITY EFFECTS ARE IMPORTANT}$$

INSIDE THE VORTICAL SPOTS; FOR x, y IN LENGTH SCALE OF H.

HIGHLIGHTS

(1) USE OF 2-SCALE METHOD.

(2) THE DECAY OF THE VORTICITY (IN SMALL SCALE) IS HANDLED ANALYTICALLY.

(3) THE TRANSPORT OF THE VORTICITY IS ANALYSED BY NUMERICAL SOLUTION OF THE EULER EQUATION. THE INTERACTION EFFECTS WITH THE MOTION AND THE INDUCED FLOW FIELD OF THE SPOTS ARE INCLUDED.

(4) THE GRID SIZE Δ FOR THE NUMERICAL ANALYSIS CAN BE $\gg \delta$ i.e. $H \gg \Delta \gg \delta$.

(5) BECAUSE OF THE "AVERAGING" BUILT INTO THE TWO-SCALE METHOD, Δt DEPENDS ONLY ON U_∞ AND Δ AND INDEP. OF δ.

(6) TREATMENT OF THE FAR FIELD BOUNDARY CONDITIONS FOR THE EULER SOLUTION.

I

BOUNDARY CONDITIONS ON THE N-S SOLUTIONS

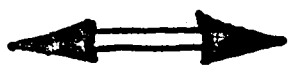

COMPATIBILITY CONDITIONS FOR THE BOUNDARY LAYER (OR WAKE) AND/OR THE POTENTIAL SOLUTIONS

FOR TWO DIMENSIONAL PROBLEMS

WE HAVE THE SAME EQUATIONS FOR BOUNDARY LAYERS AND WAKES

FOR SIMPLICITY WE SHALL ASSUME THE FLOW IS INCOMPRESSIBLE AND THE BOUNDARY LAYER(S) ARE ALONG WALL(S) PARALLEL TO x-AXIS

$\rho = 1$ $\quad U_\infty \rightarrow \quad u^*, v^*, p^*$ POTENTIAL

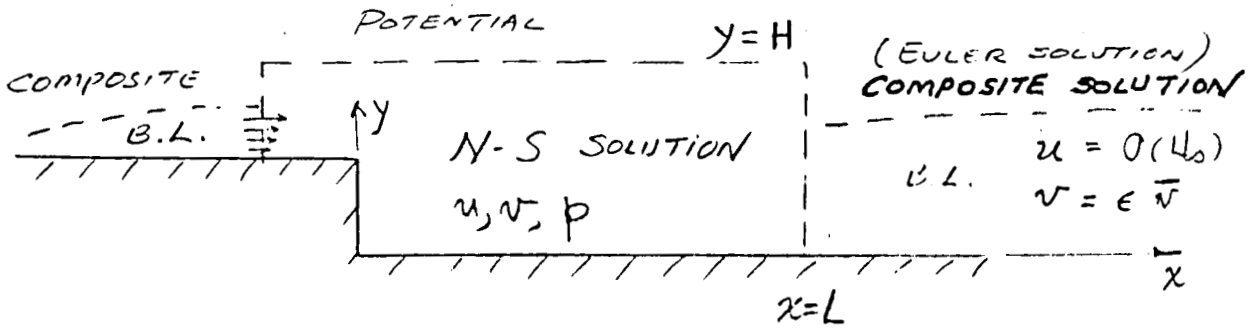

$(^*)$ FOR POTENTIAL SOLUTIONS $\quad u^*, v^*, p^*$ in (x, y)

$(\bar{\ })$ FOR BOUNDARY LAYER $\quad \bar{u}, \epsilon\bar{v}$ in $(x, \bar{y})$

STRETCHED y VARIABLE $\quad \bar{y} = y/\epsilon$

$$\epsilon = 1/\sqrt{Re}$$

WE SHALL DEVELOP THE B.C. ON THE DOWNSTREAM SIDE $x = L$.

WE NOTE THE EQS. FOR B.L. SOLUTION ($x \geq L$)

$$\bar{u}_x + \bar{v}_{\bar{y}} = 0 \qquad (1)$$

$$\bar{u}\bar{u}_x + \bar{v}\bar{u}_{\bar{y}} = -p^*_x(x, y=0) + \bar{u}_{\bar{y}\bar{y}} \qquad (2)$$

$$\bar{p}(x, \bar{y}) = p^*(x, y=0) \qquad (3)$$

WE CAN ONLY IMPOSE ONE INITIAL DATA $\bar{u}$ AT $x=L$. VALUES OF $\bar{v}$ AND $\bar{u}_x$, COMPATIBLE WITH $\bar{u}$, ARE DEFINED BY EQ. (1) AND (2). (E. KRAUSE AIAA J., 5, 1967, 1231-1237)

WE CAN EITHER ELIMINATE $\bar{v}$ FROM (1) & (2) TO FORM A RELATIONSHIP FOR $\bar{u}$ AND $\bar{u}_x$, i.e.

$$\bar{u}\bar{u}_x - \bar{u}_{\bar{y}} \int_0^{\bar{y}} \bar{u}_x \, d\bar{y}' = -p^*_x(L, 0) + \bar{u}_{\bar{y}\bar{y}} \qquad (4)$$

OR ELIMINATE $\bar{u}_x$ FROM (1) & (2) TO FORM A CONDITION ON $\bar{u}$ AND $\bar{v}$ AT $x=L$, i.e.

$$-\bar{u}\bar{v}_{\bar{y}} + \bar{v}\bar{u}_{\bar{y}} = -p^*_x(L, y=0) + \bar{u}_{\bar{y}\bar{y}} \qquad (5)$$

THE INITIAL DATA FOR B.L. SOLUTION $x > L$ HAVE TO BE **COMPATIBLE WITH** (3) AND (5) (OR (4)). (3) AND (5), IN TURN ARE THE TWO BOUNDARY CONDITIONS ON $x=L$ FOR THE N-S SOLUTION MERGING WITH B.L. $x \geq L$

SINCE THE BOUNDARY $x=L$ EXTENDS INTO THE (EULER) THE POTENTIAL REGION, WE SHOULD USE THE COMPOSITE SOLUTION FOR $y>\delta$ TO MODIFY (3) & (5), THE TWO BOUNDARY CONDITIONS ON $x=L$, $0 \le y \le H$ ARE:

$$p(L,y) = p^*(L,y) \qquad (6)$$

AND

$$-u v_y + v u_y = -p_x^*(L,y) + \frac{1}{Re} u_{yy} \qquad (7)$$

NOTE THAT THE LAST TERM IN (7) IS NEGLIGIBLE OUTSIDE THE BOUNDARY LAYER, (6) & (7) ARE THEN COMPATIBLE WITH THE POTENTIAL OR EULER SOLUTION.

THIS PROCEDURE CAN BE EXTENDED TO A COMPRESSIBLE FLOW.

THE DENSITY $\hat{N}$ IS RELATED TO THE TEMPERATURE $\bar{T}$ AND THE PRESSURE p OR p^* BY THE EQ. OF STATE.

THE ENERGY EQUATION FOR THE B.L. BECOMES THE OTHER COMPATIBILITY CONDITION FOR $\bar{T}$ AND $\bar{T}_x$ AND HENCE AN ADDITIONAL BOUNDARY CONDITION FOR THE N S SOLUTION.

WE CAN EXTEND THIS PROCEDURE TO AXISYMMETRIC PROBLEMS.

IT SHOULD BE NOTED HERE THAT

IT IS INCORRECT TO REPLACE CONDITION (7) BY

$$u_{xx} = 0$$

THE X-COMP. BL EQ. AND NS EQUATION DIFFER BY THE TERM u_{xx}/R_e. IT IS SMALL BECAUSE $R_e \gg 1$. WE SEE FROM BLASIUS SOLUTION

$$\bar{u}_{xx} = O(\bar{u}) \quad \text{FOR } x = O(L).$$

IF WE IMPOSE A SIMILARY BOUDARY LAYER PROFILE AT $X=L$ (WITH A MASS BALANCE CONDITION TO DEFINE THE ORIGIN OF THE SIMILARITY SOLUTION) WE HAVE TO USE A LARGE VALUE OF L SUCH THAT THE PRESSURE $p^*(x,0) \sim X^K$ AND THE NONSIMILAR PARTS OF THE B.L. SOLUTION HAVE BECOME INSIGNIFICANT FOR $X > L$.

THREE DIMENSIONAL PROBLEMS

ESSENTIAL DIFFERENCES BETWEEN (i) THE FLOWFIELD OF A BOUNDARY LAYER OVER A SMOOTH SURFACE AND (ii) THAT OF AN ASYMMETRIC WAKE (OR THE BOUNDARY LAYER NEAR THE INTERSECTION OF TWO SURFACES)

(i) BOUNDARY LAYER OVER A SMOOTH SURFACE

x, y SURFACE COORDINATES

y NORMAL "

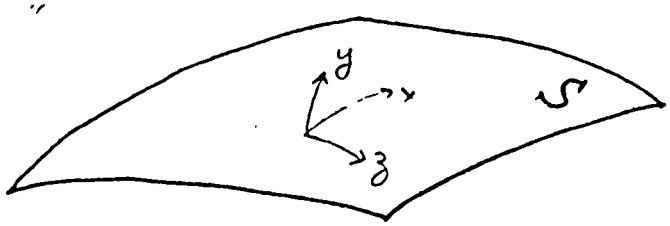

$\frac{\partial}{\partial y} >> \frac{\partial}{\partial x}$, $\frac{\partial}{\partial y} >> \frac{\partial}{\partial z}$

$v << u$ and w

STRETCH y $\bar{y} = y/\epsilon$, $v = \epsilon \bar{v}$

y-comp. momentum equation $\Rightarrow$ $\bar{p}_{\bar{y}} = 0$

OR $\bar{p}(x, \bar{y}, z) = p^*(x, y=0, z)$

(ii) ASYMMETRIC WAKE (EULER)

x — ARC LENGTH ALONG A POTENTIAL STREAM LINE NEAR THE WAKE

(x — ARC LENGTH ALONG THE INTERSECTION OF TWO SURFACES)

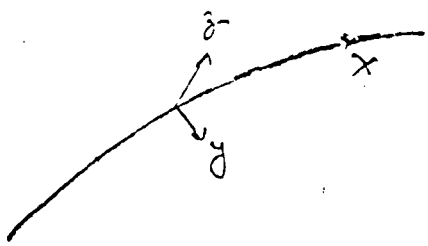

$\frac{\partial}{\partial y} >> \frac{\partial}{\partial x}$, $\frac{\partial}{\partial z} >> \frac{\partial}{\partial x}$, v & $w << u$

STRETCH y & z $\bar{y} = y/\epsilon$, $\bar{z} = z/\epsilon$, $v = \epsilon \bar{v}$, $w = \epsilon \bar{w}$

BOTH y- & z- momentum eq. YIELD $\bar{p}(x, \bar{y}, \bar{z}) = p^*(x, 0, 0)$

ONE MISSING EQ. IS SUPPLIED BY THE x- COMP OF THE VORTICITY EQ. (CARRIER QUART. APPL MATH 4, 1946, 367-370)

(i) N - S SOLUTION

MERGING WITH A BOUNDARY LAYER OVER A SMOOTH SURFACE ($y = 0$)

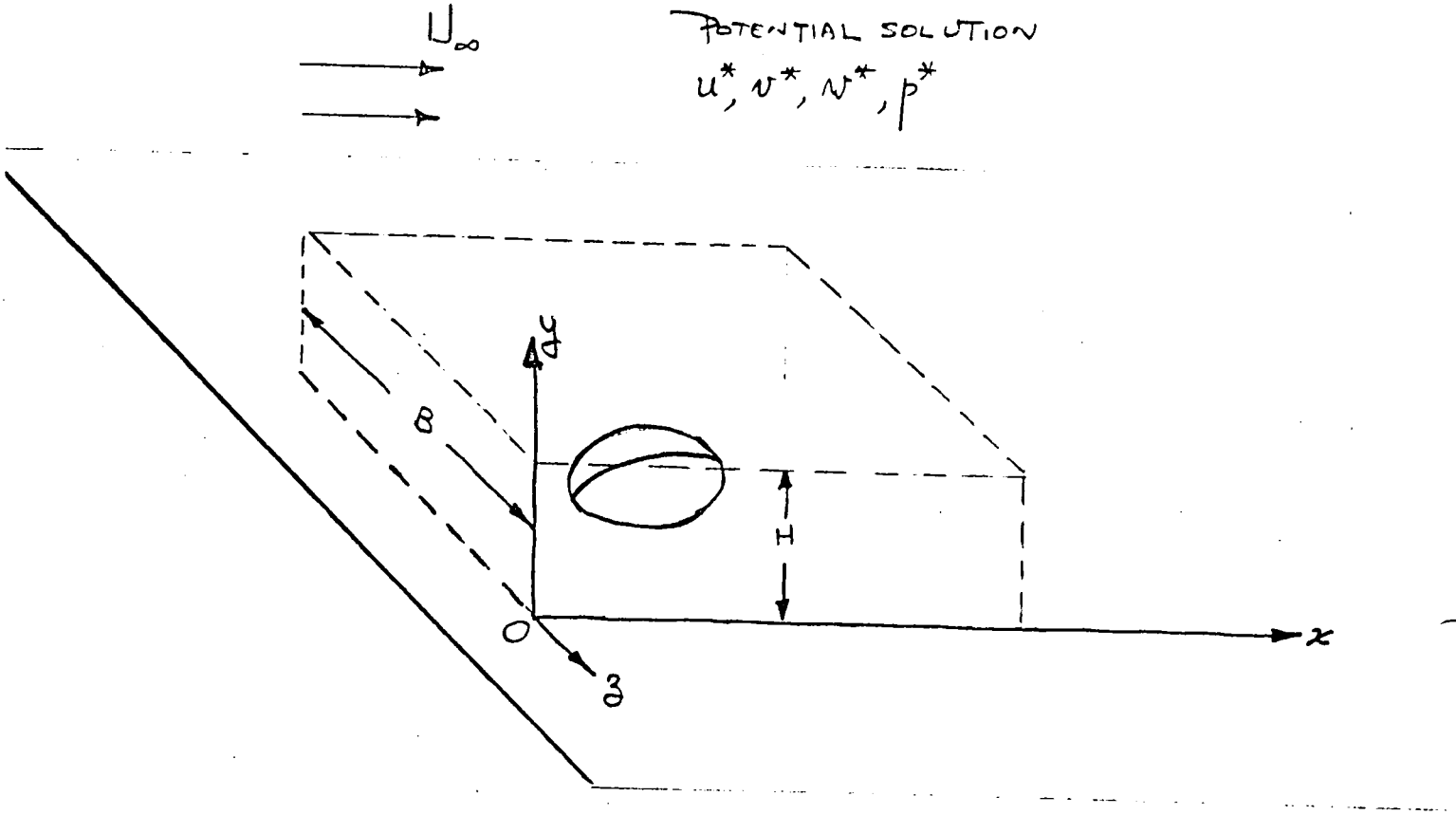

N - S SOLUTION

u, v, w, p

$0 < x < L$

$0 < y < H$

$-B < z < 0$

BOUNDARY LAYER EQUATIONS $(\bar{y}>0,\ x\geq L)$, $\bar{y}=y/\epsilon$

$u=\bar{u}$, $w=\bar{w}$, $v=\epsilon\bar{v}$

$$\bar{u}_x+\bar{v}_{\bar{y}}+\bar{w}_z=0 \qquad (8)$$

$$\bar{u}\bar{u}_x+\bar{v}\bar{u}_{\bar{y}}+\bar{w}\bar{u}_z=-p^*_x(x,y=0^+,z)+\bar{u}_{\bar{y}\bar{y}} \qquad (9)$$

$$\bar{u}\bar{w}_x+\bar{v}\bar{w}_{\bar{y}}+\bar{w}\bar{w}_z=-p^*_z(x,y=0^+,z)+\bar{w}_{\bar{y}\bar{y}} \qquad (10)$$

$$\bar{p}(x,\bar{y},z)=p^*(x,y=0^+,z) \qquad (11)$$

PROPER INITIAL CONDITIONS:

$\bar{u}(L,\bar{y},z)$, $\bar{w}(L,\bar{y},z)$ PRESCRIBED

EQS (8), (9) AND (10) THEN DEFINE $\bar{v}$ AND $\bar{u}_x$, $\bar{w}_x$ AT $x=L$.

SIMILAR TO THE TWO DIMENSIONAL CASE, WE EITHER ELIMINATE $\bar{v}$ FROM (8) (9) (10) TO FORM TWO COMPACTIBILTY CONDITIONS FOR $\bar{u}$, $\bar{u}_x$ $\bar{w}$ AND $\bar{w}_x$ OR ELIMINATE $\bar{u}_x$. WE CHOOSE THE LATTER. FROM (8) AND (9) WE HAVE

$$-\bar{u}(\bar{v}_{\bar{y}}+\bar{w}_z)+\bar{v}\bar{u}_{\bar{y}}+\bar{w}\bar{u}_z=-p^*_x(x,0,z)+\bar{u}_{\bar{y}\bar{y}} \qquad (12)$$

EQS. (11), (12) AND (10) IN TURN SERVE AS THE BOUNDARY CONDITION FOR THE N-S SOLUTION AT $X=L$.

IN GENERAL $y=0$ WILL BE THE NO-SLIP SURFACE AND $x=L$ WILL BE THE SURFACE NORMAL TO $y=0$ AND TO THE POTENTIAL FLOW NEAR $y=0$.

(ii) N-S SOLUTIONS MERGING WITH AN ASYMMETRIC WAKE

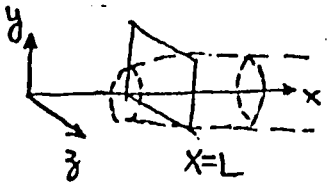

(ALONG x-axis for $x > L$,

e.g. "FAR" WAKE BEHIND A BODY SYMMETRIC WITH xy AND xz PLANE.)

D.E. FOR THE WAKE (INCOMPRESSIBLE, $\rho = 1$)

NOTE
$\bar{z} = z/\epsilon$, $\bar{y} = y/\epsilon$
$u = \bar{u}$, $v = \epsilon\bar{v}$, $w = \epsilon\bar{w}$ (13)

CONTINUITY, $\bar{u}_x + \bar{v}_{\bar{y}} + \bar{w}_{\bar{z}} = 0$ (12)

y-, z-MOMENTUM, $\bar{p}(x, \bar{y}, \bar{z}) = p^*(x, y=0, z=0)$

x-MOMENTUM, $\bar{u}\bar{u}_x + \bar{v}\bar{u}_{\bar{y}} + \bar{w}\bar{u}_{\bar{z}} = -p_x^* + (\bar{u}_{\bar{y}\bar{y}} + \bar{u}_{\bar{z}\bar{z}})$. (14)

X-COMP. OF VORTICITY EQ. ($\frac{\partial}{\partial \bar{z}}$ y-MOMENTUM $- \frac{\partial}{\partial \bar{y}}$ z-MOMENTUM EQ.)

$$\bar{u}\bar{\xi}_x + \bar{v}\bar{\xi}_{\bar{y}} + \bar{w}\bar{\xi}_{\bar{z}} + \bar{w}_x\bar{u}_{\bar{y}} - \bar{v}_x\bar{u}_{\bar{z}} + \bar{u}_x\bar{\xi} = \bar{\xi}_{\bar{y}\bar{y}} + \bar{\xi}_{\bar{z}\bar{z}} \quad (15a)$$

WHERE $\bar{\xi} = \bar{w}_{\bar{y}} - \bar{v}_{\bar{z}}$ (CARRIER 1946 Q. Appl. MATH), OR

$$\left[(\bar{u}\bar{w})_{\bar{y}} - (\bar{u}\bar{v})_{\bar{z}}\right]_x = (\bar{v}\bar{w})_{\bar{z}\bar{z}} - (\bar{v}\bar{w})_{\bar{y}\bar{y}} - (\bar{w}^2 - \bar{v}^2)_{\bar{y}\bar{z}} + \bar{\xi}_{\bar{y}\bar{y}} + \bar{\xi}_{\bar{z}\bar{z}} \quad (15b)$$

THE PROPER INITIAL CONDITIONS ARE: (TING J. MATH. PHYS. XLIV 1965, 353-367)

$\bar{u}(L, \bar{y}, \bar{z})$ AND

$\bar{q} = (\bar{u}\bar{w})_{\bar{y}} - (\bar{u}\bar{v})_{\bar{z}}$ AT $X = L$ PRESCRIBED.

$\bar{v}$, $\bar{w}$, $\bar{u}_x$ AND $\bar{q}_x$ ARE THEN DEFINED BY (12) (13) (14) AND (15b).

AGAIN, ELIMINATE $\bar{u}_x$ FROM (12) AND (14),

$$-\bar{u}(\bar{v}_y+\bar{w}_z)+\bar{v}\bar{u}_y+\bar{w}\bar{u}_z=-p_x^*(L,0,0)+\bar{u}_{yy}+\bar{u}_{zz} \quad (16)$$

EQS. (13), (16) AND (15b) ARE IN TURN THE THREE BOUNDARY CONDITIONS FOR THE N-S SOLUTIONS. THEY ARE ON $\underline{x=L}$, $\underline{0\le y\le H}$, $\underline{-B\le z\le 0}$

$$p=p^*(L,y,z) \quad (17)$$

$$-u(v_y+w_z)+vu_y+wu_z=-p_x^*(L,y,z)+\frac{1}{Re}(u_{yy}+u_{zz}) \quad (18)$$

AND

$$[(uw)_y-(uv)_z]_x=(vw)_{zz}-(vw)_{yy}-(w^2-v^2)_{yz}+\frac{1}{Re}\left(\frac{\partial^2}{\partial y^2}+\frac{\partial^2}{\partial z^2}\right)(w_y-v_z) \quad (19)$$

IN THE REGION OUTSIDE THE WAKE, THE LAST TERMS IN (18) AND (19) INVOLVING THE FACTOR $1/Re$ ARE NEGLIGIBLE, AND EQS (18) AND (19) BECOME RESPECTIVELY THE X-COMP. OF EULER EQ. AND THAT OF THE VORTICITY EQUATION FOR INVISCID FLOW. IN GENERAL p^* IN (17) AND (18) SHOULD BE THE "OUTER" EULER SOLUTION WHICH INCLUDES THE VORTICITY CARRIED INTO THE COMPOSITE REGION BEHIND $x=L$.

SOLUTION ADAPTIVE GRID GENERATION

Peter R. Eiseman

Columbia University

(25)

PROPERTIES FOR A GENERAL ADAPTIVE METHOD

- Efficiency
- Reliability
- Simplicity
- Versatility
  - Numerical algorithms
  - Physical problems
  - Complicated Regions
  - Multiple valued solutions
- Control
  - Resolution
  - Alignment
  - Structure
  - Application
    - how, when, where, directness

SOLUTION GENERATED SURFACE

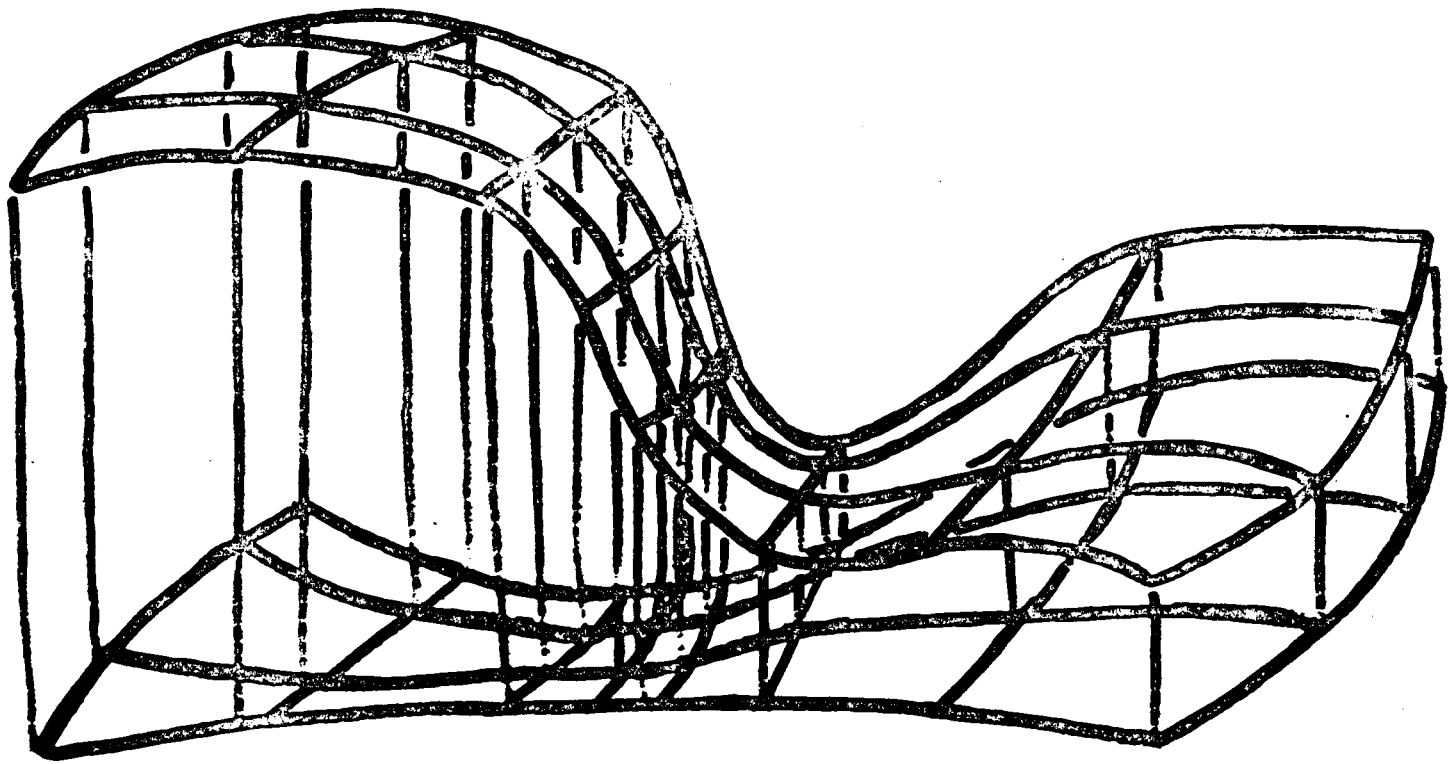

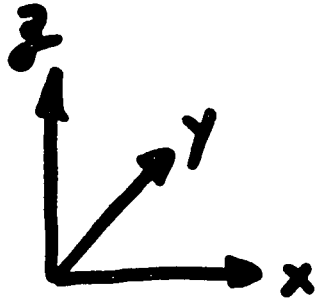

SOLUTION GENERATED SURFACES

- Definition
  - Salient solution properties
  - Discrete
  - Scaling
  - Can be smoothed if necessary
- Generate New Surface Mesh
  - More accurate view of surface
  - Enhanced solution accuracy
- Control
  - Curvature
  - Weights
- Application
  - Direct — multivalued solutions
  - Upon projection

SURFACE MESH GENERATION STRATEGIES

- Mean Value Relaxation
  - ASME Proc. on Advances in Grid Generation, FED-Vol.5, Houston 1983 pgs. 29-34.
- Alternating Direction
  - AIAA 6th CFD Conf., Danvers 1983, pgs. 339-348
- Triangular
  - Jointly with Gordon Erlebacher
  - Thesis of Gordon Erlebacher for Columbia PhD – this semester
  - Future reporting will be directed towards AIAA, JCP, ...
- Parameter Variation in Multi Surface Method
- Variational
  - Jointly with P.J. Roache & S. Steinberg
- Add and Subtract Points

1 D MOVEMENT

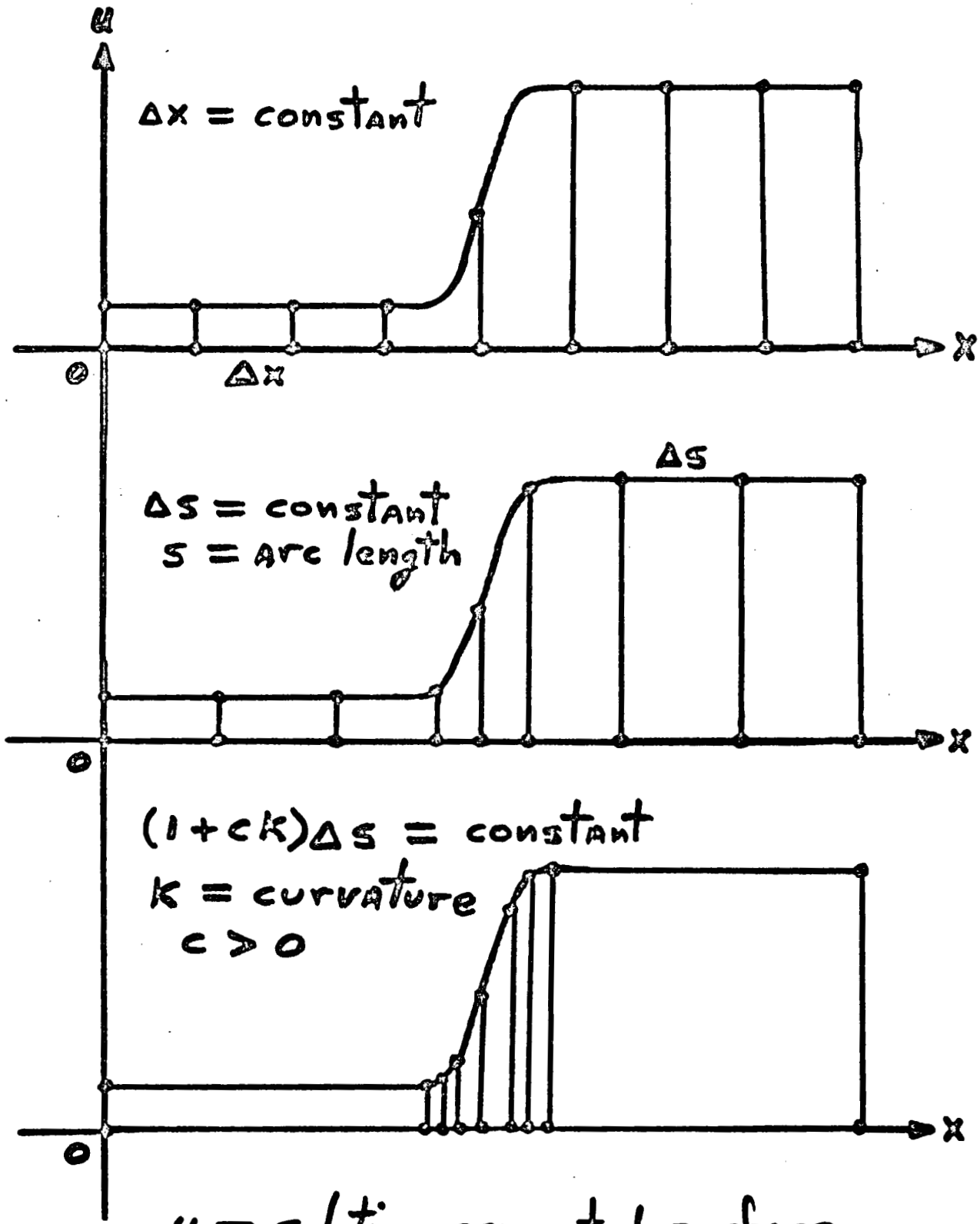

u = solution generated surface

GRADIENT CLUSTERING FROM SOLUTION ARC LENGTH

Equal arc length increments

$$\Delta s = \text{constant}$$

In physical space

$$\sqrt{1 + u_x^2}\,\Delta x = \text{constant}$$

Limiting behavior

- When $|u_x| \ll 1$

$$\Delta x \simeq \text{constant}$$

- When $|u_x| \gg 1$

$$|u_x|\,\Delta x \simeq \text{constant}$$

Altogether, there is a continuous transition between uniform and gradient spacing

1-D BURGER EQUATION

$$u_t + uu_x = \frac{1}{R_e} u_{xx}$$

at $R_e = 200$

Crank-Nicolson from $t = 0$ to $t = 2$ with $\Delta t = .01$

Movement steps with weight

$$w = 1 + 50 \left| \frac{K}{K_{max}} \right|$$

where

$$K = \frac{u_{xx}}{[1 + u_x^2]^{3/2}}$$

$$ds = \sqrt{1 + u_x^2}\, dx$$

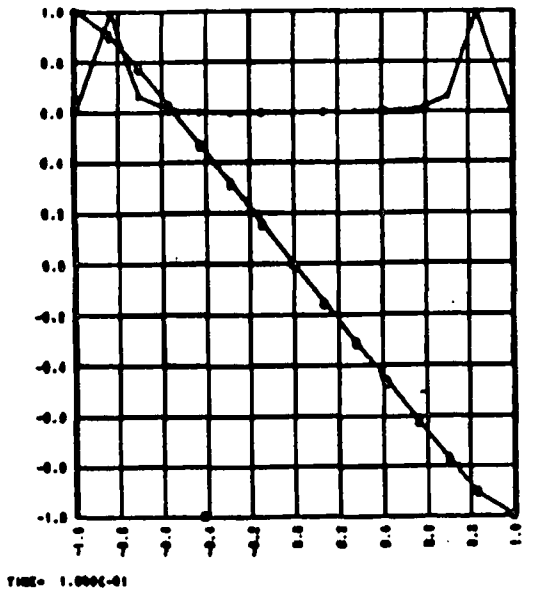

$t = .1$

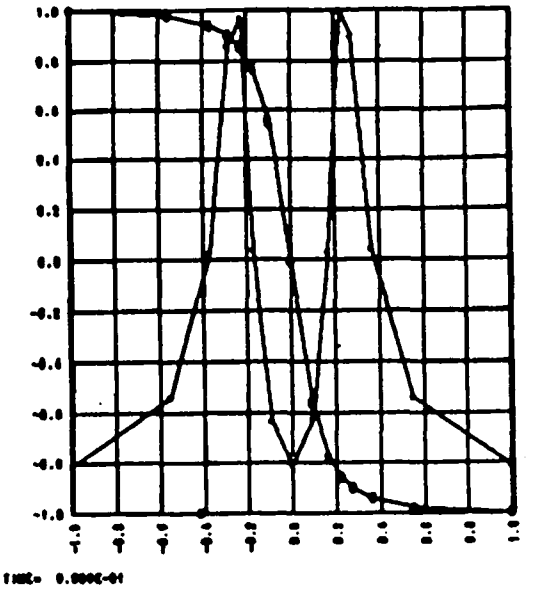

$t = .9$

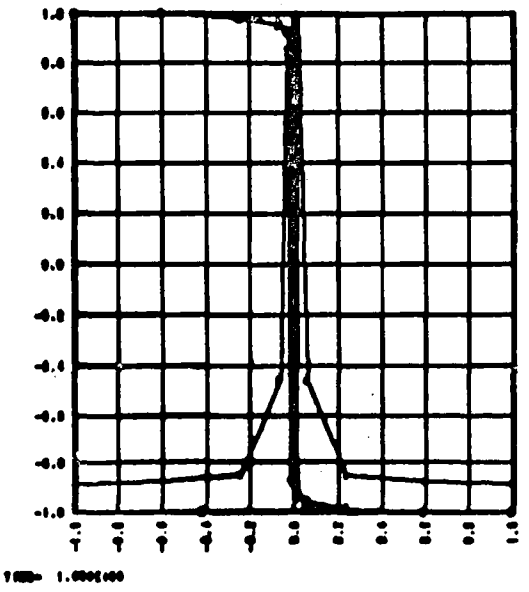

$t = 1.6$

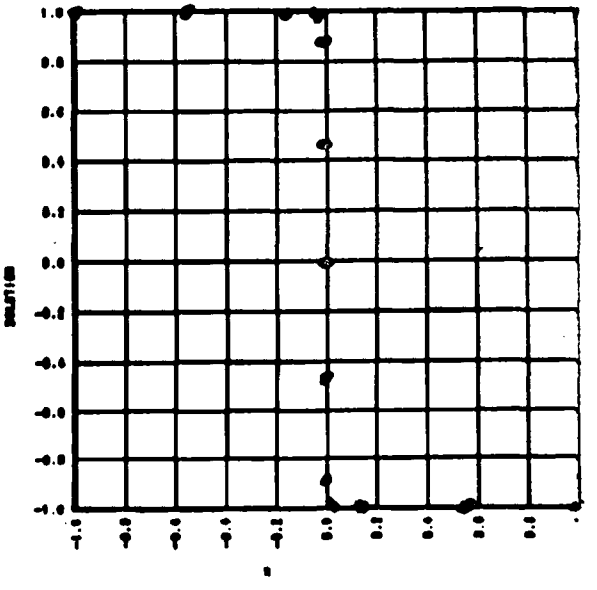

$t = 2.$

ALTERNATING DIRECTION METHOD

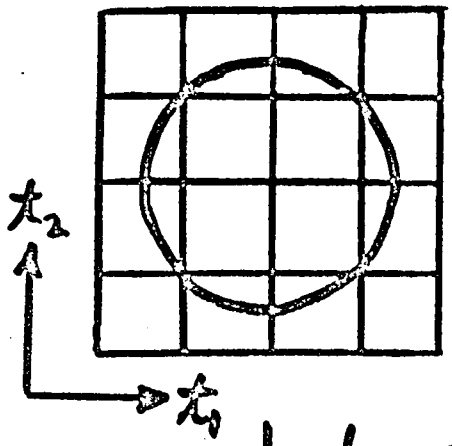

$\downarrow t_1$-Sweep

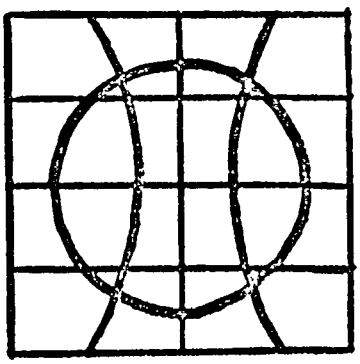

$\downarrow t_2$-Sweep

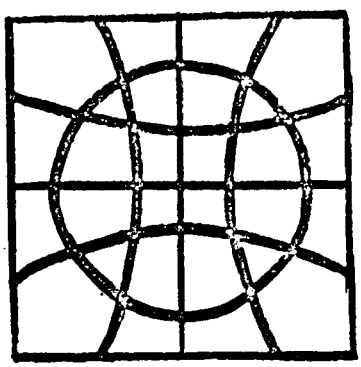

$\vdots$

$$dt \propto W\,ds$$

$$W = 1 + \sum_{j=1}^{m} c_j M_j$$

$$t = \frac{T(s)}{T(s_{MAX})}$$

where

$$T(s) = \int_0^s W\,dr$$

TANGENT PLANES ALONG A CURVE

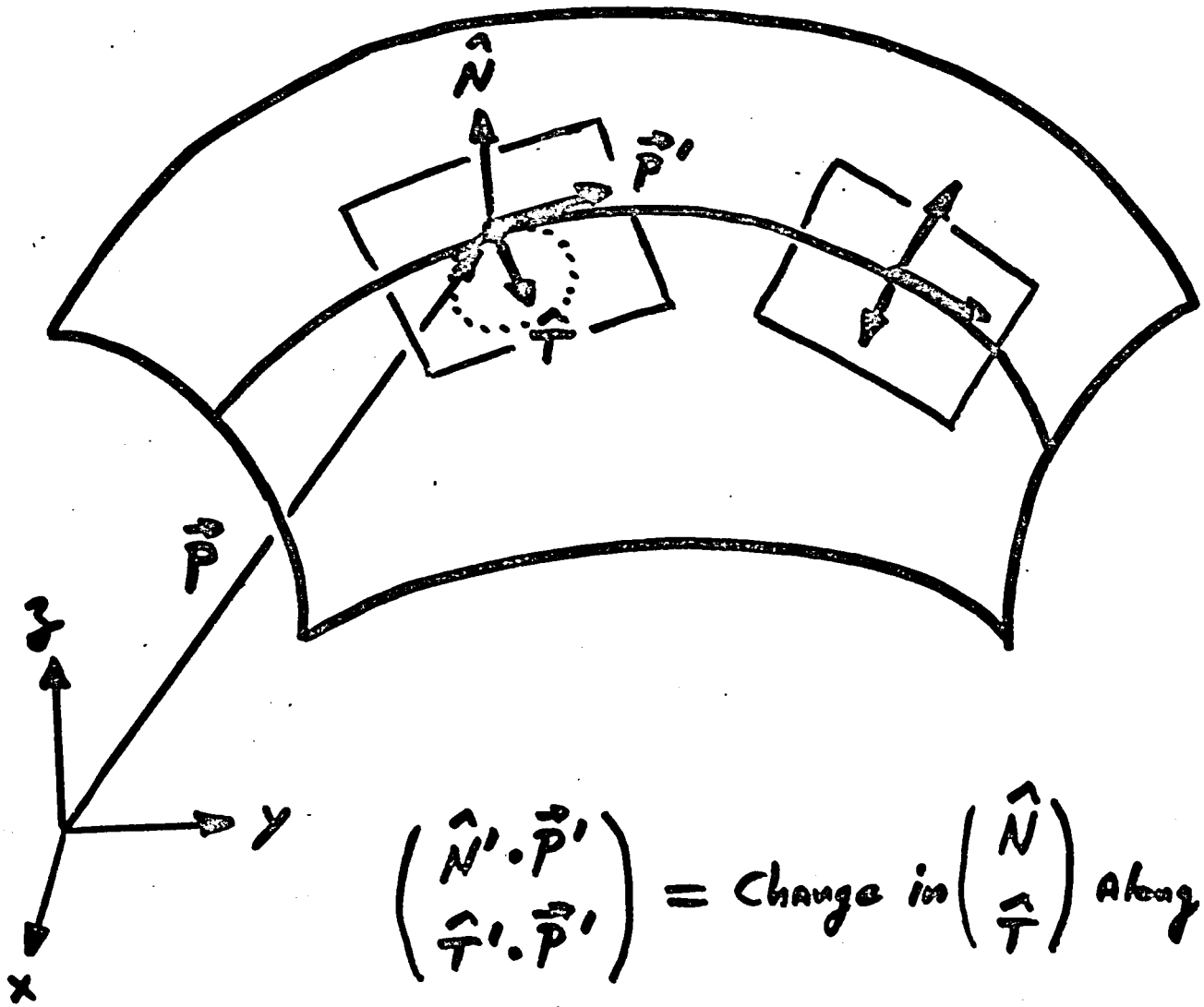

$$\begin{pmatrix} \hat{N}' \cdot \vec{P}' \\ \hat{T}' \cdot \vec{P}' \end{pmatrix} = \text{Change in} \begin{pmatrix} \hat{N} \\ \hat{T} \end{pmatrix} \text{ Along } \vec{P}' \text{ wrt. s}$$

CHOICE OF WEIGHTS

Normal Curvature χ_N

Basic Surface Geometry

Geodesic Curvature χ_g

Boundary Resolution

Jacobian

Equal Area

Function of Curvilinear Variables

Independent of Image Location

Metric Coefficients

Structure

g_{11} and g_{22} — spacing

g_{12} — orthogonallity

CURVATURE

$$\vec{P}'' = \kappa \hat{n} = k_g \hat{T} + k_N \hat{N}$$

$\kappa = \hat{n} \cdot \vec{P}''$ = full curvature

$k_g = \hat{T} \cdot \vec{P}''$ = geodesic curvature

$k_N = \hat{N} \cdot \vec{P}''$ = normal curvature

From

$$\vec{P}(u,v) = (x(u,v), y(u,v), z(u,v))$$

we compute

$$\vec{B} = \frac{\partial \vec{P}}{\partial u} \times \frac{\partial \vec{P}}{\partial v}$$

$$\hat{N} = \frac{\vec{B}}{\|\vec{B}\|}$$

$$\hat{T} = \vec{P}' \times \hat{N}$$

and then the curvatures

CURVATURE WEIGHT

$$W(s) = 1 + c\,|X_N(s)|$$

Transformation

$$t = \frac{s + c\,I(s)}{s_{max} + c\,I(s_{max})}$$

where

$$I(s) = \int_0^s |X_N(r)|\,dr$$

Specify fractions (Dwyer)

$$f = \frac{c\,I(s_{max})}{s_{max} + c\,I(s_{max})}$$

inversion yields

$$c = \frac{f\,s_{max}}{(1-f)\,I(s_{max})}$$

DYNAMIC SHIFTING

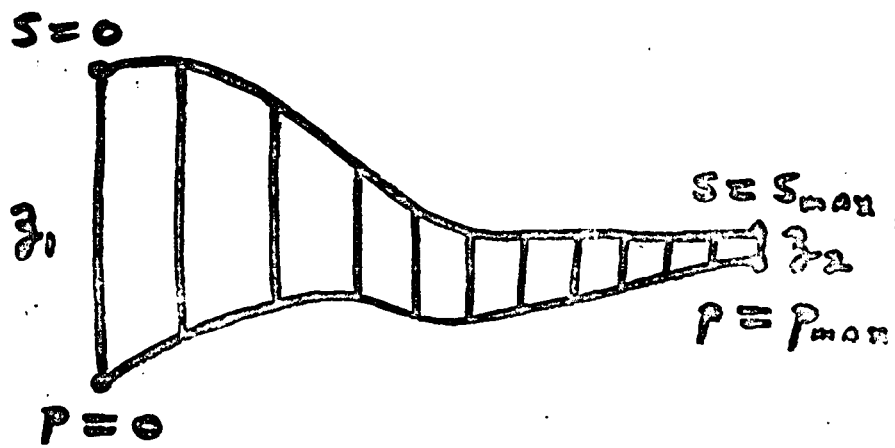

$$\Delta z = z_2 - z_1$$

$$R = \frac{S_{max}}{\sqrt{P_{max}^2 + (\Delta z)^2}}$$

Specify <u>maximum</u> fraction f and <u>rate</u> of transition D

$$c = \frac{f\, S_{max} \tanh D(R-1)}{(1-f)\, I(S_{max}) + \varepsilon}$$

Process can be extended to

$$W(S) = 1 + c_1 |X_N(S)| + c_2 |X_g(S)|$$

...

TEST CASES

① $z(x,y) = \frac{1}{2}\{1 + \tanh 3(1 - x^2 - y^2)\}$

from Cartesian on $-2 \le x, y \le 2$

② $z(x,y) = \frac{1}{2}\tanh 3(x - \alpha y^2 + \frac{3}{2})$

from a sheared system on

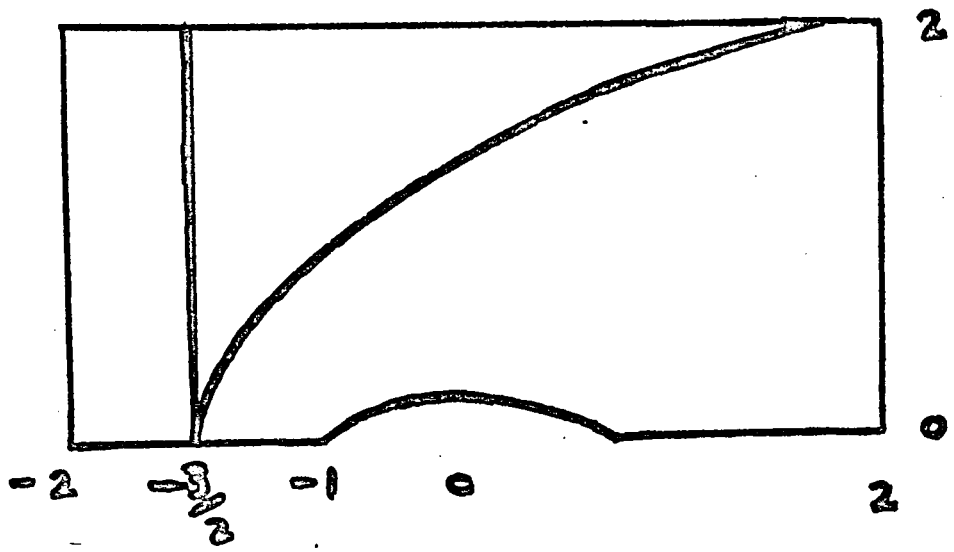

where α is increased from 0.

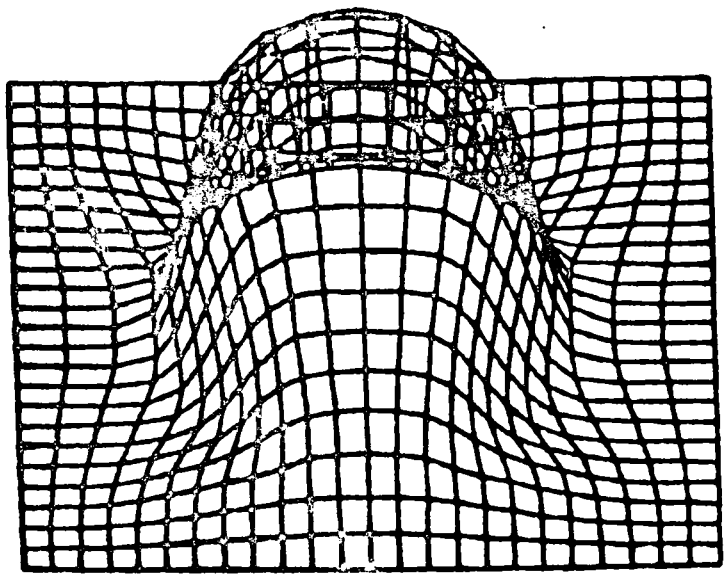

Surface With No Curvature Pull

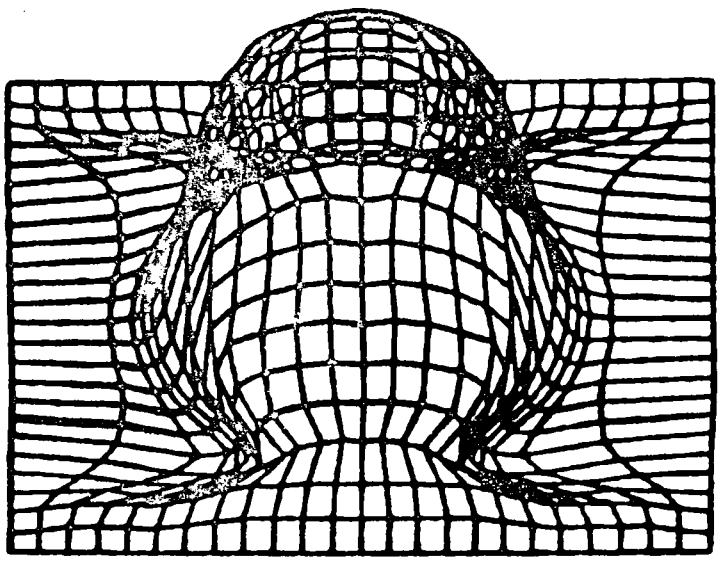

Surface With Curvature Pull In One Direction

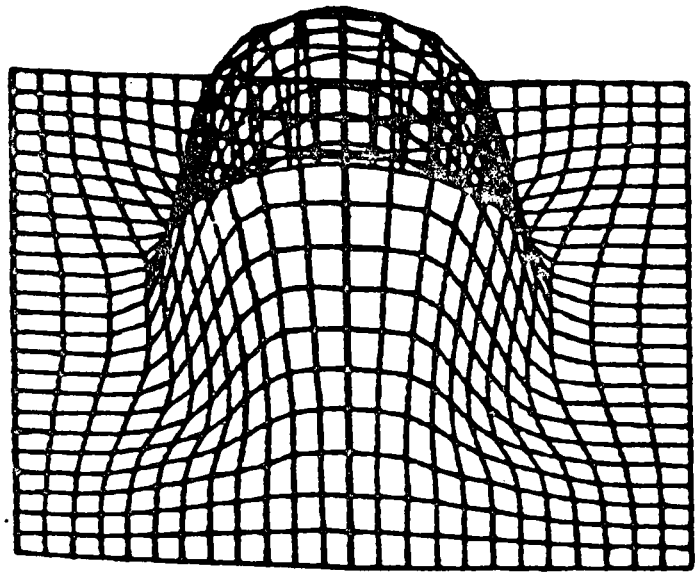

No Curvature Pull

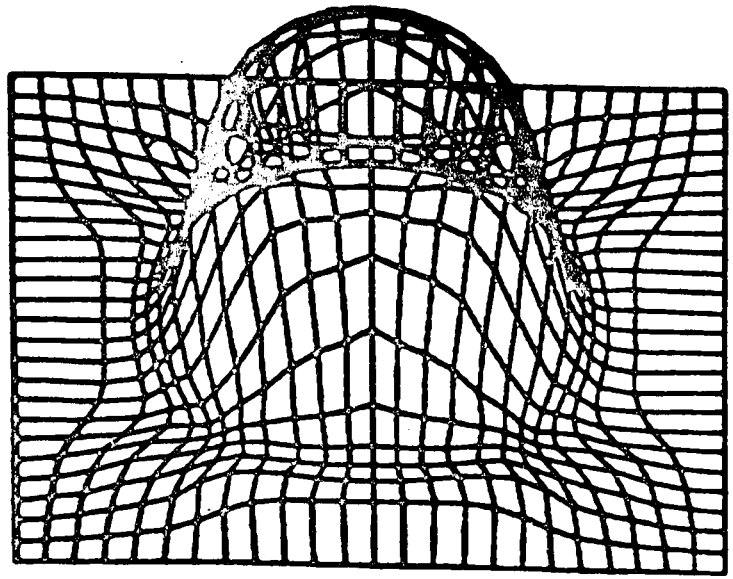

Curvature Pull In Both Directions

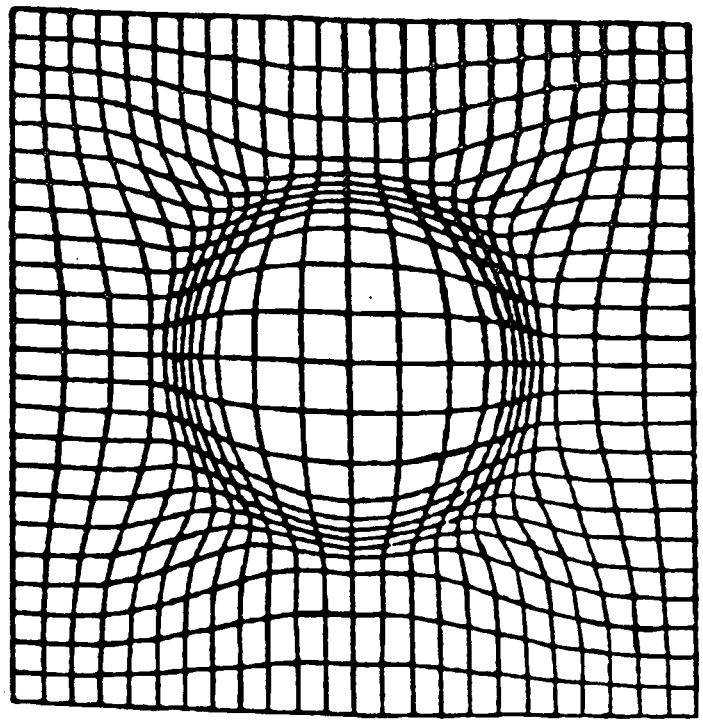

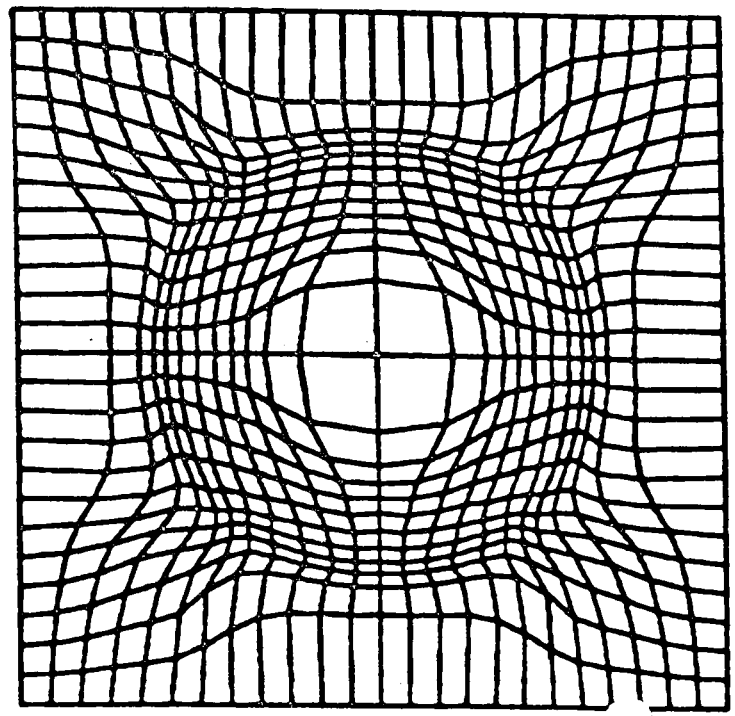

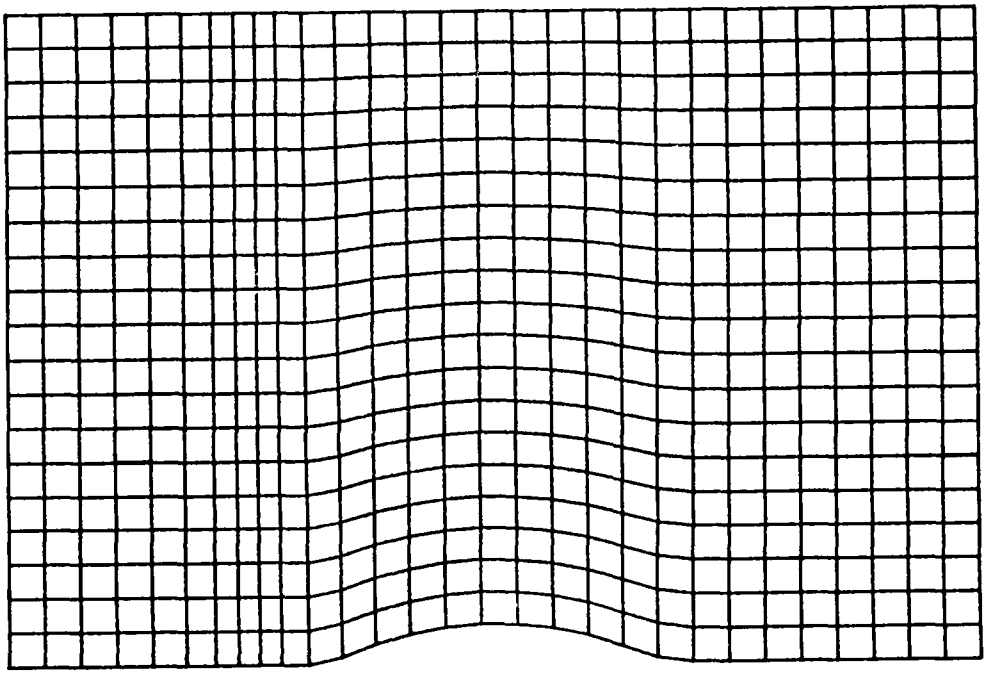

Without Curvature

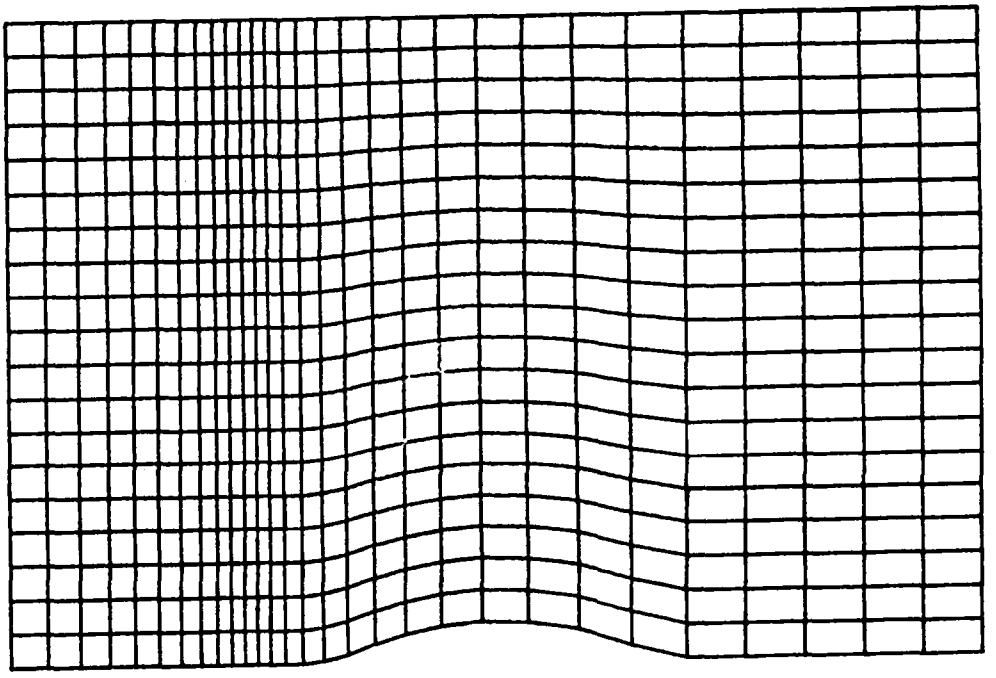

With Curvature

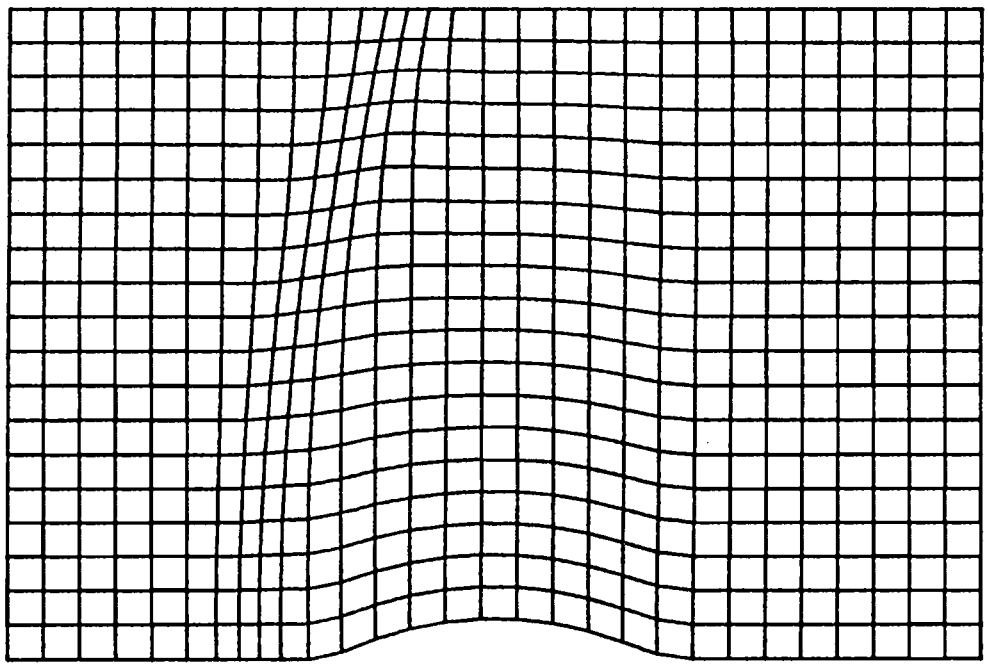

Without Curvature

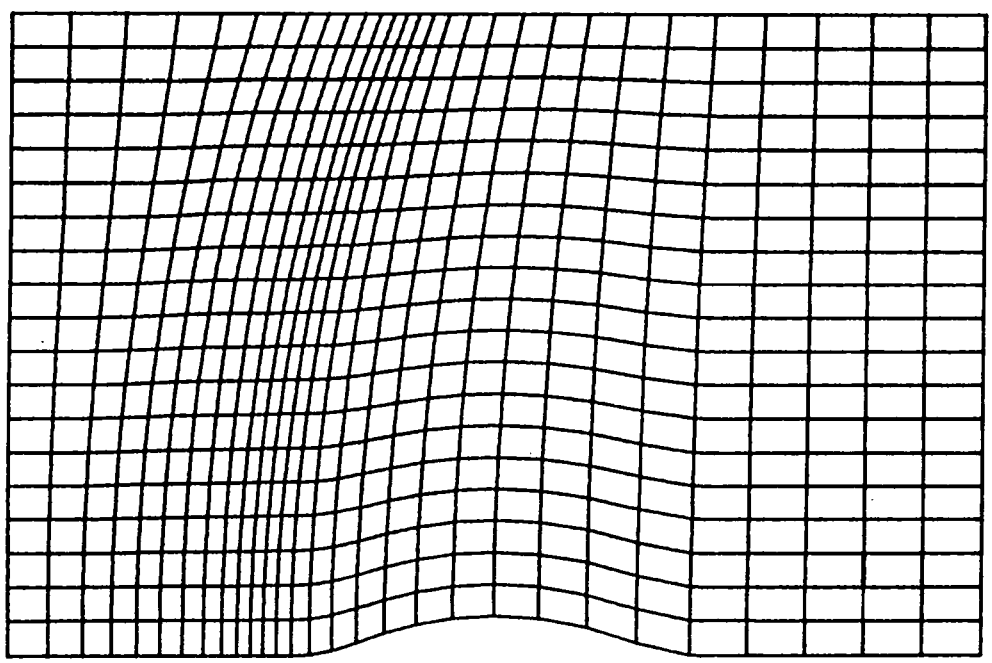

With Curvature

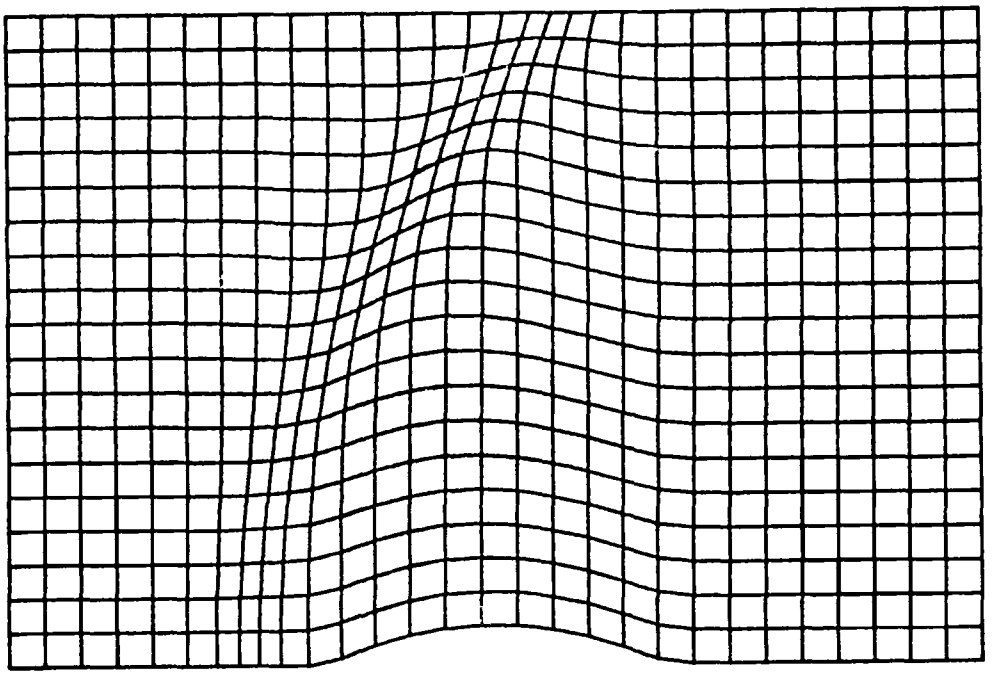

Without Curvature

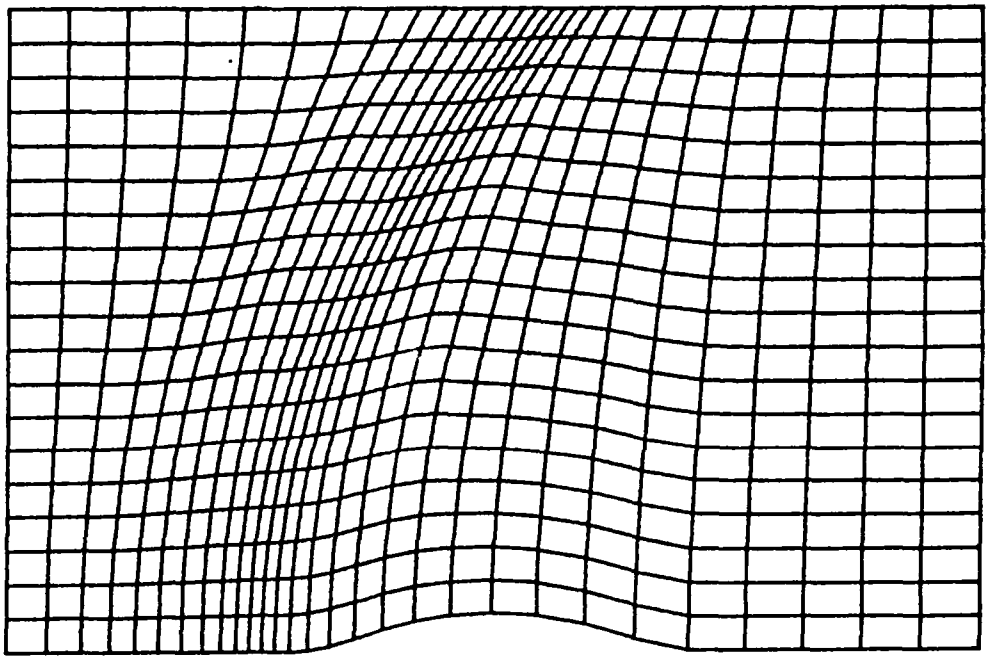

With Curvature

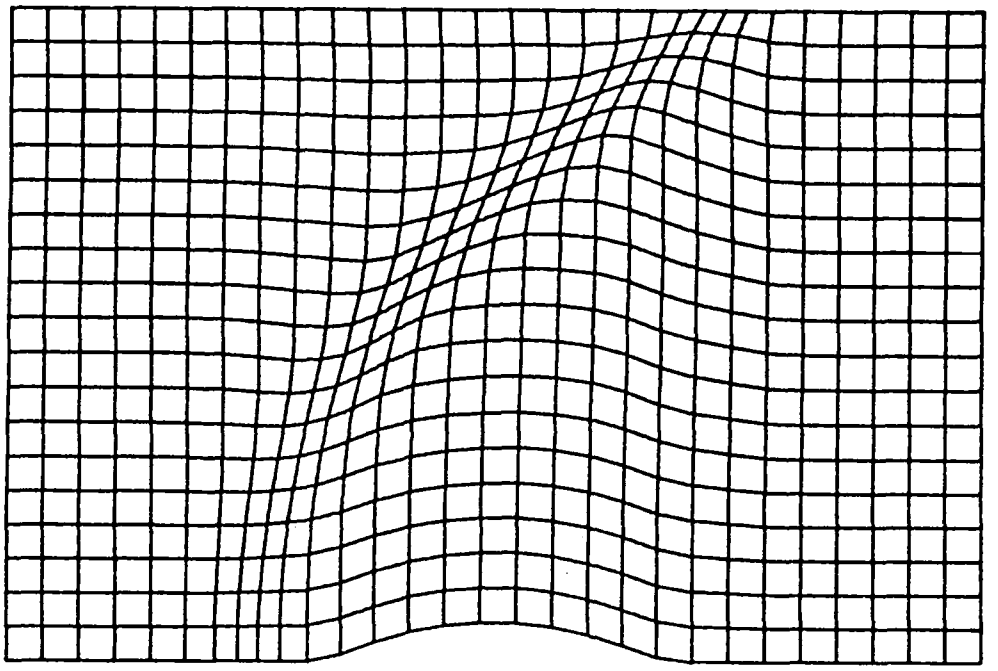

Without Curvature

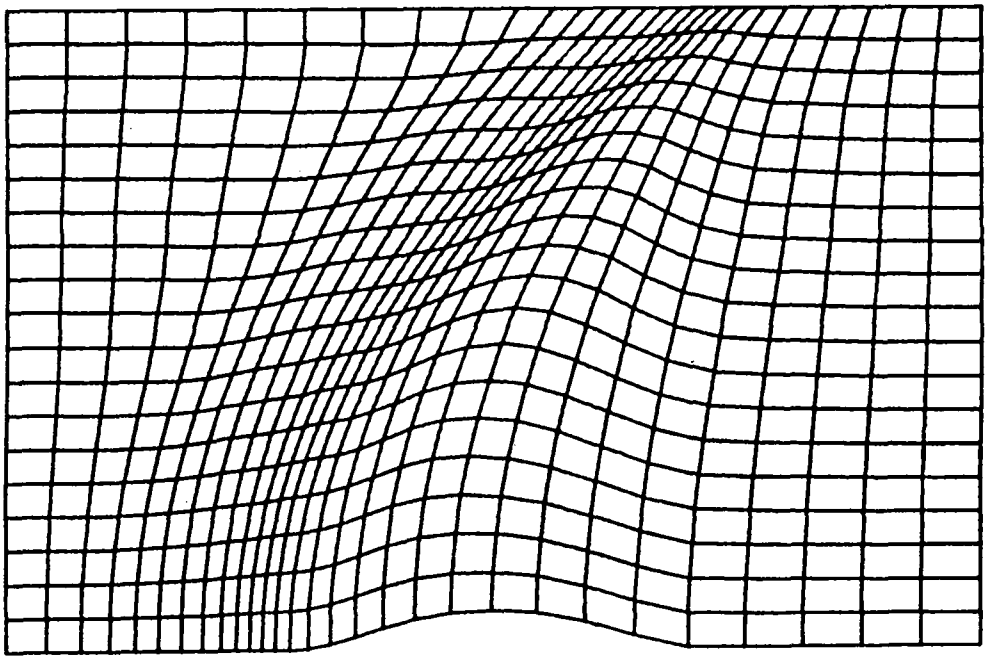

With Curvature

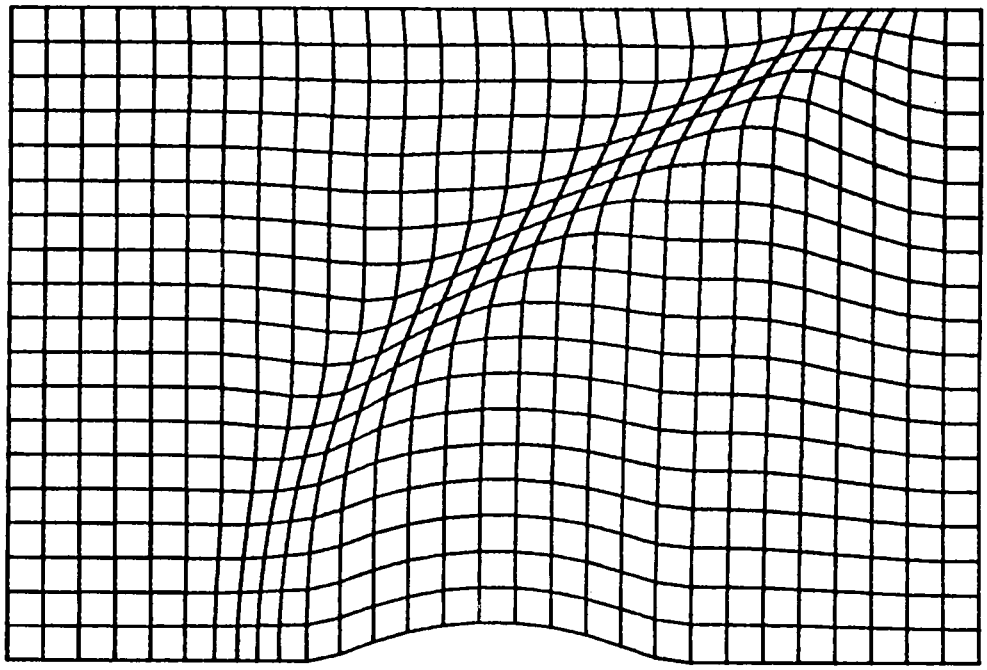

Without Curvature

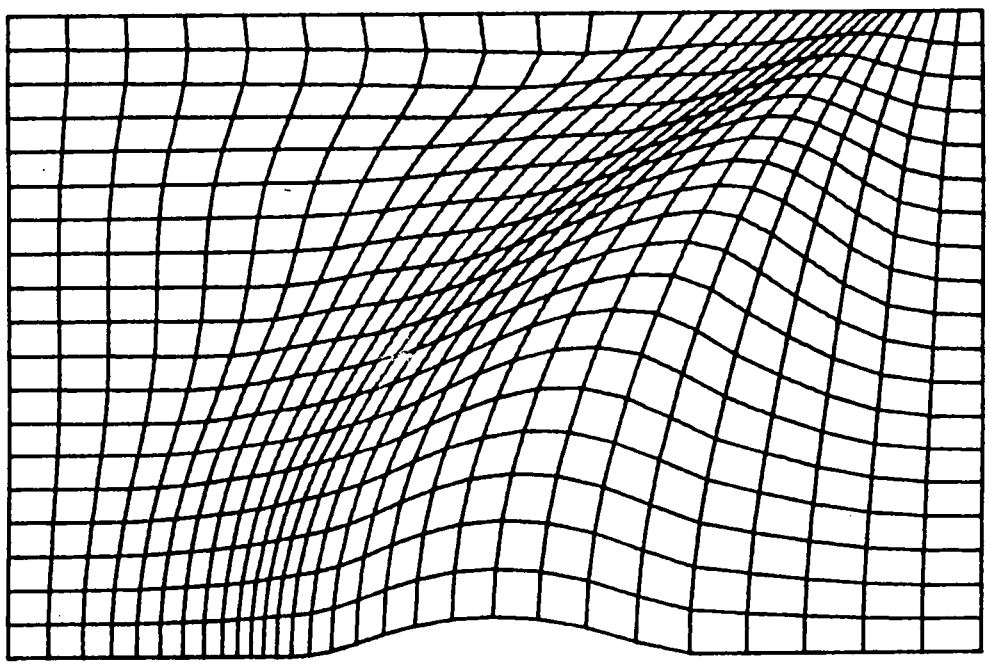

With Curvature

MOVEMENT FOR A TRIANGULAR MESH

Physical Space Projection:

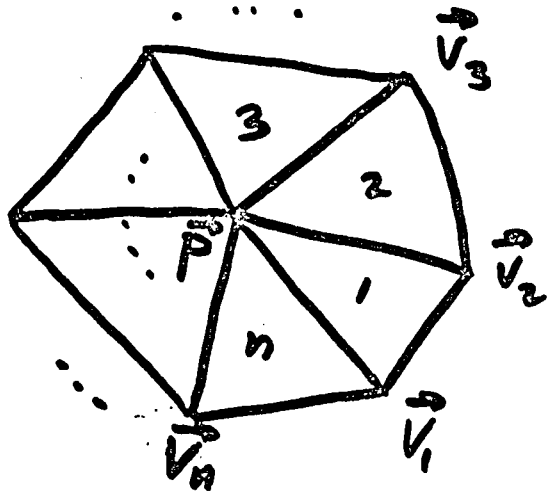

Barycenters:

$$\vec{b}_i = \frac{1}{3}(\vec{P} + \vec{V}_i + \vec{V}_{i+1})$$

Weights:

$$w_i = (1 + \sum_{j=1}^{m} c_j M_j) A_i$$

where

A_i = Area of surface triangle i

New Position:

$$\vec{P}_{new} = \vec{P} + \frac{\sum_{i=1}^{n} (\vec{b}_i - \vec{P}) w_i}{\sum_{i=1}^{n} w_i} = \frac{\sum_{i=1}^{n} \vec{b}_i w_i}{\sum_{i=1}^{n} w_i}$$

PLASMA EQUILIBRIUM

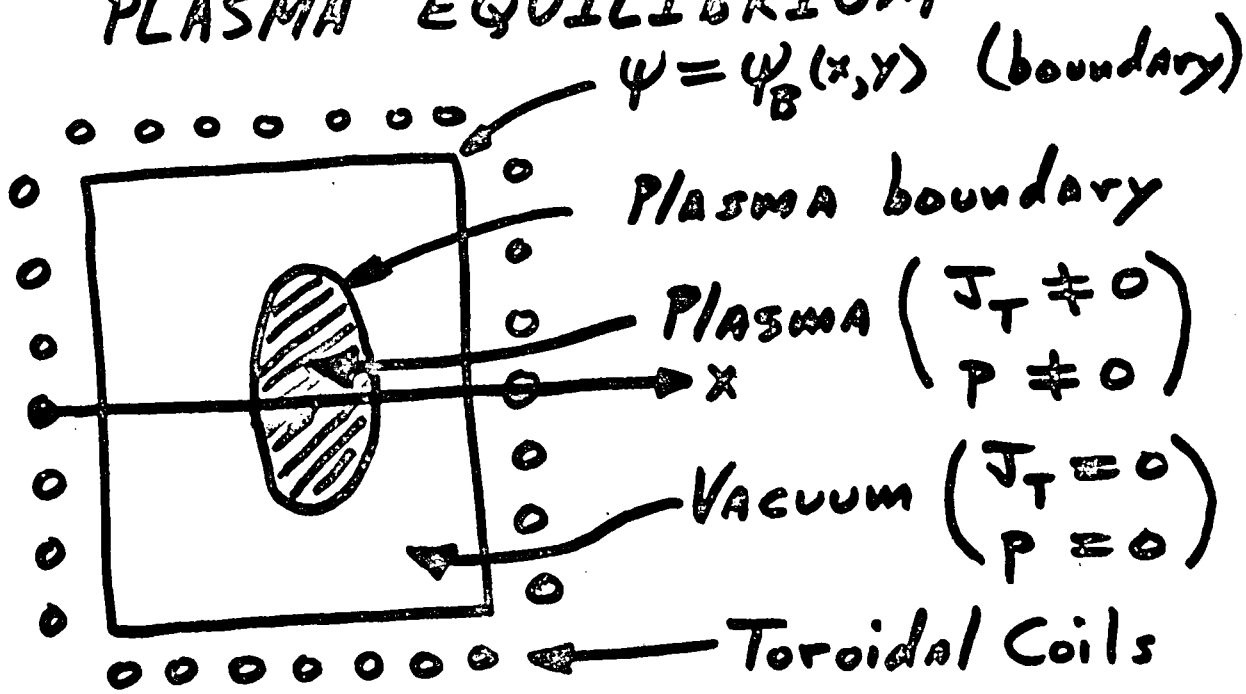

J_T = Toroidal Current Density

p = pressure

$I = x B_T \propto$ Poloidal Current

B_T = Toroidal Magnetic Field

PRESCRIBE

Total Toroidal Current

Plasma Width

PLASMA EQUILIBRIUM

Solve

$$\Delta^* \psi = -x J_T \equiv -x^2 p'(\psi) - \frac{1}{2}\left[I^2(\psi)\right]'$$

where

$$\Delta^* = x \frac{\partial}{\partial x} \frac{1}{x} \frac{\partial}{\partial x} + \frac{\partial^2}{\partial z^2}$$

and

$$p(\psi) = \left[\frac{\psi}{\psi_{MAX}}\right]^{\alpha}$$

$$I^2(\psi) = I_0^2 \left[1 - \gamma \left(\frac{\psi}{\psi_{MAX}}\right)^{\beta}\right]$$

with γ chosen to maintain a prescribed toroidal current $I_{tot.}$

The flux at the boundary is due to both the plasma and the coils. Consequently, it is determined by the solution.

MESH MOVEMENT

Solution Generate Surface

$$u = 1 \cdot \frac{J_T}{(J_T)_{MAX}} + 2 \cdot \frac{|\nabla\psi|^{-2}}{|\nabla\psi|^{-2}_{MAX}}$$

Resolve Δ^* operator

Resolve magnetic axis

Weight

$$w = 1 + c\,k$$

$k \simeq$ Mean Curvature

Smooth u before evaluation of k

(Physical quantities remain unsmoothed)

EXACT EQUILBRIUM
(Fixed Boundary)

- Solove'v

$$\psi = 1 - \left[x^2 z^2 - \frac{1}{4}(x^2 - R^2)^2 \right]$$

$$\Delta^* \psi = -4x^2$$

Thus $p(\psi) = 4\psi$ and $B_T \propto \frac{1}{x}$

ψ(mag. axis) = 1

ψ(Boundary) = 0

$J_T = 4x$

Favorable comparisons were <u>also</u> obtained against a code by

EVANS

the results of which were reported in 197

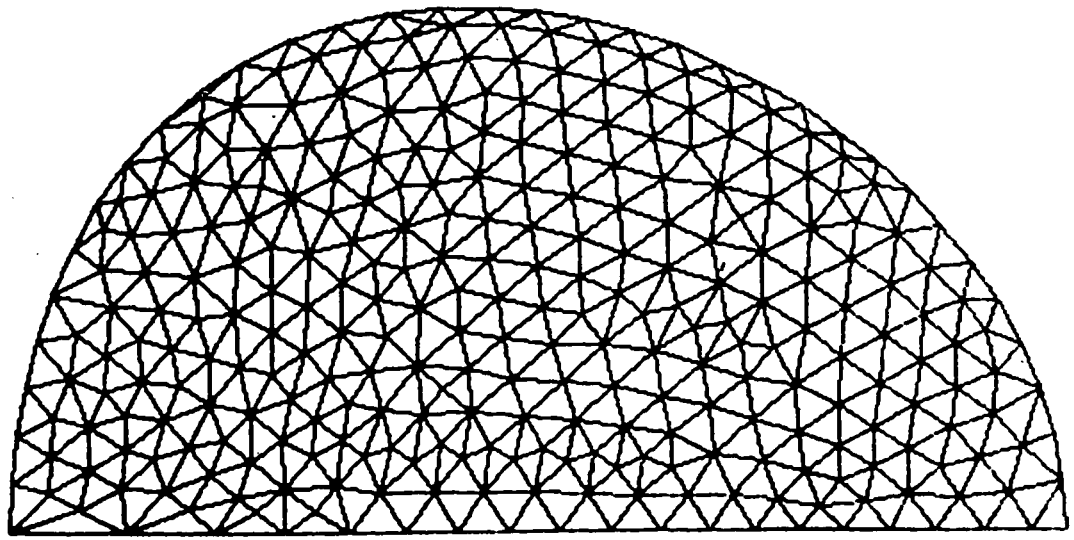

		VERT	308	GRAD	5.000E+01
ITER	0	EDGE	868	LAPL	3.000E+01
		TRIAN	561		

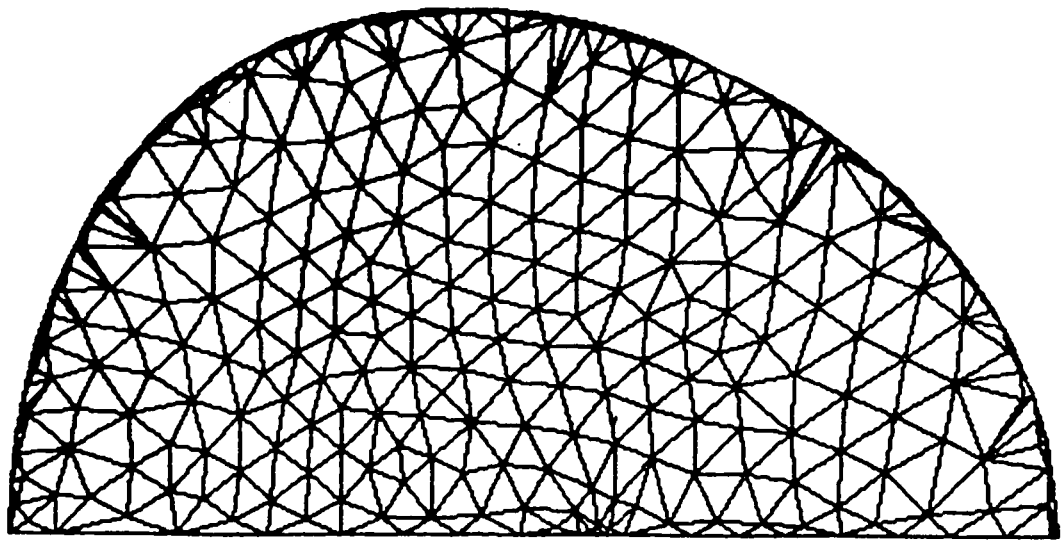

		VERT	30 MIN	GRAD.	5.000E+01
ITER	3 0	EDGE	86 MAX	LAPD.	3.000E+01
		TRIAN	561		

frame # 6.

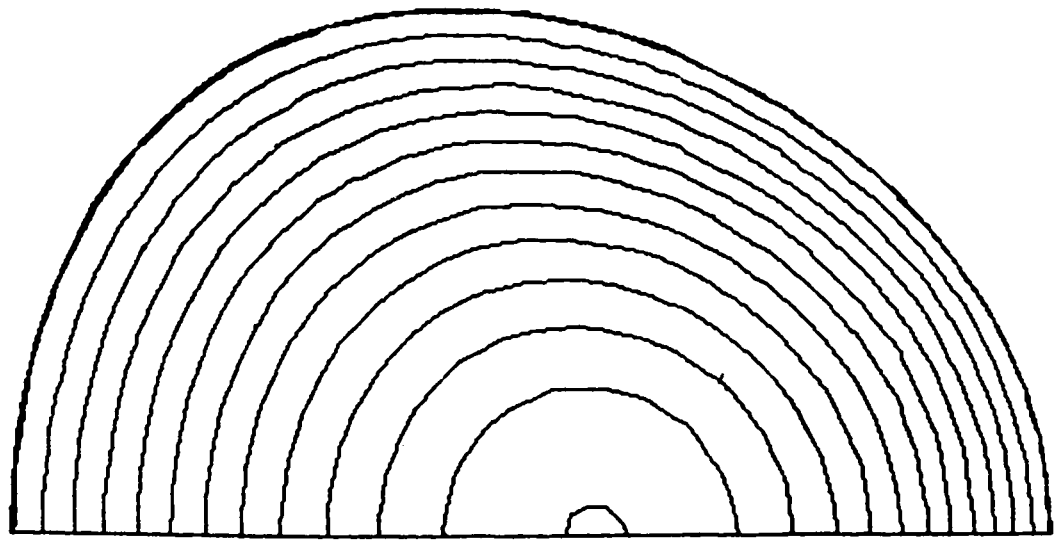
5.010E-03
8.768E-02
1.704E-01
2.530E-01
3.357E-01
4.184E-01
5.010E-01
5.837E-01
6.664E-01
7.491E-01
8.317E-01
9.144E-01
9.971E-01
L2 ERROR
0.
POL FLUX
ITER
3
MIN
0.
MAX
1.002E+00

frame # 7.

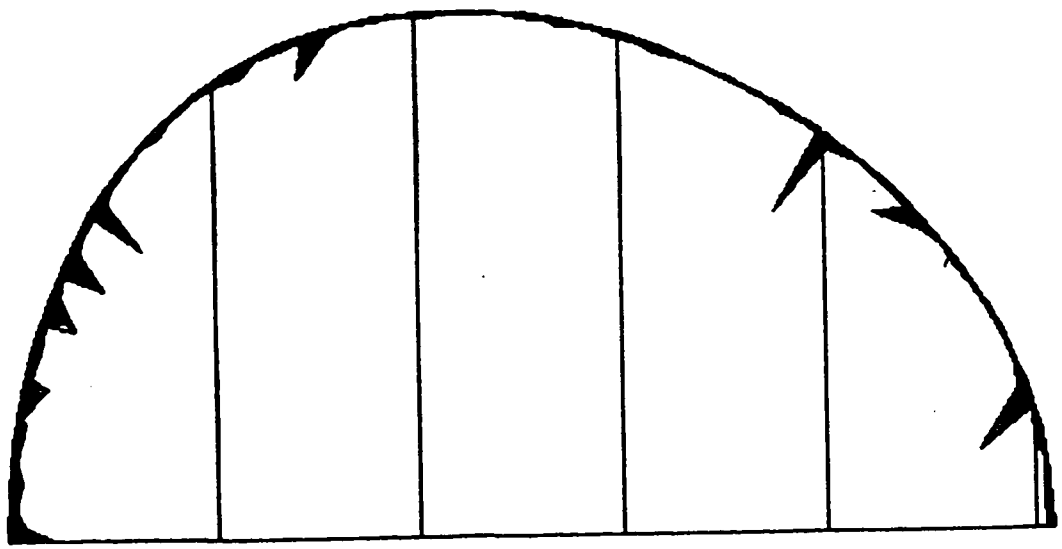
4.884E-02
8.548E-01
1.661E+00
2.467E+00
3.273E+00
4.078E+00
4.884E+00
5.690E+00
6.496E+00
7.302E+00
8.108E+00
8.914E+00
9.720E+00
L2 ERROR
0.
CURRENT
ITER
3
MIN
0.
MAX
9.769E+00

682

rame # 8.

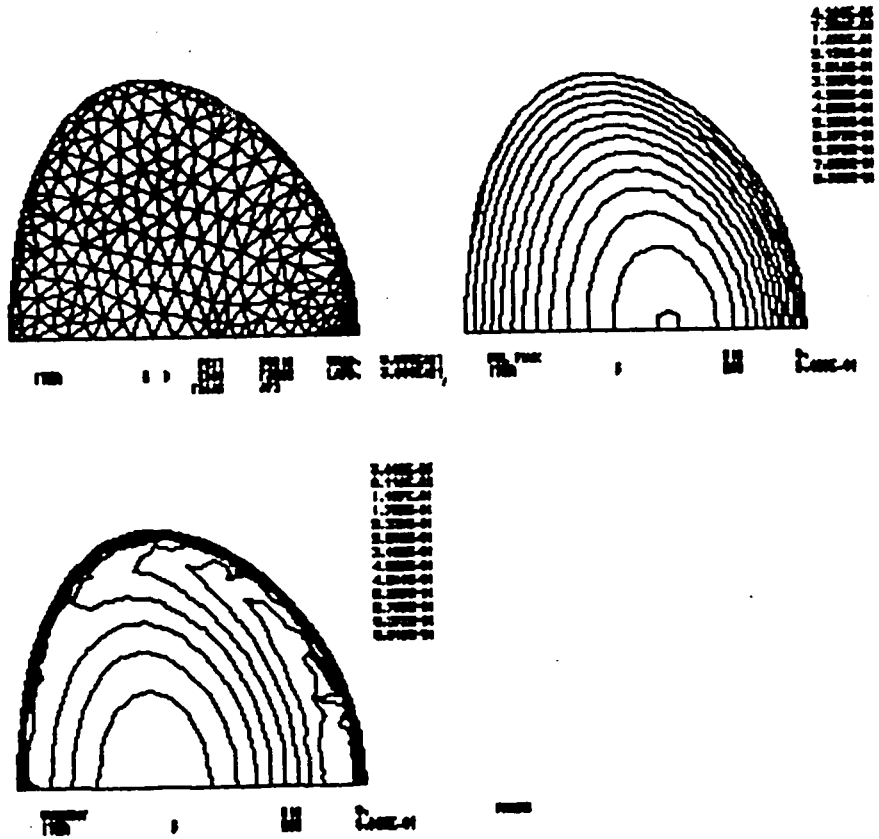

HtH
frame # 9.

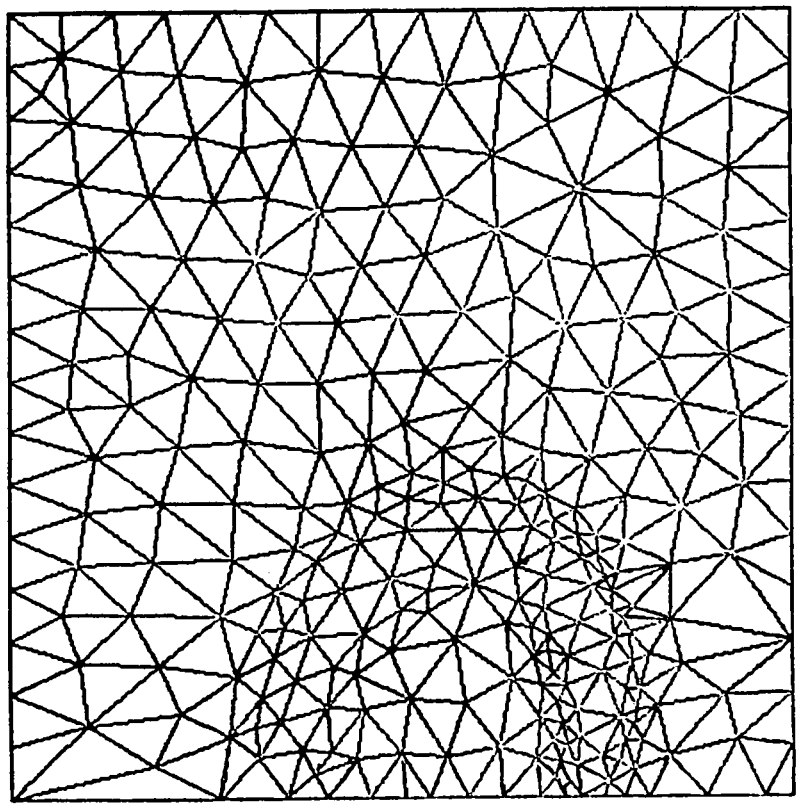

		VERT	288	GRAD	5.000E+01
ITER	1	EDGE	799	LAPL	4.500E+01
		TRIAN	512		

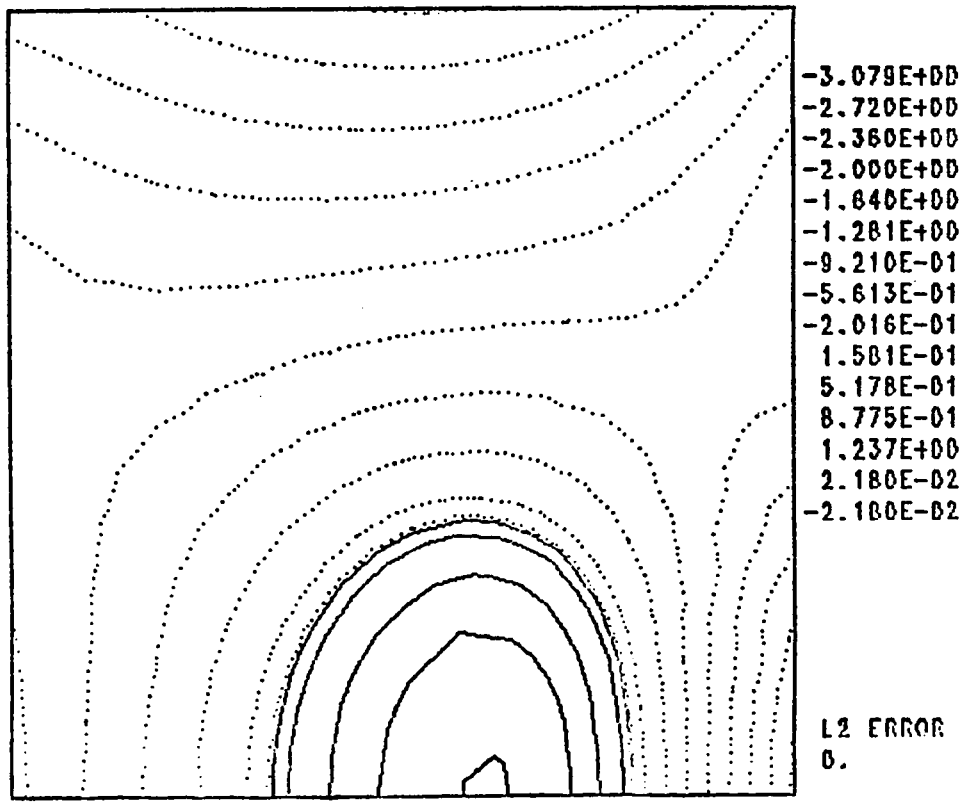
-3.079E+00
-2.720E+00
-2.360E+00
-2.000E+00
-1.640E+00
-1.281E+00
-9.210E-01
-5.613E-01
-2.016E-01
1.581E-01
5.178E-01
8.775E-01
1.237E+00
2.180E-02
-2.180E-02
L2 ERROR
0.
POL FLUX
ITER
1
MIN
-3.101E+00
MAX
1.259E+00

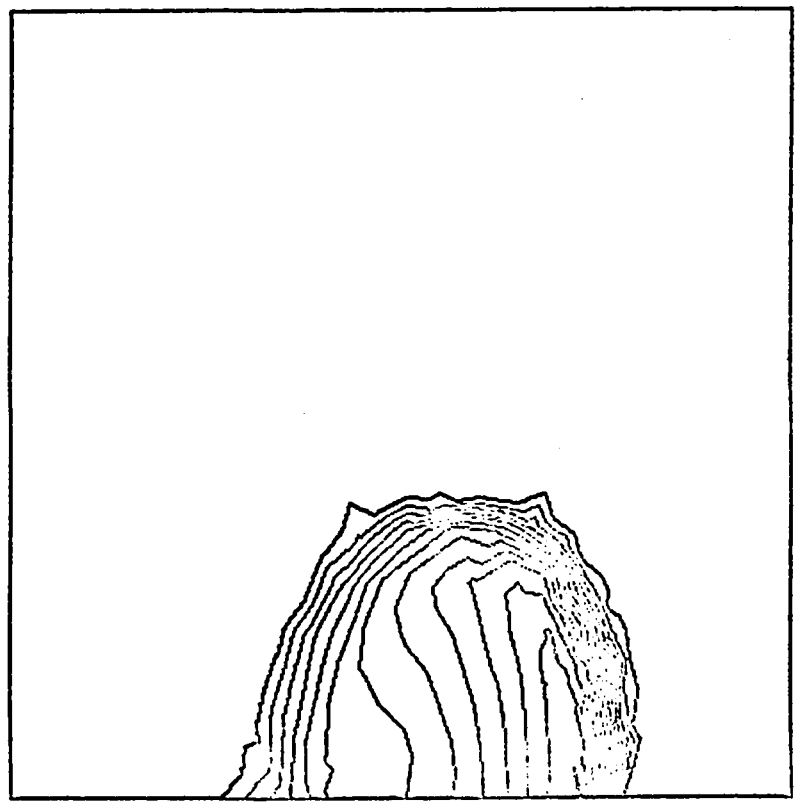
3.497E-03
6.120E-02
1.189E-01
1.766E-01
2.343E-01
2.920E-01
3.497E-01
4.074E-01
4.651E-01
5.228E-01
5.805E-01
6.382E-01
6.959E-01
L2 ERROR
0.
CURRENT DENSITY
ITER 1
MIN 0.
MAX 6.

PROPERTIES OF THE METHODS

- Direct Application of Control
- Analytic Nonsingularity
- Simple Algorithms
- Independent of Solution Techniques
- Minimal User Specified Data Required
- Works in Any Spatial Dimension
- Works on Arbitrary Surfaces

(26)

Application of Variational Methods for Generating Adaptive Grids

689

Richard I. Kreis

North Carolina State University

KREIS

OUTLINE

I. ADAPTIVE GRIDS – WHY ARE THEY USED?

II. CHOICE OF METHOD TO ADAPT GRID

III. DESCRIPTION OF METHOD
- DEVELOPMENT
- APPLICATION

IV. TEST PROBLEM

V. FUTURE EFFORTS

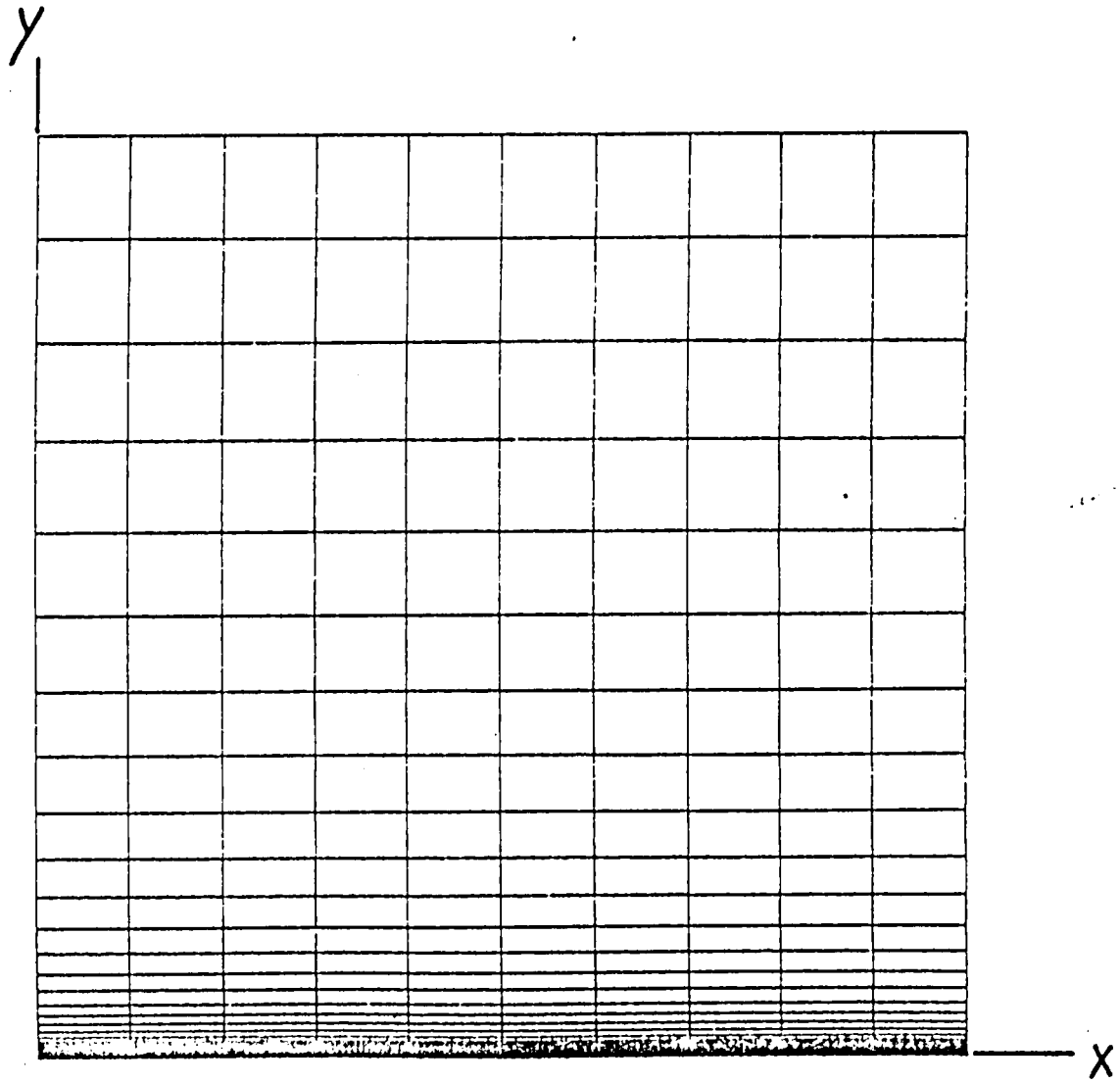
Y
X

SMOOTHNESS

$$I_S = \int_D [(\nabla\xi)^2 + (\nabla\eta)^2]\, dV = \iint d\xi\, d\eta\, \frac{x_\eta^2 + x_\xi^2 + y_\xi^2 + y_\eta^2}{J}$$

WEIGHTED VOLUME VARIATION

$$I_v = \int_D w J\, dV = \iint d\xi d\eta\, w J^2$$

$w = w(x, y)$

ORTHOGONALITY

$$I_o = \int_D (\nabla\xi \cdot \nabla\eta)^2 J^3\, dV = \iint d\xi d\eta\, (x_\xi x_\eta + y_\xi y_\eta)^2$$

TO MINIMIZE $I = \iint f \, d\xi d\eta$, SET $\delta I = 0$

THE CORRESPONDING EULER EQUATIONS ARE:

$$\begin{cases} \left(\frac{\partial}{\partial x} - \frac{\partial}{\partial \xi}\frac{\partial}{\partial x_\xi} - \frac{\partial}{\partial \eta}\frac{\partial}{\partial x_\eta}\right) f = 0 \\ \left(\frac{\partial}{\partial y} - \frac{\partial}{\partial \xi}\frac{\partial}{\partial y_\xi} - \frac{\partial}{\partial \eta}\frac{\partial}{\partial y_\eta}\right) f = 0 \end{cases}$$

693

$$\begin{cases} b_1 x_{\xi\xi} + b_2 x_{\xi\eta} + b_3 x_{\eta\eta} + a_1 y_{\xi\xi} + a_2 y_{\xi\eta} + a_3 y_{\eta\eta} = g_1 \\ a_1 x_{\xi\xi} + a_2 x_{\xi\eta} + a_3 x_{\eta\eta} + c_1 y_{\xi\xi} + c_2 y_{\xi\eta} + c_3 y_{\eta\eta} = g_2 \end{cases}$$

$$I = I_s + \lambda_v I_v + \lambda_o I_o$$

$$\begin{cases} b_1 x_{\mu\mu} + b_2 x_{\mu\eta} + b_3 x_{\eta\eta} + a_1 y_{\mu\mu} + a_2 y_{\mu\eta} + a_3 y_{\eta\eta} = \dfrac{-J^2}{2w} \dfrac{\partial w}{\partial x} \lambda_v \\ a_1 x_{\mu\mu} + a_2 x_{\mu\eta} + a_3 x_{\eta\eta} + c_1 y_{\mu\mu} + c_2 y_{\mu\eta} + c_3 y_{\eta\eta} = \dfrac{-J^2}{2w} \dfrac{\partial w}{\partial y} \lambda_v \end{cases}$$

WHERE:

$$a_i = a_{si} + \lambda_v a_{vi} + \lambda_o a_{oi}$$
$$b_i = b_{si} + \lambda_v b_{vi} + \lambda_o b_{oi}$$
$$c_i = c_{si} + \lambda_v c_{vi} + \lambda_o c_{oi}$$

$$A \Delta S = R$$

$$\Delta S = S^{n+1} - S^n \qquad S = \begin{bmatrix} x \\ y \end{bmatrix}$$

$$J = x_\xi y_\eta - x_\eta y_\xi \simeq \frac{\Delta x}{\Delta \xi}\frac{\Delta y}{\Delta \eta}$$

$$\therefore J \to \mathcal{O}\left(\frac{\Delta x}{\Delta \xi}\right)^2$$

$$\text{"s"} \Rightarrow \frac{1}{J}\left(x_\xi^2 + x_\eta^2 + y_\xi^2 + y_\eta^2\right) \simeq \frac{1}{J}\left(\frac{\Delta x}{\Delta \xi}\right)^2 \to \mathcal{O}(1)$$

$$\text{"v"} \Rightarrow wJ^2 \to \mathcal{O}\left(\frac{\Delta x}{\Delta \xi}\right)^4 \; ; \; w \to \mathcal{O}(1)$$

$$\text{"o"} \Rightarrow \left(x_\xi x_\eta + y_\xi y_\eta\right)^2 \to \mathcal{O}\left(\frac{\Delta x}{\Delta \xi}\right)^4$$

CHOOSE:

$$\lambda_v = \frac{\lambda_v^\circ}{(\Delta x/\Delta y)^4}$$

$$\lambda_o = \frac{\lambda_o^\circ}{(\Delta x/\Delta y)^4}$$

WHERE

$$\lambda_v^\circ \Rightarrow \mathcal{O}(1)$$

$$\lambda_o^\circ \Rightarrow \mathcal{O}(1)$$

- CHOICE OF FORCING FUNCTION, w :

$$w = f(u) \quad \text{OR} \quad w = f(\nabla u)$$

- TRY:

$$w = (\nabla u)^p$$

$$w = (u_x^2 + u_y^2)^{p/2}$$

$$p > 0$$

- OTHER CHOICES FOR w MAY ALSO BE ACCEPTABLE

TEST PROBLEM

- LINEAR, 2-D BURGER'S EQ.

$$u_t + a_1 u_x + a_2 u_y = \epsilon (u_{xx} + u_{yy})$$

- TRANSFORM FROM (x, y, t) TO (ξ, η, t)

$$u_t + \bar{a}_1 u_\xi + \bar{a}_2 u_\eta = \bar{\epsilon} (g_{22} u_{\xi\xi} - 2 g_{12} u_{\xi\eta} + g_{11} u_{\eta\eta})$$

$\bar{a}_1, \bar{a}_2, \bar{\epsilon}, g_{11}, g_{12}, g_{22}$ } FUNCTIONS OF a_1, a_2, ϵ & METRICS

TEST PROBLEM B.C.'S

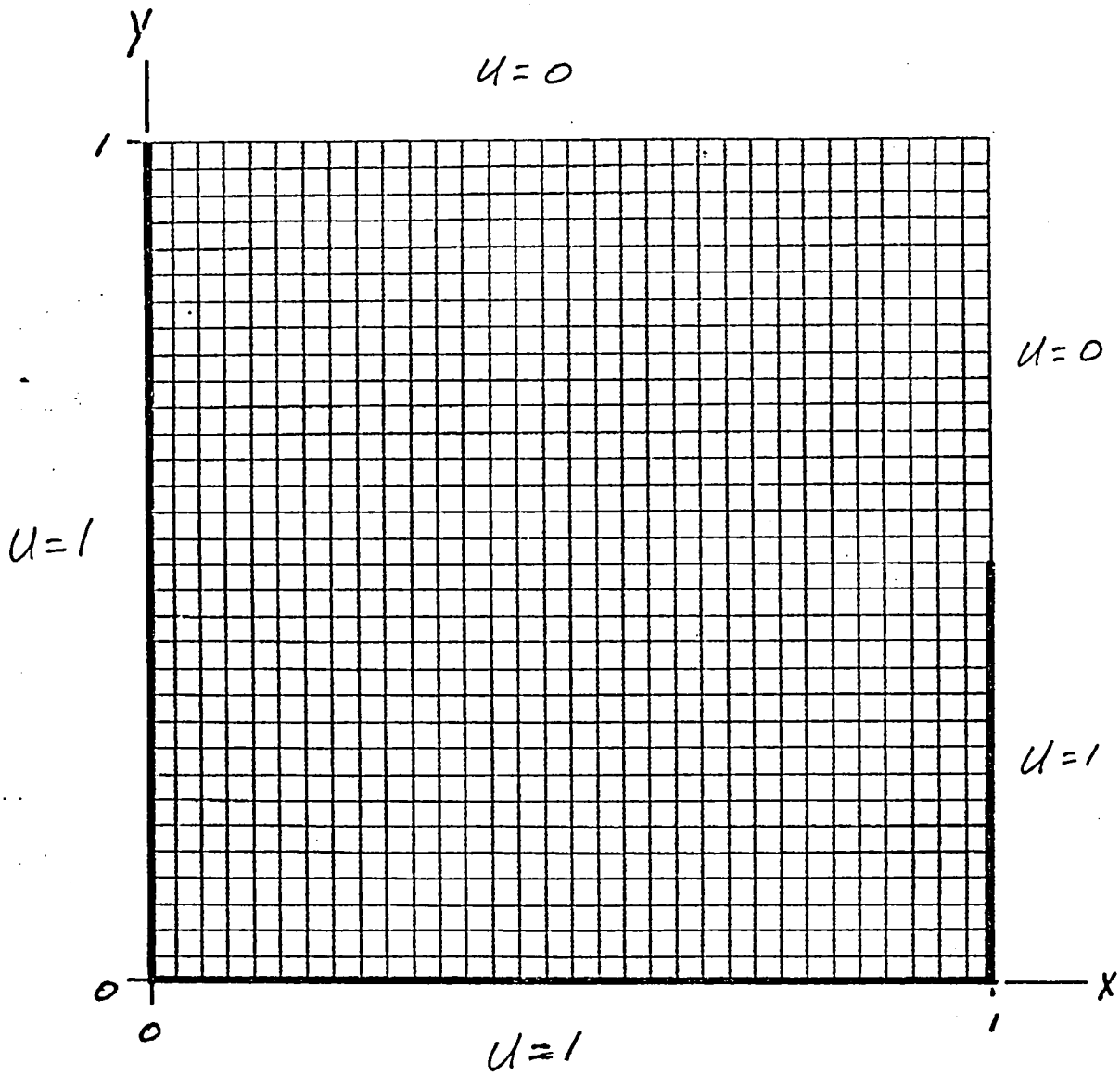

Solution to Burgers Eq.

$$u_t + a_1 u_x + a_2 u_y = \epsilon (u_{xx} + u_{yy})$$

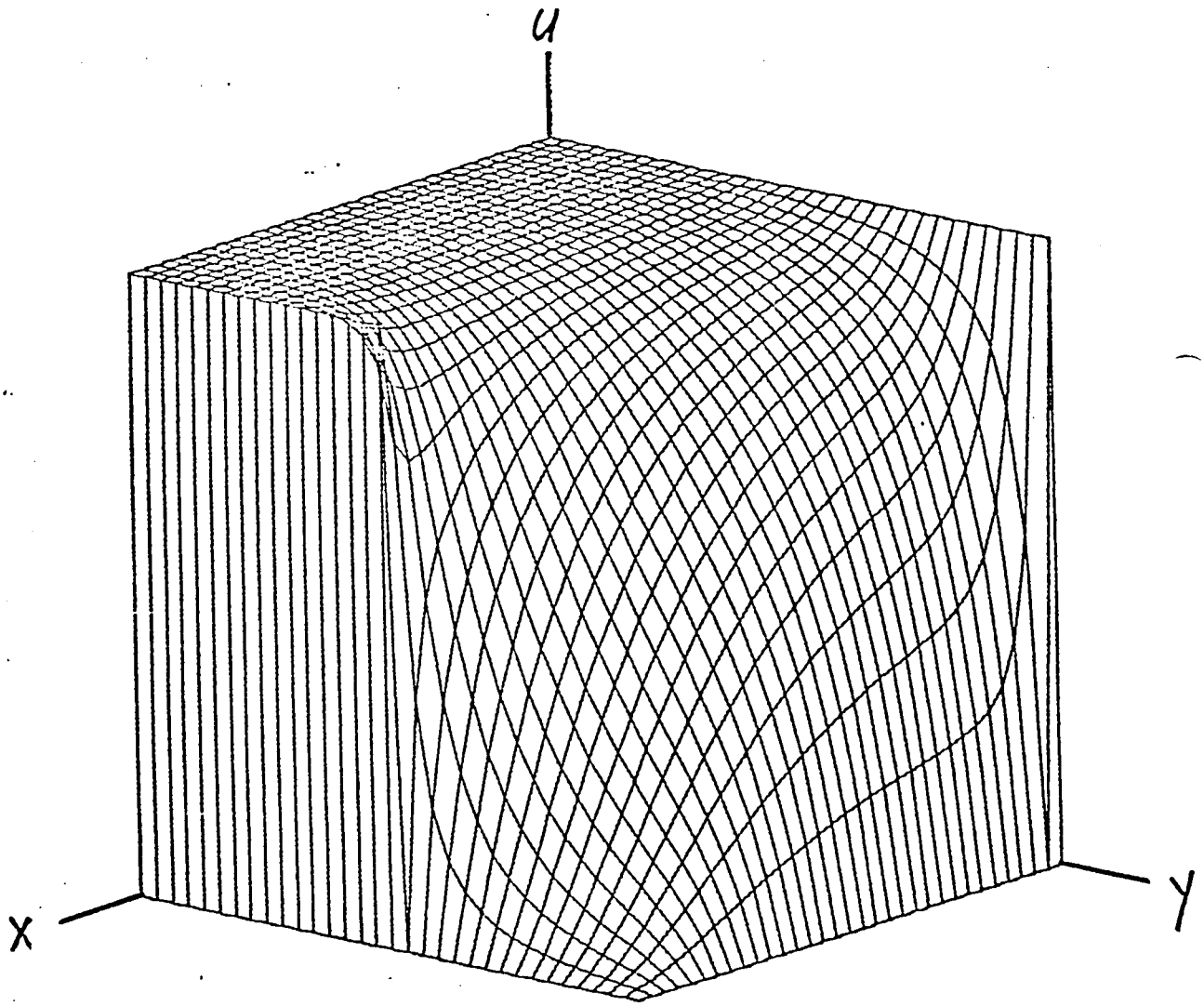

$$W = (\nabla u)^{\frac{1}{2}}$$

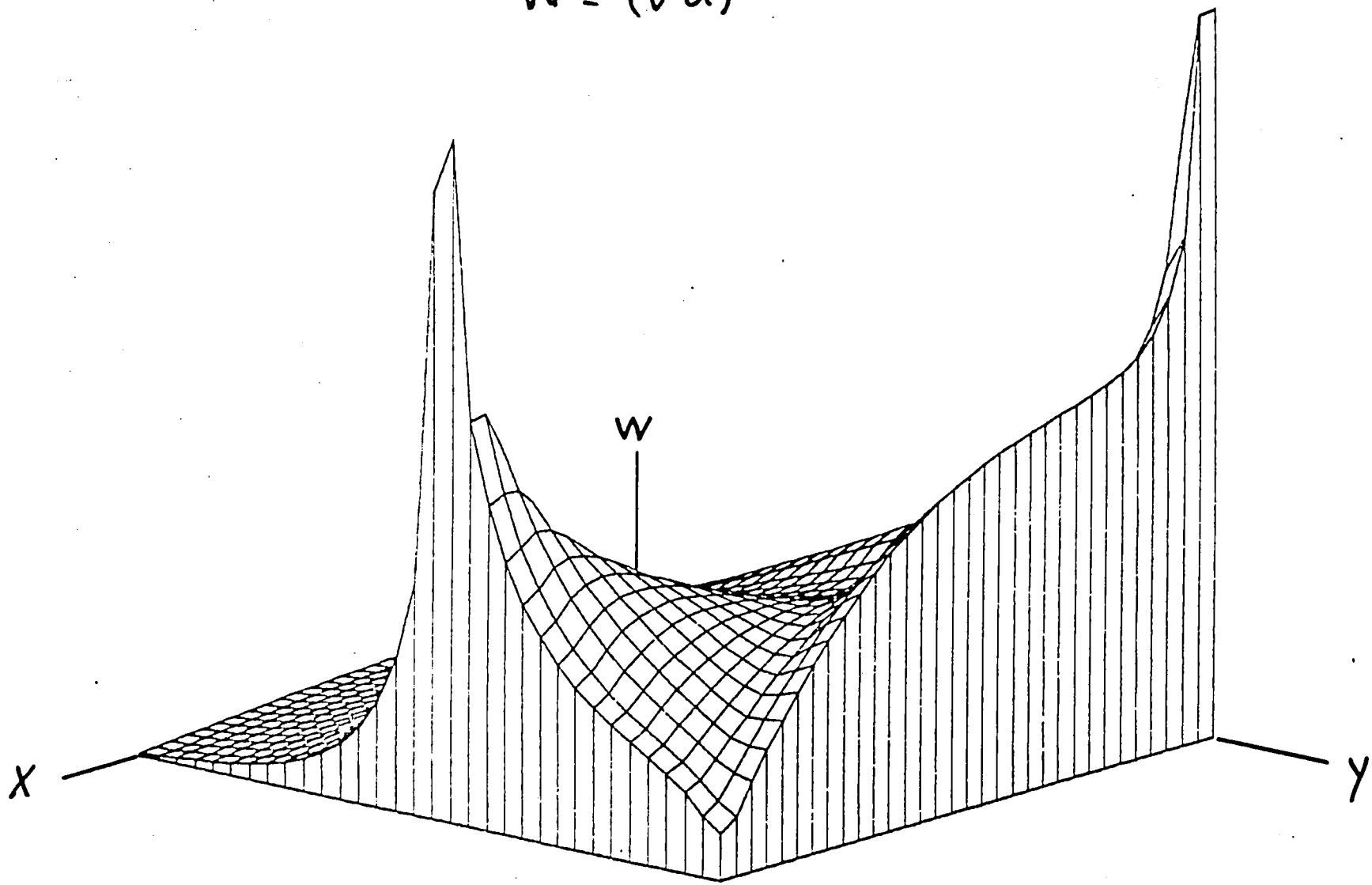

$W = DU$

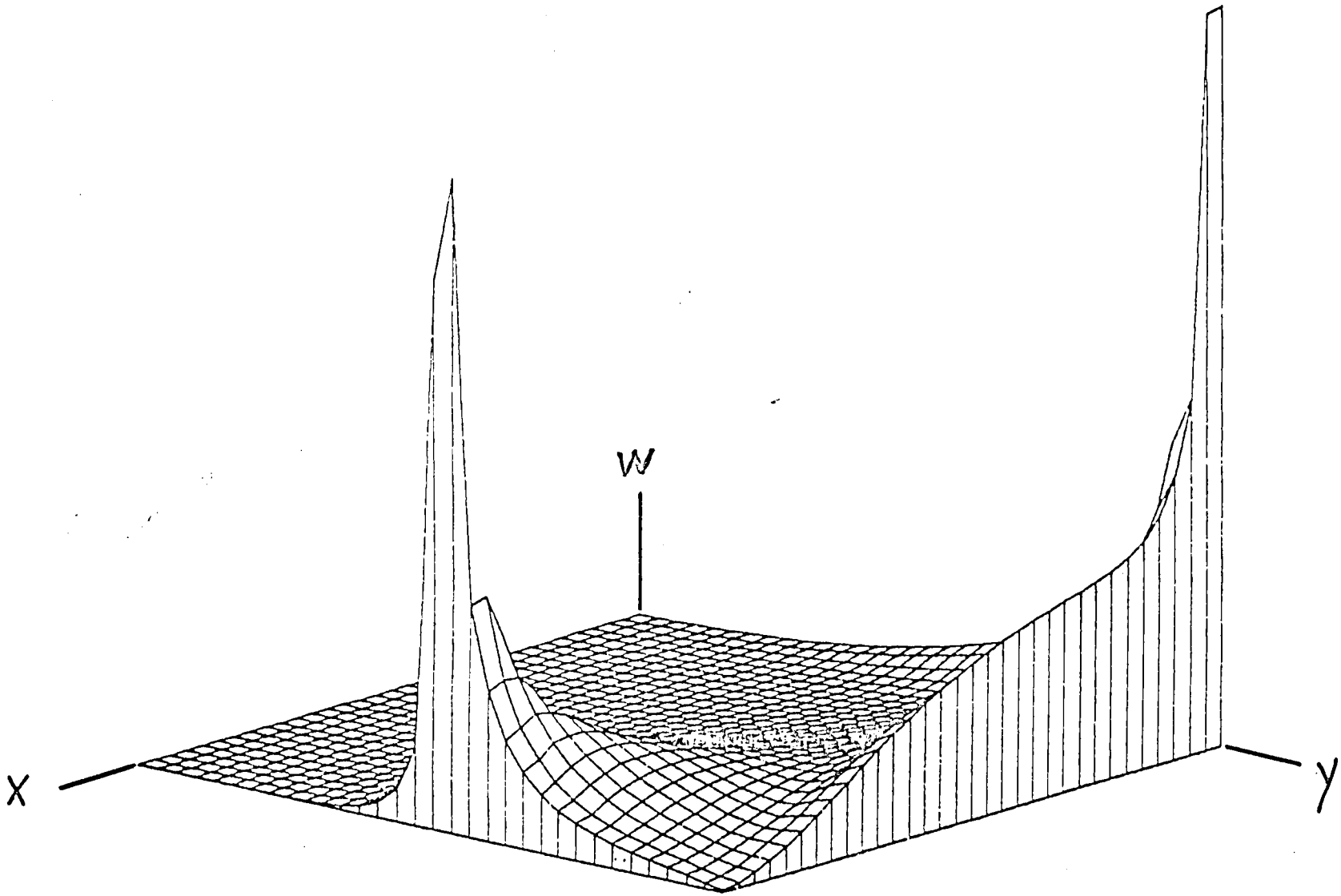

ADAPTED GRID

32×32

$w = (\phi\psi)^{1/2}$

$\lambda_v = 20$

$\lambda_0 = 0$

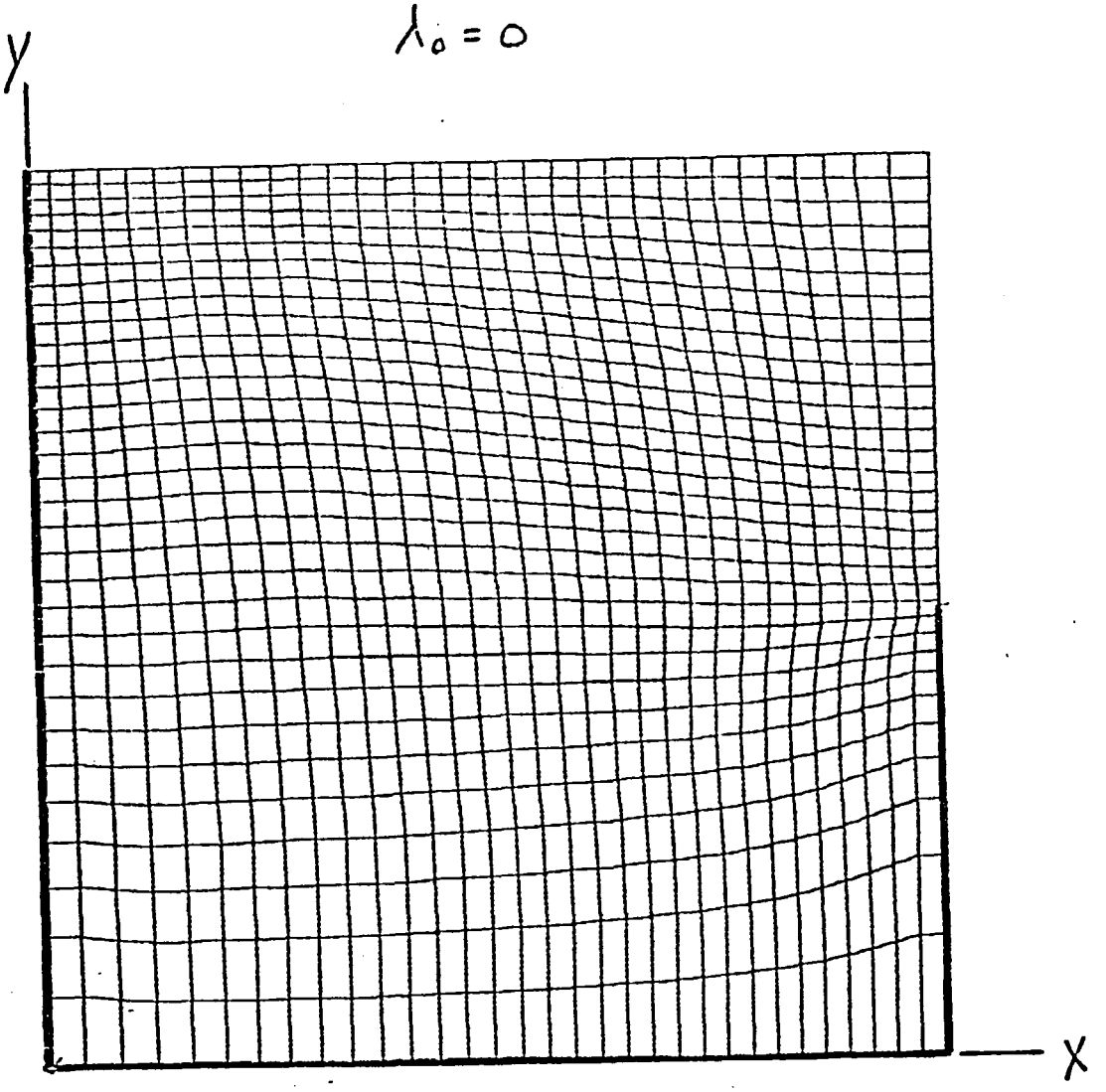

SOLUTION TO BURGERS EQ.
ON AN
ADAPTED GRID

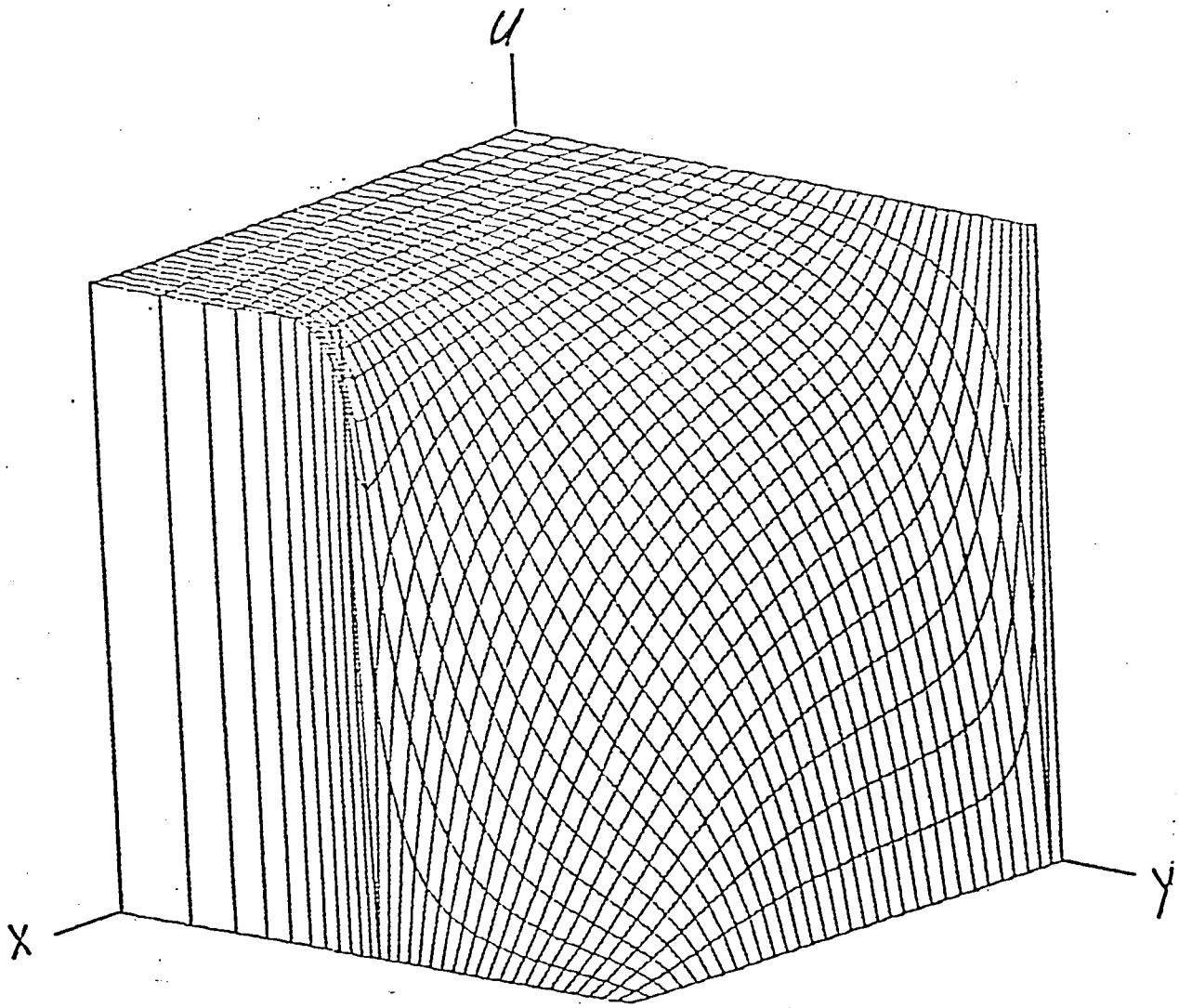

$$W = |UU|^{1/2}$$

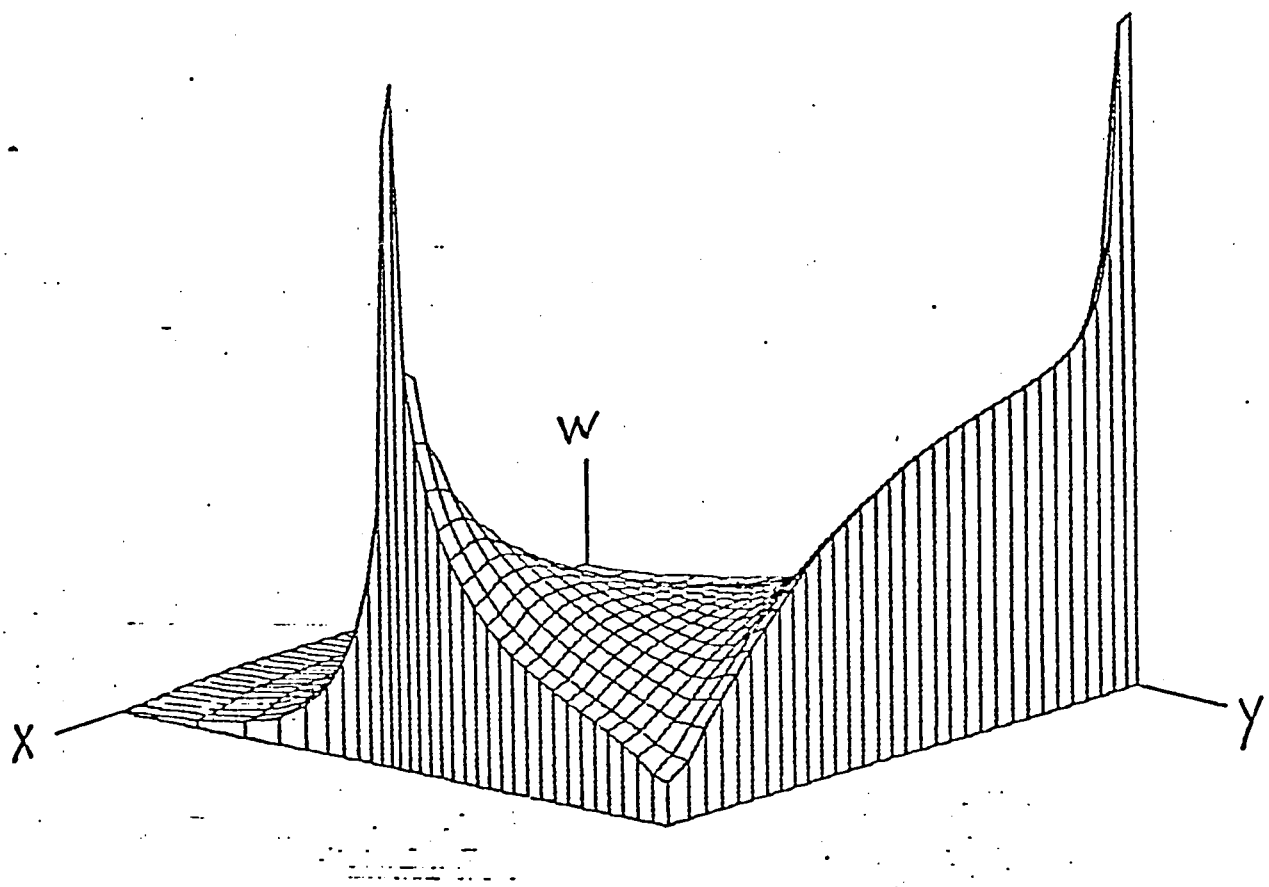

JACOBIAN VARIATION

$$J = x_\xi y_\eta - x_\eta y_\xi$$

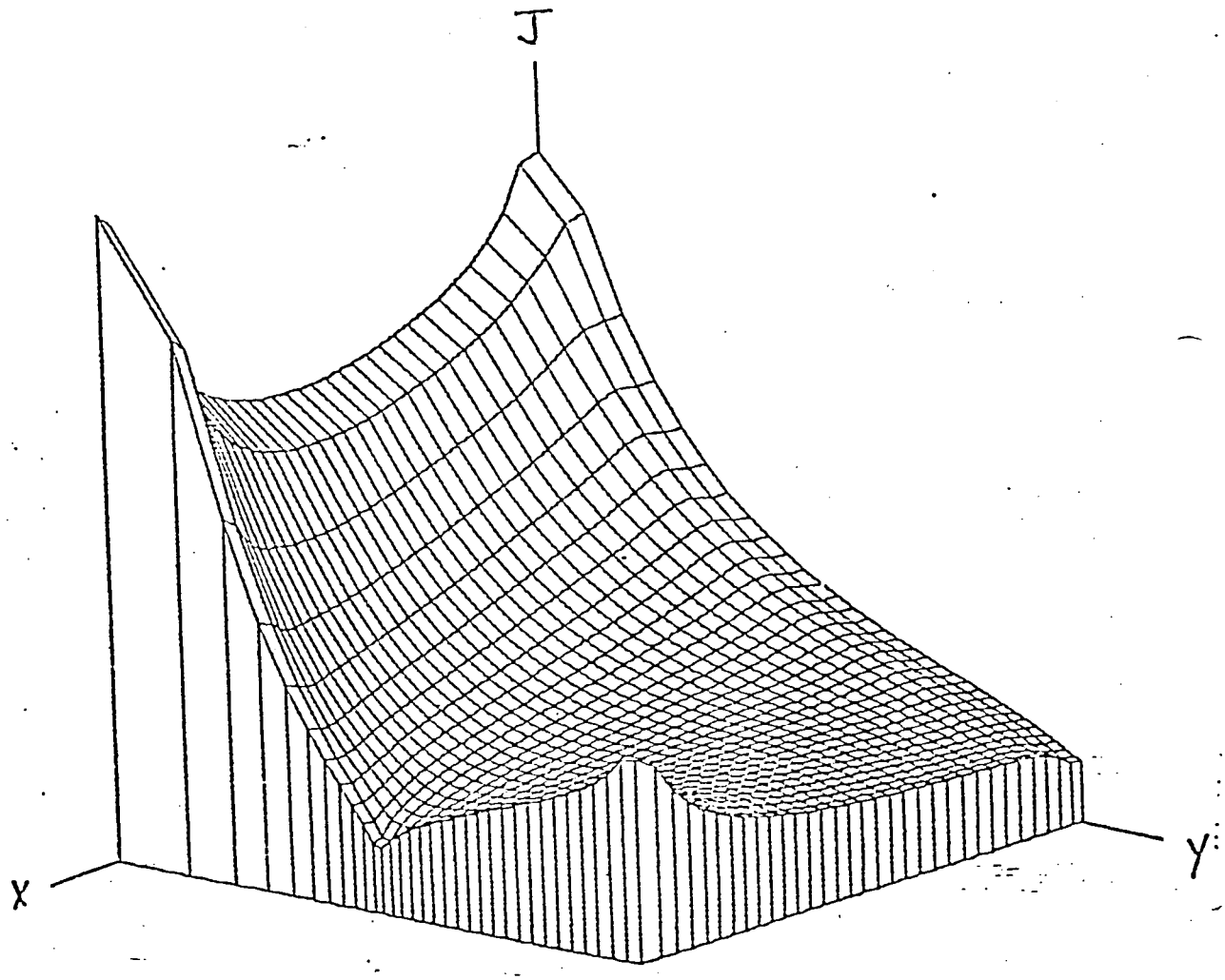

32×32

$\omega = (0.4)^{1/2}$

$\lambda_J = 20$

$\lambda_0 = 0$

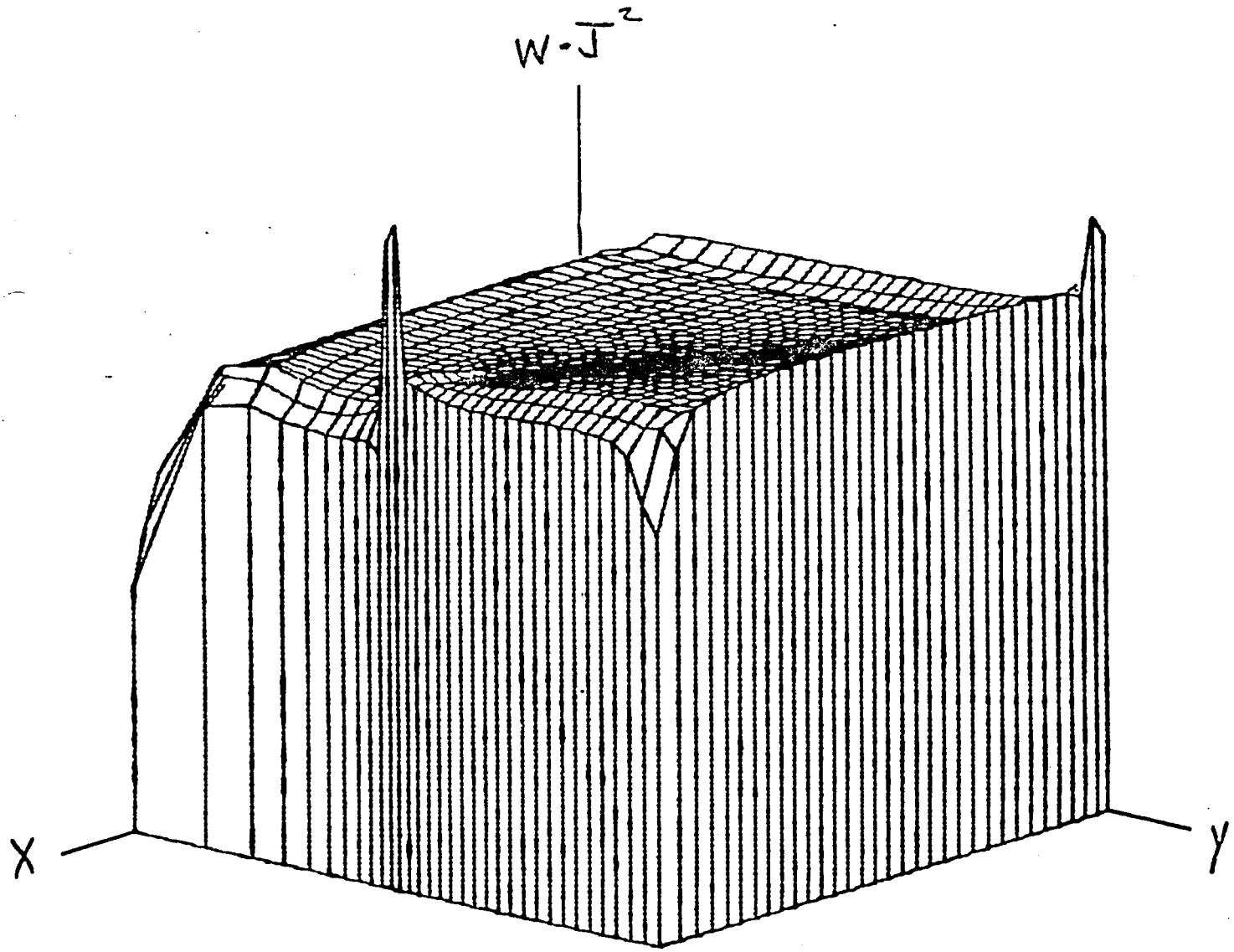

20×20

$\omega = (\nabla u)^{1/2}$

$\lambda_v = 10$

$\lambda_0 = 0$

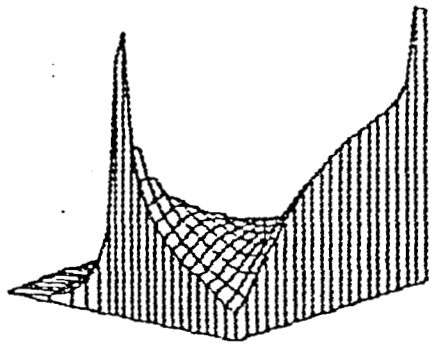

w(x,y)
Max = 1.000

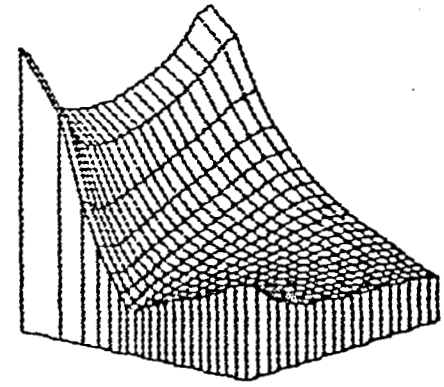

J(x,y)
Max = .8014e-02

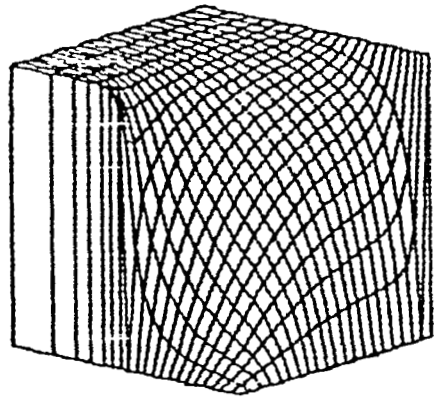

U(x,y)
Max = 1.000

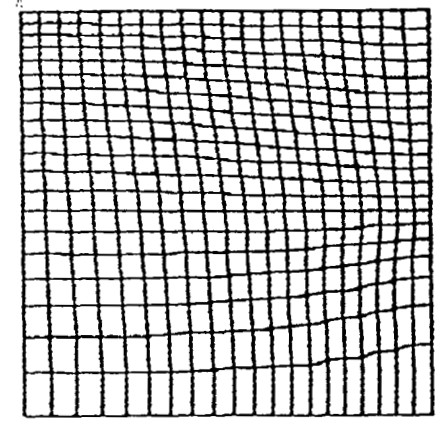

Grid: Normal View
Max = 0.

TEST4 /A,LAMVI=10,LAMO=0,POWW=0.5,NS=0
Date & Time Generated: 83/10/04., 14.03.27.
Date & Time Plotted: 83/10/04., 19.49.14.
IMAX= 21 JMAX= 21 IL= 1 IU= 21 JL= 1 JU= 21

20X20

$\omega = 0.4$

$\lambda_v = 1$

$\lambda_0 = 0$

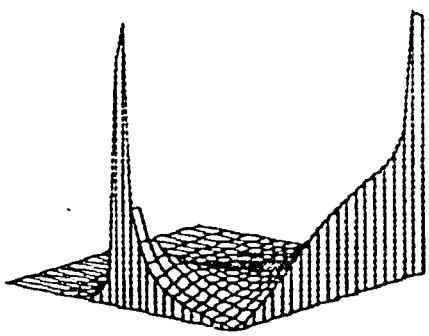

w(x,y)
Max = 1.000

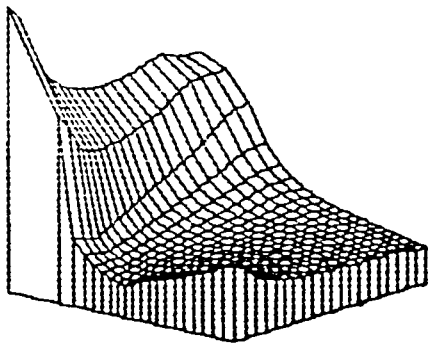

J(x,y)
Max = .1151e-01

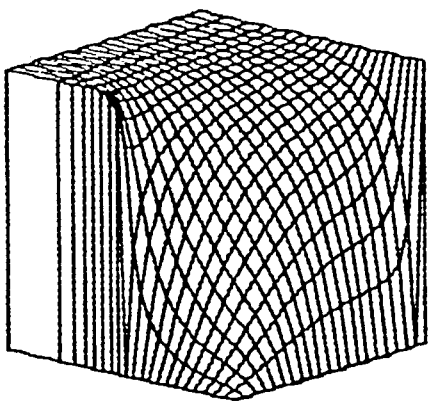

U(x,y)
Max = 1.000

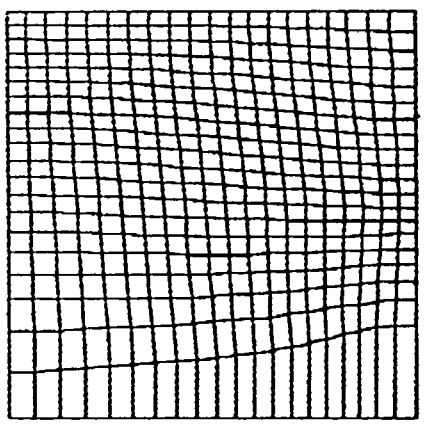

Grid: Normal View
Max = 0.

TEST18/A,LAMV1=1,LAMO=0,POWW=1.0,NS=0
Date & Time Generated: 83/10/14., 08.31.38.
Date & Time Plotted: 83/10/14., 14.39.11.
IMAX= 21 JMAX= 21 IL= 1 IU= 21 JL= 1 JU= 21

20 x 20

$\omega = 1.0$

$\lambda_v = 1$

$\lambda_o = 5$

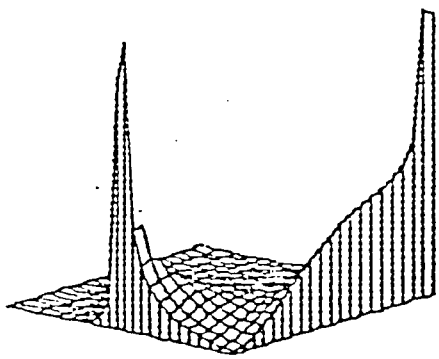

w(x,y)
Max = 1.000

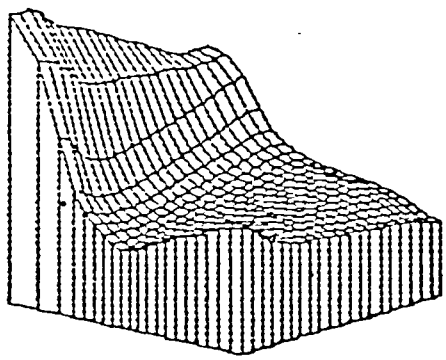

V(x,y)
Max = .6511e-02

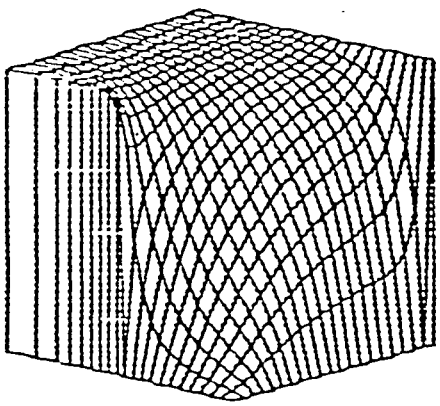

U(x,y)
Max = 1.000

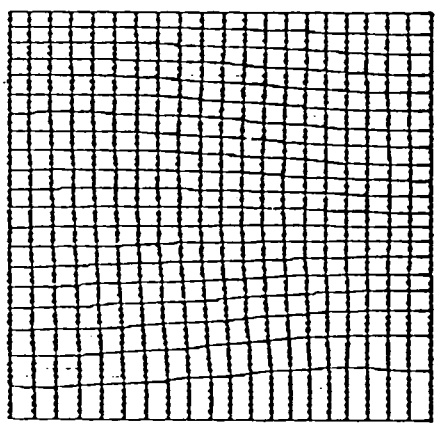

Grid: Normal View
Max = 0.

TEST18/C,LAMV=1,LAMO=5,POWW=1.0,NS=0
Date & Time Generated: 83/10/14., 08.36.47.
Date & Time Plotted: 83/10/14., 17.15.56.
IMAX= 21 JMAX= 21 IL= 1 IU= 21 JL= 1 JU= 21

20×20

$w = |ou|$

$\lambda_v = 5$

$\lambda_o = 0$

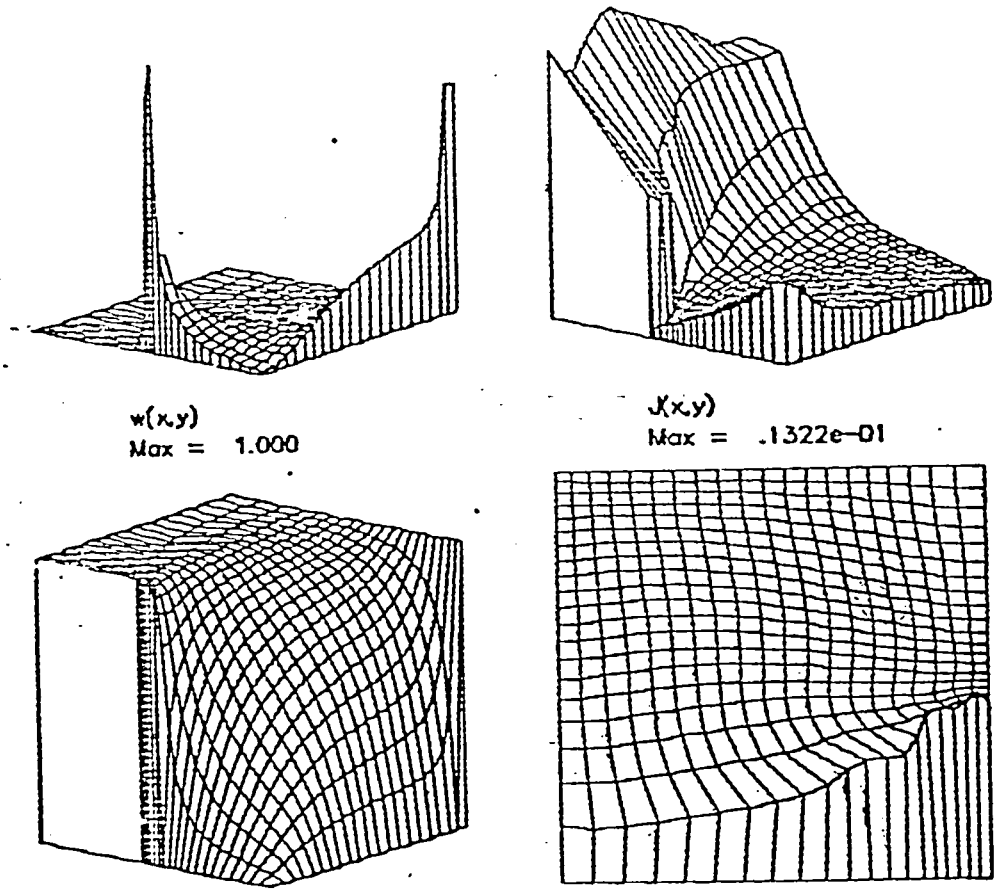

TEST1 /A,LAMVI=5,LAMO=0,POWW=1.0,NS=0
Date & Time Generated: 83/10/05.. 08.48.05.
Date & Time Plotted: 83/10/05.. 10.04.09.
IMAX= 21 JMAX= 21 IL= 1 IU= 21 JL= 1 JU= 21

20×20

$w = |DU|$

$\lambda_v = 5$

$\lambda_0 = 5$

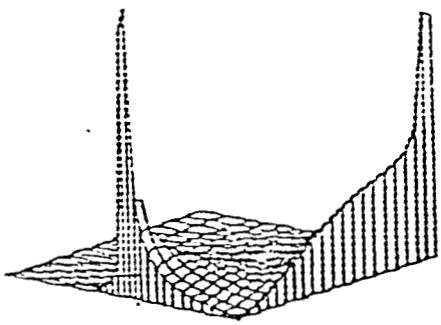

w(x,y)
Max = 1.000

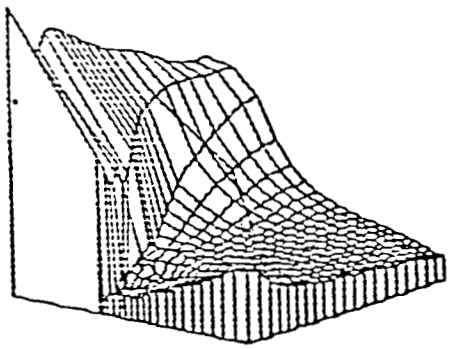

J(x,y)
Max = .1328e-01

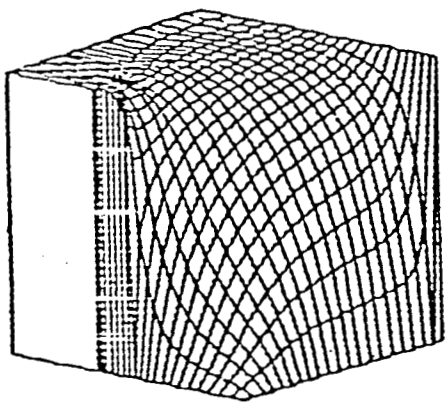

U(x,y)
Max = 1.000

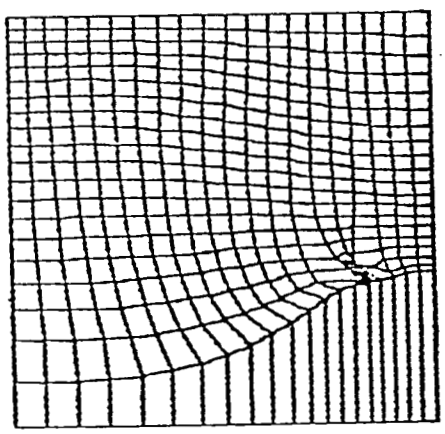

Grid: Normal View
Max = 0.

TEST16/C,LAMVI=5,LAM0=5,POWW=1.0,NS=0
Date & Time Generated: 83/10/14.. 08.33.22.
Date & Time Plotted: 83/10/14.. 14.28.06.
MAX= 21 JMAX= 21 IL= 1 IU= 21 JL= 1 JU= 21

20 × 20

$w = 0.4$ $\lambda_v = 5$

$\lambda_0 = 10$

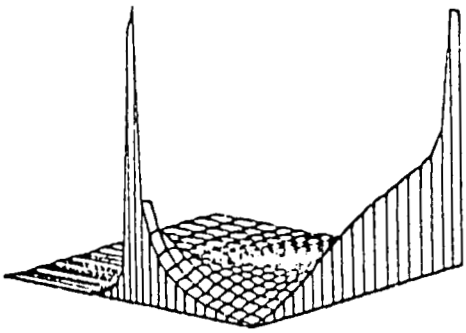

w(x,y)
Max = 1.000

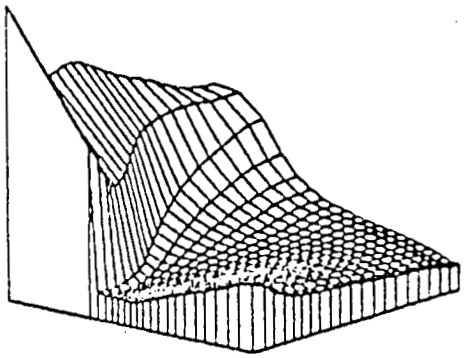

J(x,y)
Max = .1400e-01

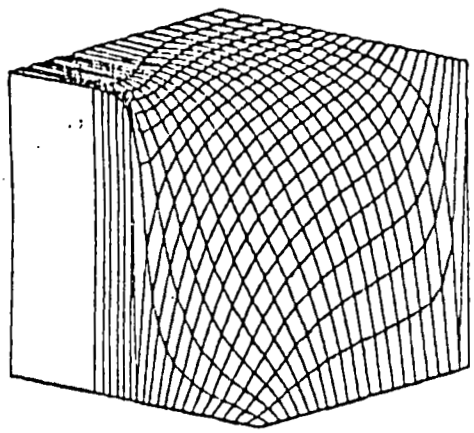

U(x,y)
Max = 1.000

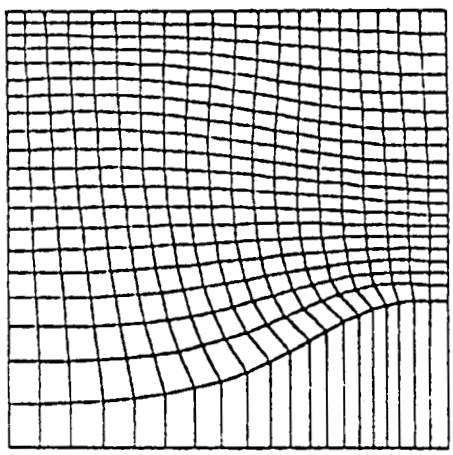

Grid: Normal View
Max = 0.

TEST17/A,LAMVI=5,LAMO=10,POWW=1.0,NS=0
Date & Time Generated: 83/10/14., 17.36.55.
Date & Time Plotted: 83/10/17., 17.05.23.
IMAX= 21 JMAX= 21 IL= 1 IU= 21 JL= 1 JU= 21

FURTHER WORK

- COMPARE ANALYTICAL SOLUTION TO THOSE OBTAINED ON ADAPTED & NON-ADAPTED GRIDS.

- OPTIMIZE GRID GENERATION CODE - IS IT REALLY WORTH THE EFFORT?

- APPLY TO OTHER TYPES OF PROBLEMS